Dimension sociale de l'espace péri-personnel des primates

Audrey Dureux

N° d'ordre NNT : 2021LYSE1262

THESE de DOCTORAT DE L'UNIVERSITE DE LYON
opérée au sein de
l'Université Claude Bernard Lyon 1

Ecole Doctorale N° 476
Neurosciences et Cognition (NSCo)

Spécialité de doctorat :
Neurosciences

Soutenue publiquement le 19/11/2021, par :
Audrey DUREUX

Dimension sociale de l'Espace Péri-personnel des primates

Devant le jury composé de :

Dorine VERGILINO-PEREZ	Professeure des universités, Paris-Descartes	Présidente/Rapporteure
Andrea SERINO	Professeur, Université de Lausanne	Rapporteur
Julia SLIWA	C.R., CNRS Paris	Examinatrice
Yves ROSSETTI	PU-PH, Université Lyon 1	Examinateur
Alessandro FARNÈ	D.R., INSERM Lyon	Directeur de thèse
Fadila HADJ-BOUZIANE	C.R., CNRS Lyon	Co-directrice de thèse

Université Claude Bernard – LYON 1

Président de l'Université	M. Frédéric FLEURY
Président du Conseil Académique	M. Hamda BEN HADID
Vice-Président du Conseil d'Administration	M. Didier REVEL
Vice-Président du Conseil des Etudes et de la Vie Universitaire	M. Philippe CHEVALLIER
Vice-Président de la Commission de Recherche	M. Petru MIRONESCU
Directeur Général des Services	M. Pierre ROLLAND

COMPOSANTES SANTE

Département de Formation et Centre de Recherche en Biologie Humaine	Directrice : Mme Anne-Marie SCHOTT
Faculté d'Odontologie	Doyenne : Mme Dominique SEUX
Faculté de Médecine et Maïeutique Lyon Sud - Charles Mérieux	Doyenne : Mme Carole BURILLON
Faculté de Médecine Lyon-Est	Doyen : M. Gilles RODE
Institut des Sciences et Techniques de la Réadaptation (ISTR)	Directeur : M. Xavier PERROT
Institut des Sciences Pharmaceutiques et Biologiques (ISBP)	Directrice : Mme Christine VINCIGUERRA

COMPOSANTES & DEPARTEMENTS DE SCIENCES & TECHNOLOGIE

Département Génie Electrique et des Procédés (GEP)	Directrice : Mme Rosaria FERRIGNO
Département Informatique	Directeur : M. Behzad SHARIAT
Département Mécanique	Directeur M. Marc BUFFAT
Ecole Supérieure de Chimie, Physique, Electronique (CPE Lyon)	Directeur : Gérard PIGNAULT
Institut de Science Financière et d'Assurances (ISFA)	Directeur : M. Nicolas LEBOISNE
Institut National du Professorat et de l'Education	Administrateur Provisoire : M. Pierre CHAREYRON
Institut Universitaire de Technologie de Lyon 1	Directeur : M. Christophe VITON
Observatoire de Lyon	Directrice : Mme Isabelle DANIEL
Polytechnique Lyon	Directeur : Emmanuel PERRIN
UFR Biosciences	Administratrice provisoire : Mme Kathrin GIESELER
UFR des Sciences et Techniques des Activités Physiques et Sportives (STAPS)	Directeur : M. Yannick VANPOULLE
UFR Faculté des Sciences	Directeur : M. Bruno ANDRIOLETTI

Résumé

Même si nous percevons l'espace qui nous entoure comme un continuum cartésien, la région de l'espace près du corps où se déroulent les interactions physiques avec l'environnement est une région spéciale, appelée espace péri-personnel (EPP). L'EPP a d'abord été défini sur la base des propriétés de neurones enregistrés chez le singe dans des régions cérébrales prémotrices et pariétales spécifiques. Plus récemment, un réseau homologue putatif a été identifié chez l'homme en utilisant l'Imagerie par Résonance Magnétique fonctionnelle (IRMf). La représentation de cet espace ne fait pas référence à une région bien délimitée avec des frontières claires mais est au contraire flexible, nous permettant d'adapter notre comportement en fonction du contexte. En particulier, le monde des hommes et des singes est avant tout un monde social. Dans ce monde social, une zone de confort est nécessaire pour réguler la distance entre soi et les autres et ainsi éviter l'inconfort, voire l'anxiété. Cependant, on sait encore peu de choses sur cette dimension sociale de l'EPP comparé à celle liée aux objets. Dans ce contexte, mon travail de thèse visait d'abord à combler le fossé entre les propriétés enregistrées dans les neurones individuels du singe et les activations cérébrales identifiées en neuroimagerie du réseau prémoteur-pariétal humain. Deuxièmement, il visait à apporter un nouvel éclairage sur la dimension sociale de l'EPP, un sujet qui a été largement négligé jusqu'à présent alors qu'il est de la plus haute importance pour tous les animaux. Pour répondre à ces questions, j'ai développé des protocoles utilisant un environnement de réalité virtuelle (RV), avec un casque de RV ou avec un projecteur 3D dans le scanner IRM, permettant une manipulation et un contrôle très précis des informations visuelles à différentes distances de notre corps.

Pour réaliser mon premier objectif, j'ai utilisé des procédures expérimentales similaires chez l'homme et le singe afin de comparer l'activité cérébrale en IRMf chez ces deux espèces. À travers deux tâches, où des objets réels ou virtuels étaient présentés dans l'espace proche ou éloigné du corps, j'ai identifié un réseau prémoteur-pariétal homologue sous-jacent à la représentation de l'EPP chez les deux espèces. Pour réaliser mon deuxième objectif, j'ai utilisé une approche multi-échelle chez l'homme. Plus précisément, mon objectif était de comprendre comment les informations sociales (expressions faciales émotionnelles) dans notre EPP affectent nos capacités de perception, notre état physiologique en utilisant des mesures de diamètre pupillaire et de fréquence cardiaque, et notre activité cérébrale en utilisant l'IRMf.

Au niveau comportemental, mes résultats ont montré que nos capacités de discrimination visuelle étaient améliorées lorsque les visages émotionnels étaient présentés dans l'EPP par rapport à l'espace lointain, même lorsque la taille rétinienne était similaire pour les images proches et lointaines. Cette amélioration des capacités perceptives s'accompagnait d'une augmentation de la fréquence cardiaque lorsque les visages émotionnels étaient dans l'espace proche du corps. Enfin, au niveau neuronal, j'ai identifié un réseau occipito-prémoteur-pariétal avec une activité accrue en présence de visages émotionnels présentés dans l'espace proche par rapport aux visages dans l'espace loin. Mes résultats montrent également qu'un réseau commun code de manière similaire des stimuli sociaux et non sociaux dans l'EPP. Parallèlement à ce travail réalisé chez des volontaires sains, j'ai également établi un lien direct entre des lésions unilatérales médio-temporales et un déficit dans la régulation appropriée des distances sociales.

En résumé, mes résultats démontrent que la présence sociale dans l'EPP facilite nos performances comportementales, augmente notre niveau de vigilance et recrute un réseau neuronal prémoteur-pariétal central quel que soit le type d'information (sociale ou non sociale). Ainsi, un réseau neuronal commun pourrait être principalement recruté dans n'importe quelle situation se produisant dans notre EPP, nous permettant d'agir plus rapidement, et des régions cérébrales supplémentaires pourraient entrer en jeu afin d'affiner notre comportement en fonction du contexte.

Abstract

Even though we perceive the space surrounding us as a cartesian continuum, the region of space near the body where physical interactions with the environment take place is a special region, termed peripersonal space (PPS). PPS was first defined on the basis of neuronal properties recorded in the monkey in specific premotor and parietal brain regions. More recently, a putative homologous network has been identified in humans using functional Magnetic Resonance Imaging (fMRI). The representation of this space does not refer to a well-demarcated region with clear borders but is instead flexible allowing us to adapt our behavior depending on the context. In particular, the world of human and non-human animals is first and foremost a social world. In this social world, a comfort zone is necessary to regulate the distance between selves and others and thus avoid discomfort or even anxiety. Much less is known about this social dimension of PPS than about the physical, object-related function of PPS. In this context, my PhD work aimed first at bridging the gap between the properties recorded in the monkey's individual neurons and the neuroimaging measure of the human premotor-parietal network. Second, it aimed at shedding new light on the social dimension of PPS, a topic that has largely been overlooked up to now although it is of utmost importance for all animals. To address these questions, I have developed protocols in virtual reality (VR) environment with a virtual reality headset or with a 3D projector in the MRI scanner because it allows for very precise manipulation and control of visual information at different distances from our body.

To carry out my first objective, we used similar experimental procedures in both humans and monkeys to compare cerebral activity with fMRI. Through two tasks, where either real or virtual objects were presented at different distances (close and far) from the body, I identified a homologous premotor-parietal network underlying PPS representation in the two species. To carry out my second objective, I used a multiscale approach. Specifically, my goal was to understand how social information (emotional facial expressions) in our PPS affects our perceptual abilities, our physiological state using measures of pupil diameter and heart rate, and our brain activity using fMRI. At the behavioral level, my results showed that our visual discriminating abilities were improved when emotional faces were presented in PPS compared to the far space, even when retinal size was equated for close and far images. This improvement in perceptual abilities was accompanied by an increase in heart rate frequency, reflecting an

arousing response when emotional faces were close to the body. Finally, at the neuronal level, I have identified an occipito-premotor-parietal network with increased activity in the presence of close compared to far emotional faces. Interestingly, my results also show that a common network encoded similarly social and non-social stimuli in PPS. In parallel to this work in healthy volunteers, I also established a direct link between unilateral medial-temporal lesions and a deficit in the regulation of appropriate social distances.

In summary, my results demonstrate that social presence in PPS facilitates our behavioral performance, increases our level of arousal, and recruits a central premotor-parietal neural network regardless of the type of cue (social or non-social). Thus, a common neural network might allow a rapid response that might be primarily recruited in any situation occurring in our PPS and additional brain regions might come into play to fine tune our behavior depending on the context.

Remerciements

Quelques 300 pages plus tard, c'est avec beaucoup d'émotions que je suis en train d'écrire ces remerciements qui marquent la fin de ma thèse …
Bien que ce soient les premiers mots que vous lisez, (avant tout le reste qui suit derrière pour les plus courageux), pour moi ce sont mes dernières lignes. Dans ces quelques lignes, j'aimerais remercier toutes les personnes qui ont contribué à mon travail de thèse, à ma vie de thésarde ou qui m'ont simplement soutenue au cours de ces quelques années importantes de ma vie.

Tout d'abord, je tiens à remercier l'ensemble des membres du jury qui ont gentiment accepté d'évaluer mon travail de thèse, mes examinateurs Julia Sliwa et Yves Rossetti ainsi que mes rapporteurs, Dorine Vergilino-Perez et Andrea Serino, qui ont également accepté d'analyser dans les détails l'ensemble de mon manuscrit.

J'aimerais maintenant remercier mes directeurs de thèse sans qui ce travail n'aurait jamais pu voir le jour.
Un remerciement tout particulier à toi, Fadila, pour avoir dirigé ma thèse durant ces quelques années. Je n'ai pas assez de mots pour t'exprimer ma gratitude, mais je voudrais déjà commencer par te dire MERCI ! Merci de m'avoir transmis tes connaissances, ta rigueur scientifique, ta capacité de réflexion et d'interprétation qui ont largement contribué à l'avancement de mon travail de thèse. J'ai pu voir mon évolution à travers ces années et c'est en grande partie grâce à toi. Tu m'as appris à prendre de la hauteur sur mon travail (avec ton expression favorite : « so what ? ») et tu as continué à me pousser chaque jour pour donner le meilleur de moi-même. C'est avec une grande satisfaction que je peux dire que nous avons réussi à travailler main dans la main pour réaliser ce travail de thèse conséquent dont je suis très fière. Ma thèse aura été très riche et tu y as énormément contribué. Grâce à toi je suis maintenant prête pour continuer à « chercher » dans une autre contrée ! Merci encore infiniment.

Merci aussi à toi Alessandro pour nos échanges constructifs et tes précieux conseils sur mon travail ainsi que ton soutien dans cette dernière ligne droite.

Je souhaiterais également remercier les personnes qui ont contribué de différentes façons à la mise en place de mes expériences. Merci Fred pour tes superbes constructions, Clément et Roméo pour votre aide dans le développement et la mise en place de la 3D à l'IRM, qui n'a pas été facile ! Merci Franck et Danielle pour toutes ces heures passées à l'IRM et pour vos conseils précieux. Et merci à toi, Gislène, pour la transmission de ton amour et de ton savoir-faire avec nos grosses bébêtes poilues ainsi que ces heures partagées ensembles à l'animalerie.

Je voudrais également remercier les membres de l'équipe Impact qui m'ont accueilli à bras ouverts et qui ont pu égayer ces longues journées de travail par des moments de rigolades et de détente durant les pauses midi ou les pauses thé. Je pense notamment à Alexis, Leslie, Audrey, François, Amélie, Samy, Éric, Cécile, Bertrand, et la petite dernière arrivée au labo Clara, mais également aux collègues du SBRI, Camille, Vincent et Clément qui ont aussi contribué à ces moments de rigolades, surtout en dehors du labo.
Une dédicace un peu plus particulière pour vous Alexis, François, Leslie, Audrey puisque vous avez partagé un peu plus que des moments mais plutôt un petit bout de ma vie. Merci pour tous ces jours passés ensemble et de tout ce que nous avons pu partager au cours de nos sessions bars, brunch (le plus souvent chez Alexis et Nico ;)), espace game et j'en passe. Merci à toi aussi Nico d'avoir été là.

Alexis, tu as été ma première rencontre au labo et je ne l'oublierai jamais. On s'est suivis de la première à la dernière année de thèse, dans les bons comme dans les mauvais moments, et c'est pour cela que tu resteras ma grande rencontre amicale de la thèse.

Camille petite pensée à toutes ces heures éprouvantes que nous avons passé à l'IRM ces derniers mois mais qui nous aurons permis de nous rencontrer, tu es maintenant devenue une amie.

Enfin, bien que tu sois reparti en Italie, je pense aussi à toi Elvio ! Merci d'avoir été là pour me soutenir, surtout dans les premières années de ma thèse (parfois autour d'un verre à Saxe Gambetta ;)), mais également de m'avoir transmis ton savoir-faire inconditionnel pour coder sur R. Ces premières années n'auraient pas été pareil sans toi !

Un GRAND MERCI à mes amies les plus fidèles et ma famille qui ont toujours été présents quand j'avais besoin d'eux. Merci de faire partie de ma vie et de m'accompagner chaque jour un peu plus.

Ma Gagathe… trop de mots s'emmêlent dans mon l'esprit mais la chose principale à laquelle je pense c'est que tu es l'une des rares personnes les plus importantes de ma vie. Merci d'être mon pilier depuis maintenant tellement d'années… Sans toi ma vie ne serait pas la même.
Je n'oublie pas mon petit Kéké que je n'aurais jamais rencontré sans toi ;) Vous êtes deux personnes géniales alors merci d'être à mes côtés tout simplement !

Ma Blanblan… que dire... déjà 7 ans de folie à tes côtés. Ta rencontre a littéralement bouleversé ma vie. Tu as été là chaque jour pendant 2 ans lorsqu'on vivait côte à côte à Paris et tu continues et tu continueras à occuper une place considérable dans ma vie, même si des centaines ou des milliers de kilomètres nous séparent. Tu es tellement importante dans ma vie !

Ma Clara… loin des yeux mais près du cœur comme on dit ! On n'aura pas réussi à se voir beaucoup ces dernières années, mais tu es et tu resteras toujours une personne qui compte énormément à mes yeux.

Toto et Cyp, je ne vous ai pas oubliés ! Mes deux petits frères qui m'apportent tant chaque jour. Merci de m'avoir toujours supportée et d'avoir contribué à tous ces moments de bonheur. Je suis fière d'être votre grande sœur et de voir votre évolution au fil des années.

Maman, Papa, tout simplement MERCI ! Merci pour tout ce que vous avez toujours fait pour moi. Merci d'avoir toujours cru en moi et de m'avoir toujours soutenue dans toutes les décisions que j'ai pu prendre. Si j'en suis arrivée jusque-là aujourd'hui c'est grâce à vous qui m'avez toujours poussé à donner le meilleur de moi-même. Simplement merci d'être des parents extraordinaires.

Enfin, merci à toi, Ale, qui partage ma vie chaque jour. Tu resteras la plus belle chose qui me sois arrivée pendant cette thèse. Merci d'être là pour moi et de m'épauler chaque jour. Merci du soutien que tu m'apportes et que tu as pu m'apporter pendant ces derniers mois difficiles. Ta joie de vivre, ta bonne humeur et tes bons petits plats ont su me remonter le moral. Merci aussi d'avoir supporté mon vilain caractère quand j'étais fatiguée et stressée. Je suis heureuse de ce que nous avons construit ensemble et de la nouvelle vie qui nous attend au Canada. Simplement, merci de me rendre heureuse !

Table des matières

Synopsis 15

Chapitre 1 : Introduction 19

***AXE 1* : Espace péri-personnel, un espace autour du corps pour interagir avec l'environnement** 21

I. Retour aux origines : qu'est-ce que l'espace péri-personnel ? 21

II. Propriétés neuronales de l'espace péri-personnel chez le primate non-humain 23

Le cortex prémoteur 25

Le cortex pariétal 27

Le putamen 29

Deux différents circuits fonctionnels potentiels : F4-VIP et 7b-F5 30

III. Fonctions de l'EPP d'un point de vue théorique 32

IV. Fonctions de l'EPP définies par les études comportementales 38

La mesure de l'EPP à travers une variété de procédures expérimentales 39

Un traitement de l'information plus efficace dans l'EPP 43

Une représentation de l'EPP flexible 47

Des réponses défensives dans l'EPP 48

V. Substrats neuronaux de l'espace péri-personnel chez l'homme : études de neuro-imagerie 50

Un réseau prémoteur-pariétal commun : méta-analyse de Grivaz et al., 2017 50

Études de neuroimagerie utilisant des stimuli multisensoriels pour identifier les mécanismes fonctionnels de l'EPP chez l'homme 53

Études de neuroimagerie utilisant des stimuli unisensoriels pour identifier les mécanismes fonctionnels de l'EPP chez l'homme 56

VI. Comparaison des réseaux de l'EPP chez l'homme et le singe 61

***AXE 2* : L'EPP dans un contexte social** 69

I. L'espace personnel, une définition issue de l'éthologie et de la psychologie sociale 69

II. La dimension sociale de l'EPP : modulation de la représentation de l'EPP en fonction du contexte 70

III. Espace personnel et EPP, des espaces différents ou similaires ? 72

IV. Corrélats neuronaux de l'espace personnel chez l'homme 74

V. Lien entre l'EPP, l'intéroception et la conscience corporelle de soi 82

Questions posées et démarche expérimentale 105

Chapitre 2 : Comparaison des réseaux fonctionnels impliqués dans la représentation de l'EPP chez l'homme et le macaque 111

ETUDE 1 : **Comparaison de la représentation de l'espace péri-personnel chez l'homme et le singe avec un objet réel** 113

ETUDE 2 : **Comparaison de la représentation de l'espace péri-personnel chez l'homme et le singe avec un objet virtuel** 179

Chapitre 3 : Étude de la dimension sociale de l'EPP chez l'homme à travers une approche multi-échelle *221*

ETUDE 3 : **Les visages émotionnels présentés dans l'espace péri-personnel facilitent les capacités de discrimination visuelle et augmentent les réponses physiologiques** **223**

ETUDE 4 : **Les informations sociales et non sociales présentées dans l'espace péri-personnel recrutent-elles un réseau neuronal fronto-pariétal commun ?** **243**

ETUDE 5 : **Régulation de l'espace personnel chez les patients avec des lésions unilatérales médio-temporales** **281**

Chapitre 4 : Discussion générale *313*

I. Quelles sont les homologies concernant les réseaux neuronaux de la représentation de l'EPP chez l'homme et le singe ? 315

II. Comment l'information sociale module nos capacités de perception, notre état physiologique et notre activité cérébrale ? 323

III. Les réponses cérébrales de la représentation de l'EPP sont-elles influencées en fonction de la nature de l'information (sociale vs non-sociale) ? 330

IV. Mécanisme neuronal de l'espace personnel pour réguler les distances entre individus 334

V. Perspectives 339

VI. Conclusion 340

Bibliographie *343*

Synopsis

Dans la vie de tous les jours, nous évoluons et interagissons dynamiquement dans un environnement composé d'un ensemble d'objets et d'événements. Même si nous percevons l'espace qui nous entoure comme une représentation unitaire, en réalité notre cerveau code diverses représentations fonctionnelles distinctes de l'espace qui pourraient être assimilées à différentes 'bulles' invisibles autour de notre corps, partant d'une bulle très proche de la peau qui pourrait être vue comme une combinaison et s'éloignant petit à petit jusqu'à devenir très éloignée comme une sorte de zone de quarantaine. Des réseaux neuronaux élaborés permettent de contrôler ces différentes bulles et en particulier, un réseau spécifique permet de contrôler une région « spéciale » près du corps appelée espace péri-personnel (EPP). Il a été proposé que cette bulle spécifique nous permet de réaliser des actions physiques simples qui nous permettent d'évoluer dans notre vie quotidienne comme attraper une tasse de café, traverser une pièce encombrée en se faufilant sans effort autour des meubles, éviter un livre qui serait en train de tomber d'une étagère ou encore esquiver un pigeon qui vole vers notre tête dans la rue. Elle nous permet également de réaliser des actions défensives face par exemple à un prédateur qui tenterait de nous approcher. Cependant, afin de ne pas en arriver au point de fuir un prédateur qui s'approcherait trop proche de nous, dans certaines situations, cet espace pourrait nous permettre également de nous protéger des potentiels dangers ou simplement de nous éviter de l'inconfort en nous permettant de garder des distances appropriées. Prenons le cas par exemple d'une femme assise seule sur un banc dans une salle d'attente. Si un parfait inconnu vient s'asseoir à côté d'elle et se rapproche de plus en plus, il y a un moment où, à partir d'une certaine distance, la femme en question se sentira mal à l'aise, et cet inconfort arrivera d'autant plus tôt si la personne semble menaçante. En revanche, si cette personne est une personne familière, celle-ci laissera pénétrer dans son espace plus facilement la personne, mais se tiendra toujours un peu plus loin de son patron que de son ami, et beaucoup plus proche de son amant. Ainsi, nous passons beaucoup de temps à essayer de garder les individus hors de cet espace et les laisser entrer pourrait être interprété comme un signe de confiance et d'intimité. L'EPP ne se réfère donc pas à une région bien délimitée avec des frontières nettes et stables. Au lieu de cela, c'est un espace flexible qui nous permet de nous adapter rapidement et de manière

optimale en fonction du contexte. L'EPP pourrait donc être interprété comme une bulle spatiale entre nous-même et le monde, à la fois pour protéger son corps du danger immédiat et pour interagir avec l'environnement mais également avec les individus tout en gardant des distances appropriées en fonction des situations, affectant chaque partie de l'expérience humaine.

Les interactions qui se produisent dans l'espace proche du corps ont été étudiées dans un large éventail de disciplines dont l'éthologie, la neurophysiologie, les sciences sociales et la philosophie. Les méthodes d'études vont de l'enregistrement de l'activité électrique des neurones grâce à l'électrophysiologie chez l'animal, à la mesure de l'activité des aires du cerveau par détection des flux sanguins grâce à l'imagerie par résonance magnétique fonctionnelle (IRMf) chez l'homme, et à l'enregistrement de nos réactions comportementales ou physiologiques. De telles études ont montré que l'ensemble de ces mesures sont modulées lorsque des événements se produisent près du corps conduisant à l'activation d'un réseau neuronal qui serait fondamental pour notre survie.

En résumé, les recherches ayant investigué cette représentation de l'espace qui nous entoure, l'EPP, soulignent son rôle déterminant dans les interactions quotidiennes que nous entretenons avec notre environnement, sociales et non sociales. Cependant, la composante sociale de l'EPP a été étudiée que très récemment et surtout au niveau comportemental, il reste donc beaucoup à élucider au niveau neuronal pour mieux comprendre ses propriétés fonctionnelles. L'aspect que j'ai donc choisi d'approfondir pendant ma thèse est la dimension sociale de l'EPP afin de mieux comprendre comment les informations sociales, c'est à dire celles qui concernent nos pairs, en fonction de leur position dans l'espace, autrement dit, dans notre EPP, influencent notre perception de l'environnement, et par conséquent notre interaction avec cet environnement. En utilisant la réalité virtuelle, qui nous permet de contrôler rigoureusement la présence d'éléments dans différentes parties de l'espace (proches ou éloignées de nous), mon travail a été de comprendre comment la présence d'individus affecte nos capacités mentales, notre état physiologique et notre activité cérébrale, en fonction de leur état émotionnel.

Le manuscrit est organisé sous forme d'articles publiés ou en préparation. Le premier chapitre de ma thèse est composé d'une introduction que j'ai divisé en deux axes. Le premier axe introduit la notion d'EPP dans son ensemble, donnant un aperçu des propriétés neuronales de l'EPP mises en évidence chez le primate non-humain grâce aux études menées en électrophysiologie, des fonctions de l'EPP identifiées chez l'homme par un ensemble d'études

comportementales variées mais également des substrats neuronaux de l'EPP mis en évidence chez l'homme grâce aux études de neuroimagerie. Enfin, dans une dernière partie, je compare les réseaux neuronaux obtenus chez ces deux espèces, afin d'introduire le premier chapitre de mes travaux expérimentaux (études 1 et 2) qui m'ont permis d'établir une comparaison directe des réseaux neuronaux fonctionnels chez l'homme et le singe en utilisant des méthodologies similaires chez les deux espèces dans l'IRM.

Ensuite, l'axe II de mon introduction sera focalisé tout particulièrement sur la composante sociale de l'EPP. Il sera appuyé par une revue de littérature que nous avons récemment publiée sur l'EPP dans un monde social, celle-ci sera accolée à la fin de mon introduction. Dans cet axe, j'exposerai les études qui ont été conduites jusqu'ici permettant de mieux caractériser cette dimension au niveau comportemental ainsi que les quelques études ayant utilisé la neuroimagerie chez l'homme. Dans une dernière partie, j'exposerai les travaux reliant la représentation de l'EPP et l'intéroception, définie comme la sensibilité à percevoir nos signaux internes comme notre activité physiologique. Cet axe servira à introduire la deuxième partie de mes travaux expérimentaux qui porte sur la caractérisation de l'EPP dans un contexte social au niveau comportemental, physiologique et neuronal. Comme je le décris dans la partie « questions posées et démarche expérimentale », dans le troisième chapitre de ma thèse j'exposerai les trois études que j'ai réalisées sur la composante sociale de l'EPP. Dans l'étude 3, je me suis intéressée à la manière dont l'information sociale module nos capacités de discrimination visuelle et nos réponses physiologiques dans l'EPP. Dans l'étude 4, j'ai identifié le réseau neuronal impliqué dans la représentation de l'EPP en fonction de différents contextes : non-sociaux, sociaux neutres et sociaux émotionnels. Dans l'étude 5, j'ai pu établir un lien direct entre les conséquences de lésions cérébrales et un déficit dans la régulation appropriée des distances chez trois patients. Finalement, dans le quatrième et dernier chapitre de ma thèse, j'ai synthétisé et discuté les résultats de l'ensemble de ces travaux.

Chapitre 1 :

Introduction

AXE 1 :

Espace péri-personnel, un espace autour du corps pour interagir avec l'environnement

I. Retour aux origines : qu'est-ce que l'espace péri-personnel ?

Bien que l'espace soit perçu comme un continuum, il existe de nombreuses cartes spatiales dans notre cerveau, nous permettant de représenter l'espace qui nous entoure (Colby & Duhamel, 1996 ; Gross & Graziano, 1995). En particulier, le concept d'une division de l'espace en fonction de sa représentation proche du corps (espace péri-personnel) ou loin du corps (espace extra-personnel) a été initialement suggéré par Brain en 1941 proposant une dissociation entre distance « d'atteinte » et distance « de marche » pour expliquer une déficience sélective dans l'une ou l'autre de ces dimensions spatiales chez les patients cérébro-lésés de l'hémisphère droit (Làdavas et al., 1998 ; Làdavas & Farnè, 2004). Ces patients souffraient d'extinction ou d'héminégligence, deux pathologies liées à des fonctions altérées de la perception spatiale.

L'héminégligence conduit la personne atteinte à « oublier » la moitié de l'espace qui l'entoure et de tout ce qui s'y présente. Ainsi, cette personne ne répond plus aux signaux qui lui sont présentés du côté opposé à la partie touchée de son cerveau. Leur déficit se présente sous diverses formes, et est souvent testé avec des tâches de représentation d'objets ou des tâches de bissection. Dans cette dernière tâche, il leur est demandé de diviser une ligne horizontale en deux, en général à l'aide d'un stylo : alors que les sujets sains ont tendance à couper la ligne en deux avec un léger biais vers la gauche (phénomène appelé pseudo-négligence), les patients héminégligents coupent la ligne sur la droite. Ce biais est dû à la méconnaissance de l'existence et/ou de l'étendue de la moitié gauche de la ligne chez les patients. Ces études ont notamment pu mettre en évidence une dissociation entre espace proche et espace loin, démontrant une

double dissociation entre héminégligence et l'espace proche et loin (Bisiach et al., 1986). En effet, la sévérité du déficit chez certains patients est influencée par la région de l'espace dans laquelle la tâche de bissection est réalisée, réussissant lorsque celle-ci était réalisée sur une feuille avec un stylo dans l'espace proche et échouant lorsque la même tâche était réalisée avec un pointeur lumineux sur des lignes placées loin (Berti & Frassinetti, 2000 ; Beschin & Robertson, 1997 ; Bisiach et al., 1986 ; Halligan & Marshall, 1991 ; Ortigue et al., 2006). Cependant, d'autres études ont montré des cas d'héminégligence spécifiques à l'espace loin (Cowey et al., 1994 ; Ortigue et al., 2006 ; Vuilleumier et al., 1998). Ces études ont ainsi pu démontrer que l'espace n'est pas représenté de manière uniforme dans notre cerveau, mais serait divisé en plusieurs secteurs distincts.

Simultanément, les premières données démontrant une interaction multisensorielle préférentielle dans l'espace proche du corps ont été obtenues chez les patients souffrant d'extinction. Ces patients sont capables d'identifier sans problème les stimulations visuelles ou tactiles lorsqu'elles sont présentées individuellement, qu'elles soient ipsi- ou contralésionnelles. Cependant, lorsqu'elles sont présentées simultanément, le patient est capable de ne rapporter que le stimulus ipsilésionnel (Bender et Feldman, 1951). L'extinction se produit également lorsque des stimuli de différentes modalités sensorielles, par exemple des stimuli tactiles ou visuels, sont administrés des deux côtés de l'espace (Mattingley et al., 1997). Ce phénomène, qui survient principalement à la suite de lésions pariétales de l'hémisphère droit (Becker & Karnath, 2007), semble être dû à une compétition sensorielle entre les stimuli (Duncan, 1996), dans laquelle l'un des deux " l'emporte" sur l'autre (de Haan et al., 2012 ; Di Pellegrino & De Renzi, 1995 ; Jacobs et al., 2011). L'étude de ces patients a permis de démontrer que le degré d'extinction dépend de la distance à laquelle les stimuli sont présentés par rapport au corps. Par exemple, lorsqu'un stimulus tactile était présenté sur la main gauche du patient, la stimulation visuelle sur la main droite était significativement plus affectée lorsque celle-ci était présentée proche par rapport à loin (Di Pellegrino et al., 1997 ; Ladavas et al., 1998). Une même modulation du degré d'extinction par rapport à la distance a été rapportée autour du visage pour des stimulations visuo-tactiles (Farnè et al., 2005 ; Ladavas et al., 1998) et audio-tactiles (Farnè & Làdavas, 2002). En effet, le degré de sévérité de l'extinction de la stimulation tactile contralésionnelle était réduit lorsque la stimulation visuelle ou auditive ipsilésionnelle était présentée loin du visage par rapport à proche. Ces preuves démontrent donc l'existence de

différentes représentations multisensorielles de l'espace autour de différentes parties du corps (di Pellegrino & Làdavas, 2015 ; Làdavas & Farnè, 2004 ; Làdavas, 2002).

Ces différentes représentations spatiales mais plus en particulier la notion d'une représentation séparée dans le cerveau pour l'espace proche et loin du corps a également pu être mise en évidence par des études neurophysiologiques. En particulier, Rizzolatti et ses collègues (1981) ont été les premiers à introduire le terme d'espace péri-personnel (EPP) pour décrire cette région de l'espace proche du corps où ont lieu les interactions physiques avec les objets de l'environnement, c'est à dire dans laquelle les objets peuvent être saisis et manipulés. L'EPP a pu être dissocié de l'espace extrapersonnel, référé comme l'espace au-delà de la distance d'atteinte. En utilisant des enregistrements en électrophysiologie chez le singe, ils ont été les premiers à identifier un ensemble de neurones dans la région postérieure péri-arquée, à l'intérieur du cortex ventral prémoteur (PMv, F4), qui répondaient préférentiellement aux objets qui étaient présentés dans l'espace proche du corps, dans l'EPP, comparé à des objets présentés loin. Deux ensembles de neurones ont pu être mis en évidence. On a ensuite dû attendre la fin des années 1990 pour une exploration neurophysiologique plus détaillée de cet espace décrivant des neurones possédant des champs récepteurs bimodaux répondant à la fois à des stimuli tactiles et visuels dans des régions corticales et sous-corticales bien définies.

II. Propriétés neuronales de l'espace péri-personnel chez le primate non-humain

La représentation neuronale de l'EPP est construite à travers un réseau neuronal constitué d'aires corticales et sous corticales qui interagissent. Des ensembles spécifiques de neurones ont été décrits dans différentes régions des aires fronto-pariétales. Ce réseau fronto-pariétal inclut le cortex prémoteur ventral, dans l'aire rostral 6, en particulier les régions F4 et F5 (Fogassi et al., 1996 ; Graziano et al., 1994 ; Gross & Graziano, 2016 ; Rizzolatti et al., 1988 ; Rizzolatti et al., 1981) et dans le cortex pariétal, la section ventrale du sillon intrapariétal (VIP ; Colby et al., 1993), la section médiale du sillon intrapariétal (MIP ; Colby & Duhamel, 1996) et l'aire 7b (Graziano & Cook, 2006). Graziano & Gross (1993) ont aussi montré que ces neurones étaient présents dans les aires sous-corticales et spécifiquement dans le putamen

(Graziano & Gross, 1993). Une particularité majeure des neurones de ces régions est qu'ils sont multisensoriels, répondant à la fois aux stimulations tactiles et visuelles et parfois auditives présentées à quelques centimètres du singe (Avillac et al., 2007 ; Colby et al., 1993 ; Duhamel et al., 1998 ; Gentile et al., 2011 ; Graziano et al., 1997 ; Rizzolatti et al., 1981). Également, ces neurones sont codés avec un cadre de référence centré sur les parties du corps, c'est-à-dire que les champs récepteurs visuels sont ancrés sur les champs récepteurs tactiles et suivent la partie du corps qui peut bouger dans l'espace. Enfin, ces neurones peuvent présenter des sélectivités pour certaines directions avec par exemple certains neurones qui ont montré des préférences pour les objets s'approchant (Graziano et al., 1997).

Pour mieux comprendre, j'ai résumé ci-dessous les propriétés communes que partagent les neurones du réseau fronto-pariétal de l'EPP à l'aide d'une figure adaptée de Graziano et al. (1997) schématisant la propriété bimodale des neurones du PMv :

1) Comme on peut le voir dans la figure 1A, ci-dessous, les champs récepteurs tactiles (représentés par la partie hachurée) et visuels (représentés par les cercles ou boxes autour de la partie de corps) se situent au même endroit et sont limités à l'espace entourant immédiatement la partie du corps. En effet, les neurones sont plus fortement activés par les stimuli présentés proches.
2) Également représentés dans la figure 1A, les champs récepteurs visuels et tactiles fonctionnent dans des systèmes de coordonnées centrés sur les parties du corps, restant ancrés à la partie du corps lorsque celle-ci est déplacée.
3) Dans la figure 1B, on peut voir que les neurones ont une propriété dynamique montrant une sélectivité pour certaines directions des stimuli tactiles et visuels.

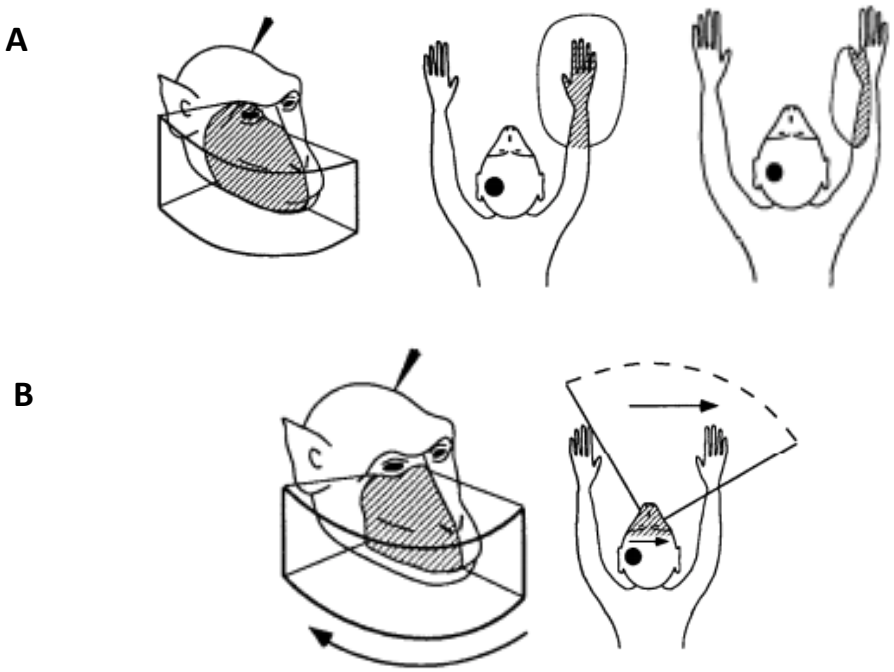

Figure 1. Schémas illustrant les propriétés communes des neurones bimodaux tactiles et visuels du réseau fronto-pariétal, répondant plus fortement aux stimuli dans l'EPP. A. Figures schématisant la superposition des champs récepteurs tactiles et visuels et également localisés sur des parties bien définies du corps. **B.** Figures schématisant la préférence pour certaines directions des stimuli tactiles et visuels. Figure adaptée de Graziano et al., 1997.

Nous allons maintenant voir en détail les propriétés neuronales de chacune des régions contenues dans les aires prémotrices et pariétales ainsi que le putamen, impliquées dans la représentation de l'EPP.

Le cortex prémoteur

Le cortex prémoteur (aire 6) est impliqué dans la préparation, l'orientation et l'exécution des mouvements (Wise, 1985). La partie ventrale de cette région (PMv) possède des neurones bimodaux, c'est-à-dire qu'ils répondent à la fois aux stimuli tactiles et visuels dans l'espace autour du corps. En particulier, les champs récepteurs visuels suivent les champs récepteurs tactiles de ces neurones qui sont principalement situés sur la main, le bras et le visage du singe (Fogassi et al., 1996 ; Graziano et al., 1994 ; Rizzolatti et al., 1981). Ces neurones bimodaux sont particulièrement nombreux dans la partie postérieure du PMv, dans l'aire F4 (Gentilucci et al., 1988, voir Figure 2A pour la localisation), répondant plus fortement à des objets en

mouvement proche de l'animal, dans son EPP, comparé à loin (Gentilucci et al., 1983, 1988 ; Rizzolatti et al., 1981). Une partie de ces neurones répondait uniquement aux stimuli qui étaient présentés très proche du corps, à moins de 10 cm de l'animal, tandis qu'une autre partie préférait les stimuli présentés un peu plus loin mais toujours dans l'espace d'atteinte de l'animal. Une autre propriété importante des neurones F4 est que le champ récepteur visuel est indépendant des mouvements des yeux. En effet, bien que la plupart des aires visuelles du cerveau possèdent des champs récepteurs ancrés sur la rétine et donc bougeant en fonction du mouvement des yeux, pour la plupart des neurones bimodaux situés dans l'aire F4, le champ récepteur ne bouge pas avec les mouvements des yeux. Celui-ci reste ancré dans la même région de l'espace, proche du champ récepteur visuel et/ou tactile indépendamment de la position du regard de l'animal (Fogassi et al., 1992). En effet, Graziano et al., 1997 ont montré que les neurones du PMv répondaient même aux stimuli visuels qui étaient présentés dans l'espace proche lorsque l'objet ne pouvait plus être vu. Les neurones du PMv codent donc la localisation du stimulus visuel en fonction du corps et non de la rétine, possédant des champs récepteurs visuels centrés sur des parties du corps (Gentilucci et al., 1983).

Une autre région faisant face à l'aire F4, le frontal eye field (FEF, aire 8), possède des neurones qui sont modulés par la distance à laquelle un objet visuel est présenté. Bien qu'une préférence pour l'EPP n'ait pas été directement montrée, ces neurones seraient modulés par la vergence (Alkan et al., 2011 ; Cléry et al., 2015), qui correspond aux mouvements oculaires conjugués permettant aux deux yeux de se focaliser sur un objet visuel donné, et également par les indices visuels de disparité binoculaire (Ferraina et al., 2000), qui correspond à la différence d'endroit où l'image d'un objet donné tombe sur la rétine gauche et droite. En combinant ces signaux de vergence oculaire avec les informations de disparité binoculaire, il serait possible d'estimer l'emplacement d'un stimulus visuel dans l'espace.

Une zone adjacente à F4, l'aire F5, située le long de la branche inférieure du sillon arqué (voir figure 2A), contient des neurones répondant à la saisie manuelle à la fois dans la lumière et dans l'obscurité dont la moitié répondaient également à des objets visuels en 3D qui étaient saisissables (Murata et al., 1997 ; Raos et al., 2006 ; Rizzolatti et al., 1988). Ces neurones possèdent des champs récepteurs tactiles localisés principalement sur le bras et/ou le visage (Gentilucci et al., 1988 ; Murata et al., 1997 ; Raos et al., 2006). En revanche, les champs récepteurs visuels semblent plus difficiles à définir. En effet, bien que des neurones répondent

plus fortement à des stimuli présentés dans l'espace d'atteinte de l'animal (Gentilucci et al., 1988), leurs réponses reposent principalement sur le fait que l'objet vu soit saisissable ou non (Bonini et al., 2014). Ils possèdent une sélectivité visuelle correspondant à une sélectivité motrice, répondant mieux à l'objet qui appelle la configuration de saisie de la main (Murata et al., 1997 ; Raos et al., 2006).

Le cortex pariétal

Des neurones avec des propriétés bimodales répondant à des stimuli tactiles et visuels, similaires aux neurones du PMv, ont aussi été retrouvés dans le lobe pariétal postérieur, en particulier dans l'aire ventrale intrapariétale (VIP ; Colby et al., 1993 ; Duhamel et al., 1998, voir Figure 2 A et B pour la localisation) et l'aire 7b (Graziano & Cooke, 2006). Bien que les neurones des aires VIP et 7b partagent des propriétés similaires, répondant aux stimuli visuels s'avançant en direction du singe à environ 10 cm du champ récepteur tactile ou un peu plus loin mais toujours dans la distance d'atteinte de l'animal, la différence majeure concerne la localisation de leurs champs récepteurs. Alors que les neurones VIP possèdent une représentation de leurs champs récepteurs centrés autour de la tête et du visage, caractérisant l'aire VIP comme étant impliquée dans la représentation de l'espace proche de la tête (Colby et al., 1993 ; Duhamel et al., 1998), les neurones de l'aire 7b possèdent des champs récepteurs qui sont distribués sur la main, le bras et le visage. Cependant, Duhamel et al, en 1997, ont montré que les neurones VIP étaient organisés le long d'un continuum, dans un gradient de référence des yeux à la tête. En effet, une partie des neurones possédaient des champs récepteurs visuels et tactiles qui restaient situés autour de la tête, quelle que soit la position des yeux du singe, tandis que pour l'autre partie des neurones, les champs récepteurs visuels et tactiles étaient ancrés sur la rétine, dépendant de la direction du regard (Bremmer et al., 2013 ; Duhamel et al., 1997).

En plus des aires VIP et 7b, d'autres régions du cortex pariétal ont été identifiées comme possédant des réponses spécifiques lorsque des objets apparaissaient dans l'espace proche du corps. Cependant, les champs récepteurs de leurs neurones étaient plus souvent centrés sur les yeux que sur les parties du corps contrairement aux neurones des régions VIP et 7b. Dans la partie médiale du cortex pariétal, l'aire V6A (Luppino et al., 2005), une portion des neurones

possède une activité qui est modulée par la position du regard dans l'espace en 3D et par les signaux envoyés par le système de vergence lors de la fixation d'un objet se déplaçant en profondeur (Breveglieri et al., 2012). Ces neurones préféraient également des distances de fixation proche du corps du singe, dans l'espace d'atteinte de l'animal. Une préférence similaire pour des fixations dans l'espace proche du corps, dans l'espace d'atteinte, a été reportée dans l'aire 7a (Sakata et al., 1980). Une autre région dans l'aire latérale intrapariétale, l'aire LIP, possède les trois quarts de ses neurones qui sont préférentiellement activés lors de fixations dans l'EPP (Genovesio & Ferraina, 2004 ; Gnadt & Mays, 1995, voir Figure 2A et B pour la localisation) et également par les stimuli visuels qui étaient présentés entre le corps de l'observateur et la localisation de la fixation. Les neurones de l'aire LIP montrent une préférence pour les indices de disparité visuelle qui indiquent des objets apparaissant proche par rapport au point de fixation lui-même présenté dans l'EPP (Genovesio & Ferraina, 2004). Toujours dans le sillon intrapariétal, mais cette fois dans l'aire médiale intrapariétale, l'aire MIP aurait un codage préférentiel pour la portion de l'espace proche du corps (Bhattacharyya et al., 2009, voir Figure 2 B pour la localisation). Les neurones de l'aire MIP ont des champs récepteurs qui sont à la fois ancrés sur la position des yeux et sur la position des mains, leurs permettant de déplacer la main efficacement pour atteindre l'objet visuel (Colby & Duhamel, 1996). Cette région est d'ailleurs également surnommée la région pariétale d'atteinte (« Parietal reach region », PRR ; Andersen & Buneo, 2002) puisque c'est une aire critique impliquée dans des comportements d'atteinte comme la saisie d'objets (Andersen et al., 1997).

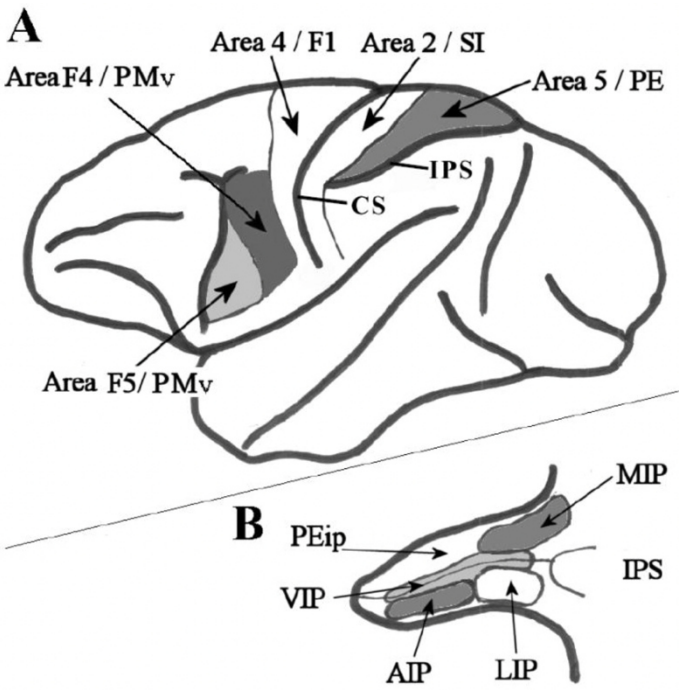

Figure 2. **A.** Représentation des régions prémotrices (F4, F5) et pariétales (IPS : VIP, MIP, LIP) de l'EPP chez le singe. **B.** Le sillon intrapariétal a été ouvert pour révéler la localisation des régions le composant. *IPS – Sillon intrapariétal ; MIP – sillon intrapariétal médian ; LIP – sillon intrapariétal latéral ; AIP – sillon intrapariétal antérieur ; VIP –sillon intrapariétal ventral ; PEip – l'aire PE de la portion intrapariétale.* Figure de Holmes et al., 2004.

Le putamen

Des propriétés similaires aux neurones bimodaux décrits dans les aires prémotrices et pariétales ont été identifiées dans une structure sous-corticale faisant partie des ganglions de la base, le putamen, qui forme avec le cortex frontal les boucles fronto-striatales. Cette région contient des neurones qui répondent aux stimuli tactiles et visuels dans l'espace proche autour du singe, n'étant pas sélectifs au type de stimuli (couleur, forme) (Graziano & Gross, 1993). Comme pour les régions décrites précédemment, le putamen possède des propriétés bimodales qui fournissent une carte de l'espace visuel entourant immédiatement le singe et organisée de manière somatotopique, c'est-à-dire par partie du corps, plutôt que rétinotopique.

Les différentes régions décrites précédemment sont fortement connectées anatomiquement. En plus de leurs connexions anatomiques, certaines régions peuvent être également reliées à travers les différentes fonctions qu'elles partagent ou encore en fonction des parties du corps qu'elles codent. Dans leur revue, Cléry et al. (2015) ont suggéré deux circuits fonctionnels fronto-pariétaux distincts, tous deux possédant des neurones bimodaux répondant à la fois aux stimuli tactiles et visuels présentés dans l'espace proche. Le premier réseau reliant l'aire pariétale VIP à l'aire prémotrice F4 semblerait correspondre à un réseau défensif de l'EPP (Figure 3). En effet, bien que ces régions présentent des propriétés divergentes avec une représentation de l'EPP plus marquée autour du visage dans VIP et plus marquée autour du bras dans F4, des études utilisant des micro-stimulations électriques dans VIP et F4 ont produits des mouvements de défense chez l'animal comme des clignements de yeux, des levés de bras, un haussement des épaules etc. (Cooke & Graziano, 2003 ; Thier & Andersen, 1998). Lorsque les micro-stimulations étaient réalisées dans F4, il a aussi été décrit un retrait rapide de la main vers une posture protectrice derrière le dos (Cooke & Graziano, 2004 ; Graziano et al., 2002 ; Graziano & Cooke 2006). Le deuxième réseau serait composé de l'aire pariétale 7b et l'aire prémotrice F5 et serait plus associé aux comportements d'approche (Figure 3). Les neurones situés dans l'aire 7b répondent aux stimuli visuels et tactiles et déchargent lors d'une activité motrice (Leinonen et al., 1979 ; Robinson et al., 1978). L'aire F5 possède des neurones qui déchargent à la vue de certains stimuli mais également à l'action générée vers les objets mentionnés (Murata et al., 1997 ; Raos et al., 2006).

Cependant, les auteurs ont également proposé une autre distinction basée sur la représentation de l'EPP autour de différentes parties du corps plutôt que les fonctions de chaque région identifiée plus haut. En effet, la représentation de l'EPP autour du visage est plus marquée dans les aires VIP (Colby et al., 1993 ; Duhamel et al., 1998), les neurones VIP possédant leurs champs récepteurs centrés autour du visage et traitant les informations relatives à la direction du regard et de la tête. Les neurones du PMv présentent, eux, une représentation de l'EPP plus centrée autour du bras (Graziano et al., 1997) et les neurones de l'aire 7b possèdent des champs récepteurs recouvrant le tronc et la partie proximale du membre supérieur (Graziano & Gross 1995). Ils ont donc suggéré qu'il existerait finalement une multitude de

représentations de l'EPP qui pourrait être soit définie en fonction des différentes parties du corps ou en fonction de leur rôle.

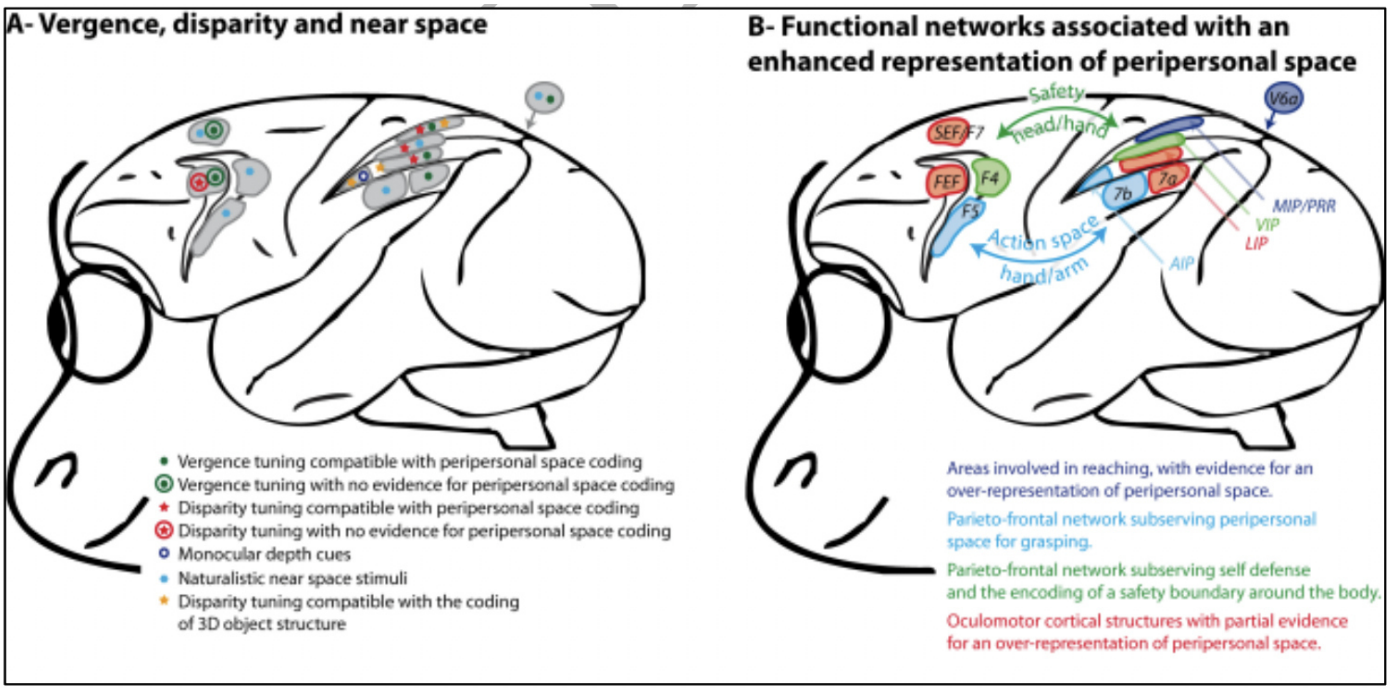

Figure 3. A. Régions fonctionnelles montrant une modulation des réponses en fonction des indices de profondeur (système de vergence et disparité binoculaire) compatibles ou non avec le codage de l'EPP. Pour plus de détails, se référer à la légende associée à la figure. **B.** Représentation des réseaux fonctionnels associés à la représentation de l'EPP dans le cerveau du singe d'après Cléry et al., 2015. En bleu foncé sont représentées les aires impliquées dans les actions d'atteintes, et en rouge les régions oculomotrices modulées par la disparité binoculaire et par le système de vergence mais pour lesquelles aucune évidence pour une préférence dans l'EPP n'a été montrée. En bleu clair et en vert sont représentés les réseaux suggérés par les auteurs pouvant être séparés en différentes fonctions. Les aires du réseau fronto-pariétal qui pourraient potentiellement être impliquées dans les comportements d'approche (aires pariétales 7b et le sillon intrapariétal antérieur AIP avec l'aire prémotrice F5) sont représentées en bleu clair, alors que le réseau fronto-pariétal qui pourrait potentiellement être impliqué dans les comportements d'évitement (défensif) (zone intrapariétale ventrale VIP avec la zone prémotrice F4) est représenté en vert.

III. Fonctions de l'EPP d'un point de vue théorique

Comme je l'ai présenté dans le premier paragraphe de mon introduction, l'existence d'un système de l'EPP chez l'homme a d'abord été suggéré par des preuves en neuropsychologie sur des patients atteints de lésions cérébrales souffrant d'extinction et d'héminégligence.

Par la suite, d'autres études convergentes de la psychologie expérimentale et des études utilisant la neuroimagerie sont venues confirmer l'existence de cette région spécifique, proche du corps, traitant et intégrant des stimuli tactiles, visuels ou auditifs. Avant de rentrer dans le détail de ces études comportementales et de neuroimagerie, je vais d'abord décrire la notion d'EPP d'un point de vue théorique, que des chercheurs ont tenté d'expliquer.

Dans le paragraphe précédent, nous avons vu qu'il pouvait exister plusieurs représentations de l'EPP en fonction de différents facteurs, à savoir, en fonction de la partie du corps ciblée et/ou de la fonction sollicitée. D'un point de vue théorique, de Vignemont & Iannetti, en 2015, ont proposé un modèle de la représentation de l'EPP sur la base d'une distinction fonctionnelle, sensorielle et motrice. Selon eux, la représentation de l'EPP serait considérée comme un modèle spécialiste qui conduirait à l'existence de deux types d'EPP : la protection du corps et l'action dirigée vers un but. L'EPP agirait donc comme une interface privilégiée pour éviter les menaces potentielles proche du corps et comme une interface de travail qui permettrait au corps d'agir dans l'environnement proche (Figure 4).

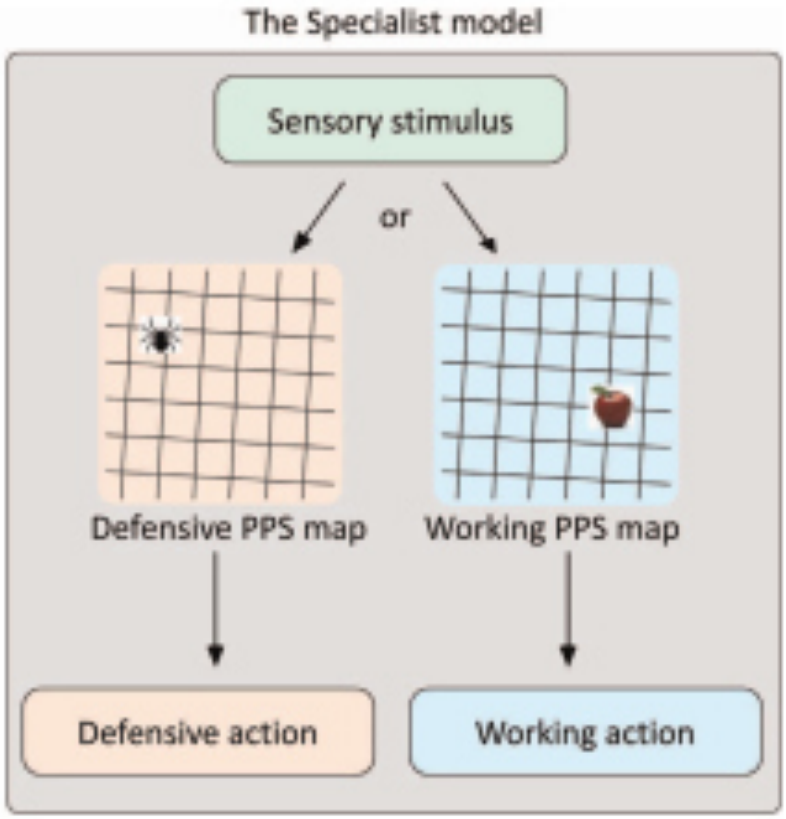

Figure 4. Le model spécialiste de l'EPP à partir de la revue de Vignemont & Iannetti (2015). Ce modèle spécifique défini la représentation de l'EPP selon deux types de fonctions : soit une représentation de l'EPP impliquée dans la protection du corps, un espace défensif ou une représentation de l'EPP impliquée dans l'action dirigée par un but, un espace de travail. La signification du stimulus définirait la représentation de l'EPP adaptée.

Plus récemment, Bufacchi & Iannetti (2018) ont proposé un modèle alternatif, dans lequel l'EPP est défini comme un ensemble de zones (définies dans la revue comme des « fields » en anglais) graduées où chaque zone serait reflétée en fonction de la pertinence comportementale d'un stimulus pour une action donnée, c'est-à-dire des actions comportementales visant à créer ou éviter le contact entre les objets et le corps.

Les propriétés spatiales de l'EPP seraient déterminées par la proximité du corps ou d'une partie du corps mais également par un ensemble de facteurs. En effet, un certain nombre de travaux ont pu montrer qu'un ensemble de facteurs affectaient les propriétés de l'EPP, influencées par exemple par la position du stimulus (Colby et al., 1993 ; Graziano, 2017), sa direction (Serino et al., 2015) ainsi que sa trajectoire (Cléry et al., 2015), mais également par les signaux gravitationnels (Bufacchi & Iannetti, 2016), le mouvement des parties du corps

(Brozzoli et al., 2009, 2010), la marche (Noel et al., 2014 ; Amemiya et al., 2017), ou encore des facteurs de plus haut niveau tels que la valence du stimulus (Taffou and Viaud-Delmon, 2014 ; Ferri et al., 2015 ; de Hann et al., 2016 ; Cartaud et al., 2010) ou l'environnement (Sambo et al., 2012). Selon les auteurs, ces effets fournissent des preuves à l'idée que la représentation de l'EPP ne peut pas être expliquée uniquement par la proximité du stimulus. Ainsi, ils suggèrent que la différence de sensibilité de l'EPP en fonction de différents facteurs indique que l'EPP n'agirait pas comme une entité unique mais serait plutôt considéré comme un ensemble de zones continues, appuyant le fait que la représentation de l'EPP change de manière non-monotone avec la proximité du corps. La figure 5 ci-dessous, tirée de la revue de Bufacchi & Iannetti (2018), illustre justement cette idée que l'EPP ne serait pas une entité unique mais un ensemble de zones qui dépendent de la proximité et sont modulées par certains facteurs. Les exemples ci-après, représentés dans la figure, montrent différents types de facteurs affectant les mesures liées à l'EPP et pouvant provoquer une expansion ou une réduction de ces zones. Ces facteurs incluent par exemple le mouvement d'un stimulus visuel (i) ou le mouvement d'une partie du corps (ii) ou encore du corps entier (iii), l'utilisation d'outils (iv), la présence d'un objet, un écran de protection, dans l'espace proche (v) ou encore la présence de sons menaçants (v). Dans ces différents exemples, chaque couleur indique la partie du corps où la zone de l'EPP est représentée (vert : visage, bleu : main et rouge : corps entier).

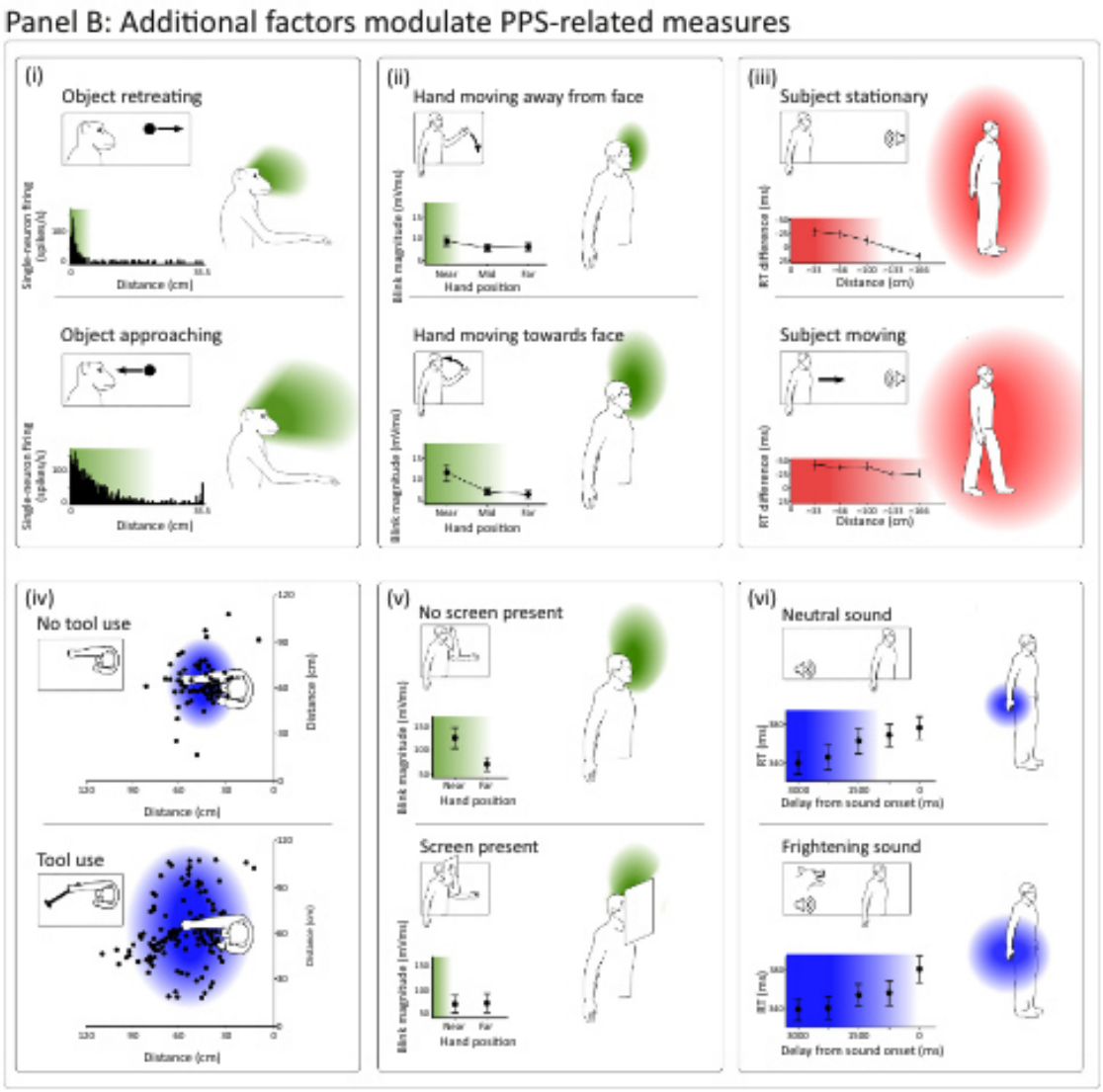

Figure 5. Reconceptualisation de l'EPP comme un ensemble de zones reflétant la pertinence des actions visant à créer ou éviter le contact entre les objets et le corps qui dépendent de la proximité spatiale mais également de facteurs additionnels. Figure de la revue de Bufacchi & Iannetti, 2018.

Enfin, un autre modèle proposé par Magosso et Serino décrit dans la récente revue de Serino (2019) a permis de synthétiser comment la représentation de l'EPP pouvait être implémentée dans le cerveau. Ils ont ainsi proposé un modèle neuronal computationnel décrivant comment les stimuli tactiles sur la main ainsi que les stimuli visuels et auditifs présentés proche du corps étaient intégrés (Magosso, 2010 ; Magosso, Serino, et al., 2010 ; Magosso, Zavaglia, et al., 2010 ; Serino, Canzoneri, et al., 2015). Dans ce modèle neuronal computationnel, une série de couches unisensorielles représentant les zones tactiles, visuelles et auditives sont connectées les unes aux autres à une couche multisensorielle. Le réseau reproduit la force des connexions

synaptiques entre ces couches en cas de stimulations situées à l'intérieur ou à l'extérieur de l'EPP (Magosso, Zavaglia, et al., 2010). Ainsi, une stimulation tactile sur la main et/ou une stimulation visuelle ou auditive proche de la main est suffisante pour activer les neurones multisensoriels. A l'inverse, une stimulation visuelle ou auditive loin de la main n'est pas assez forte pour induire une activité multisensorielle (Figure 6A).

En réalisant une série d'expériences in-silico, ce modèle a permis de simuler les données comportementales chez les sujets sains et les patients en modélisant la perception tactile comme le résultat de l'activation des neurones multisensoriels. Ces simulations ont réussi à reproduire des données comportementales montrant une perception plus rapide et plus précise lorsque la stimulation tactile était couplée à des stimuli visuels (Magosso, 2010 ; Magosso, Serino, et al., 2010) ou auditifs (Serino, Canzoneri, et al., 2015) proche du corps, et ils ont été capables de reproduire la modulation graduée de l'espace de traitement tactile en fonction de la position des sons dans l'espace, comme le montre l'étude de Canzoneri et al. (2012) qui sera expliquée plus en détail dans le paragraphe suivant.

Les interactions physiques entre le corps et les objets externes se produisent au sein de l'EPP. L'utilisation d'outils permet une interaction physique avec des stimuli externes plus éloignés spatialement, ce qui peut étendre la représentation de l'EPP. Leur modèle a donc été élargi afin de proposer un mécanisme neuronal sous-jacent à cette plasticité dépendante de l'expérience dans l'EPP, en modifiant la force des synapses afin qu'elle ne soit pas fixe mais qu'elle soit définie en continu par l'expérience selon une règle d'apprentissage Hebbian visant à simuler l'intégration main-objets de la vie quotidienne. Dans des conditions classiques, la stimulation tactile est couplée à une stimulation visuelle ou auditive se produisant à proximité de la main (activant des neurones unisensoriels visuels ou auditifs avec des champs récepteurs dans l'espace proche) alors que les neurones possédant des champs récepteurs pour l'espace lointain sont beaucoup plus rarement associés à une stimulation tactile. De cette façon, les connexions synaptiques entre les neurones visuels ou auditifs unimodaux avec des champs récepteurs dans l'espace proche du corps se renforcent continuellement en raison du déclenchement simultané des neurones multisensoriels post-synaptiques (activés par la stimulation tactile), tandis que ceux avec des neurones visuels ou auditifs unimodaux avec des champs récepteurs loin se dégradent. Cependant, une stimulation multisensorielle proche et lointaine médiée par l'utilisation d'un outil synchrone entrainerait un renforcement des synapses entre les neurones unisensoriels avec des champs récepteurs lointains et les neurones multisensoriels. Dans cette condition, les neurones multisensoriels sont activés par les neurones tactiles unisensoriels en

raison de la stimulation de la main et les neurones visuels/auditifs unisensoriels avec des champs récepteurs lointains sont activés par des informations sensorielles lointaines liées à l'outil renforçant ainsi les synapses entre les deux ensembles de neurones (Figure 6B). Une série d'expériences de simulation (Serino, Canzoneri, et al., 2015) ont ainsi pu montrer que ce modèle était capable de reproduire l'extension de l'EPP induite par l'utilisation d'outils telle que mesurée par les résultats comportementaux chez les sujets sains (Canzoneri et al., 2013).

Par conséquent, à travers ce modèle, Serino (2019) a proposé que l'extension de l'EPP, défini par la taille des champs récepteurs multisensoriels des neurones de l'EPP, est constamment façonnée par l'expérience en fonction du couplage de la stimulation somatosensorielle et des signaux externes visuels et/ou auditifs.

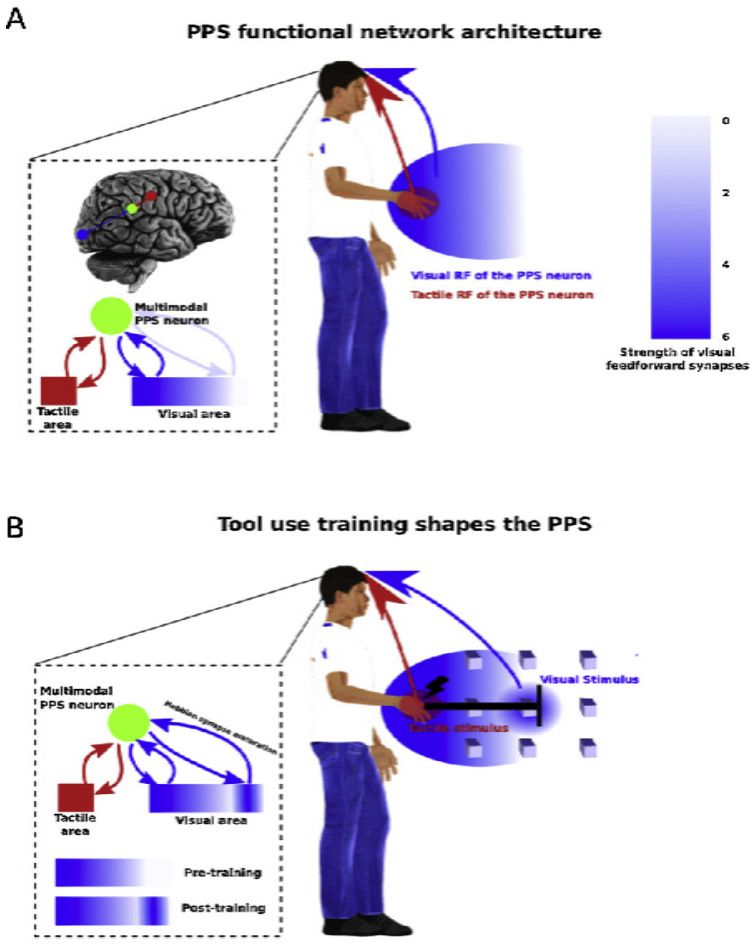

Figure 6. A. Structure du modèle de simulation du réseau de neurones de l'EPP (Magosso, Ursino, et al., 2010 ; Magosso, Zavaglia, et al., 2010). La représentation de l'espace péri-main visuo-tactile est reconstruite par la communication d'aires unisensorielles tactiles (rouge) et visuelles (bleu), qui ont des champs récepteurs centrés sur la main (tactile) ou sur l'espace qui l'entoure (visuel), et les zones d'intégration multisensorielle par le biais de synapses. Afin de reproduire la caractéristique principale de la représentation de l'EPP, c'est-à-dire une interaction plus forte pour les stimuli multisensoriels proche du corps, la force des synapses des neurones unisensoriels aux neurones multisensoriels est plus forte à partir des neurones visuels avec des champs récepteurs proche de la main et plus faible à partir des neurones avec des champs récepteurs lointains. **B.** L'utilisation d'un outil conduit à coupler des stimulations tactiles à des stimulations visuelles éloignées de la main, renforçant les synapses entre les régions multisensorielles et les régions visuelles avec des champs récepteurs centrés sur l'espace lointain via un mécanisme de type hebbian. Cela provoque une extension de l'EPP.
Figure modifiée à partir de Serino, 2019.

Le résumé de ces différentes théories montre la complexité associée au concept de représentation de l'EPP. Je vais maintenant examiner plus en détail les principaux paradigmes expérimentaux qui ont été utilisés pour étudier l'EPP chez l'homme ainsi que les principaux résultats obtenus, définissant les propriétés de cet espace.

IV. Fonctions de l'EPP définies par les études comportementales

Depuis les études de neurophysiologie chez le singe, une littérature abondante s'est accumulée pour comprendre les caractéristiques de la représentation de l'EPP ainsi que ses fonctions. Ces études ont révélé une caractéristique clé de la représentation de l'EPP, à savoir,

sa flexibilité. Cette flexibilité dépend de facteurs externes, c'est-à-dire les caractéristiques du stimulus présent dans l'EPP, des facteurs internes liés par exemple aux traits de personnalité, et à l'utilisation d'outils (Canzoneri et al., 2013 ; Serino et al., 2007). Des modulations de la représentation de l'EPP ont également été mises en évidence pendant la marche (Berger et al., 2019 ; Noel, Grivaz, et al., 2015) ou encore en présence d'autres individus (Pellencin et al., 2018 ; Teneggi et al., 2013).

Sur la base de ces propriétés et compte tenu notamment de leur position anatomique à l'interface avec les régions motrices, il a été suggéré que la représentation de l'EPP jouait un rôle clé dans nos actions lors de nos interactions avec les objets dans l'environnement, nous permettant également d'interagir de manière efficace et optimale.

Je vais maintenant décrire l'étendue de ces recherches comportementales conduites à travers une variété de procédures expérimentales qui se sont développées ces dernières années pour mesurer l'EPP et mettre en évidence l'ensemble des propriétés clés de cet espace.

La mesure de l'EPP à travers une variété de procédures expérimentales

Depuis plusieurs années, la diversité des méthodologies qui se sont développées et ont été employées pour étudier la représentation de l'EPP a eu des implications importantes dans la caractérisation de ses fonctions et de sa conceptualisation.

Un certain nombre de procédures expérimentales ont été utilisées exploitant principalement des stimuli dynamiques ou statiques multisensoriels et, plus récemment, unisensoriels. Dans des conditions statiques, les méthodologies comparent généralement les conséquences comportementales en réponse à des stimuli apparaissant soit dans l'espace proche (à l'intérieur de l'EPP), soit dans l'espace lointain (à l'extérieur de l'EPP) alors que dans des conditions dynamiques, ce sont les réponses à des stimuli qui se rapprochent ou s'éloignent des participants. Outre les tâches audio ou visuo-tactiles décrites précédemment utilisées chez les patients souffrant d'extinction, la première tâche chez le sujet sain démontrant un traitement tactile plus fortement affecté par les stimuli visuels ou auditifs présentés dans l'espace proche du corps plutôt que loin était la tâche de congruence intermodale (« cross-modal congruency task » en anglais). Dans cette tâche, les participants devaient discriminer l'élévation des cibles

vibro-tactiles administrées soit au pouce (dans une position inférieure) soit à l'index (position supérieure), tout en ignorant les repères visuels présentés à la même élévation ou à une élévation différente (voir Figure 7). Les réponses des participants étaient plus rapides et plus précises lorsque la cible tactile et le repère visuel étaient présentés à la même altitude (conditions de congruence) : un effet appelé « effet de congruence intermodale » (CCE ; Spence et al., 2000 ; Spence et al., 2004). Mais la découverte qui nous intéresse ici est que le CCE était plus fort lorsque les repères visuels étaient présentés près de la main, par rapport à lorsqu'ils étaient présentés dans un endroit éloigné (Maravita et al., 2003 ; Pavani et al., 2000), démontrant que la force du CCE dépendait de la distance relative entre les cibles tactiles et les repères visuels. Des effets CCE dépendant de l'espace ont également été démontrés en stimulant d'autres régions du corps telles que la tête et le dos (Aspell et al., 2010).

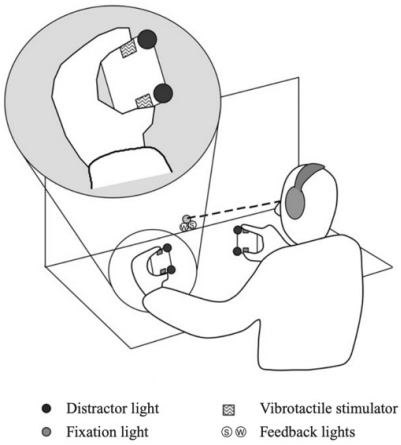

Figure 7. Schéma expérimental de la tâche de congruence intermodale, à partir de Spence et al., 2004. Le participant tient un cube en mousse dans chaque main où sont présents deux stimulateurs vibrotactiles (cf. rectangles avec zigzag) et deux lumières de distraction visuelle (cf. cercles noirs), positionnés à côté du pouce ou de l'index du participant. Les sujets devaient répondre aux cibles vibrotactiles en levant soit les orteils pour indiquer une cible supérieure ou le talon du pied droit pour indiquer une cible inférieure.

Par la suite, d'autres tâches expérimentales ont été développées et ont montré des résultats similaires. C'est le cas de la tâche d'interaction multisensorielle, utilisant des stimuli dynamiques multisensoriels audio ou visuo-tactiles. Une stimulation tactile était délivrée pendant qu'un stimulus visuel ou auditif non pertinent était présenté proche ou loin. Les sujets devaient détecter la stimulation tactile pendant que le stimulus non pertinent était plus ou moins proche du participant (Figure 8). Cette tâche a permis d'évaluer les réponses aux stimulations tactiles dans l'espace proche et loin (Canzoneri et al., 2012 ; Serino et al., 2007) mais également d'interpréter une « limite » de l'EPP en présentant les stimuli tactiles à différents

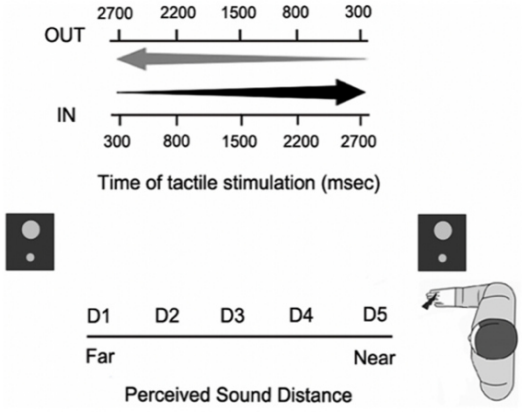

Figure 8. Paradigme de la tâche d'interaction multisensorielle audio-tactile à partir de Serino et al., 2015. Les participants devaient répondre à un stimulus tactile sur leur main, pendant que des sons non pertinents s'approchaient (sons IN) ou s'éloignaient (sons OUT) de leur main. À chaque essai, le stimulus tactile était délivré à un délai différent depuis l'apparition du son, donc perçu à une distance différente du corps du sujet (de D1, loin, à D5, proche).

délais temporels à partir de l'apparition du son, donc perçus à différentes distances du corps (Noel, Grivaz, et al., 2015 ; Serino, Noel, et al., 2015).

D'autres tâches comportementales ont été utilisées comme la tâche de bissection de ligne servant d'indicateur de l'étendue de l'EPP en mesurant l'endroit où le biais présent légèrement à gauche pour diviser les lignes près du corps se transforme en un biais vers la droite dans l'espace lointain (Longo & Lourenco, 2006) ou encore la tâche de jugement d'atteinte (« reachability judgment task » en anglais), couramment utilisée pour mesurer les limites de l'EPP. Dans cette tâche, un objet se déplace vers les participants et ceux-ci doivent l'arrêter lorsqu'il est accessible (Iachini et al., 2014 ; Quesque et al., 2017 ; Ruggiero et al., 2017).

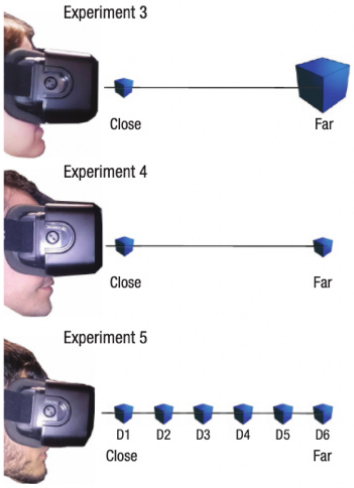

Figure 9. Paradigme de Blini et al., 2018, tâche de discrimination visuelle. Dans un environnement virtuel en 3D, des formes étaient présentées proche (50 cm) ou loin (300 cm) étant corrigées (exp 3) ou non (exp 4) pour la taille rétinienne. Six différentes distances de 50 à 300 cm ont également été utilisées où, comme pour l'exp 4, la taille de l'objet sur la rétine était mise à l'échelle en fonction de la distance. Les participants devaient discriminer entre deux formes (cube et sphère) à l'aide d'un clavier.

Récemment, au sein de notre groupe, nous avons développé une tâche de discrimination visuelle avec des stimuli statiques présentés proche et loin dans un environnement virtuel à l'aide d'un casque de réalité virtuelle (Blini et al., 2018, Figure 9). Les participants discriminaient plus rapidement les objets qui étaient présentés dans l'espace proche par rapport à loin. J'ai ensuite utilisé cette même tâche avec des stimuli sociaux afin de mettre en évidence les propriétés de l'EPP dans un contexte social, découvertes que je vous exposerai en détail dans mon Chapitre 3.

Enfin, une autre tâche utilisant une mesure physiologique, le réflexe de clignement des yeux par la main (« hand-blink reflex » en anglais, HBR), a été développée afin d'évaluer la dimension de l'EPP autour du visage (Figure 10). En particulier, ils ont démontré que la force des clignements des yeux, induite par la stimulation du nerf médian sur le poignet, variait en fonction de la distance entre la main du

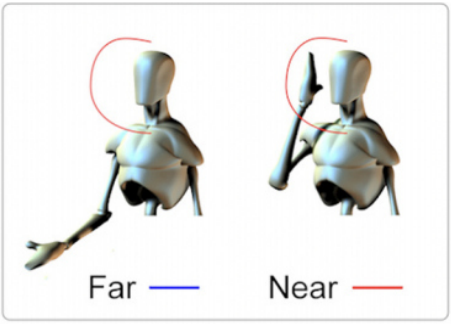

Figure 10. Paradigme du réflexe de clignement des yeux par la main, utilisé par Sambo et al., 2012. Dans la condition à gauche, la main est maintenue loin du visage, dans la condition à droite elle est maintenue proche, pendant que des stimuli tactiles étaient délivrés sur chaque main. L'amplitude de l'HBR était mesurée dans chaque condition.

bras stimulé et le visage (Bisio et al., 2017; Bufacchi, 2017; Sambo et al., 2012; Sambo & Iannetti, 2013).

Toutes ces études ont été développées pour explorer les propriétés des différentes fonctions de l'EPP, à savoir, ses capacités d'une perception améliorée, la planification d'action ou encore les réponses défensives. Le détail de ces différentes expériences est résumé dans le tableau 1 ci-dessous et est également décrit dans notre revue récemment publiée et accolée à la fin de mon introduction (Bogdanova, Boganov, Dureux, Farnè & Hadj-bouziane, 2021). Ce tableau répertorie l'ensemble des tâches utilisées pour étudier la représentation de l'EPP. Je vais maintenant détailler une à une chaque fonction supposée de l'EPP en développant certaines découvertes comportementales que je viens de résumer dans ce paragraphe.

Tableau 1. Les différentes approches expérimentales pour étudier la représentation de l'EPP chez l'homme.

Table 1 – Experimental approaches used to probe PPS in human behavioral research.

Tasks	Main results	References
Perception and PPS representation: Detection or discrimination tasks		
Crossmodal congruency	Stronger Cross-modal Congruency Effect (CCE), with close vs. far visual stimuli.	(Aspell, Lavanchy, Lenggenhager, & Blanke, 2010; Spence et al., 2004)
Audio- or Visuo-tactile extinction	Inability to detect a visual stimuli presented in the contralesional side if presented concurrently with a competing ipsilesional event of another modality (in near space)	(Brozzoli et al., 2006; Farnè et al., 2000, 2005)
Multisensory interaction	Faster tactile stimuli detection in the presence of approaching audio or visual stimuli	(Canzoneri et al., 2012; Serino et al., 2015; Stone, Kandula, Keizer, & Dijkerman, 2018)
Line bisection	Bias to bisect lines slightly to the left close to the body and slightly to the right in the far space	(Hunley, Marker, & Lourenco, 2017; Lourenco et al., 2011)
Visual detection/discrimination	Faster response to stimuli close to the body or hand; faster target discrimination in near space (vs. in the far space)	(Blini et al., 2018; Dureux et al., 2021; Plewan & Rinkenauer, 2017; Reed, Grubb, & Steele, 2006)
Action-related PPS representation:		
A. Action planning and execution in near space with or without movement		
Reachability judgment	Modulation of the size of reachable space as a function of the stimuli	(Iachini et al., 2014; Quesque et al., 2017; Ruggiero et al., 2017)
Spatial alignment	Facilitation of the behavioral response when the target is in a congruent position to an intended or executed grasping movement in close space	(Costantini et al., 2010; Stefani et al., 2014)
Action planning and execution	Stronger multisensory integration effects during interactive compared to non-interactive movements.	(Belardinelli et al., 2018; Brozzoli et al., 2009, 2010; Patané et al., 2018; Senna et al., 2019)
B. Defensive responses		
Hand blink reflex	Increase of HBR amplitude as a function of the position the hand and a nociceptive stimulation applied on the hand	(Bisio et al., 2017; Bufacchi, 2017; Sambo et al., 2012; Sambo & Iannetti, 2013)
Multisensory interaction	Facilitation of tactile detection with approaching stimuli with negative emotional valence; Facilitation of nociceptive detection with approaching visual stimuli; Increase of skin conductance response with approaching noxious stimuli	(De Paepe, Crombez, & Legrain, 2016; Ferri et al., 2015; Rossetti et al., 2015);
Reachability judgment	Increase of skin conductance response with approaching angry faces	Cartaud et al. (2018)
Time to collision/temporal order judgment	Privileged temporal judgements with visual stimuli in close space	(De Paepe, Crombez, Spence, & Legrain, 2014)

L'ensemble de ces tâches ont permis de mettre en évidence un traitement plus efficace des informations sensorielles dans l'espace proche par rapport à loin. Décrite chez les patients et chez les sujets sains, la tâche de congruence intermodale (« Crossmodal congruency task ») a permis de montrer un traitement de l'information tactile plus efficacement influencé par les stimuli visuels ou auditifs qui se produisaient proche du corps (Spence et al., 2004). Ensuite, ce traitement plus efficace de l'information dans l'EPP a été vérifié avec les tâches d'interactions multisensorielles de plus en plus utilisées pour étudier la représentation de l'EPP, impliquant des stimulations bimodales où le participant devait détecter un stimulus tactile couplé à un stimulus visuel ou auditif non pertinent délivré à différentes distances dans l'espace. Ces tâches ont permis de mettre en évidence une facilitation dans l'interaction multisensorielle lorsque le stimulus tactile était superposé avec le stimulus visuel ou auditif non pertinent présenté proche du corps (Canzoneri et al., 2012 ; Maravita et al., 2003 ; Spence et al., 2004 ; Teneggi et al., 2013). C'est-à-dire que le temps de réaction pour détecter le stimulus tactile était plus rapide lorsque le stimulus non pertinent était délivré à de proches distances, avec une détection du stimulus tactile de moins en moins rapide au fur et à mesure que le stimulus non pertinent s'éloignait. La modélisation psychophysique du traitement de l'information tactile a permis d'estimer un point approximatif à partir duquel l'interaction multisensorielle ne se produisait plus, permettant ainsi d'identifier une « limite » entre l'EPP et l'espace extrapersonnel. La modélisation psychophysique a suggéré qu'une fonction sigmoïde pouvait capturer ce pattern avec un point d'inflexion de la courbe servant d'indicateur de la « limite » de l'EPP (Canzoneri et al., 2012 ; Noel et al., 2015 ; Teneggi et al., 2013). C'est cette tâche qui a également permis de démontrer que la distance à partir de laquelle l'interaction multisensorielle se produisait variait en fonction de la partie du corps stimulée. En administrant des stimulations tactiles sur différentes parties du corps, à savoir la main, le visage et le tronc, Serino et al. (2015) ont montré que cette distance était la plus proche pour la main (30-45 cm) et la plus large pour le tronc (70-80 cm), avec une distance intermédiaire pour le visage (50-60 cm), faisant le lien avec les données neurophysiologiques chez le singe décrites dans le paragraphe 2 (Figure 11).

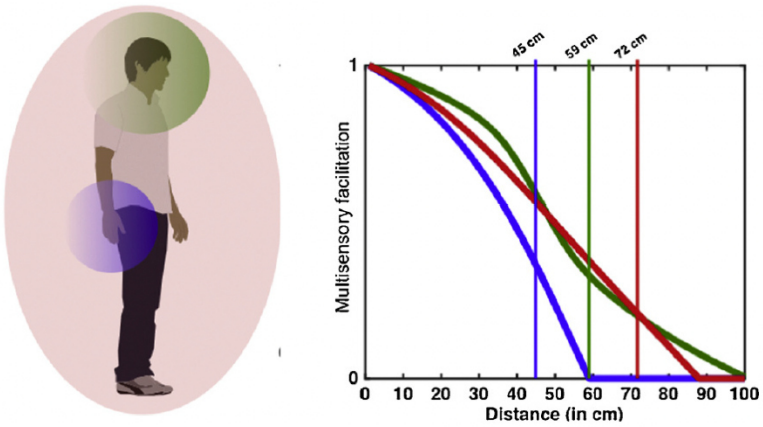

Figure 11. A. Représentation schématique de la taille relative de la représentation de l'EPP autour de la main (bleu), du visage (vert) et du tronc (rouge) identifiée par le degré d'interaction multisensorielle mis en évidence dans la tâche comportementale de Serino et al., 2015. **B.** Représentation de la facilitation multisensorielle induite sur la détection du stimulus tactile par un stimulus non pertinent délivré en fonction de sa distance sur différentes parties du corps dans la tâche de Serino et al., 2015. L'estimation de la limite de la représentation de l'EPP autour de ces parties du corps a été obtenue par modélisation psychophysique en utilisant le point d'intersection de la fonction sigmoïde pour la main (bleu) et le visage (vert) ou l'intersection entre la fonction linéaire et la borne inférieure de l'intervalle de confiance 95% pour le tronc (rouge). Ces figures sont tirées de la revue de Serino, 2019.

A ce stade, la plupart des tâches développées pour étudier le traitement de l'EPP impliquaient uniquement des stimulations sensorielles bimodales avec une facilitation d'interaction multisensorielle dans l'EPP. Les avantages purement visuels survenant dans l'EPP, impliquant donc seulement une stimulation unimodale, ont été rarement rapportés (mais voir de Vignemont, 2018). Une étude récente de notre groupe a tenté d'étudier comment la perception des objets, et en particulier de leur forme, était affectée par la proximité (Blini et al., 2018). Dans un environnement virtuel immersif, les participants devaient discriminer entre plusieurs formes 3D présentées à différentes distances des participants, dans l'EPP, à 50 cm, ou à l'extérieur de l'espace d'atteinte, à 300 cm. A travers différentes expériences pouvant faire varier certains paramètres (comme la hauteur des formes, leur taille ou encore l'absence d'indices oculomoteurs), à chaque fois, une facilitation dans la discrimination des formes (c'est-à-dire une discrimination plus rapide) a été mise en évidence lorsque celles-ci étaient présentées proche du corps, dans l'EPP. En effet, comme la taille physique évolue avec la profondeur et impacte certainement les capacités visuelles, dans les expériences 1, 2 et 3 une correction de la taille rétinienne a été appliquée, égalant la taille des formes qui étaient présentées proche et loin

(Figure 12). De plus, afin d'éviter une confusion entre le champ visuel supérieur et inférieur, dans l'expérience 3, les formes étaient présentées à la même hauteur (même hauteur que la croix de fixation) (Figure 12). Dans l'expérience 2, afin d'éviter les mouvements oculaires de la vergence, les indices de profondeur ont été supprimés en utilisant une illusion mettant en scène des repères de perspective permettant de percevoir illusoirement les formes disposées à des hauteurs différentes plus ou moins proche ou loin dans l'espace (« ponzo illusion » en anglais, Figure 12). Enfin, dans les expériences 4 et 5, la taille des stimuli s'adaptait naturellement à la distance. Dans cette dernière, afin de capturer la distribution spatiale de la facilitation de discrimination en fonction de la distance, les formes étaient présentées à six distances différentes (équidistantes de 50 à 300 cm). Comme observé dans les études utilisant la tâche d'interaction multisensorielle, signature caractéristique du traitement de l'EPP, la modélisation psychophysique a démontré une tendance sigmoïde pour expliquer les performances comportementales en termes de précision et de temps de réaction (Figure 12).

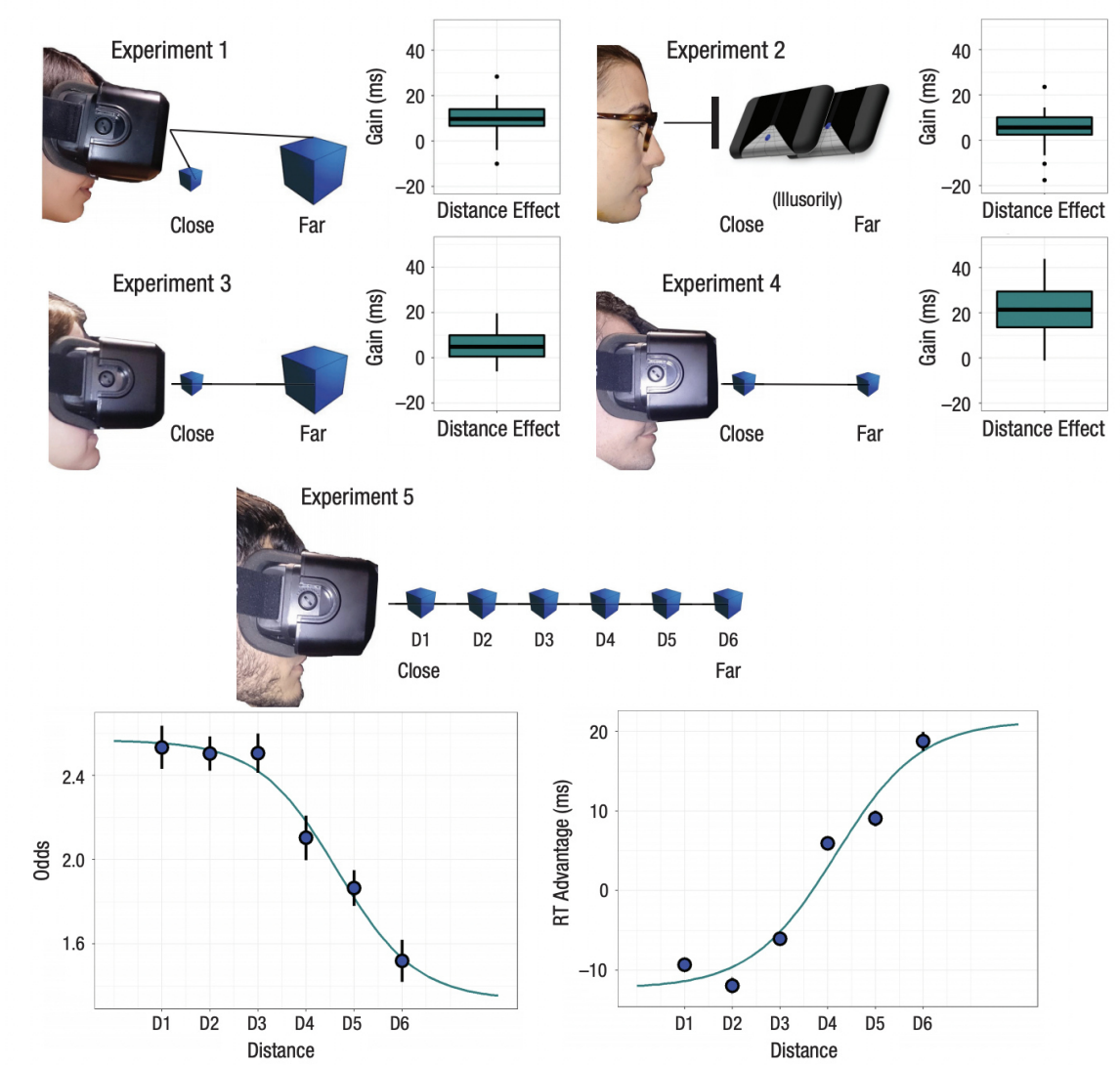

Figure 12. Résumé des expériences réalisées dans l'étude de Blini et al. (2018) pour évaluer les capacités de discrimination perceptive de stimuli unimodaux visuels présentés dans l'environnement virtuel à différentes distances (proche, 50 cm, et loin, 300 cm). Dans l'expérience 1, les formes dans l'espace proche étaient présentées dans la partie inférieure du champ visuel des participants alors que les formes lointaines étaient présentées dans le champ supérieur, avec une taille rétinienne maintenue constante pour les stimuli proche et loin. Dans l'expérience 2, les formes étaient présentées en 2D et une illusion visuelle de profondeur a été créée percevant les objets présentés dans le champ inférieur proche et dans le champ supérieur loin (« ponzo illusion ») toujours avec une taille rétinienne constante. Dans l'expérience 3, les formes apparaissant dans l'espace proche et loin et égalées pour leur taille, étaient présentées à la même hauteur que la croix de fixation. Dans l'expérience 4, les formes étaient également présentées à la même hauteur que la croix de fixation mais cette fois-ci la taille des objets était naturellement adaptée avec la distance. Enfin, dans l'expérience 4, les formes étaient présentées à six distances différentes (de 50 à 300 cm). Les box-plots dans chaque expérience représentent la facilitation de discrimination des formes lorsque celles-ci étaient présentées dans l'espace proche comparé à loin (= « Distance Effect »), observée dans chacune des expériences 1, 2, 3 et 4. Dans l'expérience 5, l'utilisation de 6 distances a permis de mettre en évidence une

tendance sigmoïde pour capturer la distribution spatiale de cet avantage dans les performances comportementales de discrimination visuelle (précision et temps de réponse). Figure reproduite à partir de Blini et al., 2018.

Cette étude a été la première preuve que l'EPP ne se limitait pas à une facilitation de l'interaction multisensorielle mais que des stimulations unimodales présentées dans l'EPP pouvaient à elles seules induire un traitement favorisé. On pourrait donc avancer la prédiction que tout serait amélioré à proximité du corps d'une manière générale.

Une représentation de l'EPP flexible

Comme nous l'avons déjà évoqué, l'EPP pourrait permettre d'interagir physiquement avec les objets externes. Cependant, les données comportementales suggèrent que la représentation de l'EPP serait dynamique et flexible. Une des propriétés fondamentales de l'EPP est sa plasticité.

Les premières études qui ont mis en évidence une modulation de l'EPP ont été démontrées par des expériences mettant en scène l'utilisation d'outils. Chez le singe, il a d'abord été montré que si le singe tenait un outil pour atteindre de la nourriture en dehors de son espace d'atteinte, les champs récepteurs visuels des neurones du sillon intrapariétal s'étendaient vers l'outil (Iriki et al., 1996). Ensuite, chez des patients atteints d'extinction, Farnè et Ladavas (2000) ont montré pour la première fois un effet similaire chez l'homme. Ils ont montré que les stimuli visuels présentés à droite et dans l'espace loin du patient, à proximité d'un long râteau, induisaient une extinction plus importante des stimulations tactiles à gauche mais immédiatement après utilisation de l'outil par le patient. Plus tard, d'autres études ont ensuite mis en évidence une extinction intermodale plus forte à un endroit éloigné de la main après l'utilisation de l'outil, suggérant une extension de l'EPP entourant la main le long de l'axe de l'outil (Làdavas & Serino, 2010 ; Maravita et al., 2002 ; Maravita & Iriki, 2004). Néanmoins, cela nécessitait l'utilisation réelle de l'outil dans une tâche, il ne suffisait pas simplement de tenir l'outil pour étendre la représentation de l'EPP (Farnè et al., 2007; Ishibashi et al., 2004) même après une expérience passive prolongée avec l'outil (Farnè et al., 2005). Cependant, certaines personnes sont habituées à utiliser des outils quotidiennement et pendant de longues périodes, comme c'est le cas par exemple des personnes aveugles qui utilisent une canne pour naviguer dans

l'environnement. Serino et al. (2007) ont montré que la représentation de l'EPP était étendue chez les sujets aveugles dès qu'ils prenaient possession de leur canne, alors que chez les sujets voyants, la représentation de l'EPP était limitée à la zone entourant leur main, suggérant une extension de l'EPP de manière durable chez les personnes non-voyantes même sans utilisation temporaire active de l'outil.

Il n'y a pas seulement les études impliquant l'utilisation d'outils qui ont permis de mettre en évidence la flexibilité de la représentation de l'EPP. En effet, la tâche d'interaction multisensorielle dont je vous ai parlé dans le paragraphe précédent ou encore la tâche de jugement d'atteinte (« reachability judgment task ») ont également permis de démontrer une modulation de la représentation de cet espace en fonction du type de stimuli et du contexte. Les études utilisant la tâche d'interaction multisensorielle ont montré que le point d'inflexion de la fonction sigmoïde, signature caractéristique du traitement de l'EPP et interprété comme la « limite » de l'EPP, se déplaçait vers le participant ou à l'inverse s'éloignait du participant en fonction de plusieurs paramètres comme la simple présence d'un autre individu dans l'espace (Teneggi et al., 2013). Ce déplacement du point d'inflexion vers le participant était perçu comme une réduction de la représentation de l'EPP alors que l'éloignement de ce point par rapport au participant signifiait une augmentation de la représentation de l'EPP (Canzoneri et al., 2012). Dans la tâche de jugement d'atteinte, la distance où le participant stoppe l'objet en mouvement lorsque celui-ci devient atteignable est également interprétée comme la « limite » de la représentation de l'EPP. Cette distance variait en fonction de différents paramètres comme une réduction de l'EPP lorsque les participants faisaient face à un avatar comparé à un objet ou un robot (Iachini et al., 2014), mais également dans des contextes sociaux (Cartaud et al., 2018 ; Costantini et al., 2010 ; Iachini et al., 2016 ; Iachini et al., 2015 ; Ruggiero et al., 2017). Ces modulations, surtout observées dans des études investiguant l'EPP dans un contexte sociale, seront exposées plus en détail dans mon axe 2 « l'EPP dans un contexte sociale ».

Des réponses défensives dans l'EPP

La fonction défensive de l'EPP a pu être mise en évidence par les études mesurant le réflexe de clignement des yeux par la main (« hand-blink reflex », HBR) induit par une stimulation électrocutanée du nerf médian sur le poignet (Bisio et al., 2017 ; Buffachi, 2017 ; Sambo et al., 2012 ; Sambo et Iannetti, 2013). L'amplitude des clignements des yeux qui est mesurée via

l'activité électromyographique enregistrée à partir des muscles orbiculaires de l'œil, augmentait lorsque la main stimulée s'approchait du visage, dans l'EPP (Figure 13). Ces résultats montrant que l'HBR était largement augmentée lorsque la main stimulée se situait dans l'espace proche du visage, ont permis de suggérer l'existence d'un « EPP défensif » pouvant servir comme marge de sécurité protégeant l'organisme d'un danger potentiel dans l'environnement comme suggéré par les études de neurophysiologie chez le singe (Graziano & Cooke 2006).

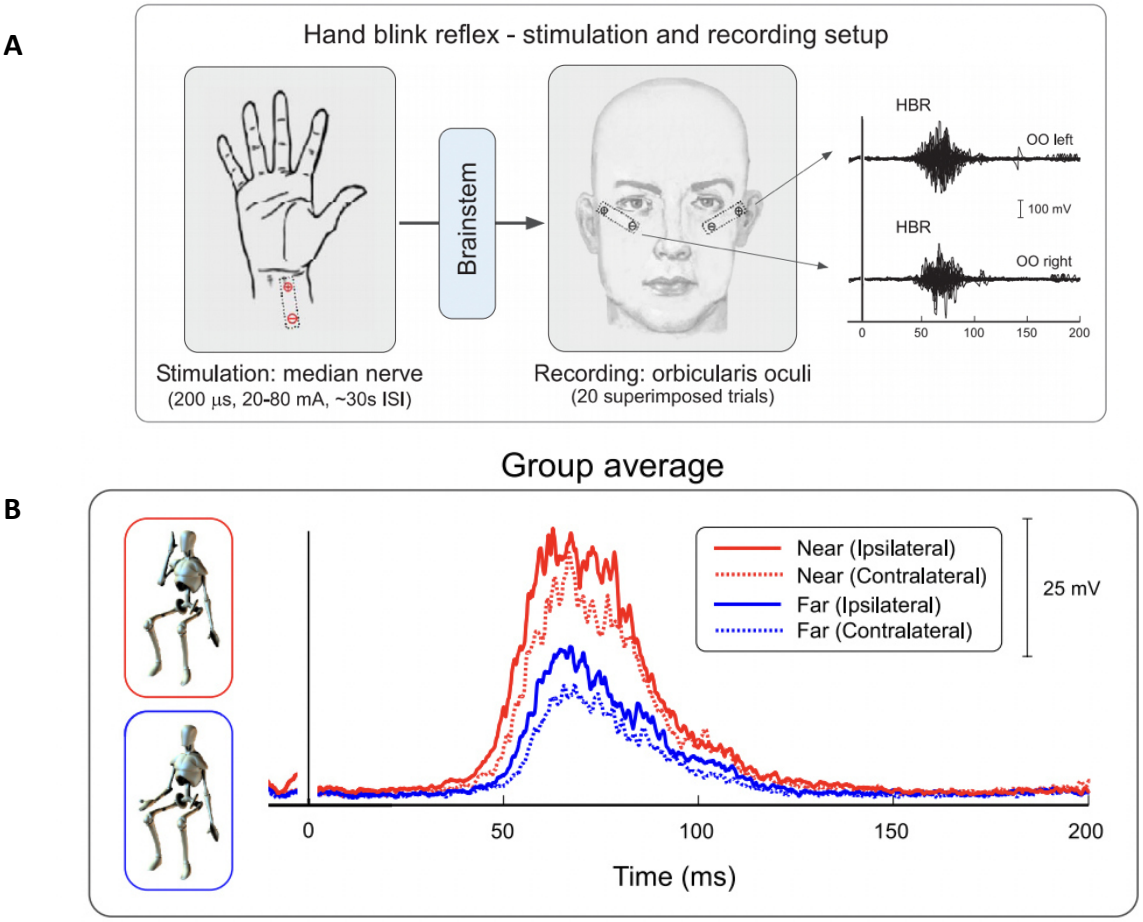

Figure 13. **A.** Schéma du réflexe de clignement des yeux par la main (HBR) à partir de Sambo et al., 2012. Le clignement des yeux est provoqué par une stimulation électrique du nerf médian au poignet et enregistré à partir du muscle orbiculaire des yeux (orbicularis oculi). **B.** Amplitude du clignement des yeux mesurée, ipsilatérale et controlatérale à la main stimulée qui pouvait être placée soit proche du visage (rouge) ou loin du visage (bleu). Ces résultats obtenus par Sambo et al., 2012, montrent une amplitude de l'HBR plus élevée lorsque la main est proche du visage.

V. Substrats neuronaux de l'espace péri-personnel chez l'homme : études de neuro-imagerie

Comme nous l'avons vu à travers ces études comportementales, l'idée d'une représentation de l'espace fragmentée en différentes cartes spatiales et plus en particulier d'une division de l'espace en fonction de sa représentation proche ou loin du corps s'est de plus en plus développée depuis les premières études chez le singe. L'EPP n'est plus seulement le domaine de l'électrophysiologie chez l'animal, mais est devenu un sujet d'étude au niveau humain grâce à ces études comportementales mais également par des études de neuroimagerie. L'utilisation de la neuroimagerie chez l'homme, depuis plusieurs années, a permis de représenter un potentiel homologue de ce réseau prémoteur-pariétal décrit chez le singe avec des propriétés multisensorielles mais également unisensorielles.

Après avoir étudié les bases neuronales de l'EPP chez le singe dans le paragraphe II, je vais donc maintenant faire un tour des différentes études conduites en IRMf chez l'homme, répertoriant les aires cérébrales qui codent pour la représentation de l'EPP et plus en particulier le réseau fonctionnel de l'EPP dans son ensemble.

Un réseau prémoteur-pariétal commun : méta-analyse de Grivaz et al., 2017

Des expériences de neuroimagerie ont récemment commencé à démêler les mécanismes cérébraux associés à la représentation de l'EPP autour de différentes parties du corps comme la main, le visage et le tronc. Récemment, Grivaz et al. (2017) ont réalisé une méta-analyse basée sur les coordonnées mises en évidence dans 18 études différentes conduites en IRMf afin d'identifier les régions communes du cerveau humain qui traitaient les informations multisensorielles ou unisensorielles dans l'EPP (Grivaz et al., 2017). Parmi ces 18 expériences, 9 avaient étudié l'espace autour de la main (Brozzoli et al., 2013 ; Brozzoli et al., 2011, 2012 ; Ferri et al., 2015 ; Gentile et al., 2011, 2013 ; Huang et al., 2012 ; Makin et al., 2007 ; Schaefer et al., 2012), 8 l'espace autour du visage (Bremmer et al., 2001 ; Cardini et al., 2011 ; Holt et al., 2014 ; Huang et al., 2012 ; Quinlan & Culham, 2007 ; Sereno & Huang, 2006 ; Tyll et al., 2012 ; Wittmann et al., 2010) et 1 l'espace autour du tronc (Huang et al., 2012). Ce réseau,

activé par des évènements unisensoriels ou multisensoriels au sein de l'EPP, se situe principalement dans le cortex prémoteur et pariétal postérieur. En effet, 7 clusters en commun de ces études ont pu être mis en évidence dans le cortex pariétal supérieur bilatéral (Bremmer et al., 2001 ; Brozzoli et al., 2013 ; Brozzoli et al., 2012, 2011 ; Gentile et al., 2013, 2011 ; Holt et al., 2014 ; Huang et al., 2012 ; Makin et al., 2007 ; Schaefer et al., 2012 ; Sereno and Huang, 2006), dans le cortex temporo-pariétal bilatéral (Brozzoli et al., 2013, 2012, 2011 ; Gentile et al., 2013, 2011) et dans le cortex prémoteur bilatéral (gyrus précentral) (Brozzoli et al., 2012, 2011 ; Ferri et al., 2015 ; Gentile et al., 2013, 2011 ; Holt et al., 2014). Dans le cortex pariétal, deux clusters incluaient le cortex somatosensoriel primaire SI (aire 1, 2, 3), le lobule supérieur pariétal (SPL, aire 5), le lobule pariétal inférieur (IPL, aire 40), le sillon intrapariétal (IPS). Les deux clusters temporo-pariétaux étaient principalement localisés dans la partie ventrale de l'IPL et dans l'opercule pariétal. Enfin, les clusters du gyrus précentral correspondaient aux régions du cortex prémoteur situées dans la partie ventrale dans l'hémisphère gauche (PMv) et dans la partie plus dorsale dans l'hémisphère droit (PMv/PMd). Ces différents clusters sont représentés dans la figure 14 ci-dessous.

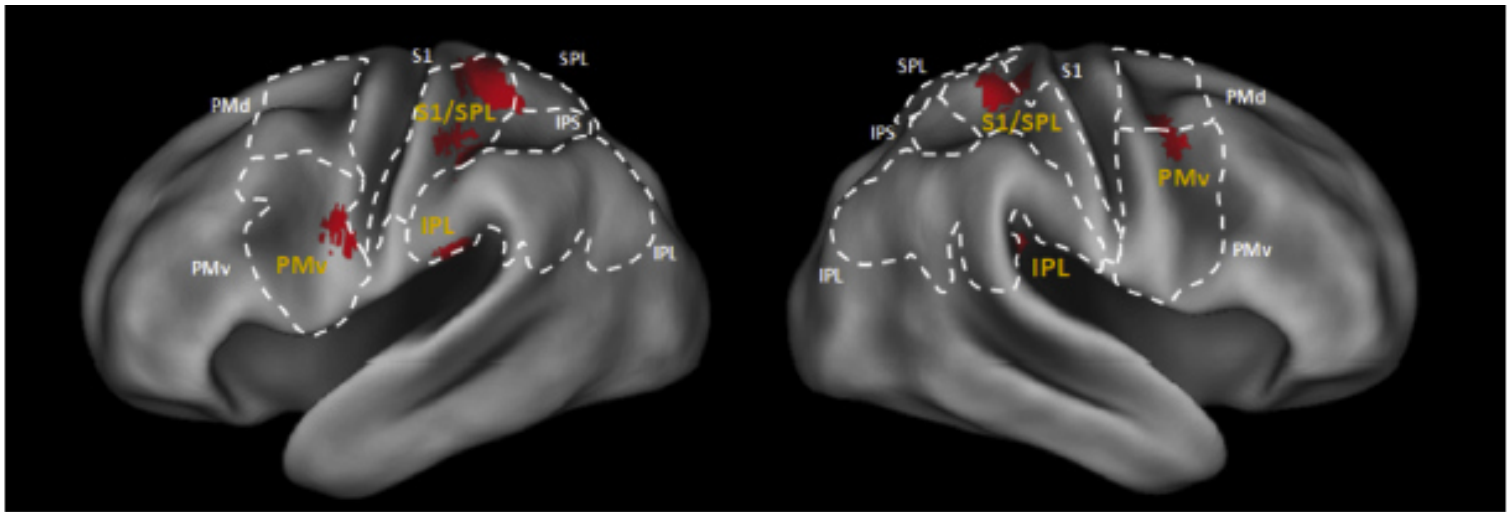

Figure 14. Régions cérébrales montrant des activations communes dans 18 études de neuroimagerie chez l'homme à partir de la méta-analyse de Grivaz et al., 2017. Figure obtenue à partir de la revue de Serino, 2019.
SPL : lobule pariétal supérieur ; S1 : cortex somatosensoriel primaire ; IPL : lobule pariétal inférieur ; IPS : sillon intrapariétal ; PMv : cortex prémoteur ventral ; PMd : cortex prémoteur dorsal.

Également, en utilisant une technique de cartographie de coactivation méta-analytique, ils ont pu mettre en évidence deux modèles de connectivités fonctionnelles, l'un impliquant les régions IPL, SI et IPS, et l'autre limité aux régions prémotrices et le SPL, démontrant que ces clusters étaient interconnectés.

Ainsi, cette méta-analyse a permis d'identifier des régions pariétales, temporo-pariétales et prémotrices principalement retrouvées dans la plupart des études investiguant les bases neurales de l'EPP chez l'homme, mettant en évidence un réseau central fronto-pariétal impliqué dans les interactions entre l'individu et l'environnement proche.

Cependant, il convient de prendre en considération le fait que toutes ces études ont été réalisées par des groupes différents utilisant des paradigmes expérimentaux variés. Alors, bien qu'un réseau principal se dessine pour coder la représentation de l'EPP, nos interactions avec l'environnement proche ne se fait pas uniquement par l'intermédiaire des régions prémotrices et pariétales décrites ici mais impliquerait également d'autres régions en fonction du type de paradigme utilisé. Ce réseau prémoteur-pariétal engloberait donc un plus grand nombre de régions qui pourraient dépendre de différents facteurs et du type de stimulation, qu'elle soit unisensorielle ou multisensorielle.

Au cours de ma thèse, j'ai choisi d'utiliser des stimuli unisensoriels visuels puisque jusqu'ici très peu d'études se sont concentrées sur cet aspect de l'EPP, l'EPP ayant été décrit tout d'abord comme un espace d'interaction multisensoriel. Il est important de ne pas négliger le fait que les stimulations unimodales à elles seules peuvent capturer les propriétés de l'EPP, de la même manière qu'en utilisant des stimulations bimodales, comme nous l'avons vu dans le paragraphe IV, à travers la découverte d'un traitement favorisé dans une tâche de discrimination visuelle (Blini et al., 2018).

Dans la suite du paragraphe, j'ai donc choisi de séparer les différentes études de neuroimagerie en deux groupes : les études ayant utilisé des stimulations multisensorielles et les études ayant utilisé des stimulations unisensorielles, afin d'essayer de mieux comprendre les similitudes et les différences qui pourraient leur être associées. Dans chacun de ces paragraphes, je vais détailler la récente génération d'études qui ont identifié les fondements anatomiques et les mécanismes fonctionnels de la représentation de l'EPP chez l'homme. Enfin

dans un dernier paragraphe, je comparerai les réseaux neuronaux qui ont été obtenus chez les espèces homme et singe.

Études de neuroimagerie utilisant des stimuli multisensoriels pour identifier les mécanismes fonctionnels de l'EPP chez l'homme

Les toutes premières études de neuroimagerie ayant exploré un réseau neuronal du cerveau humain étant impliqué dans les interactions entre l'individu et l'EPP ont utilisé des évènements multisensoriels avec en général des stimulations tactiles additionnées à des stimuli visuels et/ou auditifs. Bremmer et al. (2001) ont été les premiers à étudier le pattern neuronal de l'EPP à travers l'utilisation de stimuli multisensoriels. En effet, dans leur étude, ils ont mis en évidence les régions préférentiellement activées par des stimulations tactiles appliquées au visage ou encore pendant que des stimulations visuelles ou auditives se déplaçaient vers le visage. Les auteurs ont observé un chevauchement des réponses pour les trois stimulations au niveau du cortex pariétal supérieur, en particulier dans la partie plus profonde de l'IPS, du PMv et de la partie latérale inférieure du gyrus postcentral. Au vu du profil de réponse, Bremmer et al. (2001) ont proposé un homologue humain de la zone VIP chez le singe dans une partie de l'IPS. Sereno et Huang, en 2006, ont par la suite montré que la région IPS présentait une cartographie somatosensorielle et visuelle autour du visage, cette région répondait à la fois aux stimulations tactiles appliquées au visage mais aussi aux stimuli visuels proche du visage. Sereno et Huang (2006) ont donc corroboré la proposition de Bremmer et al., en 2001, en démontrant également un homologue putatif dans l'IPS qui présentait des propriétés similaires à celles des neurones du VIP observées chez le singe (Colby et al., 1993 ; Duhamel et al., 1998 ; voir paragraphe II ci-dessus). Quelques années plus tard, le même groupe a testé l'intégration multisensorielle visuo-tactile autour de plusieurs parties du corps, à savoir la tête, les épaules, les mains, les doigts, les jambes et les orteils (Huang et al., 2012). Ils ont ainsi pu mettre en évidence une cartographie somatotopique activée par les stimulations tactiles et une cartographie rétinotopique activée par des boules qui s'approchaient. Les cartes somatototopiques et rétinotopiques se chevauchaient le plus dans les zones pariétales du visage et des lèvres alors que des niveaux inférieurs de chevauchements ont été observés dans les parties postérieures des zones pariétales de l'épaule, de la jambe et des orteils. Les zones pariétales des doigts possédaient le plus faible niveau de chevauchement. Sur la base de ces cartes, ils ont pu

proposer un modèle d'homonculus multisensoriel dans le cortex pariétal supérieur partant de la zone du visage pariétal et se déplaçant médialement et postérieurement dans les zones du bas du corps.

Plusieurs autres études en IRMf ont par la suite également démontré que les régions du cortex pariétal et du cortex prémoteur répondaient à des stimulations multisensorielles. L'étude de Gentile et al. (2011) a examiné comment ces régions intégraient des stimuli visuels et tactiles délivrés dans l'espace proche de la main. Alors que les participants étaient dans le scanner en train de regarder leur main, des stimuli unisensoriels et multisensoriels ont été présentés dans l'espace entourant immédiatement la main. Des réponses superadditives ont été observées dans l'IPS antérieur ainsi que dans l'opercule pariétal, dans le cortex prémoteur dorsal (PMd), dans l'insula, dans le putamen ainsi que dans le cervelet au cours de la stimulation visuo-tactile multisensorielle, c'est-à-dire que ces régions possédaient une réponse à la stimulation visuo-tactile qui était significativement supérieure à la somme des deux stimuli unisensoriels. L'analyse de conjonction des effets principaux des deux stimuli unisensoriels, stimulations tactiles et visuelles séparément, a révélé les mêmes régions cérébrales avec des clusters supplémentaires significativement activés par les deux modalités dans le PMv et le supramarginal gyrus (SMG). Plus tard, une étude du même laboratoire a révélé que les réponses dans les mêmes aires pariétales et prémotrices dépendaient de la congruence spatiale et temporelle des signaux visuels et tactiles (Gentile et al., 2013).

Enfin, des études utilisant des stimulations multisensorielles visuo-auditives (Tyll et al., 2012) ou audio-tactiles (Ferri et al., 2015) ont également analysé les réponses neuronales aux stimulations multisensorielles délivrées proche du corps. Dans leur étude, bien qu'ils ne mentionnent pas spécifiquement l'EPP, en 2012, Tyll et al. ont étudié les profils neuronaux des réponses multisensorielles lorsque des informations auditives et visuelles congruentes s'approchaient ou s'éloignaient du corps. L'analyse a révélé des activations préférentielles pour une stimulation audiovisuelle congruente s'approchant (comparé à s'éloignant) dans les zones cérébrales visuelles (gyrus calcarine/cuneus) et auditives, le sillon temporal supérieur (STS), le lobe pariétal supérieur et le gyrus cingulaire. Cette étude suggère que d'autres régions cérébrales interagiraient avec le réseau principal prémoteur-pariétal décrit dans la plupart des études investiguant les bases neurales de l'EPP, en fonction du type de stimuli utilisé. Ferri et al. (2015), eux, ont recherché les régions cérébrales qui étaient sensibles aux sons s'approchant du corps. Les régions du cortex prémoteur, du gyrus frontal inférieur ainsi que du STS

présentaient des activations préférentielles comparé à un son monotone. Également, ils ont montré une spécificité de l'interaction audio-tactile dans le cortex prémoteur et dans le gyrus frontal médian.

J'ai listé dans le tableau 2 ci-dessous l'ensemble des études répertoriant les principales régions du cerveau mises en évidence lors de stimulations multisensorielles dans l'espace proche de la main, du visage ou du corps en général en fonction également de la tâche réalisée, comme décrit dans ce paragraphe.

Tableau 2. Résumé des études de neuroimagerie ayant investigué les bases neurales de l'EPP à travers des stimulations multisensorielles ciblées sur différentes parties du corps. Les études sont classées par ordre chronologique et dans chaque étude sont indiqués le type de stimulus utilisé, la partie du corps ciblée ainsi que les analyses réalisées et les résultats principaux mis en évidence dans ce paragraphe.

Études	Stimuli	Partie du corps ciblée	Analyses concernées	Résultats principaux
Bremmer et al., 2001	Visuel, Tactile et auditif	Visage	Analyse de conjonction pour révéler les régions corticales activées par les 3 types de stimuli.	Augmentation de l'activité neuronale à la fois pour les simuli visuels, tactiles et auditifs dans **l'IPS, le PMv et le gyrus postcentral**.
Sereno and Huang, 2006	Visuel et Tactile	Visage	Alignement des données de cartographies somatosensorielles et visuelles, répondant à la fois aux stimulations tactiles sur le visage et aux stimuli visuels proche du visage.	Mise en évidence d'une cartographie tactile et visuelle autour du visage dans l'**IPS**.
Gentile et al., 2011	Visuel et Tactile	Main	**1)** Identification des régions montrant des réponses superadditives révélant les voxels où la stimulation visuotactile de la main produit une réponse significativement supérieure à la somme des deux stimuli unisensoriels présentés isolément. **2)** Analyse de conjonction des deux stimulations unisensoriels.	**1)** Réponses supperadditives dans **l'IPS antérieur, l'opercule pariétale, le PMd, l'insula, le putamen et le cervelet.** **2)** Activations communes pour les deux stimulations dans **l'IPS antérieur, l'opercule pariétale, le PMd, l'insula, le putamen, le cervelet, le PMv et le SMG.**
Huang et al., 2012	Visuel et Tactile	Main/Visage/ Épaules/Doigts/ Jambes/Orteils	Superposition des cartographies somatotopiques et rétinotopiques pour identifier les niveaux de chevauchements des stimulations tactiles et visuelles et ainsi proposer un modèle d'homonculus multisensoriel.	Identification d'un modèle d'homonculus multisensoriel dans le **cortex pariétal supérieur** partant de la zone du visage pariétal et se déplaçant médialement et postérieurement dans les zones du bas du corps.
Gentile et al., 2013	Visuel et Tactile	Main	Deux contrastes linéaires mettant en évidence les régions intégrant spécifiquement des stimuli visuels (V) et tactiles (T) de la main congruents dans le temps et l'espace : **1) VT Conguent vs VT Time Incongruent et 2) VT Congruent vs VT Space Incongruent.**	Réponses aux stimuli V et T sur la main significativement modulées à la fois par la congruence temporelle et spatiale des signaux sensoriels dans **l'IPS, le PMv, le PMd, le SMG, le LOC, l'opercule pariétale, le gyrus postcentral, l'insula, le putamen, et le cervelet.**
Tyll et al., 2012	Visuel et Auditif	Corps	Identification des régions montrant une activation préférentielle pour les stimulation audio (A)-visuelles (V) congruentes s'approchant vs. s'éloignant du corps : **contraste VA s'approchant > VA s'éloignant.**	Activations préférentielles dans les zones cérébrales visuelles et auditives, le **STS, le lobe pariétal supérieur et le gyrus cingulaire** lors d'une stimulation audiovisuelle congruente s'approchant.
Ferri et al., 2015	Auditif et Tactile	Main/Corps	**1)** Identification des régions sensibles aux sons s'approchant du corps **2)** Mise en évidence des régions impliquées dans l'interaction audio-tactile pendant que le son était perçu proche	**1)** Activations préférentielles pour les sons s'approchant comparé aux sons monotones dans **le cortex prémoteur, le gyrus frontal inférieur ainsi que le STS**. **2)** Activations préférentielles lors des stimulations à la fois tactiles sur la main et auditives s'approchant du corps dans **le cortex prémoteur et dans le gyrus frontal médian.**

Études de neuroimagerie utilisant des stimuli unisensoriels pour identifier les mécanismes fonctionnels de l'EPP chez l'homme

L'exploration des aires cérébrales impliquées dans la représentation de l'EPP mesurée par des stimuli unisensoriels, et plus en particulier par des stimuli visuels, a débuté seulement en 2007 avec l'étude de Makin et al. La plupart de ces études se sont concentrées sur le traitement des signaux dans l'espace autour de la main. Dans leur étude, Makin et al. ont identifié que les régions de l'IPS, du complexe occipital latéral (LOC) et du cortex prémoteur, en particulier le PMv, montraient des activations préférentielles en réponse à une balle réelle qui était présentée proche de la main du participant par rapport à la même stimulation visuelle mais présentée à une distance lointaine de la main. Quelques années plus tard, ces résultats ont été confirmés et étendus par Brozzoli et al., en 2011, à travers un paradigme d'adaptation en IRMf qu'ils ont développé afin d'identifier les spécificités neuronales lors d'une stimulation visuelle dans l'EPP de la main. Ce type de paradigme permet de révéler des sous-populations de neurones qui présentent une sélectivité à la répétition de stimuli, induisant une suppression de la réponse de ces neurones spécifiquement à l'une des caractéristiques (Grill-Spector et al., 2006). En utilisant une démarche expérimentale très proche de celle de Makin et al., 2007, c'est-à-dire en présentant une balle en mouvement proche ou loin de la main, ils ont pu mettre en évidence une adaptation, donc une réduction du signal BOLD, à la suite de la stimulation visuelle répétée proche de la main dans les régions de l'IPS, du SMG, du PMd, du PMv, du putamen et du cervelet (Figure 15). Ces régions n'étaient pas retrouvées lorsque la stimulation visuelle répétée était réalisée loin de la main ou encore lorsque la main était rétractée.

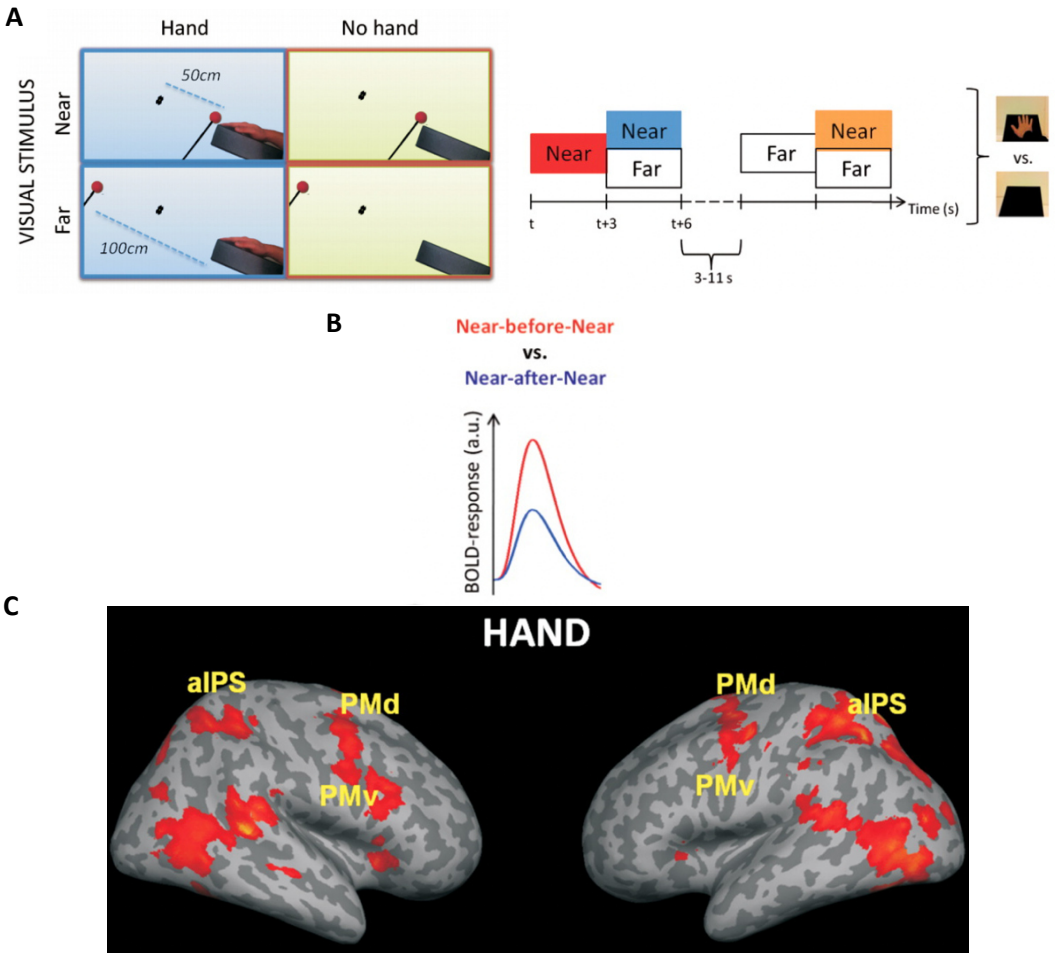

Figure 15. Figure adaptée de Brozzoli et al., 2011. **A.** Procédure expérimentale utilisée dans l'étude de Brozzoli et al., 2011. À gauche, est représenté un schéma expliquant la démarche expérimentale. Pendant que le participant maintenait son regard sur un point cible (représenté par un point noir), un stimulus visuel, une sphère réelle, était présenté proche (à 2 cm) ou loin (à 100 cm) de la main droite du participant placée sur un support. Le bras pouvait soit être étendu pour que la main soit placée sur la table bien en vue (colonne de gauche) ou rétracté avec la main posée sur la poitrine du participant (colonne de droite). À droite, le design expérimental comprenait quatre combinaisons de stimuli : proche-proche, proche-loin, loin-proche, loin-loin, chacune étant divisée par deux parties pour une durée totale de stimulation de 6 sec par combinaison, chaque stimulation durant 3 sec. **B.** Le graphique schématise le principe d'adaptation dans cette étude. Une réduction du signal BOLD est attendue dans la condition proche-proche lorsque le stimulus visuel est répété donc dans la deuxième partie de la condition (proche-après-proche) par rapport à la première partie (proche-avant-proche). **C.** Visualisation des résultats obtenus dans l'étude de Brozzoli et al., 2011, à savoir, les régions montrant une adaptation BOLD à la stimulation visuelle proche de la main obtenue par le contraste (proche-avant-proche) vs. (proche-après-proche). a*IPS : sillon intrapariétal antérieur ; PMv : cortex prémoteur ventral ; PMd : cortex prémoteur dorsal.*

Dans l'année qui a suivi, le même groupe a réalisé une étude exploitant également la méthode d'adaptation en IRMf pour déterminer si, de la même manière que chez le singe, les aires pariétales et prémotrices suivaient l'espace proche de la main lorsque celle-ci se déplaçait dans l'espace, c'est-à-dire si la sélectivité visuelle pour l'espace autour de la main possédait un encodage dynamique de l'espace centré sur la main. En présentant un objet réel proche ou loin de la main droite qui était positionnée dans deux postures différentes (la stimulation était présentée à gauche ou à droite de la main rendant la stimulation proche ou loin en fonction de la position de la main, voir figure 16), ils ont observé une plus grande adaptation (plus grande réduction du signal BOLD) lorsque le stimulus visuel était présenté proche de la main par rapport à loin dans les deux positions de la main, dans les régions du cortex prémoteur (PMd et PMv) ainsi que dans l'IPS. Ces résultats suggèrent que ces régions possèdent un traitement visuel privilégié dans l'espace proche de la main et « ancré » sur la main lors de son déplacement dans l'espace.

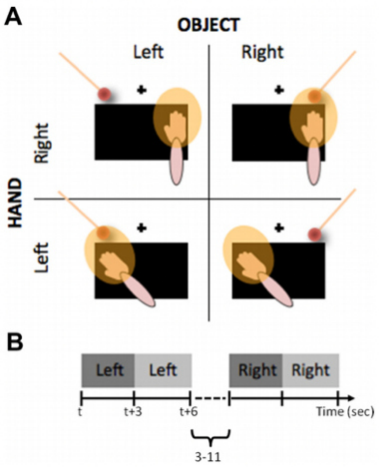

Figure 16. Procédure expérimentale de l'étude de Brozzoli et al., 2012. A. Un objet réel était présenté à gauche ou à droite du point de fixation pendant que la main droite du participant pouvait être positionnée à deux endroits différents, c'est-à-dire que la stimulation pouvait être proche ou loin selon la position de la main. **B.** Dans chaque essai, l'objet était présenté à gauche ou à droite pendant 6 sec (répétition de chaque stimulation de 3 sec).

Une étude de Quinlan et Culham (2007), utilisant un autre type de paradigme et ciblant cette fois le visage, a examiné les réponses neuronales à des disques en mouvement qui s'approchaient ou s'éloignaient du visage, présentés à des distances spécifiques : très proche du visage (de 13-17 cm), proche du corps (33-43 cm) et loin du corps (73-95 cm), en dehors de l'espace d'atteinte. Les réponses étaient examinées dans le cortex occipital, pariétal, et en particulier dans l'homologue humain supposé de la région VIP (Colby et al., 1993) après avoir utilisé une tâche de localisation qui impliquait une balle se déplaçant proche et loin du visage et pouvant également toucher le visage. Étonnement, les résultats n'ont pas montré de préférence pour l'espace proche dans l'homologue putatif fonctionnel de la région VIP ou dans le cortex pariétal, répondant de la même manière dans les trois conditions. Cependant, ils ont identifié une région à l'extrémité dorsale du sillon pariéto-occipitale (dPOS), suggérée comme homologue putatif des régions V6 et V6A chez le singe, qui montrait une préférence pour les objets dans l'espace proche et un gradient d'activation dépendant de la distance du stimulus par rapport au participant.

D’autres groupes de recherche ont également investigué les régions répondant aux stimuli visuels présentés proche du corps avec des démarches expérimentales beaucoup plus éloignées que celles de Brozzoli et al., 2011, 2012, Makin et al., 2007, et Quinlan et Culham, 2007, n’utilisant pas d’objets réels mais des stimuli en 2D présentés sur un écran. Wittman et al. (2010) ont utilisé des disques centrés sur un écran qui changeaient de taille afin de créer une illusion d’approche lorsque la taille des disques augmentait ou une illusion d’éloignement lorsque les disques diminuaient en taille. Bien qu’ils ne mentionnent pas le terme exact d’EPP dans leur étude, ils ont identifié des activations préférentielles lorsque les disques s’approchaient par rapport à s’éloignaient dans le gyrus frontal médian, le gyrus cingulaire postérieur et le precuneus. Schaefer et ses collègues (Schaefer et al., 2012) ont utilisé des clips vidéo mettant en scène une main présentée dans une position anatomiquement congruente où un pinceau apparaissait proche de la main et dans certains cas pouvait toucher la main. A travers cette expérience, ils ont montré une réponse préférentielle dans l’aire somatosensorielle primaire (SI) lorsque le pinceau était visible dans l’espace proche de la main par rapport à lorsque la main était touchée. Plus récemment, d’autres études utilisant également des stimuli visuels sur un écran s’approchant ou s’éloignant du corps ont investigué l’EPP avec des stimuli sociaux (Holt et al., 2014 ; Vieira et al., 2017, 2020), mais je détaillerai ces études plus spécifiquement dans l’Axe 2 de mon introduction, que j’ai spécialement dédié à la dimension sociale de l’EPP, je n’en parlerai donc pas dans cette partie.

Comme pour le paragraphe précédent, j’ai répertorié dans le tableau 3 ci-joint l’ensemble des études qui ont identifié les régions du cerveau impliquées dans le traitement des stimulations unisensorielles visuelles présentées dans l’EPP.

Tableau 3. Résumé des études de neuroimagerie ayant investigué les bases neurales de l'EPP à travers des stimulations unisensorielles ciblées sur la main ou le visage.

Études	Stimuli	Partie du corps ciblée	Analyses concernées	Résultats principaux
Makin et al., 2007	**Visuel :** Balle réelle	Main	Identification des régions montrant une activation préférentielle pour la balle présentée proche comparé à loin de la main : **contraste proche vs loin.**	Activation préférentielle en réponse à la balle proche de la main par rapport à loin dans **le cortex occipital, l'IPS, le LOC et le PMv.**
Quinlan et Culham, 2007	**Visuel :** Disque réel en mouvement	Visage	Identification des régions répondant aux disques en mouvement présentés proche du visage comparé à loin : contraste **proche en mouvement vs. loin en mouvement.**	Aucune préférence d'espace proche dans pVIP ou même n'importe où dans le pariétal mais la région **dPOS** montrait une préférence pour les objets proches.
Wittman et al., 2010	**Visuel :** Disque en 2D sur un écran	Visage	Explorations des réponses neuronales préférentiellement activées par les disques s'approchant du corps : **contraste disque s'approchant vs. s'éloignant.**	Activations préférentielles dans **le gyrus frontal médian, le gyrus cingulaire postérieur et le precuneus** lorsque les disques s'approchaient.
Brozzoli et al., 2011	**Visuel :** Balle réelle	Main	**1)** Identification des régions montrant une adaptation significative à la stimulation visuelle proche de la main : contraste linéaire **Proche-avant-proche vs. Proche-après-proche**. **2)** Évaluation de la nature de ces réponses centrées sur la main en soustrayant les contrastes linéaires proche de la main et proche de la main rétractée : **(proche-avant-proche vs. proche-avant-proche)Main – (proche-avant-proche vs. proche-après-proche)Retractée**	**1)** Réduction du signal BOLD (donc adaptation du signal) à la suite de la stimulation visuelle répétée proche de la main, dans les régions de **l'IPS, du SMG, du PMd, du PMv, du putamen et du cervelet.** **2)** Mêmes résultats.
Brozzoli et al., 2012	**Visuel :** Balle réelle	Main	Identification de l'interaction entre l'adaptation BOLD pour la position du stimulus visuel (OD = objet présenté à droite et OG = objet présenté à gauche) et la position de la main : **contraste [(OD1 vs OD2)maindroite + (OG1 vs OG2)maingrauche] *vs.* [(OD1 vs OD2)maingauche + (OG1 vs OG2)maindroite)]**	Réduction du signal plus importante (= adaptation) dans **le PMd, le PMv et l'IPS** lorsque le stimulus visuel était présenté proche de la main par rapport à loin dans les deux positions du bras.
Schaefer et al., 2012	**Visuel :** Pinceau en 2D sur un écran	Main	Exploration des activations associées à la condition visuelle proche de la main : **contraste pinceau visible proche de la main > pinceau touche la main.**	Réponse préférentielle dans **SI** lorsque le pinceau était visible dans l'EPP.

Ensemble, ces études d'IRMf ont permis de démontrer qu'un réseau principal et commun d'aires prémotrices et pariétales (impliquant également le putamen et le cervelet) serait recruté pour traiter l'information proche du corps, dans l'EPP, qu'elle soit unisensorielle ou multisensorielle avec quelques différences en fonction du type de stimuli (voir le paragraphe suivant pour plus de détails concernant ces divergences).

VI. Comparaison des réseaux de l'EPP chez l'homme et le singe

Comme je l'ai évoqué au début de mon introduction, les propriétés neuronales de l'EPP ont pu être décrites à l'aide des études de neurophysiologie chez le singe, Rizzolatti et al. (1981) étant les premiers à avoir introduit le terme d'EPP. Par la suite, comme je viens de l'exposer à l'instant, un certain nombre d'études en neuroimagerie chez l'homme ont été développées afin de définir un réseau neuronal putatif de l'EPP chez l'homme. Cependant, les études en électrophysiologie se sont concentrées sur des régions spécifiques prédéfinies, à savoir des régions du cortex prémoteur et pariétal ainsi que le putamen. Cette technique ne permettait pas d'obtenir une mesure de l'activité d'un réseau à l'échelle du cerveau entier même avec des enregistrements multi-sites. Alors que les enregistrements en électrophysiologie fournissent une mesure directe de l'activité neuronale d'un seul neurone, l'approche IRMf du cerveau entier fournit une mesure indirecte de l'activité cérébrale, échantillonnant l'activité de milliers de neurones (le signal BOLD). C'est pourquoi les données neurophysiologiques du singe ne peuvent pas être directement transposées à l'homme et l'application de l'IRMf aux deux espèces est une étape nécessaire pour combler le fossé entre ces deux sources majeures de connaissances sur le cerveau des primates. Jusqu'à présent, une seule étude a tenté de dévoiler les corrélats neuronaux de la représentation de l'EPP chez le singe à l'aide de l'IRMf (Cléry et al., 2018). De la même manière que pour les études en électrophysiologie, Cléry et al. (2018) ont utilisé un environnement naturaliste où un cube 3D de différentes tailles était présenté proche (à 15 cm) ou loin du corps (à 150 cm) du singe pendant que celui-ci devait fixer une LED située dans une position spatiale intermédiaire (Figure 17). Ils ont mis en évidence le réseau neuronal activé

préférentiellement par le cube proche par rapport au cube présenté loin mais également les régions préférentiellement activées par le cube dans l'espace loin par rapport à l'espace proche.

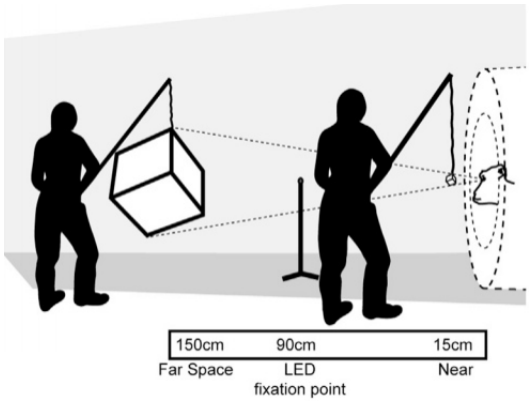

Figure 17. Protocole expérimentale de l'étude de Cléry et al., 2018. Le singe devait fixer une LED située à 90 cm pendant que deux cubes pouvaient être présentés soit proche de la tête du singe (15 cm) ou loin (150 cm).

Le réseau de l'espace proche comprenait des régions corticales bilatérales dont l'activation était statistiquement plus élevée pour l'espace proche que pour l'espace lointain. Ce réseau incluait des régions du cortex temporal (l'aire occipital temporo-pariétale rostrale TPOe dans le STS, l'aire associée au sillon intrapariétal IPa, l'aire temporale inférieure TEAa-m, la portion dorsale de la subdivision TE1-3), des régions du cortex pariétal, à savoir le sillon intrapariétal postérieur (VIP et MIP) et antérieur (AIP), le cortex pariétal médial (PGm) et la région operculaire pariétale 7op, mais également des régions préfrontales et prémotrices identifiées comme le cortex prémoteur dorsal F2, les aires prémotrices 4C ou F4/F5, le SEF, le FEF, l'aire préfrontale 46p, l'aire préfrontale 45B et enfin également une région frontale (la zone orbitofrontale postérieure 12), l'aire somatosensorielle II et le cortex insulaire (PI), voir Figure 18 A et B).

Concernant l'espace loin, la présentation du cube loin par rapport à proche activait préférentiellement l'ensemble du cortex visuel strié et extra-strié (aires V1, V2, V3, V3A et V4), le sillon intrapariétal postérieur (PIP), latéral (LIP) et caudal (CIP, PRR « parietal reach region »), et la convexité pariétale médiale (aire 5v) et latérale (aires 7a, 7ab et 7b). Ce réseau s'étendait ensuite vers le cortex pariéto-occipital (incluant les aires V6 et V6A) ainsi que le cortex temporal (aires temporales médiales et supérieures MT et MST).

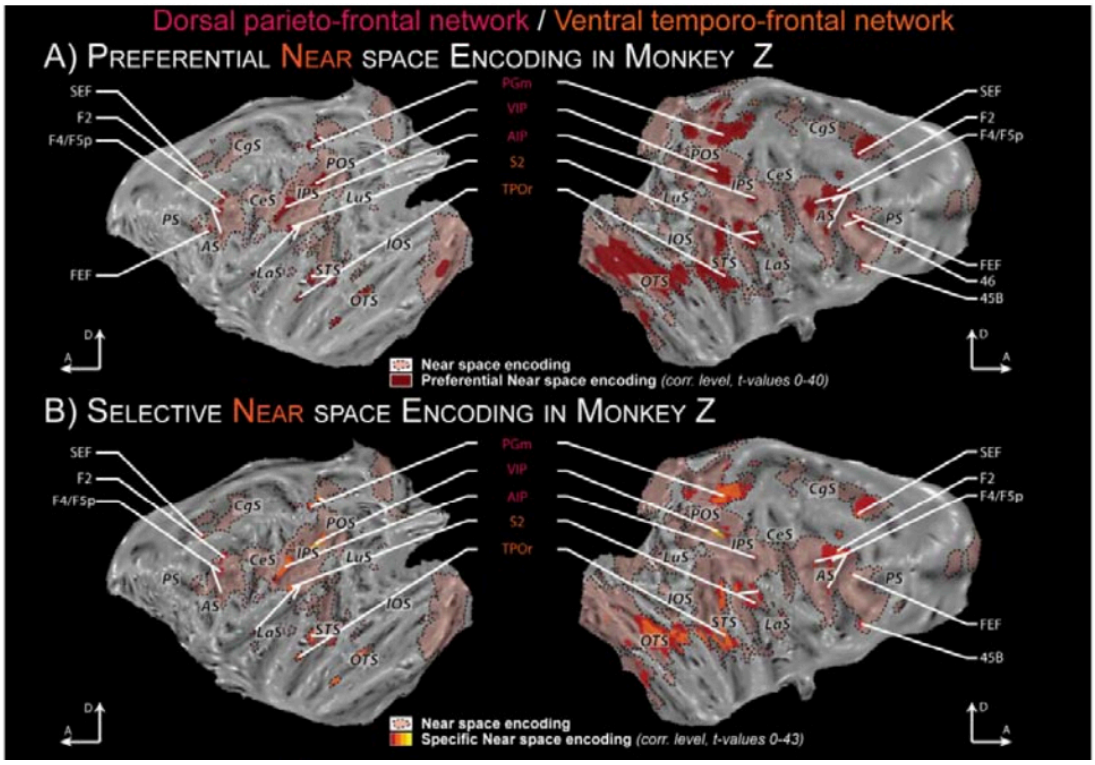

Figure 18. Réseaux corticaux fonctionnels préférentiels à l'espace proche par rapport à loin. Figure adaptée de Cléry et al., 2018. Représentation du codage préférentiel dans l'espace proche pour chacun des deux singes (A et B), c'est-à-dire les régions préférentiellement activées lors de la présentation du cube proche par rapport à loin. Les contours rouges externes sur les deux cartes correspondent à un codage non sélectif dans l'espace proche (espace proche versus fixation).

Dans l'ensemble, cette étude vient appuyer les recherches antérieures menées en électrophysiologie chez le singe montrant une implication d'un réseau pariéto-frontal dans le codage de l'espace proche avec des activations dans le VIP (Colby et al., 1993 ; Duhamel et al., 1998), le MIP (Bhattacharyya et al., 2009) et dans les aires prémotrices F4 (Fogassi et al., 1992, 1996 ; Gentilucci et al., 1988 ; Graziano et al., 1997 ; Graziano et al., 1994 ; Rizzolatti et al., 1981) et F5 (Gentilucci et al., 1983, 1988; Murata et al., 1997; Raos et al., 2006). Cependant, Cléry et al. (2018) ont mis en évidence un réseau beaucoup plus étendu que celui qui a été décrit chez l'homme en IRMf, néanmoins identifié avec un paradigme expérimental et une analyse différente. Concernant le traitement de l'espace loin, le réseau était également très étendu impliquant des régions du cortex occipital et temporal. Cependant quelques divergences peuvent être remarquées par rapport à ce qui a été observé chez l'homme par exemple avec une préférence pour l'espace loin dans la région dPOS qui pourrait être suggéré comme étant une région homologue aux aires V6 et V6A chez le singe et qui a été montrée comme impliqué dans

le traitement préférentiel de l'espace proche (Quinlan et Culham, 2007). Les auteurs supposent que ces différences pourraient être expliquées par les différences méthodologiques employées.

Afin d'y voir plus clair sur les activations obtenues chez les deux espèces, j'ai répertorié dans un tableau ci-dessous (Tableau 4), les différentes régions mises en évidence chez le singe et chez l'homme. Ce tableau rapporte les activations obtenues dans l'ensemble des études ayant enregistré l'activité des neurones chez le singe, décrites dans le paragraphe II « propriétés neuronales de l'espace péri-personnel chez le primate non-humain », celles obtenues dans l'étude de Cléry et al. (2018) en IRMf ainsi que les activations mises en évidence dans les études en IRMf chez l'homme, résumées dans le paragraphe V précédent.

Tableau 4. Résumé des régions identifiées dans les études en électrophysiologie chez le singe et en IRMf chez l'homme et le singe.

		Lobe occipital	Lobe temporal	Lobe pariétal	Lobe frontal	Régions sous-corticales
Études Electrophysiologie	**Singe avec stimuli uni et multisensoriels :** -Sakata et al. 1980 -Rizzolatti et al. 1981 -Gentilucci et al. 1983, 1988 -Fogassi et al. 1992, 1996 -Colby et al. 1993 -Colby et Duhamel, 1996 -Graziano et al. 1993, 1994, 1997, 2006 -Gnadt et Mays, 1995 -Murata et al. 1997 -Duhamel et al. 1998 -Genovesio et Ferraina, 2004 -Raos et al. 2006 -Bhattacharyya et al. 2009 -Breveglieri et al. 2012	-V6A		-VIP -LIP -MIP (PRR) -Aire 7a -Aire 7b -(AIP)	-F4 -F5	-Putamen
Études IRMf	**Singe avec stimulus unisensoriel visuel :** -Cléry et al. 2018		-TPOr dans STS -IPa -TEAa-m -TE1-3	-VIP -MIP -AIP -PGm -7op -SII	-F2 -F4/F5 -Aire 45b -SEF -FEF -Aire 46p -Aire orbitofrontale 12 -Insula	
	Homme avec stimuli multisensoriels : -Bremmer et al. 2001 -Sereno et Huang, 2006 -Gentile et al. 2011 -Huang et al. 2012 -Gentile et al. 2013 -Tyll et al. 2012 -Ferri et al 2015	-LOC	-STS	-IPS -SMG -Opercule pariétal (SII) -Gyrus postcentral	-PMv -PMd -Gyrus frontal médian -Insula -Gyrus cingulaire	-Putamen -Cervelet
	Homme avec stimuli unisensoriels visuels : -Makin et al. 2007 -Quinlan et Culham. 2007 -Wittman et al. 2010 -Brozzoli et al. 2011 -Brozzoli et al. 2012 -Shaefer et al. 2012	-LOC -Occipital gyrus inférieur et médian -Calcarine sulcus -Posterior collateral sulcus (pCOlS) -Occipital transverse intrapariétal (IPTO) -dPOS		-IPS -SMG -Gyrus postcentral -Precuneus -SI	-PMv -PMd -Gyrus frontal médian -Gyrus cingulaire	-Putamen -Cervelet

Pour résumer, ce tableau reflète une étendue des activations principalement dans les cortex frontaux et pariétaux chez les deux espèces. Tout d'abord, si nous nous concentrons au sein des études réalisées chez l'homme, il ne semble pas y avoir de grandes différences en termes d'activations neuronales en fonction du type de stimuli utilisé (uni vs. multisensoriels), du moins au niveau du réseau général fronto-pariétal. Cela suggère qu'un système de codage « central » de l'EPP, impliquant un réseau de neurones dans les aires fronto-pariétales, serait optimisé pour surveiller l'espace proche du corps lors du traitement des informations visuo-tactiles ou simplement visuelles. Cependant, quelques différences minimes semblent apparaître. Par exemple, les stimuli unisensoriels dans l'espace proche sembleraient recruter plus de régions occipitales, ce qui n'est pas surprenant puisqu'elles codent les informations visuelles en général mais également certaines régions du cortex occipital auraient une préférence pour les signaux visuels de vergence comme c'est notamment le cas de la région dPOS (Quinlan et Culham, 2007). Les stimuli multisensoriels présentés dans l'espace proche du corps, eux, semblent recruter plus particulièrement la région STS du cortex temporal, mais également l'opercule pariétal qui fait partie de l'aire secondaire somatosensorielle (SII) ainsi que le cortex insulaire. Ici encore, il n'est pas surprenant de voir un recrutement de l'aire SII puisque celle-ci était systématiquement activée par un large éventail de stimuli somatiques dans un certain nombre d'études de neuroimagerie (Banati et al., 2000 ; Bodegård et al., 2000 ; Ledberg et al., 1995). L'insula a également été suggéré comme étant un site cortical important pour l'intégration multisensorielle (Bushara et al., 2001 ; Naghavi et al., 2007), particulièrement associée à des tâches intermodales de traitement ou de reconnaissance visuo-tactile (Banati et al. 2000).

Maintenant, si nous examinons plus en détail les résultats obtenus chez le singe à l'aide de la technique d'IRMf, Cléry et al. (2018) ont identifié un réseau neuronal préférentiellement activé lors du traitement des informations présentées proche par rapport à loin incluant un certain nombre de régions ayant auparavant été identifiées à l'aide de l'électrophysiologie. Plus spécifiquement, ils ont montré une implication des aires F4 et F5 dans le cortex frontal ainsi que les aires VIP et MIP dans le cortex pariétal lors du traitement de l'information visuelle proche du corps, comme il l'avait été montré dans les études de neurophysiologie. Cependant, certaines régions n'ont pas été retrouvées comme impliquées dans ce réseau général de l'espace proche, à savoir les aires 7a et 7b ainsi que le putamen. En revanche, un certain nombre d'autres régions ont pu être identifiées, en particulier des régions du cortex temporal ou encore des

régions connues comme étant modulées par le système de vergence (FEF, SEF, Alkan et al., 2011). Jusqu'ici les études en électrophysiologie avaient montré que les neurones de la région FEF étaient modulés par la disparité binoculaire (Ferraina et al., 2000), cependant aucune de ces études mettaient en évidence un codage préférentiel de l'espace proche.

Si nous comparons ensuite les réseaux neuronaux chez les deux espèces, obtenus à l'aide de l'IRMf, il semblerait tout d'abord que ce réseau soit plus étendu chez le singe. Par exemple, un certain nombre de régions frontales impliquées dans le traitement du système de vergence (Alkan et al., 2011) semblent recrutées uniquement chez le singe. Également, plus de régions dans le cortex temporal seraient recrutées dans le traitement de l'espace proche du singe, contrairement à l'homme qui montre que très peu d'activations dans ces régions. Cependant, chez l'homme, les études en IRMf suggèrent que la représentation de l'EPP recrute d'autres régions qui incluent le putamen, le gyrus cingulaire, le cervelet et des régions dans le cortex occipital, ces régions n'étant pas retrouvées dans l'étude de Cléry et al. (2018).

Cependant, il faut être prudent lorsque nous comparons ces études et ne pas tirer de conclusions hâtives. En effet, dans le paragraphe IV décrivant les fonctions de l'EPP à l'aide des études comportementales chez l'homme, nous avons vu que les résultats pouvaient varier en fonction des méthodologies (nous verrons que ces différences seront d'autant plus importantes lorsque des facteurs sociaux sont en jeu, ce que je détaillerai dans l'axe 2). Pour le moment, il est donc difficile voire impossible de conclure sur des similitudes ou des différences « réelles » entre ces deux espèces concernant le réseau neuronal du traitement de l'espace proche au vu de l'hétérogénéité dans les méthodologies utilisées. A ce jour, aucune étude n'a permis de comparer directement les réseaux neuronaux de l'EPP chez ces deux espèces.

C'est pourquoi j'ai consacré les deux premières études de ma thèse à comparer les réseaux neuronaux impliqués dans le traitement de l'EPP chez l'homme et le singe en utilisant la même procédure afin de réconcilier les sources de connaissances, à savoir de combler le fossé entre les mesures neuronales en IRMf chez l'homme et les enregistrements en électrophysiologie chez le singe. Ces deux études constitueront le Chapitre 2 de ma thèse.

AXE 2 :

L'EPP dans un contexte social

Dans mon premier axe, je me suis concentrée sur la représentation de l'EPP telle qu'elle a été décrite à la fois chez les primates humains et non-humains, comme un espace autour de notre corps pour interagir avec les objets présents dans notre environnement. Cependant, les mécanismes multisensoriels et unisensoriels sous-jacents de la représentation de l'EPP seraient impliqués non seulement dans les interactions physiques entre le corps et les objets, mais également dans d'autres contextes. En effet, notre monde n'est pas seulement fait d'objets, il est davantage un monde social. L'espace proche qui nous entoure n'est donc pas seulement la région privilégiée de l'espace pour saisir et manipuler des objets mais servirait aussi pour interagir avec d'autres individus. En conséquence, récemment, un certain nombre d'études ont commencé à explorer comment l'information sociale pouvait moduler notre représentation de l'EPP. Dans ce second axe, je vais donc me focaliser sur un autre versant de l'EPP, à savoir l'influence du contexte social et des interactions sociales sur notre représentation de l'EPP.

Dans cet axe, je me suis particulièrement appuyée sur la récente revue que nous avons publiée, décrivant les différents aspects de l'EPP dans un monde social (Bogdanova, Boganov, Dureux, Farnè & Hadj-Bouziane, 2021).

I. L'espace personnel, une définition issue de l'éthologie et de la psychologie sociale

Les psychologues et les éthologues savent depuis longtemps qu'une zone de confort est nécessaire pour réguler la distance entre nous-même et les autres. Hediger, directeur du zoo de Zurich en 1955, a introduit pour la première fois le concept de « zone de fuite » (« flight zone »

en anglais), appelée plus tard marge de sécurité, pour décrire la distance que les animaux gardaient entre eux et les autres animaux, et servant à la fois pour les fonctions de communication et de survie. L'anthropologue américain Edward T. Hall a ensuite adapté ce concept chez l'homme à une zone de confort ou espace personnel, que nous gardons entre nous et les autres pour réguler la distance interpersonnelle et éviter l'inconfort, voire l'anxiété (Hall, 1966 ; 2014). Le test typiquement utilisé pour évaluer l'espace personnel est le paradigme de distance d'arrêt (« stop distance paradigm » en anglais). Dans la version qu'on appelle passive, les participants font face à un expérimentateur et au fur et à mesure que l'expérimentateur se déplace vers les participants (ou vice versa pour la version active), ils doivent arrêter l'expérimentateur (ou eux-mêmes pour la version active) lorsqu'ils commencent à se sentir mal à l'aise avec la proximité de l'autre (Hayduk, 1983 ; Nishihara & Okubo, 2015). Ce jugement de distance de confort permet de fournir une mesure de l'espace personnel du sujet, la violation de ces limites invisibles créant un sentiment d'inconfort chez les individus. Cet espace personnel est une entité omniprésente qui permet de déterminer les interactions sociales avec quelques variations selon les espèces animales et chez l'homme (Baldwin & Baldwin, 1974 ; Kennedy et al., 2009). Cette autre dimension de la perception spatiale pourrait donc se rapporter à la représentation de l'EPP. Ce sont Graziano & Cooke, en 2006, qui ont été les premiers à mettre en relation l'EPP et le concept d'espace personnel. Malgré leurs origines différentes, tant l'espace personnel que la représentation de l'EPP renvoient à l'espace ancré autour du corps. En tant que tels, ils peuvent partager certains points communs. Une question intéressante est de savoir si et dans quelle mesure les mécanismes sous-jacents de la représentation de l'EPP décrits plus haut sont impliqués dans la définition de l'espace personnel. Ces aspects seront discutés plus en détail ci-dessous.

II. La dimension sociale de l'EPP : modulation de la représentation de l'EPP en fonction du contexte

Dans le récent débat des fonctions de l'EPP, différents groupes ont cherché à savoir si l'information sociale pouvait affecter la représentation de l'EPP. A travers ces récentes études, il a été montré que les caractéristiques des facteurs sociaux mais également la relation de ces facteurs avec l'autre, notamment sa familiarité et ses traits de personnalité, pouvaient exercer

une influence sur la représentation de l'EPP. Par conséquent, sous l'influence d'éléments sociaux et selon le contexte, la représentation de l'EPP serait affectée, s'élargissant, se rétrécissant ou se remodelant par rapport à l'autre. Nous avons résumé dans la Table 2 de notre revue ci-joint les différents résultats obtenus concernant la modulation de l'EPP en fonction des caractéristiques sociales. Déjà décrites dans l'axe 1, la tâche d'interaction multisensorielle ou encore la tâche de jugement d'atteinte ont été les tâches les plus largement utilisées pour étudier la dimension sociale de l'EPP. A l'aide de la première tâche, il a été montré que la simple présence d'une autre personne réduisait la « limite » de l'EPP (Teneggi et al., 2013). Cependant, après une tâche sociale coopérative, la représentation de l'EPP était plus étendue, incluant l'autre personne en face (Teneggi et al., 2013). Cette première étude a suggéré que la présence d'autres personnes autour de nous pouvait jouer un rôle important dans la représentation de l'EPP et donc dans les interactions sociales. Par la suite, d'autres études utilisant la même tâche ont pu mettre en évidence cette plasticité de l'EPP en fonction de différents paramètres avec une représentation de l'EPP s'élargissant ou diminuant en fonction par exemple du caractère émotionnel (Ellena et al., 2020 ; Ferri et al., 2015), du jugement moral (Pellencin et al., 2017) ou encore du type de coopération (Hobeika et al., 2020). A l'aide de la tâche de jugement d'atteinte, la distance d'atteinte utilisée comme « limite » de l'EPP variait également en fonction du type de stimulus présenté, à savoir un avatar comparé à un objet (Iachini et al., 2014), ou encore en fonction de l'émotion (Cartaud et al., 2018) et de la moralité (Iachini et al., 2015) de l'avatar. L'utilisation d'outils affectait également la distance d'atteinte après une coopération avec un congénère (Candini et al., 2019 ; Patané et al., 2017). D'autres tâches comme la tâche de congruence visuo ou audio-tactile (Heed et al., 2010) ou encore la tâche de réflexe de clignement des yeux par la main (HBR, Fossataro et al., 2016), ont montré une modulation des réponses en présence d'autres personnes.

Il est important de noter que l'ensemble de ces résultats comportent des variations en fonction de la tâche utilisée. Globalement, comme nous l'avons souligné dans la partie 2.2 « Social modulation of PPS representation » et schématisé dans la figure 1 de notre revue, avec la tâche d'interaction multisensorielle, une interaction positive entre les participants et le congénère ou encore une valence positive du stimulus social (émotion positive ou moralité) suscitait un élargissement de l'EPP du participant alors qu'une valence négative du stimulus social (émotion négative ou immoralité) provoquait un rétrécissement de l'EPP du participant (mais voir Ferri et al., 2015). A l'inverse, avec la tâche de jugement d'atteinte, un facteur social

positif provoquait une diminution des distances alors qu'un facteur social négatif suscitait de plus grandes distances atteignables. Ces différentes modulations observées en présence de stimuli sociaux positifs ont suggéré que les interactions avec nos congénères pourraient être perçues différemment en fonction de la tâche réalisée. En effet, une expansion de l'EPP observée à travers la tâche d'interaction multisensorielle pourrait suggérer que nous souhaitons inclure notre propre EPP vers l'autre personne afin de vouloir interagir avec elle alors que ce même désir d'approche vers l'autre personne serait à l'inverse observé par une constriction de l'EPP à travers la tâche de jugement d'atteinte.

Ces différences de résultats peuvent donc être interprétées différemment en fonction de la tâche, recrutant certainement des réseaux neuronaux communs (comme le réseau central de l'EPP décrit plus haut) mais possédant également des spécificités comme le recrutement des régions motrices et prémotrices ainsi que le cortex pariétal postérieur lors de la perception de ce qui est atteignable (Filimon, 2010; Lara et al., 2018; Monaco et al., 2011; Pitzalis et al., 2013), d'ailleurs corroboré par une étude comportementale récente mettant en avant les différences des représentations spatiales de l'EPP et l'espace d'atteinte (Zanini et al., 2021).

III. Espace personnel et EPP, des espaces différents ou similaires ?

Une question qui reste intrigante est de savoir comment relier l'EPP tel que défini par les neuroscientifiques, et l'espace personnel tel que défini par les psychologues. De toute évidence, ces deux concepts peuvent (au moins en partie) se chevaucher, car ils se rapportent tous deux à l'espace entourant notre corps. Mais pouvons-nous vraiment dire que ces espaces sont similaires ? Quelques études ont essayé de comparer directement ces deux espaces avec deux tâches bien particulières : la tâche de distance d'arrêt, que je vous ai décrite plus haut comme étant le paradigme typique pour évaluer l'espace personnel, et la tâche de distance d'atteinte. Dans la plupart des études, il a été montré que l'espace personnel et l'EPP se chevauchaient, avec une modulation des distances de confort et d'atteinte allant dans le même sens en fonction des différents facteurs testés comme la nature du stimuli (Iachini et al., 2014), le jugement moral (Iachini et al., 2015), l'âge et le sexe (Iachini et al., 2016), ou encore l'expression faciale (Ruggiero et al., 2017). Cependant, le fait que les deux représentations soient affectées par les

mêmes manipulations n'implique pas qu'elles sous-tendent la même fonction, ni même qu'elles se chevauchent. En effet, comme je l'ai décrit précédemment, selon le paradigme expérimental utilisé pour étudier l'EPP, les résultats divergent et ne vont plus dans le même sens. Par exemple dans l'étude de Iachini et al. (2015), les deux tâches de jugement d'atteinte et de distance d'arrêt ont montré une diminution de l'espace face à une personne morale alors que lorsque l'EPP a été estimé avec la tâche d'interaction multisensorielle, sa représentation s'étendait vers l'agent moral ou coopératif (Pellencin et al. 2017 ; Teneggi et al., 2013). Ces différences de résultats peuvent donc refléter de véritables différences entre les représentations de l'espace personnel et de l'EPP ou simplement refléter des différences méthodologiques, soulignant à nouveau l'importance des procédures expérimentales utilisées pour évaluer la représentation de l'EPP. En revanche, ces deux espaces faisant référence à des représentations spatiales proche du corps étant toutes les deux sensibles à la présence des autres individus et étant modulées par certains types de facteurs sociaux, cela suggère qu'ils partagent certaines caractéristiques mais qu'ils peuvent sonder différents aspects de l'espace comme observé avec les dissociations expérimentales. Cela fait référence à la revue de Iannetti et Bufacchi (2018) proposant une reconceptualisation de l'EPP en différentes zones en fonction du contexte (voir paragraphe III « Fonctions de l'EPP d'un point de vue théorique » dans l'axe I de l'introduction), suggérant donc qu'il y aurait différentes zones en fonction de la pertinence des actions disponibles pour l'individu dépendant non seulement de la position des autres congénères dans l'espace, mais aussi de l'ensemble des actions dont ils disposent. L'espace personnel pourrait donc être compris comme des zones d'actions de l'EPP où la distance est dictée par la pertinence des actions disponibles à la fois pour l'individu et les autres (Iannetti et Bufacchi, 2018), ce qui pourrait expliquer les différences en termes de distances en fonction de la procédure expérimentale utilisée, testant des actions différentes.

IV. Corrélats neuronaux de l'espace personnel chez l'homme

Les premières preuves neuronales montrant que la représentation de l'EPP était affectée par la présence d'autres individus proviennent de Ishida et al. (2010) qui ont identifié certains neurones dans la région VIP du singe qui répondaient à une stimulation tactile sur une partie du corps de l'animal pendant que des stimuli visuels approchaient en direction de l'animal mais aussi en direction de l'expérimentateur face à l'animal. Chez l'homme, Brozzoli et al. (2013) ont démontré que l'activité dans le PMv, ayant été définie comme une région impliquée dans la représentation de l'EPP, était modulée non seulement en fonction de la distance d'un objet présenté vers la main du participant mais aussi par la distance du même objet vers la main d'une autre personne visible par le participant. Ces résultats montrent que le réseau de l'EPP met également en œuvre un mécanisme pour cartographier la représentation de l'EPP d'autres personnes dans l'espace proche.

Plus tard, des études conduites en IRMf chez les sujets sains se sont concentrées sur le réseau fonctionnel impliqué dans le traitement de l'espace personnel, permettant de maintenir les distances appropriées entre les individus. En 2014, Holt et ses collègues ont mesuré les réponses neuronales à différents types de stimuli qui s'approchaient ou s'éloignaient du corps (Holt et al., 2014). Ils ont utilisé des stimuli sociaux, c'est-à-dire des avatars humains avec une expression neutre, et des stimuli non sociaux, des voitures et sphères, présentés sur un écran qui s'élargissaient en taille ou se contractaient, les faisant apparaître de manière illusoire plus proche ou plus loin. Une activité préférentielle pour les visages s'approchant par rapport à s'éloignant a été identifiée dans la région dorsale et ventrale du sillon intrapariétal (dIPS et vIPS), dans le PMv, le PMd, le gyrus cingulaire, le precuneus, le gyrus frontal médian, le gyrus occipital médian et le gyrus temporal inférieur. En revanche, aucune activation préférentielle n'a été mise en évidence pour les stimuli non sociaux qui s'approchaient. Lorsqu'ils ont mesuré la taille de l'espace personnel en utilisant le paradigme de distance d'arrêt en dehors du scanner, ils n'ont pas identifié de corrélation entre la taille de l'espace personnel et l'activation biaisée par l'approche dans le dIPS et le PMV, cependant la taille de l'espace personnel était négativement corrélée avec la force du couplage fonctionnel entre dIPS et PMv.

Dans la même lignée, Vieira et ses collègues ont mené une série de deux études afin d'identifier également les corrélats neuronaux de l'espace personnel mais cette fois en utilisant des stimuli émotionnels. Dans une première étude (Vieira et al., 2017), ils ont évalué les réponses neuronales pendant que des visages véhiculant 5 expressions émotionnelles (colère, peur, joie, tristesse et neutre) augmentaient ou diminuaient de taille sur un écran en 2D créant une illusion d'approche ou d'éloignement. Dans chaque essai, les participants devaient évaluer leur niveau d'inconfort à l'aide d'une échelle à 5 points (Figure 19 A). En dehors du scanner, avec les mêmes stimuli, les participants devaient réaliser une tâche dans laquelle des essais d'approche et de retrait était présentés et le participant devait appuyer sur un bouton réponse pour choisir de rapprocher le visage ou sur un autre pour le repousser jusqu'à atteindre la distance souhaitée, c'est-à-dire la distance qu'ils garderaient normalement lors d'une conversation avec un étranger (Figure 19 B). Les régions qui montraient une activation accrue pour les visages en approche par rapport aux visages en retrait, indépendamment de l'émotion, comprenaient le sillon intrapariétal incluant les lobules pariétaux supérieurs et inférieurs (SPL et IPL), le cortex prémoteur, l'aire motrice supplémentaire (SMA), le cortex préfrontal dorsolatéral (DLPFC), le gyrus frontal inférieur, le gyrus occipital médian, l'amygdale, l'insula et le cervelet. L'interaction entre l'émotion et la direction a révélé des activations préférentielles dans le precuneus, le cortex préfrontal ventrolatéral (vIPFC), le gyrus frontal inférieur et l'insula. En particulier, l'insula et le gyrus frontal inférieur montraient une préférence pour les visages heureux et en colère s'approchant et le vlPFC pour les visages heureux uniquement. Lorsqu'ils ont extrait le pourcentage de changement de signal dans l'amygdale, obtenu pour le contraste visage s'approchant vs. s'éloignant indépendamment de l'émotion, ils ont identifié une corrélation significative entre l'activité de cette région et les résultats obtenus dans la tâche réalisée en dehors du scanner, c'est-à-dire une association avec de plus grandes distances pour les visages en colère et peureux. Ce résultat est en accord avec une étude précédente montrant que cette région jouait un rôle clé dans la représentation de l'espace personnel afin d'établir des distances appropriées entre les individus (Kennedy et al., 2009).

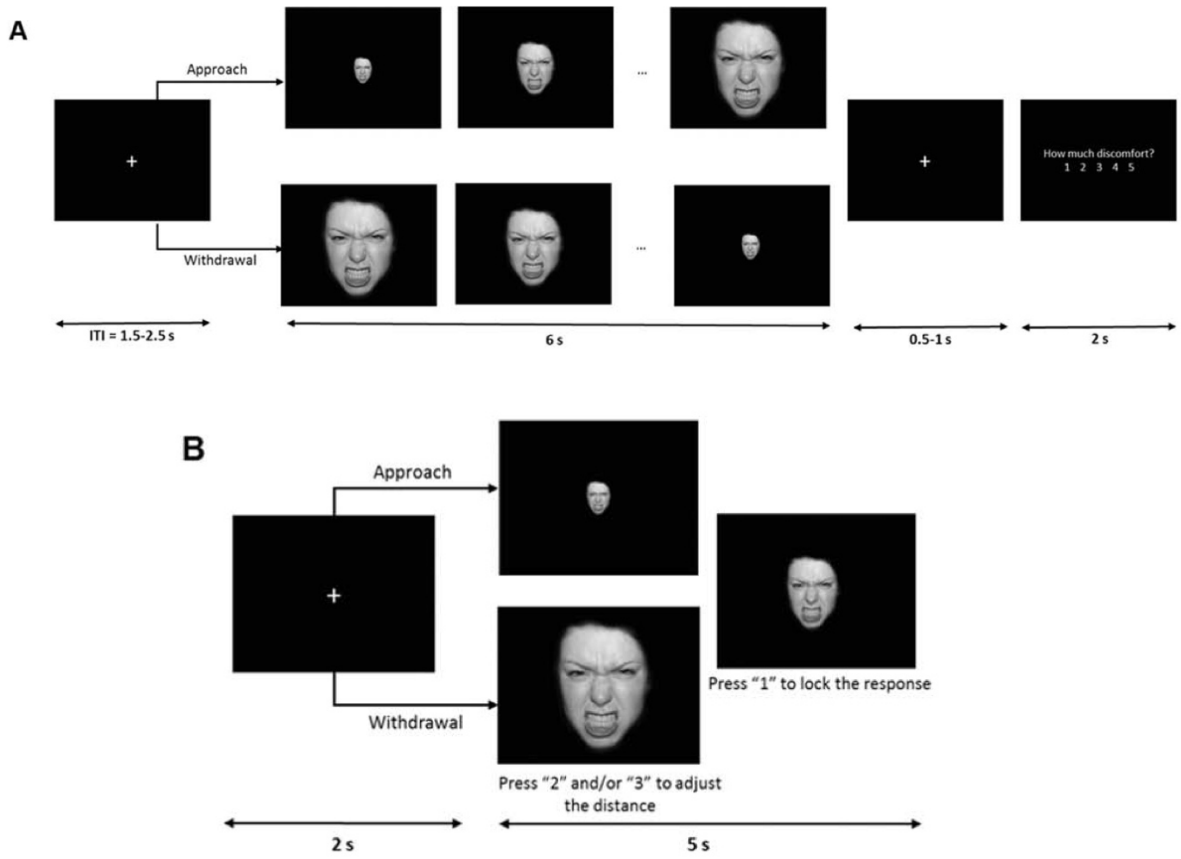

Figure 19. Tâches expérimentales réalisées dans l'IRM (A) et à l'extérieur de l'IRM (B) dans l'étude de Vieira et al., 2017. Ces tâches impliquent l'utilisation de visages émotionnels (5 émotions : joie, colère, peur, tristesse, et neutre) en 2D sur un écran apparaissant illusoirement plus proche ou plus loin du corps.

Plus récemment, dans une seconde étude, Vieira et al. (2020) ont exploré les corrélats neuronaux de l'espace personnel dans une situation défensive. Des stimuli sociaux et non sociaux avec différents niveaux de menace ont été utilisés dans les tâches expérimentales. Les stimuli sociaux représentaient des visages affichant une expression faciale neutre ou en colère alors que les stimuli non sociaux étaient des photographies prises à partir de spécimens entomologiques réhydratés, notamment une tarentule, un scorpion, un longicorne et trois coléoptères colorés différents (Figure 20). La tâche réalisée dans le scanner afin d'évaluer les réponses neuronales associées aux stimuli sociaux et non sociaux proches du corps par rapport à loin était la même tâche que celle utilisée dans leur précédente étude (Vieira et al., 2017). Également, comme précédemment, ils ont utilisé une

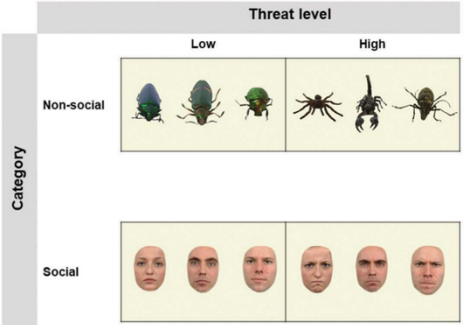

Figure 20. Stimuli sociaux et non-sociaux utilisés dans la tâche expérimentale de Vieira et al., 2020.

tâche d'évaluation des distances en dehors du scanner où il était demandé aux participants d'ajuster la distance avec les stimuli sociaux et non sociaux en changeant leur taille sur un écran jusqu'à atteindre la distance qu'ils garderaient normalement avec ces stimuli. L'approche des stimuli, indépendamment du type et du niveau de menace, a provoqué une activation accrue dans le mésencéphale (la substance grise périaqueducale, PAG), l'insula, le thalamus, le PMv s'étendant au cortex préfrontal dorsolatéral et le SPL (Figure 21). L'analyse de conjonction réalisée entre les stimuli sociaux et non-sociaux menaçants s'approchant comparé à s'éloignant du corps a montré des activations préférentielles communes dans le mésencéphale, le PMv, le SPL et le gyrus occipital médian (Figure 21). Lorsque la première image statique de chaque essai a été utilisée, créant des stimuli proches et lointains (au lieu de s'approchant et s'éloignant), des activations assez similaires étaient observées. Enfin, afin d'identifier les régions présentant une augmentation du couplage fonctionnel avec le mésencéphale en réponse aux intrusions dans l'espace personnel par des stimuli sociaux par rapport à des stimuli non sociaux, ils ont effectué une analyse d'interaction psychophysiologique généralisée (PPI) permettant d'analyser les changements dans la connectivité fonctionnelle pour le contraste stimuli sociaux s'approchant vs. non sociaux s'approchant en utilisant le mésencéphale PAG comme région d'intérêt. Ils ont pu mettre en évidence une augmentation de la connectivité fonctionnelle entre le PAG et le cortex prémoteur ainsi que le cortex préfrontal dorsolatéral. En outre, l'analyse de corrélation a montré que l'augmentation du couplage fonctionnel entre le PAG et le PMv était associée à des distances préférées plus courtes, obtenues dans la tâche réalisée en dehors du scanner, suggérant que le mésencéphale PAG et le cortex prémoteur permettrait de guider les interactions sociales appropriées lors de la régulation des distances entre les individus (espace personnel).

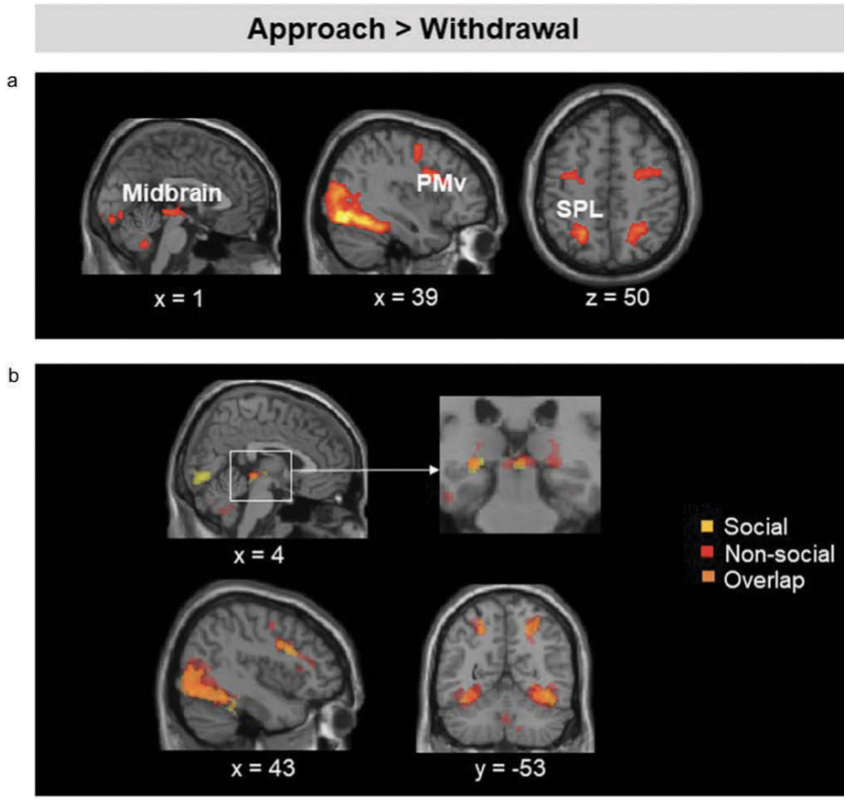

Figure 21. Résultats obtenus dans la tâche en IRMf de l'étude de Vieira et al., 2020. (a) Régions neuronales montrant une activation préférentielle pour les stimuli s'approchant par rapport aux stimuli s'éloignant, indépendamment de la catégorie (sociale ou non sociale) et du niveau de menace. **(b)** Résultats de l'analyse de conjonction montrant les régions communes aux stimuli sociaux et non-sociaux menaçants s'approchant. *PMv : cortex ventral prémoteur ; SPL : lobule pariétal supérieur.*

Trois autres études ont également investigué les corrélats neuronaux de l'espace personnel mais chez d'autres types de sujets ou patients. Schienle et al. (2016), ont montré que les délinquants violents (ainsi que le groupe témoin non criminel) présentaient une activation préférentielle pour un réseau fronto-pariétal (cortex prémoteur, SI, DLPFC, SPL, IPL) ainsi que l'insula lorsque des photos de visages d'hommes et femmes avec une expression neutre s'approchaient d'eux. Cependant, les délinquants présentaient une plus grande activation de l'insula à l'approche des visages par rapport aux sujets contrôles. Holt et al. (2015), ont constaté que les patients schizophrènes ainsi que les sujets sains présentaient des réponses préférentielles dans le DIPS et le PMv ainsi que dans les cortex occipitaux et temporaux pour les visages s'approchant comparé à s'éloignant du corps. Cependant, la région DIPS était plus activée chez les patients schizophrènes comparé aux sujets contrôles. Également, conformément à leur étude précédente (Holt et al., 2014), aucun des deux groupes n'a montré de réponses biaisées par

l'approche pour les stimuli non sociaux. Lorsqu'ils ont évalué la connectivité fonctionnelle de DIPS avec le PMv, ils ont révélé une connectivité significativement plus faible entre le DIPS et le gyrus fusiforme (FFA) chez les patients schizophrènes par rapport aux sujets sains. De plus, après avoir réalisé la tâche de distance d'arrêt en dehors du scanner, les patients schizophrènes possédaient une taille de leur espace personnel significativement plus grande par rapport aux témoins. Très récemment, Massaccesi et al. (2021) ont développé une nouvelle tâche évaluant l'espace personnel chez des sujets atteints d'un trouble du spectre autistique (TSA). Les participants étaient informés qu'une caméra compatible IRM montée sur le scanner enregistrait et diffusait en ligne deux expérimentateurs qui marchaient vers eux. Les participants pouvaient voir les images sur un écran accessible via un système de miroir (en réalité les vidéos étaient préenregistrées). Après avoir vu les expérimentateurs s'approcher d'eux, il a été demandé aux participants de juger leur confort quant à la distance à laquelle les compères s'arrêtaient. Les sujets atteints de TSA ont montré un confort général inférieur en réponse à l'approche d'un expérimentateur indiquant une préférence pour un espace personnel plus large par rapport au groupe contrôle. Cette préférence était accompagnée d'une activité réduite dans le DIPS et le FFA. De plus, ils ont observé des différences de connectivités fonctionnelles entre le DIPS, le FFA et l'amygdale chez les sujets atteints de TSA par rapport aux sujets contrôles, observé par une augmentation de la connectivité entre l'amygdale et le DIPS et une réduction de la connectivité entre le DIPS et le FFA. Ils ont également révélé une différence de connectivité en fonction du niveau de confort ressenti. À mesure que le confort diminuait, les sujets atteints de TSA présentaient une connectivité accrue du DIPS à l'amygdale et une connectivité réduite du FFA à l'amygdale par rapport aux sujets sains.

Le tableau 5 ci-dessous résume les analyses ainsi que les principaux résultats obtenus dans ces études.

Tableau 5. Résumé des études de neuroimagerie ayant investigué les bases neurales de l'espace personnel.

Études	Stimuli	Partie du corps ciblée	Analyses concernées	Résultats principaux
Holt et al. 2014 (Sujets sains)	**Visuel :** Sociaux (avatars humains avec expression neutre) et non sociaux (photos de voitures et sphères) en 2D sur un écran	Corps	Localisation des régions dont l'activité est biaisée par l'approche en fonction du type de stimuli : **contrastes 1) visages s'approchant vs. s'éloignant et 2) voitures ou sphères s'approchants vs. s'éloignant.**	Activité préférentielle **uniquement** pour les visages s'approchant par rapport à s'éloignant dans le **dIPS, le vIPS, le PMv, le PMd, le gyrus cingulaire, le precuneus, le gyrus frontal médian, le gyrus occipital médian et le gyrus temporal inferieur**
Vieira et al. 2017 (Sujets sains)	**Visuel :** Photos de visages humains émotionnels (heureux, en colère, peureux, triste, et neutre) en 2D sur un écran	Corps	Identification des régions avec des activations neuronales montrant une préférence pour les visages s'approchant indépendamment de l'émotion et en fonction de l'émotion : **contrastes 1) visages s'approchant vs. s'éloignant et 2) visages émotionnels s'approchants vs. s'éloignant.**	1) Activation préférentielle pour les visages en approche par rapport au visage en retrait dans **l'IPS (SPL et IPL), le cortex prémoteur, le SMA, le DLPFC) le gyrus frontal inférieur, le gyrus occipital médian, l'amygdale, l'insula et le cervelet.** 2) Interaction entre l'émotion et la direction a dans le **precuneus, le vlPFC, le gyrus frontal inférieur et l'insula.**
Vieira et al. 2020 (Sujets sains)	**Visuel :** Photos de visages humains en 2D sur un écran	Corps	**1)** Évaluation des clusters répondant préférentiellement aux stimuli s'approchant indépendamment du type de stimuli : **contraste approche vs. éloignement ;** **2)** Analyse de conjonction mettant en évidence les régions similaires pour les stimuli sociaux et non sociaux menaçants : **conjonction non social menaçant ^ social menaçant** **3)** Mêmes analyses de contraste et de conjonction en utilisant la première image statique de chaque essai conduisant à des stimuli proche et loin au lieu de s'approchant et s'éloignant. **4)** Identification du pattern de connectivité fonctionelle du mécenséphale PAG pour les stimuli sociaux versus non-sociaux s'approchant : **analyse PPI sociaux s'approchant > non sociaux s'approchant.**	1) Activation accrue avec l'approche des stimuli dans le **PAG, l'insula, le thalamus, le PMv s'étendant au cortex préfrontal dorsolatéral et le SPL** 2) Activations préférentielles communes entre les stimuli sociaux et non-sociaux menaçants s'approchant comparé à s'éloignant du corps dans le **PAG, le PMv, le SPL et le gyrus occipital médian.** 3) Augmentation du couplage fonctionnel entre le PAG et le PMv associé avec des distances préférées plus courte, obtenues dans la tâche de stop distance réalisée en dehors du scanner.
Schienle et al. 2016 (Délinquants violents)	**Visuel :** Photos de visages humains en 2D sur un écran	Corps	Identification des régions montrant une préférence pour les visages s'approchant **1)** pour chaque groupe (délinquants et témoins) et **2)** comparaison des groupes : contrastes **visages s'approchant vs. s'éloignant.**	1) Activations préférentielles dans le **SI, DLPFC, SPL, IP l'insula** par l'approche de visages chez les deux groupes. 2) **Plus grande activation de l'insula** à l'approche des visages **chez les délinquants.**
Holt et al. 2015 (Patients schizophrènes)	**Visuel :** Sociaux (avatars humains avec expression neutre) et non sociaux (photos de voitures) en 2D sur un écran	Corps	Localisation des régions dont l'activité est biaisée par l'approche en fonction du type de stimuli **1)** pour chaque groupe, **2)** comparaison des groupes : contrastes **visages s'approchant vs. s'éloignant** et **voitures s'approchant vs. s'éloignant,** Puis **3)** analyse de connectivité fonctionnelle de DIPS.	1) Réponses préférentielles dans **le DIPS, le PMv et les cortex occipitaux et temporaux** chez les patients schizophrènes et les sujets sains pour les visages en approche. 2) Région **DIPS plus activée chez les patients schizophrènes.** 3) Connectivité fonctionnelle plus faible entre le DIPS et le FFA chez les patients schizophrènes.
Massaccessi et al. 2021 (Sujets atteints de TSA)	Visuel : Vidéos d'expérimentateurs en 2D sur un écran	Corps	**1)** Évaluation des régions répondant préférentiellement chez les sujets TSA comparé aux contrôles : **contraste TSA vs. CTR.** **2)** Exploration de la connectivité fonctionnelle entre DIPS, FFA et amygdale pendant la tâche : **analyses DCM.**	**1) Activité réduite dans le DIPS et le FFA chez les sujets TSA** par rapport aux contrôles. **2)** Différences de connectivités fonctionnelles entre le DIPS, le FFA et l'amygdale chez les sujets atteints de TSA par rapport aux témoins, et dépendant du niveau de confort.

Ces quelques découvertes ont démontré que les structures fronto-pariétales impliquées dans la représentation de l'EPP, en particulier les régions PMv, PMd et IPS, seraient recrutées par l'approche d'éléments sociaux dans l'espace proche du corps, interprété comme une implication de ces régions dans l'espace personnel et donc jouant un rôle potentiel dans la régulation des distances sociales. Lorsque ces éléments sociaux étaient menaçants, le mésencéphale (PAG) était additionnellement recruté à ce réseau, suggérant un réseau défensif (Vieira et al., 2020). Cependant, par quels mécanismes notre cerveau agit lorsque des stimuli sociaux nous approchent ?

Au début de mes travaux de thèse, nous faisions l'hypothèse que lors de l'approche d'un élément social, comme un visage, des signaux intéroceptifs, provenant de l'intérieur de notre corps, seraient envoyés aux régions sous-corticales impliquées dans la régulation autonome telles que l'hypothalamus, l'amygdale, le striatum et le cervelet (Azzalini et al., 2019 ; Critchley & Harrison, 2013) et que ces signaux pourraient donc moduler directement ou indirectement l'activité du réseau prémoteur-pariétal de l'EPP. Dans le paragraphe V qui suit, je fais justement le lien entre notre état intérieur, l'intéroception, et le façonnement de notre représentation de l'EPP. Mais comme nous l'avons vu dans l'étude de Schienle et al. (2016) ou de Vieira et al. (2017), l'approche des visages induisait l'activation de l'insula qui peut être considérée comme une région intégrant les entrées sensorielles extéroceptives et les signaux intéroceptifs (Uddin et al., 2017). Il est important de noter que l'insula est fonctionnellement et anatomiquement liée à l'amygdale (Mufson et al., 1981 ; Uddin et al., 2017), une région jouant un rôle essentiel dans la régulation des distances lors des interactions sociales (Kennedy et al., 2009 ; Schienle et al., 2016 ; Vieira et al., 2017). En effet, Kennedy et al. (2019) ont montré une réduction de l'espace personnel chez une patiente qui présentait des lésions bilatérales de l'amygdale comparé aux sujets contrôles. Enfin, le FFA, une région sélective dans la perception et la reconnaissance des visages, pourrait également jouer un rôle dans l'interaction avec nos pairs dans l'espace proche de notre corps puisque Holt et al. (2015) ont rapporté une réduction du couplage fonctionnel entre le sillon intrapariétal dorsal et le FFA chez les patients schizophrènes lors de l'approche de visages, une pathologie qui a récemment été associée à une modification de la représentation de l'EPP (Lee et al., 2021) mais également à un déficit de leur espace personnel (Corbo et al., 2017 ; Di Cosmo et al., 2018) par rapport aux sujets sains.

V. Lien entre l'EPP, l'intéroception et la conscience corporelle de soi

L'intéroception fait référence au processus par lequel le système nerveux détecte, intègre et interprète les signaux provenant de l'intérieur du corps (Khalsa et al., 2018). L'intéroception, régit par nos réponses autonomes, pourrait servir à modifier notre comportement et nos sensations causées par des stimuli extérieurs (extéroception). Récemment, quelques études se sont justement penchées sur la relation entre la perception de l'état intérieur du corps et la représentation de l'EPP (Ardizzi & Ferri, 2018 ; Cartaud et al., 2018 ; Noel et al., 2018 ; Noel, Pfeiffer, et al., 2015 ; Rabellino et al., 2020 ; Rossetti et al., 2015 ; Scandola et al., 2020). Ces quelques études ont démontré que l'activation du système nerveux sympathique ou parasympathique, mesurée à travers les signaux physiologiques, pouvait être directement reliée à la proximité d'éléments sociaux proche de notre corps, comme il a pu être observé par une activité électrodermale augmentée avec l'approche de visages en colère (Cartaud et al., 2018, 2020 ; Ellena et al., 2020). Mais d'autres signaux corporels fortement liés à notre état intérieur agiraient également sur notre représentation de l'EPP, comme les traits de personnalité (anxiété, claustrophobie) qui seraient fortement liés à nos réponses comportementales face à des situations stressantes apparaissant proche de notre corps (Iachini et al., 2015 ; Lebert et al., 2020 ; Lourenco et al., 2011).

Le codage de l'EPP pourrait donc être le résultat d'une interaction à un niveau plus complexe, comprenant non seulement des signaux externes, mais également internes pouvant potentiellement expliquer que le sentiment intrinsèque d'inconfort qui délimite l'espace personnel et dépend de la personnalité de l'individu qui nous fait face puisse dépendre des interactions entre l'EPP et l'intéroception.

Récemment il a été suggéré que le mécanisme d'intégration multisensoriel qui sous-tend la représentation de l'EPP contribuerait à la représentation de soi comme étant distinct de l'environnement et plus particulièrement à la conscience corporelle de soi (« Bodily Self-Consciousness » en anglais). En effet, la conscience de son propre corps a pour élément fondamental l'intégration continue de signaux multisensoriels cohérents provenant non seulement de l'environnement extérieur, mais aussi du corps lui-même. Le sentiment

d'appropriation fait partie de l'expérience corporelle subjective nous donnant le sentiment que différentes parties de notre corps nous appartiennent (« body ownership » en anglais ; Gallagher, 2000 ; Jeannerod, 2003). Ce sentiment coïncide avec l'auto-identification correspondant à l'expérience de soi comme lié à un corps qui est le sien. La notion de conscience corporelle de soi est définie comme l'idée d'un « soi » incorporé dans un corps qui nous appartient (auto-identification), qui occupe une position spécifique dans l'espace (auto-localisation) et qui regarde le monde avec sa propre perspective (Serino, 2019). Depuis quelques années, certaines études ont proposé que les composants de la conscience corporelle de soi était un mécanisme clé de la représentation de l'EPP (Blanke, 2012 ; Makin et al., 2008 ; Serino et al., 2013 ; Tsakiris, 2010). En effet, l'établissement du sentiment d'appropriation à travers des expériences induisant des illusions portées sur la main dans lesquelles une main en caoutchouc était placée dans une posture compatible avec la vraie position du bras (appelée « rubber hand illusion » en anglais), serait corrélé à l'activité des régions neuronales de l'EPP, et en particulier au niveau du cortex pariétal prémoteur et postérieur (Brozzoli et al., 2012 ; Ehrsson et al., 2004, 2005 ; Makin et al., 2007). Une autre preuve a montré que si après quelques minutes où un participant percevait un contact sur le visage tout en voyant un visage étranger être touché de manière spatialement et temporellement cohérente créant une illusion sur le visage (« enfacement illusion » en anglais), l'activité des neurones de l'IPS augmentait (Apps et al., 2015). Cette région a été associée à la représentation de l'EPP aussi bien chez le singe et chez l'homme, et ici on peut voir que son activation lors de l'illusion appliquée au visage est liée à un recodage de l'espace proche d'un visage inconnu, comme si c'était notre propre visage (Bufalari et al., 2015 ; Maister et al., 2015). D'autres études suscitant une sensation de propriété envers un corps différent (« body swap illusion » en anglais ; Petkova et al., 2011 ; Petkova & Ehrsson, 2008) ou une dislocation du « soi » vers une position extérieure au corps (« full-body illusion » en anglais) ont pu mettre en évidence les mêmes propriétés de l'EPP que lorsque ces illusions n'avaient pas lieu. Par exemple, avec la première illusion, lorsque les participants percevaient une stimulation tactile sur la poitrine mais, regardant vers le bas, percevaient à travers le casque de réalité virtuelle, le corps d'un mannequin recevant la même stimulation, synchrone temporellement et spatialement, le PMv présentait des modèles d'activité spécifique à l'illusion (Gentile et al., 2015 ; Petkova et al., 2011). Avec la deuxième illusion, en appliquant une stimulation visuo-tactile synchrone sur la poitrine du participant et sur celle d'un mannequin virtuel dans une position différente, la représentation de l'EPP semblait s'étendre en direction de la nouvelle position virtuelle du corps, avec des performances facilitées dans la tâche de

détection tactile associée à la présence de stimuli auditifs proche du corps (Noel, Pfeiffer, et al., 2015).
Par conséquent, l'EPP ne reflète pas uniquement la position physique du corps mais également sa position intérieure (« Self » en anglais) et un chevauchement des régions neuronales impliquées dans la représentation de l'EPP semble également relatif à la sensation de possession du corps.

Ces différentes preuves sur la conscience corporelle de soi ainsi que les quelques études qui se sont penchées sur les mesures intéroceptives suggèrent qu'en fusionnant les informations extéroceptives de l'environnement et les influences de l'intérieur, à savoir les signaux internes provenant du corps, cela pourrait contribuer à notre propre représentation de l'EPP, donc favoriser une représentation intégrée de soi distincte de l'environnement, afin de façonner dynamiquement nos interactions et fournir une meilleure compréhension des processus mis en jeu lors des interactions sociales.

Pour conclure, à travers ce second axe, j'ai pu montrer le rôle déterminant de cette représentation de l'espace qui nous entoure, l'EPP, dans les interactions quotidiennes que nous entretenons avec notre environnement social. Les recherches menées sur la composante sociale de l'EPP sont en expansion dans le domaine mais il reste encore des questions ouvertes concernant cet espace actif durant nos interactions sociales. Des aspects qui me semblent essentiels pour une meilleure compréhension de son rôle seraient d'étudier comment notre représentation de l'EPP est construite à travers l'intégration des signaux physiologiques et des réponses comportementales mais également les corrélats neuronaux qui y sont associés, pour le moment seulement étudiés au travers de tâches « mesurant » l'espace personnel, en présentant des visages humains 2D dont la taille était augmentée (donc s'approchant) ou réduite (donc s'éloignant).

Au travers de ma thèse, j'ai donc décidé d'approfondir ces questions en caractérisant l'impact des éléments sociaux sur notre représentation de l'EPP au niveau comportemental, physiologique et neuronal en menant 3 études complémentaires. J'ai choisi pour cela d'utiliser une méthode plus écologique en développant des tâches utilisant la réalité virtuelle pour contrôler précisément les informations visuelles à différentes distances du corps. Ces études constituent le Chapitre 3 de ma thèse.

Dans la partie qui suit, j'expose les différentes questions que je me suis posées tout au long de mon travail de thèse ainsi que les méthodologies utilisées pour y répondre.

CORTEX 142 (2021) 28–46

Available online at www.sciencedirect.com

ScienceDirect

Journal homepage: www.elsevier.com/locate/cortex

Review

The Peripersonal Space in a social world

Olena V. Bogdanova [a,b,f,*], Volodymyr B. Bogdanov [a,b,e], Audrey Dureux [a,b], Alessandro Farnè [a,b,c,d] and Fadila Hadj-Bouziane [a,b,**]

[a] Integrative Multisensory Perception Action & Cognition Team (Impact), INSERM U1028, CNRS UMR5292, Lyon Neuroscience Research Center (CRNL), Lyon, France
[b] University of Lyon 1, France
[c] Hospices Civils de Lyon, Neuro-Immersion Platform, Lyon, France
[d] Center for Mind/Brain Sciences (CIMeC), University of Trento, Italy
[e] Ecole Nationale des Travaux Publics de l'Etat, Laboratoire Génie Civil et Bâtiment, Vaulx-en-Velin, France
[f] INCIA, UMR 5287, CNRS, Université de Bordeaux, France

ARTICLE INFO

Article history:
Received 26 June 2020
Reviewed 30 November 2020
Revised 27 February 2021
Accepted 19 May 2021
Action Editor Giuseppe Vallar
Published online 28 May 2021

Keywords:
PeriPersonal Space
Social
Interpersonal distance
Interoception
Shared representations

ABSTRACT

The PeriPersonal Space (PPS) has been defined as the space surrounding the body, where physical interactions with elements of the environment take place. As our world is social in nature, recent evidence revealed the complex modulation of social factors onto PPS representation. In light of the growing interest in the field, in this review we take a close look at the experimental approaches undertaken to assess the impact of social factors onto PPS representation. Our social world also influences the personal space (PS), a concept stemming from social psychology, defined as the space we keep between us and others to avoid discomfort. Here we analytically compare PPS and PS with the aim of understanding if and how they relate to each other. At the behavioral level, the multiplicity of experimental methodologies, whether well-established or novel, lead to somewhat divergent results and interpretations. Beyond behavior, we review physiological and neural signatures of PPS representation to discuss how interoceptive signals could contribute to PPS representation, as well as how these internal signals could shape the neural responses of PPS representation. In particular, by merging exteroceptive information from the environment and internal signals that come from the body, PPS may promote an integrated representation of the self, as distinct from the environment and the others. We put forward that integrating internal and external signals in the brain for perception of proximal environmental stimuli may also provide us with a better understanding of the processes at play during social interactions. Adopting such an integrative stance may offer novel insights about PPS representation in a social world. Finally, we discuss possible links between PPS research and social cognition, a link that may contribute to the understanding of intentions and feelings of others around us and promote appropriate social interactions.

* *Corresponding author*. Neuroscience Research Center, ImpAct Team, 16 Avenue Doyen Lépine 69500 Bron, France.
** *Corresponding author*. Neuroscience Research Center, ImpAct Team, 16 Avenue Doyen Lépine 69500 Bron, France.
E-mail addresses: olena.bogdanova@u-bordeaux.fr (O.V. Bogdanova), fadila.hadj-bouziane@inserm.fr (F. Hadj-Bouziane).
https://doi.org/10.1016/j.cortex.2021.05.005

1. Introduction: what is PeriPersonal Space?

In everyday life, humans and animals evolve in a complex environment composed of various kinds of objects with which they interact. Appropriate interactions require solving many computationally demanding sensorimotor problems, including the effective optimization of the distance between the agent's body/effector and objects in space. Even though we perceive the space surrounding us as a Cartesian continuum, our brain actually encodes for modular representations of space. This concept was introduced by Brain (Brain, 1941), following neuropsychological evaluations of hemispatial neglect, a condition that frequently follows right brain damage in which patients fail to attend to stimuli presented on the contralesional side. Brain suggested dissociation between 'a grasping' and a 'walking' distance to account for rather selective impairments of some of these patients for either one of these spatial dimensions (Làdavas, Zeloni, & Farnè, 1998; Làdavas & Farnè, 2004).

This notion was then supported by seminal electrophysiological studies, in particular by Rizzolatti, Scandolara, Matelli, and Gentilucci (1981) (Rizzolatti, Scandolara, Matelli, & Gentilucci, 1981), who first introduced the term PeriPersonal Space (PPS) to describe this region of space near the body where physical interactions with objects in the environment take place. PPS was distinguished from the extrapersonal space that referred to the space outside the mouth/hand grasping distance. Using electrophysiological recordings in monkeys, Rizzolatti, Scandolara, Matelli, and Gentilucci (1981) first identified a set of neurons in the posterior periarcuate regions, within the ventral premotor cortex, which responded more to objects presented in the peripersonal space compared to objects presented outside this sector of space. Several studies have shown that activities of single neurons in ventral premotor cortex (Graziano, Yap, & Gross, 1994; Rizzolatti, Scandolara, Matelli, & Gentilucci, 1981), the putamen (Graziano & Gross, 1993) and the parietal cortex (Colby, Duhamel, & Goldberg, 1993) were selectively modulated by the presence of objects near the hand or the face. In the parietal cortex, several subregions exhibited this selective coding, namely the ventral intraparietal area (Colby et al., 1993), the medial intraparietal area (Colby & Duhamel, 1996), and area 7b of the parietal lobe (Graziano & Cooke, 2006). Another critical feature of these neurons is that they are multisensory, they respond to visual, tactile, and auditory stimuli (Avillac, Hamed, & Duhamel, 2007; Colby et al., 1993; Duhamel, Colby, & Goldberg, 1998; Gentile, Petkova, & Ehrsson, 2011; Graziano, Hu, & Gross, 1997; Rizzolatti, Scandolara, Matelli, & Gentilucci, 1981). Neurons with responses to either tactile and visual stimuli were coded in body part-centered coordinates: for example, visual receptive fields were anchored to the tactile ones and followed the hand in space if it moved. They also display selectivity in several directions, with some neurons exhibiting preference for looming objects (Graziano et al., 1997).

Since the seminal work in monkeys, an abundant literature has accumulated to understand the characteristic of PPS coding/representation and its functions (Avillac, Ben Hamed, et al., 2007; Brozzoli, Makin, Cardinali, Holmes, & Farnè, 2012; Caggiano, Fogassi, Rizzolatti, Thier, & Casile, 2009; Cléry, Guipponi, Wardak, & Ben Hamed, 2015, 2018; di Pellegrino & Làdavas, 2015; Graziano & Cooke, 2006; Grivaz, Blanke, & Serino, 2017). These studies revealed one key feature of PPS representation, hence its flexibility. This flexibility depends on external factors, that is the characteristics of the stimulus within PPS (its nature, valence and the context), internal factors related to individual traits (physical—e.g., arm length or height; personality traits, bodily states) and exposure to different procedures such as tool use (Berti & Frassinetti, 2000; Biggio et al, 2017, 2019; Farnè, Pavani, Meneghello, & Làdavas, 2000; Maravita, Spence, Clarke, Husain, & Driver, 2000; Serino et al., 2015) or following body (Makin, Wilf, Schwartz, & Zohary, 2010) or spinal cord injuries (Scandola et al., 2020).

Ongoing, fast modulations of PPS representations following tool use (Canzoneri et al., 2013; Farnè, Iriki, & Làdavas, 2005; Serino, Bassolino, Farnè, & Làdavas, 2007) or body illusions (D'Angelo, di Pellegrino, & Frassinetti, 2019; Maister, Cardini, Zamariola, Serino, & Tsakiris, 2015; Noel, Pfeiffer, Blanke, & Serino, 2015) have also been reported during motion (Berger, Neumann, & Gail, 2019; Noel, Grivaz, et al., 2015), or in the presence of other individuals (Pellencin, Paladino, Herbelin, & Serino, 2017; Teneggi, Canzoneri, di Pellegrino, & Serino, 2013). Developmental studies also show the existence of early predisposition to stimuli processing in the PPS in newborns or in first-year infants (Drew, Meltzoff, & Marshall, 2018; Orioli, Filippetti, Gerbino, Dragovic, & Farroni, 2018). Along the same lines, multisensory integration of spatial cues, a key property of PPS representation, develops gradually across the lifespan (Bremner, Holmes, & Spence, 2008; Burr & Gori, 2012; Sorrentino et al., 2021).

Based on these properties and owing to their anatomical position at the interface with motor regions, it was suggested that PPS brain regions play a key role in visually guided actions or in more general terms facilitate the interactions with objects in our environment. In recent years, the diversity of methodologies employed to study PPS representation has had important implications for its theoretical conceptualization (de Vignemont & Iannetti, 2015), leading to different frameworks describing PPS representations in terms of a network of body-part centered representations (Hunley & Lourenco, 2018), a set of continuous action fields (Bufacchi & Iannetti, 2018) or an index of multisensory body–environment interactions (Serino et al., 2019). Closely related to the current topic, it has been suggested that PPS could contribute to the representation of the self (Noel, Pfeiffer, et al., 2015; Serino, 2019). While discussing these different theoretical accounts is beyond the scope of the present review article, we posit that they are all compatible with a role of PPS representation in social interactions. In particular, we will argue that, by merging exteroceptive information from the environment and internal signals that come from the body (that is a physiological representation of the state of the body, including somatosensory, proprioceptive, visceral afferents etc.), the PPS may indeed underlie an integrated representation of the self, as distinct from the environment and the others.

Adding to this complexity, one should also consider that the mere presence of conspecifics around us affects our behavior. This phenomenon has been long studied in social

psychology and is well documented in human and animal research (Bond & Titus, 1983; Reynaud, Guedj, Hadj-Bouziane, Meunier, & Monfardini, 2015). Indeed, another dimension of spatial perception, stemming from ethology and social psychology and that could relate to PPS representation, has been termed 'personal space' (Altman & Chemers, 1984; Hayduk, 1983). The notion of flight zone, later termed margin of safety, to describe the distance animals keep between themselves and other animals has first been introduced by Hediger, the director of the Zurich Zoo in 1955, and was though to serve both communicative and survival functions. The American anthropologist Edward T. Hall adapted this concept to a comfort zone or personal space, that we keep between us and others to regulate the interpersonal distance and to avoid discomfort, or even anxiety (Hall, 1966; 2014). This distance governing social interactions is a ubiquitous entity, present with some variations across the animal kingdom and in humans (Baldwin & Baldwin, 1974; Kennedy, Gläscher, Tyszka, & Adolphs, 2009; Vestal, 1977). Graziano & Cooke (2006) were the first to relate PPS and the ethological concept of a flight zone and the psychological concept of personal space (Graziano & Cooke, 2006). Despite their different origins, both personal space and PPS representation broadly refer to the space anchored to the body. As such, they may share some commonalities.

In this review, we depart from the classical 'action-related' features of PPS, to rather focus on the social dimension(s) of PPS representation, which has seen an exponentially growing interest in recent years (Heed, Habets, Sebanz, & Knoblich, 2010; Patané, Farnè, & Frassinetti, 2017; Pellencin et al., 2017; Teneggi et al., 2013). First, we will review findings describing the influence on PPS of social elements depending on the context (emotional valence, moral judgment, interaction with partners, etc.) making the PPS enlarge, shrink or remap. Second, we will frame the comparison between PPS and Personal Space (PS) at both the theoretical and empirical level, aiming at clarifying these concepts. Third, we will discuss whether and how the internal states of the organism relate to PPS representation in social environments. Finally, we will consider possible mechanisms allowing for the interactions between body signals and brain networks to adapt behavioral responses according to varying social contexts. We ultimately advance that these represent important dimensions along which PPS and its relation with social behaviors will be better understood, and provide some perspectives on PPS in the field of social cognition and its role in social interactions.

2. PeriPersonal Space representation in a social world

2.1. *PPS through different lenses: a variety of experimental procedures*

Since Rizzolatti et al.'s findings in monkeys (Rizzolatti, Scandolara, Gentilucci, & Camarda, 1981; Rizzolatti, Scandolara, Matelli, & Gentilucci, 1981), several experimental approaches have been employed in humans to study PPS representation, to better understand and characterize its features and functions (Brozzoli, Dematte, Pavani, Frassinetti, & Farnè, 2006; Farnè et al., 2000, 2005). Different methods focused on either perceptual abilities, action planning or defensive responses (Table 1). Most typically, participants were exposed to static or dynamic multisensory stimulations and, more recently also uni-sensory ones. What follows is a brief, non-exhaustive description of the experimental procedures used to investigate PPS representation. Regardless of the methods, a stimulus presented within PPS typically induces a modulation of the cognitive processes taking place, made observable via several measures.

In static conditions, methods typically compare the behavioral outcome in response to stimuli appearing either in close (within PPS), or far space (outside PPS). This is the case for the crossmodal congruency task, in which the difference in performance between incongruent and congruent trials, known as Cross-modal Congruency Effect (CCE), measures the amount of the cross–modal interaction (Spence, Nicholls, Gillespie, & Driver, 1998). This method revealed larger CCE for visual distractors close to (vs. far from) the stimulated hand (Spence et al., 1998, 2004). This finding extends to static conditions before an upcoming movement: merely planning to reach an object increased crossmodal congruency effects (Belardinelli, Lohmann, Farnè, & Butz, 2018; Brozzoli et al., 2009, 2010; Patané et al., 2018). Such behavioral effects may be accompanied by changes in motor cortex excitability (Job, de Fockert, & van Velzen, 2016; Wamain, Gabrielli, & Coello, 2016).

In dynamic conditions, stimuli typically move toward or away from participants and behavioral responses are probed along the spatiotemporal displacement. An influential example of such a multisensory interaction paradigm consists of a speeded tactile detection task concurrent to an irrelevant (visual or auditory) approaching stimulus (Canzoneri, Magosso, & Serino, 2012). The stimulus being delivered at different timings, being thus more or less close to the participant, this method measures multisensory boosting of touch perception by an approaching stimulus. It allows to model behavioral responses along the sagittal plane with a sigmoidal function, whose inflexion point is interpreted as the PPS 'boundary'. The displacement of this point toward or away from participants is typically interpreted as a reduction or an enlargement of PPS extent, respectively (Canzoneri et al., 2012; Teneggi et al., 2013).

Another method leveraged the reachability judgment task (Coello et al., 2008). Here, participants view an object (either static at a certain distance, or moving toward them) and have to judge whether (or stop the object movement when) it is reachable. The reachability distance, used as a proxy of PPS representation, is also interpreted as the boundary of PPS representation, and has been assessed in different contexts, including social ones (Cartaud, Ruggiero, Ott, Iachini, & Coello, 2018; Costantini, Ambrosini, Tieri, Sinigaglia, & Committeri, 2010; Iachini et al., 2016; Iachini, Ruggiero, Ruotolo, Schiano di Cola, & Senese, 2015; Quesque et al., 2017).

Not last, other studies probed the defensive nature of PPS, measuring the hand-blink reflex (HBR), in which an electrocutaneous stimulation of the median nerve at the wrist elicits a blink reflex (Bisio et al., 2017; Bufacchi, 2017; Sambo, Liang, Cruccu, & Iannetti, 2012). Its amplitude, as measured via the electromyographic activity recorded from orbicularis oculi

Table 1 – Experimental approaches used to probe PPS in human behavioral research.

Tasks	Main results	References
Perception and PPS representation: Detection or discrimination tasks		
Crossmodal congruency	Stronger Cross-modal Congruency Effect (CCE), with close vs. far visual stimuli.	(Aspell, Lavanchy, Lenggenhager, & Blanke, 2010; Spence et al., 2004)
Audio- or Visuo-tactile extinction	Inability to detect a visual stimuli presented in the contralesional side if presented concurrently with a competing ipsilesional event of another modality (in near space)	(Brozzoli et al., 2006; Farnè et al., 2000, 2005)
Multisensory interaction	Faster tactile stimuli detection in the presence of approaching audio or visual stimuli	(Canzoneri et al., 2012; Serino et al., 2015; Stone, Kandula, Keizer, & Dijkerman, 2018)
Line bisection	Bias to bisect lines slightly to the left close to the body and slightly to the right in the far space	(Hunley, Marker, & Lourenco, 2017; Lourenco et al., 2011)
Visual detection/discrimination	Faster response to stimuli close to the body or hand; faster target discrimination in near space (vs. in the far space)	(Blini et al., 2018; Dureux et al., 2021; Plewan & Rinkenauer, 2017; Reed, Grubb, & Steele, 2006)
Action-related PPS representation:		
A. Action planning and execution in near space with or without movement		
Reachability judgment	Modulation of the size of reachable space as a function of the stimuli.	(Iachini et al., 2014; Quesque et al., 2017; Ruggiero et al., 2017)
Spatial alignment	Facilitation of the behavioral response when the target is in a congruent position to an intended or executed grasping movement in close space	(Costantini et al., 2010; Stefani et al., 2014)
Action planning and execution	Stronger multisensory integration effects during interactive compared to non-interactive movements.	(Belardinelli et al., 2018; Brozzoli et al., 2009, 2010; Patané et al., 2018; Senna et al., 2019)
B. Defensive responses		
Hand blink reflex	Increase of HBR amplitude as a function of the position the hand and a nociceptive stimulation applied on the hand	(Bisio et al., 2017; Bufacchi, 2017; Sambo et al., 2012; Sambo & Iannetti, 2013)
Multisensory interaction	Facilitation of tactile detection with approaching stimuli with negative emotional valence; Facilitation of nociceptive detection with approaching visual stimuli; Increase of skin conductance response with approaching noxious stimuli	(De Paepe, Crombez, & Legrain, 2016; Ferri et al., 2015; Rossetti et al., 2015);
Reachability judgment	Increase of skin conductance response with approaching angry faces	Cartaud et al. (2018)
Time to collision/temporal order judgment	Privileged temporal judgements with visual stimuli in close space	(De Paepe, Crombez, Spence, & Legrain, 2014)

muscles, increases when the stimulated hand comes closer to the face, thus 'entering' the PPS surrounding it. This suggests that the brainstem circuits mediating the HBR are under the influence of higher-level brain regions coding space representation in relation to body parts proximity (as is PPS), likely to protect the body from potential danger in the environment.

To sum-up, PPS extent has been estimated with a variety of methods that manipulated distance as the main variable. The task conditions and the behavioral outcome may thus tap into a given property or function of the PPS construct, as the guidance of voluntary action and the enabling of self-defensive reactions. Such modulatory effects appear to occur gradually along the sagittal plane. Several studies have shown that PPS representation is shaped depending on a variety of intrinsic and environmental factors and likely result from complex computations integrating both internal and external signals. Such computations could get even more complex when we consider real-world situations with multiple layers of interactions with objects and peers. The following sections will attempt to frame this complexity.

2.2. *Social modulation of PPS representation*

When investigating the influence of a modulator, and in particular social factors that involve the presence of *others* (e.g., partners, conspecifics, confederates, intruders etc.), the characteristics of the latter(s) matters. One needs to consider their physical attributes, that could appear as salient features with a bottom up influence, such as their sex or emotional signals, as well as more subtle features that may involve a top-down influence, such as participants' prior beliefs about the other (i.e., moral judgements). As summarized in Table 2, both the characteristics of the participant and his/her relationships with the other, notably their familiarity and personality traits, may also matter for PPS representation. Under the influence of social elements, depending on the context, PPS representation is affected and its boundary enlarges, shrinks or remaps in relation to the other (Fig. 1).

In studies using the visuo-tactile or audio-tactile congruency task, participants hold vibrotactile stimulators while a task irrelevant visual (or auditory) stimulus is presented at incongruent or congruent position in regard to the vibrotactile stimuli. Spence et al. (2004) showed that the CCE was stronger when the visual stimulus appeared close as compared to far from the tactile stimulation (Spence et al., 2004). Using this procedure, Heed et al. found that performing this task alone or with another person differently affected performance (Heed et al., 2010). CCE was significantly reduced in the presence of the other participant, only when he/she sat within the participant's PPS and when the two protagonists were concurrently performing the task. No effect was found when the other stood outside the participant's PPS, or when she/he did not perform the task, suggesting that for the effect to take place, the participant needed to know that the other was also engaged by responding to the tactile stimulus. Interestingly, the mere attribution of object ownership also affects PPS representation during both observed and executed grasping actions performed by participants facing each other as measuring using CCE (Patané, Brozzoli, Koun, Frassinetti, & Farnè, 2020). In this study, the authors manipulated the ownership status of an object to be grasped by the participants ("is mine or other's") and found ownership-dependent modulation of PPS, such that this modulation only occurred when observing or executing grasping action toward objects that has been assigned to oneself. This study highlights the link between PPS and the notion of self that might also be extended with tools as previously mentioned but also with object ownership.

Studies using the multisensory interaction task showed that the mere presence of another person *vs* a mannequin shrinks the participant's PPS boundary (Teneggi et al., 2013) (Table 2). By contrast, after a cooperative game with the other, the PPS boundary enlarges toward the confederate (Hobeika, Taffou, & Viaud-Delmon, 2019; Teneggi et al., 2013). A similar change, i.e., PPS enlargement, was also found when facing a moral other as compared to an immoral one (Pellencin et al., 2017). Finally, another type of PPS plasticity, termed *shared or merged* PPS, has been revealed in tasks involving either synchronous stimulation to the participants and the confederate (Maister et al., 2015) or when they both performed the same task concurrently (Teramoto, 2018) (see Fig. 1B for illustration). These settings yielded faster detection time with stimuli approaching the confederate when the two persons experienced the same condition, mimicking 'a shift of PPS representation' between them, beyond physical spatial proximity. Interestingly, Iachini et Ruggiero (Iachini & Ruggiero, 2021), recently revealed that the representation of one's own and others' PPS was affected by physical distance but also by the possibility of the protagonists to move or not their arms, suggesting that the representation of others' PPS might be triggered by a motor simulation of one's own PPS. In the same vein, the amplitude of the hand blink reflex was enhanced both when the stimulated hand belonged to the participant and to another person; it was also enhanced when the stimulated hand was brought close to the face of another individual and this enhancement was dependent on the participants' empathic traits (Fossataro, Sambo, Garbarini, & Iannetti, 2016). That is, not only purely physical spatial proximity between agents modulates PPS, but their level of familiarity, social proximity and the interactions between them come into play. For instance, enhancement of touch perception in a participant, induced by the observation of a photograph depicting another person being touched in the same location, depended on the degree of familiarity or social proximity between the observer and the observe (Serino, Giovagnoli, & Làdavas, 2009). Such shared PPS representations may facilitate interactions with others via multisensory predictive coding mechanisms (Fanghella, Era, & Candidi, 2021).

Other researchers applied the reachability judgment task, as a proxy of PPS representation (Fig. 1), reporting it was shorter facing an avatar as compared to an object, or a robot (Iachini, Coello, Frassinetti, & Ruggiero, 2014). This distance increased with angry emotional faces (Cartaud et al., 2018, 2020) and avatars that were tagged with immoral statements (Iachini, Pagliaro, & Ruggiero, 2015). Another set of experiments assessed the impact of social factors onto PPS plasticity before and after tool use, thought to modify both spatial and body representation (Bassolino, Finisguerra, Canzoneri, Serino, & Pozzo, 2015; Canzoneri et al., 2013; Cardinali, Brozzoli, & Farnè, 2009). The studies consistently found that tool use affected reachability distance after a cooperation with the confederate, leading to larger reachability distance toward

Table 2 – Social modulation of PeriPersonal (PPS) and Personal Space (PS) measures.

Social manipulation	PPS	PS
	Multisensory interaction task Variable: Sigmoidal central point	**Stop-distance paradigm** Variable: comfort distance
Presence of the other outside PPS (Real person vs. mannequin) (Teneggi et al., 2013)	⇐ with real unfamiliar other	
Before and after non-cooperative or cooperative game (Teneggi et al., 2013)	⇒ (Faster RT in the far space) after cooperative game	
Emotional sounds (Ferri et al., 2015)	⇒ with negative sound (vs. neutral or positive sounds)	
Moral judgment (moral vs. immoral) (Pellencin et al., 2017)	⇒ with moral other	⇐ with moral other
Facial emotions of conferderate(neutral, happy, fearful) (Ellena et al., 2020)[a]	Visual attention redistribution in near space with fearful faces	
After synchronous multisensory stimulation (only participants responding) (Maister et al., 2015)	Shared PPS (faster tactile detection with auditory stimuli near the other only after synchronous multisensory stimulation	
Cooperation (Hobeika et al., 2019)	⇒ right hemispace and independently of the location of the partner only when participants collaborated with a partner	
	Reachability judgment task Variable: Reachability distance	**Stop-distance paradigm** Variable: comfort distance
Standing still (passive) or walking toward stimuli (active) (avatar, object, robot in VR) (Iachini et al., 2014)	⇐ with avatar vs cylinder	⇐ with avatar vs cylinder
Moral judgment (moral vs. immoral) (Iachini, Pagliaro, & Ruggiero, 2015)	⇐ with moral other	⇐ with moral other
Facial expressions (neutral, happy, angry) (Ruggiero et al., 2017)	⇐ with happy other	⇐ with happy other
Facial expressions of other (positive vs negative) with point-light walkers (Cartaud et al., 2018)[a]	reachability judgments were not influenced by the facial expression	⇐ with happy or neutral other vs with angry one
Cooperative tool use (before and after) (Candini et al., 2019; Patané et al., 2017)	⇒ after vs. before	⇐ after vs. before
Individual tool use (before and after) Exp2 in (D'Angelo et al., 2017) (Patané et al., 2016)	⇒ after vs. before	⇔ after vs. before
Individual tool use (before and after) with point-light walkers (Quesque et al., 2017)	⇒ after vs. before	⇒ after vs. before
Invisible body illusion Exp1 in (D'Angelo et al., 2017)	⇔ after body illusion	⇐ after body illusion
	Hand Blink Reflex	
Presence of other inside PPS (Fossataro, Sambo, et al., 2016)	Increase of HBR amplitude when stimulated hand close to confederate's face	
	Cross congruency task	
Presence of other (Heed et al., 2010)	Reduced interference cost (CCE) with confederate inside but not outside PPS	
	Audio-(visuo-) tactile interaction task	
After joint task performance (Dell'Anna et al., 2020)	no facilitation in near space in non-cooperative condition	

(*continued on next page*)

Table 2 – (continued)

Social manipulation	PPS	PS
	Multisensory interaction task Variable: Sigmoidal central point	**Stop-distance paradigm** Variable: comfort distance
After joint task performance (Teramoto, 2018)	Shared PPS (faster tactile responses with visual stimuli near the confederate)	
	Spatial alignment task	
Presence of other (Saccone et al., 2018)	Shared PPS (equal affordance responses for space near self and the other)	
	Spatial encoding task	
Collaborative interactions (Rocca, Wallentin, Vesper, & Tylén, 2019)	Linguistic coding of proximal space is shifted towards the other in a collaborative condition	

⇒ Expansion, ⇐ reduction, ⇔ unchanged.

[a] Cartaud et al. (2018) and Ellena et al. (2020) reported an increase of electrodermal activity; Dureux et al. (2021) reported increase of heart rate for faces presented in close vs. far space.

the cooperative confederate (Candini, Giuberti, Santelli, di Pellegrino, & Frassinetti, 2019; Patané et al., 2017).

Importantly, as discussed in the previous paragraphs, when considering PPS boundary, one needs to keep in mind the way this boundary is defined and measured: 1) using the central point of the sigmoid fitting the performance along the sagittal plan in multisensory interaction task or 2) measuring the reaching distance with the reachability judgement task. Note that in the former setting, the confederate was typically static and located outside participants' PPS, while participants' performance was measured with a visual probe approaching them. This implies that in such setting the social element is 'indirectly' interfering with the participant's PPS representation. By contrast, in the reachability judgement task, the confederate is typically positioned outside the participant's PPS and then moves toward the participants (in the passive version of the task, or the participant moves toward the confederate, in the active version of the task). Here, the social element is 'directly' interfering with the participant's PPS representation. With the multisensory interaction task, a positive interaction between the participants and the confederate or the presence of a social factor with a positive valence, or valued judgement (morality), elicited an enlargement of the participant's PPS. By contrast, a social factor with a negative valence, or unvalued judgement (immorality), most often elicited shrinkage of the participant's PPS. With the reachability judgement task, a social factor with a positive valence or valued judgement (morality) typically elicited shorter reachable distances while a social factor with a negative valence, or unvalued judgement (immorality), elicited larger reachable distances (Fig. 1).

This opposing direction of the effects could reflect either real differences between measures, and thus spatial representations they tackle, or may only be apparent. A PPS expansion measured by multisensory interaction might signify an inclusion of the other's PPS into one's own PPS (Teneggi et al., 2013) leading to a larger 'avenue' for potential interactions between the agents. A shrinkage of PPS, when measured by the reachability judgment task, might similarly emphasize participants are keener to 'come closer'. Perceiving what is reachable indeed activates motor representation of reaching actions, whose neural bases are reported to include motor and premotor regions (the dorsal premotor cortex, the supplementary motor area), as well as posterior parietal cortex (V6A and parietal reach region in anterior and medial intraparietal sulcus) (Filimon, 2010; Lara, Cunningham, & Churchland, 2018; Monaco et al., 2011; Pitzalis et al., 2013). As such, PPS and reachability circuitries involve partly common, but also some specific brain machinery. While this might account for some of the opposite effects measured behaviorally, recent evidence also points to genuine differences between these spatial representations (Zanini et al., 2020).

3. PeriPersonal and personal space: how do they relate to each other?

As posited earlier, despite their different origins, both PS and PPS refer to the space surrounding the body. Are they similar, but different concepts? The literature shows that in some instances, they either converge or diverge. The next section will

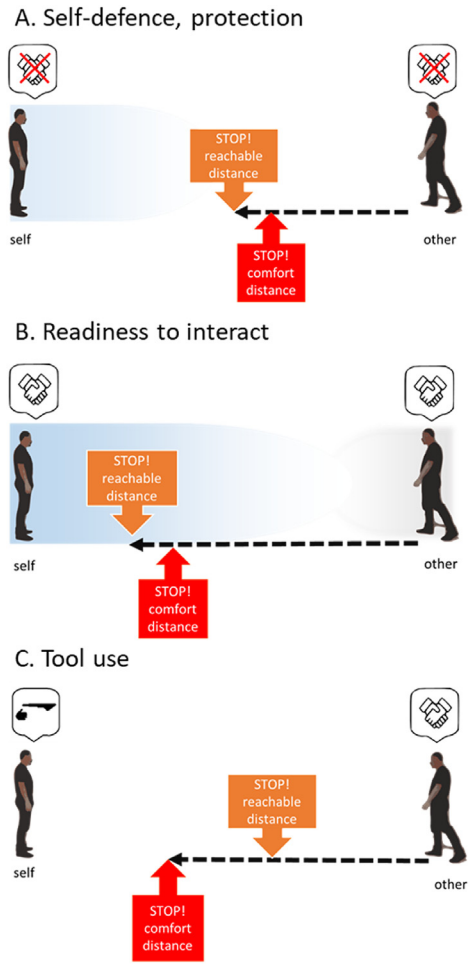

A. In the presence of an immoral, angry/fearful, non-cooperative confederate:
PPS: Shrinkage of PPS estimated with the multisensory interaction task (Dell'Anna et al., 2020; Pellencin et al., 2017; Teneggi et al., 2013) vs extension of reachability distance (Cartaud et al., 2018; Iachini, Pagliaro, et al., 2015; Ruggiero et al., 2017) ;
PS: extension of comfort distance (Cartaud et al., 2018; Iachini, Pagliaro, et al., 2015; Ruggiero et al., 2017).

B. In the presence of moral, happy, cooperative confederate:
PPS: Extension of PPS estimated with the multisensory interaction task (Hobeika et al., 2019; Pellencin et al., 2017; Teneggi et al., 2013) vs shrinkage of reachability distance (Cartaud et al., 2018; Iachini, Pagliaro, et al., 2015; Ruggiero et al., 2017);
Self-other shared or merged PPS estimated with the multisensory interaction task (Maister et al., 2015; Rocca et al., 2019; Saccone et al., 2018; Teneggi et al., 2013; Teramoto, 2018) ;
PS: Shrinkage of comfort distance (Cartaud et al., 2018; Iachini, Pagliaro, et al., 2015; Ruggiero et al., 2017).

C. After tool use:
PPS: Extension of reachability distance (Candini et al., 2019; Patané et al., 2017)
PS: Shrinkage of comfort distance (Candini et al., 2019; Patané et al., 2017, Candini et al., 2019; Patané et al., 2017).

Fig. 1 – Changes in PPS and PS representations measurements in different social contexts. In the examples depicted, PPS boundary was estimated with the multisensory interaction task (illustrated here as grey shadow, msi PPS) or the reachability judgement task (orange block), while PS boundary (comfort distance) was estimated with the stop distance paradigm (red block). The multiplicity of the experimental approaches leads to divergent results and interpretations.

summarize the studies that have directly compared these two spatial concepts in the same subjects (Table 2). Before, as we have exemplified above for PPS, it is important to recall how PS is measured. Typically, the reference measure considered in this field is the comfort distance, which is most frequently assessed with the 'stop-distance paradigm'. A participant faces another person (the experimenter) walking toward her/him. In the passive version of this task, participants stay still and have to stop the approaching experimenter at the latest separating distance they feel comfortable with. In the active version, roles are reversed and the experimenter stays still while participants move towards him/her to stop at a comfortable separating distance (Shin, Song, Kim, & Biocca, 2019; Sorokowska et al., 2017). The procedure can include measures from different perspectives, egocentric (first person) or allocentric (third person view). It has been evaluated in real world situations (Hayduk, 1983), in virtual environments (Nishihara & Okubo, 2015), or even using a paper-pencil version (Duke & Kiebach, 1974). Importantly, it always includes two agents (the participant and the confederate) facing each other and, contrary to the reachability judgement where a motor representation of a reaching action toward the confederate is prompted, with the stop-distance paradigm the emphasis is put on the participant's inner state, to avoid discomfort or anxiety (Gifford, 1982; Hayduk, 1983).

The majority of the studies that have directly compared PPS and PS have used the reachability judgment task as a proxy for PPS representation. In such a case, PS and PPS mostly overlapped. Both reachability and comfort distances strongly depended on the context (Iachini et al., 2014, 2016). When participants performed the stop distance and reachability paradigms in their passive version (being approached), both measures were larger than in the active situation (Iachini et al., 2014, 2016). Both reachability and comfort distances depended similarly on the participant's level of anxiety and her/his sex. They were also influenced by the others' attributes: their facial expressions (Cartaud et al, 2018, 2020; Ruggiero et al., 2017), the judgements that can be attributed to them such as morality (Iachini, Pagliaro, & Ruggiero, 2015), as well as age and sex (Iachini et al., 2016; Iachini, Ruggiero, et al., 2015; Ruggiero, Rapuano, & Iachini, 2019). For instance, smaller distances were typically reported for female and young person compared to male or adult person.

Yet, depending on the experimental paradigm to probe PPS representation, results may also diverge. In the study of (Iachini, Pagliaro, & Ruggiero, 2015), both reachability judgement and stop distance tasks decreased when facing a moral person. However, when PPS was estimated with the multisensory interaction task, PPS representation expanded towards a moral/cooperative agent (Teneggi et al., 2013). As anticipated above, this discrepancy may reflect true differences between PS and PPS representations, as well as merely reflect methodological differences across their measures, again underlying how experimental procedures used to evaluate PPS representation might matter.

A different, more bottom-up approach for testing PS and PPS similarities and differences has been undertaken by looking at the impact that tool-use may exert on them. In this respect, the measure of reachable and comfort distances after tool use also lead to mixed results (Candini et al., 2019; Patané et al., 2017). The use of a long tool consistently increased reachability distance estimated either alone (Bourgeois, Farnè, & Coello, 2014), or in the presence of a point-light walker (Quesque et al., 2017), a real confederate (D'Angelo, Pellegrino, & Frassinetti, 2017; Patané, Iachini, Farnè, & Frassinetti, 2016), as well as following cooperative tool use (Patané et al., 2017). These findings are in keeping with studies showing that tool use modulates PPS boundaries. However, these studies reported differences in terms of the impact of tool use on PS, as measured by the stop distance paradigm. Some researchers (D'Angelo et al., 2017; Patané et al., 2016) showed that this measure remained unchanged when facing an unfamiliar person, while it decreased after cooperative tool use in the same paradigm (Candini et al., 2019; Patané et al., 2017). By contrast, Quesque et al., 2017 reported an increase of PS towards a light-point walker after tool use (Quesque et al., 2017). It is possible that the use of a light-point walker -compared to a real person—may be responsible for this difference. Another manipulation, the illusion of having a tall body (200 cm of height) also significantly reduced interpersonal distance and enlarged reachability distance (D'Angelo et al., 2019). Interpersonal distance is typically reduced towards kids (Iachini et al., 2016), people also preferring to enter into personal space of short, but not tall others (Caplan & Goldman, 1981).

To sum-up, both spatial representations depend on other individuals and their interaction with the environment, to manipulate it or protect from it (de Vignemont & Iannetti, 2015; Graziano & Cooke, 2006). Both depend on the subjects' personality traits, for example anxiety level (Iachini, Ruggiero, et al., 2015; Sambo & Iannetti, 2013). The different effects induced by the same sensory-motor manipulation on either spatial representations may result from differences in terms of bottom-up (tool use) or top-down (sense of agency, PPS remapping) processes, or signify that they probe different aspects of the space surrounding us. Since both PPS and PS refer to spatial representations in relation to the body, they might loosely share some features but to date the empirical dissociations reported above (see also (Zanini et al., 2020) and the different experimental approaches suggest some cautions should be kept in mind when trying to delineate a unifying conceptual framework.

4. PPS, interoception and bodily self-consciousness

Interoception refers to the process by which the nervous system senses, integrates and interprets signals originating from inside the body, providing a moment-by-moment mapping of the body's internal landscape across conscious and unconscious levels (Khalsa et al., 2018). Salient stimuli in the space surrounding the body may induce changes in autonomic responses, as for example, during the observation of a noxious stimulus approaching and either touching the hand or stopping close or far from it (Rossetti, Romano, Bolognini, & Maravita, 2015). Electrodermal activity also increased in response to approaching angry faces (Cartaud et al, 2018, 2020; Ellena, Starita, Haggard, & Làdavas, 2020). Strong interoceptive signals in response to salient features, such as an angry or happy person approaching us, are likely to exert different impacts on our body, brain and behavior, likely promoting approach or avoidance reactions and fine-tuning our motor behavior. When surrounded by others, the estimation of appropriate physical distances should ideally be computed considering affective and social relationships, on top of their physical distance. This is even possibly reflected through metaphors with which we describe our relationships in many languages: 'this is my closest friend', 'a noble with its entourage', 'he is distancing himself from me' (Lakoff & Johnson, 1980). Yet, interoceptive signals are highly dependent on the subjects and interoceptive sensitivity can provide some insights about these inter-individual differences. For instance, in the study by Ferri, Ardizzi, Ambrosecchia, & Gallese, 2013 (Ferri et al., 2013), only people with high interoceptive sensitivity showed higher autonomic response in a social situation (observation of the experimenter's hand performing a caress-like movements at different distances from their own hand, as compared to a similarly moving metal stick), particularly when the experimenter's hand was moving at shorter distances. Higher interoceptive accuracy, measured with the heartbeat perception task, has also been related to sharper PPS boundary, as computed by the central point of sigmoid curve in audio-tactile multisensory task, in subjects with high self-consciousness (Ardizzi & Ferri, 2018). In addition, participants who were able to improve their interoceptive accuracy show more pronounced changes in sigmoid curve slope in the visual-tactile task and changes in their subjective experience of the self in space assessed by means of questionnaires (Noel, Park, et al., 2018). *Interoceptive* awareness, based on the perception of inner state of the body may thus be related to PPS representation (Ardizzi & Ferri, 2018; Cartaud et al., 2018; Noel, Park, et al., 2018; Noel, Pfeiffer, et al., 2015; Rabellino, Frewen, McKinnon, & Lanius, 2020; Rossetti et al., 2015; Scandola et al., 2020).

Interestingly, it has recently been suggested that the multisensory mechanism of PPS representation contributes to a representation of the self as distinct from the environment and the others and contributes to Bodily Self-Consciousness (Blanke, Slater, & Serino, 2015; Noel, Bertoni, et al., 2020; Noel, Failla, et al., 2020; Noel, Lytle, Cascio, & Wallace, 2018; Scandola et al., 2020; Serino, 2019). As quoted from Serino (Serino, 2019), page 150): the notion of "Bodily Self-

Consciousness reflects the experience of the self as a subject of the experience grounded into a body that is felt as one's own (self-identification), which occupies a specific location in space (self-location) and which faces the world from a specific perspective (first-person perspective)." It is tempting to suggest that the first two 'selves', namely self-identification and self-location, may reflect sensorimotor and spatial aspects of the relationship between the body (my body) and the external world (Jeannerod, 2006). As such, illusory or real changes in body dimensions, or body position in space may change PPS representation (Berger et al., 2019; Cardini, Fatemi-Ghomi, Gajewska-Knapik, Gooch, & Aspell, 2019; D'Angelo et al., 2017; Noel, Grivaz, et al., 2015; Pfeiffer, Noel, Serino, & Blanke, 2018). The full-body illusion, induced with virtual reality, indeed shifted the self-PPS boundary towards VR avatars (Ehrsson, 2007; Lenggenhager, Tadi, Metzinger, & Blanke, 2007; Noel, Pfeiffer, et al., 2015).

Thus, these relationships seem to be mainly determined by the constraints between the environment and the body. Instead, interoceptive signals beyond proprioceptive and vestibular inputs might have a more prominent influence on one's first-person perspective. By this, we do not imply that these are three different entities; we rather suggest that multiple influences from outside and inside the body are complementarily contributing to PPS representation of oneself and that such influences may dynamically shape our interactions with the environment. For instance, hand amputees display a sort of neglect for the space closely surrounding their missing limb (Makin et al., 2010). Even the mere temporary immobilization of one upper limb has proven to shrink PPS around that limb (Bassolino et al., 2015). In spinal cord injured patients, PPS is selectively reduced around the body parts below the lesion level, while it remained preserved around the body parts above the lesion level (Scandola et al., 2016, 2020). Passive movement induced by the experimenter partly restored PPS representation. Note that recovery induced by another person, thus with social components, need to be more deeply investigated as promising direction for future research. In addition, an evaluation of interoceptive awareness through questionnaires suggested that in subjects with incomplete lesion, greater interoceptive sensibility was associated with a better representation of PPS. When explicitly asked, the participants were able to accurately identify the presence of movement (even though it was not visible), again pointing toward a link between interoception and PPS representation. In autistic patients, altered bodily self-consciousness and disrupted integration of exteroceptive and interoceptive signaling are observed in addition to abnormalities in PPS representation, and both processes seem to be related to deficits in multisensory integration (Mul et al., 2019). These deficits might account for some of the social interactions difficulties encountered in these patients (Rabellino et al., 2020).

The handful of studies that measured physiological signals when stimuli enters PPS, support the idea that these stimuli—and more so those socially connoted—not only change overt behavioral responses, but also body responses. For instance, a recent study revealed that facial emotions displayed in the PPS enhance the observers' heart rate and facilitate their perceptual discrimination compared to facial emotions displayed outside the PPS (Dureux et al., 2021). As such, PPS coding might result from interactions at a more complex level than previously thought, including not only external, but also internal signals. Keeping in mind that bodily signals may impact social cognition through interoception (Gao, Ping, & Chen, 2019) and that PPS representations contribute to bodily self-consciousness (Serino, 2019), the role of PPS representation in social interactions may be more important than previously thought. It is for instance possible that the intrinsic sense of discomfort which delineates personal space and strongly depends on the personality of the intruder may depend on interactions between PPS and interoception. Recent evidence in support to this possibility comes from a study showing enhanced skin conductance response in participants when a confederate approached compared to when he moved farther away in the stop distance paradigm (Candini, Battaglia, Benassi, di Pellegrino, & Frassinetti, 2021). However future investigations are needed to explore that question by measuring interoceptive signals in protocols probing PPS and PS.

Indeed, very few studies have so far included interoceptive measures when assessing changes of PPS representation depending on the context. These signals might help better understanding the direction of the effects measured, their dependency from context, and more so when involving social factors (Cartaud et al., 2018). As a direct measure of sympathetic or parasympathetic nervous system activation following psychological or physiological arousal (Baig & Kavakli, 2019; Taylor & Epstein, 1967), they could inform us about the inner state of the subjects facing diverse contexts. They might track the impact of the proximity of others, whether the emphasis is put on the participant's inner state (to avoid discomfort or anxiety, as it is typically measured with the stop-distance paradigm) or whether instead the emphasis is on perception of surrounding stimuli, or the reachable space.

In other words, protecting our body, as well as interacting with stimuli in the environment, starts from and within the body. Needs, goals and concurrent bodily states may thus contribute to define bodily self and self-PPS, which likely govern the complex interplay between social and visuomotor processes within our social world. Multisensory processing may be one of the underlying mechanisms for this interplay between internal and external signals. A few available evidences indeed suggest a link between bodily signals and PPS representation. In addition, accumulating evidence suggest that personality traits (anxiety, claustrophobia) also contribute defining one's own PPS representation and personality traits are highly related to our inner state and responses to stressful situations (Iachini, Ruggiero, et al., 2015; Lourenco, Longo, & Pathman, 2011; Sambo & Iannetti, 2013) see also (Lebert, Chaby, Garnot, & Vergilino-Perez, 2020). Adding measures of internal physiological states in the future might help gathering a deeper understanding of PPS, its relationships with PS and possibly reconciling the discrepancies between different studies/methodologies. We thus suggest that by merging exteroceptive information from the environment and internal signals that come from the body, PPS may promote an integrated representation of the self, as distinct

from the environment and the others to provide us with a better understanding of the processes at play during social interactions.

5. PPS representation and brain–body interactions

In humans, neuroimaging studies revealed that PPS network includes frontoparietal regions and the putamen (Brozzoli et al, 2011, 2012, 2014; Bremmer et al., 2001; Cléry et al., 2015; Gentile et al., 2011; Grivaz et al., 2017; Sereno & Huang, 2006) and is thought to represent a putative homologue of the premotor-parietal PPS network described in monkeys. More recently, neuroimaging studies have provided some insights on how PPS network may be modulated by social factors. Holt et al. (2014) revealed a selective brain activation in response to approaching vs. receding faces (compared to spheres) in PPS network, namely the dorsal intraparietal sulcus and ventral premotor cortex (Holt et al., 2014). A greater coupling between those PPS regions was correlated with a higher self-estimated social activity and shorter comfort distance between the participant and the experimenter, measured outside the scanner.

How could approaching social stimuli specifically shape PPS network activation? A constant reciprocal adjustment of brain-body interactions is essential to adapt behavioral responses during such interaction. One possible pathway through which PPS coding could be modulated is via the adrenal medulla that has direct links with the motor cortex (Dum, Levinthal, & Strick, 2016). In addition, ascending interoceptive signals are relayed to several brainstem nuclei, including the nucleus of the solitary tract (NTS), parabrachial nucleus (PB), and periaqueductal gray matter (PAG), that in turns regulate neuromodulatory inputs to subcortical and cortical brain regions (Azzalini, Rebollo, & Tallon-Baudry, 2019; Critchley & Harrison, 2013). For instance, an approaching threat induces an increased activation of the PAG, likely preparing the body to protect itself and possibly escape from a potential danger (Mobbs et al., 2007). Ascending interoceptive signals are also sent to subcortical regions involved in autonomic regulation, such as the hypothalamus, amygdala, striatum, and cerebellum (Azzalini et al., 2019; Critchley & Harrison, 2013). These signals are thus in a position to modulate directly or indirectly the activity of PPS network. For instance, the default mode and salience networks support interoception and allostasis and continuously interact with other networks underlying different cognitive functions (Khalsa et al., 2018; Kleckner et al., 2017).

Approaching faces also induced activation of the insula (Schienle, Wabnegger, Leitner, & Leutgeb, 2017). The insula can be considered as a hub integrating exteroceptive sensory inputs and interoceptive signals (Uddin, Nomi, Hébert-Seropian, Ghaziri, & Boucher, 2017), and linking external and internal experiences. This structure regulates functions of the autonomic system and participates in forming bodily self-awareness, sense of agency and body ownership (Seghezzi, Giannini, & Zapparoli, 2019; Uddin et al., 2017). In a study leveraging intracranial EEG recordings, multisensory neurons sensitive to both audio and tactile stimuli were found in the insular region (Bernasconi et al., 2018). The activity of these neurons was modulated by the distance of the stimulus from the body; their activation was observed during very early stages (~50 ms); while later (~200 ms) distance-related responses were recorded in precentral and postcentral gyri (Bernasconi et al., 2018). Moreover, activation of the insula was uncovered using functional magnetic resonance imaging during observation of a moving object close to the hand (Schaefer, Heinze, & Rotte, 2012) and electric stimulation of insular regions induced both social approach or withdrawal reactions (Caruana, Jezzini, Sbriscia-Fioretti, Rizzolatti, & Gallese, 2011). Importantly, the insula is functionally and anatomically connected with the amygdala (Mufson, Mesulam, & Pandya, 1981; Uddin et al., 2017), a region playing a critical role in regulating distances during social interactions (Kennedy et al., 2009; Schienle, Wabnegger, Schöngassner, & Leutgeb, 2015; Vieira, Tavares, Marsh, & Mitchell, 2017). Patients with bilateral amygdala lesions show a marked reduction of interpersonal distance (Kennedy et al., 2009). These patients also exhibited deficits in retrieving socially relevant knowledge from unfamiliar faces and tended to judge unfamiliar faces as more approachable and more trustworthy than did control subjects (Adolphs, Tranel, & Damasio, 1998). Theta burst stimulation of regions of the PPS network, the inferior parietal lobule and the ventral premotor cortex affected amygdala responses to neutral *vs* negative emotional stimuli (Engelen, Zhan, Sack, & de Gelder, 2018). Such interactions might lead for example to the expansion of PPS representation with social negative sounds (Ferri, Tajadura-Jiménez, Väljamäe, Vastano, & Costantini, 2015). Not surprisingly, the amygdala activity is enhanced with looming stimuli invading near space (Coker-Appiah et al., 2013). Similarly, atypical amygdala activity (Lough et al., 2015) in autistic subjects has also been related to abnormal decrease of interpersonal distance (Kennedy & Adolphs, 2014; Massaccesi et al., 2021). A recent study found increased functional connectivity from the amygdala to the dorsal intraparietal sulcus and the fusiform gyrus (FFA), a region selective for face perception and recognition, in autistic patients compared to controls (Massaccesi et al., 2021). In this pathology, atypical interoception and bodily self-consciousness have also been documented (Mul et al., 2019; Quadt, Critchley, & Garfinkel, 2018); and may lead to altered PPS and/or PS representation (Mul et al., 2019; Noel, Cascio, Wallace, & Park, 2017) but see (Candini et al., 2019). In schizophrenic patients, Holt et al. (2015) found an increase of the dorsal intraparietal sulcus activity in response to approaching faces that was correlated with larger interpersonal distance. Interestingly, they also reported a reduction of the functional coupling between the dorsal intraparietal sulcus and FFA in these patients. This suggests that an abnormal dialogue between the regions processing face recognition and the region processing PPS representation might lead to difficulties in the interaction with elements, including peers, in the close surrounding space (Di Cosmo et al., 2017).

In sum, PPS network might integrate external and internal information to promote our interactions with the surrounding space within spatial and temporal frames (Belardinelli et al., 2018; Cléry et al., 2020; Serino, 2019). From that perspective, PPS may serve to estimate the probability of interaction with

the surrounding three-dimensional environment (Kandula, Hofman, & Dijkerman, 2015), guide our behavior depending on the context (Dijkerman & Farnè, 2015), and adjust behavior even during movement (Senna, Cardinali, Farnè, & Brozzoli, 2019), which is extremely important in social relations. In terms of PPS representation, the integration of multisensory information coming from the outside with bodily signals, including vestibular signals might not only contribute to self-consciousness (Noel, Park, et al., 2018), but also to distinguish self from others, as indicated by studies with bodily illusions and studies with pathological embodiment in neurological patients (Fossataro, Gindri, Mezzanato, Pia, & Garbarini, 2016; Makin, Holmes, & Ehrsson, 2008; Noel, Pfeiffer, et al., 2015).

6. PPS and social interactions

Beyond it sensitivity to the intrusion of objects and agents into one own's space, PPS representation is also sensitive to the intrusion of objects into the near space of others; this vicarious response was found in both human and animal studies (Brozzoli, Ehrsson, & Farnè, 2014; Brozzoli, Gentile, Bergouignan, & Ehrsson, 2013; Fossataro, Sambo, et al., 2016; Iachini & Ruggiero, 2021; Ishida, Nakajima, Inase, & Murata, 2010; Patané et al., 2020; Schaefer et al., 2012). When surrounded by others, the estimation of distance can be affected not only by the physical depth, but also by the relationships or the interactions we share with these individuals. These factors also influence our inner states. The fact that the degree of such vicarious PPS responses (Fossataro, Sambo, et al., 2016) was related to the perceived proximity between individuals beyond the physical distance, might suggest that PPS contributes to intention reading and action understanding (Kilner, Vargas, Duval, Blakemore, & Sirigu, 2004), essential for appropriate social interactions (Hunnius & Bekkering, 2014; Woodward, Sommerville, Gerson, Henderson, & Buresh, 2009). Iachini and Ruggiero (2021) found that sharing a partner's perspective influences the estimation of an object location within one own's PPS (Iachini & Ruggiero, 2021). Furthermore, manipulating the ownership status of an object ("whose object this is") also revealed a modulation of PPS in relation to this notion of ownership (Patané et al., 2020). Thus, PPS could have been exapted to map, and to maybe "understand" the ownership status of others' actions. It is possible that by integrating both external and internal signals to promote an integrated representation of the self, as distinct from the environment and the others, PPS might be equipped to face these challenging computational situations we encounter in our social world.

The phenomenon of shared PPS representation in the presence of others (Costantini, Ambrosini, Scorolli, & Borghi, 2011; Pellencin et al., 2017; Saccone, Szpak, Churches, & Nicholls, 2018) also opens questions on how PPS may be related to the development and regulation of various kinds of social relationships, including interaction, self-others coordination, and cooperation (Fanghella et al., 2021). The need to interact and cooperate with others modifies low-level perceptive mechanisms in PPS task (Hobeika et al., 2019), participating in what one could call 'supraindividual' representation of space. Emotional faces in the near space modulate our perceptual abilities and bodily signals (Dureux et al., 2021; Ellena et al., 2020). It is thus possible that self-PPS activation may contribute to shared, or joint attention during performance of the same task (cooperative action) (Mundy, 2018) which strongly depends on synchronization between partners (Fabbri, Frisoni, Martoni, Tonetti, & Natale, 2017). It is also possible that shared PPS may play a role in learning processes, as modelled in (Juett & Kuipers, 2019). Being close to cooperative vs non-cooperative partners modulates responses in multisensory tasks, enlarging or merging PPS boundary between the cooperative individuals or shrinking of PPS in non-cooperative case (Dell'Anna et al., 2020; Teneggi et al., 2013).

Greater self-other overlap is related to increased sensorimotor responses to others' sensations (Riečanský, Lengersdorff, Pfabigan, & Lamm, 2020) and enlarges self-PPS towards the partner (Pellencin et al., 2017). In that sense, self-PPS activation may contribute to the prediction and understanding of others' feelings. Notably, individuals' empathic responses are modulated by the physical distance with others (Lomoriello, Meconi, Rinaldi, & Sessa, 2018; Mahayana et al., 2014; Mencl & May, 2009). In addition, only individuals with high empathic traits develop significant vicarious defensive PPS response with approaching threats (Fossataro, Sambo, et al., 2016).

The level of self-other overlap and the intention to interact with a stranger affects the multisensory representations of the space between oneself and the other (Pellencin et al., 2017). The level of self-other overlap is defined by two related factors, 'feeling close' and 'behaving close' (Myers & Hodges, 2012). Therefore, perceived social proximity may be dependent on the 'closeness' between another (stranger) subject's behavior and one's own pre-existing implicit expectations. Via mechanism of shared representations, self-PPS may participate in perspective taking, impression and judgments about others, e.g., "if you behave, act and react as myself", you are more similar, closer to me, and "I understand you better". In this way, self PPS may contribute to gaining social, temporal and physical proximity with the others around us in addition to the regulation of social distances (Parkinson, Liu, & Wheatley, 2014; Ruggiero et al., 2019; Sorokowska et al., 2017). At this stage of our knowledge, it is difficult to precisely delineate the extent to which PPS might play a role in social cognition. Yet, in light of the growing studies interested in the influence of social factors on PPS, here we hope that future studies will provide insights on the exciting issue.

7. Concluding remarks

Since the discovery of the PPS, its definition and functional roles have been continuously expanding (Bufacchi & Iannetti, 2018; Hunley & Lourenco, 2018) and re-conceptualizing (Serino, 2019). To date, an increasing consensus exists on some basic functional roles of PPS: it may allow a subject to rapidly and flexibly interact with 3D environment, and to optimize behavioral responses towards both inanimate and animate objects around and avoid threatening and harmful elements. Yet, recent years have seen an ever-growing interest into higher level, contextual dependent modulations of these functions that seem to propel PPS roles well beyond its basic, though critical functions for survival (Ardizzi & Ferri, 2018; Rabellino et al., 2020; Salomon et al., 2017). While these expanding possibilities are in keeping with the idea that this spatial representation is susceptible to both bottom-up and top-down modulations (Coello, Quesque, Gigliotti, Ott, &

Bruyelle, 2018), the study of the social dimension of PPS may face novel challenges, notably because the role of PPS representation in the domain of social interactions may require the PPS processing to involve predictive abilities and sensory remapping to efficiently help understanding other people's actions and intentions.

We believe a critical aspect for future investigations of PPS social role is to account for its dependency on subjects' individual personalities and interoceptive states. So far, the impact of social factors produced somewhat contradictory outcomes. We argue that one possible reason for that relates to the use of 'classical' available methodologies, typically used so far to probe PPS basic sensorimotor functions. The recent development in PPS literature in relation to social elements has opened new avenues for investigators, combining physiological and psychological aspects of PPS space and its relation to other measurements of social interaction, such as interpersonal distance.

New dimensions of modern research relate PPS and self-body perception, putting the emphasis on the participation of interoceptive inputs into perception of proximal environmental stimuli. We advance that both novel and well-established methodologies should be coupled with physiological indexes, to fully embrace the view that interoceptive signals may contribute critical insights on how the PPS network works. Gathering brain and body activity while interacting with (or in the mere presence of) conspecifics, may help understanding how social PPS processing shapes our behavior.

CRediT author statement

Olena V. BOGDANOVA: Conceptualization; Writing - Original Draft.

Volodymyr B. BOGDANOV: Visualization; Writing - Review & Editing.

Audrey DUREUX: Writing - Review & Editing.

Alessandro FARNE: Writing - Review & Editing.

Fadila HADJ-BOUZIANE: Funding acquisition; Project administration; Supervision; Conceptualization; Writing - Review & Editing.

Acknowledgements

The work was funded by the French National Research Agency (ANR; ANR-15-CE37-0003, funding received by Dr Hadj-Bouziane), the IHU CeSaMe ANR-10-IBHU-0003 and ANR-16-CE28-0015 awarded to AF and has been performed within the framework of the LABEX CORTEX (ANR-11-LABX-0042).

REFERENCES

Adolphs, R., Tranel, D., & Damasio, A. R. (1998). The human amygdala in social judgment. *Nature, 393*(6684), 470–474. https://doi.org/10.1038/30982

Altman, I., & Chemers, M. M. (1984). *Culture and environment*. CUP Archive.

Ardizzi, M., & Ferri, F. (2018). Interoceptive influences on peripersonal space boundary. *Cognition, 177*, 79–86. https://doi.org/10.1016/j.cognition.2018.04.001

Aspell, J. E., Lavanchy, T., Lenggenhager, B., & Blanke, O. (2010). Seeing the body modulates audiotactile integration. *The European Journal of Neuroscience, 31*(10), 1868–1873. https://doi.org/10.1111/j.1460-9568.2010.07210.x

Avillac, M., Hamed, S. B., & Duhamel, J.-R. (2007). Multisensory integration in the ventral intraparietal area of the macaque monkey. *Journal of Neuroscience, 27*(8), 1922–1932. https://doi.org/10.1523/JNEUROSCI.2646-06.2007

Azzalini, D., Rebollo, I., & Tallon-Baudry, C. (2019). Visceral signals shape brain dynamics and cognition. *Trends in Cognitive Sciences*. https://doi.org/10.1016/j.tics.2019.03.007, 0(0).

Baig, M. Z., & Kavakli, M. (2019). A survey on psycho-physiological analysis & measurement methods in multimodal systems. *Multimodal Technologies and Interaction, 3*(2), 37. https://doi.org/10.3390/mti3020037

Baldwin, J. D., & Baldwin, J. I. (1974). The dynamics of interpersonal spacing in monkeys and man. *The American Journal of Orthopsychiatry, 44*(5), 790–806. https://doi.org/10.1111/j.1939-0025.1974.tb01157.x

Bassolino, M., Finisguerra, A., Canzoneri, E., Serino, A., & Pozzo, T. (2015). Dissociating effect of upper limb non-use and overuse on space and body representations. *Neuropsychologia, 70*, 385–392. https://doi.org/10.1016/j.neuropsychologia.2014.11.028

Belardinelli, A., Lohmann, J., Farnè, A., & Butz, M. V. (2018). Mental space maps into the future. *Cognition, 176*, 65–73. https://doi.org/10.1016/j.cognition.2018.03.007

Berger, M., Neumann, P., & Gail, A. (2019). Peri-hand space expands beyond reach in the context of walk-and-reach movements. *Scientific Reports, 9*(1), 3013. https://doi.org/10.1038/s41598-019-39520-8

Bernasconi, F., Noel, J.-P., Park, H. D., Faivre, N., Seeck, M., Spinelli, L., et al. (2018). Audio-tactile and peripersonal space processing around the trunk in human parietal and temporal cortex: An intracranial EEG study. *Cerebral Cortex (New York, NY), 28*(9), 3385–3397. https://doi.org/10.1093/cercor/bhy156

Berti, A., & Frassinetti, F. (2000). When far becomes near: Remapping of space by tool use. *Journal of Cognitive Neuroscience, 12*(3), 415–420.

Biggio, M., Bisio, A., Avanzino, L., Ruggeri, P., & Bove, M. (2017). This racket is not mine: The influence of the tool-use on peripersonal space. *Neuropsychologia, 103*, 54–58. https://doi.org/10.1016/j.neuropsychologia.2017.07.018

Biggio, M., Bisio, A., Ruggeri, P., & Bove, M. (2019). Defensive peripersonal space is modified by a learnt protective posture. *Scientific Reports, 9*(1), 6739. https://doi.org/10.1038/s41598-019-43258-8

Bisio, A., Garbarini, F., Biggio, M., Fossataro, C., Ruggeri, P., & Bove, M. (2017). Dynamic shaping of the defensive peripersonal space through predictive motor mechanisms: When the "near" becomes "far." *The Journal of Neuroscience: the Official Journal of the Society for Neuroscience, 37*(9), 2415–2424. https://doi.org/10.1523/JNEUROSCI.0371-16.2016

Blanke, O., Slater, M., & Serino, A. (2015). Behavioral, neural, and computational principles of bodily self-consciousness. *Neuron, 88*(1), 145–166. https://doi.org/10.1016/j.neuron.2015.09.029

Blini, E., Desoche, C., Salemme, R., Kabil, A., Hadj-Bouziane, F., & Farnè, A. (2018). Mind the depth: Visual perception of shapes is better in peripersonal space. *Psychological Science, 29*(11), 1868–1877. https://doi.org/10.1177/0956797618795679

Bond, C. F., & Titus, L. J. (1983). Social facilitation: A meta-analysis of 241 studies. *Psychological Bulletin, 94*(2), 265–292.

Bourgeois, J., Farnè, A., & Coello, Y. (2014). Costs and benefits of tool-use on the perception of reachable space. *Acta Psychologica, 148*, 91–95. https://doi.org/10.1016/j.actpsy.2014.01.008

Brain, W. R. (1941). Visual disorientation with special reference to lesions OF the right cerebral hemisphere. *Brain: a Journal of Neurology, 64*(4), 244–272. https://doi.org/10.1093/brain/64.4.244

Bremmer, F., Schlack, A., Shah, N. J., Zafiris, O., Kubischik, M., Hoffmann, K., et al. (2001). Polymodal motion processing in posterior parietal and premotor cortex: A human fMRI study strongly implies equivalencies between humans and monkeys. *Neuron, 29*(1), 287–296. https://doi.org/10.1016/s0896-6273(01)00198-2

Bremner, A. J., Holmes, N. P., & Spence, C. (2008). Infants lost in (peripersonal) space? *Trends in Cognitive Sciences, 12*(8), 298–305. https://doi.org/10.1016/j.tics.2008.05.003

Brozzoli, C., Cardinali, L., Pavani, F., & Farnè, A. (2010). Action-specific remapping of peripersonal space. *Neuropsychologia, 48*(3), 796–802. https://doi.org/10.1016/j.neuropsychologia.2009.10.009

Brozzoli, C., Demattè, M. L., Pavani, F., Frassinetti, F., & Farnè, A. (2006). Neglect and extinction: Within and between sensory modalities. *Restorative Neurology and Neuroscience, 24*(4–6), 217–232.

Brozzoli, C., Ehrsson, H. H., & Farnè, A. (2014). Multisensory representation of the space near the hand: From perception to action and interindividual interactions. *The Neuroscientist: a Review Journal Bringing Neurobiology, Neurology and Psychiatry, 20*(2), 122–135. https://doi.org/10.1177/1073858413511153

Brozzoli, C., Gentile, G., Bergouignan, L., & Ehrsson, H. H. (2013). A shared representation of the space near oneself and others in the human premotor cortex. *Current Biology: CB, 23*(18), 1764–1768. https://doi.org/10.1016/j.cub.2013.07.004

Brozzoli, C., Gentile, G., Petkova, V. I., & Ehrsson, H. H. (2011). FMRI adaptation reveals a cortical mechanism for the coding of space near the hand. *The Journal of Neuroscience: the Official Journal of the Society for Neuroscience, 31*(24), 9023–9031. https://doi.org/10.1523/JNEUROSCI.1172-11.2011

Brozzoli, C., Makin, T. R., Cardinali, L., Holmes, N. P., & Farnè, A. (2012). Peripersonal space: A multisensory interface for body–object interactions. In M. M. Murray, & M. T. Wallace (Eds.), *The neural bases of multisensory processes*. CRC Press/Taylor & Francis. http://www.ncbi.nlm.nih.gov/books/NBK92879/.

Brozzoli, C., Pavani, F., Urquizar, C., Cardinali, L., & Farnè, A. (2009). Grasping actions remap peripersonal space. *Neuroreport, 20*(10), 913–917. https://doi.org/10.1097/WNR.0b013e32832c0b9b

Bufacchi, R. J. (2017). Approaching threatening stimuli cause an expansion of defensive peripersonal space. *Journal of Neurophysiology, 118*(4), 1927–1930. https://doi.org/10.1152/jn.00316.2017

Bufacchi, & Iannetti, G. D. (2018). An action field theory of peripersonal space. *Trends in Cognitive Sciences*. https://doi.org/10.1016/j.tics.2018.09.004

Burr, D., & Gori, M. (2012). Multisensory integration develops late in humans. In M. M. Murray, & M. T. Wallace (Eds.), *The neural bases of multisensory processes*. CRC Press/Taylor & Francis. http://www.ncbi.nlm.nih.gov/books/NBK92864/.

Caggiano, V., Fogassi, L., Rizzolatti, G., Thier, P., & Casile, A. (2009). Mirror neurons differentially encode the peripersonal and extrapersonal space of monkeys. *Science (New York, N.Y.), 324*(5925), 403–406. https://doi.org/10.1126/science.1166818

Candini, M., Battaglia, S., Benassi, M., di Pellegrino, G., & Frassinetti, F. (2021). The physiological correlates of interpersonal space. *Scientific Reports, 11*(1), 2611. https://doi.org/10.1038/s41598-021-82223-2

Candini, M., Giuberti, V., Santelli, E., di Pellegrino, G., & Frassinetti, F. (2019). When social and action spaces diverge: A study in children with typical development and autism. *Autism: the International Journal of Research and Practice*. https://doi.org/10.1177/1362361318822504, 1362361318822504.

Canzoneri, E., Magosso, E., & Serino, A. (2012). Dynamic sounds capture the boundaries of peripersonal space representation in humans. *Plos One, 7*(9), Article e44306. https://doi.org/10.1371/journal.pone.0044306

Canzoneri, E., Ubaldi, S., Rastelli, V., Finisguerra, A., Bassolino, M., & Serino, A. (2013). Tool-use reshapes the boundaries of body and peripersonal space representations. *Experimental Brain Research, 228*(1), 25–42. https://doi.org/10.1007/s00221-013-3532-2

Caplan, M. E., & Goldman, M. (1981). Personal space violations as a function of height. *The Journal of Social Psychology, 114*(2), 167–171. https://doi.org/10.1080/00224545.1981.9922746

Cardinali, L., Brozzoli, C., & Farnè, A. (2009). Peripersonal space and body schema: Two labels for the same concept? *Brain Topography, 21*(3–4), 252–260. https://doi.org/10.1007/s10548-009-0092-7

Cardini, F., Fatemi-Ghomi, N., Gajewska-Knapik, K., Gooch, V., & Aspell, J. E. (2019). Enlarged representation of peripersonal space in pregnancy. *Scientific Reports, 9*(1), 8606. https://doi.org/10.1038/s41598-019-45224-w

Cartaud, A., Ott, L., Iachini, T., Honoré, J., & Coello, Y. (2020). The influence of facial expression at perceptual threshold on electrodermal activity and social comfort distance. *Psychophysiology*. , Article e13600. https://doi.org/10.1111/psyp.13600

Cartaud, A., Ruggiero, G., Ott, L., Iachini, T., & Coello, Y. (2018). Physiological response to facial expressions in peripersonal space determines interpersonal distance in a social interaction context. *Frontiers in Psychology, 9*. https://doi.org/10.3389/fpsyg.2018.00657

Caruana, F., Jezzini, A., Sbriscia-Fioretti, B., Rizzolatti, G., & Gallese, V. (2011). Emotional and social behaviors elicited by electrical stimulation of the insula in the macaque monkey. *Current Biology, 21*(3), 195–199. https://doi.org/10.1016/j.cub.2010.12.042

Cléry, J., Guipponi, O., Odouard, S., Wardak, C., & Ben Hamed, S. (2018). Cortical networks for encoding near and far space in the non-human primate. *Neuroimage, 176*, 164–178. https://doi.org/10.1016/j.neuroimage.2018.04.036

Cléry, J., Guipponi, O., Wardak, C., & Ben Hamed, S. (2015). Neuronal bases of peripersonal and extrapersonal spaces, their plasticity and their dynamics: Knowns and unknowns. *Neuropsychologia, 70*, 313–326. https://doi.org/10.1016/j.neuropsychologia.2014.10.022

Cléry, J. C., Schaeffer, D. J., Hori, Y., Gilbert, K. M., Hayrynen, L. K., Gati, J. S., et al. (2020). Looming and receding visual networks in awake marmosets investigated with fMRI. *Neuroimage*. https://doi.org/10.1016/j.neuroimage.2020.116815, 116815.

Coello, Y., Bartolo, A., Amiri, B., Devanne, H., Houdayer, E., & Derambure, P. (2008). Perceiving what is reachable depends on motor representations: Evidence from a transcranial magnetic stimulation study. *Plos One, 3*(8), Article e2862. https://doi.org/10.1371/journal.pone.0002862

Coello, Y., Quesque, F., Gigliotti, M.-F., Ott, L., & Bruyelle, J.-L. (2018). Idiosyncratic representation of peripersonal space depends on the success of one's own motor actions, but also the successful actions of others! *Plos One, 13*(5). https://doi.org/10.1371/journal.pone.0196874

Coker-Appiah, D., White, S., Clanton, R., Yang, J., Martin, A., & Blair, R. (2013). Looming animate and inanimate threats: The response of the amygdala and periaqueductal gray. *Social Neuroscience, 8*(6), 621–630. https://doi.org/10.1080/17470919.2013.839480

Colby, C. L., & Duhamel, J. R. (1996). Spatial representations for action in parietal cortex. *Brain Research. Cognitive Brain Research, 5*(1–2), 105–115. https://doi.org/10.1016/s0926-6410(96)00046-8

Colby, C. L., Duhamel, J. R., & Goldberg, M. E. (1993). Ventral intraparietal area of the macaque: Anatomic location and visual response properties. *Journal of Neurophysiology, 69*(3), 902–914. https://doi.org/10.1152/jn.1993.69.3.902

Costantini, M., Ambrosini, E., Scorolli, C., & Borghi, A. M. (2011). When objects are close to me: Affordances in the peripersonal space. *Psychonomic Bulletin & Review, 18*(2), 302–308. https://doi.org/10.3758/s13423-011-0054-4

Costantini, M., Ambrosini, E., Tieri, G., Sinigaglia, C., & Committeri, G. (2010). Where does an object trigger an action? An investigation about affordances in space. *Experimental Brain Research, 207*(1–2), 95–103. https://doi.org/10.1007/s00221-010-2435-8

Critchley, H. D., & Harrison, N. A. (2013). Visceral influences on brain and behavior. *Neuron, 77*(4), 624–638. https://doi.org/10.1016/j.neuron.2013.02.008

D'Angelo, M., di Pellegrino, G., & Frassinetti, F. (2019). The illusion of having a tall or short body differently modulates interpersonal and peripersonal space. *Behavioural Brain Research, 375*, 112146. https://doi.org/10.1016/j.bbr.2019.112146

D'Angelo, M., Pellegrino, G. Di, & Frassinetti, F. (2017). Invisible body illusion modulates interpersonal space. *Scientific Reports, 7*(1), 1302. https://doi.org/10.1038/s41598-017-01441-9

De Paepe, A. L., Crombez, G., & Legrain, V. (2016). What's coming near? The influence of dynamical visual stimuli on nociceptive processing. *Plos One, 11*(5), Article e0155864. https://doi.org/10.1371/journal.pone.0155864

De Paepe, A. L., Crombez, G., Spence, C., & Legrain, V. (2014). Mapping nociceptive stimuli in a peripersonal frame of reference: Evidence from a temporal order judgment task. *Neuropsychologia, 56*, 219–228. https://doi.org/10.1016/j.neuropsychologia.2014.01.016. ISSN 0028-3932.

de Vignemont, F., & Iannetti, G. D. (2015). How many peripersonal spaces? *Neuropsychologia, 70*, 327–334. https://doi.org/10.1016/j.neuropsychologia.2014.11.018

Dell'Anna, A., Rosso, M., Bruno, V., Garbarini, F., Leman, M., & Berti, A. (2020). Does musical interaction in a jazz duet modulate peripersonal space? *Psychological Research*. https://doi.org/10.1007/s00426-020-01365-6

Di Cosmo, G., Costantini, M., Salone, A., Martinotti, G., Di Iorio, G., Di Giannantonio, M., et al. (2017). Peripersonal space boundary in schizotypy and schizophrenia. *Schizophrenia Research*. https://doi.org/10.1016/j.schres.2017.12.003

di Pellegrino, G., & Làdavas, E. (2015). Peripersonal space in the brain. *Neuropsychologia, 66*, 126–133. https://doi.org/10.1016/j.neuropsychologia.2014.11.011

Dijkerman, H. C., & Farnè, A. (2015). Sensorimotor and social aspects of peripersonal space. *Neuropsychologia, 70*, 309–312. https://doi.org/10.1016/j.neuropsychologia.2015.03.005

Drew, A. R., Meltzoff, A. N., & Marshall, P. J. (2018). Interpersonal influences on body representations in the infant brain. *Frontiers in Psychology, 9*. https://doi.org/10.3389/fpsyg.2018.02601

Duhamel, J. R., Colby, C. L., & Goldberg, M. E. (1998). Ventral intraparietal area of the macaque: Congruent visual and somatic response properties. *Journal of Neurophysiology, 79*(1), 126–136. https://doi.org/10.1152/jn.1998.79.1.126

Duke, M. P., & Kiebach, C. (1974). A brief note on the validity of the comfortable interpersonal distance scale. *The Journal of Social Psychology, 94*(2), 297–298. https://doi.org/10.1080/00224545.1974.9923221

Dum, R. P., Levinthal, D. J., & Strick, P. L. (2016). Motor, cognitive, and affective areas of the cerebral cortex influence the adrenal medulla. *Proceedings of the National Academy of Sciences, 113*(35), 9922–9927. https://doi.org/10.1073/pnas.1605044113

Dureux, A., Blini, E., Grandi, L. C., Bogdanova, O., Desoche, C., Farnè, A., et al. (2021). Close facial emotions enhance physiological responses and facilitate perceptual discrimination. *Cortex; a Journal Devoted To the Study of the Nervous System and Behavior*. https://doi.org/10.1016/j.cortex.2021.01.014

Ehrsson, H. H. (2007). The experimental induction of out-of-body experiences. *Science (New York, N.Y.), 317*(5841), 1048. https://doi.org/10.1126/science.1142175

Ellena, G., Starita, F., Haggard, P., & Làdavas, E. (2020). The spatial logic of fear. *Cognition, 203*, 104336. https://doi.org/10.1016/j.cognition.2020.104336

Engelen, T., Zhan, M., Sack, A. T., & de Gelder, B. (2018). Dynamic interactions between emotion perception and action preparation for reacting to social threat: A combined cTBS-fMRI study. *ENeuro, 5*(3). https://doi.org/10.1523/ENEURO.0408-17.2018. Article 3.

Fabbri, M., Frisoni, M., Martoni, M., Tonetti, L., & Natale, V. (2017). Synchrony effect on joint attention. *Experimental Brain Research, 235*(8), 2449–2462. https://doi.org/10.1007/s00221-017-4984-6

Fanghella, M., Era, V., & Candidi, M. (2021). Interpersonal motor interactions shape multisensory representations of the peripersonal space. *Brain Sciences, 11*(2), 255. https://doi.org/10.3390/brainsci11020255

Farnè, A., Iriki, A., & Làdavas, E. (2005). Shaping multisensory action-space with tools: Evidence from patients with cross-modal extinction. *Neuropsychologia, 43*(2), 238–248. https://doi.org/10.1016/j.neuropsychologia.2004.11.010

Farnè, A., Pavani, F., Meneghello, F., & Làdavas, E. (2000). Left tactile extinction following visual stimulation of a rubber hand. *Brain: a Journal of Neurology, 123*(Pt 11), 2350–2360.

Ferri, F., Ardizzi, M., Ambrosecchia, M., & Gallese, V. (2013). Closing the gap between the inside and the outside: Interoceptive sensitivity and social distances. *Plos One, 8*(10). https://doi.org/10.1371/journal.pone.0075758. Article 10.

Ferri, F., Tajadura-Jiménez, A., Väljamäe, A., Vastano, R., & Costantini, M. (2015). Emotion-inducing approaching sounds shape the boundaries of multisensory peripersonal space. *Neuropsychologia, 70*, 468–475. https://doi.org/10.1016/j.neuropsychologia.2015.03.001

Filimon, F. (2010). Human cortical control of hand movements: Parietofrontal networks for reaching, grasping, and pointing. *The Neuroscientist: a Review Journal Bringing Neurobiology, Neurology and Psychiatry, 16*(4), 388–407. https://doi.org/10.1177/1073858410375468

Fossataro, C., Gindri, P., Mezzanato, T., Pia, L., & Garbarini, F. (2016). Bodily ownership modulation in defensive responses: Physiological evidence in brain-damaged patients with pathological embodiment of other's body parts. *Scientific Reports, 6*. https://doi.org/10.1038/srep27737

Fossataro, C., Sambo, C. F., Garbarini, F., & Iannetti, G. D. (2016). Interpersonal interactions and empathy modulate perception of threat and defensive responses. *Scientific Reports, 6*, 19353. https://doi.org/10.1038/srep19353

Gao, Q., Ping, X., & Chen, W. (2019). Body influences on social cognition through interoception. *Frontiers in Psychology, 10*, 2066. https://doi.org/10.3389/fpsyg.2019.02066

Gentile, G., Petkova, V. I., & Ehrsson, H. H. (2011). Integration of visual and tactile signals from the hand in the human brain: An fMRI study. *Journal of Neurophysiology, 105*(2), 910–922. https://doi.org/10.1152/jn.00840.2010

Gifford, R. (1982). Projected interpersonal distance and orientation choices: Personality, sex, and social situation. *School Psychology Quarterly: the Official Journal of the Division of School Psychology, American Psychological Association, 45*(3), 145–152. https://doi.org/10.2307/3033647

Graziano & Cooke. (2006). Parieto-frontal interactions, personal space, and defensive behavior. *Neuropsychologia*, 845–859.

Graziano, M. S., & Gross, C. G. (1993). A bimodal map of space: Somatosensory receptive fields in the macaque putamen with

corresponding visual receptive fields. *Experimental Brain Research, 97*(1), 96–109. https://doi.org/10.1007/bf00228820

Graziano, M. S., Hu, X. T., & Gross, C. G. (1997). Visuospatial properties of ventral premotor cortex. *Journal of Neurophysiology, 77*(5), 2268–2292. https://doi.org/10.1152/jn.1997.77.5.2268

Graziano, M. S., Yap, G. S., & Gross, C. G. (1994). Coding of visual space by premotor neurons. *Science (New York, N.Y.), 266*(5187), 1054–1057. https://doi.org/10.1126/science.7973661

Grivaz, P., Blanke, O., & Serino, A. (2017). Common and distinct brain regions processing multisensory bodily signals for peripersonal space and body ownership. *Neuroimage, 147*, 602–618. https://doi.org/10.1016/j.neuroimage.2016.12.052

Hall. (1966). *The hidden dimension garden city*. N.Y.: Doubleday, 1966 (Doubleday).

Hall, E. (2014). *Proxemics (understanding personal space)*. https://laofutze.wordpress.com/2014/01/03/e-t-hall-proxemics-understanding-personal-space/.

Hayduk, L. A. (1983). Personal space: Where we now stand. *Psychological Bulletin, 94*(2), 293–335. https://doi.org/10.1037/0033-2909.94.2.293

Heed, T., Habets, B., Sebanz, N., & Knoblich, G. (2010). Others' actions reduce crossmodal integration in peripersonal space. *Current Biology: CB, 20*(15), 1345–1349. https://doi.org/10.1016/j.cub.2010.05.068

Hobeika, L., Taffou, M., & Viaud-Delmon, I. (2019). Social coding of the multisensory space around us. *Royal Society Open Science, 6*(8), 181878. https://doi.org/10.1098/rsos.181878

Holt, D. J., Cassidy, B. S., Yue, X., Rauch, S. L., Boeke, E. A., Nasr, S., et al. (2014). Neural correlates of personal space intrusion. *The Journal of Neuroscience: the Official Journal of the Society for Neuroscience, 34*(12), 4123–4134. https://doi.org/10.1523/JNEUROSCI.0686-13.2014

Holt, D. J., Boeke, E. A., Coombs, G, DeCross, S. N., Cassidy, B. S., Stufflebeam, S., et al. (2015). Abnormalities in personal space and parietal-frontal function in schizophrenia. *NeuroImage: Clinical, 9*, 233–243. https://doi.org/10.1016/j.nicl.2015.07.008. Erratum in: Neuroimage Clin. 2016;11:538. PMID: 26484048; PMCID: PMC4573090.

Hunley, S. B., & Lourenco, S. F. (2018). What is peripersonal space? An examination of unresolved empirical issues and emerging findings. *Wiley Interdisciplinary Reviews. Cognitive Science*, e1472. https://doi.org/10.1002/wcs.1472

Hunley, S. B., Marker, A. M., & Lourenco, S. F. (2017). Individual differences in the flexibility of peripersonal space. *Experimental Psychology, 64*(1), 49–55. https://doi.org/10.1027/1618-3169/a000350

Hunnius, S., & Bekkering, H. (2014). What are you doing? How active and observational experience shape infants' action understanding. *Philosophical Transactions of the Royal Society of London. Series B, Biological Sciences, 369*(1644), 20130490. https://doi.org/10.1098/rstb.2013.0490

Iachini, T., Coello, Y., Frassinetti, F., & Ruggiero, G. (2014). Body space in social interactions: A comparison of reaching and comfort distance in immersive virtual reality. *Plos One, 9*(11). https://doi.org/10.1371/journal.pone.0111511

Iachini, T., Coello, Y., Frassinetti, F., Senese, V. P., Galante, F., & Ruggiero, G. (2016). Peripersonal and interpersonal space in virtual and real environments: Effects of gender and age. *The Journal of Economic Perspectives: a Journal of the American Economic Association, 45*, 154–164. https://doi.org/10.1016/j.jenvp.2016.01.004

Iachini, T., Pagliaro, S., & Ruggiero, G. (2015). Near or far? It depends on my impression: Moral information and spatial behavior in virtual interactions. *Acta Psychologica, 161*, 131–136. https://doi.org/10.1016/j.actpsy.2015.09.003

Iachini, T., & Ruggiero, G. (2021). Can I put myself in your shoes? Sharing peripersonal space reveals the simulation of the action possibilities of others. *Experimental Brain Research*. https://doi.org/10.1007/s00221-021-06040-9

Iachini, T., Ruggiero, G., Ruotolo, F., Schiano di Cola, A., & Senese, V. P. (2015). The influence of anxiety and personality factors on comfort and reachability space: A correlational study. *Cognitive Processing, 16*(Suppl 1), 255–258. https://doi.org/10.1007/s10339-015-0717-6

Ishida, H., Nakajima, K., Inase, M., & Murata, A. (2010). Shared mapping of own and others' bodies in visuotactile bimodal area of monkey parietal cortex. *Journal of Cognitive Neuroscience, 22*(1), 83–96. https://doi.org/10.1162/jocn.2009.21185

Jeannerod, M. (2006). From my self to other selves: A revised framework for self/other differentiation. In P. Haggard, Y. Rossetti, & M. Kawato (Eds.), *Sensorimotor foundations of higher cognition. Attention & performance XXII*. Oxford University Press.

Job, X. E., de Fockert, J. W., & van Velzen, J. (2016). Action preparation modulates sensory perception in unseen personal space: An electrophysiological investigation. *Neuropsychologia, 89*, 445–452. https://doi.org/10.1016/j.neuropsychologia.2016.07.021

Juett, J., & Kuipers, B. (2019). Learning and acting in peripersonal space: Moving, reaching, and grasping. *The Florida Nurse, 13*, 4. https://doi.org/10.3389/fnbot.2019.00004

Kandula, M., Hofman, D., & Dijkerman, H. C. (2015). Visuo-tactile interactions are dependent on the predictive value of the visual stimulus. *Neuropsychologia, 70*, 358–366. https://doi.org/10.1016/j.neuropsychologia.2014.12.008

Kennedy, D. P., & Adolphs, R. (2014). Violations of personal space by individuals with autism spectrum disorder. *Plos One, 9*(8). https://doi.org/10.1371/journal.pone.0103369. Article 8.

Kennedy, D. P., Gläscher, J., Tyszka, J. M., & Adolphs, R. (2009). Personal space regulation by the human amygdala. *Nature Neuroscience, 12*(10), 1226–1227. https://doi.org/10.1038/nn.2381

Khalsa, S. S., Adolphs, R., Cameron, O. G., Critchley, H. D., Davenport, P. W., Feinstein, J. S., et al. (2018). Interoception and mental health: A roadmap. *Biological Psychiatry: Cognitive Neuroscience and Neuroimaging, 3*(6), 501–513. https://doi.org/10.1016/j.bpsc.2017.12.004

Kilner, J. M., Vargas, C., Duval, S., Blakemore, S.-J., & Sirigu, A. (2004). Motor activation prior to observation of a predicted movement. *Nature Neuroscience, 7*(12), 1299–1301. https://doi.org/10.1038/nn1355

Kleckner, I. R., Zhang, J., Touroutoglou, A., Chanes, L., Xia, C., Simmons, W. K., et al. (2017). Evidence for a large-scale brain system supporting allostasis and interoception in humans. *Nature Human Behaviour, 1*. https://doi.org/10.1038/s41562-017-0069

Làdavas, E., & Farnè, A. (2004). Visuo-tactile representation of near-the-body space. *Journal of Physiology, Paris, 98*(1–3), 161–170. https://doi.org/10.1016/j.jphysparis.2004.03.007

Làdavas, E., Zeloni, G., & Farnè, A. (1998). Visual peripersonal space centred on the face in humans. *Brain: a Journal of Neurology, 121*(Pt 12), 2317–2326.

Lakoff, G., & Johnson, M. (1980). *Metaphors we live by* (p. 242p). University of Chicago Press.

Lara, A. H., Cunningham, J. P., & Churchland, M. M. (2018). Different population dynamics in the supplementary motor area and motor cortex during reaching. *Nature Communications, 9*(1), 2754. https://doi.org/10.1038/s41467-018-05146-z

Lebert, A., Chaby, L., Garnot, C., & Vergilino-Perez, D. (2020). The impact of emotional videos and emotional static faces on postural control through a personality trait approach. *Experimental Brain Research, 238*(12), 2877–2886. https://doi.org/10.1007/s00221-020-05941-5. Epub 2020 Oct 14. PMID: 33057868.

Lenggenhager, B., Tadi, T., Metzinger, T., & Blanke, O. (2007). Video ergo sum: Manipulating bodily self-consciousness. *Science (New York, N.Y.), 317*(5841), 1096–1099. https://doi.org/10.1126/science.1143439

Lomoriello, A. S., Meconi, F., Rinaldi, I., & Sessa, P. (2018). *Out of sight out of mind: Perceived physical distance between the observer and someone in pain shapes observer's neural empathic reactions*. ArXiv:1808.01805 [q-Bio] http://arxiv.org/abs/1808.01805.

Lough, E., Hanley, M., Rodgers, J., South, M., Kirk, H., Kennedy, D. P., et al. (2015). Violations of personal space in young people with autism spectrum disorders and williams syndrome: Insights from the social responsiveness scale. *Journal of Autism and Developmental Disorders, 45*(12), 4101–4108. https://doi.org/10.1007/s10803-015-2536-0

Lourenco, S. F., Longo, M. R., & Pathman, T. (2011). Near space and its relation to claustrophobic fear. *Cognition, 119*(3), 448–453. https://doi.org/10.1016/j.cognition.2011.02.009

Mahayana, I. T., Banissy, M. J., Chen, C.-Y., Walsh, V., Juan, C.-H., & Muggleton, N. G. (2014). Motor empathy is a consequence of misattribution of sensory information in observers. *Frontiers in Human Neuroscience, 8*. https://doi.org/10.3389/fnhum.2014.00047

Maister, L., Cardini, F., Zamariola, G., Serino, A., & Tsakiris, M. (2015). Your place or mine: Shared sensory experiences elicit a remapping of peripersonal space. *Neuropsychologia, 70*, 455–461. https://doi.org/10.1016/j.neuropsychologia.2014.10.027

Makin, T. R., Holmes, N. P., & Ehrsson, H. H. (2008). On the other hand: Dummy hands and peripersonal space. *Behavioural Brain Research, 191*(1), 1–10. https://doi.org/10.1016/j.bbr.2008.02.041

Makin, T. R., Wilf, M., Schwartz, I., & Zohary, E. (2010). Amputees "neglect" the space near their missing hand. *Psychological Science, 21*(1), 55–57. https://doi.org/10.1177/0956797609354739

Maravita, A., Spence, C., Clarke, K., Husain, M., & Driver, J. (2000). Vision and touch through the looking glass in a case of crossmodal extinction. *Neuroreport, 11*(16), 3521–3526. https://doi.org/10.1097/00001756-200011090-00024

Massaccesi, C., Groessing, A., Rosenberger, L. A., Hartmann, H., Candini, M., di Pellegrino, G., et al. (2021). Neural correlates of interpersonal space permeability and flexibility in autism spectrum disorder. *Cerebral Cortex (New York, N.Y.: 1991)*. https://doi.org/10.1093/cercor/bhaa404

Mencl, J., & May, D. R. (2009). The effects of proximity and empathy on ethical decision-making: An exploratory investigation. *Journal of Business Ethics, 85*(2), 201–226. https://doi.org/10.1007/s10551-008-9765-5

Mobbs, D., Petrovic, P., Marchant, J. L., Hassabis, D., Weiskopf, N., Seymour, B., et al. (2007). When fear is near: Threat imminence elicits prefrontal-periaqueductal gray shifts in humans. *Science (New York, N.Y.), 317*(5841), 1079–1083. https://doi.org/10.1126/science.1144298

Monaco, S., Cavina-Pratesi, C., Sedda, A., Fattori, P., Galletti, C., & Culham, J. C. (2011). Functional magnetic resonance adaptation reveals the involvement of the dorsomedial stream in hand orientation for grasping. *Journal of Neurophysiology, 106*(5), 2248–2263. https://doi.org/10.1152/jn.01069.2010

Mufson, E. J., Mesulam, M.-M., & Pandya, D. N. (1981). Insular interconnections with the amygdala in the rhesus monkey. *Neuroscience, 6*(7), 1231–1248. https://doi.org/10.1016/0306-4522(81)90184-6

Mul, C.-L., Cardini, F., Stagg, S. D., Sadeghi Esfahlani, S., Kiourtsoglou, D., Cardellicchio, P., et al. (2019). Altered bodily self-consciousness and peripersonal space in autism. *Autism: the International Journal of Research and Practice*. https://doi.org/10.1177/1362361319838950, 1362361319838950.

Mundy, P. (2018). A review of joint attention and social-cognitive brain systems in typical development and autism spectrum disorder. *The European Journal of Neuroscience, 47*(6), 497–514. https://doi.org/10.1111/ejn.13720

Myers, M. W., & Hodges, S. D. (2012). The structure of self–other overlap and its relationship to perspective taking. *Personal Relationships, 19*(4), 663–679. https://doi.org/10.1111/j.1475-6811.2011.01382.x

Nishihara, R., & Okubo, M. (2015). A study on personal space in virtual space based on personality. *Procedia Manufacturing, 3*, 2183–2190. https://doi.org/10.1016/j.promfg.2015.07.359

Noel, J.-P., Bertoni, T., Terrebonne, E., Pellencin, E., Herbelin, B., Cascio, C., et al. (2020a). Rapid recalibration of peri-personal space: Psychophysical, electrophysiological, and neural network modeling evidence. *Cerebral Cortex (New York, N.Y.: 1991), 30*(9), 5088–5106. https://doi.org/10.1093/cercor/bhaa103

Noel, J.-P., Cascio, C. J., Wallace, M. T., & Park, S. (2017). The spatial self in schizophrenia and autism spectrum disorder. *Schizophrenia Research, 179*, 8–12. https://doi.org/10.1016/j.schres.2016.09.021

Noel, J.-P., Failla, M. D., Quinde-Zlibut, J. M., Williams, Z. J., Gerdes, M., Tracy, J. M., et al. (2020b). Visual-tactile spatial multisensory interaction in adults with autism and schizophrenia. *Frontiers in Psychiatry, 11*. https://doi.org/10.3389/fpsyt.2020.578401

Noel, J.-P., Grivaz, P., Marmaroli, P., Lissek, H., Blanke, O., & Serino, A. (2015). Full body action remapping of peripersonal space: The case of walking. *Neuropsychologia, 70*, 375–384. https://doi.org/10.1016/j.neuropsychologia.2014.08.030

Noel, J.-P., Lytle, M., Cascio, C., & Wallace, M. T. (2018a). Disrupted integration of exteroceptive and interoceptive signaling in autism spectrum disorder. *Autism Research: Official Journal of the International Society for Autism Research, 11*(1), 194–205. https://doi.org/10.1002/aur.1880

Noel, J.-P., Park, H.-D., Pasqualini, I., Lissek, H., Wallace, M., Blanke, O., et al. (2018b). Audio-visual sensory deprivation degrades visuo-tactile peri-personal space. *Consciousness and Cognition, 61*, 61–75. https://doi.org/10.1016/j.concog.2018.04.001

Noel, J.-P., Pfeiffer, C., Blanke, O., & Serino, A. (2015). Peripersonal space as the space of the bodily self. *Cognition, 144*, 49–57. https://doi.org/10.1016/j.cognition.2015.07.012

Orioli, G., Filippetti, M. L., Gerbino, W., Dragovic, D., & Farroni, T. (2018). Trajectory discrimination and peripersonal space perception in newborns. *Infancy: The Official Journal of the International Society on Infant Studies, 23*(2), 252–267. https://doi.org/10.1111/infa.12207

Parkinson, C., Liu, S., & Wheatley, T. (2014). A common cortical metric for spatial, temporal, and social distance. *The Journal of Neuroscience: the Official Journal of the Society for Neuroscience, 34*(5), 1979–1987. https://doi.org/10.1523/JNEUROSCI.2159-13.2014

Patané, I., Brozzoli, C., Koun, E., Frassinetti, F., & Farnè, A. (2020). Me, you, and our object: Peripersonal space recruitment during executed and observed actions depends on object ownership. *Journal of Experimental Psychology. General*. https://doi.org/10.1037/xge0001001

Patané, I., Cardinali, L., Salemme, R., Pavani, F., Farnè, A., & Brozzoli, C. (2018). Action planning modulates peripersonal space. *Journal of Cognitive Neuroscience*, 1–14. https://doi.org/10.1162/jocn_a_01349

Patané, I., Farnè, A., & Frassinetti, F. (2017). Cooperative tool-use reveals peripersonal and interpersonal spaces are dissociable. *Cognition, 166*, 13–22. https://doi.org/10.1016/j.cognition.2017.04.013

Patané, I., Iachini, T., Farnè, A., & Frassinetti, F. (2016). Disentangling action from social space: Tool-use differently shapes the space around us. *Plos One, 11*(5), Article e0154247. https://doi.org/10.1371/journal.pone.0154247

Pellencin, E., Paladino, M. P., Herbelin, B., & Serino, A. (2017). Social perception of others shapes one's own multisensory peripersonal space. *Cortex; a Journal Devoted to the Study of the Nervous System and Behavior*. https://doi.org/10.1016/j.cortex.2017.08.033

Pfeiffer, C., Noel, J.-P., Serino, A., & Blanke, O. (2018). Vestibular modulation of peripersonal space boundaries. *The European Journal of Neuroscience, 47*(7), 800–811. https://doi.org/10.1111/ejn.13872

Pitzalis, S., Sereno, M. I., Committeri, G., Fattori, P., Galati, G., Tosoni, A., et al. (2013). The human homologue of macaque area V6A. *Neuroimage, 82*, 517–530. https://doi.org/10.1016/j.neuroimage.2013.06.026

Plewan, T., & Rinkenauer, G. (2017). Simple reaction time and size–distance integration in virtual 3D space. *Psychological Research, 81*(3), 653–663. https://doi.org/10.1007/s00426-016-0769-y

Quadt, L., Critchley, H. D., & Garfinkel, S. N. (2018). The neurobiology of interoception in health and disease. *Annals of the New York Academy of Sciences, 1428*(1), 112–128. https://doi.org/10.1111/nyas.13915

Quesque, F., Ruggiero, G., Mouta, S., Santos, J., Iachini, T., & Coello, Y. (2017). Keeping you at arm's length: Modifying peripersonal space influences interpersonal distance. *Psychological Research, 81*(4), 709–720. https://doi.org/10.1007/s00426-016-0782-1

Rabellino, D., Frewen, P. A., McKinnon, M. C., & Lanius, R. A. (2020). Peripersonal space and bodily self-consciousness: Implications for psychological trauma-related disorders. *The Florida Nurse*, 14. https://doi.org/10.3389/fnins.2020.586605

Reed, C. L., Grubb, J. D., & Steele, C. (2006). Hands up: Attentional prioritization of space near the hand. *Journal of Experimental Psychology. Human Perception and Performance, 32*(1), 166–177. https://doi.org/10.1037/0096-1523.32.1.166

Reynaud, A. J., Guedj, C., Hadj-Bouziane, F., Meunier, M., & Monfardini, E. (2015). Social facilitation of cognition in rhesus monkeys: Audience vs. Coaction. *Frontiers in Behavioral Neuroscience*, 9, 328. https://doi.org/10.3389/fnbeh.2015.00328

Riečanský, I., Lengersdorff, L., Pfabigan, D. M., & Lamm, C. (2020). Increasing self-other bodily overlap increases sensorimotor resonance to others' pain. *Cognitive, Affective & Behavioral Neuroscience, 20*, 19–33. https://doi.org/10.3758/s13415-019-00724-0

Rizzolatti, G., Scandolara, C., Gentilucci, M., & Camarda, R. (1981). Response properties and behavioral modulation of "mouth" neurons of the postarcuate cortex (area 6) in macaque monkeys. *Brain Research, 225*(2), 421–424.

Rizzolatti, G., Scandolara, C., Matelli, M., & Gentilucci, M. (1981). Afferent properties of periarcuate neurons in macaque monkeys. I. Somatosensory responses. *Behavioural Brain Research, 2*(2), 125–146.

Rocca, R., Wallentin, M., Vesper, C., & Tylén, K. (2019). This is for you: Social modulations of proximal vs. distal space in collaborative interaction. *Scientific Reports, 9*(1), 14967. https://doi.org/10.1038/s41598-019-51134-8

Rossetti, A., Romano, D., Bolognini, N., & Maravita, A. (2015). Dynamic expansion of alert responses to incoming painful stimuli following tool use. *Neuropsychologia, 70*, 486–494. https://doi.org/10.1016/j.neuropsychologia.2015.01.019

Ruggiero, G., Frassinetti, F., Coello, Y., Rapuano, M., di Cola, A. S., & Iachini, T. (2017). The effect of facial expressions on peripersonal and interpersonal spaces. *Psychological Research, 81*(6), 1232–1240. https://doi.org/10.1007/s00426-016-0806-x

Ruggiero, G., Rapuano, M., & Iachini, T. (2019). Perceived temperature modulates peripersonal and interpersonal spaces differently in men and women—ScienceDirect. *The Journal of Economic Perspectives: a Journal of the American Economic Association, 63*, 52–59.

Saccone, E. J., Szpak, A., Churches, O., & Nicholls, M. E. R. (2018). Close interpersonal proximity modulates visuomotor processing of object affordances in shared, social space. *Attention, Perception & Psychophysics, 80*(1), 54–68. https://doi.org/10.3758/s13414-017-1413-7

Salomon, R., Noel, J.-P., Łukowska, M., Faivre, N., Metzinger, T., Serino, A., et al. (2017). Unconscious integration of multisensory bodily inputs in the peripersonal space shapes bodily self-consciousness. *Cognition, 166*, 174–183. https://doi.org/10.1016/j.cognition.2017.05.028

Sambo, C. F., & Iannetti, G. D. (2013). Better safe than sorry? The safety margin surrounding the body is increased by anxiety. *The Journal of Neuroscience: the Official Journal of the Society for Neuroscience, 33*(35), 14225–14230. https://doi.org/10.1523/JNEUROSCI.0706-13.2013

Sambo, C. F., Liang, M., Cruccu, G., & Iannetti, G. D. (2012). Defensive peripersonal space: The blink reflex evoked by hand stimulation is increased when the hand is near the face. *Journal of Neurophysiology, 107*(3), 880–889. https://doi.org/10.1152/jn.00731.2011

Scandola, M., Aglioti, S. M., Bonente, C., Avesani, R., & Moro, V. (2016). Spinal cord lesions shrink peripersonal space around the feet, passive mobilization of paraplegic limbs restores it. *Scientific Reports, 6*, 24126. https://doi.org/10.1038/srep24126

Scandola, M., Aglioti, S. M., Lazzeri, G., Avesani, R., Ionta, S., & Moro, V. (2020). Visuo-motor and interoceptive influences on peripersonal space representation following spinal cord injury. *Scientific Reports, 10*(1), 5162. https://doi.org/10.1038/s41598-020-62080-1

Schaefer, M., Heinze, H.-J., & Rotte, M. (2012). Close to you: Embodied simulation for peripersonal space in primary somatosensory cortex. *Plos One, 7*(8). https://doi.org/10.1371/journal.pone.0042308. Article 8.

Schienle, A., Wabnegger, A., Leitner, M., & Leutgeb, V. (2017). Neuronal correlates of personal space intrusion in violent offenders. *Brain Imaging and Behavior, 11*(2), 454–460. https://doi.org/10.1007/s11682-016-9526-5

Schienle, A., Wabnegger, A., Schöngassner, F., & Leutgeb, V. (2015). Effects of personal space intrusion in affective contexts: An fMRI investigation with women suffering from borderline personality disorder. *[Social Cognitive and Affective Neuroscience Electronic Resource], 10*(10), 1424–1428. https://doi.org/10.1093/scan/nsv034

Seghezzi, S., Giannini, G., & Zapparoli, L. (2019). Neurofunctional correlates of body-ownership and sense of agency: A meta-analytical account of self-consciousness. *Cortex. a Journal Devoted to the Study of the Nervous System and Behavior, 121*, 169–178. https://doi.org/10.1016/j.cortex.2019.08.018

Senna, I., Cardinali, L., Farnè, A., & Brozzoli, C. (2019). Aim and plausibility of action chains remap peripersonal space. *Frontiers in Psychology*, 10. https://doi.org/10.3389/fpsyg.2019.01681

Sereno, M. I., & Huang, R.-S. (2006). A human parietal face area contains aligned head-centered visual and tactile maps. *Nature Neuroscience, 9*(10), 1337–1343. https://doi.org/10.1038/nn1777

Serino, A. (2019). Peripersonal space (PPS) as a multisensory interface between the individual and the environment, defining the space of the self. *Neuroscience and Biobehavioral Reviews*. https://doi.org/10.1016/j.neubiorev.2019.01.016

Serino, A., Bassolino, M., Farnè, A., & Làdavas, E. (2007). Extended multisensory space in blind cane users. *Psychological Science, 18*(7), 642–648. https://doi.org/10.1111/j.1467-9280.2007.01952.x

Serino, A., Giovagnoli, G., & Làdavas, E. (2009). I feel what you feel if you are similar to me. *Plos One, 4*(3), Article e4930. https://doi.org/10.1371/journal.pone.0004930

Serino, A., Noel, J.-P., Galli, G., Canzoneri, E., Marmaroli, P., Lissek, H., et al. (2015). Body part-centered and full body-centered peripersonal space representations. *Scientific Reports*, 5, 18603. https://doi.org/10.1038/srep18603

Shin, M., Song, S. W., Kim, S. J., & Biocca, F. (2019). Does sound make differences in an interpersonal relationship?: The effects of 3D sound on social presence, parasocial relationship, enjoyment, and intent of supportive action. *International Journal of Human-Computer Studies*. https://doi.org/10.1016/j.ijhcs.2019.02.001

Sorokowska, A., Sorokowski, P., Hilpert, P., Cantarero, K., Frackowiak, T., Ahmadi, K., et al. (2017). Preferred interpersonal distances: A global comparison. *Journal of Cross-Cultural Psychology*, *48*(4), 577–592. https://doi.org/10.1177/0022022117698039

Sorrentino, G., Franza, M., Zuber, C., Blanke, O., Serino, A., & Bassolino, M. (2021). How ageing shapes body and space representations: A comparison study between healthy young and older adults. *Cortex; a Journal Devoted To the Study of the Nervous System and Behavior*, *136*, 56–76. https://doi.org/10.1016/j.cortex.2020.11.021

Spence, C., Nicholls, M. E., Gillespie, N., & Driver, J. (1998). Cross-modal links in exogenous covert spatial orienting between touch, audition, and vision. *Perception & Psychophysics*, *60*(4), 544–557. https://doi.org/10.3758/bf03206045

Spence, C., Pavani, F., Maravita, A., & Holmes, N. (2004). Multisensory contributions to the 3-D representation of visuotactile peripersonal space in humans: Evidence from the crossmodal congruency task. *Journal of Physiology, Paris*, *98*(1–3), 171–189. https://doi.org/10.1016/j.jphysparis.2004.03.008

Stefani, E. D., Innocenti, A., Marco, D. D., Busiello, M., Ferri, F., Costantini, M., et al. (2014). The spatial alignment effect in near and far space: A kinematic study. *Experimental Brain Research*, *232*(7), 2431–2438. https://doi.org/10.1007/s00221-014-3943-8

Stone, K. D., Kandula, M., Keizer, A., & Dijkerman, H. C. (2018). Peripersonal space boundaries around the lower limbs. *Experimental Brain Research*, *236*(1), 161–173. https://doi.org/10.1007/s00221-017-5115-0

Taylor, S. P., & Epstein, S. (1967). The measurement of autonomic arousal. Some basic issues illustrated by the covariation of heart rate and skin conductance. *Psychosomatic Medicine*, *29*(5), 514–525. https://doi.org/10.1097/00006842-196709000-00010

Teneggi, C., Canzoneri, E., di Pellegrino, G., & Serino, A. (2013). Social modulation of peripersonal space boundaries. *Current Biology: CB*, *23*(5), 406–411. https://doi.org/10.1016/j.cub.2013.01.043

Teramoto, W. (2018). A behavioral approach to shared mapping of peripersonal space between oneself and others. *Scientific Reports*, *8*(1), 5432. https://doi.org/10.1038/s41598-018-23815-3

Uddin, L. Q., Nomi, J. S., Hébert-Seropian, B., Ghaziri, J., & Boucher, O. (2017). Structure and function of the human insula. *Journal of Clinical Neurophysiology: Official Publication of the American Electroencephalographic Society*, *34*(4), 300–306. https://doi.org/10.1097/WNP.0000000000000377

Vestal, B. M. (1977). *Sociability and individual distance in four species of rodents*.

Vieira, J. B., Tavares, T. P., Marsh, A. A., & Mitchell, D. G. V. (2017). Emotion and personal space: Neural correlates of approach-avoidance tendencies to different facial expressions as a function of coldhearted psychopathic traits. *Human Brain Mapping*, *38*(3), 1492–1506. https://doi.org/10.1002/hbm.23467

Wamain, Y., Gabrielli, F., & Coello, Y. (2016). EEG μ rhythm in virtual reality reveals that motor coding of visual objects in peripersonal space is task dependent. *Cortex; a Journal Devoted to the Study of the Nervous System and Behavior*, *74*, 20–30. https://doi.org/10.1016/j.cortex.2015.10.006

Woodward, A. L., Sommerville, J. A., Gerson, S., Henderson, A. M. E., & Buresh, J. (2009). The emergence of intention attribution in infancy. *The Psychology of Learning and Motivation*, *51*, 187–222. https://doi.org/10.1016/S0079-7421(09)51006-7

Zanini, A., Patané, I., Blini, E., Salemme, R., Koun, E., Farnè, A., et al. (2020). *Patterns of multisensory facilitation distinguish peripersonal from reaching space*. https://doi.org/10.1101/2020.06.01.127282

Questions posées et démarche expérimentale

Si l'on retrace en quelques lignes les travaux qui ont été menés jusqu'ici depuis la découverte d'une division de l'espace en fonction de sa représentation proche ou loin du corps, jusqu'à la définition et la compréhension du rôle de l'EPP, on peut souligner les premières études qui ont découvert les neurones « péripersonnels » en utilisant des enregistrements électrophysiologiques dans des régions des aires fronto-pariétales avec des stimuli dans l'espace proche du corps. Quelques années plus tard, la convergence d'études de psychologie expérimentale et de neuroimagerie chez l'homme sain a apporté des preuves expérimentales de l'existence d'un réseau homologue putatif. Cependant l'IRMf fournit une mesure à l'échelle des aires cérébrales et non à l'échelle du neurone, c'est pourquoi il est difficile de transposer directement les données du singe à l'homme. A ce jour, une seule étude a été conduite en IRMf chez le singe, cependant les variations entre les démarches expérimentales ne permettent pas d'apporter une comparaison précise entre les espèces.

Le premier objectif de ma thèse est donc d'identifier les homologies concernant le réseau fonctionnel impliqué dans la représentation de l'EPP chez ces deux espèces afin de réconcilier les différentes sources de connaissances existantes chez l'homme et le singe.
Ainsi, la première question à laquelle ce travail de thèse tentera de répondre est la suivante :

« Quelles sont les homologies concernant le réseau neuronal de la représentation de l'EPP chez l'homme et le singe ? »

⇒ **Étude 1 -** J'ai d'abord choisi de répondre à cette question avec une première étude utilisant une version modifiée d'une tâche d'adaptation en IRMf qui avait déjà été

utilisée chez l'homme pour étudier les propriétés neuronales unisensorielles de l'EPP (Brozzoli et al., 2011, 2012). Nous avons donc adapté ce protocole pour rendre la méthodologie la plus similaire possible chez les deux espèces. En raison des contraintes techniques et pour assurer les mêmes stimulations entre les espèces, nous avons choisi de présenter une balle réelle proche (à 2 cm) ou loin (à 100 cm) du visage, pendant que les sujets étaient incités à fixer un point central.

De plus, chez l'homme, où l'accès direct à différentes parties du corps était possible, contrairement au singe, nous avons cherché à étudier les réseaux neuronaux sous-jacents à la représentation de l'EPP centrée sur différentes parties du corps. Nous avons donc adapté ce même protocole d'adaptation IRMf en présentant également la balle réelle proche et loin de la main et du tronc. En effet, basé sur les études en électrophysiologie chez le macaque montrant la présence de neurones codant plus spécifiquement certaines parties du corps, notre prédiction était que le réseau neuronal pariétal-prémoteur sous-tendant la représentation de l'EPP chez l'homme possèderait une organisation somatotopique.

⇒ **Étude 2 –** J'ai également choisi d'établir les correspondances fonctionnelles du réseau neuronal de l'EPP entre l'homme et le singe en développant une nouvelle approche qui reposait sur l'utilisation de la réalité virtuelle (RV) stéréoscopique dans l'IRM. Le paradigme consistait en une tâche de visualisation passive où des formes géométriques en 3D étaient présentées soit proche (30 cm, dans l'EPP) ou loin (300 cm) dans l'environnement virtuel. Cette méthode novatrice jamais utilisée auparavant en IRMf pour étudier la représentation de l'EPP, a été réalisée chez les deux espèces afin de comparer directement les activations cérébrales préférentielles à l'apparition des objets 3D dans l'EPP. Cette étude était également importante pour faire le pont avec l'approche en réalité virtuelle que j'ai implémentée pour étudier la modulation sociale de l'EPP, et que je décris ci-dessous.

Ainsi, à travers ces deux premières études, mon objectif était d'établir les homologies et les différences potentielles concernant les réseaux fonctionnels traitant les informations dans l'EPP chez l'homme et le singe. Mes prédictions étaient que les aires pariétales et prémotrices seraient principalement recrutées lors du traitement d'un objet réel proche du visage ou d'un objet virtuel proche dans l'environnement virtuel, dans des régions cérébrales pour la plupart

similaires chez les deux espèces. Mon hypothèse étant que l'organisation du réseau neuronal serait similaire chez les deux espèces pour traiter l'information visuelle se produisant dans l'EPP. Le chapitre 2 de ma thèse présente les résultats de ces deux études.

Dans la deuxième partie de mon introduction, je me suis concentrée sur une branche récente d'études de l'EPP, à savoir l'exploration de la modulation de l'EPP par les informations sociales. Comme je l'ai développé dans l'axe 2, les mécanismes multisensoriels et unisensoriels sous-jacents de la représentation de l'EPP ne sont pas seulement impliqués dans les interactions physiques entre le corps et les objets, mais également dans les situations sociales impliquant nos pairs. Les fonctions de cette entité sociale ont été plutôt étudiées dans des études comportementales avec des stimulations multisensorielles démontrant que la présence des autres et ce qu'ils véhiculent, par exemple leur émotion, influence la représentation de l'EPP. Très peu d'études utilisant la neuroimagerie ont tenté de comprendre comment le réseau neuronal de l'EPP était influencé par la présence d'éléments sociaux dans notre espace proche. A ma connaissance, seulement six études avaient identifié les corrélats neuronaux au cours d'une tâche qui impliquait des visages émotionnels ou non s'approchant ou s'éloignant du corps, ciblant plus spécifiquement une autre définition de l'espace proche du corps, l'espace personnel, défini par les psychologues comme l'espace que nous gardons entre nous et les autres pour éviter l'inconfort. Malgré leurs origines différentes, ces espaces renvoient à l'espace ancré autour du corps, et pourraient partager certains points communs, comme certaines études ont tenté de le montrer. Mais c'est une question qui reste à ce jour encore à élucider.

Le deuxième objectif, et la partie la plus centrale de mon travail de thèse concerne donc la caractérisation de l'EPP dans un contexte social (c'est-à-dire la présence d'autres individus) en utilisant une approche multi-échelle permettant de définir les propriétés de la représentation de l'EPP au niveau comportemental, physiologique et neuronal. Mon hypothèse était que nos performances comportementales seraient améliorées lors du traitement des éléments sociaux dans l'EPP et que notre état intérieur pourrait aider à façonner notre comportement en fonction du contexte. Au niveau neuronal, mon hypothèse était que le réseau fronto-pariétal de l'EPP permettrait de traiter les informations sociales et non sociales dans l'EPP avec des spécificités propres à chaque type de stimulus.

Spécifiquement, les questions auxquelles j'ai essayé de répondre étaient les suivantes :

1- **« Comment les stimuli sociaux modulent nos capacités de discrimination visuelle et nos réponses physiologiques dans l'EPP ? » - Étude 3**
2- **« Quel est le réseau neuronal recruté lors du traitement des stimuli sociaux dans l'EPP et comment les expressions faciales émotionnelles influencent l'activité de ce réseau ? » - Étude 4**
3- **« Les réponses cérébrales de la représentation de l'EPP sont-elles influencées en fonction de la nature de l'information (sociale vs. non-sociale) ? » - Étude 4**
4- **« Quel est l'impact de lésions médio-temporales unilatérales sur la régulation des distances personnelles au cours des interactions sociales ? » - Étude 5**

Ma stratégie était de caractériser l'impact d'un élément social sur la représentation de l'EPP, en faisant varier son contenu émotionnel (visage neutre, joyeux ou en colère) et sa position dans l'espace qui nous entoure (proche ou loin). J'ai choisi d'explorer ces questions en développant des protocoles en RV. L'intérêt de la RV est qu'elle permet de manipuler et de contrôler de manière très précise des informations visuelles dans le plan sagittal et de faire varier leur présentation à différentes distances de notre corps.
Nous avons développé nos paradigmes expérimentaux en dehors de l'environnement de l'IRM, avec un casque de réalité virtuelle (Études 3 et 5 – voir ci-dessous), et à l'intérieur de l'environnement IRM, avec un projecteur 3D (Étude 4 – voir ci-dessous).

⇒ **Étude 3 -** A travers la troisième étude de ma thèse, mon objectif était de comprendre comment l'information sociale module nos capacités de discrimination visuelle et nos réponses physiologiques en fonction de sa position dans l'espace à travers un ensemble de mesures comportementales ainsi que physiologiques. Dans trois différentes tâches que nous avons développées en RV chez l'homme, la position des informations visuelles variait dans les espaces proches (dans l'EPP) et lointains et les participants devaient discriminer les visages féminins des visages masculins qui pouvaient varier en émotion. J'ai enregistré les mesures comportementales (temps de réaction et précision des réponses) et physiologiques (réponses pupillaires et la fréquence cardiaque) des participants.

Mes prédictions étaient que la proximité du visage faciliterait les capacités de discrimination visuelle et que cette facilitation serait modulée par les caractéristiques et serait accompagnée de changements de l'état interne mesurés grâce aux réponses physiologiques.

⇒ **Étude 4 -** Une quatrième étude m'a permis de caractériser les signatures neuronales de la représentation de l'EPP dans différents contextes, sociaux et non sociaux. En utilisant une version modifiée du paradigme utilisé dans l'étude 3, j'ai pu directement : 1) identifier le réseau neuronal sous-tendant la représentation de l'EPP impliquant des stimuli sociaux (visages émotionnels humains) ; 2) comparer les réponses neuronales permettant de traiter les informations sociales (visages émotionnels humains) et non-sociales (formes géométriques) dans l'EPP ; 3) déterminer l'influence de l'émotion faciale perçue dans l'EPP sur le réseau neuronal de la représentation de l'EPP. Mes prédictions étaient que les stimuli sociaux et non sociaux présentés dans l'EPP recruteraient un réseau commun fronto-pariétal. Je prédisais également des spécificités liées au contexte (social versus non social) avec notamment un recrutement supplémentaire d'autres régions corticales ou sous-corticales, connues comme étant impliquées dans la reconnaissance des visages et des émotions pour le contexte social. Cette étude, menée en IRMf chez l'homme, impliquait l'utilisation de la RV stéréoscopique dans l'IRM, une méthode pionnière dans le domaine.

⇒ **Étude 5 -** Enfin, dans la dernière étude de ma thèse, mon objectif était d'étendre notre compréhension sur la régulation de l'espace personnel en déterminant si la régulation appropriée des distances personnelles pouvait dépendre de l'amygdale et d'autres régions du cortex temporal médian, puisqu'à ce jour une seule étude de cas chez une patiente présentant des lésions bilatérales de l'amygdale a permis d'identifier le rôle important de cette structure dans la régulation appropriée des distances entre les individus (Kennedy et al., 2009).

J'ai donc caractérisé les signatures comportementales et physiologiques de trois patients présentant des lésions unilatérales médio-temporales, dont un avec une lésion entièrement confinée à l'amygdale gauche, en condition virtuelle et réelle.

Ma prédiction était qu'une lésion unilatérale de l'amygdale altèrerait la régulation des distances interpersonnelles et qu'une atteinte des régions avoisinantes dans le cortex temporal médian pourrait également perturber cette régulation.

Le Chapitre 3 de ma thèse regroupe l'ensemble des résultats de ces 3 autres études.

Le schéma ci-dessous permet de résumer mes objectifs de thèse mais également de mieux comprendre comment mes différents travaux s'intègrent les uns avec les autres (Figure 22).

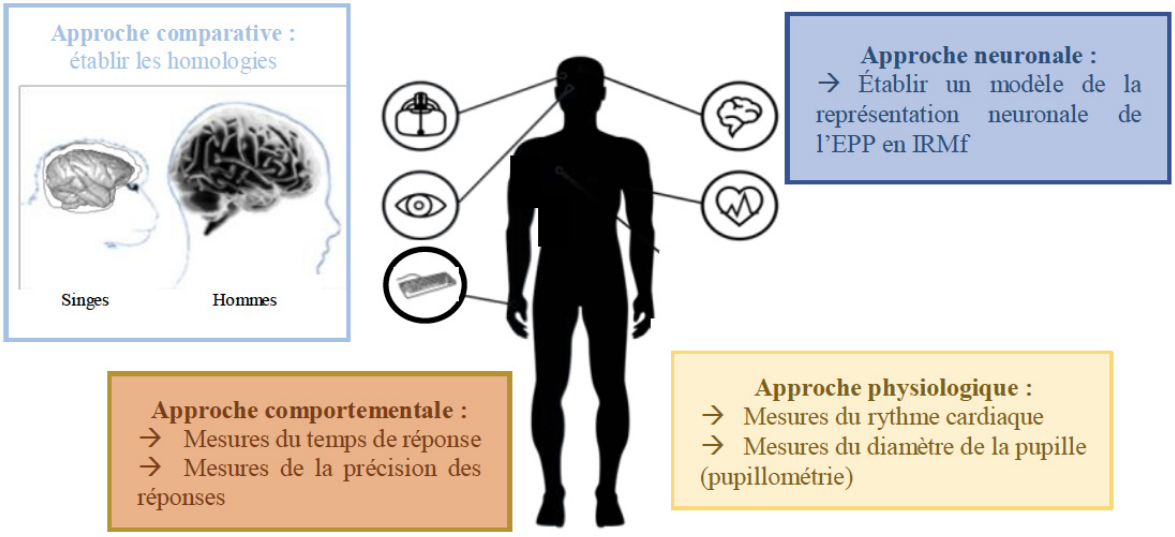

Figure 22. Schéma résumant l'ensemble des objectifs de ma thèse. L'approche centrale de ma thèse est de caractériser la représentation de l'EPP dans un contexte social en étudiant les variations de différentes réponses lors de la présence d'individus dans notre espace proche du corps. J'ai choisi d'utiliser une approche multi-échelle combinant des approches comportementales (études 3 et 5), physiologiques (études 3 et 5) et de neuroimagerie (étude 4). Ces approches sont, selon moi, complémentaires et nécessaires pour caractériser la dimension sociale de la représentation de l'EPP. Un volet important de mon travail est également l'aspect comparatif homme-singe qui permet d'établir les homologies neuronales entre les deux espèces à l'aide de la neuroimagerie (études 1 et 2), une démarche primordiale si nous souhaitons faire le lien entre nos connaissances chez l'homme et les connaissances de la réponse des neurones dans l'EPP établie chez le singe, là où les propriétés de l'EPP ont commencé à prendre tout leur sens.

Chapitre 2 :

Comparaison des réseaux fonctionnels impliqués dans la représentation de l'EPP chez l'homme et le macaque

Points essentiels de ce chapitre :

- Identification des similarités fonctionnelles des réseaux sous-tendant la représentation de l'EPP chez l'homme et le singe en utilisant des méthodologies similaires en IRMf.
- Deux méthodologies différentes exploitées : développement d'un protocole d'adaptation avec un objet réel présenté proche ou loin du visage (étude 1) et d'un protocole en réalité virtuelle où la position de l'objet en 3D variait à différentes distances dans l'environnement virtuel (étude 2).
- Mise en évidence d'un réseau fronto-pariétal central impliquant des régions prémotrices et pariétales chez les deux espèces : présence d'homologies fonctionnelles entre les espèces.

ETUDE 1

Comparaison de la représentation de l'espace péri-personnel chez l'homme et le singe avec un objet réel

---

Peripersonal space representation in humans and monkeys: a cross-species and between body-parts fMRI comparison

Audrey Dureux*, Alessandro Zanini*, Camille Giacometti, Eric Koun, Alessandro Farnè, Claudio Brozzoli and Fadila Hadj-Bouziane

Article en préparation

Peripersonal space representation in humans and monkeys: a cross-species and between body-parts fMRI comparison

Audrey Dureux*[1,2], Alessandro Zanini*[1,2], Camille Giacometti[2,3], Eric Koun[1,4], Alessandro Farnè[1,2,4,5], Claudio Brozzoli[1,2,4,6] and Fadila Hadj-Bouziane[1,2]

*These authors contributed equally to this work

1. Integrative Multisensory Perception Action & Cognition Team - ImpAct, INSERM U1028, CNRS UMR5292, Lyon Neuroscience Research Center (CRNL), Lyon, France
2. University UCBL Lyon 1, University of Lyon, Lyon, France
3. Stem Cell and Brain Research Institute U1208, 69500, Bron, France
4. Hospices Civils de Lyon, Neuro-Immersion & Mouvement et Handicap, Lyon, France
5. Center for Mind/Brain Sciences (CIMeC), University of Trento, Italy
6. Department of Neurobiology, Care Sciences and Society, Aging Research Center, Karolinska Institutet, Stockholm, Sweden

Corresponding authors:
Audrey Dureux and Fadila Hadj-Bouziane, INSERM U1028, CNRS UMR5292, Lyon Neuroscience Research Center, ImpAct Team, 16 Avenue Doyen Lépine 69500 Bron, France.
Emails: audrey.dureux@inserm.fr ; fadila.hadj-bouziane@inserm.fr.

Conflict of Interest: The authors declare that they have no conflict of interest.
Acknowledgements: This work was funded by the French National Research Agency ANR-15-CE37-0003 grant MySpace to FHB.

Funders had no role in study design, data collection and analysis, decision to publish, or preparation of the manuscript.

Abstract

Human and non-human primates are supposed to be endowed with similar neural mechanisms for coding the space closely surrounding their body, termed peripersonal space (PPS). Independent investigations through electrophysiological studies in the macaques and fMRI studies in humans have identified a set of fronto-parietal regions showing enhanced activations in response to stimuli close to the body compared to far ones. Despite the overall coherence of the findings, the differences between the two techniques have so far prevented a direct comparison between the two species. Thus, we used a similar unimodal visual stimulation protocol, recording BOLD fMRI adaptation, to reveal the existence of neuron subpopulations specific to near space coding, in both human and non-human primates. The findings demonstrate for the first time an overlap in the neural underpinnings of the PPS representation across both species within the fronto-parietal network, with activations found in premotor areas (F4-F5-PMdc/PMd-PMv), putamen and parietal regions (VIP-MIP-LIP-area 7 and their human homologues). Furthermore, in humans, we presented stimuli close to three different body parts -hand, face and trunk- in order to investigate the commonality and specificity in the neural basis of the body-part-centered reference frame of the PPS. The results point toward a common network within the fronto-parietal-supramarginal PPS network, regardless of the body-part stimulated. Importantly, we also identified specific activations for hand-, trunk- and face-based PPS representations along this network. These results provide a bridge between the results of electrophysiology in the monkey and neuroimaging in humans and broaden the knowledge about the neural basis of body-part-based PPS representations.

Abbreviations

6d/6r/6a/6mp/6v = dorsal/rostral/anterior/medial-posterior/ventral area 6

7Al/7Am = lateral/medial area 7

AIP = anterior intraparietal area

DVT = dorsal transitional visual area

FEF = frontal eye fields

LIPd/LIPv = dorsal/ventral lateral intraparietal area

LOP = lateral occipital parietal area

I6-8 = inferior 6-8 transitional area

IFJ = inferior frontal junction area

IP1/2 = intraparietal area 1/2

IPL/SPL = inferior/superior parietal lobule

IPS = intraparietal sulcus

MIP = medial intraparietal area

OP1 = S2 (secondary somatosensory area)

PEF = premotor eye fields

PIP = posterior intraparietal area

PMC = primary motor cortex (M1)

PMd/PMv = dorsal/ventral premotor cortex

PMdc = premotor dorsal caudal cortex

POS = parieto-occipital sulcus

PSL = perisylvian language area

RI = retroinsular cortex

S1 = primary somatosensory area

SMG = supramarginal gyrus

STV = superior temporal visual area

TPOJ = temporo-parieto-occipital junction

VIP = ventral intraparietal area

Vm_IPS/lat_IPS = ventro-medial / lateral IPS

1. Introduction

The peripersonal space (PPS) is the multisensory representation of objects in the region close to the body allowing us to interact with them. Its definition steams from single-unit electrophysiological studies in macaque monkeys which identified a set of neurons in the posterior periarcuate regions, within the ventral premotor cortex (PMv; F4), that responded preferentially to objects presented in the region of space close to the body (Rizzolatti et al., 1981a, 1981b). Subsequently, studies have shown that activity of single neurons in premotor (Graziano et al., 1994) and parietal cortices (Colby et al., 1993) and the putamen (Graziano and Gross, 1993) displayed similar neural properties.

In the parietal cortex, several subregions displayed selective coding for PPS, namely the ventral intraparietal (VIP) area (Colby and Duhamel, 1991; Colby et al., 1993), the medial intraparietal (MIP) area (Colby and Duhamel, 1996) and area 7b (Graziano and Cooke, 2006; Leinonen et al., 1979; Robinson et al., 1978). In addition, the visual receptive fields of area VIP formed a map of the visual space around the face (Colby and Duhamel, 1991; Colby et al., 1993), presenting a somatotopic organization with separate face, arm and hand representations (Hyvärinen and Shelepin, 1979; Leinonen et al., 1979). Also, neurons in F4 were characterized by relatively large tactile RFs, located on the monkey's face, neck, arm, hand or both hands and face (Graziano et al., 1994; Matelli and Luppino, 2001; Raos et al., 2006). These neurons were multisensory, reporting visual RFs extending for few centimeters from the skin (Rizzolatti et al., 1981b) and "anchored" to the tactile ones, following the movement of the arm (Graziano et al., 1994). Visuo-tactile neurons were also recorded in the rostral subregion F5 of area 6, RFs being located around the face, the hand or both (Rizzolatti et al., 1998). In the putamen, visual and tactile RFs were somatotopically organized on the arm, hand and face, large portion of face neurons responding best to visual stimuli presented close to the face (10-20 cm, Graziano and Gross, 1993). Altogether, these findings demonstrated that neurons in premotor-parietal-subcortical PPS network have visuo-tactile responses with a hand/arm-centered, head- or trunk-based representation. Based on these properties, it was suggested that these regions play a key role in visually guided actions, and that they would more particularly be engaged in the preparation of appropriate motor plans, especially given their anatomical position, at the interface with motor regions (Rizzolatti et al., 1997a, 1997b).

More recently, studies have investigated PPS representation in humans using functional magnetic resonance imaging (fMRI). These experiments have measured sensitivity to either

unisensory or multisensory dynamic visual stimuli presented in the space near the hand, the face or the trunk (Bremmer et al., 2001; Brozzoli et al., 2011, 2012, 2013; Ferri et al., 2015; Gentile et al., 2011, 2013; Holt et al., 2014; Huang et al., 2012; Makin et al., 2007; Schaefer et al., 2012; Sereno and Huang, 2006), identifying regions within parietal and premotor cortices that displayed enhanced or selective activation when stimuli were close to the body, without a clear and direct comparison between PPS representations depending on the part of the body stimulated (but see Grivaz et al., 2017). Brozzoli and coworkers identified through fMRI adaptation a reduction of neural activity following the repetition of near visual stimuli close to the hand within a parieto-premotor network including supramarginal gyrus (SMG), intraparietal sulcus (IPS) and dorsal and ventral premotor cortices (PMd, PMv, Brozzoli et al., 2011). Other investigations relying on different fMRI paradigms converge to indicate the involvement of this network in coding stimuli in close space in humans (Bremmer et al., 2001; Brozzoli et al., 2011, 2012; Gentile et al., 2013; Holt et al., 2014; Makin et al., 2007; Quinlan and Culham, 2007) reporting further activations in the insula (Gentile et al., 2011; Schaefer et al., 2012) and, subcortically, in the putamen (Brozzoli et al., 2011; Gentile et al., 2011). A recent meta-analysis (Grivaz et al., 2017) also points toward a common denominator subserving PPS representation, which includes the postcentral gyrus, IPS, SMG and precentral gyrus (i.e. PMv). How does the network revealed in humans using fMRI relate to that observed in monkeys through single-cell recordings? Can we identify specificities in the neural correlates of PPS representation depending on the body parts stimulated in the same individual?

In light with the first question and to the best of our knowledge, only one study has attempted to unveil the neural correlates of PPS representation in monkeys using fMRI. Cléry et al. (2018) used a naturalistic 3D environment where a cube was presented either close or far from the monkey's body and also found the involvement of a parieto-premotor network in the processing of stimuli near the body (VIP and premotor area F4, Bremmer et al., 2013; Duhamel et al., 1998; Graziano et al., 1994; Rizzolatti et al., 1981a, 1981b). Yet, the network described in their study was far more extended than that previously described by both electrophysiological studies in macaques and fMRI studies in humans, also including regions in posterior and medial parietal areas, area SII and the STS. Single-unit electrophysiological studies in macaque monkeys have focused on specific predefined regions (putamen, premotor and parietal cortices), thus failing to observe the activity of an entire network and its interactions with other brain regions, even with multi-site recordings. Their advantageous spatial resolution comes thus

at the expense of a reliable comparison with the neuroimaging results available in humans, which have the advantage to provide more holistic information on the whole-brain network of areas involved in PPS representation. Furthermore, electrophysiological recordings provide a direct measure of neural activity of a single neuron, whereas whole brain fMRI approach provides an indirect measure of brain activity, sampling the responses of thousands of neurons (i.e. BOLD signal). To compare human fMRI and monkey electrophysiology suffers from discrepancies which are also due to the different experimental paradigms (Boynton, 2011). Applying fMRI to both species, employing the same protocol of stimulation for investigating PPS, the first aim of the current study is to bridge the gap between these two major sources of knowledge about the primate brain. To develop two experimental protocols as similar as possible, considering the different positions of the human (lying in the scanner) and non-human participants (sphinx in an fMRI-compatible chair), the visual stimulation used for the comparison between species was presented only close to the face. In this way, it was possible to ensure the equal distance between face and stimulation and the absence of any physical barrier between the stimulus and the body part, which is not possible in stimulations near the trunk or hand of the macaques, due to technical constraints with the presence of the chair the animals are tested in.

In addition, in humans, where direct access to different body parts was possible, we sought to investigate the neural underpinning of body-part-centered coding of stimuli in the near space within the fronto-parietal network underlying PPS representation. We thus adapted the fMRI adaptation protocol to address this issue by presenting stimuli close to three different body parts -hand, face and trunk. Based on the previous findings described above in particular in monkeys, we predicted a somatotopically organized reduction of BOLD signal in response to repeated presentations of visual stimuli near to the hand, the trunk or the face.

2. Methods

2.1. Participants

For this study, we included two monkeys (two female rhesus monkeys, *Macaca mulatta*, 21-9 years old, hereafter M1 and M2 respectively), to minimize the use of animals, in line with the 3Rs requirements. The monkeys have been trained daily in a mock scanner to maintain fixation on a central point with their head fixed, while seated in a sphinx position in a plastic

primate chair. Animals were maintained on a water and food regulation schedule, individually tailored to maintain a stable level of performance for each monkey. All procedures follow the guidelines of European Community on animal care (European Community Council, Directive No. 86–609, November 24, 1986) and were approved by French Animal Experimentation Ethics Committee #42 (CELYNE).

Human participants (N=2, 24-30 years old, hereafter H1 and H2) were healthy volunteers with no history of neurologic or psychiatric disorders and with normal or corrected-to-normal vision (through eye-lenses). Participants were screened for MRI safety and only after meeting the previous requirements they were enrolled in the study. Written informed consent was obtained from all participants prior to participation. The study follows the Declaration of Helsinki standards and was approved by the Institut National de la Santé et de la Recherche Médicale (INSERM) Ethics Committee (SUD EST IV, ID RCB: 2010-A01180-39).

2.2. Apparatus and procedures

Human participants

During the scanning sessions, participants were lying down comfortably on the scanner bed and foam paddings have been used around their head and knees. A head coil was positioned around their head and stimuli were perceived using a mirror system attached to the scanner head coil. Participants were being told about the importance of keeping still in the scanner. Ear plugs have been used to reduce scanner noise. An MR-compatible stand for the hand (23x16 cm) was mounted on the bed above the participants' waist and was adjusted to allow them to place their (right) arm and hand comfortably at the same position across sessions. An infrared MR-compatible camera (MRC Systems) was mounted on the stand at around 60 cm of the eyes of the participants to monitor eye-movements. The task was controlled by the Presentation® program. Participants were asked to fixate at the camera while a 3D visual stimulus was presented at different distances from their face, trunk or hand (see 2.3 Experimental set-up and task), which could be placed on the stand or alongside the body, in a retracted posture.

Macaque monkeys

Macaque monkeys were surgically implanted with a MR-compatible head post under anesthesia and sterile conditions. During the surgical procedure, the animals were intubated

with a mixture of O_2 and air and their head was immobilized in a stereotactic apparatus. After an incision of the skin along the skull midline, the head fixation device was positioned on the skull, and put in place using ceramic sterile screws and dental cement following approved procedures based on the guidelines of European Community on animal care (European Community Council, Directive No. 86–609, November 24, 1986). After the surgery, monkeys recovered for at least one month. Monkeys were then trained daily to sit in a sphinx position in a plastic chair with their heads fixed, in a mock scanner mimicking the actual MRI environment. Before the scanning sessions, monkeys will undergo training every weekday for 2 to 3 hours.

During the scanning sessions, the monkeys seated in a sphinx position in a plastic chair. Their head was restrained using the surgically implanted head post and they were required to fixate a LED placed at 60 cm away from their face, at eye level, aligned with their sagittal axis. Eye position was monitored at 1000 Hz during scanning using an eye-tracking system (Eyelink 1000 Plus Long Range). The horizontal (X) and vertical (Y) eye positions in degrees have been recorded from the right eye of each monkey in each run. The calibration procedure involved the central LED and 4 additional LEDs (10° eccentricity), placed in the same plane as the fixation LED. All five LEDs were sequentially switched on and off and the monkey was rewarded for orienting and maintaining its gaze towards the illuminated LED. Monkeys were rewarded with splashes of juice dispensed by a computer-controlled reward delivery system (Crist®) through a plastic tube placed in their mouth. The reward volume increased as fixation duration increased. When the animal stopped fixating, the reward was suspended to encourage the monkey to keep the gaze onto the fixation point. Fixation was considered successful if the eyes remained within a window of 4° around the fixation point. The mean percentage of gaze time spent within the fixation window across runs was respectively 86% and 57% for M1 and M2. The task and all behavioral parameters were controlled by the Presentation® program.

2.3. Experimental set-up and task

Humans and monkeys were instructed or trained to maintain their gaze during all scanning sessions. One experimenter stimulated the space around the participant by moving a visual stimulus either close (at 2 cm) or far (at 100 cm) from the body-part or the stand, depending on the experimental condition. These distances correspond to those used in single-cell recording experiments in monkeys (Rizzolatti et al., 1981b) and in fMRI studies on humans (Brozzoli et al., 2011). The visual stimulus consisted of two fluorescent plastic balls (2 cm

diameter) mounted on the tip of two carbon sticks (150 cm long for the close ball and 100 cm for the far ball). Real physical objects were used, rather than artificial computer-generated stimuli, to increase the similarity between our protocol and those used in electrophysiological studies. As humans or monkeys maintained central fixation, the ball appeared in their right peripheral visual field. Only the last portion of the carbon stick and the ball attached to it were visible to the subjects. For the monkeys, because of their sphinx position, a curtain was attached at the edge of the scanner bore to allow the vision of only the last part of the stick and the ball, equaling the experimental conditions of human participants. The experimenter listened to audio instructions regarding the location of the forthcoming stimuli and to a metronome set to a pace of 1 Hz, to guide him to perform up and down movements of 5 cm amplitude of the ball at each position. Ball's movements were video-recorded to check for the accuracy of stimulation offline.

During the scanning session, at the beginning of each run, the position of human participants' right hand was adjusted to keep it on the stand or to retract it along the right side of the body. The experimenter moved the ball either close to the hand on the stand (HAND condition), the face (FACE condition, hand retracted and non-visible) or the empty stand (TRUNK condition, hand retracted and non-visible), in order to assess hand, face and trunk-based PPS representations, respectively. To investigate the neural underpinnings of these PPS representations, looking for both overlaps and possible differences, the three stimulation conditions were compared in human participants. Monkeys maintained their hands retracted inside the chair, and the experimenter could only move the ball close to or far from the face (FACE condition). This type of protocol allowed us to investigate the hand-, trunk- and face-based PPS representations in healthy humans and, at the same time, to compare human's and non-human primate's face-centered PPS.

The fMRI adaptation protocol we adopted included four combinations of visual stimuli: Near-Near, Near-Far, Far-Near, and Far-Far, each combination lasting a total of 6 s divided into a first and second part of equal length. Therefore, each stimulation period lasting 3 s was modelled with 8 separate regressors: Near before Near, Near after Near, Near before Far, Far after Near, Far before Near, Near after Far, Far before Far and Far after Far (Figure 2). Each run was composed of these 4 combinations of stimuli repeated 12 times (48 stimuli per run). Consecutive trials were separated by a jittered inter-trials baseline interval (3 to 11 s) with no

stimulation (see Figure 1). During these baseline periods, humans and monkeys should maintain their gaze on the central fixation point. In each human session, a total of 6 runs were collected: 1) two runs with the right hand visible and visual stimulation close to or far from it, 2) two runs with hands retracted and visual stimulation close to or far from the stand 3) two runs with hands retracted and visual stimulation close to or far from the face. The order of the 3 different types of runs was counterbalanced across sessions. For monkeys, a total of 17 and 15 runs, respectively for M1 and M2, with the visual stimulation close to or far from the face have been collected across different sessions.

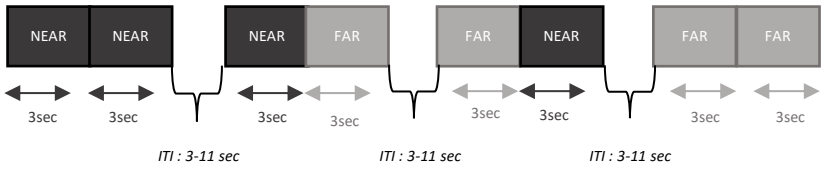

Figure 1: Task design. The four combinations of stimuli adopted in the study: Near-Near, Near-Far, Far-Near and Far-Far. Each combination was split into two parts of 3 sec each for a total duration of 6 sec. One run was composed of these 4 combinations of stimuli repeated 12 times. Conditions were separated by a jittered inter-trial interval (ITI, 3-to-11 s) with no stimulation.

2.4. MRI Data acquisition

Neuroimaging data have been collected using a 3T Siemens Magnetom Prisma scanner. In humans, we used a Siemens 64-channel head coil. An anatomical MRI has been collected for each participant at the beginning of the experiment using a T1-weighted MPRAGE 3D (voxel size=1x1x1 mm; 192 slices, TR=3000 ms, TE=3.34 ms, TI=1100 ms, flip angle=8°, matrix: 224x256). For each fMRI volume, 40 slices covering the whole brain have been collected in an ascending order (BOLD-sensitive T2* weighted echo planar sequence, TR=2200 ms, TE=29 ms, flip angle=90°, FOV=546x546mm, matrix size=78x78, voxel size=2.7 mm^3). Each run consisted of 320 volumes for a total of 2100 volumes per session.
In monkeys, MRI images have been collected with a custom-made 8 channels receive surface coil, positioned around the head. A circular transmit coil was positioned above the head (Mareyam et al., In: Proceedings of the 19th Annual Meeting of ISMRM, Montreal, Canada, 2011). For each fMRI volume, 38 slices covering the whole brain have been collected in an ascending order (BOLD-sensitive T2* weighted echo planar sequence, TR=2500 ms, TE=30

ms, flip angle=90°, FOV=588x532 mm, matrix size=84x76, voxel size=1.25 mm^3). Each run consisted of 350 volumes for a total of 1980 volumes per session. The anatomical MRI data have been collected at the beginning of the experiment in high-resolution T1-weighted MPRAGE 3D in the sagittal plane (voxel size=0.5 mm^3 thickness, TR=3000 ms, TE=3.62 ms, FOV=320 x 210).

2.5. MRI Data preprocessing

fMRI data have been preprocessed with SPM12 software (Wellcome Department of Cognitive Neurology). For humans, functional images have been realigned to correct for head movements and underwent slice timing correction. The anatomic and functional volumes have been coregistered with the high-resolution structural scan from each individual participant and normalized to Montreal Neurological Institute (MNI) standard brain space. The anatomical images have been segmented into white matter, gray matter, and CSF partitions and also normalized to the MNI space. For monkeys, the same preprocessing has been applied to anatomical and to all functional volumes except for the normalization. The functional images have been then spatially smoothed with an 8 and 4 mm FWHM isotropic Gaussian kernel, in humans and monkeys, respectively, based on the respective voxel size for each species.

2.6. Regions of Interest

The regions of interest (ROIs) of the e humans ROIs, the following regions of the AAL3v1 atlas (Rolls et al., 2020) were considered bilaterally: precentral gyrus, postcentral gyrus, superior and inferior parietal lobule, supramarginal gyrus and putamen (Bremmer et al., 2001; Brozzoli et al., 2011, 2012; Gentile et al., 2011, 2013; Holt et al., 2014; Makin et al., 2007; Quinlan and Culham, 2007; Schaefer et al., 2012b; and see Grivaz et al., 2017 for a meta-analysis). To refine the localization of the activation peaks, we then used the Glasser multi-modal Atlas parcellation (Glasser et al., 2016), carried out on four different features, including both anatomical and functional criterion: cortical thickness, myelin maps, task fMRI and resting state fMRI (Glasser et al., 2016). Similarly, the results from the literature on the neural basis of the monkeys' PPS suggested bilateral extraction of the premotor area, S1, ventro-medial and lateral IPS, area 7 and area 5 (Bremmer et al., 2013; Colby and Duhamel, 1991, 1996; Colby et al., 1993; Graziano and Cooke, 2006; Graziano et al., 1994; Leinonen et al., 1979; Rizzolatti et al., 1981b; Robinson et al., 1978) ROIs from the fourth level of the CHARM atlas (Jung et al.,

2021). Furthermore, from the fourth level of the SARM atlas (Hartig et al., 2021) the ROI of the putamen was extracted at bilateral level (Graziano and Gross, 1993). As for human participants, a more detailed localization of activation peaks was achieved thanks to the 6 levels of the CHARM and SARM atlases, which also feature fined-grained anatomical and functional descriptions of brain areas.

2.7. Imaging Data Analyses

Our aim is to identify brain regions that are sensitive to the presentation of visual stimuli in near space (i.e. PPS) in humans and macaques within the ROIs mask. We performed first-level univariate and adaptation analyses on smoothed data, by defining a general linear regression model to all runs concatenated across sessions, depending on the body-part stimulated. We further performed multi-voxel pattern analysis (MVPA) on the unsmoothed data (see description below). Furthermore, we performed conjunction and disjunction analyses on both univariate and MVPA results on human participants to investigate both overlapping and specificities of the three body-part-based PPS representations. Details about adaptations analyses, tables and results could be found in Supplementary Materials.

Univariate fMRI analysis: neural correlates of near space processing in macaques and humans

First, in order to identify brain regions implicated in near space processing independently of the body part stimulated we defined regressors of interest corresponding to near or far space in each run: Near-before-Near, Near-after-Near, Near-before-Far and Near-after-Far for the near space processing and Far-before-Far, Far-after-Far, Far-before-Near and Far-after-Near for the far space processing. These 8 regressors have been modeled with the standard SPM12 hemodynamic response function. In addition, 6 regressors of no interest have been modeled, corresponding to the head movement parameters in each run. In the first level analysis, we compared near stimulations (combining Near-before-Near, Near-after-Near, Near-before-Far and Near-after-Far regressors of interest) with far stimulation (combining Far-before-Far, Far-after-Far, Far-before-Near and Far-after-Near regressors of interest) including all conditions (i.e. 6 runs per session in total: face, hand and trunk, which means a total of 30 runs per subjects) (**Table 1**). The results from this analysis provided beta estimates, obtained by contrasting these two groups of conditions for each subject. We first thresholded the

activations at $p<0.001$ uncorrected and reported only the clusters surviving a significance cluster threshold of $p<0.05$, corrected using Family-wise error rate (FWE) implemented in SPM12.

Multi-voxel pattern analysis: specific activation patterns for representations of space centered on different body parts

It is possible that the differences between near and far stimulations are represented by patterns of activations within the selected ROIs, rather than specific and punctual variations of activation within these areas. In the first case, a general linear model could not capture these differences, and even adaptation analyses (see Supplementary Materials), despite the greater spatial resolution power of the reported signal, could not provide information regarding the spatial distribution of specific activations. For this reason, we conducted MVPA at the single subject level. For this purpose, the acquired images were subjected to the same preprocessing described above, but without proceeding with the final smoothing.

Firstly, we calculated the β weights of the eight stimulation conditions (Near before Near, Near after Near, Near before Far, Near after Far and vice versa for far stimulations) for each run of each human and non-human primates participant, within the ROI mask previously described. In this way, 30 β weights were obtained for each condition for each human participant and 17 and 15 β weights respectively for M1 and M2. To investigate the difference between stimulations close to and distant from specific body-parts, we selected the four Near conditions (Near-before-Near, Near-after-Near, Near-before-Far, Near-after-Far) and the four Far conditions (Far-before-Far, Far-after-Far, Far-before-Near, Far-after-Near) of each body district (HAND, FACE, TRUNK) and for each voxel within the ROI mask we defined a spherical neighborhood of 100 voxels (searchlight). Considering the different extension of the investigated surface in human participants (7519 voxels) and in non-human primates (1697 voxels), the extension of the searchlight was also adapted according to the species: 100 voxels in human participants, 20 voxels in monkeys (the results of the analyses conducted with a searchlight of 100 voxels in the two macaques were in line with those that will be reported here). We then conducted a searchlight analysis using the linear discriminant analysis (LDA) classifier implemented in CoSMoMVPA (Oosterhof et al., 2016) with a leave-one-out approach (see Table 1): the accuracy map was then obtained by training the classifier on the near versus far difference in n-1 runs (n=10 for human participants, 17 and 15 for monkeys) and testing this

difference on the remaining run. To compare the accuracy map of the classification thus obtained against the chance level, we performed a threshold-free cluster enhancement (TFCE) analysis (through cosmo_montecarlo_cluster_stat, implemented in CoSMoMVPA) defining a mean of 0.5 under the null hypothesis and comparing the initial accuracy map versus 1000 maps with permuted targets (the Near and Far conditions used in training and test). Finally, we reported the voxelwise corrected statistical map ($z=1.65$; $p<0.05$, one-sided t test) for each participant and each spatial district investigated.

Complementary to the MVPA analysis described above, we conducted cross-validation analyses to investigate the discriminability of the activation patterns linked to the specific body districts stimulated. As in the previous analysis, the β weights of each condition in each run were introduced into an LDA classifier with a leave-one-out cross-validation approach (see Table 1). In this method, the classifier is trained on n-1 runs of the conditions of one of the investigated body districts (i.e., the face) and tested on the remaining run of another district (i.e., the hand). A searchlight including 100 voxels (20 voxels for non-human primates) around the central voxel was then conducted for each voxel in the ROI mask. In addition to the statistical map obtained in this way, another 1000 maps were obtained by randomly permuting the training and testing runs. As previously described, these maps were subjected to a TFCE analysis with a mean of 0.5 under the null hypothesis, in order to report the voxelwise-corrected maps for each participant ($z=1.65$; $p<0.05$, one-sided t test).

Conjunction analysis in humans: common and specific representations of space centered on different body parts

To test our second hypothesis, concerning the possible specificities at the level of brain activations for the different body parts, we conducted disjunction analysis between the HAND, FACE and TRUNK conditions using the AFNI *3dcalc-step* function, using as input the thresholded maps of these three conditions obtained through the univariate analyses. In this way, it is possible to observe the specific activations of each condition, with the hypothesis that stimuli close to different body-parts induce spatially distinct activation peaks within the same ROIs. Furthermore, we studied the conjunction between the different conditions, highlighting the common activations induced by stimulations close to the hand, the face and the trunk, regardless of the body-parts.

Table 1: **Summary of the planned fMRI analysis.** On the left, univariate analysis to compare near and far stimulations, for all conditions (HAND, TRUNK and FACE). On the right, MVPA classifier within condition, trained and tested on the near vs far difference with a leave-one-out method. In the lower panel, cross-validation MVPA, training the classifier on the near vs far difference in one condition and testing it on a different condition, with a leave-one-out method.

	Univariate Analyses
Selectivity for NEAR stimulations	**Near Condition**
	Near-Before-Near
	Near-After-Near
	Near-Before-Far
	Near-After-Far
	versus
	Far Condition
	Far-Before-Far
	Far-After-Far
	Far-Before-Near
	Far-After-Near

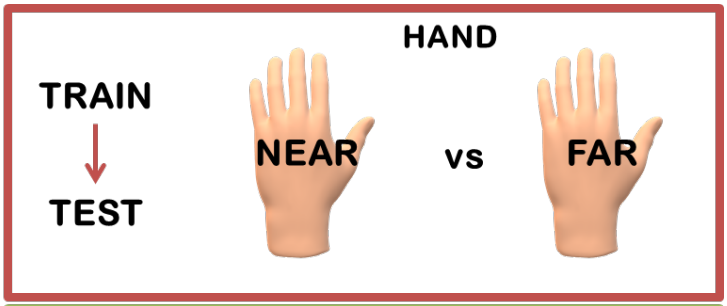

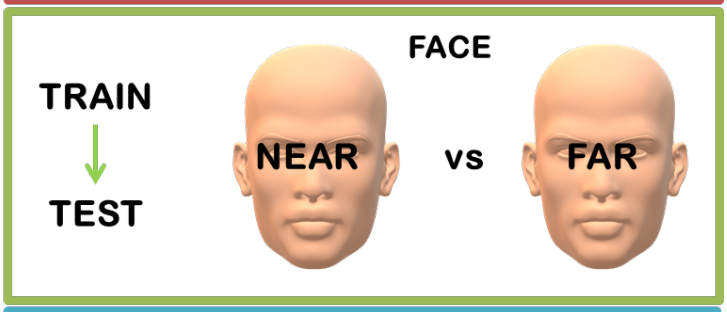

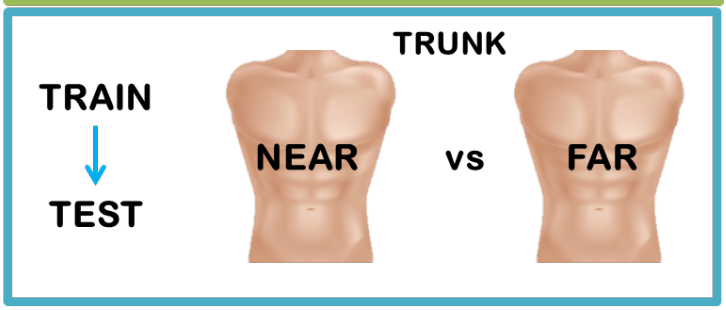

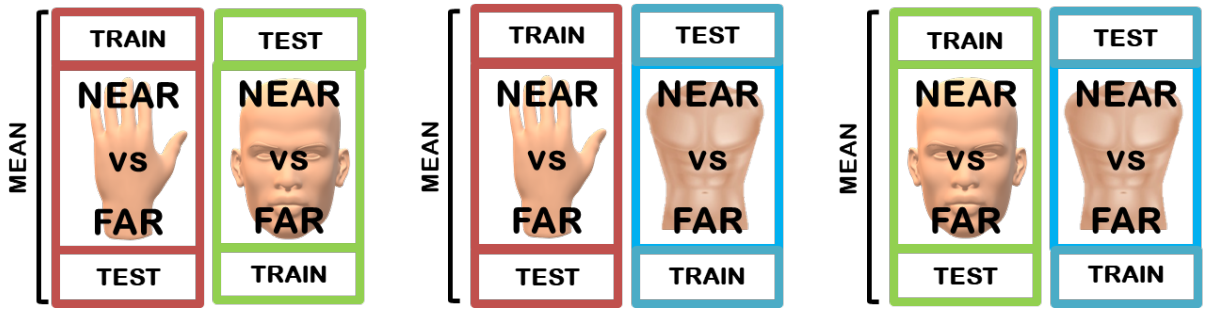

3. Results

3.1. First Aim: cross-species comparison of head-based PPS

Human's univariate and MVPA fMRI analyses

First-level analyses of brain responses associated to stimuli near to or far from the face stimulations on human participants highlighted the broadest network of activations. Comparing the Near versus the Far regressors, it was possible to find five different clusters in the subject H1, three in the right hemisphere and two in the left one. In the right hemisphere, such clusters include SMG, S1 ($k=269$, $t_{peak}=16.21$), the IPS ($k=519$, $t_{peak}=14.45$) and several portion of the premotor cortex, including PMd and PMv ($k=220$, $t_{peak}=8.83$). The two clusters on the left cover the homologous contralateral areas: the IPS ($k=394$, $t_{peak}=12.2$), S1 and large portions of both the SMG and the premotor cortex ($k=1331$, $t_{peak}=9$). The activations observed for subject H2 are consistent with those observed for H1, with two significant clusters per cerebral hemisphere. The two right-hemisphere clusters include broad regions of the SMG, IPS, S1 ($k=1436$, $t_{peak}=15.74$) and premotor cortex ($k=292$, $t_{peak}=10.94$). The left clusters include the contralateral homologous areas: IPS ($k=421$, $t_{peak}=14.35$), SMG, S1 and a large part of the premotor cortex ($k=1120$, $t_{peak}=12.02$). An exhaustive list of the clusters of activation can be found in Table 2A, significant clusters are also displayed in Figure 2A.

The results obtained by the LDA classifier used to investigate the discriminability between stimulations near and far from the face revealed activation patterns similar to those observed for the hand and the trunk (displayed in Figure 3A). In particular, a bilateral pattern of activations is observed for both H1 and H2, with a cluster in the left hemisphere ($k=1851$, $z_{peak}=3.09$ and $k=2107$, $z_{peak}=3.09$ for H1 and H2 respectively) including wide portions of the SMG, the premotor region, the IPS and the postcentral gyrus. In the right hemisphere, both subjects show activation clusters ($k=2064$, $z_{peak}=3.09$ and $k=2411$, $z_{peak}=3.09$ for H1 and H2 respectively) that include the same areas described for the left hemisphere: SMG, PMd, PMv, S1 and IPS among the others. The exhaustive list of the areas involved in this broad activation pattern is reported in Table 3A.

To summarize, the results obtained with the univariate and MVPA analyses (as well as with the adaptation analyses, see Supplementary Materials) on human participants are consistent with

each other in showing a fronto-parieto-supramarginal activation network underlying the encoding of visual stimuli close to the head.

Monkey's univariate and MVPA analysis

Consistent with what has been observed for humans, brain responses to stimulation near the face involve a large bilateral network in monkeys. In M1, three significant clusters ($p<0.05$ FWE corrected) are observed, two of which lateralized to the left and including the areas F4, F5, PMdc ($k=97$, $t_{peak}=11.02$) and the putamen ($k=100$, $t_{peak}=6.68$). The remaining cluster is very large ($k=727$, $t_{peak}=16.29$) and covers both hemispheres, reporting activation peaks in multiple PPS-related areas, such as MIP, VIP, LIPd and area 7 bilaterally plus area 5, the putamen and somatosensory areas 1-2 in the right hemisphere.
Also for the second monkey, close-to-the-face stimuli activate a large bilateral network. Four significant clusters are found, of which only one on the left ($k=624$, $t_{peak}=17.15$) and including LIPv, VIP, areas 7a and 7b, premotor areas F4, F5 and PMdc, areas 1-2 and the putamen. The three clusters of the right hemisphere, in turn, cover premotor areas, such as F5 and PMdc ($k=107$, $t_{peak}=10.93$), parietal areas, such as LIPv, VIP and the right area 3a/b ($k=241$, $t_{peak}=8.93$) and the putamen ($k=136$, $t_{peak}=8.69$). Results of this analysis are reported in Table 2B and displayed in Figure 2B.

As observed in human participants, also in monkeys the activation pattern related to the Face condition is very extensive, and reports activation peaks in both hemispheres, both at cortical and subcortical level. For M1, a pattern consisting of two clusters in the left hemisphere and two in the right one is observed. In both hemispheres one of the clusters is located frontally, including the entire premotor cortex (F4, F5, PMdc and PMdr) on the left ($k=108$, $z_{peak}=3.09$) and the premotor cortex (F4, F5) plus the putamen on the right ($k=55$, $z_{peak}=3.09$). The other cluster of each hemisphere is located in a more posterior position, at the parietal level; on the left ($k=204$, $z_{peak}=3.09$) it involves PPS-related areas such as VIP, MIP, area 5, different portions of area 7 (7b, 7a, 7_OP) and the lateral section of the IPS (AIP, LIPv, LIPd). On the right ($k=105$, $z_{peak}=3.09$) we find activations consistent with the contralateral cluster, with the exception of AIP. M2 also shows an activation pattern sensitive to the difference between close- to and far-from the face stimulations involving PPS-related fronto-parietal areas of both hemispheres. A large cluster in the left hemisphere ($k=738$, $z_{peak}=3.09$) reports activation peaks

at the subcortical level (putamen), frontal cortex (premotor regions such as F4, F5 and PMdc, but also somatosensory regions such as areas 1, 2 and 3a/b) and parietal cortex (large portions of area 7, area 5 and the lateral and ventro-medial regions of the IPS). On the right, the pattern consists of two different clusters, one subcortical (putamen, k=71, z_{peak}=3.09) and one cortical (k=506, z_{peak}=3.09), including premotor regions F4 and F5, somatosensory areas and parietal areas located in area 5, area 7 and in the lateral and ventromedial portions of the IPS. These results are reported in Table 3B and illustrated in Figure 3B.

To summarize, univariate and MVPA analyses on non-human primates also identified a fronto-parietal network of areas associated with the encoding of stimuli close to the head. These results, in addition to being in line with what has been observed in the literature (see Cléry et al., 2015a for review), are similar to those observed in human participants (see Discussion).

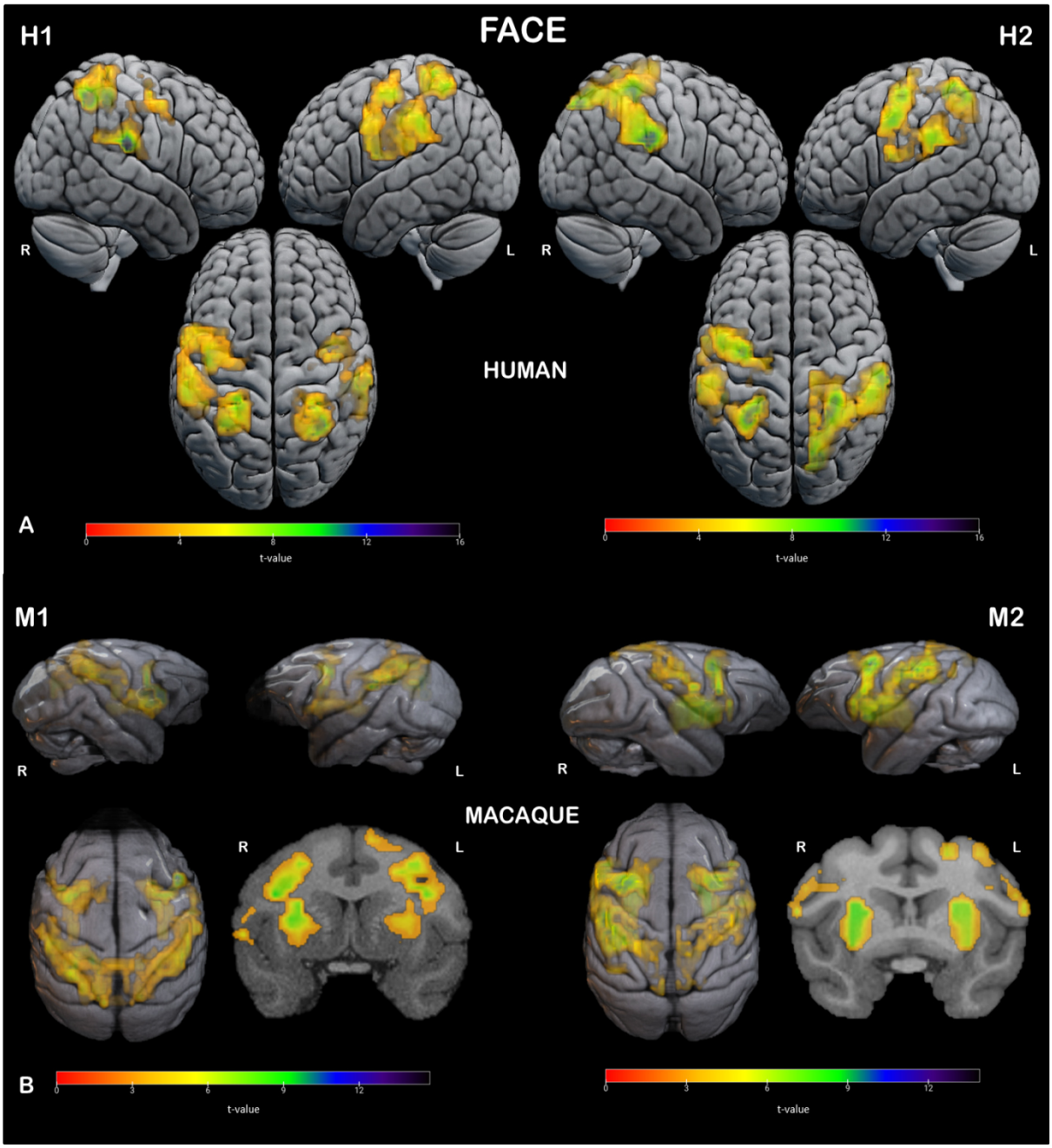

Figure 2. Results from univariate analyses comparing visual stimuli close to or far from the FACE in humans (A) and non-human primates (B). t-maps of significant clusters ($p<0.05$, cluster-based FWE corrected) for Near vs Far stimulations for H1 (upper left), H2 (upper right), M1 (lower left) and M2 (lower right).

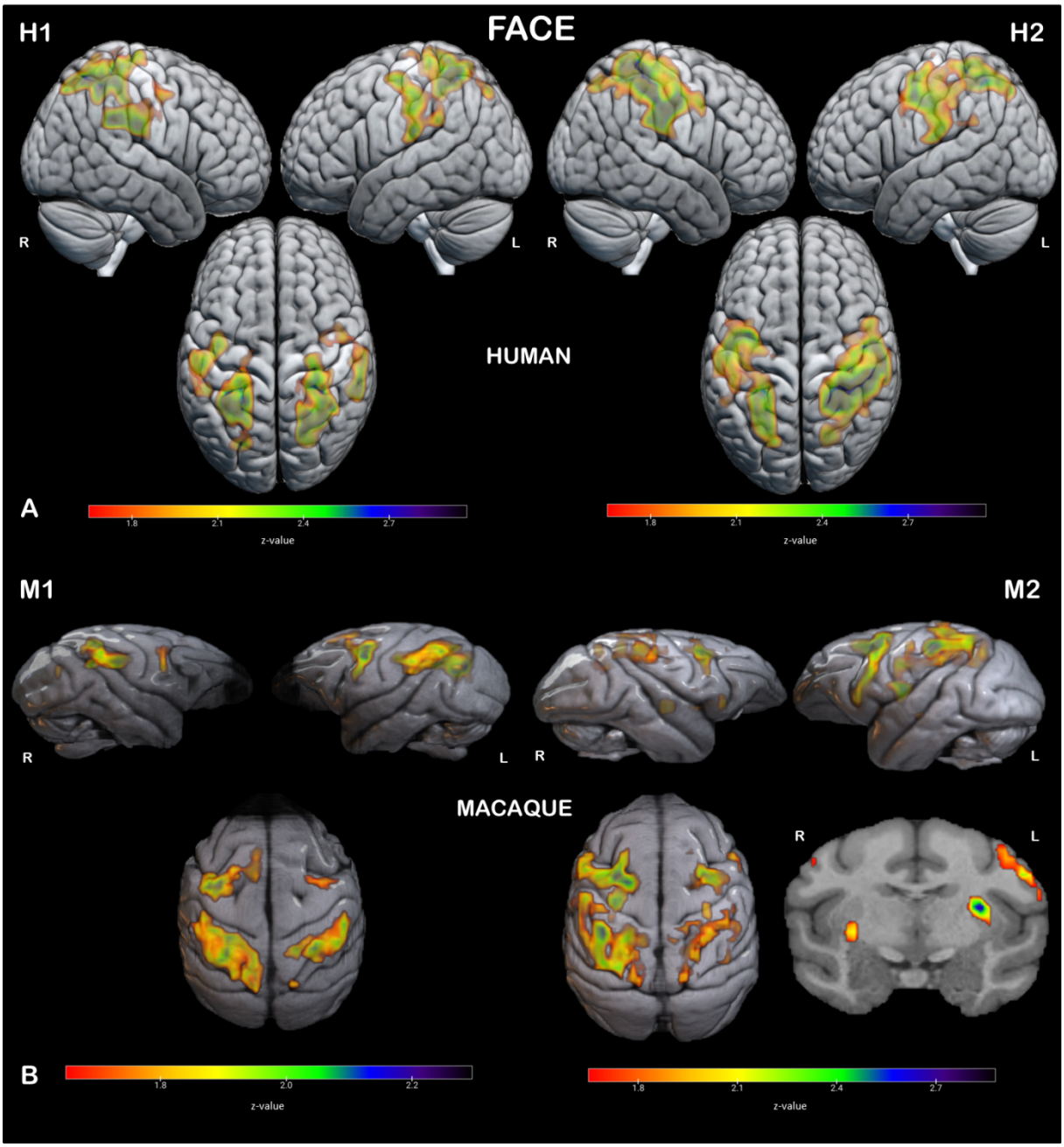

Figure 3. Results from MVPA comparing visual stimuli close to or far from the FACE in human (A) and non-human primates (B). z-maps of significant clusters (z<1.65, one-sided t test) for Near vs Far stimulations for participants H1 (upper left), H2 (upper right), M1 (lower left) and M2 (lower right). For illustrative purposes, z-maps were smoothed after statistics (6 and 2 voxels smoothing for humans and monkeys respectively).

3.2. Second Aim: between body-parts-based PPS comparisons in humans

Visual stimulation presented near the face showed activation clusters consistent with what has been observed in the literature (see Grivaz et al., 2017), including a network of fronto-parietal areas involving the dorsal and ventral premotor cortices, large portions of bilateral SMG, IPS and adjacent parietal regions. To compare the specific and common neural activations for the three body districts investigated, we conducted univariate, adaptation and MVPA analyses (the last two approaches reported in Supplementary Materials) also on the responses observed following stimulations presented near to or far from the hand and trunk.

Univariate fMRI analysis: Hand

We performed a first-level analysis by defining a general linear regression model to the data. We compared all Near regressors with all Far regressors**,** corresponding respectively to visual stimulation near to and far from the hand. For H1, the univariate contrast between near and far hand stimulations revealed two significant activation clusters, one in the left hemisphere (k=1627, t_{peak}=18.56) including several peaks of activation in all the ROIs (SMG, IPL, SPL, Precentral and Postcentral gyri), and a smaller one in the right hemisphere (k=309, t_{peak}=13.54), including SMG and the postcentral gyrus. H2 reported an activation cluster at the level of the right SMG (k=168, t_{peak}=10.41) and three clusters in the left hemisphere, including several IPS portions and S1 (k =426 t_{peak}=16.3), the SMG (k=366, t_{peak}=14.53) and the premotor region (k=137, t_{peak}=8.78). These results are displayed in Figure 4; peak of activations and the respective MNI coordinates are reported in Table 4.

Univariate fMRI analysis: Trunk

As already described for the hand, first-level analyses were conducted to compare the Near versus the Far regressors in the trunk condition. In H1, the contrast shows two significant clusters, one in the left hemisphere (k=959, t_{peak}=11.37), including areas in the SMG, the IPS and S1, the other in the right hemisphere (k=150, t_{peak}=9.58), involving several portions of the SMG ROI. The second participant, on the other hand, reports a significant cluster (k=316, t_{peak}=11.93), lateralized to the left and including several portions of the IPS and S1. These results are displayed in Figure 4; peak of activations in MNI coordinates are reported in Table 5.

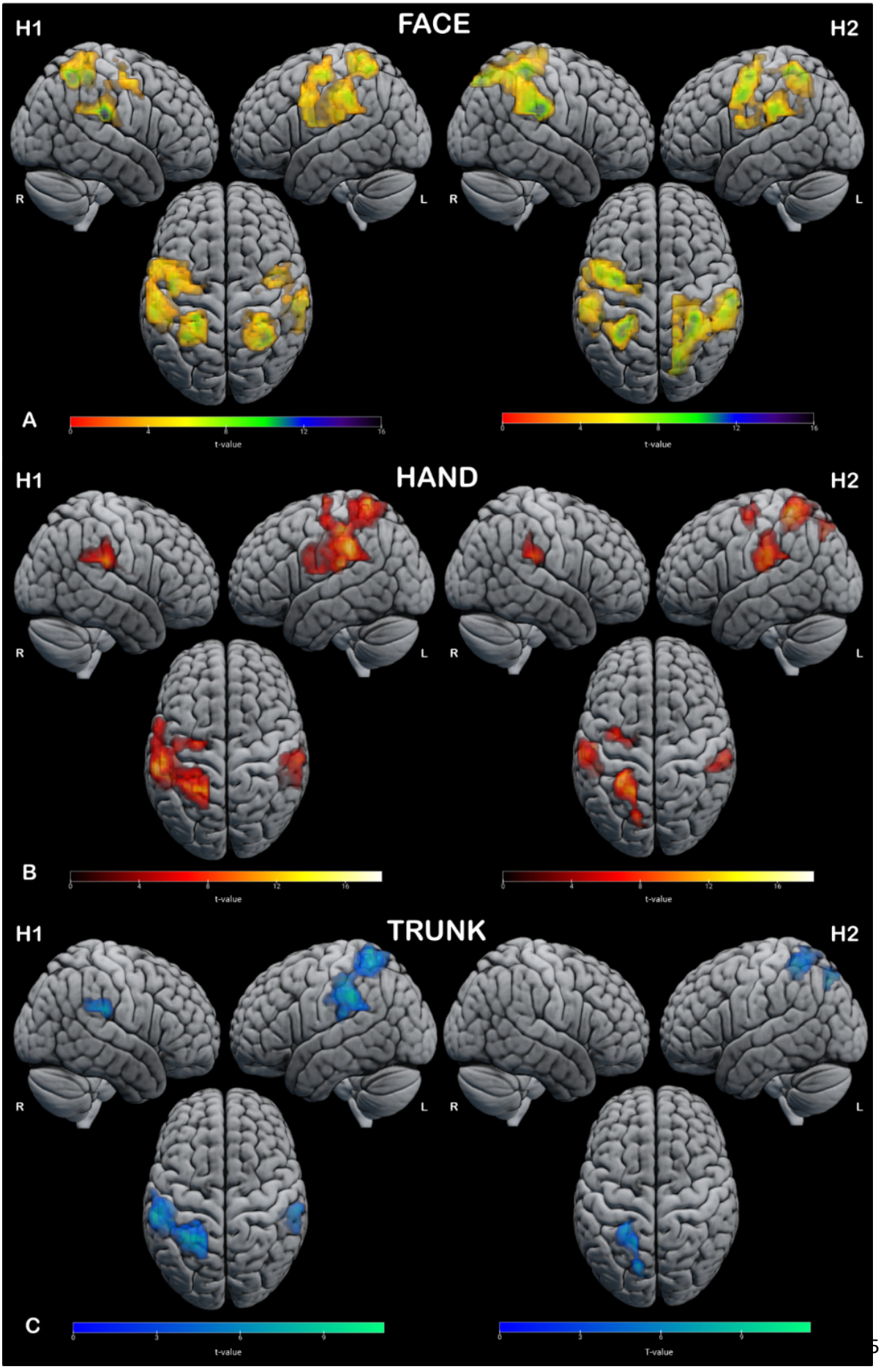

Figure 4. Results from univariate analyses comparing visual stimuli close to or far from the FACE (A), the HAND (B) or the TRUNK (C) in human participants. t-maps of significant clusters ($p<0.05$, cluster-based FWE corrected) for Near vs Far stimulations for H1 (left side) and H2 (right side).

Cross-classification between different body-parts

In search of an activation pattern sensitive to the difference between close-to or far-from the body stimulations, regardless of the stimulated body-part, we conducted cross-classification MVPA analyses between the three conditions (HAND, TRUNK and FACE). By training the classifier on the activation associated with stimulations near or far from a specific part of the body and testing it on the pattern related to this difference but associated with a different body-part (see Table 1), it is indeed possible to investigate common activations across body sectors. The results relating to the three different dyads tested (Hand-Trunk, Hand-Face and Trunk-Face) are shown in Table 6. The activation loci are reported in MNI coordinates.

By training the classifier on the near-far difference associated with the Hand condition and testing it on the Trunk one, it was possible to observe a pattern of activations common to these body districts in both H1 and H2. The pattern of responses common to these two conditions is quite broad in both participants, and involves a bilateral network of fronto-parietal areas. In H1 a large cluster is observed in the left hemisphere (k=2664, z_{peak}=3.09) with activations in all the ROIs tested and in particular in PMd, PMv, and several portions of the IPS (VIP, LIPd, LIPv) and of the PF complex. These activations are also found in the right hemisphere, divided into three different clusters (respectively k = 842, z_{peak} = 3.09; k = 211, z_{peak} = 3.09; k = 36, z_{peak} = 2.17). Moreover, both hemispheres reported activations in somatosensory areas as 1, 2, 3a and 3b. Similarly, a left cluster (k = 2313, z_{peak} = 3.09) is found in H2 response pattern including the same areas described for participant H1, and including also MIP and AIP regions within the IPS. Finally, the two clusters observed in the right hemisphere reported peaks of activation in the same areas (respectively k = 1918, z_{peak} = 3.09 and k = 9, z_{peak} = 1.94).

The common response pattern to hand and trunk conditions appears to be the largest, in both participants. However, the other two dyads tested also report common responses. Regarding Hand-Face cross-validation, for example, H1 reports two clusters in the left hemisphere including SMG (PFcm, PFop, PFt and PSL), premotor regions (PMd and PMv), several portions of postcentral gyrus such as S1 and M1 (k = 884, z_{peak} = 3.09) and a small cluster in the IPS (k = 10, z_{peak} = 1.91). In the right hemisphere, common activations are divided into a cluster at the SMG level (k = 341, z_{peak} = 3.09), including a broad portion of the PF complex, and one in the postcentral gyrus (k = 45, z_{peak} = 2.47), including areas 2 and 3b. Also for H2 the activation

pattern is distributed bilaterally, with a left cluster (k = 836, z_{peak} = 3.09) including SMG, PMd, PMv, M1, S1 and IPS (LIPv and AIP) and a right cluster (k = 960, z_{peak} = 3.09) involving PMd, IPS (VIP and AIP), area 7 in the superior parietal lobule, the PF complex and different portions of S1 (areas 2, 3a and 3b).

The third dyad investigated, Trunk-Face, is the one that reported the least extensive pattern of common activations. However, a strong overlap of activations in PPS-related areas is observed. H1 reports indeed an activation cluster at the level of the right SMG (k = 254, z_{peak} = 3.09), including a large part of the PF complex, and three clusters in the left hemisphere, located at the level of the SMG (k = 551, z_{peak} = 3.09), of the postcentral gyrus (k = 98, z_{peak} = 3.09), including areas 1 and 3b, and IPS (k = 58, z_{peak} = 3.09), particularly VIP and LIPv. The clusters at the level of SMG and IPS in the left hemisphere are also found in H2 (respectively k = 168, z_{peak} = 3.09 and k = 173, z_{peak} = 3.09), to which however a small more frontal cluster is added, at the level of PMd (k = 22, z_{peak} = 2.87). In the right hemisphere, activations in SMG are confirmed and an activation peak in premotor region is added (k = 480, z_{peak} = 3.09).

To summarize, the cross-validation analyses carried out between the three different dyads of body parts investigated allowed us to observe that, although important similarities are present, the fronto-parieto-supramarginal networks involved in the encoding of stimulations near different parts of the body have some differences. These results, treated in more detail in the Discussion, are consistent with the body-part-centered reference frame of the PPS highlighted in the literature.

Conjunction analyses: a common pattern of activations for hand-, face- and trunk-based PPS representation

In order to compare the activation pattern in response to stimuli close to the body elicited by the three experimental conditions (HAND, FACE and TRUNK), we then conducted conjunction analyses on the human participants using the thresholded maps of activations obtained through the univariate analyses of each condition.

Consistent with the MVPA results, these analyses revealed the existence of a common activation cluster, in both subjects, at the level of the superior and inferior left parietal lobules. In particular, both H1 and H2 reported activations in different portions of the left IPS, such as LIPv, the lateral section of area 7a and area 7PC. Within this activation cluster, a peak is also

found in the postcentral gyrus, within area 2 (S1). However, the activations common to HAND, FACE and TRUNK conditions are not limited to this region for H1, whose left hemisphere cluster also includes other regions of the superior (medial 7A, area 5 and VIP) and inferior parietal lobule (PFt and PFcm) and a large part of the supramarginal gyrus (including the areas OP4, PFop, PFt, PF and PSL). Moreover, H1 also reports activations in the right hemisphere, again at the level of the supramarginal region including the two sections of the PF complex, PFop and PFcm, the perisilvian region (PSL) and the superal temporal visual area.
These results therefore confirm the existence of a core of brain areas that seem to respond to the distance of stimulations from the body independently of the body-part involved.

In addition to this overlapping between the neural response to close to the hand, the face and the trunk stimulations, we investigated brain regions that reported preferential responses only to stimuli presented near the hand or face. Evidence in the literature reports, especially at the premotor level, the existence of neurons active in response to stimulations close to the hand or to the mouth (Rizzolatti et al., 1981a, 1981b), or able to respond to stimulations near the face and movements of the hand towards the mouth (Gentilucci et al., 1988). We therefore wondered if it was possible, through our experimental protocol, to observe brain regions in human participants capable of responding to close to the hand or to the face stimulations.
We observed areas in which the response to stimulations close to the two different body districts overlaps, especially at the level of the left precentral and supramarginal gyrus, for both participants. Indeed, both H1 and H2 report an activation cluster in the left premotor cortex, including different portions of area 6 (including its dorsal, ventral, anterior and medial-posterior parts). It is interesting to observe that this cluster seems to interpose itself between premotor regions with preferential response to close to the hand stimuli and regions with face-specific preferential responses, in both participants. The same appears to be true in left SMG, where both participants report an activation cluster that includes several portions of the PF complex, including PFt and PFop. In this case, however, the activation cluster of H1 are less extended and more lateralized than that of H2, but this is due to the greater extension in H1 of the supramarginal cluster in which the conjunction of the responses to the three stimulated parts of the body is found. In both subjects, however, this cluster of response to close to the hand or the face stimuli is localized between the hand-specific areas at the postcentral / precentral level and the more posterior and superior supramarginal areas, where in H2 specific responses are found for stimuli within the peri-head space and in H1 nonspecific responses for all stimuli close to

the body. Finally, both subjects show a small cluster at the level of the SPL, where the conjunction between the three parts of the body takes over, centered in both cases in the most dorsal section of the 7Al area.

In the right hemisphere, on the other hand, overlapping clusters between hand and face are found only in the SMG, including the more anterior and posterior portions of the PF complex in H1, bordering the area in which the triple conjunction takes place, and the central portion in H2, which did not display triple conjunction in this hemisphere. In this second case, hand-face activations were surrounded by face-specific response regions.
Results of these conjunction analyses are reported in Table 7 and displayed in Figure 5.

Specific neural activations for hand-, face- and trunk-based PPS

Besides the common activations for stimulations within different body-part-based PPS representation, our initial hypothesis concerns the possible differences, at the neural level, of these latter. For this reason, we identified regions that selectively responded to visual unimodal stimulations presented near the face, hand or trunk. The activation peaks for each body part are reported in Table 8 and displayed for both participants in Figure 8. Qualitatively, the results show that the representation of each body part stimulation has a different spatial pattern and extension, with a more restricted territory for trunk representation. The representation of the space around the head and hand shows more extensive and bilateral activations, especially at the supramarginal and premotor level. It is in these two regions that the greatest overlaps are found between the activations associated with these two body districts, while the neural responses associated with stimulations close to the trunk are more represented at the parietal level, and particularly in the left hemisphere.

Specifically, the trunk (represented in light blue in Figure 5) appears to be the body part with less specific activation: H2 does not exhibit any significant activation and in H1 only a small cluster can be observed at the parietal level, including the posterior part of area 7PC and the central portion of the VIP.
The second specific network body-part, in order of extension, is the one related to the hand (depicted in orange in Figure 5). In this case, indeed, bilateral specific activations are observed for H1, which in the left supramarginal gyrus include the most rostral part of the OP4 area and

the section of OP1 bordering the previous one, but also the most superior section of the PF complex. Still in the left hemisphere, but at the level of the IPL, hand-specific activations are found in the sections of the AIP and the 7PC areas bordering area 2, but also in the upper part of the latter and, in the postcentral gyrus, in area 1. Finally, the last activation cluster of the left hemisphere is found more frontally, in the most dorsal part of area 55b. In the right hemisphere, H1 displays specific activations for close-to-the-hand stimulation at the SMG level, in particular in the border region between the PFt and PF area and in that between the PF and PSL area. Finally, more ventrally, an activation cluster is observed at the level of the temporo-parietal-occipital junction. H2 also reports multiple activation clusters specific to stimulations within the peri-hand space. In the left hemisphere, coherently with what was observed for H1, activations are found at the level of the SMG, in the central section of the OP4 area and in the anterior superior one of the PF complex. Still in the SMG, but more dorsally, activation clusters are found at the level of the upper portion of the PFt area and, on the border between SMG and IPL, of the most posterior part of area 1, at the limit with PFt. Finally, in the SPL, foci of hand-specific activation are found in area 7PC, in the most dorsal part of the VIP area and in area 5, bordering the lateral section of area 7A.

The last and largest specific network is that relating to stimulation within the peri-head space (represented in green in Figure 5). The two participants reported in this case multiple overlapping, in both hemispheres. At the level of the left precentral gyrus, H2 shows a large cluster of activation in the region of the posterior inferior frontal junction, which occupies the entire junction up to occupy the ventral part of the PEF, in which it is possible to find face-specific activation also for H1, and the dorsal portion of the rostral area 6. This cluster also extends to the ventral part of area 6 (PMv), where specific activations are also found for H1. Furthermore, both subjects reported activations in the left 55b area (H1 at the intersection with the most frontal area 8C, H2 more laterally and dorsally) and in PMd, bordering area 6a. Finally, with regard to the precentral gyrus, H1 reports activations of the dorsal part of the anterior region 6 and of the FEF, while H2 reports an activation cluster on the border between FEF and the precentral part of area 4.
Only the second participant reports specific activations for the face in the left postcentral gyrus, at the level of the ventral area 4 and at the intersection between areas 3a and 3b. However, at the margin between the postcentral and supramarginal gyrus, H2 reports a face-specific activation cluster slightly more anterior and ventral than observed for the hand network, at the

junction between areas 2 and PFt. H1 also reports different specificities in this region, with specific activations for the face in the PO4 area more lateral than those observed for the hand.
The last clusters of H1 activation in the left hemisphere are found between IPL and SPL, at the junction between area 2, AIP and the intraparietal area, and between the postcentral gyrus and dorsal SPL, at the boundary between areas 1 and 5. On the other hand, the parietal cluster of H2 is wider, with head-specific activations in the IPL, which include the intraparietal areas 1 and 2, PFm, the ventral part of the 7PC area and the most ventral portion of the posterior aspect of the LIP area.
Also in the right hemisphere the specific activations for stimuli within the peri-head space are found at the premotor, supramarginal and parietal level, for both participants.
In this case, the clusters of the precentral gyrus are less extensive than in the left hemisphere, and not overlapping between the two participants: H1 reports activations in the lateral sector of the FEF and at the border between PMd and the precentral portion of the primary motor cortex, while H2 reports only one cluster, always in PMC, but more dorsally.
In the postcentral gyrus, contrariwise, a focus of activation common to the two participants is observed, located in the most lateral portion of the opercular part of the PF complex. The face-specific network of H2 also presents activations that also extend to the contiguous PFt and PF areas, resulting in the right SMG. It is here that we found another activation cluster common to the two participants, located in the most ventral part of the PFm area, bordering the STV area and the PSL area, sites of further face-specific activation for H2. The most dorsal part of PFm, in the IPL, is part of another H2 activation cluster, which includes this region and expands into the intraparietal area and the superior parietal lobule, in which the largest overlaps between the two participants are found. These face-specific activations seem to reflect the areas of activation common to the three body districts observed in the left hemisphere and described in the previous paragraph, including the dorsal and ventral portion of the LIP area, the anterior, medial and ventral intraparietal area and several portions of area 7 (lateral and medial 7A, 7PC). Finally, both participants report a final activation cluster in the most dorsal part of the junction between SPL and postcentral gyrus, on the border between areas 5 and 2.

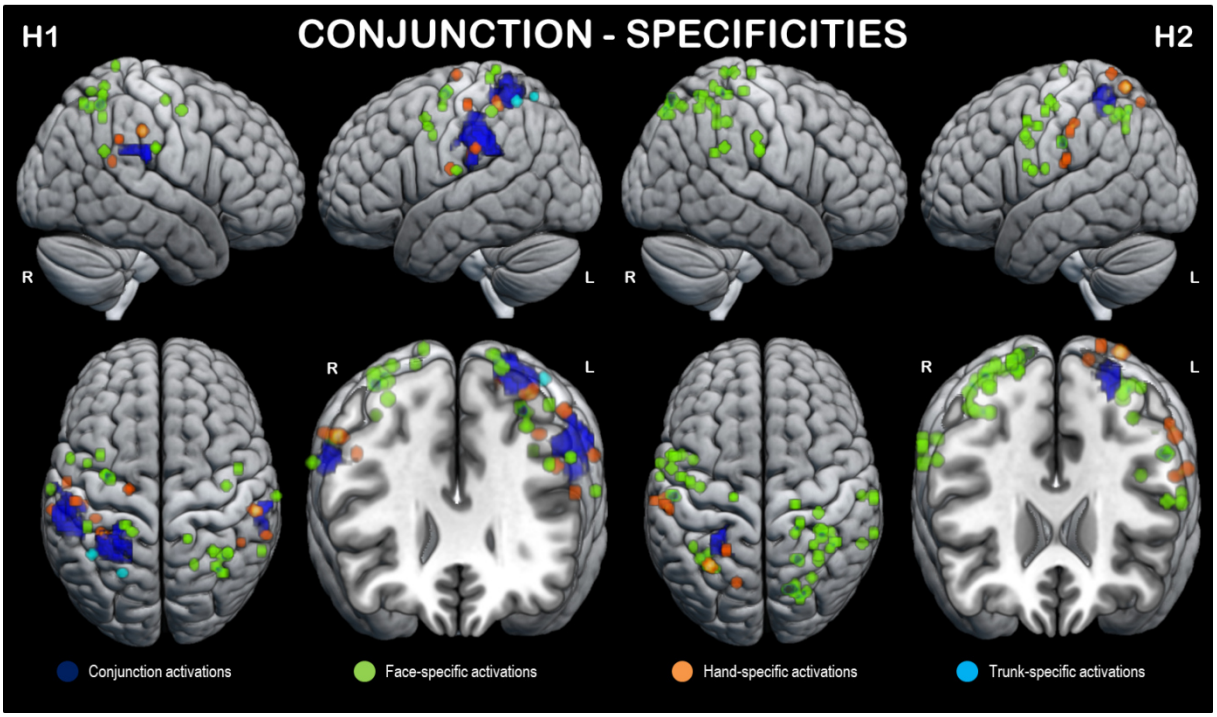

Figure 5. Peak-activation voxels reported for visual stimuli close to the face (green), the hand (orange) or the trunk (light blue) in the first (left side) and second (right side) human participants. Regions of conjunction between the activations of the three body parts are illustrated in dark blue.

4. Discussion

In our study, two human participants and two non-human primates underwent a similar experimental protocol, in which 3D visual stimuli could be presented near to or far from different body parts during fMRI recording of the respective neural responses. Main findings obtained concern the comparison of the peri-head space network between the two species and the identification of specific and common response patterns for different body-part-based PPS representations in humans.

4.1. Peri-head space underpinnings in human and non-human primates

Our study represents the first attempt to directly compare the PPS network of human and non-human primates, using the same neuroimaging technique and a similar experimental protocol. A precaution to be taken into consideration in this type of comparison concerns the possible discrepancies between the brain anatomies of the two species. A clear example

concerns the intraparietal sulcus and the regions of the SPL, including the VIP. This region, strongly involved in the encoding of stimuli within the PPS, is located on the ventral fundus of the IPS in the macaque (Colby et al., 1993), while in humans various studies have located the putative human VIP (hVIP) in different portions of the superior parietal lobule (see Foster et al., 2021). To optimize comparison, we used a brain atlas that features parcellation, based on both anatomical and functional criteria (see methods). In particular, we found a clear overlap of the neural patterns related to the decoding of the distance of the visual stimulations used. The MVPA classifier conducted on the Near-Far difference in the two species, indeed, brings out a network of bilateral areas which, in human and non-human primates, includes important portions of the premotor cortex (both ventral and dorsal), IPS (and, more generally, of the surrounding parietal cortex) and putamen. The same activation clusters in the SMG are also observed for human participants. For the first time, therefore, fMRI data allow us to observe an extensive network of subcortical and fronto-parietal cortical areas coding for the presence of a stimulus as a function of its distance from the body, both in macaques and in humans.

In monkeys, coherently with Cléry and coworkers' results (Cléry et al., 2018) and expanding the set of PPS-regions typically investigated by electrophysiological studies, we found specific responses for near visual stimuli also at the level of the premotor area F5. This area seems to be an important site for the processing of reachable stimuli and for the execution of grasping and reaching actions (Bonini et al., 2014; Murata et al., 1997; Raos et al., 2006; see Cléry et al., 2015a for review and discussion). Furthermore, its visual-tactile neurons have small receptive fields also centered on the face (Gentilucci et al., 1988; Murata et al., 1997; Raos et al., 2006; Rizzolatti and Luppino, 2001). Always in keeping with previous work, our results allow us to include within the network underlying the representation of the peri-head space also the dorsal portion of area 6 (PMdc) and the somatosensory areas 1 and 2.

The pattern of activation highlighted by the MVPA not only converge with the results obtained from the univariate analyses, but also reported the rostral dorsal premotor region (PMdr) and area 5, in particular AIP and PE, as part of the network of brain areas whose activity encodes the distance of the visual stimulus from the face. AIP, like 7a, does not seem to be directly involved in the PPS representation, but the interconnections and homologies with area 7b (Matelli and Luppino, 2001; Rizzolatti and Luppino, 2001) and the preferential response to the presentation of graspable objects (Fogassi et al., 2001; Gallese et al., 1994; Murata et al., 2000; Sakata and Taira, 1994) might explain its activation in the present study. We also found

preferential activations for stimuli close to the face found at the level of the dorsal and ventral portions of the lateral intraparietal area (LIPd and LIPv). Here, close-to-the-face stimulation, but not stimulations far away, induced bilateral LIP responses. This result appears to be in agreement with the preferential response of neurons in this region to visual stimuli presented between the monkey's body and a fixation point within the animal's reaching distance (Genovesio and Ferraina, 2004): in our experimental setting, the stimulation near the monkey's face was located within its central visual field (for which LIP neurons show a preferential response, Ben Hamed et al., 2001) and intermediate between its head and the fixation LED. Considering the similar experimental setup of Cléry and colleagues, the difference in the results could be related to the distance of the stimulation used: about 15 cm compared to about 2 cm in our study. It is interesting that, while the univariate analyses and the MVPA reported consistent results, the two adaptation analysis approaches reported small activation clusters or not sufficiently solid to resist the statistical correction. This could be due to the experimental setup used here: trials of 3 + 3 seconds may not be sufficient to induce a reduction of the response in the areas within the ROI mask adopted. It is possible that a block design (Cui and Nelissen, 2021) or a more prolonged repetition of stimulations (Kilner et al., 2014) are more suitable for eliciting this type of response, obtaining results in line with what has been observed in the other two statistical approaches.

The large network of activations described for the two monkeys is reflected in the results of the human participants, in which stimulation near the face reported the largest clusters of response that included activations at the level of the ventral premotor cortex, IPS, the primary somatosensory area and the supramarginal gyrus (Bremmer et al., 2001; Huang et al., 2012; Quinlan and Culham, 2007; Sereno and Huang, 2006), as well as more widespread activations at the level of the superior and inferior parietal cortex (which could explain any discrepancies between the coordinates of the activation peaks reported in the cited studies). The most interesting aspect, however, concerns the important overlaps of the responses observed in the two species. As for the two non-human primates, indeed, also for the two human participants the univariate analyses revealed significant activation clusters at the level of the ventral premotor cortex (homologous region of the F4 and F5 sections of the premotor area of the macaques) and of the dorsal one (reflecting the activations of the simian PMdc area). Proceeding caudally, the activations at the parietal level of the human participants are widespread, and cover large portions of the IPL and SPL, particularly in the region of the IPS.

Despite the different anatomical localization compared to the putative homologous regions of the macaques, both the ventral and the dorsal sections of the LIP area are activated, confirming what has been observed in non-human primates, and this coherence of neural responses is also confirmed for the rostral section of the simian area 7 (area 7b), activated at the level of the left hemisphere of M2. Indeed, H1 and H2 show activations of the PF/PFt complex (putative homologues region of 7b, Caspers et al., 2011) not only lateralized to the left, but also in the contralateral hemisphere. As for area 7a, activated in the left hemisphere in M2, the comparison with human participants seems more complex. The region anatomically homologous to the simian area 7a is the PFm area, which in H1 and H2 is activated only in the right hemisphere, contralaterally with respect to what is observed in M2. However, no clear homology between the two areas has so far been confirmed, and the simple rostral-caudal contiguity between PF and PFm in humans may not reflect the arrangement of 7b and 7a in macaques. Another conflicting result concerns the VIP area, activated bilaterally in the two non-human primates but absent in the activation clusters of the two human participants, at least at the level of the univariate analyses, and MIP, also activated bilaterally in M1 and M2 but found only in the right hemisphere of H2. In addition to these activations, the head-based human PPS network also extends to other regions, especially at the SMG level (multiple portions of the PF, PSL, STV and OP4 complex in particular) and parietal, in which activations of the area 7 (lateral and medial 7A and 7PC), of AIP and area 5L (putative homologue of the PE area, Scheperjans et al., 2005a, 2005b). The statistical approach of adaptation on humans allows to fill some of the inconsistencies found between the two species, reporting activations in bilateral VIP for both participants and in bilateral MIP for H2. Similarly, subcortical activations at the putamen level also emerge in human participants only through this approach, completing the comparison between the two species. However, this result is observed only through the repetition of a close-to-the-face stimulus, while the comparison between a Near-after-Near and a Near-after-Far does not report any significant result, in either human participant, following the FWE correction. Also, with regard to close-to-the-hand and to the trunk stimulations, this second adaptation approach reported clusters of activations that are less extensive than the first approach. As regards the face, in particular, it is observed that Near stimuli presented after a Far stimulus report stronger activations than a repeated Near stimulus, but this difference is not sufficiently solid to resist the correction of significance. It is possible that the first level analyses we conducted do not have sufficient power to bring out this difference, unlike the second level analyses conducted in a similar experimental paradigm (Brozzoli et al., 2011, 2012).

4.2. Body-part based PPS underpinnings in humans

In addition to near-face stimulation, human participants in our study were tested using visual stimuli presented near two other body districts, namely the right hand and the trunk. After the study by Huang and collaborators (Huang et al., 2012), ours is the first attempt to compare the neural basis of human PPS representations based on different body parts.

As previously described, the visual stimulations presented near the head, the trunk and the hand allowed to observe neural responses consistent with what has been reported in the literature (Bremmer et al., 2001; Brozzoli et al., 2011, 2012; Gentile et al., 2011, 2013; Makin et al., 2007). Although with some peculiarities related to the stimulated body district, the involvement of a fronto-parieto-supramarginal network is evident, including premotor (especially PMd), intraparietal, superior parietal and supramarginal regions (in particular large portions of the PF complex). Univariate and adaptation analyses, however, failed to report activations in the putamen, previously observed in associations with visual stimulations close to the hand (Brozzoli et al., 2011; 2012).

The MVPA classifier allowed us to deepen these results by investigating the pattern of areas involved in decoding the distance of visual stimulations close to or far from the hand. The observed results are consistent with what was described by the univariate and adaptation analyses, but with a wider bilateral involvement of PMd and extra-IPS parietal areas. Furthermore, the network included the PMv (in H1), FEF, PEF, the anterior and medial-posterior portions of the premotor area 6 (6a and 6mp) in the left hemisphere of both participants, but also the anterior segment of the IPS (AIP) bilaterally for H2 and in the right hemisphere for H1.

Ours is the first study investigating the effects of visual unimodal stimuli close to the trunk. Huang and colleagues overlapped brain activations in the posterior parietal cortex resulting from visual and tactile stimulations close to different body parts, such as the face, lips, shoulders, fingers, legs and toes (Huang et al., 2012), but they did not investigate further the neural network involved in this coding. The stimulus distance decoding pattern observed by our MVPA classifier seems similar to that observed for the previously described body parts, with bilateral involvement at the level of SMG, of the posterior parietal areas and, at least for H2, of the intraparietal and premotor areas. In H1, in these last two cases, it seems that the decoding pattern involves only the left hemisphere.

For this reason, we conducted cross-classification analyses between the patterns found for the three different parts of the body stimulated. We wondered if it was possible to train the classifier on the network of areas involved in decoding the distance of a stimulus from the hand, for example, and then test it in decoding the distance of the stimuli from the trunk. The same was done for all possible dyads: hand-face and trunk-face. The goal was to understand whether all or part of the fronto-parietal-supramarginal network described so far is involved in the decoding of the distance of a visual stimulus regardless of the part of the body involved. The areas of this network would be, more generally, sensitive to the distance of a stimulus from the body. In all dyads tested, the reported pattern covers both hemispheres, particularly for H2. H1, as reported above, appears to have a pattern more lateralized to the left. The dyad showing the broadest shared activation is that of the hand and trunk, in which the closer or farther stimuli induce activations in ventral and dorsal premotor areas, in the PF supramarginal complex, in the postcentral area S1 and in several areas at the level of the superior and inferior parietal lobules, all bilaterally. The same is observed, for H2, in the hand-face dyad, in which however the participant H1 does not report activations in PMv and lateralizes the described pattern to the left hemisphere only, with the exception of the right SMG. Finally, the pattern shared face and trunk stimulations seems to be narrow: also in this case the only region involved bilaterally by both participants is the supramarginal PF complex, with the bilateral addition of S1 and PMd for H2. H1, on the other hand, reports activations in S1 and in the region of the left IPS.

These results support the idea of a fronto-parieto-supramarginal network capable of decoding the distance of a stimulus from the body regardless of the body-part involved. The greater lateralization to the left could be due, in our experiment, to the presentation of visual stimuli, slightly lateralized in the right visual hemispace. It is interesting to observe the smaller extension of the common activation network between face and trunk; this sub-representation may be connected to less frequent interaction between these body district: if it is easy to think of hand movements in relation to the trunk and head (approaching or moving objects away from the face or trunk, for example), in which the distance of a stimulus from the two parts of the body counts, it is more difficult to imagine similar situations involving movements of the head towards the trunk or vice versa. However, this hypothesis remains only a speculation in light of the lack of motor aspects within our experimental setup and can provide interesting insights for future studies.

4.3. Commonality and differences between the neural responses underlying the different body-part based PPS representation

After investigating the decoding patterns of the distance of a stimulus common between the three parts of the body, we tried to understand if there were areas, within the PPS fronto-parietal network, having a preferential response for stimuli close to the body, regardless of which part of the body was closest. The areas belonging to this network would represent the central "core" of the PPS representation, capable of encoding the distance of a stimulus from the body, considered in this case as a whole. Grivaz and colleagues, in their meta-analysis, sought to highlight the neural basis of this PPS-core by integrating the results of 18 neuroimaging studies that tested the hand-, trunk- or face-based representation of PPS. What is reported is a response network that includes PMv at the frontal level, the areas PFop, PFcm, OP1 and OP2 in the SMG, the areas PFt, IP2 and 5 respectively in the IPL and SPL and, finally, the areas 1, 2, 3b (all included in S1) and 4 (M1 or PMC) in the postcentral gyrus (Grivaz et al., 2017). However, most of the studies involved in this meta-analysis stimulated the face (Bremmer et al., 2001; Cardini et al., 2011; Holt et al., 2014; Huang et al., 2012; Quinlan and Culham, 2007; Sereno and Huang, 2006; Tyll et al., 2013; Wittmann et al., 2010) or the hand (Brozzoli et al., 2011, 2012, 2013; Ferri et al., 2015; Gentile et al., 2011, 2013; Huang et al., 2012; Makin et al., 2007; Schaefer et al., 2012). Only one of these also stimulated the trunk (Huang et al., 2012), and in that case the stimulation was applied to the shoulders, and not the lower abdomen. Of these studies, less than half used visual unimodal stimulation (see Grivaz et al., 2017, Table 1). The characteristics of our study, and the consequent differences with respect to this literature, may be at the basis of the inconsistencies observed between our results and those just mentioned: considering the areas common to the three body districts and to both human participants, the core of the whole-body PPS seems to include mainly regions of the parietal cortex, both within the IPS (LIPv, in the left hemisphere) and in the surrounding area (lateral portion of area 7 and area 7PC, always in the left hemisphere). Finally, the last area presented by both H1 and H2 is one of those listed by Grivaz: area 2, at the level of the left postcentral gyrus. However, it is possible to confirm some of the regions described in the literature by better observing the results of the participant H1, who, in addition to the aforementioned network, also includes the supramarginal regions PFop and PFcm, the inferior parietal area PFt, the superior parietal area 5 and the somatosensory area 1. In addition, the participant also reports activations in the medial parietal area 7A, in VIP and in different portions of the SMG, including PSL and OP4, all

lateralized to the left. In the right hemisphere, only the PSL area and the superior temporal visual area, both on the border between the SMG and the temporal lobe, differ from the activations reported by Grivaz. The absence of clusters at the level of the premotor cortex stands out: no portion of area 6 seems to be part of the core of the whole-body PPS. However, as already mentioned, most studies in the literature have tested the hand-centered (Brozzoli et al., 2011, 2012, 2013; Ferri et al., 2015; Gentile et al., 2011, 2013; Huang et al., 2012; Makin et al., 2007; Schaefer et al., 2012) or head-based PPS representation (Bremmer et al., 2001; Cardini et al., 2011; Holt et al., 2014; Huang et al., 2012; Quinlan and Culham, 2007; Sereno and Huang, 2006; Tyll et al., 2013; Wittmann et al., 2010). Indeed, by considering the conjunction of specific response networks for the hand and for the face, this gap with respect to literature is bridged. We observed that both participants show a cluster of joint activation in the left precentral gyrus, which includes different portions of the premotor area 6, including PMd, PMv (in H1), the anterior and medial-posterior portions and the precentral section of the area 4 (M1 or PMC). In addition to this more frontal cluster, other specific activations are found in the SMG (bilaterally), in the SPL and in the postcentral gyrus. It therefore seems that the most frontal part of the PPS network is associated only with the encoding of stimuli near the hand or the face, indifferently. This is in line with the results from electrophysiology, which report premotor neurons characterized by multisensory receptive fields centered on the hands and face (Rizzolatti et al., 1981a, 1981b) or involved in hand-to-mouth movements (Gentilucci et al., 1988).

Another aspect that deserves attention concerns the disparity of the core-network between the two participants, caused by a left-parietal cluster only for H2 and by bilateral SMG activations for S1. This disparity seems to be due to an under-representation of the trunk at the supramarginal level by H2 (or its over-representation by H1): where H1 reports, in left SMG, a conjunction between the activation clusters associated with the hand, the face and at the trunk, H2 shows an overlap only between hand and face. Future studies, using larger samples and group-level analyses, could define in more detail the extension and localization of the PPS-core-network.

Finally, our hypothesis regarding the neural-level specificities of body-part-based PPS representations finds support in the results of the disjunction analyses. As can be seen in Figure 8, the areas of conjunction between two or more body districts are surrounded by specific body-part activations. Less extensive are those associated with the trunk, located only at the left

intraparietal level in H1. It therefore seems that the stimuli presented near the trunk induce responses mainly in non-specific areas, but associated with one or more other parts of the body. As for the hand and the face, however, the specificities are more widespread and observable in all the ROIs investigated. In particular, the underrepresentation of the trunk in H2 involves larger portions of parietal (7PC, 7Pl, VIP and area 5) and postcentral (S1, PFop, PFt) areas of the left hemisphere specifically associated with close-to-the-hand stimulations. The same is also observed for H1, in which these peaks are found at the edges of the left SMG and superior parietal cluster of the PPS core network, in both cases in the antero-ventral direction, and in the posterior and dorsal regions with respect to the right SMG cluster of conjunction already described. Finally, the last hand-specific activation is found in the most dorsal portion of the 6mp premotor area.

Lastly, the specific activations for close-to-the-face stimulations report the largest network of activations, bilaterally, for both participants. At the level of the left hemisphere, it is evident that the specific activations for the face of H1 and H2 are localized in the precentral and premotor areas more anterior than in the hand-face junction region; on the contrary, the specificities of the hand seem to be reported more posteriorly with respect to this cluster, occupying the post-central region. On the left superior parietal level, however, there does not seem to be a clear and distinct subdivision, with specific areas for face or hand intermingled with areas of conjunction. Also at the level of the right hemisphere, consistent results emerge between the two participants, with superior parietal and SMG areas associated to the encoding of stimuli close to the face. The apparent greater extent of face-specific activations in H2 actually appears to be associated with the underrepresentation of the hand in this participant's right hemisphere.

This greater extension of the network of face-specific brain regions could be due to the greater importance, in defensive terms, of the region of space surrounding the head. The stimulations used in our study also moved vertically towards the participant's face, lying on the scanner bed. In this position, the head-centered PPS representation tends to extend upwards, taking into account the gravitational cues that influence the movement of the stimuli towards the head (Bufacchi and Iannetti, 2016). Furthermore, stimuli close to the face were characterized by oscillations on the vertical axis that led to micro-movements of looming and receding directly towards the participant, as opposed to what happens for close-to-the-hand stimulation, slightly localized on the right of this body part. The possibility of impact and the

prediction of contact with the body influence the encoding of stimuli within PPS (Cléry et al., 2015b, 2017; Kandula et al., 2017), and this factor could therefore also have played a role in the over-representation observed here. Future studies can investigate this aspect, involving dynamic stimuli directed towards different body-parts in order to evaluate the consequences on the specific and joint activations reported here.

Tables

Table 2A. Significant clusters from univariate analyses for H1 and H2 by comparing stimulations close to or far from the FACE. The significant clusters ($p < 0.05$, cluster-based FWE correction) are reported with the relative activation peaks in MNI coordinates and the relative t-score.

	H1								H2							
	k	Hemisphere	AAL3v1 ROI	Glasser Area	X	Y	Z	t	k	Hemisphere	AAL3v1 ROI	Glasser Area	X	Y	Z	t
Univariate Analyses Face	269	Right	SMG	PFop	67	-25	22	16.21	1436	Right	SPL	IPS1	19	-76	48	15.74
				PF								DVT				
				PFcm								V6A				
				PFt								MIP (IPS)				
				PSL								7Am				
				OP4								7Al				
				RI								7Pl				
				STV								VIP (IPS)				
				PFm								5mv				
			Postcentral	PFop	67	-14	20	4.8				5L				
				1 (S1)							Postcentral	2 (S1)	25	-45	53	14.22
				PFt								3b (S1)				
	519	Right	IPL	PF	33	-53	53	14.45				4 (PMC)				
				AIP (IPS)								PFt				
				IP2							SMG	PF	58	-28	22	13.71
			Postcentral	2 (S1)	28	-39	53	13.14				PSL				
				7PC								PFm				
			SPL	LIPv (IPS)	33	-50	59	9.9				PFcm				
				LIPd (IPS)								Pfop				
				5L								STV				
				7Al							IPL	AIP (IPS)	36	-45	50	6.37
				VIP (IPS)								7PC				
				7Am								PFm				
	394	Left	SPL	2 (S1)	-23	-39	64	12.2				LIPv (IPS)				
				7Al								LIPd (IPS)				
				7PC					421	Left	SPL	7Al	-28	-48	56	14.35
				LIPv (IPS)							IPL	IP1	-34	-59	39	3.97
				VIP (IPS)								IP2				
				5L								LIPd (IPS)				
			Postcentral	2 (S1)	-26	-36	64	10.65				LIPv (IPS)				
			IPL	LIPv (IPS)	-33	-50	55	7.3				AIP (IPS)				
				7PC								7PC				
	1331	Left	SMG	PF	-56	-34	36	9				PFm				
				PFcm							Postcentral	2 (S1)	-29	-43	54	9.84
				PFop					1120	Left	Precentral	FEF	-34	-6	56	12.02
				PSL								PEF				
			Postcentral	4 (PMC)	-45	-11	56	8.85				6d (PMd)				
				OP4								6a				
				3a (S1)								6mp				
				3b (S1)								55b				
				1 (S1)								8Av				
				2 (S1)								i6-8				
				43							SMG	PFcm	-51	-31	22	10
				PFt							Postcentral	PFt	-56	-20	28	6
			Precentral	6d (PMd)	-42	-8	56	7.6				4 (PMC)				
				6v (PMv)					292	Right	Precentral	FEF	44	-3	48	10.94
				6r								PEF				
				6a								6v (PMv)				
				6mp								6r				
				FEF								8C				
				PEF								55b				
				8C								6a				
				i6-8								6d (PMd)				
			IPL	PFt	-54	-31	42	6.18								
				AIP (IPS)												
				IP2												
	220	Right	Precentral	6d (PMd)	42	-8	56	8.83								
				PEF												
				6v (PMv)												
				8Av												
				8C												
				55b												
			Postcentral	2 (S1)	50	-20	48	3.8								
				3b (S1)												

Table 2B. Significant clusters from univariate analyses for M1 and M2 by comparing stimulations close to or far from the FACE. The significant clusters ($p < 0.05$, cluster-based FWE correction) are reported with the relative t-score.

	M1					M2				
	k	**Hemisphere**	**CHARM/SARM 4 ROI**	**CHARM 6 Area**	**t**	**k**	**Hemisphere**	**CHARM/SARM 4 ROI**	**CHARM 6 Area**	**t**
Univariate Analyses Macaques	**727**	**Left**	**vm_IPS**	**MIP**	**16.29**	**624**	**Left**	**lat_IPS**	**LIPv**	**17.15**
				VIP	12.75			vm_IPS	VIP	12.81
			Area 7 in IPL	Area 7_OP	12.64			Area 7 in IPL	Area 7b	12.21
			lat_IPS	LIPd	9.61				Area 7a	5.92
		Right	**Premotor**	**F5**	**13.64**			S1	Areas 1-2	10.32
			Putamen	Putamen	8.91			Premotor	PMdc	11.75
			Area 7 in IPL	Area 7_PO	8.58				F4	10.1
			S1	Areas 1-2	5.99				F5	7.94
			vm_IPS	MIP	7.69			Putamen	Putamen	7.62
				VIP	5.91	**107**	**Right**	**Premotor**	**F5**	**10.93**
			lat_IPS	LIPd	5.98				PMdc	4.12
	97	**Left**	**Premotor**	**F5**	**11.02**	**241**	**Right**	**S1**	**Area 3a/b**	**8.93**
				PMdc	7.85			lat_IPS	LIPv	7.75
				F4	5.24			vm_IPS	VIP	6.08
	100	**Left**	**Putamen**	**Putamen**	**6.68**	**136**	**Right**	**Putamen**	**Putamen**	**8.69**

Table 3A. Significant clusters from MVPA on human participants training and testing the LDA classifier on the difference between near and far stimulations in the FACE condition. The significant clusters (z<1.65, one-sided t-test) are reported with the relative activation peaks in MNI coordinates and the relative z-score.

	H1								H2							
	k	Hemisphere	AAL3v1 ROI	Glasser Area	X	Y	Z	z-score	k	Hemisphere	AAL3v1 ROI	Glasser Area	X	Y	Z	z-score
MVPA Near vs Far Face	1851	Left	SMG	PFcm	-54	-25	14	3.09	2107	Left	SMG	OP4	-54	-25	14	3.09
				OP4								PFop				
				PFop								PSL				
				PFt								PFcm				
				PSL							Postcentral	3b (S1)	-51	-17	45	3.09
			Postcentral	2 (S1)	-25	-36	62	3.09				2 (S1)				
				1 (S1)								3a				
				3a								PFt				
				3b (S1)							Precentral	FEF	-34	-6	56	3.09
				5L								6v (PMv)				
			SPL	7PC	-34	-45	59	3.09				6d (PMd)				
				IPS1								4 (PMC)				
				7Al								6r				
				VIP (IPS)								IFJp				
				LIPv (IPS)								PEF				
				LIPd (IPS)								8C				
				MIP (IPS)								55b				
				DVT								8Av				
			IPL	7PC	-37	-42	48	3.09				6mp				
				PFt							SPL	7Al	-26	-56	64	3.09
				PFm								DVT				
				IP2								IPS1				
				AIP (IPS)								7Pl				
				PF								VIP (IPS)				
			Precentral	FEF	-42	-3	56	3.09			IPL	2 (S1)	-45	-28	42	3.09
				4 (PMC)								AIP (IPS)				
				6mp								LIPv (IPS)				
				6d (PMd)								LIPd (IPS)				
				8Av								MIP (IPS)				
				6a								IP2				
				55b					2411	Right	Postcentral	OP4	64	-17	14	3.09
	2064	Right	Postcentral	OP4	67	-17	14	3.09				2 (S1)				
				4 (PMC)								3a				
				1 (S1)								3b (S1)				
				PFt							SMG	PF	55	-30	44	3.09
				3a								Pfop				
				7Al								PFcm				
				5L								PSL				
			Precentral	55b	50	-3	40	3.09				RI				
				FEF								STV				
				6v (PMv)								PFt				
				6a								AIP (IPS)				
				6d (PMd)							IPL	PFm	47	-56	48	3.09
			SMG	PSL	56	-39	28	3.09				IP2				
				PFop								IP1				
				PF								IPS1				
				PFcm								LIPd (IPS)				
				PFm								7PC				
				RI							SPL	LIPv (IPS)	28	-53	59	3.09
				STV								MIP (IPS)				
			SPL	LIPv (IPS)	22	-62	53	3.09				DVT				
				LIPd (IPS)								VIP (IPS)				
				DVT							Precentral	4 (PMC)	39	-17	62	3.09
				7Pl								PEF				
				7Am								6v (PMv)				
				MIP (IPS)								6d (PMd)				
				VIP (IPS)								8Av				
			IPL	IP2	39	-48	45	3.09				FEF				
				AIP (IPS)								6a				
				IPS1								55b				
				IP1												
				7PC												

Table 3B. Significant clusters from MVPA on macaques training and testing the LDA classifier on the difference between stimulations close to and far from the face. The significant clusters (z<1.65, one-sided t-test) are reported with the relative z-score.

	M1					M2				
	k	Hemisphere	CHARM/SARM 4 ROI	CHARM 6 Area	z-score	k	Hemisphere	CHARM/SARM 4 ROI	CHARM 6 Area	z-score
MVPA Near vs Far Macaques	204	Left	V6	V6	3.09	738	Left	Putamen	Putamen	3.09
			vm_IPS	MIP	3.09				F4	3.09
				VIP	3.09			Premotor	F5	3.09
			Area 5	PEa	3.09				PMdc	3.09
			lat_IPS	LIPv	3.09			S1	Area 3a/b	3.09
				AIP	3.09				Areas 1-2	3.09
				LIPd	3.09				Area 7_OP	3.09
			Area 7 in IPL	Area 7b	3.09			Area 7 in IPL	Area 7b	3.09
				Area 7_OP	3.09				Area 7a	3.09
				Area 7a	3.09			Area 5	Pea	3.09
			S1	Areas 1-2	3.09				AIP	3.09
	108	Left	Premotor	F5	3.09			Lat_IPS	LIPv	3.09
				F4	3.09				LIPd	3.09
				PMdc	3.09				LOP	3.09
				PMdr	2.57				VIP	3.09
	55	Right	Premotor	F5	3.09			vm_IPS	MIP	3.09
				F4	3.09				PIP	3.09
				PMdc	3.09			V6	V6Ad	3.09
			Putamen	Putamen	1.85	71	Right	Putamen	Putamen	3.09
	105	Right	vm_IPS	MIP	3.09	506	Right	Premotor	F4	3.09
				VIP	3.09				F5	3.09
			lat_IPS	LIPv	3.09			S1	Area 3a/b	3.09
				LIPd	3.09				Areas 1-2	3.09
			area 5	PEa	3.09			Area 5	PEa	3.09
				PE	3.09				PEc	3.09
			Area 7 in IPL	Area 7b	3.09			Lat_IPS	AIP	3.09
				Area 7_OP	3.09				LIPv	3.09
				Area 7a	3.09			vm_IPS	VIP	3.09
			S1	Areas 1-2	3.09				MIP	3.09
									Area 7_OP	3.09
								Area 7 in IPL	Area 7b	3.09
									Area 7a	3.09

Table 4. Significant clusters from univariate analyses for the two human participants by comparing stimulations close to or far from the hand. The significant clusters ($p < 0.05$, cluster-based FWE correction) are reported with the relative activation peaks in MNI coordinates.

	H1								H2							
	k	Hemisphere	AAL3v1 ROI	Glasser Atlas	X	Y	Z	t	k	Hemisphere	AAL3v1 ROI	Glasser Atlas	X	Y	Z	t
Univariate Analyses Hand	1627	Left	SMG	PFcm	-51	-28	20	18.56	426	Left	SPL	7Al	-28	-45	52	16.3
				PFt								LIPv (IPS)				
				PFop								POS_2				
				PF								7Pl				
				PSL								7 PC				
			IPL	1 (S1)	-55	-28	47	13.63				5L				
				7PC								VIP (IPS)				
				LIPv (IPS)							Postcentral	2 (S1)	-28	-39	67	5.2
			SPL	7Al	-20	-50	67	12.29	366	Left	Postcentral	OP1	-51	-20	20	14.53
				7Am								OP4				
				VIP (IPS)								1 (S1)				
				5L								2 (S1)				
			Precentral	6d (PMd)	-40	-14	56	7.88				PFt				
				6a							SMG	PFcm	-48	-31	22	13.6
				6mp								PFop				
			Postcentral	2 (S1)	-59	-16	34	8.11				PF				
				1 (S1)								PSL				
				3b (S1)					168	Right	SMG	PFcm	47	-31	25	10.41
				4 (PMC)								PFop				
	309	Right	SMG	PFop	67	-25	22	13.54				PF				
				PFcm								PSL				
				PF								RI				
				PFm					137	Left	Precentral	FEF	-34	-6	59	8.78
				PSL								6d (PMd)				
				PFt								6a				
				STV								6mp				
			Postcentral	PFt	53	-22	45	3.78								
				1 (S1)												

Table 5. Significant clusters from univariate analyses for H1 and H2 by comparing stimulations close to or far from the TRUNK. The significant clusters ($p < 0.05$, cluster-based FWE correction) are reported with the relative activation peaks in MNI coordinates and the relative t-score.

	H1								H2							
	k	Hemisphere	AAL3v1 ROI	Glasser Atlas	X	Y	Z	t	k	Hemisphere	AAL3v1 ROI	Glasser Atlas	X	Y	Z	t
Univariate Analyses Trunk	959	Left	SMG	PFcm	-45	-36	28	11.37	316	Left	SPL	POS2	-12	-76	45	11.93
				PF								7Al				
				PFt								7Pl				
				PFop								7Pm				
				OP4								IPS1				
				OP1								DVT				
				PSL							Postcentral	2 (S1)	-25	-45	56	9.53
			SPL	7Al	-25	-50	70	9.9			IPL	LIPv (IPS)				
				LIPv (IPS)								LIPd (IPS)				
				VIP (IPS)												
				7Am												
				5L												
			Postcentral	2 (S1)	-25	-36	62	6.88								
				1 (S1)												
				3b (S1)												
			IPL	PFcm	-56	-28	48	7.9								
				AIP (IPS)												
				1 (S1)												
				IP2												
				PF												
				7PC												
	150	Right	SMG	PFop	67	-25	22	9.58								
				PF												
				PSL												
				PFcm												
				RI												
				STV												

Table 6. Significant clusters from cross-validation MVPA on human participants training and testing the LDA classifier on the difference between near and far stimulations in different dyads of conditions. The significant clusters (z<1.65, one-sided t-test) are reported with the relative activation peaks in MNI coordinates and the relative z-score.

	H1								H2							
	k	Hemisphere	AAL3v1 ROI	Glasser Area	X	Y	Z	z-score	k	Hemisphere	AAL3v1 ROI	Glasser Area	X	Y	Z	z-score
Near vs Far Hand-Face MVPA	884	Left	SMG	PFcm	-54	-25	14	3.09	836	Left	Postcentral	3a (S1)	-59	-8	20	3.09
				PFop								3b (S1)				
				PSL								2 (S1)				
				PFt								OP4				
			Postcentral	2 (S1)	-48	-26	48	3.09				55b				
				55b							SMG	PF	-56	-34	28	3.09
				OP4								PFt				
				3b (S1)							Precentral	FEF	-34	-6	56	2.58
				4 (PMC)								PEF				
			Precentral	6d (PMd)	-42	-8	58	2.17				6v (PMv)				
				6v (PMv)								6d (PMd)				
			IPL	PF	-59	-36	40	3.09				6a				
	341	Right	Postcentral	OP4	64	-16	14	3.09				6r				
				PFt								4 (PMC)				
				1 (S1)								i6-8				
			SMG	PFop	64	-22	25	3.09			IPL	2 (S1)	-32	-42	51	3.09
				PF								IP2				
				PSL								LIPv (IPS)				
				PFm								AIP (IPS)				
				PFcm							SPL	7PC	-37	-45	62	3.09
				RI								7Al				
				STV					960	Right	Postcentral	OP4	61	-17	17	3.09
	10	Left	SPL	IPS1	-25	-81	48	1.91				2 (S1)				
	45	Right	Postcentral	2 (S1)	25	-39	53	2.87				55b				
				3b (S1)								3b (S1)				
												3a (S1)				
											SMG	PFop	64	-22	31	3.09
												PF				
												PFcm				
												PFt				
												PSL				
												RI				
											IPL	IP2	48	-36	52	3.09
												AIP (IPS)				
											SPL	7PC	33	-53	64	2.75
												7Al				
												VIP (IPS)				
											Precentral	55b	53	-8	45	3.09
												6d (PMd)				
												FEF				
												4 (PMC)				

	H1								H2							
	k	Hemisphere	AAL3v1 ROI	Glasser Area	X	Y	Z	z-score	k	Hemisphere	AAL3v1 ROI	Glasser Area	X	Y	Z	z-score
Near vs Far Hand-Trunk MVPA	**2664**	**Left**	**SMG**	**PFcm**	**-54**	**-25**	**14**	**3.09**	**2313**	**Left**	**SMG**	**PFcm**	**-54**	**-25**	**14**	**3.09**
				PFt								PFop				
				PFop								PL				
				PF							**Postcentral**	**2 (S1)**	**-25**	**-36**	**62**	**3.09**
				PSL								3b (S1)				
			Postcentral	**4 (PMC)**	**-53**	**-11**	**40**	**3.09**				OP4				
				OP4								3a (S1)				
				1 (S1)								PFt				
				3b (S1)								55b				
				3a (S1)							**Precentral**	**FEF**	**-34**	**-3**	**56**	**3.09**
				2 (S1)								6v (PMv)				
			Precentral	**6r**	**-54**	**6**	**36**	**3.09**				6d (PMd)				
				6d (PMd)								6mp				
				6V (PMv)								4 (PMC)				
				6mp								6r				
				FEF								6a				
				PEF								IFJ				
				i6-8								PEF				
				6a								8C				
				55b								i6-8				
			SPL	**7Al**	**-20**	**-48**	**64**	**3.09**			**SPL**	**7Al**	**-23**	**-50**	**64**	**3.09**
				7Pl								7Pl				
				7PC								VIP (IPS)				
				IPS1								MIP (IPS)				
				5L								DVT				
				VIP (IPS)							**IPL**	**AIP (IPS)**	**-45**	**-36**	**41**	**3.09**
				LIPv (IPS)								IP2				
				DVT								LIPv (IPS)				
			IPL	**LIPd (IPS)**	**-28**	**-50**	**45**	**3.09**				7PC				
				PFm					**1918**	**Right**	**Postcentral**	**OP4**	**64**	**-17**	**14**	**3.09**
				PF								2 (S1)				
				IP2								1 (S1)				
				PGs								3b (S1)				
	842	**Right**	**Postcentral**	**OP4**	**67**	**-17**	**14**	**3.09**				5L				
				2 (S1)								7PC				
			SMG	**PFop**	**64**	**-22**	**28**	**3.09**			**SMG**	**PFcm**	**53**	**-36**	**28**	**3.09**
				PF								PF				
				PSL								PFt				
				RI								PSL				
				STV								PFop				
				PFt							**IPL**	**PFm**	**50**	**-42**	**53**	**2.88**
			IPL	**PFm**	**53**	**-48**	**48**	**2.58**				AIP (IPS)				
			Precentral	**3b (S1)**	**47**	**-11**	**53**	**3.09**				IP2				
				PEF							**SPL**	**7PC**	**42**	**-48**	**59**	**3.09**
				6v (PMv)								7Al				
				6d (PMd)								7Am				
				FEF								VIP (IPS)				
	211	**Right**	**SPL**	**LIPv (IPS)**	**30**	**-56**	**62**	**3.09**			**Precentral**	**6d (PMd)**	**32**	**-14**	**61**	**3.09**
				VIP (IPS)								6v (PMv)				
				7Am								PEF				
				7Al								FEF				
				5L								6a				
			Postcentral	**2 (S1)**	**22**	**-42**	**64**	**1.87**				8Av				
	36	**Right**	**Postcentral**	**3b (S1)**	**25**	**-31**	**62**	**2.17**				4 (PMC)				
									9	**Right**	**SPL**	**DVT**	**19**	**-76**	**48**	**1.94**
Near vs Far Trunk-Face MVPA	**551**	**Left**	**SMG**	**PFcm**	**-54**	**-25**	**14**	**3.09**	**168**	**Left**	**SMG**	**PFcm**	**-51**	**-25**	**17**	**3.09**
				PSL								PFop				
			Postcentral	**3b (S1)**	**-46**	**-22**	**55**	**2.58**			**Postcentral**	**PFt**	**-56**	**-19**	**28**	**2.75**
				OP4								OP4				
			IPL	**1 (S1)**	**-54**	**-25**	**50**	**3.09**	**480**	**Right**	**SMG**	**PF**	**58**	**-28**	**36**	**3.09**
				PF								AIP (IPS)				
				PFt							**Postcentral**	**3a (S1)**	**38**	**-24**	**50**	**3.09**
				PFm								2 (S1)				
	254	**Right**	**Postcentral**	**2 (S1)**	**59**	**-15**	**41**	**3.09**				1 (S1)				
			SMG	**OP4**	**62**	**-25**	**31**	**3.09**				PFt				
				PFop							**Precentral**	**FEF**	**36**	**-6**	**48**	**2.29**
				PF								6a				
				PFt							**IPL**	**IP2**	**50**	**-32**	**48**	**2.22**
				PSL								7PC				
				STV								PFm				
	58	**Left**	**SPL**	**LIPv (IPS)**	**-34**	**-59**	**59**	**3.09**			**SPL**	**7Al**	**30**	**-51**	**64**	**2.41**
				7PC								VIP (IPS)				
				VIP (IPS)					**173**	**Left**	**IPL**	**LIPd (IPS)**	**-31**	**-48**	**42**	**3.09**
	98	**Left**	**Postcentral**	**1 (S1)**	**-31**	**-36**	**67**	**3.09**				LIPv (IPS)				
				3b (S1)								7PC				
				55b								AIP (IPS)				
			Precentral	**4 (PMC)**	**-26**	**-24**	**70**	**2.58**			**Postcentral**	**2 (S1)**	**-31**	**-39**	**59**	**3.09**
												1 (S1)				
												3b (S1)				
									22	**Left**	**Precentral**	**4 (PMC)**	**-40**	**-14**	**59**	**2.87**
												6d (PMd)				

Table 7. Overlapping areas of activations for stimuli close to the hand and to the face (upper table) or close to one of the body part tested, indifferently (lower table). The reported MNI coordinates do not refer to peaks of greater activation but are only representative of the portion of the area involved in which the overlap occurs.

	H1						H2					
	Hemisphere	AAL3v1 ROI	Glasser Area	X	Y	Z	Hemisphere	AAL3v1 ROI	Glasser Area	X	Y	Z
Univariate Hand-Face Conjunction	Right	SMG	PFop	62	-20	25	Right	SMG	PF	63	-29	27
			PF	64	-27	36			PFop	64	-23	25
			STV	61	-49	26			PSL	61	-35	28
	Left	Precentral	6v (PMv)	-59	5	27			PFcm	57	-35	30
			6d (PMd)	-32	-15	69			RI	51	-31	24
			4 (PMC)	-58	0	23	Left	SMG	PF	-64	-32	33
			6r	-56	4	23			PFop	-60	-23	28
			6a	-32	-13	59			PFt	-58	-30	35
			6mp	-23	-17	70			PFcm	-55	-27	17
		Postcentral	1 (S1)	-46	-20	58			PSL	-51	-38	25
			2 (S1)	-59	-17	40		Precentral	6d (PMd)	-34	-9	62
			4 (PMC)	-64	-2	23			6a	-31	-13	56
			3a (S1)	-62	-5	16			6mp	-21	-17	70
		SMG	PFop	-62	-25	24		SPL	LIPv (IPS)	-34	-58	61
			PFt	-62	-21	38			7Al	-23	-44	67
			OP4	-56	-20	25		Postcentral	2 (S1)	-26	-40	58
		IPL	IP2	-49	-37	51						
		SPL	7Al	-31	-43	72						
			5L	-19	-46	74						
Univariate Hand-Face-Trunk Conjunction	Right	SMG	PF	68	-27	27	Left	Par Inf	LIPv (IPS)	-30	-49	53
			PFop	67	-26	26		Par Sup	7Al	-27	-48	65
			PSL	66	-30	30			7PC	-31	-45	65
			PFcm	56	-32	27		Post	2 (S1)	-25	-41	62
			STV	60	-42	25						
	Left	Par Sup	7Al	-27	-48	65						
			7Am	-16	-60	66						
			7PC	-31	-45	65						
			5L	-16	-53	76						
			VIP (IPS)	-22	-61	65						
		Par Inf	LIPv (IPS)	-30	-49	53						
			PFt	-47	-28	37						
			PFcm	-48	-36	26						
			2 (S1)	-51	-23	37						
		Post	2 (S1)	-25	-41	62						
			1 (S1)	-57	-25	43						
		SMG	PFcm	-49	-35	26						
			PSL	-48	-45	26						
			PF	-55	-39	35						
			OP4	-57	-21	21						
			PFt	-57	-25	30						
			PFop	-57	-27	24						

Table 8. Specific activation areas for stimulations close to the face (upper table), the hand (middle table) and the trunk (lower table). The reported MNI coordinates do not refer to peaks of greater activation but are only representative of the portion of the area involved in which specificity is present.

	H1						H2					
	Hemisphere	AAL3v1 ROI	Glasser Area	X	Y	Z	Hemisphere	AAL3v1 ROI	Glasser Area	X	Y	Z
Univariate Face Specificity	Right	Postecentral	PO4	65	-17	14	Right	SMG	PFop	66	-19	27
		SMG	PF	69	-19	29			PF	66	-21	35
			PFm	60	-51	27			PSL	66	-41	29
		Precentral	FEF	46	-3	51			STV	59	-47	26
			4 (PMC)	39	-13	57			PFt	59	-19	29
		SPL	7PC	40	-52	60			AIP	33	-39	44
			7Al	31	-51	65		IPL	IPS_2	43	-46	43
			PFm	40	-53	54			AIP	40	-40	44
			MIP	37	-64	55			PF	43	-46	51
			AIP	33	-52	47			7PC	40	-50	55
			LIPv	37	-54	54		Postecentral	2 (S1)	35	-39	60
			LIPd	33	-60	53			1 (S1)	22	-35	73
			VIP	20	-59	62			4 (PMC)	19	-24	73
			5L	16	-44	77			7PC	35	-44	62
	Left	SPL	5L	-17	-40	76			5L	19	-41	73
		Postecentral	1 (S1)	-21	-36	71		SPL	LIPv	33	-54	59
			2 (S1)	-44	-37	51			LIPd	33	-57	52
			PO4	-66	-15	16			Tal	30	-48	65
		Precentral	6a	-30	-9	63			7Am	19	-56	58
			6d (PMd)	-33	-7	61			MIP	29	-67	53
			FEF	-33	-6	54			IPS_1	26	-75	48
			PEF	-44	0	37			V6A	22	-79	49
			55b	-36	5	47			VIP	22	-57	60
			6v (PMv)	-54	3	42			DVT	19	-76	53
									7Pl	15	-74	58
							Left	Postecentral	4 (PMC)	-62	0	16
									2 (S1)	-55	-18	33
									3a (S1)	-62	-8	17
									PFt	-53	-20	32
								Precentral	6r	-55	4	19
									6v (PMv)	-55	5	37
									6d (PMd)	-44	-11	57
									PEF	-55	-3	42
									55b	-53	4	45
									FEF	-49	-8	51
									IFJ	-42	2	32
									6mp	-18	-20	75
								IPL	7PC	-42	-49	52
									PFm	-38	-56	50
									IPS_1	-33	-60	40
									IPS_2	-33	-53	47
									LIPd	-33	-60	47
								SPL	LIPv	-29	-61	52
Univariate Hand Specificity	Right	SMG	PSL	63	-42	34	Left	Postcentral	PFop	-65	-22	23
			PF	58	-28	39			PO4	-59	-20	20
			PFt	55	-27	42			PFt	-59	-24	39
			TPOJ	48	-46	21			1 (S1)	-56	-27	44
	Left	SMG	PO1	-47	-24	25		SPL	7PC	-33	-59	65
		Precentral	6mp	-19	-15	73			7Pl	-16	-70	56
		Postcentral	2 (S1)	-33	-42	54			VIP	-31	-61	65
			1 (S1)	-51	-22	55			5L	-22	-51	73
			PO4	-56	-11	17						
		SMG	PF	-65	-27	29						
		IPL	7PC (IPS)	-36	-40	57						
			AIP (IPS)	-39	-32	38						
Univariate Trunk Specificity	Left	IPL	7PC (IPS)	-41	-53	57						
		Par Sup	VIP (IPS)	-23	-64	60						

5. References

Ben Hamed, S., Duhamel, J.-R., Bremmer, F., and Graf, W. (2001). Representation of the visual field in the lateral intraparietal area of macaque monkeys: a quantitative receptive field analysis. Exp. Brain Res. 140, 127–144.

Bonini, L., Maranesi, M., Livi, A., Fogassi, L., and Rizzolatti, G. (2014). Space-Dependent Representation of Objects and Other's Action in Monkey Ventral Premotor Grasping Neurons. J. Neurosci. 34, 4108–4119.

Boynton, G.M. (2011). Spikes, BOLD, Attention, and Awareness: A comparison of electrophysiological and fMRI signals in V1. J. Vis. 11, 12–12.

Bremmer, F., Schlack, A., Shah, N.J., Zafiris, O., Kubischik, M., Hoffmann, K.-P., Zilles, K., and Fink, G.R. (2001). Polymodal Motion Processing in Posterior Parietal and Premotor Cortex. Neuron 29, 287–296.

Bremmer, F., Schlack, A., Kaminiarz, A., and Hoffmann, K.-P. (2013). Encoding of movement in near extrapersonal space in primate area VIP. Front. Behav. Neurosci. 7.

Brozzoli, C., Gentile, G., Petkova, V.I., and Ehrsson, H.H. (2011). fMRI Adaptation Reveals a Cortical Mechanism for the Coding of Space Near the Hand. J. Neurosci. 31, 9023–9031.

Brozzoli, C., Gentile, G., and Ehrsson, H.H. (2012). That's Near My Hand! Parietal and Premotor Coding of Hand-Centered Space Contributes to Localization and Self-Attribution of the Hand. J. Neurosci. 32, 14573–14582.

Brozzoli, C., Gentile, G., Bergouignan, L., and Ehrsson, H.H. (2013). A Shared Representation of the Space Near Oneself and Others in the Human Premotor Cortex. Curr. Biol. 23, 1764–1768.

Bufacchi, R.J., and Iannetti, G.D. (2016). Gravitational cues modulate the shape of defensive peripersonal space. Curr. Biol. 26, R1133–R1134.

Cardini, F., Costantini, M., Galati, G., Romani, G.L., Làdavas, E., and Serino, A. (2011). Viewing One's Own Face Being Touched Modulates Tactile Perception: An fMRI Study. J. Cogn. Neurosci. 23, 503–513.

Caspers, S., Eickhoff, S.B., Rick, T., von Kapri, A., Kuhlen, T., Huang, R., Shah, N.J., and Zilles, K. (2011). Probabilistic fibre tract analysis of cytoarchitectonically defined human inferior parietal lobule areas reveals similarities to macaques. NeuroImage 58, 362–380.

Cléry, J., Guipponi, O., Wardak, C., and Ben Hamed, S. (2015a). Neuronal bases of peripersonal and extrapersonal spaces, their plasticity and their dynamics: Knowns and unknowns. Neuropsychologia 70, 313–326.

Cléry, J., Guipponi, O., Odouard, S., Wardak, C., and Ben Hamed, S. (2015b). Impact Prediction by Looming Visual Stimuli Enhances Tactile Detection. J. Neurosci. 35, 4179–4189.

Cléry, J., Guipponi, O., Odouard, S., Pinède, S., Wardak, C., and Ben Hamed, S. (2017). The Prediction of Impact of a Looming Stimulus onto the Body Is Subserved by Multisensory Integration Mechanisms. J. Neurosci. 37, 10656–10670.

Cléry, J., Guipponi, O., Odouard, S., Wardak, C., and Ben Hamed, S. (2018). Cortical networks for encoding near and far space in the non-human primate. NeuroImage 176, 164–178.

Colby, C.L., and Duhamel, J.-R. (1991). Heterogeneity of extrastriate visual areas and multiple parietal areas in the Macaque monkey. Neuropsychologia 29, 517–537.

Colby, C.L., and Duhamel, J.R. (1996). Spatial representations for action in parietal cortex. Brain Res. Cogn. Brain Res. 5, 105–115.

Colby, C.L., Duhamel, J.R., and Goldberg, M.E. (1993). Ventral intraparietal area of the macaque: anatomic location and visual response properties. J. Neurophysiol. 69, 902–914.

Cui, D., and Nelissen, K. (2021). Examining cross-modal fMRI adaptation for observed and executed actions in the monkey brain. NeuroImage 233, 117988.

Duhamel, J.R., Colby, C.L., and Goldberg, M.E. (1998). Ventral Intraparietal Area of the Macaque: Congruent Visual and Somatic Response Properties. J. Neurophysiol. 79, 126–136.

Ferri, F., Costantini, M., Huang, Z., Perrucci, M.G., Ferretti, A., Romani, G.L., and Northoff, G. (2015). Intertrial Variability in the Premotor Cortex Accounts for Individual Differences in Peripersonal Space. J. Neurosci. 35, 16328–16339.

Fogassi, L., Gallese, V., Buccino, G., Craighero, L., Fadiga, L., and Rizzolatti, G. (2001). Cortical mechanism for the visual guidance of hand grasping movements in the monkey: A reversible inactivation study. Brain 124, 571–586.

Foster, C., Sheng, W.-A., Heed, T., and Hamed, S.B. (2021). The macaque ventral intraparietal area has expanded into three homologue human parietal areas.

Gallese, V., Murata, A., Kaseda, M., Niki, N., and Sakata, H. (1994). Deficit of hand preshaping after muscimol injection in monkey parietal cortex. Neuroreport Int. J. Rapid Commun. Res. Neurosci. 5, 1525–1529.

Genovesio, A., and Ferraina, S. (2004). Integration of Retinal Disparity and Fixation-Distance Related Signals Toward an Egocentric Coding of Distance in the Posterior Parietal Cortex of Primates. J. Neurophysiol. 91, 2670–2684.

Gentile, G., Petkova, V.I., and Ehrsson, H.H. (2011). Integration of visual and tactile signals from the hand in the human brain: an FMRI study. J. Neurophysiol. 105, 910–922.

Gentile, G., Guterstam, A., Brozzoli, C., and Ehrsson, H.H. (2013). Disintegration of Multisensory Signals from the Real Hand Reduces Default Limb Self-Attribution: An fMRI Study. J. Neurosci. 33, 13350–13366.

Gentilucci, M., Fogassi, L., Luppino, G., Matelli, M., Camarda, R., and Rizzolatti, G. (1988). Functional organization of inferior area 6 in the macaque monkey. Exp. Brain Res. 71, 475–490.

Glasser, M.F., Coalson, T.S., Robinson, E.C., Hacker, C.D., Harwell, J., Yacoub, E., Ugurbil, K., Andersson, J., Beckmann, C.F., Jenkinson, M., et al. (2016). A multi-modal parcellation of human cerebral cortex. Nature 536, 171–178.

Graziano, M.S.A., and Cooke, D.F. (2006). Parieto-frontal interactions, personal space, and defensive behavior. Neuropsychologia 44, 845–859.

Graziano, M.S.A., and Gross, C.G. (1993). A bimodal map of space: somatosensory receptive fields in the macaque putamen with corresponding visual receptive fields. Exp. Brain Res. 97, 96–109.

Graziano, M.S., Yap, G.S., and Gross, C.G. (1994). Coding of visual space by premotor neurons. Science 266, 1054–1057.

Grivaz, P., Blanke, O., and Serino, A. (2017). Common and distinct brain regions processing multisensory bodily signals for peripersonal space and body ownership. NeuroImage 147, 602–618.

Hartig, R., Glen, D., Jung, B., Logothetis, N.K., Paxinos, G., Garza-Villarreal, E.A., Messinger, A., and Evrard, H.C. (2021). The Subcortical Atlas of the Rhesus Macaque (SARM) for neuroimaging. NeuroImage 235, 117996.

Holt, D.J., Cassidy, B.S., Yue, X., Rauch, S.L., Boeke, E.A., Nasr, S., Tootell, R.B.H., and Coombs, G. (2014). Neural Correlates of Personal Space Intrusion. J. Neurosci. 34, 4123–4134.

Huang, R.-S., Chen, C. -f., Tran, A.T., Holstein, K.L., and Sereno, M.I. (2012). Mapping multisensory parietal face and body areas in humans. Proc. Natl. Acad. Sci. 109, 18114–18119.

Hyvärinen, J., and Shelepin, Y. (1979). Distribution of visual and somatic functions in the parietal associative area 7 of the monkey. Brain Res. 169, 561–564.

Jung, B., Taylor, P.A., Seidlitz, J., Sponheim, C., Perkins, P., Ungerleider, L.G., Glen, D., and Messinger, A. (2021). A comprehensive macaque fMRI pipeline and hierarchical atlas. NeuroImage 235, 117997.

Kandula, M., Van der Stoep, N., Hofman, D., and Dijkerman, H.C. (2017). On the contribution of overt tactile expectations to visuo-tactile interactions within the peripersonal space. Exp. Brain Res. 235, 2511–2522.

Kilner, J.M., Kraskov, A., and Lemon, R.N. (2014). Do monkey F5 mirror neurons show changes in firing rate during repeated observation of natural actions? J. Neurophysiol. 111, 1214–1226.

Leinonen, L., Hyvärinen, J., Nyman, G., and Linnankoski, I. (1979). I. Functional properties of neurons in lateral part of associative area 7 in awake monkeys. Exp. Brain Res. 34, 299–320.

Makin, T.R., Holmes, N.P., and Zohary, E. (2007). Is That Near My Hand? Multisensory Representation of Peripersonal Space in Human Intraparietal Sulcus. J. Neurosci. 27, 731–740.

Matelli, M., and Luppino, G. (2001). Parietofrontal Circuits for Action and Space Perception in the Macaque Monkey. NeuroImage 14, S27–S32.

Murata, A., Fadiga, L., Fogassi, L., Gallese, V., Raos, V., and Rizzolatti, G. (1997). Object Representation in the Ventral Premotor Cortex (Area F5) of the Monkey. J. Neurophysiol. 78, 2226–2230.

Murata, A., Gallese, V., Luppino, G., Kaseda, M., and Sakata, H. (2000). Selectivity for the Shape, Size, and Orientation of Objects for Grasping in Neurons of Monkey Parietal Area AIP. J. Neurophysiol. 83, 2580–2601.

Oosterhof, N.N., Connolly, A.C., and Haxby, J.V. (2016). CoSMoMVPA: Multi-Modal Multivariate Pattern Analysis of Neuroimaging Data in Matlab/GNU Octave. Front. Neuroinformatics 10, 27.

Quinlan, D.J., and Culham, J.C. (2007). fMRI reveals a preference for near viewing in the human parieto-occipital cortex. NeuroImage 36, 167–187.

Raos, V., Umiltá, M.-A., Murata, A., Fogassi, L., and Gallese, V. (2006). Functional properties of grasping-related neurons in the ventral premotor area F5 of the macaque monkey. J. Neurophysiol. 95, 709–729.

Rizzolatti, G., and Luppino, G. (2001). The Cortical Motor System. Neuron 31, 889–901.

Rizzolatti, G., Scandolara, C., Matelli, M., and Gentilucci, M. (1981a). Afferent properties of periarcuate neurons in macaque monkeys. I. Somatosensory responses. Behav. Brain Res. 2, 125–146.

Rizzolatti, G., Scandolara, C., Matelli, M., and Gentilucci, M. (1981b). Afferent properties of periarcuate neurons in macaque monkeys. II. Visual responses. Behav. Brain Res. 2, 147–163.

Rizzolatti, G., Fogassi, L., and Gallese, V. (1997a). Parietal cortex: from sight to action. Curr. Opin. Neurobiol. 7, 562–567.

Rizzolatti, G., Fadiga, L., Fogassi, L., and Gallese, V. (1997b). The Space Around Us. Science 277, 190–191.

Rizzolatti, G., Luppino, G., and Matelli, M. (1998). The organization of the cortical motor system: new concepts. Electroencephalogr. Clin. Neurophysiol. 106, 283–296.

Robinson, D.L., Goldberg, M.E., and Stanton, G.B. (1978). Parietal association cortex in the primate: sensory mechanisms and behavioral modulations. J. Neurophysiol. 41, 910–932.

Rolls, E.T., Huang, C.-C., Lin, C.-P., Feng, J., and Joliot, M. (2020). Automated anatomical labelling atlas 3. NeuroImage 206, 116189.

Sakata, H., and Taira, M. (1994). Parietal control of hand action. Curr. Opin. Neurobiol. 4, 847–856.

Schaefer, M., Heinze, H.-J., and Rotte, M. (2012). Close to You: Embodied Simulation for Peripersonal Space in Primary Somatosensory Cortex. PLOS ONE 7, e42308.

Scheperjans, F., Grefkes, C., Palomero-Gallagher, N., Schleicher, A., and Zilles, K. (2005a). Subdivisions of human parietal area 5 revealed by quantitative receptor autoradiography: a parietal region between motor, somatosensory, and cingulate cortical areas. NeuroImage 25, 975–992.

Scheperjans, F., Palomero-Gallagher, N., Grefkes, C., Schleicher, A., and Zilles, K. (2005b). Transmitter receptors reveal segregation of cortical areas in the human superior parietal cortex: Relations to visual and somatosensory regions. NeuroImage 28, 362–379.

Sereno, M.I., and Huang, R.-S. (2006). A human parietal face area contains aligned head-centered visual and tactile maps. Nat. Neurosci. 9, 1337–1343.

Tyll, S., Bonath, B., Schoenfeld, M.A., Heinze, H.-J., Ohl, F.W., and Noesselt, T. (2013). Neural basis of multisensory looming signals. NeuroImage 65, 13–22.

Wittmann, M., Van Wassenhove, V., Craig, B., and Paulus, M. (2010). The neural substrates of subjective time dilation. Front. Hum. Neurosci. 4, 2.

Supplementary Materials

S1. Adaptation analysis: brain regions selective for objects within face- and hand-based PPS in macaques and humans

We then examined neuronal adaptation by defining regressors of interest separately according to the stimulation period (i.e. first 3 sec of stimulation and second 3 sec of stimulation) and the type of body-part stimulated in each run (i.e. hand, face or trunk). Each regressor has been modeled with the standard SPM12 hemodynamic response function. We also added 6 regressors of no interest, corresponding to the head movement parameters of each run. **Table S1** provides an overview of the different analyses we performed. As in the univariate analysis, we reported clusters surviving an FWE correction ($p<0.05$).

To test our first hypothesis, namely the reduction of BOLD signal in PPS-related areas in humans and monkeys, we contrasted the conditions where the presentation of the stimuli near the hand or the face was repeated. First of all, we compared the first and the second part of the Near-Near trials, keeping separated HAND, FACE and TRUNK conditions. The repetition of the visual stimulus near the same body district should induce a reduction of the BOLD signal in areas selective for the space near this specific body-part. We then compared the activations associated with Near stimulations presented immediately after another Near stimulus (Near-after-Near condition) versus the activations associated with Near stimulations following a Far stimulus (Near-after-Far condition, see Brozzoli et al., 2011, 2012 for a similar procedure). Given the different spatial localization of the two stimuli, Near-after-Far will not undergo adaptation, thus reporting greater activations than Near-after-Near. (See Table 1, on the right, first row). In monkeys, the same contrasts were carried out on the FACE condition. As described in the introduction, we predict that different brain regions in premotor and parietal cortices and in the putamen are involved in the processing of visual stimuli presented in near space. Therein, we hypothesize a reduced BOLD signal, signature of the neuronal adaptation, when the near stimulation is repeated, suggesting that these regions contain neurons sensitive to PPS representation. Furthermore, with regard to within-face-PPS stimulation, we expect spatially coherent activations between the two species, in line with the idea that the representation of the PPS, in humans and non-human primates, involves homologous structures.

Table S1: Summary of the planned fMRI analysis. On the left, the univariate analysis will compare near and far stimulations, regardless of the order of presentation for all type of runs (HAND, TRUNK and FACE). On the right, the adaptation analysis will compare: 1) the fMRI signal in the first (Near-before-Near) and second (Near-after-Near) repetitions of the Near condition (Adaptation Near Repetition approach) and 2) the fMRI signal to near stimuli presented after a far stimulus (Near-after-Far) and after a close one (Near-after-Near, Adaptation Second Part approach). These approaches will be performed separately for HAND, TRUNK and FACE runs to identify hand-, trunk- and face-based PPS underpinnings.

	Univariate Analyses	Adaptation Analyses	
		Near Repetition	Second Part
Selectivity for NEAR stimulations	**Near Condition**		
	Near-Before-Near	Near-Before-Near	Near-After-Far
	Near-After-Near	*versus*	*versus*
	Near-Before-Far	Near-After-Near	Near-After-Near
	Near-After-Far		
	versus	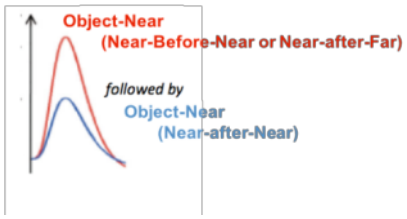	
	Far Condition		
	Far-Before-Far		
	Far-After-Far		
	Far-Before-Near		
	Far-After-Near		

S2. Human's adaptation analyses: stimulation close to the face

After the univariate analyses, we performed adaptation analysis by exploiting both approaches previously described. In the Adaptation Near Repetition approach, the Near-before-Near versus Near-after-Near contrast brings out three significant clusters for H1, two in the right hemisphere and one in the left one. The latter (k=1658, t_{peak}=9.61) report activations in all the ROIs and includes PPS-related areas such as SMG, PMd, IPS and S1. In turn, the two clusters of the right hemisphere also reported activation peaks in SMG, PMd, PMv, IPS, S1 (k=1964, t_{peak}=9.06) and in the putamen (k=334, t_{peak}=6.86).

Also for H2 we find wide activations in this first adaptation approach. Two large clusters emerge one in the left hemisphere (k=3215, t_{peak}=14.19) and one in the right one (k=2927, t_{peak}=12.25). Both clusters included activations in several portions of the IPS, the premotor cortex, the SMG and in S1. Furthermore, two smaller clusters are found at the level of the left (k=290, t_{peak}=12.32) and right (k=319, t_{peak}=11.66) putamen.

However, the pattern of activations observed in the univariate analyses and in the first approach of adaptation analyses does not seem to be repeated in the second approach. Comparing Near-

after-Far versus Near-after-Near conditions, a lack of BOLD signal reduction is observed for both participants, with no clusters able to survive the FWE correction. These results are reported in Table S2.

Table S2. Significant clusters from adaptation analyses for H1 and H2 by comparing stimulations close to or far from the FACE. The significant clusters ($p < 0.05$, cluster-based FWE correction) are reported with the relative activation peaks in MNI coordinates and the relative t-score.

	H1								H2							
	k	Hemisphere	AAL3v1 ROI	Glasser Area	X	Y	Z	t	k	Hemisphere	AAL3v1 ROI	Glasser Area	X	Y	Z	t
Adaptation Near Repetition Face	1658	Left	SMG	RI	-45	-39	25	9.61	3215	Left	SMG	PFcm	-51	-31	22	14.19
				PSL								OP4				
				PFcm								PFop				
			Precentral	6d (PMd)	-45	-8	59	8.32				PSL				
				FEF								PF				
				55b							Postcentral	2 (S1)	-23	-42	53	13.14
				4 (PMC)								3a				
				6a								1 (S1)				
				PEF								Area 43				
				Area 43								3b (S1)				
			IPL	IP2	-51	-39	50	4.94				4 (PMC)				
				PFm								PFt				
				AIP (IPS)							SPL	POS2	-14	-73	39	11.41
				LIPd (IPS)								IPS1				
				PFt								DVT				
			Postcentral	3b (S1)	-59	-11	36	4.71				LIPd (IPS)				
				1 (S1)								LIPv (IPS)				
				2 (S1)								7Pl				
				OP1								VIP (IPS)				
				OP4								7Al				
				3a								7PC				
			SPL	VIP (IPS)	-31	-59	62	6.01				5L				
				7Al							Precentral	PEF	-51	0	42	6.84
				7PC								PMr				
				LIPv (IPS)								6v (PMv)				
				IPS1								6d (PMd)				
	1964	Right	SMG	PFop	64	-25	22	9.06				8C				
				PF								IFJp				
				PSL								4 (PMC)				
				RI								FEF				
				STV								55b				
				PFcm								6a				
				PFm							IPL	AIP (IPS)	-40	-39	42	6.88
			Precentral	6d (PMd)	42	-8	59	8.48				IP2				
				PEF								IP1				
				6v (PMv)								PFm				
				Area 43								LIPd (IPS)				
				8Av								LIPv (IPS)				
				55b								PFt				
				FEF								MIP (IPS)				
				6a								7PC				
			SPL	LIPv (IPS)	30	-59	59	4.45				PF				
				LIPd (IPS)					290	Left	Putamen	Putamen	-28	-17	8	12.32
				VIP (IPS)					2927	Right	Postcentral	2 (S1)	25	-42	53	12.25
				7Al								4 (PMC)				
			IPL	AIP (IPS)	36	-48	45	4.01				3b (S1)				
				IP2								1 (S1)				
				7PC								OP4				
			Postcentral	4 (PMC)	47	-10	46	5.22			SMG	PFcm	50	-28	25	12.07
				3a								RI		-36	22	12.01
				1 (S1)								PFop				
				OP4								PF				
				3b (S1)								PSL				
				PFt								STV				
	334	Right	Putamen	Putamen	36	-11	-8	6.86				PFm				
											Precentral	55b	56	3	42	7.41
												6v (PMv)				
												IFJp				
												PEF				
												FEF				
												6r				
												6a				
												6d (PMd)				
											SPL	VIP (IPS)	19	-62	56	5.99
												MIP (IPS)				
												LIPd (IPS)				
												LIPv (IPS)				
												DVT				
												7Pl				
												7PC				
												7Al				
												7Am				
												5L				
											IPL	IP2	39	-48	45	5.93
												AIP (IPS)				
												LIPv (IPS)				
												PFm				
									319	Right	Putamen	Putamen	30	-17	8	11.66
Adaptation Second Part Face	*No suprathreshold clusters*								*No suprathreshold clusters*							

S3. Monkey's adaptation analyses: stimulation close to the face

Also for non-human primates we have conducted adaptation analyses with both approaches described above. However, in this case it seems that the wide network of activations observed in the univariate analyses does not undergo the adaptation of the response, neither following the repetition of the same close-to-the-face stimulus, nor comparing a Near-after-Far versus a Near-after-Near stimulus. Indeed, it is observed that for M1 only one significant cluster emerges (k=46, t_{peak}=15.53) located in the premotor region (F4 and PMdc) for the Adaptation Near Repetition approach, but no cluster survives the FWE correction in the Adaptation Second Part approach. For M2, moreover, neither the first nor the second approach reported significant clusters. These results are reported in Table S3.

Table S3. Significant clusters from adaptation analyses for M1 and M2 by comparing stimulations close to or far from the FACE. The significant clusters (p <0.05, cluster-based FWE correction) are reported with the relative t-score.

	M1					M2				
	k	Hemisphere	CHARM/SARM 4 ROI	CHARM 6 Area	t	k	Hemisphere	CHARM/SARM 4 ROI	CHARM 6 Area	t
Adaptation Near Repetition Macaques	46	Right	Premotor	F4	15.53	*No suprathreshold clusters*				
				PMdc	7.77					
Adaptation Second Part Macaques	*No suprathreshold clusters*					*No suprathreshold clusters*				

S4: Human's adaptation analyses: stimulation close to the hand

We identified brain areas displaying BOLD-adaptation to repeated visual stimulation near the hand. As for the univariate analysis, we performed a first-level analysis by defining a general linear regression model to the data.

In a first approach, we compared the first part and the second part of the near stimulation (condition called "Adaptation Near Repetition"). In H1, brain activations were reported only in the left hemisphere, with three clusters located in the premotor (k=116, t_{peak}=8.83), parietal (k=148, t_{peak}=6.48) and supramarginal region (k=147, t_{peak}=6.01). Also H2 has two activation clusters consistent with what was observed for H1, both in the left hemisphere and with activation peaks in the parietal (k=368, t_{peak}=11.94), postcentral and supramarginal regions (k=355, t_{peak}=9.2).

In a second approach, we compared near stimuli following a far stimulation (Near-after-Far, NaF regressor) with near stimuli following a near stimulation (i.e. near repeated, Near-after-Near, NaN regressor). We called this condition "Adaptation Second Part". We expected a reduction of the BOLD signal in the near repeated condition compared to the near stimulation followed by a far stimulation. This approach reports only one activation cluster in H1, located in the left SMG (k=164, t_{peak}=5.99) and two significant clusters for H2 in the left hemisphere, the first with activation peaks in in the IPS region (k=386, t_{peak}=10.3), the second located in more supramarginal and postcentral regions (k=333, t_{peak}=6.91).

To sum-up, both analysis (univariate and fMRI adaptation) revealed similar patterns of activation in response to stimulations in the space near the hand. The pattern of activations converges with the one described previously by Brozzoli et al. (2011) using a similar approach. In particular, we found a significant reduction of the BOLD signal in premotor and parietal regions involved in PPS representation (i.e. IPS, PMd, PMv, SMG) when the stimulation was repeated near the hand. These results are reported in Table S4.

Table S4. Significant clusters from adaptation analyses for H1 and H2 by comparing stimulations close to or far from the HAND. The significant clusters ($p < 0.05$, cluster-based FWE correction) are reported with the relative activation peaks in MNI coordinates and the relative t-score.

	H1								H2							
	k	Hemisphere	AAL3v1 ROI	Glasser Atlas	X	Y	Z	t	k	Hemisphere	AAL3v1 ROI	Glasser Atlas	X	Y	Z	t
Adaptation Near Repetition Hand	116	Left	Precentral	4 (PMC)	-40	-11	53	8.83	368	Left	Postcentral	2 (S1)	-23	-39	56	11.94
				FEF							SPL	7Al	-26	-50	59	9.88
				6d (PMd)								7Pl				
				6a								DVT				
			Postcentral	3b (S1)	-44	-18	51	6.01				IPS1				
	148	Left	Postcentral	2 (S1)	-26	-36	59	6.48				VIP (IPS)				
				1 (S1)								7PC				
			SPL	VIP (IPS)	-26	-62	64	4.91				7Am				
				LIPv (IPS)								LIPv (IPS)				
				7PC							IPL	LIPv (IPS)	-28	-49	50	5.92
				7Al								LIPv (IPS)				
	147	Left	SMG	PSL	-54	-42	25	6.01	355	Left	Postcentral	OP1	-51	-20	20	9.2
				PFcm								OP4				
				PF								1 (S1)				
			IPL	PFt	-48	-25	36	5.4				2 (S1)				
				2 (S1)								PFt				
											SMG	PFcm	-48	-31	22	8.14
												PFop				
												PSL				
Adaptation Second Part Hand	164	Left	SMG	PF	-56	-34	34	5.99	386	Left	SPL	7Al	-28	-45	62	10.3
				PSL								7Pl				
				PFcm								VIP (IPS)				
				OP4								5L				
				PFt								7PC				
			IPL	2 (S1)	-47	-27	37	3.25				7Am				
												2 (S1)				
												DVT				
											Postcentral	1 (S1)	-28	-39	67	4.03
									333	Left	Postcentral	OP1	-51	-20	20	6.91
												PFop				
												2 (S1)				
												1 (S1)				
												OP4				
											SMG	PFt	-56	-22	36	5.9
												PFcm				
											IPL	LIPv (IPS)	-26	-57	59	4.52
												AIP (IPS)				

S5: Human's MVPA: stimulation close to the hand

The LDA classifier used to investigate the activations associated to stimulations at different distances from the hand allowed to identify specific response patterns to the difference between stimulations close to and far from the hand. In particular, H1 reports a large activation cluster in the left hemisphere (k=2559, z_{peak}=3.09), whose activation peaks are found in almost all PPS-related areas: SMG, IPS, S1, PMv and PMd. These activations are part of a larger pattern that also includes two clusters in the right hemisphere, the first (k=546, z_{peak}=3.09) with response peaks in SMG, IPS and in the postcentral gyrus, the second (k=34, z_{peak}=3.09) in PMd. Secondly, the activation pattern found in H2 covers both hemispheres, with a large cluster in the left one (k=1929, z_{peak}=3.09), including almost all PPS-related areas (SMG, IPS, PMd, S1),

and a smaller cluster in the right hemisphere (k=831, z_{peak}=3.09), with activation peaks in the superior and inferior parietal lobule (IPS), in the SMG and in the precentral (PMd) and postcentral gyri (S1, PMC). Complete report of these results and peak of activations in MNI coordinates are reported in Table S5 and displayed in Figure S1.

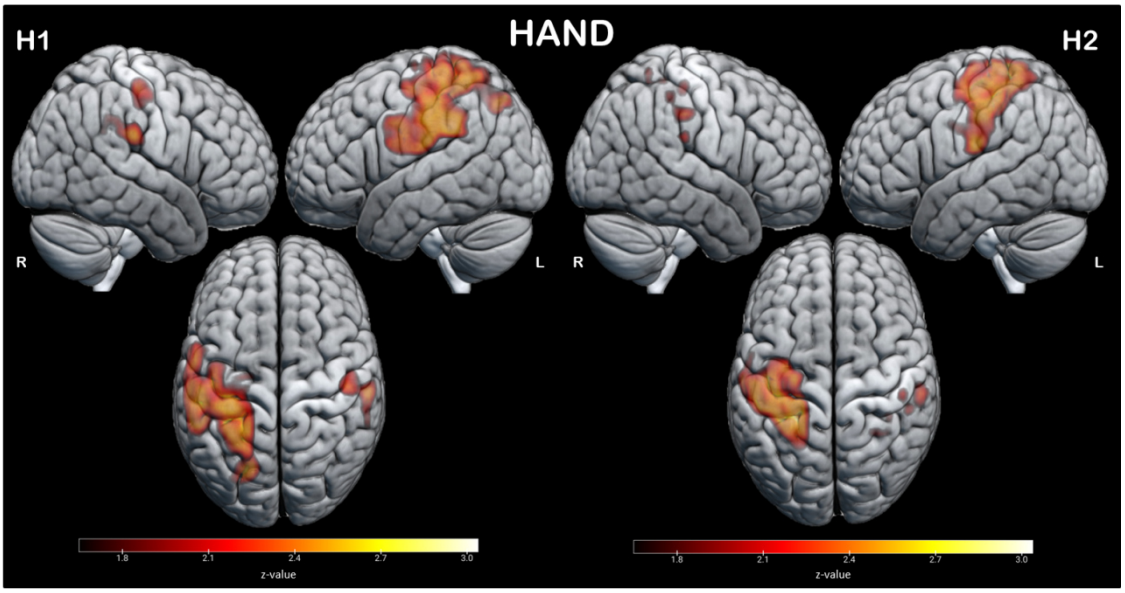

Figure S1. Results from MVPA comparing visual stimuli close to or far from the HAND. z-maps of significant clusters (z<1.65, one-sided t test) for Near vs Far stimulations for participants H1 (left) and H2 (right). For illustrative purposes, z-maps were smoothed after statistics (6 voxels smoothing).

Table S5. Significant clusters from MVPA on human participants training and testing the LDA classifier on the difference between near and far stimulations in HAND condition. The significant clusters (z<1.65, one-sided t-test) are reported with the relative activation peaks in MNI coordinates and the relative z-score.

	H1								H2							
	k	Hemisphere	AAL3v1 ROI	Glasser Atlas	X	Y	Z	z-score	k	Hemisphere	AAL3v1 ROI	Glasser Atlas	X	Y	Z	z-score
MVPA Near vs Far Hand	2559	Left	SMG	PFcm	-53	-25	14	3.09	1929	Left	SMG	PFcm	-53	-25	14	3.09
				PFt								PFt				
				PSL								PSL				
				OP1							Postcentral	2 (S1)	-28	-39	61	3.09
			Postcentral	PFop	-59	-19	25	3.09				1 (S1)				
				4 (PMC)								3b (S1)				
				1 (S1)								3a (S1)				
				2 (S1)								5L				
				3b (S1)								PFop				
				OP4								4 (PMC)				
			Precentral	6d (PMd)	-39	-6	56	3.09				OP4				
				6v (PMv)							Precentral	6d (PMd)	-36	-16	67	3.09
				6mp								6a				
				6a								6mp				
				8c								6r				
				FEF								FEF				
				PEF								PEF				
			SPL	7A	-26	-48	67	3.09				55b				
				7Pl								8C				
				7Al								i6-8				
				5L							SPL	7Al	-25	-42	61	3.09
				VIP (IPS)								7Am				
				LIPv (IPS)								VIP (IPS)				
				MIP (IPS)								7PC				
				DTV							IPL	7PC	-39	-42	50	2.75
				IPS1								LIPv (IPS)				
			IPL	7PC	-34	-42	56	3.09				IP2				
				IP1								AIP (IPS)				
				PFm								PFt				
				PF								IPS1				
	546	Right	Postcentral	OP4	66	-16	14	3.09	831	Right	SMG	PF	58	-28	20	3.09
				PFop								PFm				
				1 (S1)								PSL				
				2 (S1)							Postcentral	2 (S1)	38	-36	59	3.09
				4 (PMC)								1 (S1)				
				PFt								5L				
			SMG	AIP (IPS)	35	-33	42	2.95				PFt				
				PF							Precentral	4 (PMC)	44	-11	53	3.09
				PFop								6d (PMd)				
			Precentral	FEF	50	-11	48	2.75				3b (S1)				
				3b (S1)							SPL	7Al	22	-53	67	3.09
				6d (PMd)								IPS1				
	34	Right	Precentral	6d (PMd)	25	-14	64	3.09				7PC				
				6mp							IPL	IP2	52	-36	53	3.09
												PF				
												AIP (IPS)				
												PFm				

S6: Human's adaptation analyses: stimulation close to the trunk

Also for the trunk, the first (Adaptation Near Repetition) and the second (Adaptation Second Part) adaptation analysis approaches have been performed.

The repetition of the close-to-the-trunk stimulus induces a reduction of the BOLD signal in H1 located in two different clusters, both in the left hemisphere. The first (k=123, t_{peak}=10.43) reports an activation peak in the premotor region, while the second (k=200, t_{peak}=6.93) is located in the left SMG. H2 shows a modulation of brain activity in a cluster (k=194, t_{peak}=9.46) including the S1 area and the IPS of the left hemisphere.

Comparing the Near-after-Far condition versus the Near-after-Near condition, we observe the same supramarginal cluster (k=220, t_{peak}=6.32) of the first approach for H1, lateralized to the left. Similarly, only one significant cluster is observed for H2, again in the left hemisphere, but with activation peaks in the IPS and S1 (k=168, t_{peak}=6.57). These results are reported in Table S6.

Table S6. Significant clusters from adaptation analyses for H1 and H2 by comparing stimulations close to or far from the HAND. The significant clusters (p <0.05, cluster-based FWE correction) are reported with the relative activation peaks in MNI coordinates and the relative t-score.

	H1								H2							
	k	Hemisphere	AAL3v1 ROI	Glasser Atlas	X	Y	Z	t	k	Hemisphere	AAL3v1 ROI	Glasser Atlas	X	Y	Z	t
Adaptation Near Repetition Trunk	123	Left	Precentral	4 (PMC)	-42	-11	56	10.43	194	Left	Postcentral	2 (S1)	-23	-39	56	9.46
				6a							SPL	7Al	-20	-53	62	6.48
				FEF								VIP (IPS)				
				6d (PMd)								7PC				
	200	Left	SMG	PFcm	-45	-39	28	6.93				LIPv (IPS)				
				PSL												
				PF												
				STV												
				PFt												
			IPL	2 (S1)	-48	-25	36	5.06								
Adaptation Second Part Trunk	220	Left	SMG	PFcm	-48	-36	31	6.32	168	Left	Postcentral	S1 (area 2)	-23	-39	56	6.57
				PSL							SPL	7Al	-20	-53	62	4.95
				PF								5L				
				STV								7PC				
			IPL	2 (S1)	-48	-28	39	3.78				VIP (IPS)				

S7: Human's MVPA: stimulation close to the trunk

The Near versus Far classification conducted through an LDA classifier allowed to highlight a bilateral activation pattern in H1 and H2, which clusters and peak of activations are reported in Table S7 and displayed in Figure S2.

H1 reports a response pattern consisting of a large cluster in the left hemisphere (k=1944, z_{peak}=3.09), including peak of activations in all the ROIs and in PPS-related areas, as SMG, IPS, PMv and S1, and three clusters in the right hemisphere. The first of the latter (k=233, z_{peak}=3.09) is located at the level of the SMG, the second (k=60, z_{peak}=2.41) in IPS and the last (k=56, z_{peak}=2.58) in S1.

Similarly, activation patterns in PPS-related areas were also observed bilaterally for H2, with a cluster in the left hemisphere (k=1063, z_{peak}=3.09) and one lateralized to the right (k=1570, z_{peak}=3.09) both reporting activations in the supramarginal region, in the IPS and in S1. The cluster on the left, moreover, reported activations in PMv.

Table S7. Significant clusters from MVPA on human participants training and testing the LDA classifier on the difference between near and far stimulations in the TRUNK condition. The significant clusters (z<1.65, one-sided t-test) are reported with the relative activation peaks in MNI coordinates and the relative z-score.

	H1								H2							
	k	Hemisphere	AAL3v1 ROI	Glasser Atlas	X	Y	Z	z-score	k	Hemisphere	AAL3v1 ROI	Glasser Atlas	X	Y	Z	z-score
MVPA Near vs Far Trunk	1944	Left	SMG	OP4	-54	-25	14	3.09	1063	Left	SMG	PFcm	-54	-25	14	3.09
				OP1								PFop				
				PFop								PF				
				PFcm							Postcentral	2 (S1)	-28	-42	56	3.09
				PF								3b (S1)				
				PSL								OP4				
			Postcentral	2 (S1)	-23	-34	64	3.09				4 (PMC)				
				1 (S1)								PFt				
				4 (PMC)								3a (S1)				
				3a (S1)							SPL	7Al	-22	-56	61	3.09
				3b (S1)								IPS1				
				PFt								DVT				
			SPL	7Al	-23	-50	62	3.09				7Pl				
				IPS1								7Am				
				DVT								VIP (IPS)				
				7Pl								5L				
				VIP (IPS)							Precentral	6mp	-23	-14	67	2.51
			Precentral	6a	-34	-8	53	3.09				6v (PMv)				
				6v (PMv)								PEF				
				43								6d (PMd)				
				PEF							IPL	7PC	-37	-45	50	2.88
				FEF								AIP (IPS)				
				55b								IP2				
				6mp								LIPv (IPS)				
			IPL	PFm	-48	-53	42	2.37	1570	Right	SMG	PFop	67	-25	20	3.09
				AIP (IPS)								PSL				
				LIPd (IPS)								PFt				
				LIPv (IPS)								PFcm				
				PFt								STV				
				IP2								PF				
	233	Right	Postcentral	OP4	61	-16	16	3.09			Postcentral	2 (S1)	44	-25	45	3.09
			SMG	PFop	64	-22	28	3.09				1 (S1)				
				PF								7PC				
				PFt								3b (S1)				
				PSL								3a (S1)				
				PFm								PFt				
				STV							Precentral	4 (PMC)	44	-11	39	3.09
				PFcm								PEF				
	60	Right	SPL	7Am	16	-59	64	2.41				6a				
				VIP (IPS)								FEF				
	56	Right	Postcentral	1 (S1)	33	-36	67	2.58				8Av				
											SPL	LIPv (IPS)	28	-53	59	3.09
												5L				
												7Al				
												7Pl				
												VIP (IPS)				
												MIP (IPS)				
												DVT				
											IPL	PFm	50	-39	50	3.09
												PF				
												AIP (IPS)				
												LIPv (IPS)				
												IP1				
												IP2				

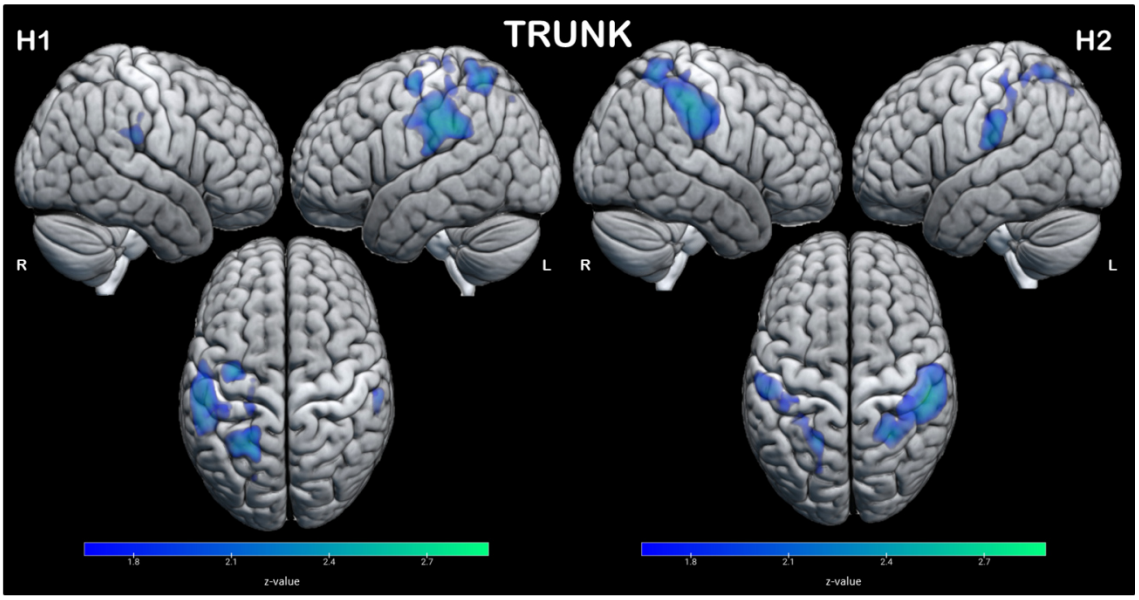

Figure S2. Results from MVPA comparing visual stimuli close to or far from the TRUNK. z-maps of significant clusters (z<1.65, one-sided t test) for Near vs Far stimulations for participants H1 (left) and H2 (right). For illustrative purposes, z-maps were smoothed after statistics (6 voxels smoothing).

ETUDE 2

Comparaison de la représentation de l'espace péri-personnel chez l'homme et le singe avec un objet virtuel

---

Bridging the gap between the Human and Macaque PPS network: a similar fMRI approach in virtual reality

Audrey Dureux, Camille Giacometti, Clément Desoche, Alessandro Farnè and Fadila Hadj-Bouziane

Article en préparation

Bridging the gap between the Human and Macaque PPS network: a similar fMRI approach in virtual reality

Audrey Dureux[1,2], Camille Giacometti[2,3], Clément Desoche[1,2,4], Alessandro Farnè[1,2,4,5] and Fadila Hadj-Bouziane[1,2]

1. Integrative Multisensory Perception Action & Cognition Team - ImpAct, INSERM U1028, CNRS UMR5292, Lyon Neuroscience Research Center (CRNL), Lyon, France
2. University UCBL Lyon 1, University of Lyon, Lyon, France
3. Stem Cell and Brain Research Institute U1208, 69500 Bron, France.
4. Hospices Civils de Lyon, Neuro-Immersion & Mouvement et Handicap, Lyon, France
5. Center for Mind/Brain Sciences (CIMeC), University of Trento, Italy.

Corresponding authors:
Audrey Dureux and Fadila Hadj-Bouziane, INSERM U1028, CNRS UMR5292, Lyon Neuroscience Research Center, ImpAct Team, 16 Avenue Doyen Lépine 69500 Bron, France.
Emails: audrey.dureux@gmail.com ; fadila.hadj-bouziane@inserm.fr.

Conflict of Interest: The authors declare that they have no conflict of interest.
Acknowledgements: This work was funded by the French National Research Agency ANR-15-GE37-0003 grant MySpace to FHB.

Funders had no role in study design, data collection and analysis, decision to publish, or preparation of the manuscript.

Abstract

Electrophysiological evidence in macaques and fMRI evidence in humans suggest the involvement of parietal and premotor areas in close space processing. However, no direct comparative approach has even been taken to relate these two sets of data between species.

Here, we used a direct comparative approach in fMRI with an paradigm in virtual reality to identify functional homologies in distance-selective areas between species. We describe the brain network dedicated to the close space processing, in the peripersonal space (PPS) in each species. Specifically, processing of 3D objects close to the body involved occipital, temporal, parietal, premotor and prefrontal areas in mostly similar brain regions in both species. These results suggest that, in each species, these regions would have a similar function for the processing of 3D information occurring in PPS. We propose that the dorsal stream of Humans and Macaques would have similar organization in the relay of visual information occurring in PPS from the ventral stream, through reciprocal interactions by principally two different parieto-premotor and parieto-prefrontal pathways, subserving visually guided action in PPS.

Using a similar paradigm in virtual reality in both Humans and Macaques, these findings constitute the first step in the identification of functionally homologous areas involved in PPS processing in these species.

1. Introduction

Growing evidence demonstrates that the brain contains a dynamic and complex representation of the space surrounding us. In particular, neuropsychological studies in brain-injured patients (e.g. di Pellegrino & Làdavas, 2015; Làdavas et al., 1998; Làdavas & Farnè, 2004) and in macaque monkeys identified a dissociation between close and far space. In macaque monkeys, specific responses for the processing of close space, termed peripersonal space (PPS, Rizzolatti et al., 1981), have been identified when real objects were presented close to the monkey compared to far, in neurons with uni – or bimodal properties (i.e., responding to visual stimulation alone or both tactile and visual) within cortical (parietal and premotor cortex; see references below) and subcortical areas (putamen; Graziano & Gross, 1993). Specifically, the cortical areas involved the ventral, medial and lateral sections of the intraparietal sulcus (VIP, MIP, LIP; Colby et al., 1993; Colby & Duhamel, 1996; Duhamel et al., 1998; Genovesio & Ferraina, 2004; Gnadt & Mays, 1995) and area 7b (Graziano & Cooke, 2006) as well as the ventral premotor cortex, in rostral area 6, especially the F4 and F5 regions (Gentilucci et al., 1983, 1988; Graziano et al., 1997; Murata et al., 1997; Rizzolatti et al., 1981). Typically, the procedure used in the monkeys, involved statistic or looming objects in different sectors of space (close or far from the body). More recently, neurons modulated by the distance at which a visual object was presented were described in the frontal eye field (FEF) (Cléry et al., 2015) and V6A area in the medial part of parietal cortex (Luppino et al., 2005) (Hadjidimitrakis et al., 2011, 2012). This modulation likely reflects pupillary movements when fixing an object at several distances moving in depth (Alkan et al., 2011).

Since the initial discovery of peripersonal space neurons in the ventral premotor cortex of the macaque monkey (Rizzolatti et al., 1981a), these neurons and especially their proposed functional role(s) in human and non-human primates have attracted a lot of attention and controversy. While PPS neurons have been identified by electrophysiological studies in brain regions of macaque monkeys, evidence of putative homolog of a PPS network in the human brain was inferred from measurements of brain activity using functional magnetic resonance imaging (fMRI) in similar settings as that used in the monkeys. These procedures could involve multisensory tasks with tactile stimuli applied to different body parts while visual or auditory stimuli moved towards the body (Bremmer et al., 2001b; Gentile et al., 2011, 2013; Sereno & Huang, 2006) and more recently they involved unisensory tasks where only visual stimuli were moved close or far from the hand or the face (Brozzoli et al., 2011, 2012; Makin et al., 2007;

Quinlan & Culham, 2007; Schaefer et al., 2012). These last years, these fMRI studies have played an important role in identifying the functional architecture of the PPS network in parietal (i.e., in superior parietal lobule, SPL; inferior parietal lobule, IPL; intraparietal sulcus, IPS) and premotor (i.e., in ventral and dorsal premotor cortex, PMv and PMd) brain regions of the human cortex with either uni- or multisensory stimuli.

So far, only one study has attempted to uncover neural correlates of PPS representation using a whole brain fMRI approach in awake macaque monkeys (Cléry et al., 2018) in order to obtain a comparative description of the PPS networks in both species, humans and monkeys. They identified a brain network with preferential responses for a real object presented close compared to far from the monkey face in some temporal areas, in the parietal cortex namely in the VIP, MIP, AIP, the medial parietal cortex (PGm) and the parietal opercular region (7op) but also in the dorsal (F2) and ventral (F4/F5) premotor cortex, in the SEF and FEF premotor regions and in prefrontal areas 46p and 45b. Although it seems established at this point that there are PPS-selective areas in both the macaque and human brain, it is not clear how these regions correspond across species given the heterogeneity in the methodologies used as well as the differences in the type of analyses carried out in both species. Using a direct, comparative approach may provide insights into the functional similarities of the distance-selective areas in the two species.

Here we developed a novel procedure relying on a virtual 3D environment inside the fMRI scanner in both macaque monkeys and humans to establish functional correspondences between brain areas involved in PPS processing across the brain in the two species. Until now, all the studies in this domain employed real visual objects or 2D visual stimuli displayed on a screen. Here we used the virtual reality inside the scanner in order to manipulate and control very precisely visual information in the sagittal plane and vary their presentation at different distances from our body, similarly to what we observed every day in our real world. We used non-social 3D stimuli (geometrical shapes) presented either close (30 cm) or far (300 cm) in the virtual environment.

We focused our analysis on identifying analogies between the macaque brain and human brain. Specifically, distance-selective areas in both species were directly compared on the basis of similarities in their spatial arrangement and mean signal responses preferentially evoked when 3D objects were presented in close compared to far space.

Using this direct comparison, we show that both species recruit a very similar network including similar set of regions mostly in occipital, parietal, premotor and prefrontal areas when a visual

3D information (i.e., a neutral object) occurred in PPS. We propose that the dorsal stream, in both species, should have a similar organization, acting with the ventral stream which should relay visual information to a core premotor-parietal network allowing us to process visual information occurring in PPS and allowing us to act accordingly.

Taken together, these findings provide an initial step toward defining functionally homologous areas in PPS processing in humans and macaques, by using similar fMRI virtual reality protocols in both species.

2. Materials and Methods

2.1. Macaque monkeys

In this study, we included 2 rhesus monkeys (*Macaca mulatta*, 5 - 6 kg): two females (Monkeys C, 21 years old and N 9.5 years old), in the appliance to the 3Rs principles of replacement, reduction and refinement (Prescott & Poirier, 2021). Reduction is about minimizing the number of animals used per experiment so achieving more science from each animal is a form of reduction and it avoids the need for additional animal use (Prescott & Poirier, 2021). Therefore, we chose to repeat several MRI sessions for each animal instead of increasing the number of animals.

Macaque monkeys were surgically implanted with a MR-compatible head post under anesthesia and aseptic conditions. During the surgical procedure, the animals were firstly sedated and intubated to maintain the animals under gas anaesthesia with a mixture of O2 and air (isoflurane 1-2%). With their head immobilized in a stereotactic apparatus, the head fixation device was positioned on the skull after an incision of the skin along the skull midline and maintain in place using ceramic sterile screws and acrylic dental cement (Palacos® Bone cements). Throughout the surgery, heart rate, respiration rate, blood pressure, expired CO2, and body temperature were continuously monitored. After the surgery, the wound was closed in anatomical layers. Analgesic and antibiotic treatment were administered for 5 days postoperatively, and monkeys recovered for at least 1 month. All procedures followed the guidelines of European Community on animal care (European Community Council, Directive No. 86–609, November 24, 1986) and were approved by French Animal Experimentation Ethics Committee #42 (CELYNE).

After recovery, monkeys were then trained daily to sit in a sphinx position in a plastic chair (Rogue Research) and acclimatized to the head-fixation system in a mock scanner mimicking

the actual MRI environment. Monkeys were trained every weekday for 1 to 2 hours to maintain their gaze on a central fixation cross presented on a screen in front of them. Throughout training, the animals were maintained on a water and food regulation schedule, individually tailored to maintain a stable level of performance for each monkey.

During the scanning sessions, the monkeys sat in a sphinx position in the plastic chair positioned within a horizontal magnet (3-T MR scanner; Siemens). Their head was restrained using the surgically implanted head post and they faced a translucent screen placed 57 cm from their eyes. Both right and left eye positions were monitored at 1000 Hz during scanning using an eye-tracking system (Eyelink 1000 plus long-range). The calibration procedure was performed with the software directly implemented in the Eyelink software and consisting in 5 points sequentially switched on and off on the screen. Monkeys were rewarded with liquid dispensed by a computer-controlled reward delivery system (Crist®) through a plastic tube placed in their mouth. As during training sessions, they were rewarded when orienting and maintaining their eyes gaze toward the fixation central cross, within a 4° window around the cross and the reward volume increased as fixation duration increased. The reward was suspended when the animal was no longer fixating (i.e. gaze outside the window of 4° around the cross) in order to encourage the animal to keep their gaze on the cross.

For each monkey and in each run, the horizontal (X) and vertical (Y) eye positions from the right and left eyes as well as the pupil size of both eyes were recorded. We computed the percentage of time the animals spent fixating within the central window. Among 28 runs for monkey N and 21 runs for monkey C (2 runs for monkey N and 9 runs for monkey C were not recorded due to technical issues), the mean percentage of time spent on the fixation cross was respectively 72% and 97% for monkeys N and C.

2.2 Human participants

We included 3 healthy volunteers where each participated in five different sessions spread over several days (S1: woman of 32 years old, S2: man of 31 years old and S3: man of 27 years old). The subjects were recruited through web advertising and provided informed consent. They were right-handed, had normal or corrected-to-normal vision and had no history of neurological or psychiatric disorders. All human experimental procedures were followed by the Declaration of Helsinki standards and was approved by the Institut National de la Santé et de la Recherche Médicale (INSERM) Ethics Committee (IRB00003888, No. 16-341).

During the scanning sessions, participants were lying down comfortably on the scanner bed and foam padding was used around their head and knees. A 64-channel head coil with a mirror system attached on the device was positioned around their head in order to visualize the task on the screen. Right eye position was monitored at 1000 Hz during scanning using an eye-tracking system (Eyelink 1000 plus long-range) to ensure the subject maintains their eye gaze on the central cross. As for monkeys, the calibration procedure consisted in 5 points sequentially switched on and off on the screen, directly implemented in the Eyelink software and the horizontal (X) and vertical (Y) right eye positions were recorded for each run and each participant. For each participant, the mean percentage of fixation across all runs exceeded 90%.

2.3 Apparatus and Stimuli

The virtual reality (VR) environment scene was rendered in a translucent screen allowing passive 3D projections with polarized light (ST-Pro-X, screen-tech) through a 3D projector using polarized system (Vpixx, screen-tech, resolution 1920 x 850, frequency of 120 Hz). In order to create the illusion of a three-dimensional environment, a polarizing filter was placed from 20 and 50 mm in front of the projector lens. Human participants visualized the scene through a first-surface-mirror (ST-GS mirror passive 3D ready, Screen-tech) as they were lying down in the scanner, while monkey subjects visualized the scene directly on the screen as they sat in sphinx position in front of the screen in the scanner. Both humans and monkeys were equipped with passive paper glasses in order to visualize the 3D image (ST-3D-Glasses, screen-tech). The augmented technology Unity software (Version 5.1.2; Unity Technologies, San Francisco, CA) was used to create the virtual environment and display the stimuli. In order to create a greater immersion effect for the subjects, as we can have it with a head-mounted display, we created an environment reproducing the inside of MRI scanner as to minimize the distractors inside the scanner and to give the impression that they are part of the 3D environment projected Visual stimuli were presented in the virtual environment at two different distances (close, 30 cm or far, 300 cm) (Figure 1).

For both species, visual stimuli consisted of non-social stimuli (objects) representing 3D coloring geometrical shapes of cubes or spheres (with red, blue, and green colors) created with the Unity software as in Blini et al. (2018). The retinal size of the stimuli was kept constant across distances, resulting in the more distant stimuli being larger. The retinal size correction was implemented directly in the Unity software by scaling up the far stimuli based on the size

and distance of the close one in order to have the exact same 3D pictures represented in close or far space (see our last study for the exact procedure and the theorem used; Blini et al, 2018; Dureux et al., 2021)

2.4 Passive viewing task

Blocks lasted 24 sec and contained 12 stimuli. Each stimulus lasted 1000 ms and was overlaid with a black fixation and was followed by 1000 ms of fixation cross only. Each block included non-social stimuli randomly selected among the distance of presentation (30 cm, close or 300 cm, far). The cross was presented at the same distance as the stimuli. The shape (cube/sphere) could vary randomly inside the block (Figure 1). Blocks of fixation only, without stimuli, were also presented at different distances lasting 20 sec.

Each run consisted of 30 blocks consisting in several repetitions of each condition (i.e., objects close and objects far) interposed by fixing blocks at different distances (i.e., fixation cross alone close and fixation cross alone far) in order to create a baseline between each block of stimulation. The order of conditions in each block was randomized across participants. The task was controlled by the Unity program.

Humans and monkeys were instructed or trained to maintain their gaze on the black fixation cross during all scanning sessions (during stimulation blocks as well as fixation blocks).

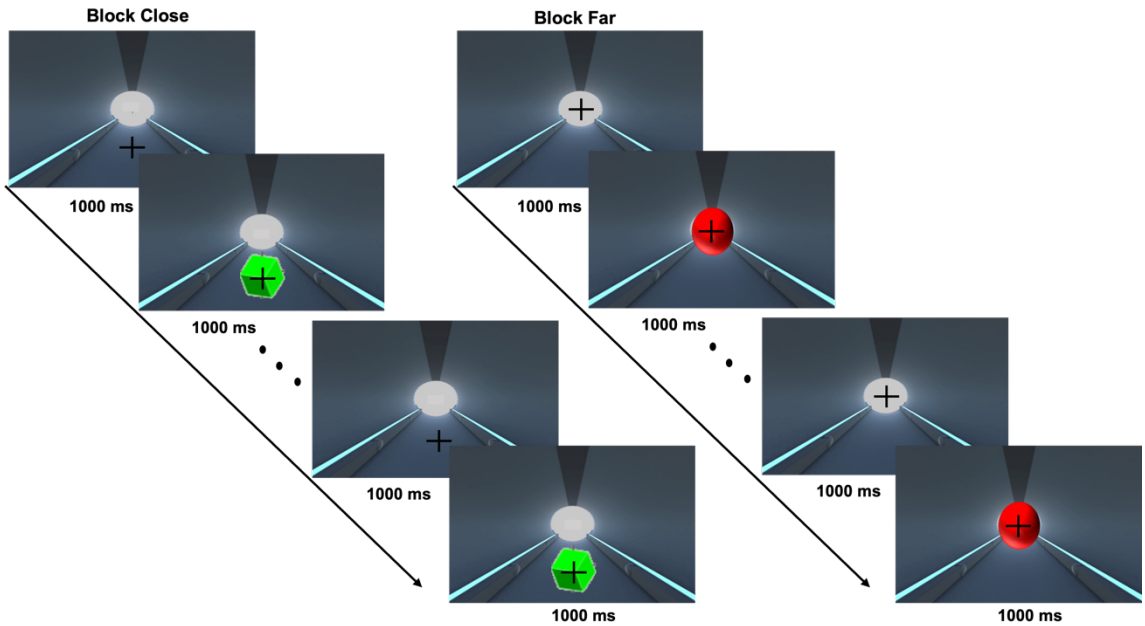

Figure 1. Experimental set up. Each block consisted of 12 geometrical 3D shapes of one distance selected randomly (close, 30 cm or far, 300 cm) lasted 24 sec. Each stimulus was presented 1 sec interspersed by fixation cross only. The task consisted to a passive viewing task where subjects were instructed to maintain their gaze on the black fixation cross.

2.5 fMRI data acquisition

The fMRI experiments took place in the same 3-Tesla Magnetom Prisma scanner (Siemens) for both humans and monkeys. Human participants were scanned using a whole-head 64-channels receive coil (Siemens) in five sessions, that included one T1-weighted anatomical scan MPRAGE 3D (TR = 3 s, TE = 3.34 ms, flip angle: 8°, matrix size = 224x256; resolution = 1x1x1 mm3) and 20 functional runs for S1 or 25 functional runs for S2 and S3 (TR = 2.2 s, TE = 29 ms, flip angle = 90°, matrix size = 78x78, resolution of 2.7x2.7x2.7 mm^3). For monkeys C and N, a T1-weighted anatomical image was acquired under general anesthesia (MPRAGE sequence, TE = 366 ms, TR = 3 s, resolution = 0.5x0.5x0.5 mm3). During functional sessions, EPI volumes were acquired using an 8-channels surface coil (KU, Leuven) around the head and a circular transmit coil positioned above the head (Mareyam et al., In: Proceedings of the 19th Annual Meeting of ISMRM, Montreal, Canada, 2011) using the following sequence parameters: BOLD sessions: TR = 2.5 s, TE = 30ms, flip angle = 90°, matrix size = 84x76, resolution = 1.25x1.25x1.25 mm^3. Across 15 sessions, we selected for each monkey the 30 runs with the higher temporal signal to noise ratio (tSNR) and with minimum brain movements computed through the six temporal derivatives (three translations and three rotations). For each run and each monkey, we computed the temporal SNR (i.e., tSNR - average intensity of time series divided by the standard deviation) across the brain using the AFNI software (Cox, 1996).

2.6 fMRI data preprocessing

For humans, fMRI data were preprocessed with Statistical Parametric Mapping - SPM12 software (Wellcome Trust Centre for Neuroimaging, University College London, UK). Functional images were realigned to correct for head movements and resliced, then a mean functional image was created. The anatomical image from each individual participant was then coregistered with the mean functional image. The anatomical images were segmented into white matter, gray matter, and CSF partitions and normalized to the Montreal Neurological Institute (MNI) standard brain space. Functional images were also normalized to the MNI

space. Spatial smoothing was then applied to the functional images using a Gaussian kernel with an isotropic FWHM of 8 mm.

For monkeys, the images were skull-stripped using the bet tool from the FSL software (https://fsl.fmrib.ox.ac.uk/fsl/fslwiki/BET, Jenkinson et al. 2005) and the same preprocessing has been applied to all functional volumes except for the normalization. For monkeys, the spatial smoothing was applied to the functional images using a Gaussian kernel with an isotropic FWHM of 4 mm. To ensure optimized inter-session and inter-subject comparisons, both anatomical and functional images were then registered in a macaque common atlas space, CHARM/SARM (Hartig et al., 2021; Jung et al., 2021; Reveley et al., 2017) using the AFNI software (Cox, 1996).

Importantly, in both humans and monkeys, we mapped our functional data onto brain atlases that feature parcellation based on both anatomical and functional criteria (Glasser et al., 2016; Jung et al., 2021) to localize the activation peaks. A recent study on cross-species functional alignment indicated some correspondences between label name used in the Glasser atlas and label name used in different macaque atlases (Xu et al., 2020), based on cross-species comparison studies (Essen & Dierker, 2007; Glasser et al., 2016; Mars et al., 2011; Neubert et al., 2014; Sallet et al., 2013). They notably argue that the VIP, LIP, AIP, area 8A of the FEF and the frontal area 9/46d as well as MT and visual areas V1 and V2 correspond in their terms between both species. V6A area In Glasser atlas was also based on the studies of Pitzalis et al. (2006) that have identified the human homologue of V6A. Moreover, the study of Orban, (2016) investigating the functional definitions of parietal areas in humans and macaques, seems to be in line with the location of VIP, LIP and AIP in both SHARM and Glasser atlases. Indeed, they proposed that the dorsal IPS anterior (DIPSA) in humans may correspond to VIP in monkeys whereas dorsal IPS medial (DIPSM) in humans may correspond to anterior LIP in monkeys and only ventral DIPSA in humans should corresponds to posterior AIP in monkeys (Orban, 2016). These locations identified in this study seem in line with the anatomical brain regions defined in the Glasser atlas redefined with similar labels between humans and monkeys (Glasser et al., 2016).

2.7. Statistical analysis of imaging data

Whole-brain univariate analysis

The general linear model, performed using SPM12, estimates the responses to objects presented close versus far. The general model included events of interest, corresponding to the 24 sec presentation of the stimuli of each block modeled as a function of the distance presented. We also included regressors of non-interest corresponding to the six head movement parameters estimated during realignment in the preprocessing of data. Therefore, for both human and monkey data, a hemodynamic response function (HRF) modeled our 2 predictors of interest as well as our 6 predictors of non-interest. Analysis was performed for each subject separately by concatenating all runs acquired across sessions for each subject, corresponding to a total of 20 and 25 runs respectively for S1, S2 and S3 as well as 30 runs for monkey C and monkey N. Cluster significance was assessed by thresholding T-maps at cluster-forming threshold of $p<0.001$ uncorrected and then corrected for multiple comparisons using Family-Wise Error (FWE)-corrected $p<0.05$ at the cluster-level as implemented in SPM12.

In humans, to identify the location of the resulting activation peaks, we used the AAL3 atlas (Rolls et al., 2020) and the most recent multi-modal cortical parcellation atlas, carried out on four different features, including both anatomical and functional criterion: cortical thickness, myelin maps, task fMRI and resting state fMRI (Glasser et al., 2016). For monkeys, we used levels 4 and 6 of the cortical CHARM atlas (Jung et al., 2021) and the level 5 of subcortical SARM atlas (Hartig et al., 2021), that also features a fined-grained anatomical and functional descriptions of brain areas.

For each significant cluster, the coordinates for each brain region were reported with their associated t values.

Univariate region-of-interest (ROI)-based analysis

In addition to the whole-brain analysis, we also performed a region-of-interest analysis of key premotor-parietal regions based on existing literature on PPS representation. This analysis was particularly interesting within this thesis framework as it allows us to compare PPS representation across species in both studies included in the thesis, that is with real objects (ici renvoie au chapitre adaptation) and here with virtual objects.

In humans, we selected regions of interest (ROIs) reported in previous fMRI studies investigating neural bases of PPS in a non-social context (Bremmer et al., 2001; Brozzoli et al., 2011, 2012; Gentile et al., 2011, 2013; Makin et al., 2007; Quinlan and Culham, 2007; Schaefer et al., 2012). All these regions were reported in the meta-analysis summarizing brain regions

consistently found in these studies (Grivaz et al., 2017). We used AAL3v1 atlas (Rolls et al., 2020) to define our anatomical ROIs, including: the precentral gyrus, the postcentral gyrus, the superior and inferior parietal lobule and the supramarginal gyrus. Although the putamen was only found in some studies (Brozzoli et al., 2011; Gentile et al., 2011, 2013) and not reported in the meta-analysis of Grivaz et al. (2017), we also selected this region according to the properties identified also in monkeys (Graziano & Gross, 1993). In order to compare activations obtained in both humans and macaques in a same way, we selected monkeys brain regions identified from seminal electrophysiological studies on PPS (Bremmer et al., 2013; Colby and Duhamel, 1991, 1996; Colby et al., 1993; Graziano and Cooke, 2006; Graziano et al., 1994; Leinonen et al., 1979; Rizzolatti et al., 1981; Robinson et al., 1978) with the fourth level of the CHARM atlas (Jung et al., 2021). Our anatomical ROIs included: the lateral and ventromedial intraparietal sulcus, the area 7 in inferior parietal lobule, the area 5, the premotor cortex and the somatosensory cortex SI. Additionally, we used the level 5 of the SARM atlas (Hartig et al., 2021) to also include the putamen as a ROI (Graziano & Gross, 1993).

Human brain ROIs were extracted from AAL3v1 atlas using SPM12 and a whole bilaterally mask including all these selected regions was created using marsbar software (Brett et al., 2002). Macaque brain ROIs were extracted from the CHARM atlas (level 4) and the SARM atlas (level 4) using AFNI and, as for humans, a whole mask including all bilateral regions extracted was created with marsbar software (Brett et al., 2002).

We then analyzed at the first level the preferential activations for close versus far with an inclusive mask containing bilateral ROIs for each subject and each monkey. Voxel significance was assessed by thresholding T-maps at $p<0.05$, corrected for multiple comparisons (FWE as implemented in SPM12). Inside each significant ROIs we define significant brain regions contained in these ROIs using Glasser atlas and level 6 of the CHARM atlas for human and monkey, respectively. We reported coordinates as well as t values associated.

3. Results

We compared the activation pattern elicited by objects presented close (30 cm) versus far (300 cm) using a similar procedure in a virtual reality environment in awake rhesus macaques (n=2) and humans (n=3). As presented below, we first applied a whole brain analysis

approach, and we then focused the analysis on a predefined bilateral mask containing ROIs based on previous evidence on PPS processing in each species.

3.1. Whole brain activations for close stimuli compared to far stimuli: identification of an extended PPS network in Humans and Monkeys

Results obtained in human subjects

The univariate analysis revealed, for the three subjects, preferential activations for close stimuli compared to far in a set of occipital, temporal, parietal, premotor and frontal brain regions as well as in the cerebellum. An exhaustive list of the clusters of activation for each subject can be found in Table 1 and depicted in Figure 2.

For subjects S1, S2 and S3, the largest significant cluster included occipital, temporal, parietal areas as well as the cerebellum and also a part of postcentral gyrus (S1, S2, S3) and precentral gyrus (S2, S3) [**S1:** cluster 1 = 7581 voxels, peak T in left middle occipital gyrus = 16.35; **S2:** cluster 1 = 16648 voxels, peak T in right superior occipital gyrus = 17.21; **S3:** cluster 1 = 11510 voxels, peak T in right inferior occipital gyrus = 14.28]. Indeed, in this cluster, bilateral activations in occipital cortex in response to close *versus* far objects extended into the inferior, middle, and superior occipital gyrus and also in the cuneus, lingual gyrus, the calcarine sulcus (activations in visual areas V1, V2, V3 and V4) as well as in the parieto-occipital sulcus (V6 and V6A). This contrast also yielded enhanced responses in the medial superior temporal area (MST) for the three subjects (left hemisphere for S1 and right hemisphere for S2 and 3), in the inferior temporal gyrus (area TE2 posterior for S1 and S2 and area PH for S3) and in the right temporo-parietal occipital junction for S2 and S3. Still in this cluster, in the parietal lobe, bilateral activations extended into the precuneus, the superior parietal lobule (SPL), the inferior parietal lobule (IPL) for S1, S2 and S3 and in supramarginal gyrus (SMG) only for S2. Of note and based of the Glasser parcellation, the activations were localized in the ventral intraparietal area (VIP), lateral intraparietal area (LIP), medial intraparietal area (MIP), anterior intraparietal area (AIP) and in area 7A (medial and lateral area 7A) and 7P (medial area 7P and area 7PC).

Other brain regions in frontal cortex in particular were also recruited for close vs. far objects including within the precentral gyrus (PMd, PMv), the postcentral gyrus (SI), and within

anterior frontal regions consistently for the 3 subjects. However, the activation pattern within the more anterior frontal regions were more variable across subjects and included the areas in the prefrontal cortex and the frontal pole for the 3 subjects, yet in subjects, the activation pattern was more extended spatially in S1 compared to subjects S2 and S3.

In more detail, for subject S1, activations for close versus far objects were found in the right postcentral gyrus (area 1 and area 2 of the somatosensory cortex SI). Other activations were distributed in two significant clusters in each hemisphere including the middle frontal gyrus in area 55b, area 9-46d, area 8C and only in area 9-46d for the left hemisphere [**S1**: cluster 2: 608 voxels, peak T in left precentral gyrus = 11.07, cluster 3: 407 voxels, peak T in right middle frontal gyrus = 11.09] and the precentral gyrus, within FEF and PMd. We also found stronger BOLD responses for close versus far objects in the right and left orbitofrontal cortex (OFC) in medial (area 10p or area 10v) and anterior part (area 11l and area 13l) [**S1**: cluster 4: 227 voxels, peak T in left OFCmed = 4.91, cluster 5: 157 voxels, peak T in right OFCmed = 5.26].

For subject S2, activations for close versus far objects were found in the left postcentral gyrus (Primary motor cortex, area 4), the left precentral gyrus (FEF, Premotor eye field (PEF), ventral area 6 (PMv) and area 8C), the left inferior frontal operculum, the left middle frontal gyrus, the left Rolandic operculum and the bilateral middle cingulate gyrus as well as the bilateral insula. We also found responses within the right precentral gyrus (PMv, PEF), the right postcentral gyrus (area 2 in SI), the right inferior frontal operculum, the right rolandic operculum, the right superior frontal gyrus and the right insula as well as within two subcortical regions, namely the putamen and the thalamus. One other cluster included the right middle frontal gyrus and the right inferior frontal gyrus in particular its orbital and triangular part [**S2:** cluster 2: 1556 voxels, peak T in right precentral gyrus = 7.36, cluster 3: 561 voxels, peak T in right middle frontal gyrus = 5.67]. Finally, one cluster included the right supplementary motor area (SMA), the right superior frontal medial and the left and right middle cingulate gyrus (area posterior 24', area p32', area 23c) and another one included the left SMA [**S2:** cluster 4: 552 voxels, peak T in right SMA = 5.47, cluster 5: 129 voxels, peak T in left SMA = 4.20].

For subject S3, activations for close versus far objects were found in the left precentral gyrus (FEF, PEF, dorsal area 6 (PMd) and PMv), the left postcentral gyrus (area 2 in SI and area 4 in M1) and in inferior frontal operculum. We also found stronger responses for close versus far

objects in bilaterally in the superior and middle frontal gyrus and its orbital part (area 10r), in the superior frontal medial (area 9), and the rectus (area 10v), and within the SMA and the left superior frontal gyrus and the right middle cingulate gyrus (area p32'). The two other clusters in the right hemisphere included the precentral gyrus (PMd, PMv, FEF) and the postcentral gyrus (area 4 of M1 and area 3b of SI) for one and the inferior frontal operculum for the last cluster [**S3:** cluster 2: 816 voxels, peak T in left superior frontal gyrus = 6.63, cluster 3: 447 voxels, peak T in left SMA = 6.10, cluster 4: 400 voxels, peak T in right precentral gyrus = 13.49, cluster 5: 157 voxels, peak T in right inferior frontal operculum = 9.10].

Results obtained in macaque monkeys

For the two macaque monkeys, the univariate analysis on the whole brain identified significant clusters with greater activation for 3D objects presented close, in PPS, compared to far in a set of visual, temporal, parietal, premotor and prefrontal brain regions. In general, the activation network elicited by this contrast was more spatially extended in monkey N compared to that of monkey C. An exhaustive list of the clusters of activation for each subject can be found in Table 2 and depicted in Figure 2.

In monkey C, three significant clusters were identified. The first cluster included activations in visual areas V1, V2, V3 and V4 as well as V6 and V6A for the right hemisphere and only in V2 for the left hemisphere. The two other clusters were separated by hemisphere and identified significant activations in premotor and prefrontal areas. Particularly in left and right FEF (periarcuate area 8A), in left and right premotor cortex in area F4 and F5 of the ventral premotor cortex and in caudal dorsal premotor cortex (PMdc), in left and right caudal and rostral ventrolateral prefrontal cortex (vlPFC; area 45b and area 46v, respectively), in left rostral dorsolateral prefrontal cortex (dlPFC; area 46d) and in right arcuate sulcus area 8B (area 8B) [**Monkey C:** cluster 1: 246 voxels, peak T in the right V2 = 6.30; cluster 2: 90 voxels, peak T in the left FEF = 5.59; cluster 3: 71 voxels, peak T in the right caudal vlPFC = 5.25].

In the monkey N, the close versus far objects contrast yielded significant activation within two significant clusters in the left hemisphere and five significant clusters in the right hemisphere. In the first cluster of the left hemisphere, preferential activations were found in visual areas (V1, V2, V3 and V4), in temporal areas and particularly in middle temporal area (MT), in fundus or dorsal bank of the superior temporal sulcus (STSf and STSd), in caudal superior

temporal gyrus (STGc) and in MST, as well as in parietal areas including the area 7 in the inferior parietal lobule (area 7a), the lateral intraparietal sulcus (IPS; dorsal and ventral LIP), the ventromedial IPS (VIP and MIP) and the area 5 (area PEa) [**Monkey N:** cluster 1: 606 voxels, peak T in the left V2 = 8.05]. Activations in mostly similar visual, temporal and parietal brain regions were found also in the right hemisphere but divided in three different clusters [**Monkey N:** cluster 2: 324 voxels, peak T in the right V2 = 7.84; cluster 3: 69 voxels, peak T in the STSf = 4.62; cluster 4: 68 voxels, peak T in the lateral IPS = 4.97]. Moreover, two significant clusters were identified in, respectively, right and left hemispheres with activations in premotor and prefrontal brain regions. Both clusters included the FEF (area 8A), the dorsal premotor cortex (PMdc), the rostral vlPFC and dlPFC (area 46) and the arcuate sulcus area 8B and only activation for the area 24 (area 24c) in the right hemisphere [**Monkey N:** cluster 5: 63 voxels, peak T in the left area 8B = 6.36; cluster 6: 57 voxels, peak T in the right rostral vlPFC = 4.29]. Finally, the last significant cluster was located in the right orbitofrontal cortex with activations in the areas 11/13 (lateral and medial area 11 and medial area 13) and in the frontal pole (area 10) [**Monkey N:** cluster 7: 41 voxels, peak T in the right areas 11/13 = 5.43].

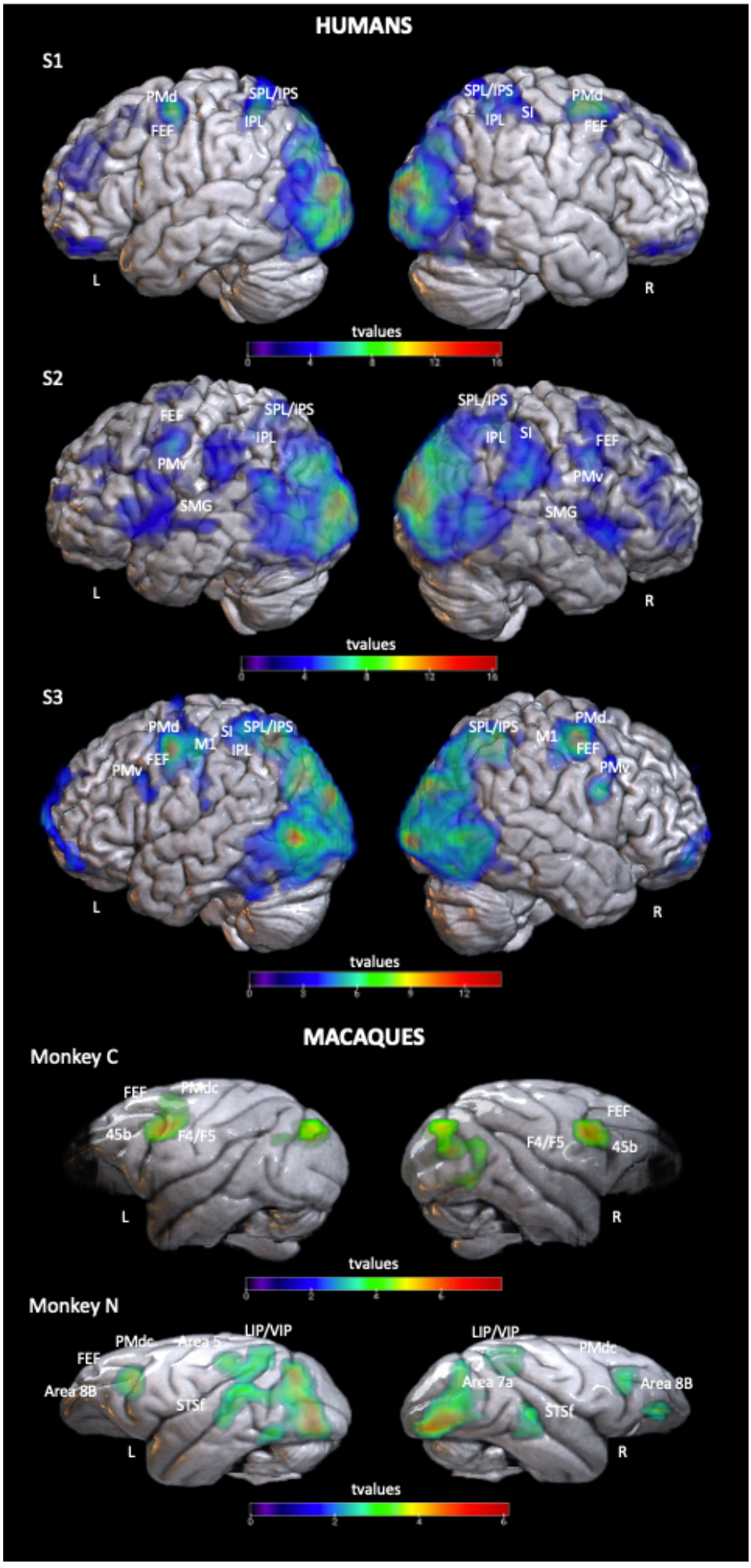
HUMANS
S1
PMd
SPL/IPS
FEF
IPL
SI
L
R
tvalues
S2
SMG
PMv
S3
M1
MACAQUES
Monkey C
45b
F4/F5
Monkey N
LIP/VIP
PMdc
Area 8B
STSf
Area 7a

Figure 2. Cerebral activations for PPS processing in humans and macaques. Brain regions showing significantly greater fMRI signal response to close versus far 3D objects (contrast close > far) for each of the three participants tested (human subjects S1, S2 and S3) **(top panel)** and each of the monkeys (Monkey C and N) **(bottom panel)**. Results are depicted on a render created from the T1 anatomical image of each subject. Activation threshold set at cluster-forming $p<0.001$ uncorrected and FEW-corrected $p<0.05$ at the cluster level.
SPL, superior parietal lobule; IPL, inferior parietal lobule; SI, primary somatosensory cortex (area 1 and area 2); M1, Primary motor cortex (area 4); PMd, dorsal premotor cortex (dorsal area 6); PMv, ventral premotor cortex (ventral area 6); SMG, supramarginal gyrus; FEF, Frontal eye fields (area 8A); PMdc, caudal dorsal premotor cortex; STSf, fundus of the superior temporal sulcus, LIP, lateral intraparietal area; VIP, ventral intraparietal area, corresponding to anatomical areas from Glasser Atlas for humans (Glasser et al., 2016) and CHARM Atlas for monkeys (Jung et al., 2021).

3.2. Brain activations for close stimuli compared to far stimuli in predefined ROIs in Humans and Monkeys

Results obtained in human subjects

Region-of-interest analysis of key premotor-parietal PPS regions in bilateral hemispheres showed that virtual 3D objects presented in close compared to far space evoked significant responses in precentral gyrus, SPL, IPL, and postcentral gyrus in the three subjects as well as in the SMG only for S1 and S2.

Particularly, in the precentral gyrus, greater activations were found in the FEF and the PEF for the three subjects as well as in the premotor cortex and in particular in the PMd for S1 and S3 and the PMv for S2. In the SPL, most of the activations were commonly found in all subjects in VIP, LIPv, lateral or medial area 7A and lateral area 7P. Activations in MIP were also found in S2 and S3. In IPS, significant preferential activations were also constantly observed in area 7PC and in AIP for S1 and S2 only. Activations in postcentral gyrus and at the border with SMG, particularly in area 1 and area 2 of the somatosensory cortex were identified in the three subjects. Only S3 also recruited the primary sensory cortex (area 3b) and the primary motor cortex (area 4). For S1 and S2, greater activations were also found in the SMG including area PF for both subjects. See Table 3 for details of results and Figure 3.

Results obtained in macaque monkeys

The region-of-interest analysis revealed significant fMRI responses for close space stimulation (compared to far space) in the premotor cortex for both monkeys and in parietal cortex only for the monkey N. More specifically, monkey N elicited greater responses in the left premotor cortex, in the PMdc, in the bilateral lateral IPS, in LIPd and LIPv, and in the left ventromedial IPS (VIP) as well as in the area 5 (Area PEa). Monkey C showed preferential significant activations in the bilateral premotor cortex and particularly in F4, F5 and in PMdc. See Table 4 for details of results and Figure 3.

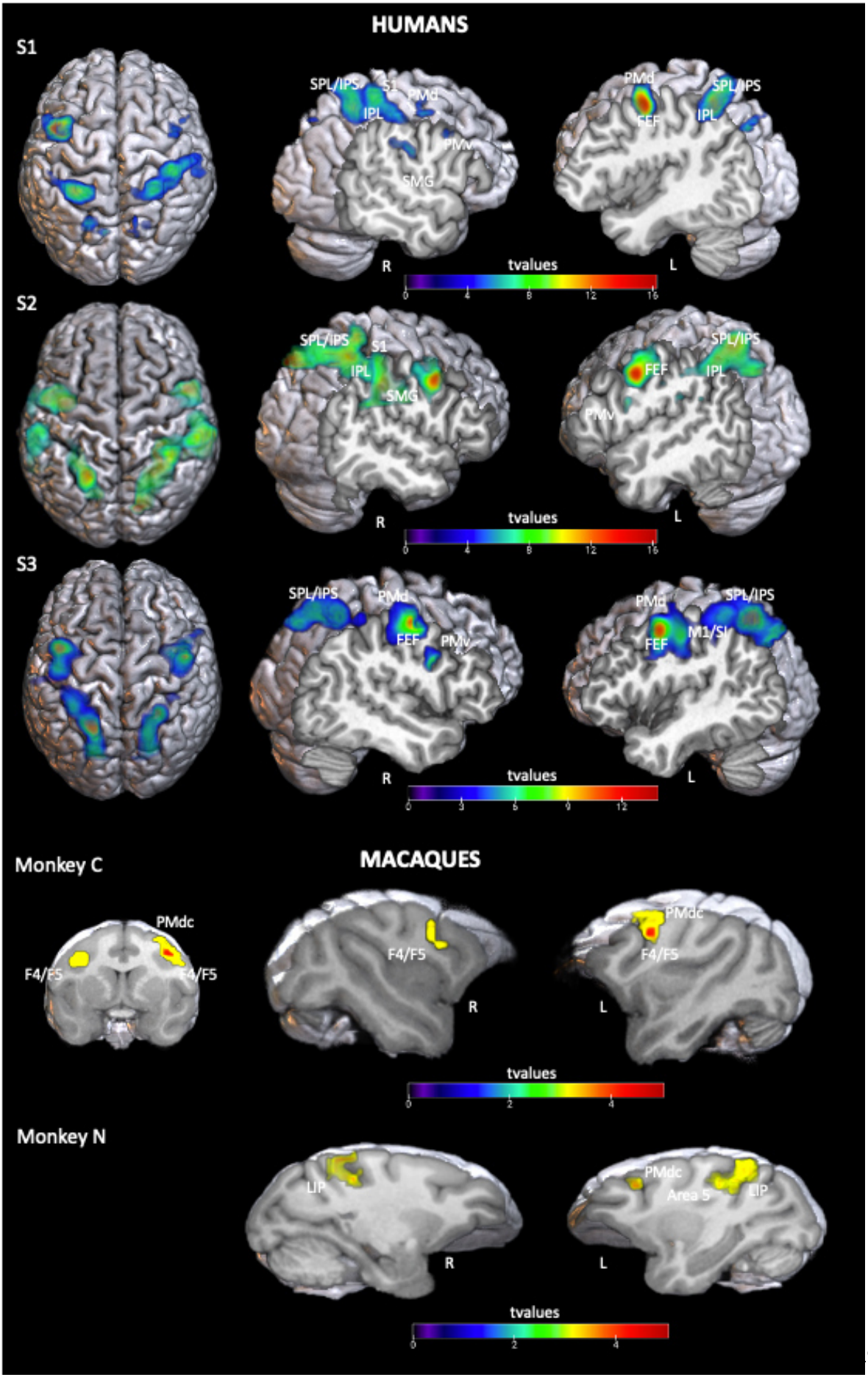
HUMANS
S1
SPL/IPS
S1
PMd
IPL
PMv
SMG
PMd
SPL/IPS
FEF
IPL
R
tvalues
0
4
8
12
16
L
S2
SPL/IPS
S1
IPL
SMG
FEF
SPL/IPS
IPL
PMv
R
tvalues
0
4
8
12
16
L
S3
SPL/IPS
PMd
FEF
PMv
PMd
SPL/IPS
M1/S1
FEF
R
tvalues
0
3
6
9
12
L
MACAQUES
Monkey C
PMdc
F4/F5
F4/F5
F4/F5
R
PMdc
F4/F5
L
tvalues
0
2
4
Monkey N
LIP
R
PMdc
Area 5
LIP
L
tvalues
0
2
4

Figure 3. ROIs-selective activations in humans and macaques. Statistical maps of the contrast close > far 3D objects masked by bilateral ROIs of interest in the three human **(top panel)** and macaque **(bottom panel)** subjects, FWE-corrected $p<0.05$. Statistical results are depicted on clipping of render brain created from the T1 anatomical image of each subject.
SPL, superior parietal lobule; IPL, inferior parietal lobule; SI, primary somatosensory cortex (area 1 and area 2); M1, Primary motor cortex (area 4); PMd, dorsal premotor cortex (dorsal area 6); PMv, ventral premotor cortex (ventral area 6); SMG, supramarginal gyrus; FEF, Frontal eye fields (area 8A); PMdc, caudal dorsal premotor cortex; STSf, fundus of the superior temporal sulcus, LIP, lateral intraparietal area; VIP, ventral intraparietal area, corresponding to anatomical areas from Glasser Atlas for humans (Glasser et al., 2016) and CHARM Atlas for monkeys (Jung et al., 2021).

4. Discussion

Using whole-brain analysis or ROIs analysis with predefined brain regions already identified in the existing literature as implicated on PPS processing, overall, our results revealed the preferential near space processing network in both human and macaque monkeys by using an ecologic virtual reality task.
In the following, we discuss each network identified in human and macaque associated with near 3D geometrical objects stimulation, in the light of the related literature. Then, we tried to compare these networks.

4.1. PPS network identified in humans

Previous studies focusing on the neural correlates of PPS representation in humans have employed different experimental procedures implying different types of stimuli which can be unisensory, involving only visual stimulation or multisensory, involving both visual and tactile stimulation. Most of these studies used a real or 2D object presented close or far from the hand (Brozzoli et al., 2011, 2012; Gentile et al., 2011, 2013; Makin et al., 2007; Schaefer et al., 2012) or the face (Bremmer et al., 2001; Sereno & Huang, 2006) as visual stimuli. These studies, as summarized in the meta-analysis of (Grivaz et al., 2017), revealed enhanced activation within a fronto-parietal network including the SPL, the IPS, the IPL, and the SI (areas 1, 2 and 3), in temporo-parietal cortex in the parietal operculum and in ventral part of the IPL and in precentral gyrus, particularly in the ventral part of the premotor cortex (PMv) but also the more dorsal part (PMd).
Here, we employed 3D geometrical shapes presented in two different sectors of space in VR, in or outside PPS, we identified similar activations. Indeed, we constantly found preferential

activations along the IPS, and the ventral or dorsal premotor areas as well as in the postcentral gyrus and the cerebellum as found in the literature (Bremmer et al., 2001; Brozzoli et al., 2011, 2012; Gentile et al., 2011, 2013; Makin et al., 2007; Schaefer et al., 2012). However, the network identified in Brozzoli et al. (2011) and in Gentile et al. (2011, 2013) also recruited the SMG and the putamen, only observed in one subject in our study. Interestingly, we also found greater activations in V6A area in all subjects which has been previously linked to be modulated by eyes position in the 3D space and by vergence system (Breveglieri et al., 2012; Luppino et al., 2005) but also showing a strong overrepresentation of PPS (Quinlan & Culham, 2007).

Depth perception involves estimating the distance between objects and determining an object's three-dimensional (3D) shape. It relies on a variety of monocular cues including perspective, but also binocular cues allowing for depth perception where the most powerful form is the stereopsis (Verhoef et al., 2016). Although dorsal visual pathways are thought to underlie visually guided actions, the ventral pathway extending from V1 through a series of visual areas such as V2, V4 and TEO to the anterior inferior temporal (IT) cortex (area TE), is implicated in object identification and categorization (Melvyn A. Goodale & Milner, 1992) and would be involved in depth representations that rely on binocular disparity. Indeed, in their review, Verhoef et al. (2016) have shown that the disparity information, combined with depth information, would recruit ventral-pathway regions prior to IT. In particular, binocular disparity activated many regions along the posterior-anterior axis of the ventral visual pathways starting in V1 area and V1 neurons transmitted the disparity information to both the ventral and the dorsal pathway. Therefore, the absolute disparity information conveyed by V1 neurons would be transmitted to regions of the dorsal pathway allowing to control visually guiding actions and vergence eyes movements, the purpose of which is to bring left and right eye images into registration (Parker, 2007), and the disparity representations becomes progressively more complex along the ventral pathway (Janssen et al., 1999; Yamane et al., 2008).
As the VR paradigm employed in our study recruited both perceptual and oculomotor depth cues, this could explain why brain regions already identified in the vergence eye movement, FEF, PEF and supplementary eye field (SEF) (Alkan et al., 2011), were systematically recruited during distance processing in our results but also why a more widespread network was also recruited within the visual cortex compared to what was previously shown. Also, we consistently observed the recruitment of inferior temporal gyrus, in particular in the area TE2, which is in line with the literature showing the implication of the ventral pathway extending

from V1 to IT in the binocular disparity. Furthermore, Verhoef et al. (2016) have pointed to the fact that several regions in this ventral pathway may interact with regions outside the ventral pathway such as AIP or VLPFC to facilitate depth perception, explaining why in our results, these regions were recruited in some subjects. Indeed, the anterior parietal area AIP has been associated with the coding of 3D structure of objects with the presence or absence of disparity cues (Orban, 2011). However, our results are also in line with other PPS fMRI studies that have shown preferential activation in the most anterior part of the IPS for the near ball (over the far) (Makin et al., 2007).

Therefore, with a VR paradigm, we identified similar premotor-parietal activations for the near space processing previously shown in studies using real objects stimulated close to the hand. Moreover, our results validate the fact that FEF, PEF and SEF, areas known to be modulated by binocular disparity and vergence-system (Alkan et al., 2011; Ferraina et al., 2000), are also allowed to identify a preferential encoding for close versus far space.

4.2. PPS network identified in macaque monkeys

In both monkeys, the whole brain analysis revealed brain responses elicited mostly in occipital, premotor and prefrontal areas by 3D objects presented in PPS (compared to far). Particularly, greater responses for close vs. far objects were observed in visual areas V1, V2, V3 and V3, in caudal dorsal premotor cortex (PMdc) as well as in prefrontal areas FEF (area 8A), in arcuate sulcus area 8B and in rostral vlPFC and dlPFC. Interestingly, in monkey C, this contrast also yielded enhanced brain responses in areas F4 and F5 of the ventral premotor cortex and within the parieto-occipital sulcus in areas V6 and V6A (Galletti et al., 1999). In monkey N, the network was more extended and encompasses temporal regions along the STS (STSf, STSd), the superior temporal gyrus (STGc), in medial superior temporal area (MST) and in middle temporal area (MT) and parietal regions along the IPS (LIPv, LIPd, VIP and MIP) and area 7 in IPL.

The ROI analysis using predefined brain areas involved in PPS processing in seminal electrophysiological studies in monkeys revealed a very restricted network recruiting all regions of the premotor cortex for monkey C (F4, F5 and PMd) whereas in monkey C recruited only the PMd of the premotor cortex but also lateral and ventromedial IPS areas (LIPd, LIPv, VIP)

and the area 5 of the parietal cortex (area PEa), reflecting as we observed in the whole brain analysis.

If we compared our results with those obtained by original electrophysiological studies describing neurons with bimodal receptive fields responding by stimuli close to the body and the study of Cléry et al. (2018) describing neural network in fMRI, we observed that similar cortical regions are involved in particular the ventral part of the premotor cortex, areas F4 and F5 (Clery et al., 2018; Gentilucci et al., 1983, 1988; Graziano et al., 1997; Graziano et al., 1994; Rizzolatti et al., 1981). In addition, we found visual preferences for close objects in the PMd. PMd has not been as thoroughly tested for responses to stimuli in the space near the body with electrophysiological recording, although at least two studies found bimodal, visual-tactile neurons only in the caudal part of PMd (Fogassi et al., 1999; Graziano & Gandhi, 2000) also observed by fMRI responding greater for objects presented near the face (Clery et al., 2018). Furthermore, in the peri-arcuate cortex facing area F4, the neurons of FEF (area 8) were modulated by the distance at which a visual object was presented and specifically by eye vergence (Alkan et al., 2011). This could explain why in our protocol involving 3D objects presented to different depth distances, FEF were coherently activated in both monkeys.

In the parietal cortex, brain responses were only detectable in monkey N and in particular in VIP, consistent with other studies showing that this region responded greater to the presentation of objects close to the face (Clery et al., 2018; Colby et al., 1993; Duhamel et al., 1998). In addition, we found increased activation within LIPv, LIPd as well as MIP for 3D close virtual objects that were presented in PPS as compared to far, in line with previous findings demonstrating a higher neural discharge rate for fixations in the near PPS in LIP (Genovesio & Ferraina, 2004; Gnadt & Mays, 1995) and MIP (Bhattacharyya et al., 2009). In PPC, in the parieto-occipital sulcus, activations observed in V6A for the monkey C is also coherent with previous findings showing preference in fixation activity of V6A neurons for representing the 3D space within reaching distance (Hadjidimitrakis et al., 2011, 2012).

In addition to the IPS, we also found greater activations in the cortical convexity of the IPL, in area 7a which is in line this the literature having described to have the majority of its neurons preferring fixations within the space close to the monkey's face (Sakata et al., 1980). However, we didn't find preferential responses in area 7b which has been found to have a response to visual stimuli presented close to their tactile receptive field (Graziano & Cooke, 2006). Finally, although area 5 of the macaque monkey has only been reported to contained

neurons activate that were more powerful driven by somatosensory stimuli and/or activated by active reaching movements (Breveglieri et al., 2006; Sakata et al., 1973) despite the fact that no discussion was offered concerning the limitation in depth of the visual receptive fields, this area was found in our fMRI results

4.3. Comparison of human and macaques PPS networks

Firstly, within the ventral visual stream, in both humans and macaques, virtual objects close to the body yielded strong activations in occipital visual areas and in part of the temporal cortex compared to virtual objects far from the body. Although Monkey N activated a more extended part of the temporal cortex compared to humans, in both species we can observe a recruitment of area TPO and MST.

Secondly, within the dorsal visual stream, in the superior parietal cortex of the PPC, the lateral and ventromedial bank of the IPS was consistently recruited in both humans and monkeys in response to objects close versus far from the body. Particularly within the intraparietal sulcus, the activity of VIP, LIP and MIP was significantly higher in both species in the presence of close virtual objects compared to far virtual objects. Stronger responses for close compared to far objects were also identified within the inferior parietal cortex in area 7a and in the anterior bank of the parieto-occipital sulcus in area V6A, in both species (Galletti et al., 1999; Pitzalis et al., 2013).

In addition, the ventral and dorsal part of the premotor cortex was systematically activated in response to virtual objects close versus far from the body in both species. In monkeys, areas F4 and F5 may correspond to the inferior or superior parts of the ventral part within the premotor cortex in humans (Ferri et al., 2015; Neubert et al., 2014; Rizzolatti & Craighero, 2004). The dorsal part of the premotor cortex was also recruited in both species and particularly the caudal part in monkeys in the processing of virtual objects within PPS. Finally, other frontal areas were also recruited in both species: the FEF (area 8) which can be situated in anterior border of the arcuate fissure or in the superior precentral sulcus in human, depending on the task used (Vernet et al., 2014) and in the arcuate gyrus in monkey (Stanton et al., 1989) as well as some other prefrontal areas as the vlPFC/dlPFC (area 9-46v/9-46d and area 45b) or orbitofrontal (area 11) and frontal pole areas (area 10).

Altogether, these results suggest a very similar PPS network in both species including occipital, temporal, parietal, premotor and prefrontal areas. However, additional brain regions were recruited in humans compared to monkeys as the somatosensory cortex (area 1 and 2), the primary motor cortex (M1), the SMG, the PEF and SEF as well as the putamen, insula and thalamus in one subject.

Moreover, our ROI analysis, focusing only on brain regions most often reported in PPS studies, have demonstrated that areas that responded the most to the virtual object in PPS commonly in both human and monkey, were mainly located in premotor areas, dorsal and ventral part, and along the IPS, in LIP and VIP. These two results, using a whole brain scale or a predefined mask, suggest that in humans and monkeys, PPS processing would act mainly in these premotor and SPL/IPS areas, corresponding to a core PPS network. However, additional brain regions would be necessary to transmit the visual information to these regions and therefore act accordingly, depending on the environment we perceive around us.

In light of the present results, we propose a similar organization of the dorsal stream in both species that could arise from visual information initially sent by the ventral stream, to process objects situated close to the body. In particular, the visual information by 3D geometrical shapes close to the body could be send in parallel from V1 and by other visual areas V2, V3 and V3A to the intermediate of V6 area, to PPC in V6A and in SPL along the IPS (VIP, LIP and MIP) as well as in superior temporal areas (MT and MST areas) which could then send information to prefrontal areas and premotor areas by reciprocal interactions, to process visual information in order to program and control the behavior. The parietal-prefrontal connections would allow a top-down control of eye movements, particularly elicited by the vergence system through the FEF, induced by the depth cues in the virtual environment. In parallel, the parietal-premotor connections, parietal subregions acting with ventral and dorsal premotor areas, would allow a specific faster processing to potentially tune our behavior depending on information occurring in PPS. This could constitute the core PPS network implicated during a visual processing occurring in PPS. We thus suggest that these processing pathways could contribute to the central PPS network, in both humans and monkeys but that additional pathways might be recruited depending on the task and the type of stimuli occurring in PPS.

Overall, by using an identical task in fMRI in two species, our study identified for the first time an equivalent, central PPS network recruited in both humans and macaques when neutral virtual objects appeared in the PPS.

Tables

Table 1. Significant clusters displaying greater activations to 3D objects in PPS in Humans. Results for whole-brain univariate analysis for contrasts close > far and far > close for each subject. Activation threshold is set at cluster-level FWE-corrected p< 0.05. Cluster size in voxels and MNI coordinates for each region in the significant clusters are reported. Only t-value of the maximum peak for each region found by AAL3 Atlas (Rolls et al., 2020) in each hemisphere are reported. Brain regions from Glasser atlas (Glasser et al., 2016) associated with each AAL3 regions are also identified.

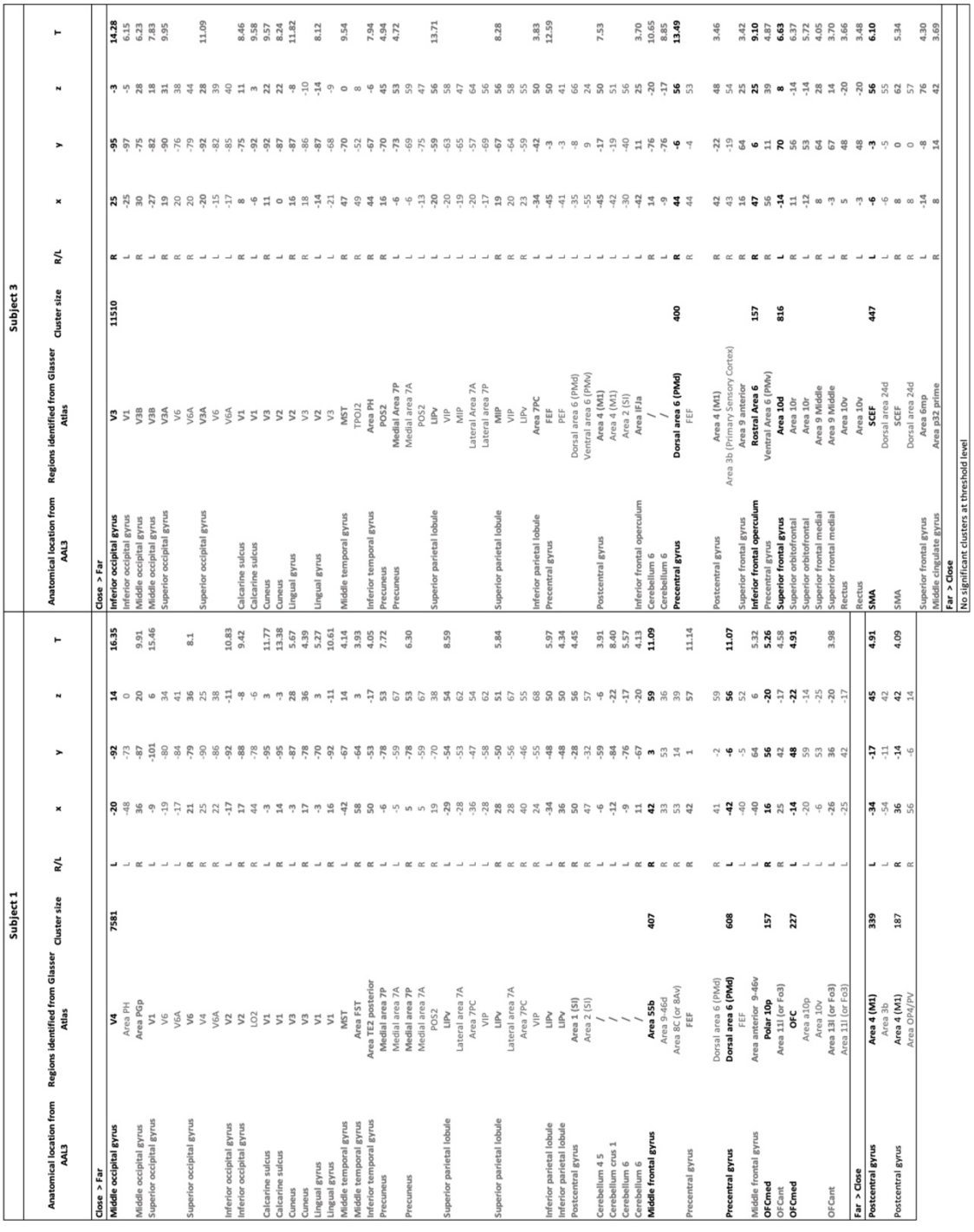

	Subject 1								Subject 3							
Anatomical location from AAL3	Regions identified from Glasser Atlas	Cluster size	R/L	x	y	z	T		Anatomical location from AAL3	Regions identified from Glasser Atlas	Cluster size	R/L	x	y	z	T
Close > Far									**Close > Far**							
Middle occipital gyrus	**V4**	**7581**	**L**	**-20**	**-92**	**14**	**16.35**		**Inferior occipital gyrus**	**V3**	**11510**	**R**	**25**	**-95**	**-3**	**14.28**
	Area PH		L	-48	-73	0			Inferior occipital gyrus	V1		L	-25	-97	-5	6.15
Middle occipital gyrus	Area PGp		R	36	-87	20	9.91		Middle occipital gyrus	V3B		R	30	-75	28	6.23
Superior occipital gyrus	V1		L	-9	-101	6	15.46		Middle occipital gyrus	V3B		L	-27	-82	18	7.83
	V6		L	-19	-80	34			Superior occipital gyrus	V3A		R	19	-90	31	9.95
	V6A		L	-17	-84	41				V6		R	20	-76	38	
Superior occipital gyrus	V6		R	21	-79	36	8.1			V6A		R	20	-79	44	
	V4		R	25	-90	25			Superior occipital gyrus	V3A		L	-20	-92	28	11.09
	V6A		R	22	-86	38				V6		L	-15	-82	39	
Inferior occipital gyrus	V2		L	-17	-92	-11	10.83			V6A		L	-17	-85	40	
Inferior occipital gyrus	V2		R	17	-88	-8	9.42		Calcarine sulcus	V1		R	8	-75	11	8.46
	LO2		R	44	-78	-6			Calcarine sulcus	V1		L	-6	-92	3	9.58
Calcarine sulcus	V1		L	-3	-95	3	11.77		Cuneus	V3		R	11	-92	22	9.57
Calcarine sulcus	V1		R	14	-95	-3	13.38		Cuneus	V2		L	0	-87	22	8.24
Cuneus	V3		L	3	-87	28	5.67		Lingual gyrus	V2		R	16	-87	-8	11.82
Cuneus	V3		R	17	-78	36	4.39			V3		R	18	-86	-10	
Lingual gyrus	V1		L	-3	-70	3	5.27		Lingual gyrus	V2		L	-14	-87	-14	8.12
Lingual gyrus	V1		R	16	-92	-11	10.61			V3		L	-21	-68	-9	
Middle temporal gyrus	MST		L	-42	-67	14	4.14		Middle temporal gyrus	MST		R	47	-70	0	9.54
Middle temporal gyrus	Area FST		R	58	-64	3	3.93			TPOJ2		R	49	-52	8	
Inferior temporal gyrus	Area TE2 posterior		R	50	-53	-17	4.05		Inferior temporal gyrus	Area PH		R	44	-67	-6	7.94
Precuneus	Medial area 7P		L	-6	-78	53	7.72		Precuneus	POS2		R	16	-70	45	4.94
	Medial area 7A		L	-5	-59	67			Precuneus	Medial Area 7P		L	-6	-73	53	4.72
Precuneus	Medial area 7P		R	5	-78	53	6.30			Medial area 7A		L	-6	-69	59	
	Medial area 7A		R	5	-59	67				POS2		L	-13	-75	47	
	POS2		R	19	-70	38			Superior parietal lobule	LIPv		L	-20	-59	56	13.71
Superior parietal lobule	LIPv		L	-29	-54	54	8.59			VIP		L	-20	-63	58	
	Lateral area 7A		L	-28	-53	62				MIP		L	-19	-65	47	
	Area 7PC		L	-36	-47	54				Lateral Area 7A		L	-20	-57	64	
	VIP		L	-28	-58	62				Lateral area 7P		L	-17	-69	56	
Superior parietal lobule	LIPv		R	28	-50	51	5.84		Superior parietal lobule	MIP		R	19	-67	56	8.28
	Lateral area 7A		R	28	-56	67				VIP		R	20	-64	58	
	Area 7PC		R	40	-46	55				LIPv		R	23	-59	55	
	VIP		R	24	-55	68			Inferior parietal lobule	Area 7PC		L	-34	-42	50	3.83
Inferior parietal lobule	LIPv		L	-34	-48	50	5.97		Precentral gyrus	FEF		L	-45	-3	50	12.59
Inferior parietal lobule	LIPv		R	36	-48	50	4.34			PEF		L	-41	-3	41	
Postcentral gyrus	Area 1 (SI)		R	50	-28	56	4.45			Dorsal area 6 (PMd)		L	-35	-8	66	
	Area 2 (SI)		R	47	-32	57				Ventral area 6 (PMv)		L	-55	9	24	
Cerebellum 4 5	/		L	-6	-59	-6	3.91		Postcentral gyrus	Area 4 (M1)		L	-45	-17	50	7.53
Cerebellum crus 1	/		L	-12	-84	-22	8.40			Area 4 (M1)		L	-42	-19	51	
Cerebellum 6	/		L	-9	-76	-17	5.57			Area 2 (SI)		L	-30	-40	56	
Cerebellum 6	/		R	11	-67	-20	4.13		Inferior frontal operculum	Area IFJa		L	-42	11	25	3.70
Middle frontal gyrus	**Area 55b**	**407**	**R**	**42**	**3**	**59**	**11.09**		Cerebellum 6	/		R	14	-76	-20	10.65
	Area 9-46d		R	33	53	36			Cerebellum 6	/		L	-9	-76	-17	8.85
	Area 8C (or 8Av)		R	53	14	39			**Precentral gyrus**	**Dorsal area 6 (PMd)**	**400**	**R**	**44**	**-6**	**56**	**13.49**
Precentral gyrus	FEF		R	42	1	57	11.14			FEF		R	44	-4	53	
	Dorsal area 6 (PMd)		R	41	-2	59			Postcentral gyrus	Area 4 (M1)		R	42	-22	48	3.46
Precentral gyrus	**Dorsal area 6 (PMd)**	**608**	**L**	**-42**	**-6**	**56**	**11.07**			Area 3b (Primary Sensory Cortex)		R	43	-19	54	
	FEF		L	-40	-5	52			Superior frontal gyrus	Area 9 anterior		R	16	64	25	3.42
Middle frontal gyrus	Area anterior 9-46v		L	-40	64	6	5.32		**Inferior frontal operculum**	**Rostral Area 6**	**157**	**R**	**47**	**6**	**25**	**9.10**
OFCmed	**Polar 10p**	**157**	**R**	**16**	**56**	**-20**	**5.26**		Precentral gyrus	Ventral Area 6 (PMv)		R	56	11	39	4.87
OFCant	Area 11l (or Fo3)		R	25	42	-17	4.58		**Superior frontal gyrus**	**Area 10d**	**816**	**L**	**-14**	**70**	**8**	**6.63**
OFCmed	**OFC**	**227**	**L**	**-14**	**48**	**-22**	**4.91**		Superior orbitofrontal	Area 10r		R	11	56	-14	6.37
	Area a10p		L	-20	59	-14			Superior orbitofrontal	Area 10r		L	-12	53	-14	5.72
	Area 10v		L	-6	53	-25			Superior frontal medial	Area 9 Middle		R	8	64	28	4.05
OFCant	Area 13l (or Fo3)		L	-26	36	-20	3.98		Superior frontal medial	Area 9 Middle		L	-3	67	14	3.70
	Area 11l (or Fo3)		L	-25	42	-17			Rectus	Area 10v		R	5	48	-20	3.66
Far > Close									Rectus	Area 10v		L	-3	48	-20	3.48
Postcentral gyrus	**Area 4 (M1)**	**339**	**L**	**-34**	**-17**	**45**	**4.91**		**SMA**	**SCEF**	**447**	**L**	**-6**	**-3**	**56**	**6.10**
	Area 3b		L	-54	-11	42				Dorsal area 24d		L	-6	-5	55	
Postcentral gyrus	**Area 4 (M1)**	**187**	**R**	**36**	**-14**	**42**	**4.09**		SMA	SCEF		R	8	0	62	5.34
	Area OP4/PV		R	56	-6	14				Dorsal area 24d		R	8	0	57	
									Superior frontal gyrus	Area 6mp		L	-14	-8	76	4.30
									Middle cingulate gyrus	Area p32 prime		R	8	14	42	3.69
									Far > Close							
									No significant clusters at threshold level							

(Table 1 continued)

Subject 2							
Anatomical location from AAL3	**Regions identified from Glasser Atlas**	**Cluster size**	**R/L**	**x**	**y**	**z**	**T**
Close > Far							
Superior occipital gyrus	**V2**	**16648**	**R**	**19**	**-98**	**17**	**17.21**
	V3		R	19	-95	25	
	V6		R	18	-79	33	
	V6A		R	21	-86	42	
Superior occipital gyrus	**V3**		**L**	**-20**	**-81**	**31**	**8.20**
	V6		L	-18	-79	33	
	V6A		L	-18	-86	37	
Middle occipital gyrus	**V3**		**L**	**-23**	**-95**	**8**	**14.94**
Middle occipital gyrus	**V4**		**R**	**30**	**-90**	**11**	**11.97**
Inferior occipital gyrus	**V3**		**R**	**33**	**-90**	**-6**	**8.33**
Inferior occipital gyrus	**V3**		**L**	**-23**	**-92**	**-6**	**9.89**
Calcarine sulcus	**V1**		**R**	**14**	**-81**	**11**	**10.52**
Calcarine sulcus	**V1**		**L**	**-3**	**-87**	**6**	**8.16**
Cuneus	**V3**		**R**	**11**	**-90**	**25**	**12.18**
Cuneus	**V2**		**L**	**-3**	**-84**	**25**	**6.83**
Lingual gyrus	**V3**		**R**	**14**	**-84**	**-8**	**10.32**
Lingual gyrus	**V2**		**L**	**-12**	**-84**	**-11**	**11.15**
Superior temporal gyrus	**PSL**		**R**	**64**	**-34**	**20**	**6.84**
Superior temporal gyrus	**A5**		**L**	**-59**	**0**	**-3**	**3.82**
	Area TA2		L	-52	11	-6	
Middle temporal gyrus	**TPOJ2**		**R**	**53**	**-59**	**3**	**6.72**
	MST		R	53	-59	7	
	STSdp		R	45	-38	3	
	TPOJ1		R	53	-45	5	
Middle temporal gyrus	**TPOJ2**		**L**	**-51**	**-53**	**14**	**7.81**
	STSdp		L	-55	-22	-6	
	Area PGi		L	-46	-52	21	
	TPOJ1		L	-46	-53	11	
Inferior temporal gyrus	**Area TE2p**		**R**	**50**	**-62**	**-6**	**6.38**
Inferior temporal gyrus	**Area TE2p**		**L**	**-45**	**-62**	**-8**	**5.65**
Superior temporal pole	**Area STGa**		**R**	**56**	**14**	**-11**	**4.89**
Superior temporal pole	**Area STGa**		**L**	**-56**	**8**	**-8**	**4.07**
Precuneus	**POS2**		**R**	**8**	**-76**	**50**	**6.19**
	Medial Area 7P		R	4	-71	56	
	Medial area 7A		R	8	-66	60	
Precuneus	**POS2**		**L**	**-6**	**-76**	**42**	**4.88**
Superior parietal lobule	**Area 7PC**		**R**	**33**	**-50**	**59**	**5.71**
	LIPv		R	36	-50	57	
	AIP		R	36	-39	48	
	VIP		R	22	-64	59	
	MIP		R	17	-65	51	
Superior parietal lobule	**VIP**		**L**	**-23**	**-59**	**59**	**7.42**
	LIPd		L	-26	-50	46	
	LIPv		L	-30	-51	48	
	Lateral Area 7A		L	-20	-58	61	
	Medial area 7A		L	-18	-62	63	
	MIP		L	-20	-65	53	
	AIP		L	-32	-39	44	
Inferior parietal lobule	**Area7PC**		**R**	**30**	**-41**	**54**	**6.17**
	AIP		R	36	-50	50	
Inferior parietal lobule	**LIPd**		**L**	**-31**	**-48**	**45**	**5.53**
	AIP		L	-33	-43	41	
Supramarginal Gyrus	**Area PF Complex**		**L**	**-62**	**-39**	**31**	**3.58**
	PSL		L	-63	-46	26	
	Area Pfop		L	-63	-28	27	
	Area PFt		L	-54	-34	42	
Supramarginal Gyrus	**Area PF Complex**		**R**	**58**	**-31**	**42**	**5.90**
Precentral gyrus	**PEF**		**L**	**-48**	**0**	**39**	**7.92**
	FEF		L	-47	-5	50	
	Ventral Area 6 (PMv)		L	-58	-3	40	
	Area 8C		L	-43	6	37	
Postcentral gyrus	**Area 4 (M1)**		**L**	**-62**	**-3**	**20**	**3.56**
Middle frontal gyrus	**Area 46**		**L**	**-37**	**42**	**34**	**4.74**
Inferior frontal operculum	**Area 44**		**L**	**-54**	**11**	**20**	**4.48**
Inferior orbitofrontal	**Area 47l**		**L**	**-42**	**22**	**-8**	**3.49**
Rolandic operculum	**RetroInsular Cortex**		**L**	**-40**	**-31**	**20**	**4.47**
Middle cingulate gyrus	**Area 23c**		**L**	**-9**	**-34**	**45**	**5.13**
Middle cingulate gyrus	**Area 23c**		**R**	**16**	**-30**	**41**	**5.1**
Insula	**Middle insular area**		**R**	**42**	**17**	**-6**	**5.63**
Insula	**Middle insular area**		**L**	**-40**	**14**	**0**	**4.03**
Cerebellum crus 1	**/**		**L**	**-17**	**-87**	**-22**	**7.29**
Cerebellum 6	**/**		**R**	**22**	**-76**	**-20**	**5.74**
Cerebellum 6	**/**		**L**	**-12**	**-73**	**-17**	**5.26**
Precentral gyrus	**PEF**	**1556**	**R**	**50**	**6**	**36**	**7.36**
	Ventral Area 6 (PMv)		R	56	1	38	
Postcentral gyrus	**Area 2**		**R**	**30**	**-36**	**48**	**6.14**
Inferior frontal operculum	**Area 47l**		**R**	**44**	**20**	**-11**	**5.92**
	Area IFJp		R	39	11	31	
Superior frontal gyrus	**Area 6 anterior**		**R**	**28**	**3**	**59**	**4.09**
Rolandic operculum	**Area 43**		**R**	**61**	**6**	**8**	**4.02**
Insula	**Area TA2**		**R**	**53**	**14**	**-6**	**5.64**
Thalamus	**/**		**R**	**8**	**-16**	**10**	**3.6**
Putamen	**/**		**R**	**30**	**0**	**8**	**3.18**
Middle frontal gyrus	**Area anterior 47r**	**561**	**R**	**44**	**59**	**-8**	**5.67**
	Area 46		R	42	45	31	
	Area IFSa		R	53	48	0	
	Area 9-46d		R	35	45	32	
Inferior frontal gyrus (triangular part)	**Area IFSp**		**R**	**47**	**34**	**14**	**4**
	Area posterior 9-46v		R	47	34	20	
Inferior frontal gyrus (orbital part)	**Area STGa**		**R**	**50**	**20**	**-8**	**5.01**
	Rostral Area 6		R	50	11	-5	
SMA	**SCEF**	**552**	**R**	**8**	**6**	**59**	**5.47**
Superior frontal medial	**Area 8BM**		**R**	**5**	**22**	**42**	**4.41**
Middle cingulate gyrus	**Area Posterior 24prime**		**L**	**-6**	**11**	**39**	**3.61**
	Area 23c		L	-10	-21	41	
	Area p32 prime		L	-6	17	41	
Middle cingulate gyrus	**Area p32 prime**		**R**	**8**	**20**	**36**	**3.80**
	Area Posterior 24prime		R	5	-5	40	
	Area 23c		R	13	-23	39	
SMA	**Area 6m anterior**	**129**	**L**	**-12**	**3**	**67**	**4.20**
	SCEF		L	-6	-6	70	
Far > Close							
No significant clusters at threshold level							

Table 2. Significant clusters displaying greater activations to 3D objects in PPS in Macaques. Results for whole-brain univariate analysis for contrasts close > far and far > close for each monkey. Activation threshold is set at cluster-level FWE-corrected p< 0.05. Cluster size in voxels and coordinates for each region in the significant clusters are reported as well as t-value associated. Regions are identified with both level 4 and 6 of CHARM atlas (Jung et al., 2021). No regions were reported with SARM atlas, as no activations were identified in subcortical areas. PMdc, caudal dorsal premotor cortex; LIPv, ventral lateral intraparietal area; LIPd, dorsal lateral intraparietal area; VIP, ventral intraparietal area; F4/F5, areas F4, F5 of ventral premotor cortex; STSf, fundus of the superior temporal sulcus; STSd, dorsal bank of the superior temporal sulcus; TPO, temporal parieto-occipital area; STGc, caudal superior temporal gyrus; CPB, caudal parabelt region.

Monkey C							
Anatomical location from CHARM Atlas (level 4)	Cluster size	R/L	x	y	z	T	Regions identified from CHARM Atlas (level 6)
Close > Far							
V2	**246**	**R**	**0**	**-32**	**15**	**6.30**	**V2**
V2		R	16	-30	11	5.07	V2
V2		L	-15	-32	16	4.98	V2
V1		R	0	-34	16	5.31	V1
V3		R	9	-30	17	4.12	V3d
V3		R	20	-23	3	3.81	V3v
V4		R	21	-23	12	3.5	V4d
V6		R	1	-30	11	3.15	V6
V6A		R	1	-30	15	4.29	V6Av
V6A		R	1	-29	17	3.6	V6Ad
FEF (area 8A)	**90**	**L**	**-18**	**4**	**16**	**5.59**	**Dorsal periarcuate area 8A (area 8Ad)**
FEF (area 8A)		L	-20	4	16	4.85	ventral periarcuate area 8A (area 8av)
Premotor cortex PM		L	-15	0	24	3.71	PMdc
Premotor cortex PM		L	-17	2	18	4.5	F5
Premotor cortex PM		L	-21	2	17	4.14	F4
caudal vlPFC		L	-20	7	14	3.85	area 45b
Rostral dlPFC		L	-18	8	16	3.09	Dorsal area 46 (area 46d)
Rostral vlPFC		L	-19	7	15	3.7	Ventral area 46 (area 46v)
Caudal vlPFC	**71**	**R**	**16**	**6**	**15**	**5.25**	**Area 45b**
Rostral vlPFC		R	16	7	16	4.51	Ventral area 46 (area 46v)
Premotor cortex PM		R	15	3	16	4.48	F5
Premotor cortex PM		R	16	2	17	3.16	F4
Premotor cortex PM		R	11	3	16	3.25	PMdc
FEF (area 8A)		R	15	5	17	4.35	Dorsal periarcuate area 8A (area 8Ad)
Area 8B		R	13	4	17	4.22	Arcuate sulcus (area 8B)
Far > Close							
No significant clusters at threshold level							

Monkey N							
Anatomical location from CHARM Atlas (level 4)	Cluster size	R/L	x	y	z	T	Regions identified from CHARM Atlas (level 6)
Close > Far							
V2	**606**	**L**	**-19**	**-37**	**-1**	**8.05**	**V2**
V2		L	-17	-32	14	7.14	V2
V1		L	-18	-38	3	5.70	V1
V3		L	-22	-24	6	3.90	V3d
V3		L	-15	-29	-3	3.44	V3v
V4		L	-24	-21	8	4.33	V4d
MT		L	-22	-22	7	4.16	MT
STSd		L	-19	-14	3	5.08	TPO
STGc		L	-26	-14	7	3.56	CPB
STSf		L	-17	-17	5	4.02	Area PGa
STSf		L	-18	-14	0	4.04	Area IPa
MST		L	-14	-21	14	3.75	MST
Area 7 in IPL		L	-17	-15	17	4.60	Area 7a
lat IPS		L	-11	-20	15	3.75	LIPv
lat IPS		L	-10	-22	17	3.69	LIPd
vm IPS		L	-10	-16	14	3.60	VIP
vm IPS		L	-4	-25	16	3.83	MIP
Area 5		L	-7	-24	19	3.95	Area PEa
V2	**324**	**R**	**21**	**-37**	**-1**	**7.84**	**V2**
V3		R	17	-32	12	5.54	V3A
V3		R	14	-33	10	4	V3d
V1		R	16	-33	7	4.64	V1
Area 8B	**63**	**L**	**-12**	**10**	**12**	**6.36**	**Area 8B**
Premotor cortex PM		L	-12	10	15	4.34	PMdc
FEF (area 8A)		L	-13	11	14	5.01	Area 8Ad
Rostral dlPFC		L	-15	12	11	3.83	Dorsal area 46 (area 46d)
Rostral vlPFC		L	-14	12	9	4.30	Ventral area 46 (area 46v)
Areas 11/13	**41**	**R**	**12**	**22**	**3**	**5.43**	**Lateral area 11 (area 11l)**
Areas 11/13		R	7	20	2	3.15	Medial area 11 (area 11m)
Areas 11/13		R	6	10	2	3.38	Medial area 13 (area 13m)
Rostral vlPFC		R	11	21	5	3.09	Ventral area 46 (area 46v)
Frontal pole (area 10)		R	2	22	1	3.09	Rostral medial frontal pole (area 10mr)
lat IPS	**68**	**R**	**14**	**-17**	**21**	**4.97**	**LIPd**
Area 7 in IPL		R	12	-25	17	3.70	Area 7a
lat IPS		R	12	-17	16	4.15	LIPv
Area 5		R	12	-18	21	3.71	Area PE
STSf	**69**	**R**	**21**	**-12**	**-3**	**4.62**	**Area IPa**
STSf		R	20	-12	-2	4.08	Area PGa
STSd		R	21	-13	2	4.11	TPO
TE in STSv		R	28	-12	1	4.03	Tem
Rostral vlPFC	**57**	**R**	**14**	**11**	**10**	**4.29**	**Area 46f**
Area 8B		R	14	10	12	3.25	Area 8B
FEF (area 8A)		R	14	12	14	3.90	Area 8Ad
Premotor cortex PM		R	12	12	15	3.42	PMdc
Premotor cortex PM		R	9	15	16	3.09	PMdr
Rostral dlPFC		R	14	13	10	3.83	Dorsal area 46 (Area 46d)
Area 24		R	6	13	12	3.09	Area 24c
Far > Close							
No significant clusters at threshold level							

Table 3. Significant activations obtained in predefined ROIs for 3D objects presented in PPS in Humans. Results for ROIs-based univariate analysis for contrasts close > far and far > close for each subject identified at FWE-corrected p< 0.05. Cluster size in voxels and MNI coordinates for each significant region are reported as well as t-value associated. Significant activation in ROIs defined by AAL3 Atlas (Rolls et al., 2020) are reported as well as corresponding region from Glasser Atlas (Glasser et al., 2016). SI, primary somatosensory cortex; PSL, perisylvian language area; PMd, dorsal premotor cortex; PMv, ventral premotor cortex; FEF, Frontal eye fields; LIPv, ventral lateral intraparietal area; LIPd, dorsal lateral intraparietal area; VIP, ventral intraparietal area; MIP, medial intraparietal area.

Subject 1							
ROIs from AAL3 Atlas	**Cluster size**	**R/L**	**x**	**y**	**z**	**T**	**Regions identified from Glasser Atlas**
Close > Far							
Precentral gyrus	**219**	**L**	**-42**	**-6**	**56**	**11.07**	**Dorsal area 6 PMd**
		L	-44	2	56	5.45	Area 55b
		L	-42	-6	50	9.26	FEF
Superior parietal lobule	**300**	**L**	**-28**	**-50**	**56**	**10.65**	**LIPv**
		L	-28	-54	64	6.98	Lateral Area 7A
		L	-21	-57	69	5.45	VIP
Inferior parietal lobule		L	-38	-47	54	5.17	Area 7PC
		L	-34	-46	49	5.46	AIP
Superior parietal lobule	**45**	**L**	**-6**	**-81**	**50**	**8.38**	**POS2**
		L	-20	-73	39	6.28	IPS1
Inferior parietal lobule	**464**	**R**	**25**	**-48**	**53**	**7.81**	**LIPv**
		R	34	-48	50	5.23	AIP
Postcentral gyrus		R	42	-39	64	6.33	Area 1 (SI)
		R	42	-39	64	6.33	Area 2 (SI)
Superior parietal lobule		R	28	-50	64	6.03	Lateral Area 7A
		R	30	-52	55	5.68	LIPv
		R	35	-42	63	4.95	Area 7PC
		R	25	-57	69	5.12	VIP
Precentral gyrus	**27**	**R**	**42**	**-6**	**50**	**5.68**	**FEF**
		R	42	-6	62	5.18	Dorsal area 6 PMd
Precentral gyrus	**9**	**R**	**50**	**8**	**36**	**4.68**	**Ventral area 6 PMv**
Supramarginal gyurs	**67**	**R**	**58**	**-20**	**31**	**4.67**	**Area PFt**
Far > Close							
Postcentral gyrus	3	L	-34	-17	45	4.91	Area 4 (M1)

Subject 2							
ROIs from AAL3 Atlas	**Cluster size**	**R/L**	**x**	**y**	**z**	**T**	**Regions identified from Glasser Atlas**
Close > Far							
Superior parietal lobule	**1296**	**R**	**14**	**-81**	**48**	**8.65**	**Lateral Area 7P**
		R	20	-63	59	4.85	VIP
		R	26	-60	56	5.31	LIPv
Supramarginal		R	64	-31	25	8.21	PSL area
		R	62	-22	37	5.15	Area PFt
		R	56	-31	39	6.07	Area PF Complex
Postcentral gyrus		R	28	-40	51	7.10	Area 2 (SI)
		R	39	-45	67	6.41	Area 7PC
Inferior parietal lobule		R	28	-42	50	7.86	Area 7PC
		R	25	-53	53	7.40	LIPv
		R	30	-36	44	6.75	AIP
Precentral gyrus	**246**	**R**	**50**	**6**	**36**	**7.36**	**PEF**
		R	56	1	38	5.05	Area ventral 6 PMv
Precentral gyrus	**482**	**L**	**-48**	**-3**	**39**	**7.96**	**PEF**
		L	-37	-6	42	6.85	FEF
		L	-56	-4	40	4.74	Area ventral 6 PMv
		L	-54	6	17	4.74	Rostral area 6
Superior parietal lobule	**411**	**L**	**-23**	**-59**	**59**	**7.42**	**VIP**
		L	-25	-58	57	6.36	LIPv
		L	-20	-65	56	4.77	MIP
		L	-19	-60	61	6.52	Medial Area 7A
		L	-12	-73	39	5.56	POS2
Inferior parietal lobule		L	-26	-48	48	7.33	LIPd
		L	-34	-48	45	4.58	AIP
Supramarginal gyrus	**355**	**L**	**-62**	**-53**	**22**	**5.89**	**PSL area**
		L	-62	-31	25	5.12	Area PF Complex
		L	-62	-31	25	5.12	Area PF opercular (Pfop)
		L	-56	-25	42	4.62	Area 1 (SI)
Far > Close							
No significant clusters at threshold level							

Subject 3							
ROIs from AAL3 Atlas	**Cluster size**	**R/L**	**x**	**y**	**z**	**T**	**Regions identified from Glasser Atlas**
Close > Far							
Superior parietal lobule	**1238**	**L**	**-20**	**-59**	**56**	**13.71**	**Lateral Area 7A**
		L	-20	-78	45	9.18	Lateral Area 7P
		L	-20	-64	56	10.86	VIP
		L	-20	-64	49	8.35	MIP
		L	-29	-57	56	7.81	LIPv
Precentral gyrus		L	-45	-3	50	12.59	FEF
		L	-41	0	40	5.61	PEF
		L	-43	-13	59	4.97	Dorsal area 6 PMD
Postcentral gyrus		L	-45	-17	50	7.53	Area 3b (Primary Sensory Cortex)
		L	-45	-13	49	6.99	Area 4 (M1)
		L	-37	-38	60	5	Area 1
		L	-38	-37	56	4.43	Area 2
Precentral gyrus	**298**	**R**	**44**	**-8**	**56**	**12.44**	**Dorsal area 6 PMD**
		R	46	-8	51	8.60	FEF
Precentral gyrus	**67**	**R**	**47**	**6**	**28**	**8.07**	**PEF**
		R	56	11	39	4.87	Ventral area 6 PMv
Postcentral gyrus	**363**	**R**	**44**	**-18**	**51**	**6.28**	**Area 3b (Primary Sensory Cortex)**
		R	42	-16	59	4.79	Area 4 (M1)
Superior parietal lobule		R	25	-50	53	11.69	LIPv
		R	20	-63	55	8.32	VIP
		R	21	-76	52	5.72	Lateral Area 7A
		R	21	-67	54	7.15	MIP
Far > Close							
No significant clusters at threshold level							

Table 4. Significant activations obtained in predefined ROIs for 3D objects presented in PPS in Macaques. Results for ROIs-based univariate analysis for contrasts close > far and far > close for each monkey identified at FWE-corrected $p < 0.05$. Cluster size in voxels and coordinates for each significant region are reported as well as t-value associated. Significant activations are identified in ROIs defined by level 4 of the CHARM atlas (Jung et al., 2021). Corresponding regions with the level 6 of the same atlas have also been reported. No regions were reported with SARM atlas, as no activations were identified in the putamen.

PMdc, caudal dorsal premotor cortex; LIPv, ventral lateral intraparietal area; LIPd, dorsal lateral intraparietal area; VIP, ventral intraparietal area; F4, area F4 of ventral premotor cortex; F5, area F5 of ventral premotor cortex.

Monkey C							
ROIs from CHARM Atlas (level 4)	**Cluster size**	**R/L**	**x**	**y**	**z**	**T**	**Regions identified from CHARM Atlas (level 6)**
Close > Far							
Premotor cortex PM	**39**	**L**	**-18**	**2**	**18**	**5.43**	**F4**
		L	-17	2	18	4.1	F5
		L	-18	1	19	4.09	PMdc
Premotor cortex PM	**16**	**R**	**14**	**2**	**16**	**4.22**	**F5**
		R	18	6	13	3.93	PMdc
		R	16	2	17	3.85	F4
Far > Close							
No significant clusters at threshold level							
Monkey N							
ROIs from CHARM Atlas (level 4)	**Cluster size**	**R/L**	**x**	**y**	**z**	**T**	**Regions identified from CHARM Atlas (level 6)**
Close > Far							
lat IPS	**43**	**R**	**14**	**-17**	**21**	**4.97**	**LIPd**
lat IPS		R	12	-17	15	4.27	LIPv
lat IPS	**84**	**L**	**-15**	**-14**	**17**	**4.95**	**LIPd**
Area 5		L	-6	-25	17	4.29	Area PEa
vm IPS		L	-6	-21	15	4.27	VIP
lat IPS		L	-12	-21	15	3.93	LIPv
Premotor cortex PM	**8**	**L**	**-12**	**10**	**14**	**5.67**	**PMdc**
Far > Close							
No significant clusters at threshold level							

5. References

Alkan, Y., Biswal, B. B., & Alvarez, T. L. (2011). Differentiation between vergence and saccadic functional activity within the human frontal eye fields and midbrain revealed through fMRi. *PLoS ONE*, *6*(11). https://doi.org/10.1371/JOURNAL.PONE.0025866

Bhattacharyya, R., Musallam, S., & Andersen, R. A. (2009). Parietal reach region encodes reach depth using retinal disparity and vergence angle signals. *Journal of Neurophysiology*, *102*(2), 805–816. https://doi.org/10.1152/JN.90359.2008

Blatt, G. J., Andersen, R. A., & Stoner, G. R. (1990). Visual receptive field organization and cortico-cortical connections of the lateral intraparietal area (area LIP) in the macaque. *Journal of Comparative Neurology*, *299*(4), 421–445. https://doi.org/10.1002/CNE.902990404

Bonini, L., Maranesi, M., Livi, A., Fogassi, L., & Rizzolatti, G. (2014). Space-Dependent Representation of Objects and Other's Action in Monkey Ventral Premotor Grasping Neurons. *Journal of Neuroscience*, *34*(11), 4108–4119. https://doi.org/10.1523/JNEUROSCI.4187-13.2014

Bremmer, F., Duhamel, J.-R., Hamed, S. Ben, & Graf, W. (1997). The Representation of Movement in Near Extra-Personal Space in the Macaque Ventral Intraparietal Area (VIP). *Parietal Lobe Contributions to Orientation in 3D Space*, 619–630. https://doi.org/10.1007/978-3-642-60661-8_33

Bremmer, Frank, Schlack, A., Kaminiarz, A., & Hoffmann, K. P. (2013). Encoding of movement in near extrapersonal space in primate area VIP. *Frontiers in Behavioral Neuroscience*, *0*(JANUARY 2013), 8. https://doi.org/10.3389/FNBEH.2013.00008

Bremmer, Frank, Schlack, A., Shah, N. J., Zafiris, O., Kubischik, M., Hoffmann, K. P., Zilles, K., & Fink, G. R. (2001). Polymodal motion processing in posterior parietal and premotor cortex: A human fMRI study strongly implies equivalencies between humans and monkeys. *Neuron*, *29*(1), 287–296. https://doi.org/10.1016/S0896-6273(01)00198-2

Brett, Matthew, Anton, Jean-Luc, Valabregue, Romain, Poline, Jean-Baptiste. Region of interest analysis using an SPM toolbox [abstract] Presented at the 8th International Conference on Functional Mapping of the Human Brain, June 2-6, 2002, Sendai, Japan. Available on CD-ROM in NeuroImage, Vol 16, No 2.

Breveglieri, R., Galletti, C., Gamberini, M., Passarelli, L., & Fattori, P. (2006). Somatosensory cells in area PEc of macaque posterior parietal cortex. *Journal of Neuroscience*, *26*(14), 3679–3684. https://doi.org/10.1523/JNEUROSCI.4637-05.2006

Breveglieri, R., Hadjidimitrakis, K., Bosco, A., Sabatini, S. P., Galletti, C., & Fattori, P. (2012). Eye Position Encoding in Three-Dimensional Space: Integration of Version and Vergence Signals in the Medial Posterior Parietal Cortex. *Journal of Neuroscience*, *32*(1), 159–169. https://doi.org/10.1523/JNEUROSCI.4028-11.2012

Brozzoli, C., Gentile, G., & Ehrsson, H. H. (2012). That's Near My Hand! Parietal and Premotor Coding of Hand-Centered Space Contributes to Localization and Self-Attribution of the Hand. *Journal of Neuroscience*, *32*(42), 14573–14582. https://doi.org/10.1523/JNEUROSCI.2660-12.2012

Brozzoli, C., Gentile, G., Petkova, V. I., & Ehrsson, H. H. (2011). fMRI Adaptation Reveals a Cortical Mechanism for the Coding of Space Near the Hand. *Journal of Neuroscience*, *31*(24), 9023–9031. https://doi.org/10.1523/JNEUROSCI.1172-11.2011

Cléry, J., Guipponi, O., Odouard, S., Wardak, C., & Ben Hamed, S. (2018). Cortical networks for encoding near and far space in the non-human primate. *NeuroImage*, *176*, 164–178. https://doi.org/10.1016/j.neuroimage.2018.04.036

Cléry, J., Guipponi, O., Wardak, C., & Ben Hamed, S. (2015). Neuronal bases of peripersonal and extrapersonal spaces, their plasticity and their dynamics: Knowns and unknowns. *Neuropsychologia*, *70*, 313–326. https://doi.org/10.1016/J.NEUROPSYCHOLOGIA.2014.10.022

Colby, C. L., Duhamel, J. R., & Goldberg, M. E. (1993). Ventral intraparietal area of the macaque: Anatomic location and visual response properties. *Journal of Neurophysiology*, *69*(3), 902–914. https://doi.org/10.1152/JN.1993.69.3.902

Colby, Carol L., & Duhamel, J. R. (1996). Spatial representations for action in parietal cortex. *Cognitive Brain Research*, *5*(1–2), 105–115. https://doi.org/10.1016/S0926-6410(96)00046-8

Cox, R. W. (1996). AFNI: Software for analysis and visualization of functional magnetic resonance neuroimages. *Computers and Biomedical Research*, *29*(3), 162–173. https://doi.org/10.1006/cbmr.1996.0014

di Pellegrino, G., & Làdavas, E. (2015). Peripersonal space in the brain. In *Neuropsychologia* (Vol. 66, pp. 126–133). Elsevier Ltd. https://doi.org/10.1016/j.neuropsychologia.2014.11.011

Duffy, C. J. (1998). MST Neurons Respond to Optic Flow and Translational Movement. *Https://Doi.Org/10.1152/Jn.1998.80.4.1816*,*80*(4),1816–1827.

Duhamel, J. R., Colby, C. L., & Goldberg, M. E. (1998). Ventral intraparietal area of the macaque: Congruent visual and somatic response properties. *Journal of Neurophysiology*, *79*(1), 126–136. https://doi.org/10.1152/JN.1998.79.1.126

Durand, J.-B., Nelissen, K., Joly, O., Wardak, C., Todd, J. T., Norman, J. F., Janssen, P., Vanduffel, W., & Orban, G. A. (2007). Anterior Regions of Monkey Parietal Cortex Process Visual 3D Shape. *Neuron*, *55*(3), 493. https://doi.org/10.1016/J.NEURON.2007.06.040

Essen, D. C. Van, & Dierker, D. L. (2007). Surface-Based and Probabilistic Atlases of Primate Cerebral Cortex. *Neuron*, *56*(2), 209–225. https://doi.org/10.1016/J.NEURON.2007.10.015

Ferraina, S., Paré, M., & Wurtz, R. (2000). Disparity sensitivity of frontal eye field neurons. *Journal of Neurophysiology*, *83*(1), 625–629. https://doi.org/10.1152/JN.2000.83.1.625

Ferri, S., Peeters, R., Nelissen, K., Vanduffel, W., Rizzolatti, G., & Orban, G. A. (2015). A human homologue of monkey F5c. *Neuroimage*, *111*, 251. https://doi.org/10.1016/J.NEUROIMAGE.2015.02.033

Fogassi, L., Raos, V., Franchi, G., Gallese, V., Luppino, G., & Matelli, M. (1999). Visual responses in the dorsal premotor area F2 of the macaque monkey. *Experimental Brain Research 1999 128:1*, *128*(1), 194–199. https://doi.org/10.1007/S002210050835

Galletti, C., Fattori, P., Kutz, D. F., & Gamberini, M. (1999). Brain location and visual topography of cortical area V6A in the macaque monkey. *European Journal of Neuroscience*, *11*(2), 575–582. https://doi.org/10.1046/J.1460-9568.1999.00467.X

Galletti, C., Gamberini, M., Kutz, D. F., Fattori, P., Luppino, G., & Matelli, M. (2001). The cortical connections of area V6: an occipito-parietal network processing visual information. *European Journal of Neuroscience*, *13*(8), 1572–1588. https://doi.org/10.1046/J.0953-816X.2001.01538.X

Genovesio, A, & Ferraina, S. (2004). Integration of retinal disparity and fixation-distance related signals toward an egocentric coding of distance in the posterior parietal cortex of primates. *Journal of Neurophysiology*, *91*(6), 2670–2684. https://doi.org/10.1152/JN.00712.2003

Gentile, G., Guterstam, A., Brozzoli, C., & Ehrsson, H. H. (2013). *Disintegration of Multisensory Signals from the Real Hand Reduces Default Limb Self-Attribution: An fMRI Study*. https://doi.org/10.1523/JNEUROSCI.1363-13.2013

Gentile, Petkova, & Ehrsson. (2011). Integration of visual and tactile signals from the hand in the human brain: an FMRI study. *Journal of Neurophysiology*, *105*(2), 910–922. https://doi.org/10.1152/JN.00840.2010

Gentilucci, M., Fogassi, L., Luppino, G., Matelli, M., Camarda, R., & Rizzolatti, G. (1988). Functional organization of inferior area 6 in the macaque monkey. *Experimental Brain Research 1988 71:3*, *71*(3), 475–490. https://doi.org/10.1007/BF00248741

Gentilucci, M., Scandolara, C., Pigarev, I., & Rizzolatti, G. (1983). Visual responses in the postarcuate cortex (area 6) of the monkey that are independent of eye position. *Experimental Brain Research*, *50*(2–3), 464–468. https://doi.org/10.1007/BF00239214

Georgieva, S., Peeters, R., Kolster, H., Todd, J. T., & Orban, G. A. (2009). The Processing of Three-Dimensional Shape from Disparity in the Human Brain. *Journal of Neuroscience*, *29*(3), 727–742. https://doi.org/10.1523/JNEUROSCI.4753-08.2009

Glasser, M. F., Smith, S. M., Marcus, D. S., Andersson, J., Auerbach, E. J., Behrens, T. E. J., Coalson, T. S., Harms, M. P., Jenkinson, M., Moeller, S., Robinson, E. C., Sotiropoulos, S. N., Xu, J., Yacoub, E., Ugurbil, K., & Essen, D. C. Van. (2016). The Human Connectome Project's Neuroimaging Approach. *Nature Neuroscience*, *19*(9), 1175. https://doi.org/10.1038/NN.4361

Gnadt, J., & Mays, L. (1995). Neurons in monkey parietal area LIP are tuned for eye-movement parameters in three-dimensional space. *Journal of Neurophysiology*, *73*(1), 280–297. https://doi.org/10.1152/JN.1995.73.1.280

Goodale, M. A., Milner, A. D., Jakobson, L. S., & Carey, D. P. (1991). A neurological dissociation between perceiving objects and grasping them. *Nature 1991 349:6305*, *349*(6305), 154–156. https://doi.org/10.1038/349154a0

Goodale, Melvyn A., & Milner, A. D. (1992). Separate visual pathways for perception and action. *Trends in Neurosciences*, *15*(1), 20–25. https://doi.org/10.1016/0166-2236(92)90344-8

Graziano, M. S. A., & Gandhi, S. (2000). Location of the polysensory zone in the precentral gyrus of anesthetized monkeys. *Experimental Brain Research 2000 135:2*, *135*(2), 259–266. https://doi.org/10.1007/S002210000518

Graziano, Michael S.A., Hu, X. T., & Gross, C. G. (1997). Visuospatial properties of ventral premotor cortex. *Journal of Neurophysiology*, *77*(5), 2268–2292.

Graziano, MS, & Cooke, D. (2006). Parieto-frontal interactions, personal space, and defensive behavior. *Neuropsychologia*, *44*(13), 2621–2635. https://doi.org/10.1016/J.NEUROPSYCHOLOGIA.2005.09.011

Graziano, MS, & Gross, C. (1993). A bimodal map of space: somatosensory receptive fields in the macaque putamen with corresponding visual receptive fields. *Experimental Brain Research*, *97*(1), 96–109. https://doi.org/10.1007/BF00228820

Graziano, MS, Yap, G., & Gross, C. (1994). Coding of visual space by premotor neurons. *Science*, *266*(5187), 1054–1057. https://doi.org/10.1126/SCIENCE.7973661

Grivaz, P., Blanke, O., & Serino, A. (2017). Common and distinct brain regions processing multisensory bodily signals for peripersonal space and body ownership. *NeuroImage*, *147*, 602–618. https://doi.org/10.1016/j.neuroimage.2016.12.052

Hadjidimitrakis, K., Breveglieri, R., Bosco, A., & Fattori, P. (2012). Three-dimensional eye position signals shape both peripersonal space and arm movement activity in the medial posterior parietal cortex. *Frontiers in Integrative Neuroscience*, *0*(JUNE 2012), 37. https://doi.org/10.3389/FNINT.2012.00037

Hadjidimitrakis, K., Breveglieri, R., Placenti, G., Bosco, A., Sabatini, S. P., & Fattori, P. (2011). Fix Your Eyes in the Space You Could Reach: Neurons in the Macaque Medial Parietal Cortex Prefer Gaze Positions in Peripersonal Space. *PLOS ONE*, *6*(8), e23335. https://doi.org/10.1371/JOURNAL.PONE.0023335

Hartig, R., Glen, D., Jung, B., Logothetis, N. K., Paxinos, G., Garza-Villarreal, E. A., Messinger, A., & Evrard, H. C. (2021). The Subcortical Atlas of the Rhesus Macaque (SARM) for neuroimaging. *NeuroImage*, *235*, 117996. https://doi.org/10.1016/J.NEUROIMAGE.2021.117996

Janssen, P., Vogels, R., & Orban, G. A. (1999). Macaque inferior temporal neurons are selective for disparity-defined three-dimensional shapes. *Proceedings of the National Academy of Sciences of the United States of America*, *96*(14), 8217. https://doi.org/10.1073/PNAS.96.14.8217

Jenkinson, M. Pechaud, and S. Smith. BET2: MR-based estimation of brain, skull and scalp surfaces. In Eleventh Annual Meeting of the Organization for Human Brain Mapping, 2005.

Jung, B., Taylor, P. A., Seidlitz, J., Sponheim, C., Perkins, P., Ungerleider, L. G., Glen, D., & Messinger, A. (2021). A comprehensive macaque fMRI pipeline and hierarchical atlas. *NeuroImage*, *235*, 117997. https://doi.org/10.1016/J.NEUROIMAGE.2021.117997

Kravitz, D. J., Saleem, K. S., Baker, C. I., & Mishkin, M. (2011). A new neural framework for visuospatial processing. *Nature Reviews. Neuroscience*, *12*(4), 217. https://doi.org/10.1038/NRN3008

Làdavas, E., & Farnè, A. (2004). Visuo-tactile representation of near-the-body space. *Journal of Physiology, Paris*, *98*(1–3), 161–170. https://doi.org/10.1016/J.JPHYSPARIS.2004.03.007

Làdavas, E., Zeloni, G., & Farnè, A. (1998). Visual peripersonal space centred on the face in humans. *Brain : A Journal of Neurology*, *121 (Pt 1*(12), 2317–2326. https://doi.org/10.1093/BRAIN/121.12.2317

Luppino, G., Hamed, S. Ben, Gamberini, M., Matelli, M., & Galletti, C. (2005). Occipital (V6) and parietal (V6A) areas in the anterior wall of the parieto-occipital sulcus of the macaque: a cytoarchitectonic study. *European Journal of Neuroscience*, *21*(11), 3056–3076. https://doi.org/10.1111/J.1460-9568.2005.04149.X

Makin, T. R., Holmes, N. P., & Zohary, E. (2007). Is That Near My Hand? Multisensory Representation of Peripersonal Space in Human Intraparietal Sulcus. *Journal of Neuroscience*, *27*(4), 731–740. https://doi.org/10.1523/JNEUROSCI.3653-06.2007

Mars, R. B., Jbabdi, S., Sallet, J., O'Reilly, J. X., Croxson, P. L., Olivier, E., Noonan, M. P., Bergmann, C., Mitchell, A. S., Baxter, M. G., Behrens, T. E. J., Johansen-Berg, H., Tomassini, V., Miller, K. L., & Rushworth, M. F. S. (2011). Diffusion-Weighted Imaging Tractography-Based Parcellation of the Human Parietal Cortex and Comparison with Human and Macaque Resting-State Functional Connectivity. *Journal of Neuroscience*, *31*(11), 4087–4100. https://doi.org/10.1523/JNEUROSCI.5102-10.2011

Murata, A., Fadiga, L., Fogassi, L., Gallese, V., Raos, V., & Rizzolatti, G. (1997). Object Representation in the Ventral Premotor Cortex (Area F5) of the Monkey. *Https://Doi.Org/10.1152/Jn.1997.78.4.2226*, *78*(4), 2226–2230. https://doi.org/10.1152/JN.1997.78.4.2226

Neubert, F. X., Mars, R. B., Thomas, A. G., Sallet, J., & Rushworth, M. F. S. (2014). Comparison of Human Ventral Frontal Cortex Areas for Cognitive Control and Language with Areas in Monkey Frontal Cortex. *Neuron*, *81*(3), 700–713. https://doi.org/10.1016/J.NEURON.2013.11.012

Orban, G. A. (2011). The Extraction of 3D Shape in the Visual System of Human and Nonhuman Primates. *Http://Dx.Doi.Org/10.1146/Annurev-Neuro-061010-113819*, *34*, 361–368. https://doi.org/10.1146/ANNUREV-NEURO-061010-113819

Orban, G. A. (2016). Functional definitions of parietal areas in human and non-human primates. *Proceedings of the Royal Society B: Biological Sciences*, *283*(1828). https://doi.org/10.1098/RSPB.2016.0118

Orban, G. A., Janssen, P., & Vogels, R. (2006). Extracting 3D structure from disparity. *Trends in Neurosciences*, *29*(8), 466–473. https://doi.org/10.1016/J.TINS.2006.06.012

Parker, A. J. (2007). Binocular depth perception and the cerebral cortex. *Nature Reviews Neuroscience 2007 8:5*, *8*(5), 379–391. https://doi.org/10.1038/nrn2131

Pitzalis, S., Sereno, M. I., Committeri, G., Fattori, P., Galati, G., Tosoni, A., & Galletti, C. (2013). The human homologue of macaque area V6A. *NeuroImage*, *82*. https://doi.org/10.1016/j.neuroimage.2013.06.026

Prescott, M. J., & Poirier, C. (2021). The role of MRI in applying the 3Rs to non-human primate neuroscience. *NeuroImage*, *225*, 117521. https://doi.org/10.1016/J.NEUROIMAGE.2020.117521

Quinlan, D. J., & Culham, J. C. (2007). fMRI reveals a preference for near viewing in the human parieto-occipital cortex. *NeuroImage*, *36*(1), 167–187. https://doi.org/10.1016/J.NEUROIMAGE.2007.02.029

Reveley, C., Gruslys, A., Ye, F. Q., Glen, D., Samaha, J., E. Russ, B., Saad, Z., K. Seth, A., Leopold, D. A., & Saleem, K. S. (2017). Three-Dimensional Digital Template Atlas of the Macaque Brain. *Cerebral Cortex*, *27*(9), 4463–4477. https://doi.org/10.1093/CERCOR/BHW248

Rizzolatti, G., & Craighero, L. (2004). THE MIRROR-NEURON SYSTEM. *Annu. Rev. Neurosci*, *27*, 169–192. https://doi.org/10.1146/annurev.neuro.27.070203.144230

Rizzolatti, G., Scandolara, C., Matelli, M., & Gentilucci, M. (1981). Afferent properties of periarcuate neurons in macaque monkeys. II. Visual responses. *Behavioural Brain Research*, *2*(2), 147–163. https://doi.org/10.1016/0166-4328(81)90053-X

Rolls, E. T., Huang, C. C., Lin, C. P., Feng, J., & Joliot, M. (2020). Automated anatomical labelling atlas 3. *NeuroImage*, *206*, 116189. https://doi.org/10.1016/j.neuroimage.2019.116189

Romero, M. C., Dromme, I. C. L. Van, & Janssen, P. (2013). The Role of Binocular Disparity in Stereoscopic Images of Objects in the Macaque Anterior Intraparietal Area. *PLOS ONE*, *8*(2), e55340. https://doi.org/10.1371/JOURNAL.PONE.0055340

Rozzi, S., Calzavara, R., Belmalih, A., Borra, E., Gregoriou, G. G., Matelli, M., & Luppino, G. (2006). Cortical Connections of the Inferior Parietal Cortical Convexity of the Macaque Monkey. *Cerebral Cortex*, *16*(10), 1389–1417. https://doi.org/10.1093/CERCOR/BHJ076

Sakata, H, Shibutani, H., & Kawano, K. (1980). Spatial properties of visual fixation neurons in posterior parietal association cortex of the monkey. *Journal of Neurophysiology*, *43*(6), 1654–1672. https://doi.org/10.1152/JN.1980.43.6.1654

Sakata, Hideo, Takaoka, Y., Kawarasaki, A., & Shibutani, H. (1973). Somatosensory properties of neurons in the superior parietal cortex (area 5) of the rhesus monkey. *Brain Research*, *64*(C), 85–102. https://doi.org/10.1016/0006-8993(73)90172-8

Sallet, J., Mars, R. B., Noonan, M. P., Neubert, F.-X., Jbabdi, S., O'Reilly, J. X., Filippini, N., Thomas, A. G., & Rushworth, M. F. (2013). The Organization of Dorsal Frontal Cortex in Humans and Macaques. *Journal of Neuroscience*, *33*(30), 12255–12274. https://doi.org/10.1523/JNEUROSCI.5108-12.2013

Schaefer, M., Heinze, H.-J., & Rotte, M. (2012). Close to You: Embodied Simulation for Peripersonal Space in Primary Somatosensory Cortex. *PLOS ONE*, *7*(8), e42308. https://doi.org/10.1371/JOURNAL.PONE.0042308

Schall, J., Morel, A., King, D., & Bullier, J. (1995). Topography of visual cortex connections with frontal eye field in macaque: convergence and segregation of processing streams. *The Journal of Neuroscience*, *15*(6), 4464. https://doi.org/10.1523/JNEUROSCI.15-06-04464.1995

Sereno, & Huang. (2006). A human parietal face area contains aligned head-centered visual and tactile maps. *Nature Neuroscience*, *9*(10), 1337–1343. https://doi.org/10.1038/NN1777

Shmuelof, L., & Zohary, E. (2005). Dissociation between Ventral and Dorsal fMRI Activation during Object and Action Recognition. *Neuron*, *47*(3), 457–470. https://doi.org/10.1016/J.NEURON.2005.06.034

Srivastava, S., Orban, G. A., Mazière, P. A. De, & Janssen, P. (2009). A Distinct Representation of Three-Dimensional Shape in Macaque Anterior Intraparietal Area: Fast, Metric, and Coarse. *Journal of Neuroscience*, *29*(34), 10613–10626. https://doi.org/10.1523/JNEUROSCI.6016-08.2009

Stanton, G., Deng, S., Goldberg, M., & McMullen, N. (1989). Cytoarchitectural characteristic of the frontal eye fields in macaque monkeys. *The Journal of Comparative Neurology*, *282*(3), 415–427. https://doi.org/10.1002/CNE.902820308

Verhoef, B.-E., Vogels, R., & Janssen, P. (2016). Binocular depth processing in the ventral visual pathway. *Philosophical Transactions of the Royal Society B: Biological Sciences*, *371*(1697). https://doi.org/10.1098/RSTB.2015.0259

Vernet, M., Quentin, R., Chanes, L., Mitsumasu, A., & Valero-Cabré, A. (2014). Frontal eye field, where art thou? Anatomy, function, and non-invasive manipulation of frontal regions involved in eye movements and associated cognitive operations. *Frontiers in Integrative Neuroscience*, *0*(AUG), 66. https://doi.org/10.3389/FNINT.2014.00066

Xu, T., Nenning, K. H., Schwartz, E., Hong, S. J., Vogelstein, J. T., Goulas, A., Fair, D. A., Schroeder, C. E., Margulies, D. S., Smallwood, J., Milham, M. P., & Langs, G. (2020). Cross-species functional alignment reveals evolutionary hierarchy within the connectome. *NeuroImage*, *223*, 117346. https://doi.org/10.1016/J.NEUROIMAGE.2020.117346

Yamane, Y., Carlson, E. T., Bowman, K. C., Wang, Z., & Connor, C. E. (2008). A neural code for three-dimensional object shape in macaque inferotemporal cortex. *Nature Neuroscience*, *11*(11), 1352. https://doi.org/10.1038/NN.2202

Chapitre 3 :

Étude de la dimension sociale de l'EPP chez l'homme à travers une approche multi-échelle

Points essentiels de ce chapitre :

- Développement d'un ensemble de protocoles en réalité virtuelle avec un visio-casque (étude 3 chez sujets sains et étude 5 chez des patients) ou avec un projecteur 3D dans l'IRM (étude 4 chez sujets sains) pour caractériser la dimension sociale de l'EPP.
- Facilitation des capacités de discrimination visuelle et augmentation du rythme cardiaque lors de la présence de visages émotionnels dans l'espace proche (EPP) par rapport à loin du corps (Étude 3).
- Identification d'un réseau fronto-pariétal commun pour le traitement des objets et des visages dans l'EPP et identification de spécificités dans le traitement neuronal en fonction de la nature des stimuli (catégorie et valence) (Étude 4).
- Altération de la régulation des distances interpersonnelles chez des patients avec des lésions unilatérales du lobe temporal médian (Étude 5).

ETUDE 3

Les visages émotionnels présentés dans l'espace péri-personnel facilitent les capacités de discrimination visuelle et augmentent les réponses physiologiques

---

Close facial emotions enhance physiological responses and facilitate perceptual discrimination

Audrey Dureux, Elvio Blini, Laura Clara Grandi, Olena Bogdanova, Clément Desoche, Alessandro Farnè and Fadila Hadj-Bouziane

Article publié dans Cortex

CORTEX 138 (2021) 40–58

Available online at www.sciencedirect.com

ScienceDirect

Journal homepage: www.elsevier.com/locate/cortex

Research Report

Close facial emotions enhance physiological responses and facilitate perceptual discrimination

Audrey Dureux [a,b,*,1], Elvio Blini [a,b,c,1], Laura Clara Grandi [a,b], Olena Bogdanova [a,b], Clément Desoche [a,b,d], Alessandro Farnè [a,b,d,e,2] and Fadila Hadj-Bouziane [a,b,**,2]

[a] Integrative Multisensory Perception Action & Cognition Team - ImpAct, INSERM U1028, CNRS UMR5292, Lyon Neuroscience Research Center (CRNL), Lyon, France
[b] University UCBL Lyon 1, University of Lyon, Lyon, France
[c] Department of General Psychology, University of Padova, Padova, Italy
[d] Hospices Civils de Lyon, Neuro-Immersion & Mouvement et Handicap, Lyon, France
[e] Center for Mind/Brain Sciences (CIMeC), University of Trento, Italy

ARTICLE INFO

Article history:
Received 11 February 2020
Reviewed 20 July 2020
Revised 22 September 2020
Accepted 26 January 2021
Action editor Holger Wiese
Published online 9 February 2021

Keywords:
Peripersonal space
Emotion
Sex
Virtual reality
Discrimination
Pupil diameter
Heart rate

ABSTRACT

Accumulating evidence indicates that the peripersonal space (PPS) constitutes a privileged area for efficient processing of proximal stimuli, allowing to flexibly adapt our behavior both to the physical and social environment. Whether and how behavioral and physiological signatures of PPS relate to each other in emotional contexts remains, though, elusive. Here, we addressed this question by having participants to discriminate male from female faces depicting different emotions (happiness, anger or neutral) and presented at different distances (50 cm–300 cm) while we measured the reaction time and accuracy of their responses, as well as pupillary diameter, heart rate and heart rate variability. Results showed facilitation of participants' performances (i.e., faster response time) when faces were presented close compared to far from the participants, even when controlling for retinal size across distances. These behavioral effects were accompanied by significant modulation of participants' physiological indexes when faces were presented in PPS. Interestingly, both PPS representation and physiological signals were affected by features of the seen faces such as the emotional valence, its sex and the participants' sex, revealing the profound impact of social context onto the autonomic state and behavior within PPS. Together, these findings suggest that both external and internal signals contribute in shaping PPS representation.

* *Corresponding author*. INSERM U1028, CNRS UMR5292, Lyon Neuroscience Research Center, ImpAct Team, 16 Avenue Doyen Lépine, 69500 Bron, France.
** *Corresponding author*. INSERM U1028, CNRS UMR5292, Lyon Neuroscience Research Center, ImpAct Team, 16 Avenue Doyen Lépine, 69500 Bron, France.
E-mail addresses: audrey.dureux@inserm.fr (A. Dureux), fadila.hadj-bouziane@inserm.fr (F. Hadj-Bouziane).
[1] These authors equally contributed to this work.
[2] These authors equally contributed to this work.
https://doi.org/10.1016/j.cortex.2021.01.014

1. Introduction

Every day, we dynamically interact with the world around us. The space closely surrounding our body, termed peripersonal space (PPS, Rizzolatti et al., 1981), is where we physically interact with objects in the environment. Its representation depends on the activity of a cortical network including premotor-parietal regions and the putamen subcortically, which displays responses to tactile stimulation, as well as stimuli in other modalities (i.e., visual and auditory) provided they occur in close proximity to the body (Ben Hamed et al., 2001; Bremmer et al., 2013; Brozzoli et al., 2011; Colby et al., 1993; Duhamel et al., 1998; Fogassi et al., 1992; Graziano et al., 1997; Makin et al., 2007; Rizzolatti et al., 1981; Sereno & Huang, 2006). At the behavioral level, the processing of stimuli in PPS is often facilitated in both uni- and multi-sensory settings, with faster detection of touches while auditory or visual stimuli approach in close space (Canzoneri et al., 2012; Ferri et al., 2015; Maister et al., 2015; Spaccasassi et al., 2019) and faster and more accurate discrimination of visual shapes (Blini et al., 2018a).

PPS representation is also characterized by a high degree of plasticity that likely facilitates interactions with the outside world. It can be shaped by experience, for instance following tool use (Farnè & Làdavas, 2000; Maravita & Iriki, 2004; Serino et al., 2007), or depending on the social context (Heed et al., 2010; Iachini et al, 2014, 2015; Maravita & Iriki, 2004; Pellencin et al., 2017; Ruggiero et al., 2017; Teneggi et al., 2013). When assessed via multisensory paradigms, PPS representation shrinks in the presence of another person: the tactile detection facilitation observed in PPS is less extended in space, as if the presence of another person was modulating the extent of one's own PPS representation (Teneggi et al., 2013). When assessed via the distance at which an approaching person is reachable, participants are influenced by the sex or the emotion the person conveys: PPS representation expands in the presence of males, angry or immoral persons, whereas it shrinks in the presence of females, happy or moral persons (Iachini et al., 2016). By contrast, multisensory tasks have shown a shrinkage or an expansion of PPS representation when facing an angry or immoral person, or a happy or moral person, respectively (Pellencin et al., 2017). PPS representation also expands when participants play a cooperative game with a partner before the task, suggesting that cooperation reconfigures the participants' PPS representation to include the space around the partner (Teneggi et al., 2013). Personality traits also influence PPS representation (Bufacchi & Iannetti, 2018; de Vignemont & Iannetti, 2015; Iachini et al., 2015; Lourenco et al., 2011; Sambo & Iannetti, 2013). For example Sambo and Iannetti (2013), found an expansion of PPS representation depending on the participants' anxiety level. Altogether, these results highlight the highly flexible nature of PPS representation that is modulated both by environmental constraints and individuals' psychological traits but also by the way this part of space is measured: whether it involves subjective judgments of reachability or sensory decisions. A handful of recent studies further suggested that the plastic features of PPS, determined by social stimuli, are associated with enhanced physiological responses (Cartaud et al., 2018; Ferri et al., 2015; Ruggiero et al., 2017). For instance, electrodermal activity increases when participants are presented with close as compared to far angry faces (Cartaud et al., 2018). Such physiological responses preferentially evoked by close emotional stimuli may reflect an increase of arousal within PPS, resulting from an activation of the sympathetic branch of the autonomic nervous system (Critchley, 2002).

However, to date the relationships between the behavioral and physiological markers of social modulations of PPS remains poorly understood. Here, we aimed at characterizing behavioral and physiological signatures of PPS representation in emotional contexts, also considering the potential role of participants' psychological traits. We thus modified an immersive virtual reality paradigm (O'Connor et al., 2014) we previously used to show advantages in visual discrimination of geometrical shapes in close space (Blini et al., 2018a). To keep distance and emotion task irrelevant, participants had to discriminate male from female faces with stimuli that could vary both in spatial location (50–300 cm) and emotion (happiness, anger, neutral). We measured participants' reaction times (RTs) and accuracy and recorded pupillary responses and heart rate.

We performed three experiments. In Experiment 1, faces were presented at 6 different distances (50–300 cm way, in 50 cm steps) and their size was scaled as a function of distance, thus farther faces appeared smaller as in natural viewing conditions. In Experiment 2, the same face stimuli were presented at two distances (50 cm, close or 300 cm, far) and, to control for the potential confound of stimulus size, they were corrected for retinal size: this way, farther faces appeared bigger than closer ones. In both experiments, we measured the participants' behavioral performance and pupil diameter. We also assessed two personality traits: anxiety (using STAI-Y and SAS questionnaires), and claustrophobia (using the CLQ questionnaire). Experiment 3 was similar to experiment 2, but participants viewed the stimuli passively to allow us for the recording of heart rate frequency and variability (HRV). We predicted that face proximity would facilitate visual discriminative abilities and this facilitation would be modulated by the facial features (sex, emotional valence), as well as the participants' sex and psychological traits. We further predicted that these behavioral changes would be associated with enhanced physiological responses.

2. Material and methods

We report how we determined our sample size, all data exclusions (if any), all inclusion/exclusion criteria, whether inclusion/exclusion criteria were established prior to data analysis, all manipulations, and all measures in the study.

2.1. *Participants*

Participants were healthy volunteers recruited through web advertising. None had history of neurologic or psychiatric disorders, and their vision was normal or corrected to normal (through contact lenses). All gave written informed consent

Table 1 – Demographic information for the three experiments.

Experiment	Demographic Information	Tasks	Measure	Retinal Size	Distances from subject
1	- 40 Subjects (20 female) - 0 Left-handed - Age (M = 22.5, SD = 3.72)	- Male/female Discrimination task - Questionnaires	- Accuracy - RTs - Pupil diameter	No correction	6 distances: 50 cm, 100 cm, 150 cm, 200 cm, 250 cm and 300 cm
2	- 40 Subjects (20 female) - 4 Left-handed - Age (M = 21.5, SD = 2.47)	- Male/female Discrimination task - Validation task - Questionnaires	- Accuracy - RTs - Pupil diameter	Correction	2 distances: 50 cm and 300 cm
3	- 24 Subjects (7 female) - 0 Left-handed	- Passive viewing task	- HR - HRV	Correction	2 distances: 50 cm and 300 cm

and were payed for their participation. A summary of participants' demographic information for each experiment is reported in Table 1. For experiments 1 and 2, we established a priori our target sample size ranged between 20 and 40 participants on the basis of what is regarded as a common sample size in the field (see, e.g., our previous study, Blini et al., 2018a). Different groups of participants took part in these experiments. For experiment 3, we managed to recruit a subset of participants who had already carried out experiment 2. In total we were able to enroll 24 subjects on the 40 who carried out experiment 2. No part of the study procedures or analyses of the three experiments was preregistered prior to the research being conducted.

The study followed the Declaration of Helsinki standards and was approved by the Institut National de la Santé et de la Recherche Médicale (INSERM) Ethics Committee (IRB00003888, No. 16-341).

2.2. *Apparatus*

In all experiments, visual stimuli were presented in a virtual reality environment. In experiment 1, the scene was rendered in an HTC Vive™ Head-Mounted Display (HMD), with a resolution of 1200 × 1080 pixels per eye, a frequency of 90 Hz and a field of view of 110°. The HMD had an embedded 250 Hz eye-tracking system (SMI). In experiments 2 and 3, the scene was rendered in an Oculus Rift DK2 HMD, with a resolution of 960 × 1080 pixels per eye, a frequency of 75 Hz, a field of view equal to 106°. The Oculus had an embedded 75 Hz eye-tracking system (SMI). The augmented technology Unity software (Version 5.1.2; Unity Technologies, San Francisco, CA) was used to create the virtual environment, display the stimuli and record participants' responses as in Blini et al. (2018a). Visual stimuli (faces) were presented in the virtual environment at different distances (see Table 1) while pupil diameter was recorded using the eye-tracking system of the HMD. In experiments 1 and 2, participants provided responses using the index and middle fingers of the dominant hand by pressing the B and N buttons on a computer keyboard. In experiment 3, a photoplethysmogram transducer (PPG, TSD200, Biopac) was attached to the right index finger of the participants to measure heart rate (HR) and heart rate variability (HRV); the signal was recorded via a Biopac system (MP150, PPGED- EDA device) at a frequency of 1 kHz.

2.3. *Stimuli*

Visual stimuli consisted of 20 individuals' faces, 10 females and 10 males, each mimicking 3 emotions (happy, neutral, angry). Legal copyright restrictions prevent public archiving of the stimuli used in our study, which were drawn from the Karolinska Directed Emotional Faces database (KDEF, Goeleven et al., 2008). These stimuli can be obtained from [www.kdef.se]. In this database, individuals were all photographed at the same distance. In detail, they were seated at a distance of approximately three meters from the camera. This distance was adapted for each subject by adjusting the camera position until the subject's eyes and mouth were at specific, predefined vertical and horizontal positions on the camera's grid screen. Then, each picture was cropped to a size of 562 pixels width and 762 pixels height. We further processed these images in the following way: stimuli were cropped to an oval shape, to remove outline and external features (e.g., hairs); images were equated for luminance, such that the mean luminance did not differ across sex or emotion of the faces. For that, we calculated the mean luminance of the face images. We then tested if luminance was different with a repeated measure ANOVA with sex and emotion of the image faces as factors; we found no significant main effects or interactions between these variables.

The size of each image was approximately 16 × 20 ° of visual angle except for the 1st experiment, in which images were scaled as a function of distance. In experiments 2 and 3, retinal size was kept constant across both distances (close and far). This was implemented in the Unity software by scaling up the far stimuli based on the size and distance of the close one, following the Basic Proportionality theorem: considering the size s of the closest stimulus displayed at a distance d, the size S of a stimulus displayed at distance D is: $S = s*D/d$. As such, in both experiments 2 and 3, the exact same 2D pictures, taken from the same position, were presented in either close or far conditions, allowing for similar object-specific spatial frequencies in both conditions. By presenting these images at different distances, they were not affected by perspective distortions, typically observed when pictures are taken from different distances (see for example Verhoff et al. (2008), Perona (2007) and Bryan et al. (2012)). Using the exact same pictures when applying retinal size correction (Experiments 2 and 3) to control for the potential confound of stimulus size,

prevented the influence of implicit distance information potentially conveyed by such perspective distortions. The 2D face images were rendered onto a VR environment over a flat surface, using a Head-Mounted Display, where geometrical distortions are marginal, only appearing in the peripheral visual field and do not differ between distances (https://github.com/facebookarchive/RiftDK2/blob/master/Documentation/DK2FirmwareSpecification.pdf).

2.4. Procedure

2.4.1. Male/female discrimination task (DT)

Participants sat in a quiet room, wearing the virtual reality headset (HDM), their head on a chinrest. The virtual environment was the same as the one used in (Blini et al., 2018a), and consisted of an empty room, as to minimize the presence of distracting elements. Different conditions were obtained by presenting the pictures of faces at different positions from the observer (6 distances in the 1st experiment: from 50 cm to 300 cm and 2 distances in the 2nd experiment: 50 cm, close and 300 cm, far). In experiment 1, retinal size was naturally scaled, as in ecological conditions (closer faces appeared bigger than farther ones). In experiment 2, retinal size of the stimuli was kept constant across distances (farther faces appeared bigger than closer ones, see Fig. 1 and Table 1).

After a 5 points calibration of the eye-tracker, trials started with a white fixation cross, presented in the center of the visual field. If the subject correctly fixated the cross for 1000 msec, its color became blue, and it was followed by the presentation of one face stimulus randomly chosen among male or female faces, its identity (10 levels for each sex), its emotion (happy, neutral, angry), and the distance of presentation. Faces were presented for 1 sec and subjects had a time-limit of 750 msec to provide an answer. A feedback text was then presented for 1 sec. The feedback reported whether a response was correct, incorrect, too slow (>750 msec), or too fast (<100 msec), as to encourage compliance with task instructions and induce time-pressure. Subjects used their index and middle fingers to report the sex of the presented face (the response keys were counterbalanced across participants). The pupil size was recorded for each trial during the sex categorization task. At the beginning of the experiment, a practice block was administered. The goal of practice trials was to ensure a stable performance across blocks. Practice

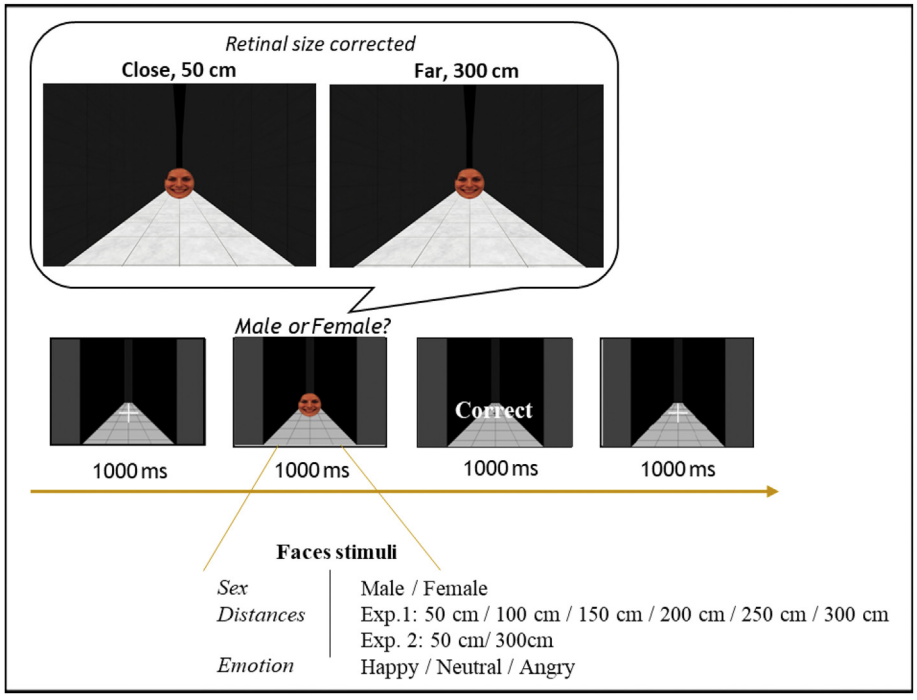

Fig. 1 – Experimental design for the male/female discrimination task in experiment 1 and 2. These experiments exploited a 3-D virtual-reality setting consisting in a simple empty room (same as the one used in Blini et al. (2018a). We used faces stimuli from the Karolinska Directed Emotional Faces database (KDEF, Goeleven et al., 2008, ID of the example face: AF06HAS). Faces stimuli with different emotions (happy, neutral, angry) were presented at different positions from participants. In the experiment 1, faces were presented at six different distances (50, 100, 150, 200, 250, and 300 cm) and retinal size was scaled as a function of distance. In the experiment 2, faces were presented at two distances (50 and 300 cm) and retinal size of the stimuli was kept constant across distances, resulting in the more distant faces appearing larger. Each trial started with a white fixation cross. If subjects correctly fixated the cross for 1000 msec, its color became blue, and it was followed by the presentation of the faces stimulus randomly chosen. Faces were presented for 1000 msec, then a feedback text was presented for 1000 msec. The feedback reported whether a response was correct, incorrect, too slow (>750 msec), or too fast (<100 msec). Participants used their index and middle fingers to report the sex of the presented face. Note that, due to lack of stereoscopic vision on 2D printing, these images do not bear any perceivable difference related to distance. Yet, their different position was clear in 3D.

blocks included 30 (experiment 1) or 24 (experiment 2) images that were also used in the ensuing experimental blocks. These stimuli were selected pseudo-randomly among the full images sample, thus including male or female faces, with various identities (10 levels for each sex), various emotions (happy, neutral, angry), and distances (6 distances from 50 to 300 cm for the experiment 1 or 2 distances for experiment 2). These categories were presented at least once in the practice trials. In addition, practice stimuli were selected randomly, according to these criteria, such that they differed for each participant.

Participants then performed 4 blocks of trials with a total of 576 trials for experiment 1, and 480 trials for experiment 2. After each block, subjects could rest and resume with the experiment by pressing the space key.

2.4.2. *Validation task (VT)*

At the end of experiment 2, we presented all the stimuli sequentially on a 2D monitor screen and asked subjects to judge whether the displayed emotion was neutral, happy or angry using a 9 points, Likert scale (range: −4–+4) presented below each face stimulus. In the scale, the minimum value (−4) indicated an angry face, the maximum (+4) a happy one, with intermediate values indicating neutral expressions. The open-source OpenSesame software (Mathôt et al., 2012) was used to display stimuli and collect responses. No time-limit was given. The aim of this task was to ensure that all the faces we presented could be correctly classified according to their emotional content.

2.4.3. *Passive viewing task*

Experiment 3 was designed to measure HR and HRV, which are typically estimated over several seconds (Shaffer & Ginsberg, 2017). Participants kept their right arm passively lying on the table in front of them with a photoplethysmogram transducer attached to their right index finger. Unlike in the first two experiments, participants had to merely look at the face stimuli. They viewed 6 blocks of 84 trials, each lasting about 4 min and followed by one-minute wash-out rest period. Also, at odds with experiment 1 and 2, here the same condition was presented within a given block. For each block, the condition was randomly selected among the different emotions (happy, neutral, angry), and distances (50 cm, close and 300 cm, far). As in experiments 1 and 2, the sex of the face stimuli (male or female), and identities (10 levels for each sex) were randomly presented in each trial within the block. The experiment started when the physiological signal (heart rate) appeared stable, typically from 5 sec to 1 min, based on the experimenter's visual inspection. At the beginning of each trial, participants had to fixate a white cross for 750 msec; then, one face stimuli appeared in the virtual environment for 2 sec and participants were instructed to look at them.

2.4.4. *Questionnaires*

At the end of experiments 1 and 2, participants filled the French versions of the following questionnaires, assessing personality traits supposedly related to PPS representation (Iachini et al., 2015; Lourenco et al., 2011; Sambo & Iannetti, 2013):

- STAI-Y questionnaire for assessing individual state and trait anxiety levels (i.e., two scores: STAY state and STAY trait scores; Gauthier & Bouchard, 1993; Spielberger & Sydeman, 1994).

- The sociality-avoidance questionnaire (SAS) for the measurement of anxiety for one own performance or for social situations, including the tendency to avoid them (i.e., six scores: Performance anxiety or fear, Social anxiety or fear, Total anxiety or fear, Performance avoidance, Social avoidance and Total avoidance scores; Radomsky et al., 2006).

- The Claustrophobia Questionnaire (CLQ), which includes two subscales assessing the specific fears of suffocation and restriction (i.e., three scores: Claustrophobia suffocation, Claustrophobia restriction and Total claustrophobia scores; Liebowitz, 1987).

The correlation between participants' scores in these questionnaires (i.e., a total of 11 different scores) and their performance on the DT was assessed by using Spearman correlations tests. The performance on the DT included RT variables for each emotion separately (i.e., angry, neutral and happy) and for all emotions regrouped. In experiment 1, we selected three variables: 1) the maximum (Max) RT and 2) the minimum (Min) RT among the 6 distances and 3) the difference between Min and Max RT (Delta RT). In addition, we computed differences in Delta RT between angry and neutral faces (Delta RTAngry-Neutral) and between happy and neutral faces (Delta RTHappy-Neutral), leading to a total of 14 variables for the correlation analysis. For experiment 2 with 2 distances (50 and 300 cm), we selected the difference between Close and Far RT for each emotion separately and for all emotion regrouped. Also, as in experiment 1, we computed differences in Delta RT between angry and neutral faces (Delta RTAngry-Neutral) and between happy and neutral faces (Delta RTHappy-Neutral), leading to a total of 6 variables for the correlation analysis. These analyses were explorative and resulted in a large number of correlation tests (exp. 1: 154 and exp. 2: 66) and as a consequence, we focused on correlations for which Bayes factors provided moderate ($3 < BF < 10$) or strong ($BF > 10$) evidence as to be more conservative with respect to false positives in the context of multiple tests (Blini et al., 2018; Gelman et al., 2012).

2.5. *Analyses*

In experiments 1 and 2, we measured accuracy, Reaction Times (RTs) and pupil diameter while the subjects performed the DT. At the end of experiment 2, we used the validation task to ensure that the emotions conveyed by the faces were correctly categorized by the participants. In experiment 3, we measured heart rate (HR) and computed heart rate variability (HRV) in the passive viewing task. Details about data processing, analyses and statistics for each variable are provided below.

2.5.1. *Behavioral performance in the male/female discrimination task (DT)*

Data were analyzed with the open-source software R (The R Core Team, 2013). Accuracy and RTs, in which both an accurate and timely response (>100 msec and <750 msec) was provided, were analyzed.

Table 2 – Psychometric functions fitted to the behavioral data (accuracy and RTs): linear, exponential, sigmoidal and gaussian. The N represents the number of participants displaying the same fitting function for all three emotions in Experiment 1. The models' goodness of fit was assessed using RMSE and AIC at the individual level. The greyed-out cells indicate that no participant presented the relative best-fitting function for all three emotions simultaneously using either goodness of fit measure (RMSE and AIC).

Curve	Equation	Measure	AIC	RMSE
Linear	y = a + b * x	Accuracy		
		RTs		
Exponential	y = a + b * exp(x/100)	Accuracy	N = 1/40	
		RTs		
Sigmoidal	y = a + b -a / 1+exp(c*(x-d))	Accuracy		N = 21/40
		RTs	N = 1/40	N = 7/40
Gaussian	y = a *exp(-1*(x-b)/c)+d	Accuracy		
		RTs	N = 4/40	N = 6/40

Experiment 1 was designed to study the spatial distribution of the effect by fitting psychometric functions: This approach is indeed well suited to study PPS, measuring performance of individuals along a continuum between far and near space. Importantly, this approach also allows for our results to be compared to several previous studies on peripersonal space, which made use of the same measures and analyses (e.g., Blini et al., 2018a; Canzoneri et al., 2012; Pellencin et al., 2017; Teneggi et al., 2013). Mean discrimination accuracy and RTs were calculated for each distance and emotion. These values were fitted at the group level and at the individual level, to four different psychometric functions: linear, exponential, sigmoidal and gaussian. The models' formulas are reported in Table 2. We performed non-linear least-squares estimations through the nls() function in R for every Emotion, using Distance as an independent predictor. We compared models' goodness of fit using both the root-mean-square error (RMSE) and the Akaike information criterion (AIC). The RMSE is a measure of dispersion of the residuals, whereas the AIC is best used for model comparison and accounts for models' complexity. The results of this analysis are provided in Tables 2 and 3. At the group level, for all emotions, the gaussian function provided the best fit for both accuracy and RTs (i.e., lower RMSE and AIC coefficients; see Table 3). At the individual level, the results indicated that the sigmoidal function best explained accuracy data for the largest number of participants while the gaussian function best explained RTs data for the largest number of participants (number of participants reported in parentheses in Table 3). Due to variability in the fitting of the four functions between individuals and emotions that lead to multiple convergence problems, we identified for each participant the best fitting function that was consistently found for the three facial expressions (Table 2). Results showed that the more consistent fitting was found for accuracy with 21 out of 40 participants, whose data were best fitted with the sigmoid function regardless of the emotion. Results were less conclusive for RTs, with <10 participants whose data were best fitted with the sigmoid or gaussian function. The inter-individual variability precluded further statistical analysis and we only provide a qualitative assessment of the results. Following previous studies (Canzoneri et al., 2012; Teneggi et al., 2013), we focused on the inflection point of the sigmoid function to identify the impact of a change in PPS representation according to facial emotions. Following the same reasoning for the gaussian fitting, we focused on the maximum peak of the gaussian curve as a putative analogous index.

In experiment 2, the results of the male/female discrimination task (i.e., Accuracy and RTs) were analyzed with mixed-effects multiple regression models (Baayen et al., 2008)

Table 3 – Results of models' goodness of fit using RMSE and AIC at the group level in Experiment 1. The number of participants who favored each model is reported in parentheses, based on analysis at the individual level.

Curve	Measure	Happy		Neutral		Angry	
		AIC	RMSE	AIC	RMSE	AIC	RMSE
Linear	Accuracy	−19.81 (N = 9)	.03 (N = 0)	−29.12 (N = 11)	.013 (N = 0)	−28.19 (N = 13)	.01 (N = 0)
	RTs	48.65 (N = 5)	8.46 (N = 0)	47.70 (N = 5)	7.82 (N = 0)	45.81 (N = 4)	6.68 (N = 0)
Exponential	Accuracy	−27.98 (N = 13)	.01 (N = 0)	−35 (N = 18)	.007 (N = 0)	−38.68 (N = 9)	.006 (N = 0)
	RTs	44.32 (N = 9)	5.90 (N = 0)	45.10 (N = 8)	6.29 (N = 0)	41.12 (N = 8)	4.52 (N = 0)
Sigmoidal	Accuracy	−30.84 (N = 7)	.008 (N = 28)	−32.60 (N = 5)	.007(N = 32)	−36.24 (N = 11)	.005(N = 33)
	RTs	44.84 (N = 9)	4.41 (N = 19)	47.42 (N = 9)	5.47 (N = 19)	39.67 (N = 12)	2.87 (N = 22)
Gaussian	Accuracy	−46.11 (N = 11)	.002 (N = 12)	−35 (N = 6)	.005 (N = 8)	−42.23 (N = 7)	.003 (N = 7)
	RTs	22.48 (N = 17)	.69 (N = 21)	37.27 (N = 18)	2.35 (N = 21)	27.36 (N = 16)	1.03 (N = 18)

using the lme4 package for R (Bates et al., 2015). These models had a logistic link-function, appropriate for binary variables, when assessing accuracy. We used Linear Mixed Effects Models (LMEM) because they allow to accommodate for both random effects of subjects and identities, most notably in this setting (e.g., Baayen et al., 2008). Thus, we could both generalize to individuals and different faces. The other advantages in the use of LMEM were that we used all the available data (trial basis, not collapsed), we could specify random effects appropriately to our design which therefore was more powerful (e.g., Jaeger, 2008).

As a first step, we defined a model containing the most appropriate random effects, striving for a parsimonious solution (Bates et al., 2015). We used an objective pipeline exposed in details elsewhere (Blini et al., 2018b). The simplest starting model included the random intercept for Subject (baseline level). We then tested: i) the random intercept for Identity (item); ii) possible nesting of the latter within Picture sex; iii) random slopes one by one. Random slopes testing started with introducing, for the random intercept of Subject, the following effects: 1) Distance; 2) Emotion; 3) Picture sex. Then, random slopes for Identity were tested in the following order: 1) Subject sex; 2) Distance; 3) Emotion. Procedures for testing fixed effects or for dealing with convergence problems were also unchanged with respect to our previous approaches (Blini et al., 2018b). We tested the role of the following four factors (fixed effects) and their interactions: Distance (2 levels: Close, Far), Emotion (3 levels: Happy, Neutral, Angry), Picture sex (2 levels: Male image, Female image) and Subject sex (2 levels: Male, Female participant). All post-hoc analyses for significant tests were computed on the basis of least-squares means (Lenth, 2016), using False Discovery Rate (FDR; Benjamini & Hochberg, 1995) correction for multiple tests.

In addition, a parametric bootstrap was used to obtain 95% confidence interval for the β coefficients, and thus to evaluate the distribution of estimated mean differences between the levels of a factor (Claridge-Chang & Assam, 2016).

2.5.2. *Pupil diameter*

Pupil diameter was retained for valid trials only, averaged across the left and right eye. A 'valid trial' corresponds to a trial in which the response was both accurate and timely (>100 msec and <750 msec). Each sample was first time-locked and aligned to the presentation of the face stimuli. To cope with inter-individuals variability, raw data were transformed in z values according to the subjects' specific distribution pattern. Z values exceeding ±2.5 SD were then treated as outliers/artifacts. We discarded trials in which more than 30% of the samples indicated such a corrupted signal, and linearly interpolated missing values in the remaining ones. Finally, each sample was normalized to (subtracted from) the first sample of each trial, which serves thus as baseline to better assess the time course of pupil dilation throughout the whole 1 sec window (corresponding to the presentation of face stimuli in each trial). To obtain a scalar index of pupil dilation/constriction for each trial, we then computed the temporal derivative (Van Den Brink et al., 2016) as the difference between the last and first sample of each epoch (submitted to statistical modelling and referred here as Gain). Positive values of Gain reflect overall pupil dilation since the beginning of the trial, negative values reflect overall constriction. Statistical modelling of the Gain followed the same pipeline of behavioral data, exposed above. For depiction purposes, smoothed curves were plotted. Since we did not correct for the influence of gaze position on pupil size measurement, results from this experiment are discussed taking into account the influence of gaze position on pupil size (see, for example, Hayes & Petrov, 2016).

2.5.3. *Heart rate and heart rate variability*

The heart rate signal was recorded and the inter-beat RR peaks were first detected with Spike2 software (Cambridge Electronic Design). The data were then imported in Kubios (Kubios software, version 2.1; Biosignal Analysis and Medical Imaging Group, Department of Applied Physics, University of Eastern Finland, Kupio, Finland) for following analysis. After extracting the HR signals, the R peaks were automatically identified. We visually inspected the automatic identification of the R peaks, and manually corrected for any missing peak. The number of R peaks during 1 min corresponds to the number of contractions (beats) of the heart per minute (bpm), i.e., heart rate frequency.

Time domain HRV indices included: 1) the number of adjacent normal to normal intervals (NN intervals or R–R interval; i.e., successive intervals between two heartbeats) differing by more than 50 msec in the entire recording (NN50, time, count); 2) mean of the standard deviations of all NN intervals for all 5-minute segments of the entire recording (SDNN, time, ms), informing about global variability and 3) the square root of the mean of the sum of the squares of differences between adjacent NN intervals (RMSSD, time, ms), expressing high frequency variability mainly of parasympathetic origin. Concerning the frequency domain analysis of the HRV, the power spectrum was obtained with a fast Fourier transform-based method (FFT; Welch's periodogram: 256 points windows with 50% overlap). The interpolation was used to resample RRi time series at 4 Hz. After the fast Fourier transform, HRV spectrum was then decomposed into two separate frequency bands: a low-frequency band (LF) with spectral components from .04 to .15 Hz and a high-frequency band (HF) comprising frequencies from .15 to .4 Hz. The ratio of LF power to HF power (LF/HF) was also calculated. We performed repeated measurement ANOVA on HR and HRV parameters, with FDR post-hoc correction ($p < .05$), with expressions (angry, happy and neutral) and distances (close and far) as factors. We ran an ANOVA instead of a LMEM approach because we didn't have multiple trials per cell, but only one value that corresponded to the mean HR and HRV parameters per block. In addition, a parametric bootstrap was used to obtain 95% confidence interval for the β coefficients, and thus to evaluate the distribution of estimated mean differences between the levels of a factor (Claridge-Chang & Assam, 2016).

3. Results

The supporting materials for this study are available on the Open Science Framework website (Supplementary Materials: https://osf.io/98mur/).

3.1. *Experiment 1: male/female discrimination task with face stimuli scaled as a function of distance*

In experiment 1, we modelled the subjects' DT performance (accuracy and RTs) as a function of depth (6 distances, from 50 to 300 cm). Due to inter-individual variability concerning the psychophysical modeling of subjects' performance and related convergence problems (see the Methods section), we reported in the part 3.1.1 only qualitative assessment of the results.

3.1.1. *Psychophysical modeling of behavioral data*

Psychophysical modeling of the subjects mean performance (accuracy and RTs) are illustrated in Fig. 2 and Table 3. Overall, visual inspection of the results show that the number of correct responses decreases (Fig. 2, on the top) while RTs increase as a function of the distance (Fig. 2, bottom), as previously reported with non-social stimuli (Blini et al., 2018a; Canzoneri et al., 2012; Ferri et al., 2015). Note that for close distances (in particular 50 cm), RTs seemed to be higher than those measured for more distant positions. At debrief, several subjects reported some 'difficulties' in focusing on stimuli at the closest distance, possibly due to the abrupt appearance of the faces in our experimental procedure.

Table 4 – Maximal peaks and of Gaussian curves and inflection points of Sigmoid curves in cm.

	Functions	Emotions		
		Happy	Neutral	Angry
Accuracy	Gaussian	122.584	95.087	96.151
	Sigmoid	255.971	266.999	268.672
RTs	Gaussian	136.530	145.576	133.452
	Sigmoid	247.191	264.581	242.383

3.1.1.1. Accuracy. Visual inspection of Fig. 2 suggests that the peak of the gaussian curve and the inflection point of the sigmoid curve change as a function of the emotional valence conveyed by the faces (Fig. 2 and Table 4). In particular, for happy faces, these parameters stand out from the other two emotions, namely neutral and angry faces, regardless of the fitting, suggesting higher accuracy for the former as compared to the latter.

3.1.1.2. Reaction times. As for accuracy, the peak of the gaussian curve and the inflexion point of the sigmoid curve for RTs seem to change as a function of the emotional valence conveyed by the faces (Fig. 2 and Table 4). Faster RTs are

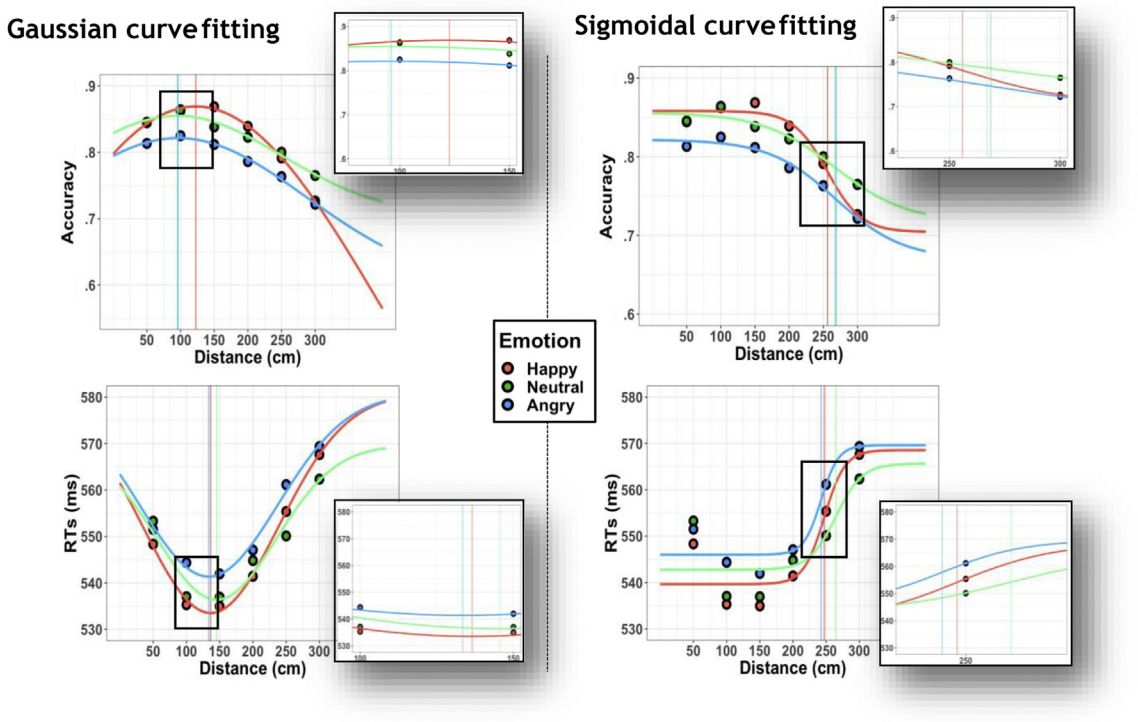

Fig. 2 – Psychophysical modeling of accuracy and RTs from Experiment 1. Fitting with gaussian (left) and sigmoidal (right) functions for the relationships between accuracy (top) or correct RTs (bottom) of the discrimination between male and female faces as a function of distance presented (in cm) with one color per emotion (red: happy faces, green: neutral faces and blue: angry faces). In each plot, the y-axis refer to the accuracy of participant's responses (correct responses) and RTs to discriminate. The x-axis refer to the distance where the stimuli were presented. The windows next to the main plot represent a zoom into the maximal peak and inflection points of the Gaussian and Sigmoidal curves, represented by the solid vertical lines for each emotion (red line: happy, green line: neutral, blue line: angry).

observed for happy faces compared to the two other emotions. Moreover, both gaussian and sigmoid fitting suggest a similar trend with a closer central point for both angry and happy faces compared to neutral faces, suggesting a modulation of PPS representation depending on the emotion conveyed by faces.

3.1.2. *Physiological analysis: pupil diameter*

The time-course of the pupil response, reflecting overall pupil dilation (positive values) or constriction (negative values) during the 1 sec time-window of stimulus presentation, is depicted in Fig. 4D Gain values for each trial were submitted to analyses with a random effect matrix which included: random slopes of Distance and Emotion for the random intercept of Subject; random intercept of Identity. We found a significant main effect of distance on pupil diameter ($\chi^2(5) = 99.98$, $p < .001$) with close faces inducing constriction and far faces inducing dilation ($\beta = 2.1$, 95% CI [1.89, 2.29]). A significant main effect was also observed for emotion (χ^2 (2) = 29.34, $p < .001$) with a difference in pupil dilation according to emotional faces. Pupil dilation was induced by the presentation of angry faces compared to the presentation of both neutral ($\beta = .05$, 95% CI [.03, .07]) and happy faces (all $|z| < 4$, all pfdr< .0001, $\beta = .05$, 95% CI [.02, .07]), while neutral and happy faces did not differ ($|z| = 1.845$, pfdr = .15, $\beta = -.007$, 95% CI [−.03, .01]). Finally, Distance and Emotion did not interact ($\chi^2(10) = 15.02$, $p = .13$).

3.1.3. *Psychological indexes and their correlation with behavioral responses*

We assessed the participants' anxiety, their sociality-avoidance and claustrophobia scores and estimated their relationship with their behavioral results on the DT. Due to large inter-individual variability in the fitting of the four functions between individuals and emotions that lead to multiple convergence problems, for the correlation analysis with personality traits, we focused on differences between the minimum and maximum RTs across the 6 distances for each participant rather than a mean RT at a fixed distance.

Our results found moderate evidence ($3 < BF < 10$) with a relation between differences between min and max RTs and claustrophobia levels. The measure of claustrophobia is composed of two separates but related items: fear of suffocation and fear of restriction (Radomsky et al., 2001). The global score and each individual item were positively correlated with the difference between min and max RTs for the neutral emotion: higher scores were associated with larger RTs differences (total.claustrophobia score: r = .36, $p = .024$; suffocation: r = .34, $p = .031$; restriction = .33, $p = .035$).

3.1.4. *Discussion*

We fitted the participants' accuracy and RTs with different theoretical curves as in previous studies (Blini et al., 2018a; Canzoneri et al., 2012; Ferri et al., 2015; Pellencin et al., 2017; Teneggi et al., 2013). When assessing gaussian and sigmoid functions fittings, our results suggest a shift of PPS representation depending on the emotional valence of the face to be discriminated. Specifically, both the maximal peak of the gaussian curve and the inflection point of the sigmoid curve occurred at closer distances for angry faces, followed by, in turn, happy and neutral faces. Emotion and distance modulated also pupil diameter. The pupillary response is tightly coupled with the vergence system (Feil et al., 2017). A decrease or increase in pupil diameter is observed when focusing the eyes from far to near distances (accommodation), or from near to far distances (disaccommodation), respectively (Kasthurirangan & Glasser, 2005). In our immersive setting, subjects moved their eyes from central fixation to either closer or farther positions, inducing a constriction and a dilation of the pupil when stimuli were presented in close and far space, respectively. In addition, we found that pupil size was larger with angry as compared to neutral, or happy faces, as in previous studies (Bradley et al., 2008; Libby et al., 1973). This increase likely reflects an activation of the sympathetic branch of the autonomic nervous system (Steinhauer et al., 2004), typically recruited to mobilize body's resources in threatening circumstances (Gordan et al., 2015).

Finally, we found a modulation of PPS that depended on participants' psychological traits and in particular their level of claustrophobia. We found that high claustrophobic fear was related to larger distance effect, suggesting that participants' psychological traits influence PPS representation.

3.2. *Experiment 2: male/female discrimination task with retinal-size corrected face stimuli*

In experiment 2, face stimuli were corrected for the retinal size and presented at either the closest or farthest distance (50 cm or 300 cm).

3.2.1. *Analysis of discrimination abilities in close and far space*

3.2.1.1. Accuracy. The mean accuracy of the 39 participants was 85.28% (SD = 6.15%). One subject was excluded from the analysis due to poor performance. Multiple convergence problems prompted us to use a matrix of random effects, which only included the random intercepts for Subject and Identity; no random slope was included. Fig. 3A illustrates the participants' accuracy depending on the distance (close/far) and the emotional valence conveyed by the faces (happy, neutral, angry). We found that accuracy was not modulated by Distance ($\chi^2(1) = .12$, $p = .73$). Emotion, on the other hand, did modulate participants' accuracy ($\chi^2(2) = 32.59$, $p < .001$). Indeed, happy faces were discriminated better than both neutral ($\beta = -.02$, 95% CI [−.03, −.008]) and angry ones (all $|z| > 3.49$, all pfdr < .001, $\beta = -.03$, 95% CI [−.04, −.02]), whereas the latter two did not differ ($|z| = .56$, pfdr = .58, $\beta = -.008$, 95% CI [−.02, .004]). There was no interaction between Distance and Emotion (χ^2 (2) = .07, $p = .97$). Three two-way interactions were also significant: Distance by Picture sex ($\chi^2(1) = 32.97$, $p < .001$); Emotion by Picture sex ($\chi^2(2) = 270.06$, $p < .001$); Picture sex by Subject sex ($\chi^2(1) = 12.54$, $p < .001$). The discrimination of male faces improved when images were presented far with respect to close ($\beta = .03$, 95% CI [.01, .04]), the pattern being reversed for female faces ($\beta = -.03$, 95% CI [-.05, −.009]). Within female faces, accuracy for the angry emotion was the lowest ($\beta_{Happy-} = -.08$, 95.0%CI [−.06, −.11], $\beta_{Neutral} = -.11$, 95.0%CI [−.08, −.13]); angry male faces were instead discriminated more

Fig. 3 – Results of male/female discrimination task from Experiment 2: A. Box-plots depicting participants' accuracy as a function of distance (close, 50 cm and far, 300 cm) and emotion depicted by faces. B. Box-plots depicting the participants' correct RTs as a function of distance (close, 50 cm and far, 300 cm) and emotion. In each plot, the vertical length of the box represents the interquartile range, the thick horizontal line represents the median, and the whiskers indicate the full range of values. Large dots inside the whiskers represent the mean. Dots outside the whiskers represent values exceeding 1.5 times the interquartile range.

accurately ($\beta_{Happy} = .02$, 95.0% CI [.003, .04], $\beta_{Neutral} = .09$, 95.0% CI [.07, .1]). Full results and graphical depictions of these tests are detailed in the supplementary materials.

3.2.1.2. Reaction times. The selected matrix of random effects included Emotion, Distance, Sex, and the Distance by Sex interaction as random slopes for Subject. No random slope was selected for the random intercept of Identity, which was included as well. Fig. 3B illustrates the participants' RTs depending on the distance (close/far) and the emotional valence conveyed by the faces (happy, neutral, angry). We found main effects of Distance ($\chi^2(1) = 25.45$, $p < .001$) and Emotion ($\chi^2(2) = 17.02$, $p < .001$). The first, as found in experiment 1 without retinal size correction, reflected faster responses for stimuli presented close with respect to far from participants ($|z| = 6.17$, $p < .001$, ($\beta = 8.75$, 95% CI [5.63, 11.4]). The second, also similar to experiment 1, reflected faster RTs for happy faces, which were discriminated faster than both neutral ($\beta = 3.48$, 95% CI [1.04, 5.92]) and angry ones (all $|z| > 3.23$, all pfdr < .002, $\beta = 7.65$, 95% CI [4.28, 11.2]); neutral faces were, in addition, discriminated faster than angry ones ($|z| = 2.79$, pfdr = .006, $\beta = 4.18$, 95% CI [.69, 7.86]). Moreover, these two effects were found to interact (Distance by Emotion: $\chi^2(2) = 7.94$, $p = .019$, depicted in Fig. 3). We thus compared the magnitude of the Distance effect between the three Emotions (i.e., the difference between RTs obtained in close and far space). We found that it was enhanced for angry faces with respect to neutral ($|z| = 2.8$, pfdr = .015, $\beta = 7.38$, 95% CI [.79, 14.2]) but not happy ones ($|z| = 1.83$, pfdr = .1, $\beta = -4.35$, 95% CI [−9.71, .85]); the magnitude of the advantage for close did not differ between neutral and happy faces ($|z| = 1.01$, pfdr = .31, $\beta = 3.03$, 95% CI [−4.02, 9.89]). As a complementary approach to post-hoc contrasts, we examined RTs for Emotion for each Distance. When images were presented close, happy faces were discriminated faster than both neutral ($\beta = 5.1$, 95% CI [1.45, 9.42]) and angry ones (all $|z| > 3.04$, all pfdr < .004, $\beta = 6.09$, 95% CI [1.62, 10.5]); when images were presented far, angry faces were discriminated slower than both happy ($\beta = -10.4$, 95% CI [−14.4, −6.7] and neutral (all $|z| > 5.48$, all pfdr < .001, $\beta = -8.37$, 95% CI [−13.5, −3.28]). Finally, three two-way interactions and one three-way interactions were significant: Distance by Picture Sex ($\chi^2(1) = 9.29$, $p = .002$); Emotion by Picture Sex ($\chi^2(2) = 292.66$, $p < .001$); Emotion by Subject Sex ($\chi^2(2) = 7.49$, $p = .023$) and Distance by Emotion by Subject Sex ($\chi^2(2) = 7.40$, $p = .024$). Concerning the two-way interactions, the first refers to female faces being discriminated faster than male ones when presented close ($\beta = 14.4$, 95% CI [8.92, 20.1]), but not far (and thus an enhanced distance effect for the discrimination of females, $\beta = 5.75$, 95% CI [−.66, 12.8]). The second indicates that female faces were consistently discriminated faster when displaying happy (~30 msec, 95% CI [27.5, 38.3]) or neutral (~23 msec, 95% CI [19.6, 30.2]) expressions with respect to angry, whereas male faces where discriminated faster if displaying angry expressions (~15 msec, 95% CI [10.3, 19.6] $_{Neutral}$, 95% CI [9.77, 19.8] $_{Happy}$). Finally, female participants were consistently faster in discriminating happy faces ($\beta_{Neutral} = 4.52$, 95% CI [2.41, 7.09], $\beta_{Angry} = 4.2$, 95.0% CI [.315, 10.1]), but there were no differences between neutral and angry faces ($\beta = -.32$, 95% CI [−3.97, 4.86]); male participants, on the contrary, showed a full gradient also indicating that angry faces were discriminated particularly slower ($\beta_{Happy} = -12.5$, 95.0% CI [−16.3, −8.95], $\beta_{Neutral} = -9.62$, 95.0% CI [−13.4, −4.92,]). The three-way interaction refers to a larger distance effect (advantage for Close) for Females for Neutral with respect to Happy faces and a larger Distance effect for Males for Happy than Neutral. All post-hoc results and graphical depictions for the last tests can be retrieved in the supplementary materials.

3.2.2. *Physiological analysis: pupil diameter*

As for experiment 1, the time-course pupil response during the whole 1 sec time-window of stimulus presentation, is depicted in Fig. 4E. Gain values for each trial were submitted to analyses using a random effect matrix, which included:

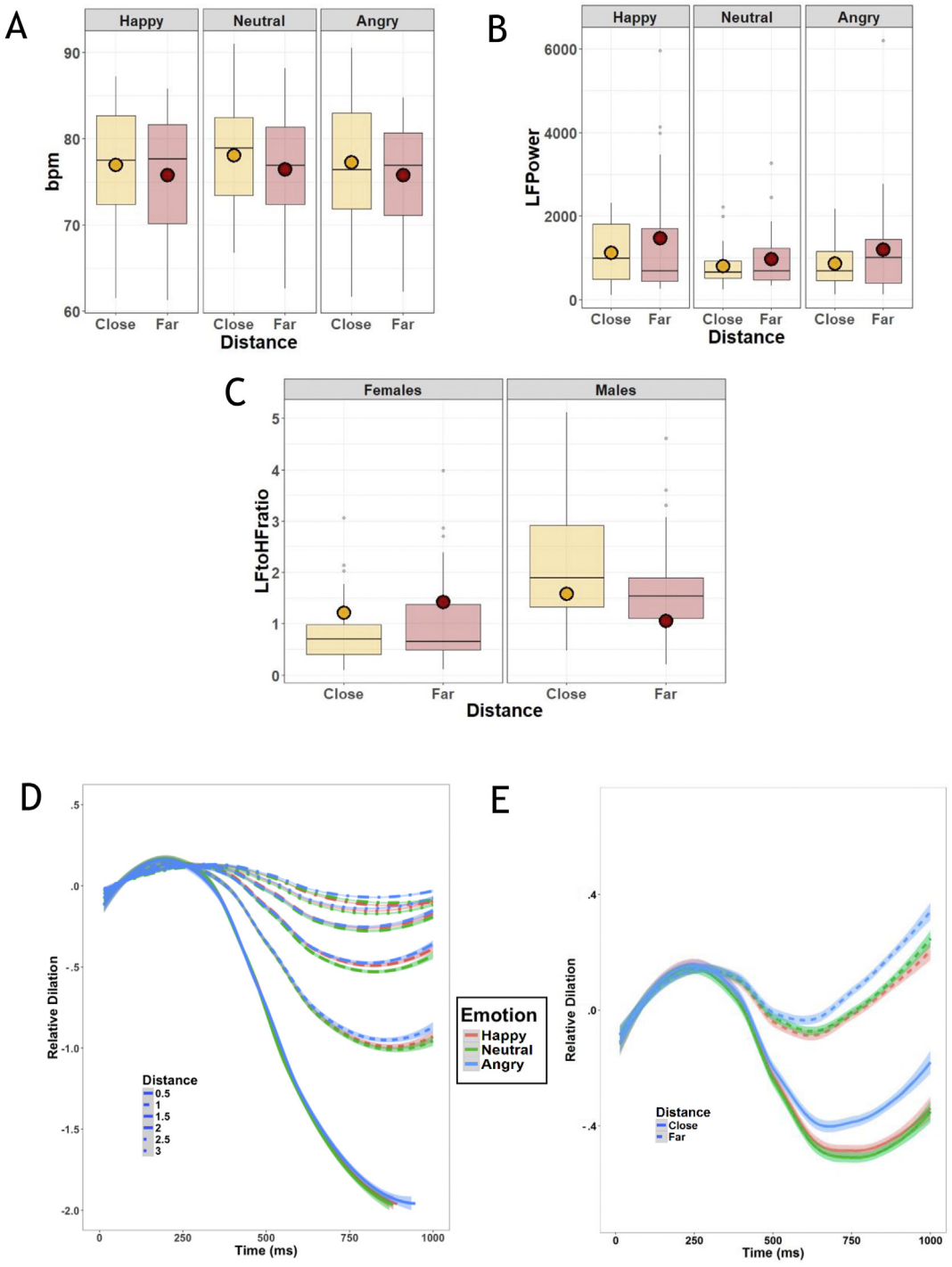

Fig. 4 – Physiological responses: A. Heart Rate results from Experiment 3. Box-plots depicting the participants' Heart Rate as a function of distance (close, 50 cm and far, 300 cm) and the emotion depicted by faces. B. and C. HRV results from Experiment 3. Box-plots depicting the LF power component of HRV as a function of distance (close, 50 cm and far, 300 cm) and the emotion depicted by faces (B) and LF to HR ratio of HRV as a function of distance (close, 50 cm and far, 300 cm) and the participants' sex (C). In each plot, the vertical length of the box represents the interquartile range, the thick horizontal line represents the median, and the whiskers indicate the full range of values. Large dots inside the whiskers represent the mean. Dots outside the whiskers represent values exceeding 1.5 times the interquartile range. D and E. Pupil diameter results from Experiment 1 and 2, respectively. Time-course of changes in pupil size, reflecting dilation or constriction during the whole 1 sec time-window of stimulus presentation represented as a function of distance and emotion depicted by faces. The lines and dashed lines correspond to the different distances where face stimuli were presented from 50 cm to 300 cm in panel C.; close, 50 cm and far, 300 cm in panel D. Locally weighted smoothing (LOESS) was applied to curves for depiction purposes.

random slopes of Distance, Emotion, and Sex for the random intercept of Subject; random slopes of Emotion and Subject Sex for the random intercept of Identity. Similarly to experiment 1, we found an effect of Distance on pupil diameter ($\chi^2(1) = 27.55$, $p < .001$) when retinal size was controlled for. Close stimuli induced pupil constriction, whereas far stimuli induced pupil dilation (|z| = 6.53, pfdr< .0001, β = .54, 95% CI [.39, .71]). Emotion had a strong effect as well ($\chi^2(2) = 34.64$, $p < .001$); angry faces caused pupil dilation with respect to both neutral (β = −.12, 95% CI [−.15, −.09]) and happy faces (all |z|> 6.97, all pfdr< .0001, β = −.13, 95% CI [−.17, −.09]), while the latter two conditions did not differ (|z| = .54, pfdr = .59, β = .01, 95% CI [−.01, .05]). Distance and Emotion did not interact ($\chi^2(2) = 2.38$, $p = .30$). The three-way interaction Distance by Subject Sex by Picture Sex was significant ($\chi^2(1) = 6.19$, $p = .01$). When viewing female faces presented far, male participants showed less dilation compared to female participants.

3.2.3. *Validation task*

We found significant main effects of Sex [F(1, 38) = 40.63, $p < .001$] and Emotion [F(2, 76) = 982.94, $p < .001$]. The first indicates that images of males were ranked on average towards the "angry" side of the continuum (β = −.19, 95% CI [−.246, −.131]). The second effect, which was the core test for this section, confirms that Emotions were clearly clustered such that angry faces obtained strongly negative rankings, happy faces strongly positive rankings, and neutral ones clustered around zero ($\beta_{Happy\text{-}Angry} = -4.94$, 95% CI [-4.66, −5.24], $\beta_{Happy\text{-}Neutral} = -2.8$, 95% CI [−2.64, −2.96], $\beta_{Neutral\text{-}Angry} = -2.14$, 95% CI [−1.99, −2.32]). However, Emotion and Sex interacted [F (2, 76) = 8.52, $p < .001$], such that males were indeed classified more often towards the "angry" side of the continuum, but only for neutral (β = .17, 95% CI [.08, .26] and angry expressions (β = .34, 95% CI [.23, .45]; rankings did not differ between male and female images for happy emotions (β = .07, 95% CI [−.008, .15].

3.2.4. *Psychological indexes and their correlation with behavioral responses*

In particular, we found strong evidence (BF > 10) for a correlation between the distance effect observed for happy faces and sociality-avoidance: the more self-reported avoidance for social situations, the smaller the deltas for happy faces (r = −.4, $p = .011$). This support, again, the notion that participants' personality traits influence PPS representation. Full details can be found in the supplementary materials.

3.2.5. *Discussion*

First, in Experiment 2, despite the retinal size was kept constant, we observed an advantage in responding to faces presented in near space, as previously found for geometrical objects shape discrimination (Blini et al., 2018a). Interestingly, this effect was modulated by the emotion conveyed by the face. Participants were fastest and more accurate in discriminating happy faces when these were presented close to them, while the slowest responses were obtained with angry faces presented far. Noteworthy, the distance effect (i.e., difference in RTs for close *vs* far faces) was more important for angry faces compared to other emotions (neutral and happy). Finally, we also observed a modulation of accuracy and RTs according to the Sex of the face stimuli (i.e., angry males were recognized faster and better than happy males, and inversely for females) and according to the participants' Sex (i.e., females were faster to discriminate happy faces, males were slower to discriminate angry faces) confirming that the impact of emotion on PPS representation may differ between males and females (Gigliotti, Soares Coelho, Coutinho, & Coello, 2019 ;Iachini et al., 2016; Ruggiero et al., 2017; Wingenbach et al., 2018).

Second, we found changes in pupil size depending on distance, emotion of the face stimulus and participant sex. The emotional- and distance-dependent modulation replicated the findings of Experiment 1, where retinal size varied as a function of distance: 1) pupil dilates for far faces and constricts for close faces, which likely reflects the tight coupling between pupil size and eye vergence and, 2) pupil dilates with angry faces, which likely reflects an increased level of arousal (Bradley et al., 2008; Steinhauer et al., 2004). In addition, we found an interaction between distance, participants' sex and the sex of the face stimuli, supporting the view that females and males process social stimuli differently in PPS, as reported in previous studies (Iachini et al., 2016; Ruggiero et al., 2017).

Third, we found that distance effect (i.e., far-close RTs) for happy faces was related to participants' self-reported avoidance scores in social situations, with larger distance effect related to smaller avoidance scores.

3.3. *Experiment 3: HR indices when viewing close and far faces*

In experiment 3, participants were merely exposed to the same emotional faces presented in the DT. Similar to experiment 2, they viewed retinal-size corrected stimuli at two distances (close: 50 cm and far: 300 cm) while we measured HR frequency and HRV.

3.3.1. *Heart rate and heart rate variability as a function of distance and emotion*

3.3.1.1. Heart rate frequency. Fig. 4A illustrates the participants' HR frequency as a function of Distance (close/far) and Emotions (happy, neutral, angry). We found a main effect of Distance [F (1, 21) = 6.94, $p = .02$], that reflected higher HR frequency for faces presented close with respect to far from participants (|t| = 2.63, $p = .015$, β = 1.4, 95% CI [.64, 2.92,]). Emotion did not modulate participants' HR [F (1.97, 41.29) = 1.31, $p = .28$] and there was no interaction between Distance and Emotion [F (1.83, 38.40) = .13, $p = .86$].

3.3.1.2. Heart Rate Variability. ANOVA tests were performed on the time domain (NN50, SDNN and RMSSD components) and the frequency domain (HF and LF components). Results on the time domain revealed no effect of Distance (NN50: F(1, 21) = .15, $p = .70$; SDNN: F(1, 21) = 1.41, $p = .25$; RMSSD: F(1, 21) = 1.61, $p = .22$), nor Emotion (NN50: F(1.72, 36.02) = .09, $p = .89$; SDNN: F(1.80, 37.76) = .004, $p = .65$; RMSSD:F(1.99, 41.74) = .06, $p = .94$). Results on the frequency domain revealed a main effect of Emotion for the LF component [F (1.46, 30.75) = 5.38, $p = .02$], but no effect of Distance [F (1, 21) = 2.67, $p = .12$], nor any interaction [F (1.98, 41.67) = .50, $p = .61$]. Fig. 4B illustrates the participant's LF component for HRV depending

on the distance (close/far) and the face emotional valence (happy, neutral, angry). Post-hoc analysis revealed that LF component was enhanced for happy faces with respect to neutral ($|t| = 3.245$, $p = .007$, $\beta = 415$, 95% CI [113, 779]), but not angry ones ($|t| = 2.028$, $p = .073$, $\beta = -264$, 95% CI [−583, 26.5]) and the latter two did not differ ($|t| = 1.217$, $p = .23$, $\beta = 151$, 95% CI [−9.31, 354]). Analysis of the LF to HF ratio showed no effect of Distance [$F(1, 21) = 3.49$, $p = .08$] nor Emotion [$F(1.88, 39.55) = .64$, $p = .52$], but there was a significant two-way interaction of Distance by Subject Sex [$F(1, 21) = 18.38$, $p = .0003$], showing that males presented larger ratios when images were presented close with respect to far ($\beta = .54$, 95% CI [.29, .85]) (Fig. 4C).

3.3.2. Discussion

We found higher HR when faces were presented close (50 cm), as compared to far (300 cm), from the participants. These results extend previous findings reporting changes of skin conductance with emotional faces within PPS (Cartaud et al., 2018), or HR in conditions involving a stimulated hand approaching the face (Chillura et al., 2018). Altogether, these findings demonstrate that emotional faces enhance physiological responses and these responses are potentiated within PPS. The increase in physiological responses typically signifies an aroused state, through the activation of the sympathetic branch of the peripheral nervous system (Gordan et al., 2015; Kreibig, 2010). In addition, our results demonstrate that distance also modulated HRV depending on the participants' sex. We found a selective increase of LF/HF ratio when faces were presented close to male participants. The ratio between the high- and low-frequency oscillations in HRV is viewed as reflecting the balance in activity between the parasympathetic and sympathetic systems. An increase of this ratio is thought to represent a sympathetic effect on the heart (Shaffer & Ginsberg, 2017). We found also that the HRV is sensitive to the emotion displayed: LF component was increased for happy faces compared to neutral faces. Both parasympathetic and sympathetic peripheral nervous system contribute to LF power (Shaffer & Ginsberg, 2017), however in some conditions sympathetic activity may dominate over parasympathetic activity (Pagani et al., 1984). The HR and HRV responses suggest an activation of the sympathetic system depending on the emotion perceived by the subject (happy faces), by the distance at which these stimuli were presented (close compared to far) and by the sex of the participants.

4. General discussion

In the present study, we investigated the impact of social stimuli (i.e., faces with emotional expressions) on the PPS advantage in visual discrimination abilities reported recently (Blini et al., 2018a) and its physiological markers. We presented emotionally connotated faces close or far from participants in an immersive virtual reality environment. Across experiments, we consistently observed a facilitation in facial discrimination within PPS. In absence of any speed accuracy trade off, participants performed sex categorization faster in close compared to far space (Exp. 1), even when retinal size was equated for close and far images (Exp. 2). Most relevant for this study's purpose, this distance-related modulation depended on the face emotional valence, its' sex, and the participant's sex, providing new evidence that PPS representation is finely tuned to both external and internal constraints. In addition, two physiological responses were also modulated by distance: the pupil size and HR indexes (frequency and variability). Interestingly, and similar to the behavioral findings, these distance-related physiological changes (pupil diameter, HR and HRV) also depended on the participant's sex and the sex of the face stimuli.

4.1. *Close emotional faces facilitate visual discriminative abilities*

We found that participants were faster in categorizing sex when faces were presented close as compared to far (8.6 msec advantage). This advantage was found even when stimuli in close and far space were equated in retinal size, without any speed accuracy trade off, as found for object shape discrimination (Blini et al., 2018a), suggesting that the faster processing in PPS, previously reported for neutral objects, extends to social stimuli.

Humans faces share the same basic prototypic structure with subtle idiosyncratic differences in the position, shape and characteristics of the elements that constitute an individual face (Logan et al., 2017). Despite these complexities, humans can extract seemingly effortlessly an important number of information such as sex. Here, we further show that the depth at which a face is presented affects this fine discrimination ability, facilitating such an ability within close space. This effect was present with unfamiliar, cropped faces, that is hair and any other external features were lacking and with faces expressing emotions that could potentially increase the difficulty in discriminating the sex of the face image. As accumulating evidence suggest that "what" and "where" information can coexist in the dorsal pathway (Freud et al., 2017), it is tempting to suggest that the PPS network seems ideally suited to subserve the advantage in discriminating close versus far objects and faces. Yet, recent evidence also demonstrates that category-selective regions in the visual ventral stream are also engaged in the processing of depth information (Nag et al., 2019). The specific contribution of these different networks in the behavioral facilitation that we report here is beyond the scope of the current study and future neuroimaging studies are needed to provide insights about the brain processes involved. Importantly, the present study provides new evidence that male/female discrimination, a fine perceptual ability, is facilitated in close space, within PPS. Interestingly, Smith and Schyns (2009) reported that changes in viewing distance affect the spatial frequency (SF) content of the stimuli and performance was differently affected across distances depending on the facial expressions. The recognition of neutral facial expressions tended to be more impaired than happy and angry across several distances. Although we report here performance related to sex discrimination, instead of emotions, we also observed that performance was differently affected depending on the emotions across the different distances. Specifically, we found that performance with angry faces tended to be more impaired than that of happy or neutral faces across several

physical distances. We did not determine the SF range of the face images depending on the emotion and viewing distance in our set of stimuli as this was beyond the scope of our current experiment, but it is possible that differences in SF across emotion and viewing distances may impact performance differently depending on the task at hand (discrimination of emotional facial expressions *vs* sex of faces). Noteworthy, Aguado et al. (2010) found both common and specific effects of SF content on sex and emotional expression discrimination in faces, suggesting that they rely on a set of features that are in part overlapping and in part independent. This is also consistent with Rotshtein et al. (2010) findings demonstrating specific effects of SF content depending on the task demand. Importantly, in experiments 2 and 3 where retinal size was equated across close and far conditions, the SF content of the images were similar across both distances and therefore did not affect our results.

Second, within PPS, participants were faster to discriminate happy faces compared to both neutral and angry ones whereas, outside PPS, participants were slower in discriminating angry faces compared to both happy and neutral ones. The psychophysical modeling (gaussian and sigmoidal fittings specifically) of accuracy and RTs as a function of distance indicates that performance is modulated according to emotions. In particular, up to 150 cm from the observer happy faces lead to faster and more accurate performance compared to the other emotions. Such a perceptual facilitation with happy faces could result from salient information extracted from the mouth region, that may speed up the processing (Calvo et al., 2010). This finding concurs in suggesting that complex stimuli appearing in PPS benefit of a much finer visual processing than previously thought. In addition, a comparison between the maximum peak of the gaussian fitting and the inflection point of sigmoid fitting for RTs, a canonical signature of PPS representation (Canzoneri et al., 2012; Pellencin et al., 2017; Teneggi et al., 2013), suggests a similar shift in representation of PPS depending on the facial emotions. These parameters are typically taken to indicate a change or a shift in PPS representation 'border', which comes closer to the body facing angry compared to happy and neutral faces. Our results are in keeping with previous work assessing PPS with multi-sensory tasks whereby, as here, distance is not relevant to the task (Pellencin et al., 2017). Together, these findings suggest a shrinkage of PPS representation in the presence of faces with negative connotations. Yet, faces with negative connotations are not always associated with a shrinkage of PPS representation. For instance, in reachability judgement task, participants favored larger distance from faces with negative connotations (Iachini et al., 2015; Ruggiero et al., 2016). This task, on the contrary, directly involves a distance judgment (participants press a button when an approaching avatar is reachable). Altogether, these results denote the highly flexible, context-dependent nature of PPS representation. This representation of the space close to the body allows us to adapt our behavioral response and interact toward and away from the different elements of our environment depending on the context, in an unconscious and automatic manner. Noteworthy, the differences observed on the flexibility of PPS representation (shrinking or enlargement with negative emotions) suggest that different methods to assess PPS representation (Iachini et al., 2015; Pellencin et al., 2017; Ruggiero et al., 2016; Teneggi et al., 2013) may refer to different concepts of PPS (de Vignemont & Iannetti, 2015). In this regard, the unisensory visual approach developed in the present study seems to capture PPS features that are typically observed in multisensory tasks (Pellencin et al., 2017; Teneggi et al., 2013).

Finally, our exploratory correlation analyses suggest that PPS representation depends also on the participants' psychological traits and in particular on their level of claustrophobia and social avoidance. In Experiment 1, high claustrophobic fear (fear of restriction or suffocation) were related to larger RT differences. Our results are in line with those of Lourenco et al. (2011) and Hunley et al. (2017) who found larger PPS representation in individuals with high claustrophobic fear and suggested that this distortion in the representation of near space might be linked to the defensive function of PPS (Graziano & Cooke, 2006). In experiment 2, we found that higher avoidance scores in social situations were related to smaller distance effect for happy faces. In both experiments with different groups of participants, the results seem to indicate that PPS representation is influenced by personality traits. Yet, it is difficult to draw strong conclusions about the specificity of this influence due the degree of subjectivity and variability associated with these types of questionnaires. Future studies – including a larger number of participants and testing more systematically psychological traits – are necessary to understand the complex relationship between psychological traits and PPS representation depending on the context at hand.

4.2. *Emotional faces in PPS enhance physiological responses*

Stimuli presented in PPS tend to be processed faster; the processing of objects conveying a potential threat, whether social or not, are even more prioritized when approaching the body (Bufacchi, 2017; Coello et al., 2012). A few recent studies suggested that physiological responses are also modulated as a function of distance (Meyer et al., 2019). For instance, Rossetti et al. (2015) reported an increase of electrodermal activity to incoming threatening stimuli (a needle) in the space close to the hand. Cartaud et al. (2018) also reported an increase of electrodermal activity for angry facial emotions presented in PPS using human-like point-light displays. Other studies investigated the relationship between interoceptive accuracy, a proxy for trait-like sensitivity to one's visceral signal determined by heartbeat tracking, and the modulation of participants' autonomic response (Ferri et al., 2013) and PPS representation (Ardizzi & Ferri, 2018). Ferri et al. (2013) found a positive correlation between heartbeat perception scores and respiratory sinus arrhythmia (RSA) responses in PPS in a social task, suggesting that high interoceptive sensitivity contribute to more efficient body-related information occurring in PPS. In addition, Ardizzi and Ferri (2018) found that higher interoceptive accuracy predicts sharper PPS boundary. These studies suggest that the level of arousal is differentially

affected by the position of stimuli in space, with an increase of interoceptive accuracy (i.e., heartbeat perception) or physiological responses in close space.

Our results add to these findings by providing novel evidence of distance-dependent modulation of pupil diameter and heart rate indexes (frequency and variability). We found a constriction of the pupil size when faces were presented in close space and a dilation when faces were presented in far space. This finding fits nicely with the modulation of the pupil diameter that is generally observed during accommodation and disaccommodation: focusing the eyes at different distances is associated with a decrease in pupil diameter when focusing from far to near (accommodation) and an increase when focusing from near to far (disaccommodation) (Kasthurirangan & Glasser, 2005), reflecting the tight coupling between pupil size the vergence system (Feil et al., 2017). Such internal signals could therefore contribute to or result from the behavioral facilitation within PPS. In addition to this general modulation though, the pupil diameter was selectively modulated by the facial emotion: angry faces induced pupil dilation, as previously reported (Bradley et al., 2008; Libby et al., 1973). The pupil diameter is controlled by two muscles, the dilator and the sphincter, differentially influenced by the sympathetic and parasympathetic nervous systems. Increased sympathetic activity leads to pupil dilation whereas increased parasympathetic activity leads to pupil constriction (Steinhauer et al., 2004). The increase in pupil diameter in response to angry faces thus suggests a stimulation of the sympathetic branch of the autonomic nervous system, preparing the body for a rapid reaction to face environmental changes, which is especially important for near-space situated stimuli (Ebitz & Moore, 2019). Although in the present study this effect did not appear to vary as a function of the distance, we prefer cautiously not excluding this possibility on this sole basis. Further, a study by Schurgin et al. (2014) on eye movements during facial emotion recognition reported an eye-gaze distinctive pattern for each type of emotional face. For example, the eyes region is less explored in expressions of happiness and disgust, as compared to faces expressing fear and shame. When additionally considering that changes in pupil size according to close and far presentation of stimuli are highly coupled with the vergence system (Feil et al., 2017), it is possible that the difference in eye movements between different facial expressions and face sizes might have affected the pupil diameter results. Yet, in the light of the similar, distance dependent pattern we observed across emotions when faces were presented either without or with retinal size correction (Exps 1 and 2, respectively) we deem this possibility is unlikely.

We also measured the heart rate (HR) and its variability (HRV) while the subjects observed the faces. As previously described, these variables were modulated by facial expressions (Appelhans & Luecken, 2006). In addition, we found that closer faces evoked significant increase of the HR, together with a modulation of its variability, which depended on the sex of the face stimuli or of the participants. As for the pupil size, sympathetic and parasympathetic systems exert antagonistic effects on the heart, either preparing the body for emergency or stressful situations (sympathetic system), or restoring the body to a restful state (parasympathetic system) (Ziegler, 2004). Both the pupil dilation and the HR/HRV increase suggest a sympathetic activation in the presence of emotional stimuli (i.e., increase of HRV for happy faces and pupil dilation with angry faces) and by their proximity to the body (i.e., increase of HR in close space compared to far). The physiological changes induced by emotional faces in PPS likely reflect an increase of the level of arousal when stimuli approach the body. Neither for the heart rate nor the pupil size, we observed any interaction between the type of emotion and distance from the body. This might suggest that they reflect a generalized arousing response when a stimulus approach the body, prompting a defensive response to protect from a potential danger (Cléry et al., 2015; Graziano & Cooke, 2006; di Pellegrino & Làdavas, 2015).

4.3. *Sex matters to the space around us*

The emotional content of a face influences both people's visual discrimination and their physiological responses and our results concur showing the profound impact that emotions can have on PPS. In addition, we also found that the sex of the face stimuli and/or that of the participants could influence behavioral and physiological responses. First, as previously reported (Hess et al., 2009), we found that male participants are slower to discriminate the sex of angry faces, when compared to other emotions. Second, the sex of the seen face influences the observer's accuracy and RT: sex categorization was better (higher accuracy) and faster (smaller RTs) for close female images (compared to far ones) and, conversely, it was better for far male images (compared to close ones). Third, the sex of the face and/or that of the participants influenced pupil size and HRV. Male participants showed less pupil dilation when female images were presented far (compared to close ones). In addition, here we report a larger LF/HF ratio for male participants exposed to closer faces. Pagani et al. (1984, 1986) have proposed that LF/HF ratio could be considered an estimate of the balance between sympathetic and parasympathetic nervous system activity. An increase in LF/HF ratio could thus be viewed as increase in sympathetic activity (Billman, 2013). According to this interpretation, our results suggest that the level of arousal in male participants is higher when emotional faces are presented next to them. Thus, both the sex of the viewer and that of the nearby conspecifics matters. These variables modulate the level of arousal, with changes that can be measured from the pupil and the heart and may also influence behavioral responses. Our results support the notion that PPS representation is highly sensitive to both external and internal milieu aspects (Bufacchi & Iannetti, 2018).

4.4. *How can interoceptive signals influence PPS brain network activity?*

The present study shows that when social elements enter the PPS, they induce a variety of specific effects at the behavioral and physiological level. Several neurophysiological and

neuroimaging studies have identified a set of neural substrates with selective activity in response to stimuli presented in PPS, including premotor-putamen-parietal regions. How is this network involved in behavioral and physiological regulations when stimuli approach the body? While future neuroimaging studies are needed to tackle this question directly, we believe it should at least be tentatively addressed here. We wish discussing the speculation that peripheral physiological changes could contribute to behavioral effects by modulating activity of this network. The central nervous system receives inputs from the internal body by ascending visceral signals (Azzalini et al., 2019; Critchley & Garfinkel, 2017). Visceral inputs reach the brain via vagal and spinal pathways targeting brainstems relay nuclei (nucleus tractus solitarius, NTS; and parabrachial nucleus, PBN). Ascending sensory fibers represent 80% of the vagus nerve (Agostoni et al., 1957). From NTS and PBN nuclei, projections are sent to noradrenergic and serotonergic pathways in the brainstem acting as relays to subcortical regions (Azzalini et al., 2019). Then, via thalamic relays, numerous cortical areas receive visceral signals, including the PPS network. Emotionally connotated stimuli in close proximity of our body may increase the level of arousal (heart rate) and this interoceptive information may be transferred via thalamocortical pathways and other subcortical regions (e.g., hippocampus, amygdala, insula), which are connected to cortical PPS brain regions. In particular, strong thalamic projections are sent to premotor and prefrontal areas including ventral premotor cortex (PMV) (Fang et al., 2006). Strong anatomic connections also exist between the amygdala and the granular frontal operculum, an adjacent and connected region to the PMv (Gerbella et al., 2014). Amygdala activation could leads to heart rate increases and HRV decreases through activation or disinhibition of sympatho-excitatory neurons in the rostral ventrolateral medulla, and inhibition of vagal activity through the nucleus ambiguous (Thayer & Sternberg, 2009). Therefore, these routes could relay visceral/sensory inputs to brain regions coding for PPS representation and shape the behavioral responses depending on the context (i.e., faster RTs and higher accuracy).

Author contributions

Audrey Dureux: Conceptualization; Methodology; Validation; Formal analysis; Investigation; Data curation; Original draft; Review & editing; Visualization; Project administration.

Elvio Blini: Conceptualization; Methodology; Validation; Formal analysis; Investigation; Data curation; Original draft; Review & editing; Visualization; Project administration.

Laura Clara Grandi: Conceptualization; Methodology; Formal analysis; Investigation; Review & editing.

Olena Bogdanova: Resources; Writing - Review & Editing.

Clément Desoche: Software; Resources.

Alessandro Farné: Conceptualization; Methodology; Validation; Review & editing; Project administration; Supervision.

Fadila Hadj-Bouziane: Conceptualization; Methodology; Validation; Original draft; Review & editing; Visualization; Supervision; Project administration; Funding acquisition.

Open practices

The study in this article earned Open Materials and Open Data badges for transparent practices. Materials and data for the study are available at https://osf.io/98mur/.

Declaration of competing interest

The authors declare that they have no conflict of interest.

Acknowledgements

This work was supported by the French National Research Agency ANR-15-CE37-0003 grant MySpace to FHB and ANR-10-IBHU-000 Neuro-Immersion to AF. EB was supported by: the European Union's Horizon 2020 research and innovation programme (Marie Curie Actions) under grant agreement MSCA-IF-2016-746154; a grant from MIUR (Departments of Excellence DM 11/05/2017 n. 262) to the Department of General Psychology, University of Padova. The study was performed within the framework of the LABEX CORTEX (ANR-11-LABX-0042) of Lyon University within the program "Investissements d'Avenir" (ANR-11-IDEX-0007) operated by the ANR. We thank S. Alouche, JL. Borach, S. Terrones for administrative and informatics support, A. Belle and R. Salemme for engineering support.

Funders had no role in study design, data collection and analysis, decision to publish, or preparation of the manuscript.

REFERENCES

Agostoni, E., Chinnock, J. E., Daly, M. D. B., & Murray, J. G. (1957). Functional and histological studies of the vagus nerve and its branches to the heart, lungs and abdominal viscera in the cat. *Journal of Physiological, 135*, 182–205.

Aguado, L., Serrano-Pedraza, I., Rodríguez, S., & Román, F. J. (2010). Effects of spatial frequency content on classification of face gender and expression. *The Spanish Journal of Psychology, 13*(2), 525–537.

Appelhans, B. M., & Luecken, L. J. (2006). Heart rate variability as an index of regulated emotional responding. *Review of General Psychology, 10*, 229–240.

Ardizzi, M., & Ferri, F. (2018). Interoceptive influences on peripersonal space boundary. *Cognition, 177*, 79–86.

Azzalini, D., Rebollo, I., & Tallon-Baudry, C. (2019). Visceral signals shape brain dynamics and cognition. *Trends in Cognition Science, 23*, 488–509.

Baayen, R. H., Davidson, D. J., & Bates, D. M. (2008). Mixed-effects modeling with crossed random effects for subjects and items. *Journal of Memory and Language, 59*, 390–412.

Bates, D., Mächler, M., Bolker, B., & Walker, S. (2015). Fitting linear mixed-effects models using lme4. *Journal of Statistical Software, 67*, 1–48.

Ben Hamed, S., Duhamel, J.-R., Bremmer, F., & Graf, W. (2001). Representation of the visual field in the lateral intraparietal

area of macaque monkeys: A quantitative receptive field analysis. *Experimental Brain Research, 140*, 127–144.
Benjamini, Y., & Hochberg, Y. (1995). Controlling the false Discovery rate: A practical and powerful approach to multiple testing. *Journal of the Royal Statistical Society: Series B (Methodological), 57*, 289–300.
Billman, G. E. (2013). The LF/HF ratio does not accurately measure cardiac sympatho-vagal balance. *Frontiers in Physiology, 4*, 26.
Blini, E., Desoche, C., Salemme, R., Kabil, A., Hadj-Bouziane, F., & Farnè, A. (2018a). Mind the depth: Visual perception of shapes is better in peripersonal space. *Psychological Science, 29*, 1868–1877.
Blini, E., Tilikete, C., Farnè, A., & Hadj-Bouziane, F. (2018b). Probing the role of the vestibular system in motivation and reward-based attention. *Cortex, 103*, 82–99.
Bradley, M. M., Miccoli, L., Escrig, M. A., & Lang, P. J. (2008). The pupil as a measure of emotional arousal and autonomic activation. *Psychophysiology, 45*, 602–607.
Bremmer, F., Schlack, A., Kaminiarz, A., & Hoffmann, K.-P. (2013). Encoding of movement in near extrapersonal space in primate area VIP. *Frontiers in Behavioral Neuroscience, 7*, 8.
Brozzoli, C., Gentile, G., Petkova, V. I., & Ehrsson, H. H. (2011). fMRI adaptation reveals a cortical mechanism for the coding of space near the hand. *The Journal of Neuroscience, 31*, 9023–9031.
Bryan, R., Perona, P., & Adolphs, R. (2012). Perspective distortion from interpersonal distance is an implicit visual cue for social judgments of faces. *Plos One, 7*(9), Article e45301. https://doi.org/10.1371/journal.pone.0045301
Bufacchi, R. J. (2017). Approaching threatening stimuli cause an expansion of defensive peripersonal space. *Journal of Neurophysiology, 118*, 1927–1930.
Bufacchi, R. J., & Iannetti, G. D. (2018). An action field theory of peripersonal space. *Trends in Cognition Science, 22*, 1076–1090.
Calvo, M. G., Nummenmaa, L., & Avero, P. (2010). Recognition advantage of happy faces in extrafoveal vision: Featural and affective processing. *Visual Cognition, 18*, 1274–1297.
Canzoneri, E., Magosso, E., & Serino, A. (2012). Dynamic sounds capture the boundaries of peripersonal space representation in humans. *Plos One, 7*, Article e44306.
Cartaud, A., Ruggiero, G., Ott, L., Iachini, T., & Coello, Y. (2018). A social interaction context. *Frontiers in Psychology, 9*, 657.
Chillura, A., Naro, A., Ciappina, F., Bramanti, A., Lauria, P., Bramanti, P., & Calabrò, R. S. (2018). Detecting peripersonal space: The promising role of ultrasonics. *Brain Behaviour, 8*(9), Article e01085.
Claridge-Chang, A., & Assam, P. N. (2016). Estimation statistics should replace significance testing. *Nature Methods, 13*(2), 108–109. https://doi.org/10.1038/nmeth.3729
Cléry, J., Guipponi, O., Wardak, C., & Ben Hamed, S. (2015). Neuronal bases of peripersonal and extrapersonal spaces, their plasticity and their dynamics: Knowns and unknowns. *Neuropsychologia, 70*, 313–326.
Coello, Y., Bourgeois, J., & Iachini, T. (2012). Embodied perception of reachable space: How do we manage threatening objects? *Cognitive Processing, 13*, 131–135.
Colby, C. L., Duhamel, J. R., & Goldberg, M. E. (1993). Ventral intraparietal area of the macaque: Anatomic location and visual response properties. *Journal of Neurophysiology, 69*, 902–914.
Critchley, H. D. (2002). Review: Electrodermal responses: What happens in the brain. *The Neuroscientist, 8*, 132–142.
Critchley, H. D., & Garfinkel, S. N. (2017). Interoception and emotion. *Current Opinion in Psychology, 17*, 7–14.
de Vignemont, F., & Iannetti, G. D. (2015). How many peripersonal spaces? *Neuropsychologia, 70*, 327–334.
di Pellegrino, G., & Làdavas, E. (2015). Peripersonal space in the brain. *Neuropsychologia, 66*, 126–133.
Duhamel, J.-R., Colby, C. L., & Goldberg, M. E. (1998). Ventral intraparietal area of the macaque: Congruent visual and somatic response properties. *Journal of Neurophysiology, 79*, 126–136.
Ebitz, R. B., & Moore, T. (2019). Both a gauge and a filter: Cognitive modulations of pupil size. *Frontiers in Neurology, 9*, 1190.
Fang, P., Stepniewska, I., & Kaas, J. H. (2006). The thalamic connections of motor, premotor, and prefrontal areas of cortex in a Prosimian primate (Otolemur garnetti). *Neuroscience, 143*, 987–1020.
Farnè, A., & Làdavas, E. (2000). Dynamic size-change of hand peripersonal space following tool use. *Neuroreport, 11*, 1645–1649.
Feil, M., Moser, B., & Abegg, M. (2017). The interaction of pupil response with the vergence system. *Graefes Archive for Clinical and Experimental Ophthalmology, 255*, 2247–2253.
Ferri, F., Ardizzi, M., Ambrosecchia, M., & Gallese, V. (2013). Closing the gap between the inside and the outside: Interoceptive sensitivity and social distances. *Plos One, 8*(10), Article e75758.
Ferri, F., Tajadura-Jiménez, A., Väljamäe, A., Vastano, R., & Costantini, M. (2015). Emotion-inducing approaching sounds shape the boundaries of multisensory peripersonal space. *Neuropsychologia, 70*, 468–475.
Fogassi, L., Gallese, V., di Pellegrino, G., Fadiga, L., Gentilucci, M., Luppino, G., Matelli, M., Pedotti, A., & Rizzolatti, G. (1992). Space coding by premotor cortex. *Experimental Brain Research, 89*, 686–690.
Freud, E., Culham, J., Plaut, D., & Behrmann, M. (2017). The large-scale organization of shape processing in the ventral and dorsal pathways. *eLIFE, 6*, Article e27576.
Gauthier, J., & Bouchard, S. (1993). Adaptation canadienne-française de la forme révisée du State–Trait Anxiety Inventory de Spielberger. [A French-Canadian adaptation of the revised version of Spielberger's State–Trait Anxiety Inventory.]. *Canadian Journal of Behavioural Science/Revue canadienne des sciences du comportement, 25*, 559–578.
Gelman, A., Hill, J., & Yajima, M. (2012). Why we (usually) don't have to worry about multiple comparisons. *Journal of Research on Educational Effectiveness, 5*, 189–211.
Gerbella, M., Baccarini, M., Borra, E., Rozzi, S., & Luppino, G. (2014). Amygdalar connections of the macaque areas 45A and 45B. *Brain Structure & Function, 219*, 831–842.
Gigliotti, M. F., Soares Coelho, P., Coutinho, J., & Coello, Y. (2019). Peripersonal space in social context is modulated by action reward, but differently in males and females. *Psychological Research, 85*(1), 181–194.
Goeleven, E., De Raedt, R., Leyman, L., & Verschuere, B. (2008). The Karolinska directed emotional faces: A validation study. *Cognition & Emotion, 22*, 1094–1118.
Gordan, R., Gwathmey, J. K., & Xie, L.-H. (2015). Autonomic and endocrine control of cardiovascular function. *World Journal of Cardiology, 7*, 204–214.
Graziano, M. S. A., & Cooke, D. F. (2006). Parieto-frontal interactions, personal space, and defensive behavior. *Neuropsychologia, 44*, 845–859.
Graziano, M. S. A., Hu, X. T., & Gross, C. G. (1997). Visuospatial properties of ventral premotor cortex. *Journal of Neurophysiology, 77*, 2268–2292.
Hayes, T. R., & Petrov, A. A. (2016). Mapping and correcting the influence of gaze position on pupil size measurements. *Behavior Research Methods, 48*(2), 510–527. https://doi.org/10.3758/s13428-015-0588-x
Heed, T., Habets, B., Sebanz, N., & Knoblich, G. (2010). Others' actions reduce crossmodal integration in peripersonal space. *Current Biology, 20*(15), 1345–1349.

Hess, U., Adams, R. B., Grammer, K., & Kleck, R. E. (2009). Face gender and emotion expression: Are angry women more like men? *Journal of Vision, 9*, 19.1–19.8.
Hunley, S. B., Marker, A. M., & Lourenco, S. F. (2017). Individual differences in the flexibility of peripersonal space. *Experimental Psychology, 64*, 49–55.
Iachini, T., Coello, Y., Frassinetti, F., & Ruggiero, G. (2014). Body space in social interactions: A comparison of reaching and comfort distance in immersive virtual reality. *Plos One, 9*(11), Article e111511.
Iachini, T., Coello, Y., Frassinetti, F., Senese, V. P., Galante, F., & Ruggiero, G. (2016). Peripersonal and interpersonal space in virtual and real environments: Effects of gender and age. *Journal of Environment Psychological, 45*, 154–164.
Iachini, T., Ruggiero, G., Ruotolo, F., di Cola, A. S., & Senese, V. P. (2015). The influence of anxiety and personality factors on comfort and reachability space: A correlational study. *Cognitive Processing, 16*, 255–258.
Jaeger, T. F. (2008). Categorical data analysis: Away from ANOVAs (transformation or not) and towards logit mixed models. *Journal of Memory and Language, 59*(4), 434–446.
Kasthurirangan, S., & Glasser, A. (2005). Characteristics of pupil responses during far-to-near and near-to-far accommodation. *Ophthalmic & Physiological Optics, 25*, 328–339.
Kreibig, S. D. (2010). Autonomic nervous system activity in emotion: A review. *Biological Psychology, 84*, 394–421.
Lenth, R. V. (2016). Least-squares means: The R package lsmeans. *Journal of Statistical Software, 69*, 1–33.
Libby, W. L., Lacey, B. C., & Lacey, J. I. (1973). Pupillary and cardiac activity during visual attention. *Psychophysiology, 10*, 270–294.
Liebowitz, M. R. (1987). Social phobia. *Modern Problems Pharmacopsychiatry, 22*, 141–173.
Logan, A. J., Gordon, G. E., & Loffler, G. (2017). Contributions of individual face features to face discrimination. *Vision Research, 137*, 29–39.
Lourenco, S. F., Longo, M. R., & Pathman, T. (2011). Near space and its relation to claustrophobic fear. *Cognition, 119*, 448–453.
Maister, L., Cardini, F., Zamariola, G., Serino, A., & Tsakiris, M. (2015). Your place or mine: Shared sensory experiences elicit a remapping of peripersonal space. *Neuropsychologia, 70*, 455–461.
Makin, T. R., Holmes, N. P., & Zohary, E. (2007). Is that near my hand? Multisensory representation of peripersonal space in human intraparietal sulcus. *The Journal of Neuroscience, 27*, 731–740.
Maravita, A., & Iriki, A. (2004). Tools for the body (schema). *Trends Cognition Science, 8*, 79–86.
Mathôt, S., Schreij, D., & Theeuwes, J. (2012). OpenSesame: An open-source, graphical experiment builder for the social sciences. *Behavior Research Methods, 44*, 314–324.
Meyer, C., Padmala, S., & Pessoa, L. (2019). Dynamic threat processing. *Journal of Cognition Neuroscience, 31*, 522–542.
Nag, S., Berman, D., & Golomb, J. (2019). Category-selective areas in human visual cortex exhibit preferences for stimulus depth. *Neuroimage, 196*, 289–301.
O'Connor, D. A., Meade, B., Carter, O., Rossiter, S., & Hester, R. (2014). Behavioral sensitivity to reward is reduced for far objects. *Psychological Science, 25*, 271–277.
Pagani, M., Lombardi, F., Guzzetti, S., Rimoldi, O., Furlan, R., Pizzinelli, P., Sandrone, G., Malfatto, G., Dell'Orto, S., & Piccaluga, E. (1986). Power spectral analysis of heart rate and arterial pressure variabilities as a marker of sympatho-vagal interaction in man and conscious dog. *Circulation Research, 59*, 178–193.
Pagani, M., Lombardi, F., Guzzetti, S., Sandrone, G., Rimoldi, O., Malfatto, G., Cerutti, S., & Malliani, A. (1984). Power spectral density of heart rate variability as an index of sympatho-vagal interaction in normal and hypertensive subjects. *Journal of Hypertension. Supplement: Official Journal of the International Society of Hypertension, 2*, S383–S385.
Pellencin, E., Paladino, M. P., Herbelin, B., & Serino, A. (2017). Social perception of others shapes one's own multisensory peripersonal space. *Cortex, 104*, 163–179.
Perona, P. (2007). A new perspective on portraiture. *Journal of Vision, 7*(9). https://doi.org/10.1167/7.9.992, 992-992.
Radomsky, A. S., Ashbaugh, A. R., Saxe, M. L., Ouimet, A. J., Golden, E. R., Lavoie, S. L., & O'Connor, K. P. (2006). Psychometric properties of the French and English versions of the social phobia inventory. *Canadian Journal of Behavioural Science/Revue canadienne des sciences du comportement, 38*, 354–360.
Radomsky, A. S., Rachman, S., Thordarson, D. S., McIsaac, H. K., & Teachman, B. A. (2001). The claustrophobia questionnaire. *Journal of Anxiety Disorders, 15*, 287–297.
Rizzolatti, G., Scandolara, C., Matelli, M., & Gentilucci, M. (1981). Afferent properties of periarcuate neurons in macaque monkeys. II. Visual responses. *Behavioural Brain Research, 2*, 147–163.
Rossetti, A., Romano, D., Bolognini, N., & Maravita, A. (2015). Dynamic expansion of alert responses to incoming painful stimuli following tool use. *Neuropsychologia, 70*, 486–494.
Rotshtein, P., Schofield, A., Funes, M. J., & Humphreys, G. W. (2010). Effects of spatial frequency bands on perceptual decision: It is not the stimuli but the comparison. *Journal of Vision, 10*(10), 25.
Ruggiero, G., Frassinetti, F., Coello, Y., Rapuano, M., di Cola, A. S., & Iachini, T. (2016). The effect of facial expressions on peripersonal and interpersonal spaces. *Psychological Research*, 1–9.
Ruggiero, G., Frassinetti, F., Coello, Y., Rapuano, M., di Cola, A. S., & Iachini, T. (2017). The effect of facial expressions on peripersonal and interpersonal spaces. *Psychological Research, 81*, 1232–1240.
Sambo, C. F., & Iannetti, G. D. (2013). Better safe than sorry? The safety margin surrounding the body is increased by anxiety. *The Journal of Neuroscience, 33*, 14225–14230.
Schurgin, M. W., Nelson, J., Iida, S., Ohira, H., Chiao, J. Y., & Franconeri. (2014). Eye movements during emotion recognition in faces. *Journal of vision, 18*(13), 14. https://doi.org/10.1167/14.13.14, 14.
Sereno, M. I., & Huang, R.-S. (2006). A human parietal face area contains aligned head-centered visual and tactile maps. *Nature Neuroscience, 9*, 1337–1343.
Serino, A., Bassolino, M., Farnè, A., & Làdavas, E. (2007). Extended multisensory space in blind cane users. *Psychological Science, 18*(7), 642–648.
Shaffer, F., & Ginsberg, J. P. (2017). An overview of heart rate variability metrics and norms. *Frontiers Public Health, 5*, 258.
Smith, F. W., & Schyns, P. G. (2009). Smile through your fear and sadness: Transmitting and identifying facial expression signals over a range of viewing distances. *Psychological Science, 20*(10), 1202–1208.
Spaccasassi, C., Romano, D., & Maravita, A. (2019). Everything is worth when it is close to my body: How spatial proximity and stimulus valence affect visuo-tactile integration. *Acta Psychol. (Amst.), 192*, 42–51.
Spielberger, C. D., & Sydeman, S. J. (1994). State-trait anxiety inventory and state-trait anger expression inventory. In *The use of psychological testing for treatment planning and outcome assessment* (pp. 292–321). Hillsdale, NJ, US: Lawrence Erlbaum Associates, Inc.
Steinhauer, S. R., Siegle, G. J., Condray, R., & Plessa, M. (2004). Sympathetic and parasympathetic innervation of pupillary dilation during sustained processing. *International Journal of Psychophysiology*, 77–86.
Teneggi, C., Canzoneri, E., di Pellegrino, G., & Serino, A. (2013). Social modulation of peripersonal space boundaries. *Current Biology, 23*, 406–411.

Thayer, J. F., & Sternberg, E. M. (2009). Neural concomitants of immunity—focus on the vagus nerve. *Neuroimage, 47*, 908–910.
Van den Brink, R. L., Murphy, P. R., & Nieuwenhuis, S. (2016). Pupil diameter tracks lapses of attention. *Plos One, 11*, Article e0165274.
Verhoff, M. A., Witzel, C., Kreutz, K., & Ramsthaler, F. (2008). The ideal subject distance for passport pictures. *Forensic Science International, 178*(2–3), 153–156. https://doi.org/10.1016/j.forsciint.2008.03.011
Wingenbach, T. S. H., Ashwin, C., & Brosnan, M. (2018). Sex differences in facial emotion recognition across varying expression intensity levels from videos. *Plos One, 13*.
Ziegler, M. G. (2004). 50 - psychological stress and the autonomic nervous system. In D. Robertson, I. Biaggioni, G. Burnstock, & P. A. Low (Eds.), *Primer on the autonomic nervous system* (2nd ed., pp. 189–190). San Diego: Academic Press.

ETUDE 4

Les informations sociales et non sociales présentées dans l'espace péri-personnel recrutent-elles un réseau neuronal fronto-pariétal commun?

Social and non-social information in peripersonal space recruit a similar fronto-parietal neural network

Audrey Dureux, Clément Desoche, Roméo Salemme, Alessandro Farnè and Fadila Hadj-Bouziane

Article en préparation

Social and non-social information presented in peripersonal space recruit a similar fronto-parietal neural network

Audrey Dureux[1,2], Clément Desoche[2,4], Roméo Salemme, Alessandro Farnè[1,2,4,5] and Fadila Hadj-Bouziane[1,2]

1. Integrative Multisensory Perception Action & Cognition Team - ImpAct, INSERM U1028, CNRS UMR5292, Lyon Neuroscience Research Center (CRNL), Lyon, France
2. University UCBL Lyon 1, University of Lyon, Lyon, France
3. Hospices Civils de Lyon, Neuro-Immersion & Mouvement et Handicap, Lyon, France
4. Center for Mind/Brain Sciences (CIMeC), University of Trento, Italy.

Corresponding authors:
Audrey Dureux and Fadila Hadj-Bouziane, INSERM U1028, CNRS UMR5292, Lyon Neuroscience Research Center, ImpAct Team, 16 Avenue Doyen Lépine 69500 Bron, France.
Emails: audrey.dureux@gmail.com ; fadila.hadj-bouziane@inserm.fr.

Conflict of Interest: The authors declare that they have no conflict of interest.
Acknowledgements: This work was funded by the French National Research Agency ANR-15-GE37-0003 grant MySpace to FHB.

Funders had no role in study design, data collection and analysis, decision to publish, or preparation of the manuscript.

Abstract

Although it is now well established that the representation of peripersonal space (PPS), defined as the region of space close to the body, plays a role in everyday life social interactions, the neural markers underpinning the PPS representation has mostly been identified for non-social physical interactions implying a parietal-premotor network. PPS representation in social situations remains poorly understood with a still open question that is if this representation of space in our brain is different according to the social or non-social context.

Here, we used a strereoscopic virtual reality ecological task to characterize brain correlates of PPS for social category (i.e., human faces) and depending on the emotional content and to compare neural signatures between social and non-social category (i.e., geometrical shapes).

We identified a common occipital-parietal-premotor network implied in the processing of social and non-social information presented in close space although we pointed out a more extended network to process social stimuli, recruiting also additional brain regions in temporal and limbic areas. We further uncovered that happy faces in close space stand out as, it also recruiting brain regions playing a role in the perception of bodily reactions, such as the insular cortex, suggesting that connections between these structures and the central PPS network would be necessary to process emotional and salient social stimuli.

These findings bring important new insights into the neural substrate of PPS in social context and the direct comparison of social and non-social PPS representation using for the first time an ecological dimension with virtual reality.

1. Introduction

Facing a happy or angry person triggers different behavioral and physiological responses. This is subserved by a special and complex brain machinery dedicated to face processing (Ghuman et al., 2014; Grill-Spector et al., 2017; Haxby et al., 2000; O'Toole et al., 2002). Importantly, our behavioral and physiological responses depend on the situation at hand and in particular on the physical proximity with this person. When physically close, our behavioral and physiological responses are typically enhanced and this is related to the way we perceive the space around us. It is thought that these enhanced responses are under the influence of the peripersonal space (PPS) network, a set of regions within the parietal and premotor cortex (see Grivaz et al., 2017 for review), that encodes the space close to the body to facilitate the interactions with objects of our environment. Accumulating evidence has recently shown that various factors related to the social factors within PPS, such as their valence, come into play and affect behavioral and physiological responses (Bogdanova et al., 2021; Cartaud et al., 2018; Dureux et al., 2021; Pellencin et al., 2018; Ruggiero et al., 2017).

To date, the neural markers of the social influence on PPS network remain poorly understood. Only few studies have attempted to investigate this issue (Holt et al., 2014, 2015; Schienle et al., 2016; Vieira et al., 2017, 2020). These studies compared the fMRI responses to looming faces (Holt et al., 2014, 2015; Schienle et al., 2016; Vieira et al., 2017, 2020) or non-social stimuli such as objects (Holt et al., 2014; Vieira et al., 2020). They found greater responses to approaching versus withdrawing faces in the PPS network as well as in subcortical brain regions. These activations were also elicited by non-social biological stimuli (Vieira et al., 2020) but not by non-social objects stimuli (Holt et al., 2014) suggesting that those structures might be sensitive specifically to the intrusions of conspecifics or non-human biological organisms. This is at odds with several studies reporting a preferential activation within the PPS network for objects presented close versus far from the participants (see Grivaz et al., 2017 for review). Therefore, there seems to be mixed evidence as to whether regions potentially coding for proximity of visual stimuli could be similar for social and non-social content.

In this study, we characterized neural signatures of PPS representation for social category (emotional faces), and we compared if these brain regions could be similarly recruited by non-social category (objects). We adapted the immersive virtual reality (VR) task from Dureux et al. (2021) to the fMRI environment. We presented virtual emotional faces close (30

cm, in PPS) versus far (300 cm, outside PPS) from the participants. This task implied similar perceptual and oculomotor depth cues for both categories of stimuli. We first identified the brain network subserving PPS processing for the social category. Second, we directly compared the neural responses to the processing of social stimuli and non-social stimuli in PPS. Finally, we aimed at determining the influence of facial emotional expressions (happy, neutral, or angry) onto the PPS network. Distance and emotion were irrelevant to the task as participants had to discriminate either the face gender (male / female) or the object shape (cube / sphere).

We predicted that a central frontoparietal network would be recruited by close stimuli, in particular in premotor (PMd, PMv) and parietal areas (superior parietal lobule, IPS, SMG, somatosensory cortex) and that this network would be similarly recruited by social and non-social stimuli. In addition, we predicted a selective interplay between the face network (including the occipital face area (OFA) and the fusiform face area (FFA) (Haxby et al., 2000)) and the PPS network.

2. Method

2.1. Participants

In total, 20 healthy volunteers were recruited through web advertising to participate in the study (8 Females, 12 Males, mean Age = 26 years old). All participants were right-handed, their vision was normal or corrected to normal (through contact lenses) and none had history of neurologic or psychiatric disorders. All gave written informed consent and were paid for their participation. The study followed the Declaration of Helsinki standards and was approved by the Institut National de la Santé et de la Recherche Médicale (INSERM) Ethics Committee (SUD EST IV, ID RCB: 2010-A01180-39).

2.2. Apparatus

In the experiment, visual stimuli were presented in a virtual reality environment. The scene was rendered in a screen allowing passive 3D projections with polarized light (ST-Pro-X, screen-tech) through a 3D projector (Vpixx, screen-tech). As the projector has a circular polarization, a polarizer needs to be placed from 20 and 50 mm in front of the projector lens. The projector has a resolution of 1920 x 850 and a frequency of 120 Hz. During the scanning sessions, participants were lying down comfortably on the scanner bed and foam padding was

used around their head and knees. A 64-channel head coil was positioned around their head and stimuli were visualized through a mirror system attached to the scanner head coil. A first-surface-mirror was used in order to avoid reflections on it by the 3D image (ST-GS mirror passive 3D ready, Screen-tech). Participants were equipped with passive paper glasses in order to visualize the 3D image (ST-3D-Glasses, screen-tech). Participants were also wearing passive 3D glasses to visualize the virtual environment through the mirror attached to the head coil.
The augmented technology Unity software (Version 5.1.2; Unity Technologies, San Francisco, CA) was used to create the 3D and 2D environment, display the stimuli and record participants' responses. The environment consisted of a graphical depiction rendering the inside, tubular space of the MRI in order to create a full immersion of the participants. The environment was presented in stereoscopic virtual reality with cues allowing a realistic depth perception (see **Figure 1**). Visual stimuli were presented in the virtual environment at two different positions from the observed: 30 cm, close and 300 cm, far. A further rendering included a cross, which was used as a fixation point across all trials. The position of the cross was midway between close and distant stimuli (175 cm).
Participants provided responses using the index and middle fingers of the right hand by pressing left and right buttons of a response box (PKG-904, Current Design) installed in the scanner.

2.3. Stimuli

Social stimuli (human faces) were pictures of female and male faces displaying three emotions (happy, neutral and angry). Pictures were taken from the Karolinska Directed Emotional Faces database (KDEF, Goeleven et al., 2008) and further processed: stimuli were cropped to an oval shape, to remove outline and external features (e.g., hairs); images were corrected for luminance, such that the mean luminance did not differ across sex of the faces. Finally, faces were transformed into a 3D rendering with the AI-powered 3D avatars software (https://itseez3D.com). A total of 20 (10 females and 10 males) were used. Non- social stimuli were colored 3D geometrical shapes (cubes and spheres) created with the Unity software. The retinal size of the stimuli (≈14° of visual angle) was kept constant across distances and type of stimuli, resulting in the more distant stimuli being perceived larger. This was implemented in the Unity software by scaling up the far stimuli based on the size and distance of the close one (see Dureux et al., 2021).

2.4. Procedure: fMRI discrimination task for social and non-social stimuli

Participants practiced the task before entering the scanner. This practice phase was performed on a computer through the OpenSesame software (http://osdoc.cogsci.nl/).

Trials started with a white fixation cross, presented in the center of the visual field. The subject was instructed to maintain the fixation during the presentation of the cross. After 1000 ms, the cross was followed by the presentation of one social (or non-social, by block) stimuli randomly chosen among the category (male/female or cube/sphere) and the distance of presentation or the part of the environment (see above). For social stimuli, the identity was also randomly chosen (10 levels for each sex). Stimuli were presented for 1000 ms and subjects had up to 750 ms to respond. A feedback text was then presented for 1000 ms followed by a intertrial jitter from 4 to 6 sec consisting of the white fixation cross. The feedback reported whether a response was correct, incorrect, too slow (> 750 ms), or too fast (< 100 ms), as to encourage compliance with task instructions and induce time-pressure. Participants were instructed to report the sex of presented faces or the shape of the presented objects by pressing buttons on a response box with their index and middle fingers.

Participants completed 5 functional runs with a total of 120 trials for each emotional face (happy, neutral, and angry) and 60 trials for objects. To minimize the cost associated with switching between categories, trials of faces and objects were blocked within each run. Every 60 trials, a fixation cross was presented during 20 sec to allow a little rest of the subject. The order of stimuli was randomized across participants.

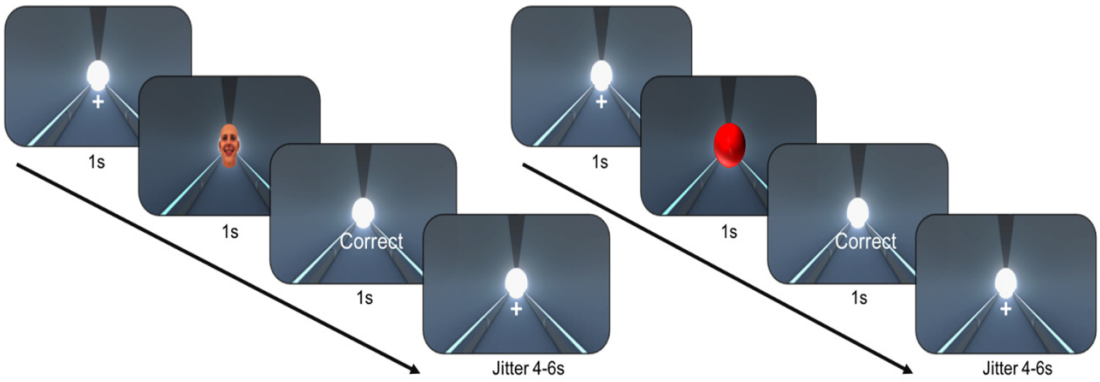

Figure 1. Trial structure of the experiment. On each trial, participants viewed a fixation cross (1000 ms), followed by the presentation of stimuli (1000 ms) which can be social (a face) or non-social (a geometrical shape). The participant needs to discriminate between the sex or type of shape during the presentation of the stimuli (750 ms of limited response time). Then feedback of the response given by the participant appeared (1000 ms). The trial ended by a jittered fixation cross (4000-6000 ms).

2.5. fMRI data acquisition

Neuroimaging data were collected using a 3T Siemens Magnetom Prisma scanner. An anatomical MRI was collected for each participant at the beginning of the experiment using a T1- weighted MPRAGE 3D (voxel size = 1x1x1 mm; 192 slices, TR = 3000 ms, TE = 3.34 ms, TI = 1100 ms, flip angle = 8°, matrix: 224 x 256). Functional images were taken with an echo-planar BOLD-sensitive T2*-weighted imaging sequence with whole-brain coverage while participants performed the task. For each fMRI volume, 40 slices covering the whole brain were collected in an ascending order (TR = 2200 ms, TE = 29 ms, flip angle = 90°, FOV = 546 x 546mm, matrix size = 78 x 78, voxel size = 2.7 mm^3).

2.6. fMRI data preprocessing

fMRI data were preprocessed using SPM12 software (Wellcome Department of Cognitive Neurology). Functional images were realigned to correct for head movements and underwent slice timing correction. The anatomic and functional volumes were then coregistered with the high-resolution structural scan from each individual participant and normalized to the Montreal Neurological Institute (MNI) standard brain space. The anatomical images were segmented into white matter, gray matter, and CSF partitions and normalized to the MNI space. Spatial smoothing was then applied to the functional images using a Gaussian kernel with an isotropic

FWHM of 8 mm only for the univariate analysis. A high-pass filter (128 s) was also applied to the time series.

2.7. Statistical analysis

Behavioral data

The results of the discrimination task were analyzed with mixed-effects multiple regression models (Baayen et al., 2008), with the open-source software R (The R Core Team, 2013) using the lme4 package (Bates et al., 2015). We analyzed accuracy and response times (RTs), in which both an accurate and timely response (>100 msec and <750 msec) was provided. We used Linear Mixed Effects Models (LMEM) because they allow to specify random effects appropriately to our design (Jaeger, 2008), similar to that of our previous study, where we tested performance (accuracy and RTs) during a male/female discrimination task with a virtual reality headset and 2D faces (Dureux et al., 2021). For each accuracy and RTs results, we used an objective pipeline exposed in our last study (Dureux et al., 2021). As a first step, we defined a model containing the most appropriate random effects, the simplest starting model including the random intercept for Subject. We then tested the random intercept for Runs as well as the random intercept for Identity item and random slopes one by one. Procedure for testing fixed effects were also identical to our previous approaches (see Blini et al., 2018 and Dureux et al., 2021 for more details). When considered social trials, we tested the role of the following three factors as fixed effect: Distance, Emotion (3 levels: Happy, Neutral, Angry) and Picture sex (2 levels: Male image, Female image) whereas when considered non-social trials we tested only the Distance as fixed effect

All post-hoc analyses for significant tests were computed on the basis of least-squares means (Lenth, 2016), using False Discovery Rate (FDR; Benjamini & Hochberg, 1995) correction for multiple tests.

fMRI data: Whole-brain univariate analysis

First-level analysis were performed on preprocessed data, by defining a general linear regression model to the data. For each correct trial (i.e., in which both an accurate and timely response (>100 ms and <750 ms) was provided), events of interest were modeled, corresponding to the 1 sec presentation of the stimuli. Events were modeled as a function of the Category (social or non-social stimuli), Emotion (happy, neutral or angry) and Distance (close

or far) of stimuli presented, resulting in 8 predictors of interest per run modeled with the standard SPM12 hemodynamic response function. In addition, 6 regressors of non-interest (3 rotations and 3 translations) were also included in the model, corresponding to the head movement parameters estimated during realignment. Events corresponding to the presentation of stimuli with a wrong or too slow response were also modeled in a regressor "errors" as predictor of no interest. We then performed a second-level analysis by entering these contrasts from all subjects into a random effect group analysis.

We adopted a cluster-forming threshold of $p< 0.001$ uncorrected, and then a False Discovery Rate (FDR)-corrected $p< 0.05$ at the cluster-level to minimize Type I errors in the analyses by controlling for multiple comparisons as implemented in SPM12.

In each significant cluster, the coordinates for each peak of activation in human brain regions were reported in the MNI space as well as the t value associated. We used AAL3 atlas (Rolls et al., 2020) to define anatomical location and also the most recent multi-modal cortical parcellation atlas including both anatomical and functional criterion (Glasser et al., 2016).

To identify brain regions implicated in the PPS processing of social cues, we examined the clusters displaying a main effect of distance in each of the social and non-social category by identifying brain regions responding preferentially to close (close social > far social and close non-social stimuli > far non-social stimuli) or Far (Far social > Close social) stimuli (results in supplementary material). We also performed similar contrasts for each emotion (close happy > far happy, close neutral > far neutral, close angry > far angry, and inversely for far).

fMRI data: Multivariate analysis (MVPA) searchlight whole-brain classification

Multi-voxel pattern analysis (MVPA) was conducted to test whether processing of distance could be decoded from multi-voxel patterns of activity, and to test the similarity of the distance decoding pattern of PPS according to the category (social vs. non-social) and the emotion presented (happy vs. neutral vs. angry). Classification analyses were conducted with a whole-brain searchlight across close and far conditions to identify the brain pattern to decode the distance effect (close vs. far) (1) for social category, (2) commonly for social and non-social category (3) commonly for the emotional content of the social category (happy, neutral and angry). For each participant, we estimated a GLM on unsmoothed data modelling each experimental condition. As for the univariate GLM convolved with the hemodynamic response function in SPM12, the same eight regressors were used consisting to a total of 40 regressors

of interest corresponding to 8 conditions x 5 runs, originating from the 4 types of stimuli (faces happy, faces neutral, faces angry and objects) x 2 distances (close, var) x 5 runs. We also modelled the six movement parameters and errors as non-interest regressors.
MVPA searchlight analysis was performed using COSMoMVPA toolbox (Oosterhof et al., 2016, http://www.cosmomvpa.org/). We performed a whole brain searchlight on beta maps for each condition for each subject to map the classification accuracy of distance effect (i.e., close vs. far) by centering a spherical neighbourhood including the 100 voxels nearest to the center voxel at each voxel of the subject-specific whole-brain mask. We adopted a Linear Discriminant Analysis (LDA) classifier. Decoding accuracy was estimated with a leave-one-run-out cross-validation approach. For each participant, the classifier was trained on 4 runs to distinguish between the two distances, close and far, and tested on the remaining 5th run, considering all the possible combinations (results were averaged across different folds of training and test dataset assignments).

First, in order to decode the distance effect of the social category, we trained and tested the classifier on the pairwise comparison of close vs. far faces pattern (see Figure 2a). Second, in order to determine if a pattern of decoding of distance could be similar for social and non-social stimuli, we adopted cross-decoding. We trained the classifier on the pairwise comparison between close vs. far for social stimuli (faces) and then tested the classifier on the same comparison but for the non-social stimuli (objects). This procedure was performed in both directions. Then, we calculated the average of the two decoding maps (see Figure 2b). Third, in order to determine the pattern of decoding of distance similarly to the three emotions depicted by the faces, we trained the classifier on the pairwise comparison between close vs. far for two emotions and then tested the classifier on the same comparison for the remaining emotion, for each possible combination. Then, we calculated the average of the three decoding maps (see Figure 2c). In the two latter analyses we balanced partitions in order that numbers of conditions occur equally in each training and test runs with the cosmo_balance_partitions function.

This first step yielded one map representing the classification accuracy score per subject. Chance level (50%) was then subtracted from these maps, which were then smoothed with a 6-mm Gaussian smoothing kernel (for the purpose of statistical inference) before being analyzed at group level using a one-sample non-parametric permutation test (Nichols & Holmes, 2002) implemented in the Statistical non-Parametric Mapping toolbox (SnPM13;

https://warwick.ac.uk/fac/sci/statistics/staff/academic-research/nichols/software/snpm31). In this procedure, we assessed in which regions classification accuracy was significantly higher than chance with the generation of a null distribution of voxel-wise pattern distinctness across multiple iterations by using a sign-permutation test. This test consists of randomly swapping the sign (positive or negative after subtracting chance, 50%) of the decoding results for each subject and voxel to obtain a null distribution of voxel-wise pattern distinctness across multiple iterations. The correct accuracy value obtained by adding all participant values is then compared to the distribution. We ran 10,000 iterations. This analysis resulted in a group-level map of distance-responsive voxels showing significant results above-chance, cluster-wise thresholded at $p < 0.05$ (FWE corrected). XJview (http://www.alivelearn.net/xjview/) was used to visually inspect the results and to derive the significant cluster information. Location of significant brain regions were identified by using AAL3 atlas (Rolls et al., 2020) to define anatomical location and also the most recent multi-modal cortical parcellation atlas including both anatomical and functional criterion (Glasser et al., 2016).

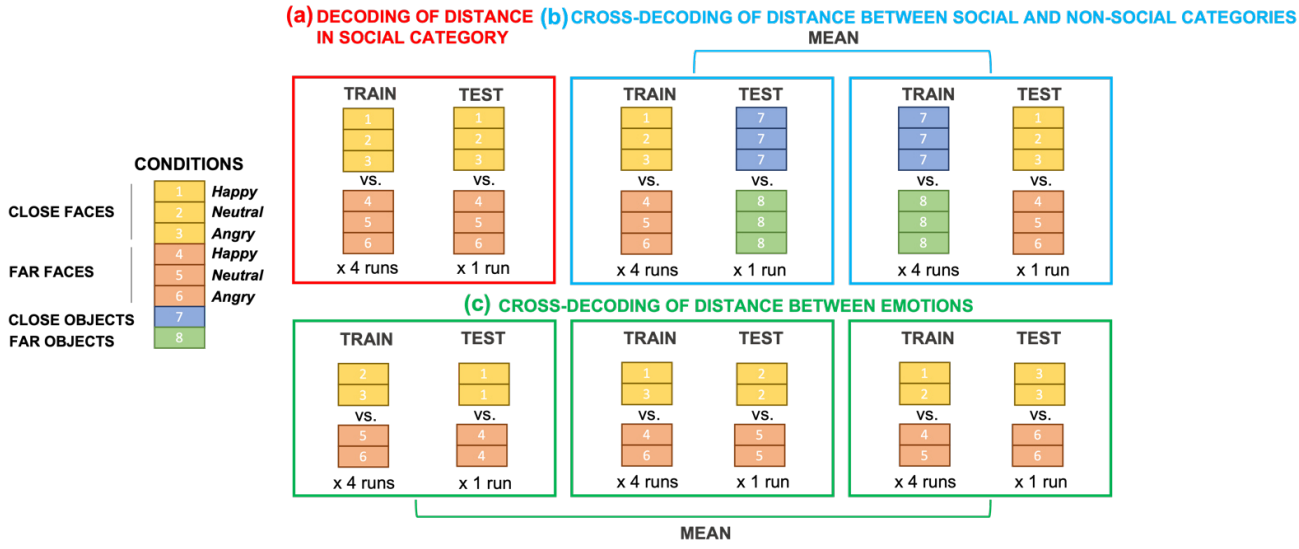

Figure 2. Schema of details analysis for MVPA searchlight classification. Cross-validation approach. Each experimental run comprised 8 conditions, 4 for close condition and 4 for far condition separated in social and non-social content. Decoding accuracy was estimated with a leave-one-run-out cross-validation approach. We trained the classifier on condition of 4 runs and then tested the classifier on the condition of the remaining run. **(a)** Decoding of distance across social stimuli: pairwise comparison of close vs. far. The classifier was trained on a specific pairwise comparison (social close conditions vs. social far conditions) of 4 runs and tested on the same pairwise comparison on the remaining run. **(b)** Cross-modality decoding of distance between social and non-social stimuli. We trained the classifier on a specific pairwise comparison (close vs. far for social stimuli) and tested the

classifier on other pairwise comparisons (close vs. far for non-social stimuli). Then, we performed the same analysis but permuting the conditions adopted for training and testing the classifier. Finally, we averaged the decoding accuracy maps of these two decoding combinations. **(c)** Cross-modality decoding of distance between the emotions depicted by face stimuli. Classifier was trained on the pairwise comparison of distance for two emotions and then tested on the same pairwise comparison for the remaining emotion (e.g., training on close vs. far for happy and neutral emotions and testing on close vs. far for angry emotion). Then, we performed the same analysis permuting the emotions adopted for training and testing the classifier. We then average the decoding accuracy maps of these three decoding combinations. For **(b)** and **(c)** classification analysis, as the number of conditions was unequal between the training and the testing (i.e. three conditions of social stimuli vs. one condition of non-social stimuli (b) and two emotions vs. one (c)), we balanced our design in order that conditions occur equally in each training and test run.

3. Results

3.1. Behavioral results

Accuracy. For the social category analysis, considering only social trials, accuracy was modulated by Distance (χ^2 (1) = 8.16, p= 0.004), far faces being discriminated better than close faces (|z|= 2.873, pfdr= 0.004). Accuracy was also modulated by emotion (χ^2 (2) = 16.79, p < 0.001) with better discrimination for happy faces than both neutral (|z| = 3.91, pfdr < 0.001) and angry ones (|z|= 3.06, pfdr=0.003), whereas the latter two did not differ (|z| = 0.93, pfdr = 0.35). Three two-way interactions where also significant: Distance by Emotion (χ^2 (2) = 8.23, p = 0.02); Distance by Picture sex (χ^2 (1) = 88.74, p < 0.001) and Emotion by Picture sex (χ^2 (2) = 109.89, p < 0.001). The discrimination of angry faces improved when images were presented far with respect to close (|z| = 3.55, pfdr < 0.001). The same pattern was observed for male faces with better discrimination for male faces when images were presented far with respect to close (|z| = 8.78, pfdr < 0.001), the patter being reversed for female faces (|z| = 4.43, pfdr < 0.001). Happy female faces were discriminated more accurately compared to both neutral and angry female faces (all |z| > 3.16, pfdr < 0.001) while Neutral male faces were better discriminated compared to happy and angry (|z| = 3.82, pfdr < 0.001). For the non-social category analysis, considering only non-social trials, accuracy was not modulated by Distance (χ^2 (1) = 0.24, p= 0.62).

Reaction times. In the social category analysis, the selected matrix included random intercepts for Subject, Runs and the Identity of faces with Distance as random slope for each of

these random intercepts. RTs was not modulated by Distance (χ^2 (1) = 2.55, p = 0.11), however Emotion did modulate RTs (χ^2 (2) = 18.64, p < 0.001), with faster RTs for discriminating happy faces compared to neutral ones (|z| = 4.57, pfdr < 0.001). Angry faces were also discriminated faster than neutral ones (|z| = 3.19, pfdr = 0.002). Moreover, two two-way interactions were significant: Distance by Picture sex (χ^2 (1) = 64.50, p < 0.001) and Emotion by Picture sex (χ^2 (2) = 134.94, p < 0.001). The first interaction refers to female faces being discriminated faster than male ones when presented close (|z| = 6.64, pfdr < 0.001) but not far, males being, on the contrary, discriminated faster when presented far (|z| = 4.69, pfdr < 0.001). The second indicates that female faces were discriminated faster when displaying happy (|z| = 10.11, pfdr < 0.001) or angry expressions (|z| = 9.58, pfdr < 0.001) with respect to neutral, whereas male faces were discriminated faster if displaying neutral expressions compared to happy (|z| = 3.72, pfdr < 0.001) and angry (|z| = 5.22, pfdr < 0.001).

For the non-social category analysis, no random slope was selected for the random intercept of Subject and Block. In this analysis, we didn't find a modulation of RTs by Distance (χ^2 (1) = 1.13, p = 0.29).

3.2. fMRI results

An extended neural network related to distance processing of social category

We extracted decoding accuracy for the pairwise comparison between close and far social stimuli for each subject, and we tested for significance at the group level (p < 0.05 FWE-corrected at cluster-level). Significant pattern distinctness was observed in a set of uni- and bilateral cortical regions (Figure 3A, Table 1). We found significant distinct activity patterns in one cluster made up of regions in the occipital cortex including the bilateral inferior, middle and superior occipital gyrus, the bilateral cuneus, the bilateral lingual gyrus, the bilateral calcarine sulcus mainly corresponding to visual areas (V1, V2, V3, V3A, V3B, V4, V6) and parieto-occipital sulcus area extending to V6A area. This cluster also contained regions in the temporal cortex, with significant decoding accuracy in bilateral middle temporal gyrus, in particular in the medial superior temporal area (MST), the middle temporal area (MT), the area FST and the temporo-parieto-occipital junction (TPOJ), and also in bilateral fusiform gyrus mostly in the fusiform face area (FFA), in the ventral visual complex (VVC) and in the ventromedial visual area (VMV). In addition, we found significant clusters including brain regions in parietal and frontal cortices. Brain regions in parietal cortex were situated in the

bilateral precuneus (lateral and medial area 7P), in the bilateral angular gyrus (area 5L), in the bilateral superior parietal lobule (SPL), along the intraparietal sulcus (IPS) including the right lateral intraparietal ventral and dorsal area (LIPv, LIPd), the left LIPv, the right and left medial intraparietal area (MIP), and the left ventral intraparietal area (VIP), and in the bilateral inferior parietal lobule (IPL) including the areas PFm and 7PC. Bilateral activations in the postcentral gyrus were also identified mostly in the primary somatosensory cortex (area 2 of SI) and also in the right primary sensory cortex (area 3b). Frontal cortex contained strong activations in the precentral gyrus, along the bilateral premotor dorsal and ventral pathways (PMv and PMd), as well as in the left primary motor cortex (M1) and in a region around the intersection of the middle frontal gyrus with the precentral gyrus, the bilateral frontal eye field area (FEF) also bounding the area 55b.

Finally, significant pattern distinctness of distance was also found in subcortical areas as the bilateral cerebellum (cerebellum 6 and crus 1), in the right parahippocampal gyrus and the right hippocampus and in the midbrain/brainstem.

The univariate analysis identifying the preferential activations for close compared to far social stimuli (i.e., close social > far social contrast) recruited almost similar brain regions in occipital, temporal, parietal and premotor cortex while no significant cluster after correction were identified for preferential activation in far space (see supplementary materials for more details).

A common premotor-parietal network to subserve PPS representation of social and non-social stimuli

We performed MVPA with cross-modality method by decoding the distance (i.e., close vs. far) in one category and try to decode the same pattern of distance on the other category. In other words, we identified if distance was decoded similarly for social and non-social categories by training the classifier on the pairwise comparison between close and far for one category and testing on the other category (i.e., training on social stimuli, testing on non-social stimuli and inversely). The average of the two decoding maps significantly higher than chance level and corrected for multiple comparisons (FWE, $p < 0.05$) is represented in Figure 3B and significant clusters are reported in Table 1. The results show that information about distance (close versus far) could be decoded in a set of regions in occipital, parietal, and frontal areas regardless of the category of the stimulus.

The most significant cluster included regions of the occipital cortex, mostly visual areas (V1, V2, V3, V3A, V3B, V4) among the bilateral superior and middle occipital gyrus, the bilateral

cuneus, the bilateral calcarine sulcus, the left lingual gyrus, and the medial parieto-occipital sulcus containing V6 and V6A regions. This cluster also included left cerebellum (6 and crus 1) as well as parietal areas, in the bilateral precuneus, in the right angular gyrus (area MIP), in the bilateral SPL (in lateral area 7P and also along the IPS in the VIP, LIPv and LIPd areas) and in the right IPL (in the inferior part of the LIPv area).

Another significant cluster in the right hemisphere included brain regions in precentral (premotor areas PMd and PMv) and postcentral gyrus (area 2 and area 3b of SI) as well as M1 and areas in bordering the middle frontal gyrus (FEF and 55b areas).

The univariate analysis performed for the non-social category to identify preferential activations for close compared to far geometrical shapes stimuli revealed only greater activation in occipital brain regions (see supplementary materials for details). Importantly, the BOLD signal for non-social stimuli was weaker than when considering all social stimuli.

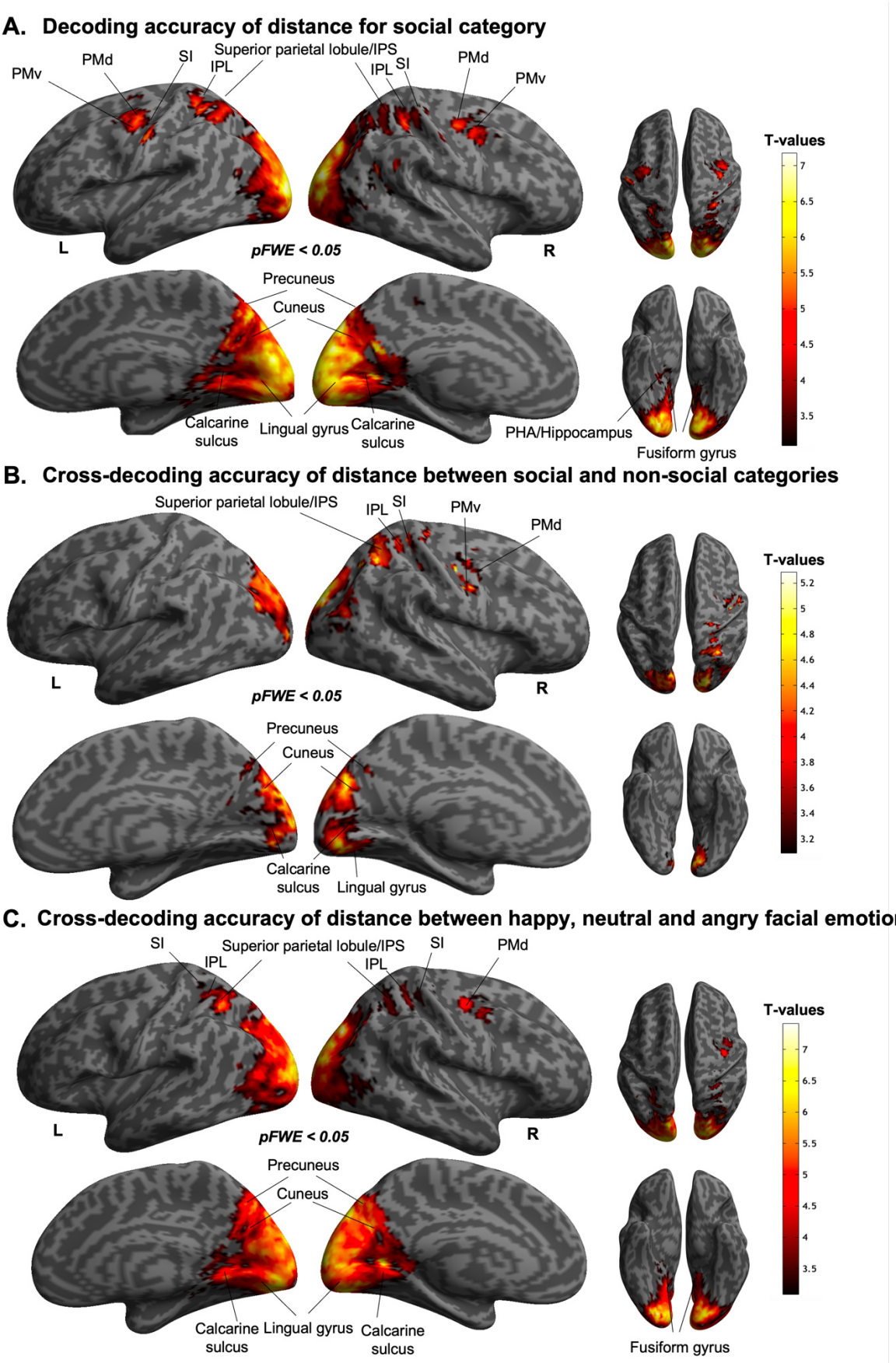
A. Decoding accuracy of distance for social category
PMv
PMd
SI
IPL
Superior parietal lobule/IPS
IPL
SI
PMd
PMv
L
pFWE < 0.05
R
Precuneus
Cuneus
Calcarine sulcus
Lingual gyrus
Calcarine sulcus
PHA/Hippocampus
Fusiform gyrus
T-values
7
6.5
6
5.5
5
4.5
4
3.5
B. Cross-decoding accuracy of distance between social and non-social categories
Superior parietal lobule/IPS
IPL
SI
PMv
PMd
L
pFWE < 0.05
R
Precuneus
Cuneus
Calcarine sulcus
Lingual gyrus
T-values
5.2
5
4.8
4.6
4.4
4.2
4
3.8
3.6
3.4
3.2
C. Cross-decoding accuracy of distance between happy, neutral and angry facial emotions
SI
IPL
Superior parietal lobule/IPS
IPL
SI
PMd
L
pFWE < 0.05
R
Precuneus
Cuneus
Calcarine sulcus
Lingual gyrus
Calcarine sulcus
Fusiform gyrus
T-values
7
6.5
6
5.5
5
4.5
4
3.5

Figure 3. Brain network involved in PPS processing according to stimulus category. A. Maps of significant group-averaged above-chance distance classification accuracy obtained with whole-brain MVPA searchlight analysis for close vs. far decoding of social category. Results of the group-level permutation-based random effects analysis represented on an inflated surface and showing the regions in which classification accuracy was significantly higher than chance (p-FWE < 0.05 cluster-level-corrected). **B.** Maps of significant group-averaged above-chance distance classification accuracy obtained with whole-brain MVPA cross-modality decoding of close vs. far between social and non-social categories. The classifier was trained on one pairwise comparison for one category and tested on the other, and inversely. Activations depicted in the inflated render show the results of the group-level permutation-based random effects analysis of the average of these two decoding maps showing the regions with significant classification accuracy found in both social and non-social categories (p-FWE < 0.05 cluster-level-corrected). **C.** Maps of significant group-averaged above-chance distance classification accuracy with whole-brain MVPA cross-modality decoding of close vs. far between happy, neutral and angry faces. The classifier was trained on two pairwise comparisons for two emotions and tested on the remaining emotion, and inversely until tested all the combinations. Activations depicted in the inflated render show the results of the group-level permutation-based random effects analysis of the average of all these decoding maps showing the regions in which classification accuracy was significantly higher than chance similarly for angry, happy, and neutral faces stimuli (p-FWE < 0.05 cluster-level-corrected).

PPS network for Happy faces is more extended compared to neutral and angry faces

We then considered each facial emotional expression separately to identify 1) the brain network with a similar pattern of decoding of distance for the three emotions and 2) specificity in neural coding depending on each emotion separately.

Firstly, we performed MVPA cross-decoding accuracy of distance by training the pattern of distance processing in one emotion (i.e., close vs far) and then tested if this pattern could be decoded on the other emotions. All combinations of emotions were performed (see figure 2 c) in methods for details) and the average of all the decoding maps has been computed in order to identify the brain regions with a common decoding pattern of distance for the three emotions. Figure 3C represents the average decoding maps with clusters significantly higher than chance level and corrected for multiple comparisons (FWE, $p < 0.05$). As for the analysis considering all faces stimuli independent of the type of emotion depicted, the network comprised several regions in the occipital, temporal, parietal cortices, and subcortical structures. A widespread significant cluster allowing to decode the same pattern of distance for the three emotions were composed of visual areas (V1, V2, V3, V3A, V4, V7) in bilateral superior, middle and inferior occipital gyrus, calcarine sulcus, lingual gyrus, cuneus, and bilateral fusiform gyrus (V8, Ventral visual complex VVC, ventromedial visual area VMV), with also activations in the left FFA, but were also composed of a set of temporal, parietal and subcortical areas. In particular

activations were situated in the bilateral parieto-occipital sulcus (V6, V6A) next to the precuneus, the right middle temporal gyrus (MT, MST and FST areas), the right MIP area in the angular gyrus, the bilateral IPS in the SPL (VIP, LIPd, LIPv), the bilateral IPL (the right area 7PC and inferior part of LIPv and the left inferior part of LIPd), and the bilateral postcentral gyrus in the area 2 of SI. The subcortical areas comprised the cerebellum (the left and right cerebellum 6 and Crus 1, the left cerebellum 4 5) and the right parahippocampal gyrus. Finally, another significant cluster included the right precentral gyrus with activations in the dorsal part of the premotor cortex (PMd), the primary motor cortex and more anteriorly, the FEF. All the significant clusters and associated peaks of activation are reported in Table 1.
Taken together, these results suggest that all these emotional faces presented in PPS recruit a common network including a set of areas, very close to the one identified in the previous analysis, when all social stimuli were considered independently of the emotion.

Secondly, through univariate whole-brain analysis, we identified each brain regions with preferential activations for either happy, neutral, and angry emotions presented in close compared to far space, in order to determine if additional brain regions could be recruited to process these emotions separately (i.e. contrasts close > far for each happy, neutral and angry emotion). Theses univariate results revealed a major significant cluster for the three emotions including brain regions in occipital lobe with higher activations for close happy, neutral and angry faces compared to far similarly particularly in the bilateral calcarine sulcus, the bilateral lingual gyrus, the bilateral cuneus, the bilateral superior occipital gyrus, the bilateral fusiform gyrus (V1, V2, V3, V3A, V8, VMV, VVC, FFA) and in the bilateral parieto-occipital sulcus (in V6, V6A) with also activations in bilateral precuneus. Activations in the bilateral middle occipital gyrus and the left inferior occipital gyrus (in V3B and V4 areas) were found with angry faces and activations in the left middle occipital gyrus (in V3B) were observed for neutral faces. In the temporal lobe, activations in the bilateral middle temporal gyrus were found with happy and angry faces (in MT, MST, TPOJ, area FST for happy and in MT, area FST for angry). Higher activations for close compared to far faces were also identified in the bilateral cerebellum 6 and in vermis (6 and 4 5) for these three emotions.
In addition, happy faces in PPS evoked a far more extended pattern of brain activity compared to the other two facial expressions as confirmed by the conjunction analysis between these three contrasts (see table S1 in supplementary materials for details). The responses were found in a set of parietal brain regions including the right precuneus, the bilateral SPL with activation in

bilateral LIPv, LIPd and the right area intraparietal 2 but also in the right SMG (area PF). Higher activations were also found in the left middle cingulate cortex (the dorsal area 24d and the area 23c), in the retrosplenial complex and in frontal brain regions distributed in two significant clusters. These clusters included the right area 2 (SI) of the postcentral gyrus, the bilateral precentral gyrus with activations in the left rostral area 6 and the right PMd, the right PMv, the right rostral area 6 and in the vicinity of the precentral sulcus and the dorsal-most portion of the superior frontal gyrus, the right FEF as well as brain regions in the middle part of the frontal gyrus (the right dorsolateral prefrontal cortex DLPFC area 46) and in the inferior part of the frontal gyrus, in the left and right opercular part. Finally, in one of this significant cluster, the right insular cortex also exhibited greater activation for close happy faces (the middle insular area and the anterior agranular insula complex).

For each of the three emotions presented in far compared to close space, no significant cluster was found after correction for all the three emotions (i.e., contrasts far happy faces > close happy faces, far neutral faces > close neutral faces and far angry faces > close angry faces).

All these results are detailed in the Table 2 and depicted in figure 4.

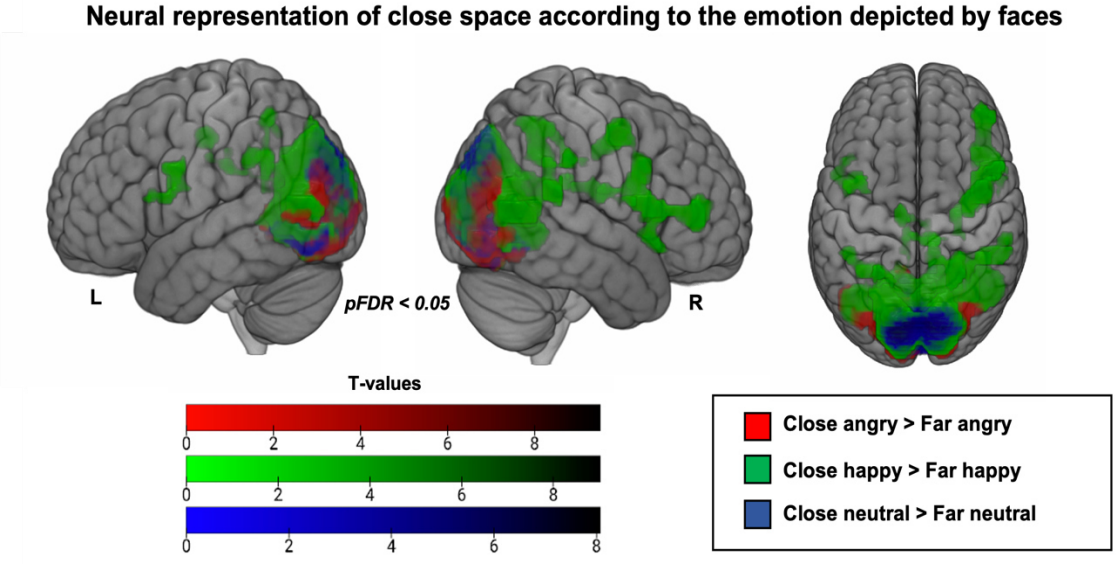

Figure 4. Brain network involved in PPS processing according to happy, neutral, and angry emotion depicted by faces. Brain regions showing significant greater activations for close angry, happy or neutral faces stimuli compared to far: whole-brain univariate analysis for the three contrasts close angry faces > far angry faces, close happy faces > far happy faces and close neutral faces > far neutral faces. The three contrasts are superimposed in a render brain: results of the group-level statistical analysis for close angry faces > far angry faces contrast is depicted in red, results of the group-level statistical analysis for close happy faces > far happy faces contrast is shown in green and results of the

group-level statistical analysis for close neutral faces > far neutral faces are in blue. Activation threshold set at cluster-forming $p< 0.001$ uncorrected, and FDR-corrected $p< 0.05$ at the cluster level.

4. Discussion

This study aimed at providing novel insights on the neural network subserving PPS representation of social faces stimuli depending on their emotional content, and at comparing this neural network with those elicited by non-social objects stimuli. In order to place ourselves in the most ecological situation, we used, for the first-time, stereoscopic virtual reality inside the scanner (3D stimuli and virtual environment) allowing us to vary the position of stimuli in space.

First, we found that social stimuli recruited an occipital-parietal-premotor network, with some structures previously linked to PPS representation (PMd, PMv, IPS, SI and SMG) but also additional brain regions known to process facial identity (OFA, FFA) (Haxby et al., 2000). Second, we found that this occipital-premotor-parietal network was similarly recruited for both faces and geometrical shapes stimuli, suggesting a similar processing for social or non-social categories presented in PPS although additional brain regions seem necessary to process social visual information. Finally, we further uncovered that the brain activations could be differently evoked depending on the emotional facial expressions in close space, especially with happy faces, that stands out recruiting more regions in frontal areas, including the cingulate cortex and the insula.

4.1. Social and non-social categories in PPS are processed by a similar occipito-parieto-premotor network which is enlarged for social stimuli

Various behavioural research has investigated whether social information may affect the regulation of PPS. By demonstrating the flexibility of PPS representation in the presence of confederates (Teneggi et al., 2013) also sensitive to various social factors (e.g., level of anxiety, emotion, morality; Dureux et al., 2021; Pellencin et al., 2018; Ruggiero et al., 2017; Sambo & Iannetti, 2013), it was suggested that the presence of other people around us may play an important role in PPS representation and its role in social interactions. These behavioral findings suggest that PPS is not only the physical space for acting on objects but is also a

physical space for social interactions depending on several social factors. Social and non-social characteristics of the stimuli presented in our close space could therefore recruit the similar brain network which could however depend on the nature of the interactions whether social or not.

Previous studies that investigated PPS neural representation of social and non-social categories in humans involved different types of depth cues. While most of fMRI studies investigated neural encoding of unisensory non-social events by using real dynamic objects presented close as opposed to far (Brozzoli et al., 2013; Brozzoli et al., 2011; Grivaz et al., 2017; Makin et al., 2007), fMRI studies that investigated neural encoding of social events used approaching vs. withdrawing visual stimuli increasing in size on a screen (Holt et al., 2014, 2015; Schienle et al., 2016; Vieira et al., 2017, 2020).

Locating a visual object in space involves a combination of both low- and high-level cues. The high-level cues are based on the visual object recognition corresponding to the cognitive interpretation of what is being perceived (e.g., the apparent size of the object perceived allow to infer its distance) whereas the low level-cues are based on oculomotor information and visual cues (Cléry et al., 2015). In our study, we used 3D faces or geometrical shapes stereoscopic stimuli presented at two distances either close, at 30 cm or far, at 300 cm in a naturalistic virtual depth environment therefore including high-level cues, with depth cues provided by the naturalistic environment as well as low-level cues of eye vergence corresponding to the conjugate eye movements that allow both eyes to focus onto the given visual stimuli providing the brain with information about where the eyes are fixating in space.

First, consistent with prior studies having studied non-social PPS representation involving high and low level-cues (Makin et al., 2007; Quinlan and Culham, 2007; Brozzoli et al., 2011, 2013), or only high-level cues of visual information recognition by varying the apparent size of the stimuli perceived (approaching vs. withdrawing, (Holt et al., 2014, 2015; Massaccesi et al., 2021; Schienle et al., 2016; Vieira et al., 2017, 2020), we found similar recruitment of parietal (IPS, somatosensory cortex SI and SMG) and premotor regions (PMd and PMv) as well as cerebellum for the processing of faces stimuli in close space. Moreover, we found an extended occipital-temporal network including visual areas (V1, V2, V3, V3A, V4) and the parieto-occipital sulcus extending to V6 and V6A areas, the occipital face area (OFA) in the inferior occipital, MST and MT areas and TPOJ as well as in the FFA, that was

also found to be preferentially activated by approaching compared to withdrawing faces in healthy subjects and patients (Holt et al., 2015; Massaccesi et al., n.d.-b). Finally, we also identified other subcortical regions sensitive to distance processing of faces, particularly in the parahippocampal gyrus, the hippocampus and a part of the midbrain previously linked to preferential activation for looming faces, particularly in the periaqueductal gray (PAG) area.
This results clearly showed that a parietal-premotor network seems fundamental to process distance information and that the perception of close faces rely on the interplay between the PPS network and regions of the "face network" such the OFA and FFA (Haxby et al., 2000; O'Toole et al., 2002).

Next, we found that part of the PPS network encodes distance regardless of the category of stimuli (social or non-social). This network included visual areas, superior parietal brain regions (V6A, MIP, VIP, LIP), the somatosensory cortex (SI), the premotor cortex (PMv and PMd), FEF, in the middle frontal gyrus and in the cerebellum. This suggests that a core brain network would be similarly recruited by proximal visual stimuli, whether they convey social information or not. The specificity depending on the context might depend on interactions between the ventral and dorsal visual pathways. All these connections would constitute a complex exchange system for processing the visual social information appearing in the PPS in order to enable us to react more quickly, as observed through the facilitation identified in a set of behavioral studies (Dureux et al., 2021; Pellencin et al., 2018; Teneggi et al., 2013).

4.2. Happy faces in PPS recruit an extended network compared to neutral and angry faces

Given that the proximity of a happy or angry person triggers different behavioral and physiological responses (Cartaud et al., 2018; Dureux et al., 2021; Ruggiero et al., 2017), it would not be surprising that they elicit different neural signatures. First, we do find some overlap in the encoding of close faces regardless of their emotional content (neutral, happy or angry). This overlap reflected the ability of these regions to decode information about distance regardless of the emotional facial expressions depicted. This property was found in occipital visual areas, middle temporal areas and the FFA, the SPL and IPL with greater activations mostly situated along the IPS (MIP, LIP, VIP), the dorsal part of premotor cortex, the somatosensory area (SI) as well as the parahippocampal gyrus and the cerebellum.

In addition, we were able to identify brain regions that preferentially encoded distance information for each emotion, specifically. Of note, the brain network was far more extended with happy faces compared to neutral and angry faces. Indeed, in addition to the majority of brain regions already identified in common for the three emotion, happy faces in PPS elicited an increase of activity in the prefrontal cortex, in the Rolandic operculum, in the cingulate cortex, in the retrosplenial complex and in the insular cortex. Some of these regions, in particular activations in the cingulate cortex and the insular cortex were previously identified by studies using facial expression (Schienle et al., 2016; Vieira et al., 2017, 2020) although Vieira et al. (2017) also identified greater activation in the amygdala, not found here. Our results suggest that in our setting, happy faces were processed differently compared to other emotions, and this could be linked to the behavioral performances. Indeed, the participants were better and faster at discriminating happy faces compared to the other emotions. This is also in line with our previous behavioral study showing facilitation of behavioral performances but also an increase of heart rate variability with happy faces (Dureux et al., 2021). It is possible that the insula, that contribute to the perception of bodily reactions induced by emotions (Gogolla, 2017 for review) constitute a privileged area to integrate sensory inputs and interoceptive signals (Uddin et al., 2017) to then send this information to the core PPS network and shape our behavioral responses according to the social context. The analysis of the functional relationships between these regions depending on the distance will clarify these issues in the future.

In sum, these findings bring important new insights into the neural substrate of PPS in a social context, never studied in stereoscopic virtual reality mimicking an ecological dimension and allowed to directly compare neural correlates of PPS representation for social and non-social categories.

Tables

Table 1. Clusters showing significant accuracy of distance for a whole-brain MVPA at cluster-level inference of FWE p< 0.05 corrected. **(1)** Distance encoding for the social category **(Close vs. Far social stimuli)**, **(2)** average decoding accuracy for the two distance decoding combinations for social and non-social stimuli separately (classifier trained on **Close vs. Far social** and tested **on Close vs. Far non-social**, and inversely) and **(3)** average decoding accuracy for the three distance decoding combinations for each emotional stimuli separately (happy, neutral and angry; each combination of classifier trained on Close vs. Far of two emotions and tested on Close vs. Far of one emotion). All these significant accuracy clusters were tested against 50% chance with permutation Monte Carlo Test and FWE corrected ($p < 0.05$, FWE corrected). Cluster size in voxels and MNI coordinates of the peak voxel for each region in the significant cluster are reported with the t-values associated. Locations of the corresponding cluster and brain regions associated are reported from anatomical AAL3 atlas (Rolls et al., 2020) and from the multi-modal cortical parcellation Glasser atlas (Glasser et al., 2016).

			MNI coordinates				
Anatomical location from AAL3 atlas	**R/L**	**Cluster size**	**x**	**y**	**z**	**T**	**Glasser Atlas labels**
(1) Decoding of distance for social category							
Close vs. Far							
	R	**12788**	**2**	**-84**	**22**	**7.5**	**V2**
Cuneus	R		8	-92	25		V3
	L		**-6**	**-92**	**17**	**6**	**V2**
	L		-3	-84	34		V3
	R		**8**	**-90**	**3**	**5.51**	**V1**
Calcarine sulcus	R		9	-61	17		POS1
	L		**-14**	**-78**	**6**	**4.91**	**V1**
	L		-15	-62	6		POS1
	R		**33**	**-87**	**-11**	**5.06**	**V4**
Inferior occipital gyrus	R		44	-84	-11		OFA
	L		**-23**	**-92**	**-6**	**5.51**	**V3**
	L		-44	-84	-11		OFA
	R		**33**	**-81**	**34**	**6.01**	**Area PG**
	R		33	-86	23		IP0
	R		33	-78	23		V3B
Middle occipital gyrus	**L**		**-20**	**-92**	**6**	**7.03**	**V3**
	L		-20	-90	17		V3A
	L		-31	-89	27		Area PG
	L		-31	-79	20		IP0
	R		**22**	**-87**	**-11**	**6.08**	**V3**
	R		17	-87	-7		V2
	R		16	-62	-4		VMV1
Lingual gyrus	**L**		**-14**	**-84**	**-8**	**6.13**	**V2**
	L		-9	-52	3		POS1
	L		-14	-84	-8		V3
	L		-17	-63	-4		VMV1
	R		**22**	**-92**	**20**	**6.58**	**V3A**
	R		22	-81	34		V6
	R		22	-78	45		V6A
Superior occipital gyrus	**L**		**-20**	**-92**	**25**	**5.22**	**V3A**
	L		-20	-79	37		V6
	L		-20	-78	40		DVT
	L		-20	-83	46		V6A
	R		**44**	**-67**	**11**	**3.51**	**MST**
	R		44	-67	13		MT
	R		42	-66	5		FST
Middle temporal gyrus	**L**		**-48**	**-70**	**17**	**3.48**	**TPOJ**
	L		-48	-70	10		MT
	L		-49	-70	9		FST
	R		**28**	**-78**	**-11**	**5.85**	**V8**
	R		28	-45	-14		Ventral Visual Complex
Fusiform gyrus	R		39	-71	-16		FFA
	L		**-26**	**-69**	**-11**	**4.6**	**VMV3**
	L		-26	-73	-14		V8
	R		**25**	**-78**	**-20**	**4.73**	**/**
Cerebellum 6	**L**		**-9**	**-73**	**-17**	**5.05**	**/**
	R		**19**	**-87**	**-22**	**3.80**	**/**
Cerebellum crus1	**L**		**-20**	**-87**	**-22**	**4.41**	**/**
	R		**8**	**-73**	**53**	**4.22**	**Lateral area 7P**
Precuneus	**L**		**-6**	**-78**	**48**	**4.43**	**POS2**
	L		-6	-78	52		Medial area 7P
	R		**46**	**-48**	**25**	**3.74**	**STV**
Angular	R		46	-48	22		Area 5L
	R		**33**	**-62**	**59**		**LIPv**
Superior parietal lobule	R		28	-50	46		LIPd
	R		26	-667	49		MIP
	R		**32**	**-35**	**56**		**Area 2 (SI)**
Postcentral gyrus	R		33	-30	58		area 3B
	R		**22**	**-34**	**-17**	**3.61**	**ParahippocampalArea1**
ParaHippocampal	R		19	-31	-12		PreSubiculum
Hippocampus	**R**		**20**	**-29**	**-8**		**Hippocampus**
Midbrain/brainstem			**11**	**-25**	**-8**	**3.23**	**/**
Postcentral gyrus	**L**	**531**	**-59**	**-11**	**48**	**5.3**	**Area 1**
	L		-54	-9	50		Area 55b
	L		-55	-16	44		area 3B
Precentral gyrus	**L**		**-42**	**-6**	**48**	**4.54**	**FEF**
	L		-45	-10	59		Dorsal area 6 PMd
	L		-60	-5	44		Ventral area 6 PMv
	L		-37	-8	54		Area 6 anterior
	L		-42	-13	50		M1
Precentral gyrus	**R**	**514**	**47**	**-6**	**53**	**5**	**FEF**
	R		44	-8	57		Dorsal area 6 PMd
	R		44	2	45		PEF
	R		36	-6	49		Area 6 anterior
	R		44	4	47		Area 55b
Superior frontal gyrus	**R**		**30**	**0**	**62**	**3.53**	**i6-8**
Postcentral gyrus	**L**	**479**	**-26**	**-45**	**53**	**5.44**	**Area 2**
Superior parietal lobule	**L**		**-34**	**-64**	**59**	**4.76**	**LIPv**
	L		-34	-64	52		MIP
	L		-29	-67	62		VIP
Inferior parietal lobule	**L**		**-34**	**-56**	**50**	**3.81**	**Area PFm complex**
	L		-38	-55	58		Area 7PC

(Table 1 continued)

(2) Cross-decoding of distance between social and non-social categories Close vs. Far social/non-social stimuli							
	R	**4461**	**22**	**-90**	**28**	**5.73**	**V3A**
	R		22	-81	34		V6
	R		22	-82	39		V6A
Superior occipital gyrus	R		28	-73	38		IPS1
	L		**-17**	**-78**	**30**	**4.46**	**V6**
	L		-17	-87	28		V3A
	L		-17	-86	40		V6A
	L		-20	-82	51		DVT
	R		**47**	**-70**	**25**	**4.26**	**Area PGp**
	R		36	-83	40		Area PGs
Middle occipital gyrus	R		41	-73	21		Area Lateral occipital 3
	L		**-40**	**-87**	**22**	**4.73**	**Area PGp**
	L		-31	-89	20		V4
	L		-27	-82	22		V3B
	R		**14**	**-98**	**8**	**4.96**	**V1**
Cuneus	R		14	-93	12		V2
	L		**-6**	**-81**	**34**	**4.58**	**V3**
	L		-6	-83	25		V2
Calcarine sulcus	**R**		**11**	**-90**	**3**	**3.98**	**V1**
	L		**-17**	**-78**	**-14**	**3.78**	**V1**
Lingual gyrus	**R**		**5**	**-83**	**-7**	**4.13**	**V2**
	L		**-15**	**-76**	**-11**	**3.64**	**V3**
Angular gyrus	**R**		**28**	**-59**	**45**	**5.23**	**MIP**
Precuneus	**R**		**14**	**-76**	**46**	**3.20**	**POS2**
	L		**-3**	**-76**	**42**	**5.35**	**POS2**
	R		**22**	**-53**	**59**	**4.44**	**VIP**
Superior parietal lobule	R		24	-53	54		LIPv
	R		25	-56	50		LIPd
	L		**-20**	**-78**	**50**	**3.37**	**Lateral area 7P**
Inferior parietal lobule	**R**		**36**	**-50**	**50**	**3.45**	**LIPv**
Cerebellum Crus 1	**L**		**-20**	**-81**	**-28**	**3.79**	**/**
Cerebellum 6	**L**		**-9**	**-73**	**-22**	**4.45**	**/**
	R	**212**	**39**	**-14**	**42**	**4.99**	**M1**
Precentral gyrus	R		44	-5	61		Dorsal area 6 PMd
	R		48	-3	51		FEF
	R		54	1	34		Ventral area 6 PMv
Postcentral gyrus	**R**		**30**	**-34**	**62**	**4.36**	**Area 2 (SI)**
	R		30	-30	62		Area 3b
Middle frontal gyrus	**R**		**53**	**3**	**56**	**3.65**	**Area 55b**

(Table 1 continued)

(3) Cross-decoding of distance between happy, neutral and angry emotions							
Close vs. Far happy/neutral/angry faces							
	R	**12079**	**28**	**-84**	**31**	**7.42**	**V7**
	R		28	-74	40		IPS1
	R		21	-82	40		V6A
	R		21	-78	34		V6
Superior occipital gyrus	R		21	-90	29		V3A
	L		**-20**	**-70**	**28**	**5.65**	**DVT**
	L		-21	-86	42		V6A
	L		-17	-80	31		V6
	L		-17	-89	29		V3A
	R		**36**	**-84**	**28**	**4.64**	**Area PGp**
	R		36	-91	17		V4
	R		27	-97	5		V3
Middle occipital gyrus	**L**		**-18**	**-96**	**9**	**6**	**V3**
	L		-28	-92	3		V4
	L		-28	-84	25		V7
	L		-28	-89	29		Area PGp
	R		**36**	**-90**	**-11**	**3.83**	**V4**
	R		36	-84	-4		PIT (OFA)
Inferior occipital gyrus	**L**		**-35**	**-87**	**2**	**4.5**	**V4**
	L		-42	-78	-8		FFA
	L		-42	-74	-2		Area PH
	L		-39	-83	-11		PIT (OFA)
	R		**14**	**-98**	**0**	**5.76**	**V1**
Calcarine sulcus	**L**		**-26**	**-59**	**6**	**7.38**	**ProStriate Area**
	L		-20	-67	6		V1
Lingual gyrus	**R**		**11**	**-84**	**-8**	**6.48**	**V2**
	L		**-12**	**-84**	**-8**	**5.92**	**V2**
	R		**8**	**-90**	**20**	**5.67**	**V2**
Cuneus	R		8	-86	31		V3
	L		**0**	**-84**	**22**	**5.50**	**V2**
	L		2	-78	31		V3
	R		**25**	**-81**	**-11**	**7.30**	**V8**
	R		27	-72	-14		VVC
Fusiform gyrus	R		25	-67	-11		VMV3
	L		**-26**	**-70**	**-14**	**4.16**	**V8**
	L		-26	-68	-15		VVC
	L		-26	-69	-12		VMV3
Precuneus	**R**		**8**	**-76**	**48**	**4.78**	**POS2**
	L		**0**	**-76**	**42**	**5.28**	**POS2**
	R		**53**	**-70**	**6**	**3.51**	**MT**
Middle temporal gyrus	R		46	-69	6		MST
	R		56	-68	3		Area FST
	R		51	-76	3		Area V4t
Cerebellum 6	**R**		**11**	**-73**	**-20**	**5.20**	**/**
	L		**-9**	**-73**	**-14**	**5.45**	**/**
Cerebellum Crus 1	**R**		**28**	**-84**	**-22**	**3.59**	**/**
	L		**-23**	**-84**	**-22**	**5.16**	**/**
Cerebellum 4 5	**L**		**-6**	**-59**	**-6**	**3.86**	**/**
Parahippocampal gyrus	**R**		**22**	**-39**	**-8**	**3.38**	**ParahippocampalArea1**
Angular gyrus	**R**		**32**	**-64**	**48**	**3.5**	**MIP**
	R		**28**	**-53**	**59**	**3.42**	**LIPv**
	R		30	-52	46		LIPd
Superior parietal lobule	**L**		**-28**	**-62**	**53**	**4.49**	**LIPv**
	L		-28	-61	62		VIP
	L		-35	-60	50		LIPd
Postcentral gyrus	**R**		**30**	**-36**	**56**	**3.74**	**Area 2 (SI)**
	L		**-23**	**-42**	**62**	**3.21**	**Area 2 (SI)**
	R		**30**	**-44**	**54**	**3.5**	**Area 7PC**
Inferior parietal lobule	R		36	-50	50		LIPv
	L		**-34**	**-56**	**50**	**4.26**	**LIPd**
	R	**325**	**44**	**-6**	**53**	**4.98**	**Dorsal area 6 PMd**
Precentral gyrus	R		44	-8	53		M1
	R		45	-4	51		FEF
	R		36	-4	52		Area 6 anterior

Table 2. Brain regions displaying greater activation for close relative to far stimuli for happy **(Close happy > Far happy)**, angry **(Close angry > Far angry)** and neutral **(Close neutral > Far neutral)** faces stimuli **(1).** Results for contrasts of far relative to close stimuli for each emotion are also reported **(2).** Activation threshold is set at cluster-level FDR-corrected $p < 0.05$. Cluster size in voxels and MNI coordinates of the peak voxel for each region in significant clusters are reported with the t-values associated. Locations of the corresponding cluster and brain regions associated are reported from anatomical AAL3 atlas (Rolls et al., 2020) and from the multi-modal cortical parcellation Glasser atlas (Glasser et al., 2016).

			MNI coordinates				
Anatomical location from AAL3 atlas	**R/L**	**Cluster size**	**x**	**y**	**z**	**T**	**Glasser Atlas labels**
(1) Univariate analysis : close effect contrasts							
Close Happy > Far Happy							
Calcarine sulcus	**R**	**6497**	**8**	**-90**	**8**	**9.09**	**V1**
	L		0	-87	8	7.48	**V1**
Lingual gyrus	R		11	-84	-3	8.74	**V2**
	L		-8	-64	0	6.09	**V2**
	R		12	-80	39	6.15	**V3**
Cuneus	R		12	-70	29		V2
	L		-6	-81	31	7.24	**V3**
	L		-6	-83	26		V2
	R		25	-84	31	6.59	**V3A**
	R		22	-72	35		DVT
	R		22	-72	26		V6
	R		19	-79	41		V6A
Superior occipital gyrus	L		-12	-81	34	7.35	**V6**
	L		-20	-87	31		V3A
	L		-18	-74	29		DVT
	L		-18	-76	31		V6
	L		-21	-83	40		V6A
Precuneus	R		11	-73	45	4.74	**POS2**
	R		50	-64	11	4.78	**MST**
	R		51	-65	12		MT
Middle temporal gyrus	R		50	-60	9		TPOJ2
	L		-48	-67	11	3.85	**MST**
	L		-48	-75	10		MT
	L		-48	-69	10		Area FST
Superior temporal gyrus	R		53	-39	20	4.10	**Superior TemporalVisual area**
	R		53	-38	17		TPOJ1
Middle cingulate gyrus	L		-12	-16	42	4.8	**Dorsal area 24d**
	L		-9	-17	42		Area 23c
Retrosplenial complex	L		-6	-27	26	3.6	**Retrosplenial complex**
SupraMarginal gyrus	R		58	-31	39	3.67	**Area PF**
	R		22	-56	56	3.38	**LIPv**
	R		27	-53	47		LIPd
Superior parietal lobule	R		33	-47	36		Area Intraparietal 2
	L		-28	-50	59	3.24	**LIPv**
	L		-26	-50	40		LIPd
	R		28	-67	-8	3.70	**VMV3**
Fusiform gyrus	L		-26	-73	-11	3.74	**V8**
	L		-26	-58	-8		VMV2
Cerebellum 6	R		11	-73	-17	3.61	**/**
	L		-6	-73	-14	4.94	**/**
Vermis 6			0	-70	-8	4.10	/
Vermis 4 5			0	-62	-3	5.16	/
Postcentral gyrus	R		27	-40	60	3.6	**Area 2 (SI)**
	R	787	42	-6	50	4.85	**FEF**
	R		42	-5	57		Dorsal area 6 PMd
Precentral gyrus	R		54	11	34		Ventral area 6 PMv
	R		50	11	31		Rostral area 6
	R		33	-11	42		Area 6 anterior
Triangular part of inferior frontal gyrus (pars triangularis)	R		42	22	8	4.24	**Area FrontalOpercular**
	R		42	18	6		Frontal opercular area 4
Opercular part of inferior frontal gyrus	R		50	17	11	3.92	**Area 44**
Insula	R		41	14	-3	3.52	**Middle insular area**
	R		37	18	-6		Anterior AgranularInsula Complex
Middle fontral gyrus	R		39	45	8	4.21	**9-46v**
	R		39	43	12		Area 46
Precentral gyrus	L	139	-50	9	17	3.5	**Rostral area 6**
Frontal inferior opeculum	L		-42	3	28	3.56	**Area IFJp**

(Table 2 continued)

Close Angry > Far Angry							
	R	**5221**	**11**	**-84**	**-3**	**9.67**	**V2**
Lingual gyrus	R		11	-75	-5		V3
	L		-9	-81	-6	6.40	**V2**
	L		-11	-74	-8		V3
	R		5	-90	0	9.28	**V1**
Calcarine sulcus	L		-9	-90	-3	9.04	**V1**
	R		14	-81	28	6.63	**V6**
Cuneus	R		11	-86	26		V3
	L		-6	-81	28	6.47	**V3**
	L		-15	-79	31		V6
	R		25	-81	31	6.43	**V3A**
	R		25	-78	31		V7
Superior occipital gyrus	R		21	-78	39		V6A
	L		-17	-90	25	7.66	**V3A**
	L		-17	-78	37		DVT
	L		-18	-81	39		V6A
Middle occipital gyrus	R		30	-76	25	4.78	**V3B**
	L		-23	-81	20	5.1	**V3B**
Inferior occipital gyrus	L		-28	-84	-8	4.04	**V4**
Precuneus	R		11	-75	45	4	**POS2**
	R		42	-67	14	4.55	**MT**
	R		42	-68	16		LO3
Middle temporal gyrus	R		41	-67	6		Area FST
	L		-48	-67	8	4.01	**Area FST**
	L		-46	-69	10		MT
	R		28	-59	-14	3.37	**VVC**
	R		28	-76	-8		V8
Fusiform gyrus	R		28	-69	-8		VMV3
	R		35	-68	-8		FFA
	L		-28	-76	-14	3.60	**V8**
	L		-28	-70	-11		VMV3
	R		11	-73	-17	5.11	**/**
Cerebelum 6	L		-9	-73	-14	7.30	**/**
Vermis 6			2	-73	-14	3.20	/
Vermis 4 5			2	-62	-3	3.16	/
Close Neutral > Far Neutral							
	R	**3438**	**11**	**-87**	**6**	**7.03**	**V1**
Calcarine sulcus	L		2	-92	0	8.14	**V1**
	R		11	-84	-3	8.12	**V2**
Lingual gyrus	R		11	-74	-5		V3
	L		-12	-84	-8	7.30	**V2**
	R		-12	-67	-4		V3
	R		14	-79	36	6	**V6**
	R		11	-78	37		V3
Cuneus	R		14	-87	26		V3A
	L		-12	-84	31	8.05	**V6**
	L		-12	-79	25		V3
	L		-12	-89	26		V3A
	R		19	-77	40	4.85	**V6A**
	R		25	-84	31		V3A
Superior occipital gyrus	R		19	-72	31		DVT
	L		-20	-81	28	6.35	**V3A**
	L		-20	-83	37		V6A
	L		-20	-78	37		DVT
Middle occipital gyrus	L		-23	-84	17	3.98	**V3B**
	R		14	-76	45	4.68	**POS2**
Precuneus	L		-3	-78	45	3.97	**POS2**
	R		28	-78	-14	3.48	**V8**
Fusiform gyrus	R		23	-69	-7		VMV3
	L		-26	-73	-14	3.83	**V8**
	R		11	-73	-17	5.04	**/**
Cerebelum 6	L		-9	-73	-14	6.80	**/**
Vermis 6			2	-73	-14	3.81	/
Vermis 4 5			2	-62	-3	3.23	/
(2) Univariate analysis : far effect contrasts							
Far Happy > Close Happy							
No significant clusters							
Far Angry > Close Angry							
No significant clusters							
Far Neutral > Close Neutral							
No significant clusters							

5. References

Baayen, R. H., Davidson, D. J., & Bates, D. M. (2008). Mixed-effects modeling with crossed random effects for subjects and items. Journal of Memory and Language, 59(4), 390–412. https://doi.org/10.1016/J.JML.2007.12.005

Bates, D., Mächler, M., Bolker, B. M., & Walker, S. C. (2015). Fitting linear mixed-effects models using lme4. Journal of Statistical Software, 67(1). https://doi.org/10.18637/jss.v067.i01

Benjamini, Y., & Hochberg, Y. (1995). Controlling the False Discovery Rate: A Practical and Powerful Approach to Multiple Testing. Journal of the Royal Statistical Society: Series B (Methodological), 57(1), 289–300. https://doi.org/10.1111/j.2517-6161.1995.tb02031.x

Bogdanova, O. V., Bogdanov, V. B., Dureux, A., Farnè, A., & Hadj-Bouziane, F. (2021). The Peripersonal Space in a social world. Cortex, 142, 28–46. https://doi.org/10.1016/J.CORTEX.2021.05.005

Bremmer, F., Schlack, A., Shah, N. J., Zafiris, O., Kubischik, M., Hoffmann, K. P., Zilles, K., & Fink, G. R. (2001). Polymodal motion processing in posterior parietal and premotor cortex: A human fMRI study strongly implies equivalencies between humans and monkeys. Neuron, 29(1), 287–296. https://doi.org/10.1016/S0896-6273(01)00198-2

Brozzoli, C, Gentile, G., Bergouignan, L., & Ehrsson, H. (2013). A shared representation of the space near onself and others in the human premotor cortex. Curr Biol, 23.

Brozzoli, Claudio, Gentile, G., Petkova, V. I., & Ehrsson, H. H. (2011). FMRI adaptation reveals a cortical mechanism for the coding of space near the hand. Journal of Neuroscience, 31(24), 9023–9031. https://doi.org/10.1523/JNEUROSCI.1172-11.2011

Cartaud, A., Ruggiero, G., Ott, L., Iachini, T., & Coello, Y. (2018). Physiological Response to Facial Expressions in Peripersonal Space Determines Interpersonal Distance in a Social Interaction Context. Frontiers in Psychology, 9(MAY), 657. https://doi.org/10.3389/fpsyg.2018.00657

Cléry, J., Guipponi, O., Wardak, C., & Ben Hamed, S. (n.d.). Neuronal bases of peripersonal and extrapersonal spaces, their plasticity and their dynamics: knowns and unknowns. https://doi.org/10.1016/j.neuropsychologia.2014.10.022

Dureux, A., Blini, E., Grandi, L. C., Bogdanova, O., Desoche, C., Farnè, A., & Hadj-Bouziane, F. (2021). Close facial emotions enhance physiological responses and facilitate perceptual discrimination. Cortex, 138, 40–58. https://doi.org/10.1016/j.cortex.2021.01.014

Gentile, Petkova, & Ehrsson. (2011). Integration of visual and tactile signals from the hand in the human brain: an FMRI study. Journal of Neurophysiology, 105(2), 910–922. https://doi.org/10.1152/JN.00840.2010

Ghuman, A. S., Brunet, N. M., Li, Y., Konecky, R. O., Pyles, J. A., Walls, S. A., Destefino, V., Wang, W., & Richardson, R. M. (2014). Dynamic encoding of face information in the human fusiform gyrus. Nature Communications, 5, 5672. https://doi.org/10.1038/ncomms6672

Glasser, M. F., Smith, S. M., Marcus, D. S., Andersson, J., Auerbach, E. J., Behrens, T. E. J., Coalson, T. S., Harms, M. P., Jenkinson, M., Moeller, S., Robinson, E. C., Sotiropoulos, S. N., Xu, J., Yacoub, E., Ugurbil, K., & Essen, D. C. Van. (2016). The Human Connectome Project's Neuroimaging Approach. Nature Neuroscience, 19(9), 1175. https://doi.org/10.1038/NN.4361

Gogolla, N. (2017). The insular cortex. Current Biology, 27(12), R580–R586. https://doi.org/10.1016/J.CUB.2017.05.010

Graziano, M., & Cooke, D. (2006). Parieto-frontal interactions, personal space, and defensive behavior. Neuropsychologia, 44.

Grill-Spector, K., Weiner, K. S., Kay, K., & Gomez, J. (2017). The Functional Neuroanatomy of Human Face Perception. In Annual Review of Vision Science (Vol. 3, pp. 167–196). Annual Reviews Inc. https://doi.org/10.1146/annurev-vision-102016-061214

Grivaz, P., Blanke, O., & Serino, A. (2017). Common and distinct brain regions processing multisensory bodily signals for peripersonal space and body ownership. NeuroImage, 147, 602–618. https://doi.org/10.1016/j.neuroimage.2016.12.052

Haxby, J. V., Hoffman, E. A., Gobbini, M. I., Haxby, J. V., Hoffman, E. A., Gobbini, M. I., Haxby, J. V., Hoffman, E. A., & Gobbini, M. I. (2000). The distributed human neural system for face perception. Trends in Cognitive Sciences, 4(6), 223–233. https://doi.org/10.1016/S1364-6613(00)01482-0

Holt, D. J., Boeke, E. A., Coombs, G., Decross, S. N., Cassidy, B. S., Stufflebeam, S., Rauch, S. L., & Tootell, R. B. H. (2015). Abnormalities in personal space and parietal–frontal function in schizophrenia. NeuroImage: Clinical, 9, 233–243. https://doi.org/10.1016/J.NICL.2015.07.008

Holt, D. J., Cassidy, B. S., Yue, X., Rauch, S. L., Boeke, E. A., Nasr, S., Tootell, R. B. H., & Coombs Iii, G. (2014). Neural Correlates of Personal Space Intrusion. https://doi.org/10.1523/JNEUROSCI.0686-13.2014

Jaeger, T. F. (2008). Categorical Data Analysis: Away from ANOVAs (transformation or not) and

towards Logit Mixed Models. Journal of Memory and Language, 59(4), 434. https://doi.org/10.1016/J.JML.2007.11.007

Lenth, R. V. (2016). Least-squares means: The R package lsmeans. Journal of Statistical Software, 69. https://doi.org/10.18637/jss.v069.i01

Makin, T. R., Holmes, N. P., & Zohary, E. (2007). Is that near my hand? Multisensory representation of peripersonal space in human intraparietal sulcus. Journal of Neuroscience, 27(4), 731–740. https://doi.org/10.1523/JNEUROSCI.3653-06.2007

Massaccesi, C., Groessing, A., Rosenberger, L. A., Hartmann, H., Candini, M., Di Pellegrino, G., Frassinetti, F., & Silani, G. (2021). Neural correlates of interpersonal space permeability and flexibility in autism spectrum disorder Running Title: Interpersonal space regulation in autism. https://doi.org/10.1101/2020.10.14.339291

Nichols, T. E., & Holmes, A. P. (2002). Nonparametric permutation tests for functional neuroimaging: A primer with examples. Human Brain Mapping, 15(1), 1–25. https://doi.org/10.1002/hbm.1058

O'Toole, A. J., Roark, D. A., & Abdi, H. (2002). Recognizing moving faces: a psychological and neural synthesis. Trends in Cognitive Sciences, 6(6), 261–266. https://doi.org/10.1016/S1364-6613(02)01908-3

Oosterhof, N. N., Connolly, A. C., & Haxby, J. V. (2016). CoSMoMVPA: Multi-modal multivariate pattern analysis of neuroimaging data in matlab/GNU octave. Frontiers in Neuroinformatics, 10(JUL), 27. https://doi.org/10.3389/fninf.2016.00027

Pellencin, E., Paladino, M. P., Herbelin, B., & Serino, A. (2018). Social perception of others shapes one's own multisensory peripersonal space. Cortex, 104, 163–179. https://doi.org/10.1016/J.CORTEX.2017.08.033

Quinlan, D. J., & Culham, J. C. (2007). fMRI reveals a preference for near viewing in the human parieto-occipital cortex. NeuroImage, 36(1), 167–187. https://doi.org/10.1016/J.NEUROIMAGE.2007.02.029

Rolls, E. T., Huang, C. C., Lin, C. P., Feng, J., & Joliot, M. (2020). Automated anatomical labelling atlas 3. NeuroImage, 206, 116189. https://doi.org/10.1016/j.neuroimage.2019.116189

Ruggiero, G., Frassinetti, F., Coello, Y., Rapuano, M., di Cola, A. S., & Iachini, T. (2017). The effect of facial expressions on peripersonal and interpersonal spaces. Psychological Research, 81(6), 1232–1240. https://doi.org/10.1007/s00426-016-0806-x

Sambo, C. F., & Iannetti, G. D. (2013). Better Safe Than Sorry? The Safety Margin Surrounding the Body Is Increased by Anxiety. Journal of Neuroscience, 33(35), 14225–14230. https://doi.org/10.1523/JNEUROSCI.0706-13.2013

Schienle, A., Wabnegger, A., Leitner, M., & Leutgeb, V. (2016). Neuronal correlates of personal space intrusion in violent offenders. https://doi.org/10.1007/s11682-016-9526-5

Sereno, & Huang. (2006). A human parietal face area contains aligned head-centered visual and tactile maps. Nature Neuroscience, 9(10), 1337–1343. https://doi.org/10.1038/NN1777

Teneggi, C., Canzoneri, E., Pellegrino, G. di, & Serino, A. (2013). Social modulation of peripersonal space boundaries. Curr Biol, 23.

Uddin, L. Q., Nomi, J. S., Hebert-Seropian, B., Ghaziri, J., & Boucher, O. (2017). Structure and function of the human insula. Journal of Clinical Neurophysiology : Official Publication of the American Electroencephalographic Society, 34(4), 300. https://doi.org/10.1097/WNP.0000000000000377

Vieira, J. B., Pierzchajlo, S. R., & Mitchell, D. G. V. (2020). Neural correlates of social and non-social personal space intrusions: Role of defensive and peripersonal space systems in interpersonal distance regulation. Social Neuroscience, 15(1), 36–51. https://doi.org/10.1080/17470919.2019.1626763

Vieira, J. B., Tavares, T. P., Marsh, A. A., & Mitchell, D. G. V. (2017). Emotion and personal space: Neural correlates of approach-avoidance tendencies to different facial expressions as a function of coldhearted psychopathic traits. Human Brain Mapping, 38(3), 1492–1506. https://doi.org/10.1002/hbm.23467

Supplementary materials

S1. Whole-brain univariate analysis: brain regions responding to social or non-social stimuli presented in close space

The close social > far social contrast revealed brain regions eliciting greater responses in bilateral brain regions of the occipital and temporal cortex with activations in the middle and superior occipital gyrus, the calcarine sulcus, the lingual gyrus, the cuneus, the fusiform gyrus, the middle temporal gyrus and the left inferior occipital cortex. Another significant cluster in premotor and parietal cortex showed preferential activations for close compared to far social stimuli. These clusters included brain regions in the bilateral precuneus, the right SMG, the right superior parietal cortex (IPS), the premotor cortex (i.e PMv and PMd). The processing of close non-social stimuli (close non-social > far non-social contrast) engaged only one significant cluster in the occipital cortex (bilateral superior occipital cortex, lingual gyrus, calcarine sulcus and cuneus, and left middle occipital cortex). Similar results were obtained when we performed the conjunction analysis between close social > far social and close non-social > far non-social contrast. The same brain regions were found with in addition activations in the left inferior occipital gyrus, the bilateral precuneus and the left cerebellum 6. No significant clusters survived the correction for multiple comparisons for far stimuli (i.e., Far social > close social and far non-social > close non-social contrasts). All results are detailed in the table 1 and depicted in figure 4.

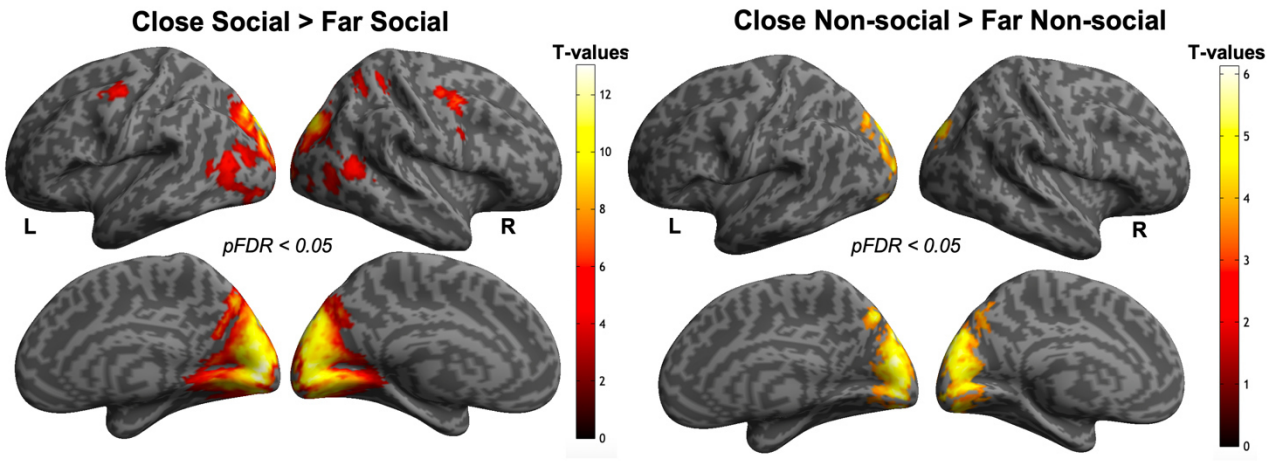

Figure S1. Brain regions showing significant preferential activations for close social (human faces) or non-social (objects representing shapes) stimuli compared to far: whole-brain univariate analysis for close social > far social and close non-social > far non-social contrast. Both contrasts are superimposed in a render brain: results of the group-level statistical analysis for close social > far social contrast is depicted in red and results of the group-level statistical analysis for close non-social > far non-social contrast is shown in green. Activation threshold set at cluster-forming $p < 0.001$ uncorrected, and FDR-corrected $p < 0.05$ at the cluster level.

Table S1. Brain regions displaying greater activation for close relative to far stimuli for social **(Close social > Far social)** and non-social stimuli **(Close non-social > Far non-social) (1),** and results for contrasts of far relative to close stimuli **(3).** Results of conjunction analysis are also reported, the first between the social and non-social of close relative to far contrasts and the second between happy, neutral and angry of close relative to far contrasts as detailed in the main text of the paper **(2).** Activation threshold is set at cluster-level FDR-corrected $p < 0.05$. Cluster size in voxels and MNI coordinates of the peak voxel for each region in significant clusters are reported with the t-values associated. Anatomical locations of the corresponding cluster and brain regions associated are reported from AAL3 atlas (Rolls et al., 2020).

			MNI coordinates			
Anatomical location	R/L	Cluster size	x	y	z	T
(1) Univariate analysis : close effect contrasts						
Close social > Far social						
Lingual gyrus	**R**	**6686**	**11**	**-84**	**-3**	**13.34**
	L		-14	-73	-6	8.77
Calcarine sulcus	R		14	-84	8	10.15
	L		-6	-84	8	10.35
Middle occipital gyrus	R		30	-76	28	5.20
	L		-42	-76	8	5.24
Cuneus	R		11	-84	34	11.23
	L		-6	-84	28	10.49
Superior occipital gyrus	R		22	-81	31	10.06
	L		-20	-87	28	9.83
Precuneus	R		11	-73	45	6.30
	L		-3	-78	45	5.49
Middle temporal gyrus	R		44	-64	11	4.95
	L		-45	-64	8	4.90
Fusiform gyrus	R		28	-78	-14	5.41
	L		-28	-76	-14	4.99
Inferior occipital gyrus	L		-28	-84	-8	5.63
Cerebellum 6	R		11	-73	-17	6.89
	L		-12	-73	-17	8.65
Precentral gyrus (*dorsal premotor, PMd)	**R**	**223**	**42**	**-3**	**53**	**6.50**
	L	**125**	**-42**	**-6**	**50**	**5.33**
Superior parietal lobule (*IPS)	**R**	**133**	**25**	**-53**	**53**	**5.03**
SupraMarginal gyrus	**R**	**102**	**58**	**-31**	**39**	**4.43**
Close Non-social > Far Non-social						
Cuneus	**L**	**2478**	**2**	**-78**	**20**	**6.15**
	R		11	-84	36	5.15
Calcarine sulcus	R		8	-87	6	5.34
	L		2	-84	11	4.80
Lingual gyrus	R		14	-84	-6	6.14
	L		-12	-84	-8	4.94
Superior occipital gyrus	R		22	-84	34	5.13
	L		-17	-87	28	5.08
Middle occipital gyrus	L		-20	-95	0	5.01
(2) Univariate analysis : conjunction						
(Close social > Far social) ^ (Close Non-social > Far Non-social)						
Cuneus	L	**2433**	**2**	**-78**	**20**	**6.15**
	R		8	-78	20	5.14
Calcarine sulcus	R		8	-87	3	5.38
	L		0	-90	0	4.55
Lingual gyrus	R		14	-84	-6	6.14
	L		-9	-81	-8	4.08
Superior occipital gyrus	R		25	-81	34	4.40
	L		-20	-84	28	4.29
Middle occipital gyrus	L		-20	-92	6	4
Inferior occipital gyrus	L		-26	-87	-8	4.54
Precuneus	R		11	-73	45	4.44
	L		-3	-76	42	3.66
Cerebellum 6	L		-9	-76	-17	3.75
(Close happy > Far happy) ^ (Close neutral > Far neutral) ^ (Close angry > Far angry)						
Lingual gyrus	**R**	**3183**	**11**	**-84**	**-3**	**8.12**
	L		-12	-84	-6	6.66
Calcarine sulcus	R		14	-84	6	6.27
	L		0	-79	10	6.14
Cuneus	R		11	-81	28	6.32
	L		-3	-81	28	6.85
Superior occipital gyrus	R		22	-84	28	5.33
	L		-20	-84	25	6.34
Fusiform gyrus	R		28	-78	-8	3.26
	L		-26	-73	-14	3.44
Precuneus	R		8	-76	48	3.73
Cerebellum 6	R		11	-70	-17	3.70
	L		-9	-73	-14	5.51
Vermis 6			2	-70	-8	3.76
(3) Univariate analysis : far effect contrasts						
Far social > Close social						
No significant clusters						
Far Non-social > Close Non-social						
No significant clusters						
(2) Univariate analysis : conjunction						

ETUDE 5

Régulation de l'espace personnel chez les patients avec des lésions unilatérales médio-temporales

---

Personal space regulation in patients with unilateral medio-temporal lesions

Audrey Dureux, Luca Zigiotto, Silvio Sarubbo, Clément Desoche, Alessandro Farnè, Nadia Bolognini and Fadila Hadj-Bouziane

Article en préparation

Personal space regulation in patients with unilateral medio-temporal lesions

Audrey Dureux[1,2], Luca Zigiotto[3], Silvio Sarubbo[3], Clément Desoche[2,4], Alessandro Farnè[1,2,4,5], Nadia Bolognini[6,7] and Fadila Hadj-Bouziane[1,2]

1. Integrative Multisensory Perception Action & Cognition Team - ImpAct, INSERM U1028, CNRS UMR5292, Lyon Neuroscience Research Center (CRNL), Lyon, France
2. University UCBL Lyon 1, University of Lyon, Lyon, France
3. Department of Neurosurgery, Azienda Provinciale per i Servizi Sanitari (APSS), "Santa Chiara Hospital", Trento, Italy
4. Hospices Civils de Lyon, Neuro-Immersion & Mouvement et Handicap, Lyon, France
5. Center for Mind/Brain Sciences (CIMeC), University of Trento, Italy.
6. Department of Psychology, University of Milano Bicocca, Milano, Italy
7. Laboratory of Neuropsychology, IRCCS Istituto Auxologico Italiano, Milano, Italy

Corresponding authors:
Audrey Dureux, and Fadila Hadj-Bouziane, INSERM U1028, CNRS UMR5292, Lyon Neuroscience Research Center, ImpAct Team, 16 Avenue Doyen Lépine 69500 Bron, France.
Emails: audrey.dureux@inserm.fr; fadila.hadj-bouziane@inserm.fr.

Conflict of Interest: The authors declare that they have no conflict of interest.
Acknowledgements: This work was funded by the French National Research Agency ANR-15-GE37-0003 grant MySpace to FHB.

Funders had no role in study design, data collection and analysis, decision to publish, or preparation of the manuscript.

Abstract

In everyday life, we constantly face situations involving interactions with others. These social interactions require individuals to automatically adjust their physical distance to avoid discomfort and anxiety. This physical distance is termed personal or interpersonal space and depends on various factors such as the type of relationships shared by individuals, their physical appearance and their emotional state and personality traits. To the best of our knowledge, only a single case study with selective bilateral lesions of the amygdala, has provided strong support for a role of the amygdala in the regulation of personal distances (Kennedy et al., 2009). This study shows that the integrity of both amygdalae is essential to regulate these distances. While unilateral lesion to the amygdala and lesion to other sectors of the medial temporal cortex also affects social behavior, their implication in the regulation of interpersonal distances has never been investigated.

Here we sought to fill this gap by testing three patients with unilateral temporal lesions, including one with lesion which was entirely confined to the amygdala while the amygdala was spared in the other two patients. Our results showed that a unilateral damage to the temporal lobe, including or not the amygdala, appears to be sufficient to cause inappropriate regulation of social distances. All 3 patients chose shorter interpersonal distance compared to neurotypical control subjects. Compared to controls, the patients did not adjust the distances depending on the facial emotional expression of the approaching face despite a preserved ability to categorize the emotion. Finally, the patients and the control group also had different heart rate (HR) responses when viewing approaching faces.

This study brings new evidence demonstrating that the unilateral lesion within the medial temporal cortex, restricted or not to the amygdala, is sufficient to alter the interpersonal distance that governs our social interaction.

1. Introduction

Social situations make people adjust their distance automatically between each other. This physical distance, termed personal or interpersonal space, depends on the relationships between individuals and the social context where the interaction takes place (Hall et al., 1968; Hayduk, 1983). In everyday life our social distances continuously adapt, for example if we take part in a family meeting, if we are in a work environment or when we are in a crowded train, elevator, or street with strangers.

In the laboratory, interpersonal space is typically assessed with the "stop-distance paradigm". Participants face an experimenter located about 3 meters away and moving toward them (or vice versa). They have to stop the experimenter (or themselves) nearest to the distance they start feeling uncomfortable with the other's proximity. Violation of this invisible boundary creates a sense of discomfort in individuals. In healthy participants, the interpersonal distance typically varies between 60 cm and 160 cm depending on the condition (i.e. active or passive version of the task) (Iachini et al., 2014a, 2015, 2016; Ruggiero et al., 2017). Its extent also depends on the participant's personality traits and is also influenced by the confederates' attributes, such as its age and sex (Iachini et al., 2015, 2016; Ruggiero et al., 2019) or their emotional states (Cartaud et al., 2018; Ruggiero et al., 2017).

Previous studies revealed that the amygdala is a critical node in this regulation of physical distances between individuals. The most direct evidence of this implication comes from a case study of a patient (SM) with a rare genetic disease (Urbach-wiethe), that leads to selective, bilateral damage to the amygdala (Kennedy et al., 2009). Compared to controls, SM did not feel any discomfort with the proximity of others. Her interpersonal distance with the experimenter was 34 cm, half shorter compared to that of neurotypical control subjects. In addition, in the same study, the authors reported increased amygdala activation as measured with fMRI, when control subjects were made to believe that another person was close, as compared to far from them. Based on these findings, Kennedy and collaborators suggested that the amygdala is crucial for those feelings of discomfort with close physical proximity that help maintain socially appropriate interpersonal distance. This proposal may also be related to the alteration in patients with bilateral amygdala lesions of physiological and subjective responses to emotionally salient stimuli, particularly fear-related responses (Adolphs et al., 1999; Davis & Whalen, 2001; Ledoux & Brown, 2017) (Masaoka et al., 2003). This suggests that the feeling of discomfort

when one violates our personal space might be triggered by the stimulation of the autonomic system following amygdale activation. This is supported by a recent study demonstrating that amygdala stimulation in controls subjects strongly modulated autonomic activity (i.e. large changes in HR) (Inman et al., 2020). This seems also coherent with the role of the amygdala in social approach and avoidance (Capitanio et al., 2006; Emery et al., 2001; Kennedy et al., 2009) and more generally, in its contribution to the processing of emotionally and socially relevant information (Adolphs, 2010; Martin & Weisberg, 2003; Noack et al., 2015).

Thus far, available evidence suggests that, compared to bilateral amygdala lesions, patients with unilateral amygdala damage exhibit less marked deficits (Adolphs et al., 1995) and the degree of impairment seem to depend on the side of lesion (Adolphs et al., 2001; Fowler et al., 2006). Yet, the impact of a unilateral lesion involving the amygdala onto the regulation of interpersonal distance has never been tested. In addition, and beyond the amygdala, other brain regions of the temporal lobe are thought to play a role in social cognition (Duffau, 2021; Sarubbo et al., 2015, 2020; Vilasboas et al., 2017), yet their implication in the regulation of interpersonal distances has also never been investigated to the best of our knowledge. Studies in monkeys for instance have revealed that after bilateral temporal pole (TP) lesions, the animals showed marked deficits in social interactions, in particular they exhibited a loss of emotional attachments to their infants and to other conspecifics (Bucher et al., 1970; Kling & Steklis, 1976). A similar clinical picture was reported in a case study describing a patient who underwent right temporal lobectomy and lost all emotional attachments to his family members, although he was still able to recognize all of them (Lipson et al., 2003). Given that electrical stimulation of the human TP, like the amygdala, alters autonomic responses such as heart rate, respiratory rate and blood pressure, it is possible that the lesion prevented this physiological response reflecting social attachment (Gloor et al. in 1982).

Based on this evidence, it is tempting to suggest that the regulation of interpersonal distance that governs our social interactions may not be strictly dependent on the integrity of both amygdalae, but rather might depend in part on a set of regions within the temporal cortex. In this context, we sought to investigate whether and to what extent unilateral temporal lobe lesion may cause deficits onto the regulation of personal distances during social interactions. Our goal was to characterize behavioral and physiological signatures of three patients with unilateral medial-temporal lesions, including one entirely confined to the left amygdala, in the regulation of distance in emotional contexts. As no other study has so far been reported, we aim to extend our understanding in personal space regulation by investigating whether a unilateral

amygdala lesion elicits similar deficit in personal space regulation in different emotional contexts, also exploring the impact of a lesion largely confined to the amygdala to that of lesions comprising nearby regions of the temporal lobe.

We therefore tested such patients on the stop distance paradigm in a virtual reality (VR) environment (experiment 1) and in a real setting (experiment 2). In both experiments, the participants were asked to stop virtual faces or real confederates moving towards them at the nearest distance they start feeling uncomfortable with the confederates' proximity. In the 1st experiment with VR setting, faces depicted three different emotions: happy, neutral, or angry. The participants' heart rate frequency was also recorded during the 1st experiment to evaluate the impact of unilateral medial-temporal lesions onto the physiological state.

2. Materials and Methods

2.1. Participants

We recruited three patients with postsurgical unilateral temporo-mesial resections. Patients underwent awake (P1 and P2) or asleep surgery (P3) for glioma or metastasis resection at the Department of Neurosurgery of the Azienda Sanitaria per i Servizi Sanitari (APSS, "S. Chiara Hospital", Trento, Italy). For awake surgery, the cortical and subcortical mapping was performed with 60Hz, 1ms and amplitude ranging between 2-4mA, setting the threshold when eliciting speech arrest at the level of the ventral pre-motor cortex (VPMC)(Zacà et al., 2018), stopping the resection when functional responses were elicited at cortical and subcortical stimulation of the eloquent structures; intraoperative neuropsychological assessment had been customized for every patient, as already reported (Dallabona et al., 2017; Sarubbo et al., 2021; Zigiotto et al., 2020). For the asleep procedure, the resection stopped after the complete resection of the enhancing area. All the surgeries were assisted by neuronavigation (Steatlh Station 7, Medtronic, Minneapolis, MN, USA). Before taking part in the experiments, all three patients signed an informed consent, and the study was approved also by the ethical committee of the Azienda Provinciale per i Servizi Sanitari (Rep. Int. 14854 del 12/09/2019, Verbale VI/2019). Every patient underwent a complete neuropsychological assessment within 1 week of the experiment, including tests for Language, Attention, Executive functions, Memory, Visuo-spatial cognition, Praxis and, importantly, Social cognition, as previously reported (Zigiotto et al., 2020). Interestingly none of them showed cognitive deficit in any domain, with

the exception of P3 who had a mild impairment in long-term verbal memory (Rey's 15 words delayed recall score under cut-off). Moreover, the Frontal Behavioral Inventory (FBI) (Alberici et al., 2007), a psychological scale useful to detect behavior and personality changes especially in behavioral fronto-temporal dementia, was administered to every patient's caregiver (i.e. wife) in order to identify changes and/or inappropriate behavior in patient's social interactions. For P1 mild/occasional changes in "aspontaneity", "disorganization" and "loss of insight" were reported; for P2 mild/occasional changes were observed in "apathy", "indifference", "perseveration", "irritability" and "restlessness", with a moderate change in "inflexibility"; finally, P3 showed mild/occasional changes in "aspontaneity", "indifference", "disorganization", "inattention", "loss of insight" and a moderate change "hyperorality". Importantly, no difference was reported for any patient in "inappropriateness" items, which is focused on the ability to keep and maintain social rules.

Concerning the lesion assessment, firstly lesion surgical cavities were mapped by a neurosurgeon, blind to the experimental results, based on each subject structural T1 with gadolinium MRI, acquired within 1 month of the testing days. Then, lesion volume estimates were made by transforming each subject' MR T1 to the standard MNI space using SPM (Friston et al., 2007) and were then aligned on the AAL3 atlas (Rolls et al., 2020). For each subdivision of the AAL3 atlas (i.e. 170 ROIs across all the brain), we computed the percent of lesioned voxels for each patient by dividing the number of voxels that intercepted between the lesion surgical cavity and each ROI by the total number of voxels within each ROI. Figure 1 shows the surgical lesions cavities superimposed on postsurgical MR T1 images of the three patients.

We compared these 3 male patients to 10 neurologically and psychiatrically healthy males recruited through web advertising. The healthy control group was selected to match to patients on age and level of education (age: 54.8 ± 4.98 (mean ± SD), education: 14.4 ± 1.65 (mean ± SD) and were tested on all the experimental tasks at the Impact laboratory (Lyon, France). All gave written informed consent and were paid for their participation. The study followed the Declaration of Helsinki standards and was approved by the Institut National de la Santé et de la Recherche Médicale (INSERM) Ethics Committee (IRB00003888, No. 16-341).

Table 1. Details concerning each patient and their lesion (i.e. location and ratio in percent for each brain region impacted).

							Brain regions impacted by the lesion				
	Sex	**Age**	**Education**	**Type of surgery**	**Lesion location**	**Testing since surgery**	**PHC (%)**	**HC (%)**	**AMY (%)**	**FUSI (%)**	**TP (%)**	**MT (%)**
P1	M	53	13	Awake surgery for Low Grade Glioma in February 2014 (47 years old)	Left medial-temporal lobe	Tested in 2019 (60 months after surgery)	11.35	5.69	64.43	-	32.7	0.31
P2	M	58	13	Awake surgery for Low Grade Glioma in January 2019 (57 years old)	Left medial-temporal lobe	Tested in 2019 (10 months after surgery)	7.48	-	-	8.14	4.83	11.37
P3	M	61	8	Asleep surgery for Renal Metastasis in January 2020 (61 years old)	Right medial-temporal lobe	Tested in 2020 (1 month after surgery)	22.43	3.59	0.96	9.46	-	13.57

Brain regions damaged by the lesion: values represent the ratio (in percent) of lesioned voxels for each patient. This ratio has been obtained by divided the number of voxels that intercepted between the lesion mask and each ROIs from the AAL3 atlas (Rolls et al., 2020) by the number of voxels within each ROI. PHC= parahippocampal cortex; HC= hippocampus; AMY= amygdala; FUSI= fusiform gyrus; TP= Temporal Pole; MT= Middle Temporal Gyrus.

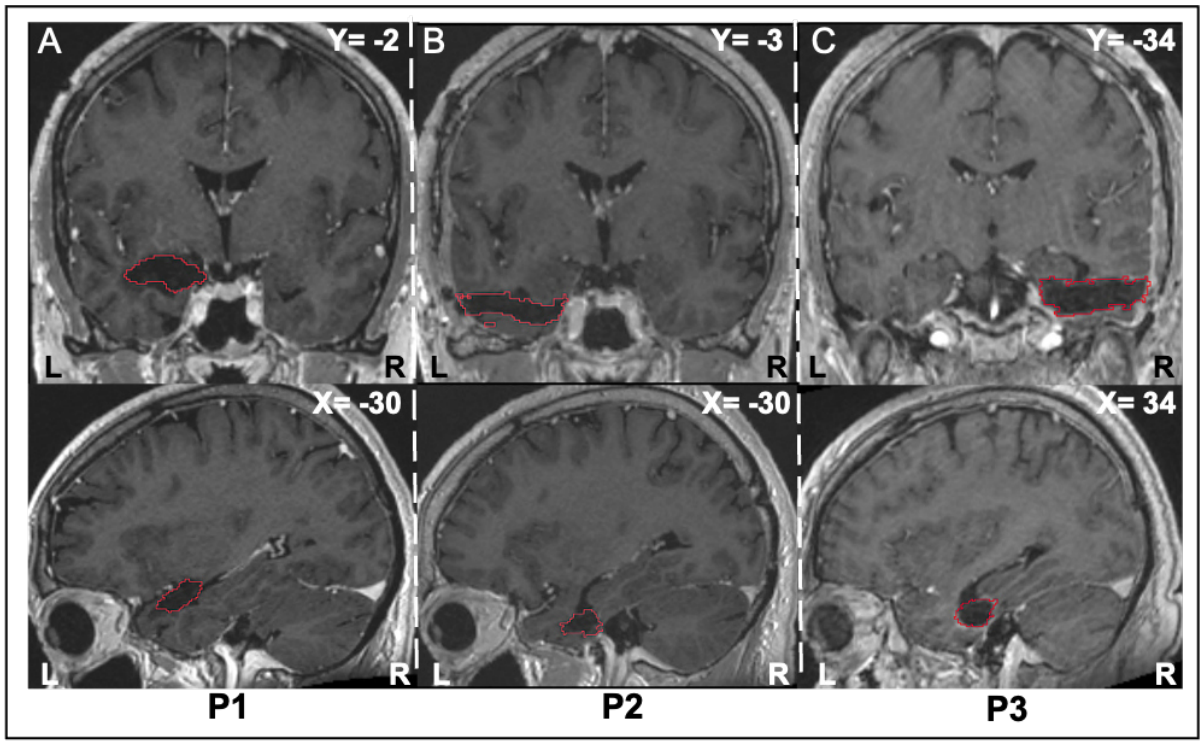

Figure 1. Postsurgical MR T1 images of three patients with surgical cavity of their unilateral temporo-mesial lesions superimposed. For each patient **(A=P1, B=P2, C=P3)**, surgical cavity of lesions are represented in each anatomical T1 sequence in coronal (upper images) and sagittal (lower images) planes. **A.** Patient P1 was submitted to a large resection involving the left amygdala extending toward the temporal pole and the middle temporal gyrus and incorporating the parahippocampal cortex and the hippocampus. **B.** Patient P2 was submitted to a resection centered to the left anterior temporal lobe including the temporal pole, the left middle temporal gyrus, the left fusiform gyrus and the left parahippocampal cortex. **C.** Patient P3 was submitted to a resection involving the right middle temporal gyrus, the right amygdala, the right fusiform gyrus, the right hippocampus and the right parahippocampal cortex.

2.2. Experimental protocols

2.2.1 Stop distance paradigms: measure of interpersonal distance

We carried out two versions of the stop distance paradigm. The participants first completed this task in a virtual reality environment with faces depicting three different emotions (experiment 1, virtual setting) and then completed the traditional version of the task, involving a setting in which the experimenter moves toward the participants (experiment 2, real setting) In the first experiment, we also measured the heart rate frequency. The aim of the second experiment was to assess the ecological validity of the VR experiment.

Experiment 1: Stop distance task in virtual reality setting

Apparatus and stimuli

Visual stimuli were presented in a VR environment. The scene was rendered in an Oculus Rift DK2 Head-Mounted Display (HMD), with a resolution of 960x1080 per eye, a frequency of 75Hz, a field of view equal to 106°. The HMD had an embedded 75 Hz eye-tracking system (SMI). The augmented technology Unity software (Version 5.1.2; Unity Technologies, San Francisco, CA) was used to create the virtual environment, display the stimuli and record participants' responses. Visual stimuli were presented in the VR environment and participants provided responses using the index fingers of the dominant hand by pressing the spacebar on a computer keyboard. During the whole course of the experiment, a photoplethysmogram transducer (PPG, TSD200, Biopac) was attached to the right index finger of the participants to measure heart rate (HR); the signal was recorded via a Biopac system (MP150, PPGED- EDA device) at a frequency of 1kHz. Visual stimuli consisted of 4 individuals' faces (2 females and 2 males) each mimicking 3 emotions (happy, neutral, angry). They were drawn from the Karolinska Directed Emotional Faces database (KDEF, Goeleven et al., 2008). We further processed these images in the following way: stimuli were cropped to an oval shape, to remove outline and external features (e.g. hairs); images were corrected for luminance, such that the mean luminance did not differ across sex or emotion of the faces. Each image measured 30 cm and the size was scaled as a function of distance as the faces were presented in looming direction.

Procedure

Participants sat in a quiet room, wearing a virtual reality headset (HDM). The VR environment consisted of an empty room, as to minimize the presence of distracting elements (Dureux et al., 2021). The instruction gave to the participants was to: "press the button as soon as the distance between you and the face makes you feel uncomfortable".

After a 5 points calibration of the eye-tracker, trials started with a white fixation cross, presented in the center of the visual field. If the subject correctly fixated the cross for 4000 ms, its color became blue, and it was followed by the presentation of one face stimulus randomly chosen among male or female faces, its identity (2 levels for each sex) and its emotion (happy, neutral, angry). The virtual stimulus then loomed towards them at a constant speed (0.5 m/s) (Iachini et

al., 2016; Ruggiero et al., 2016) until they stopped them by pressing the button and the face disappeared. The starting distance from the virtual face to the participant was randomized between 3 distances: 2.8 m, 3 m and 3.2 m to avoid the habituation of the starting line for the participant.

Each virtual stimulus was presented a total of 36 times per emotion (18 for each male or female face), with a total of 108 trials, except for P3 where a total of 18 trials per emotion was presented (54 trials in total). The task lasted about 20 min and a break could be introduced at any time during the experience by removing the HMD.

During the whole experiment, participants kept their left arm passively lying on the table in front of them with a photoplethysmogram transducer attached to their left index finger. The experiment started when the physiological signal (heart rate) appeared stable, typically from 5 sec to 1 minute, based on the experimenter's visual inspection.

Experiment 2: Stop distance task in real setting

Apparatus and confederates

The experimental session took place in an empty rectangular room in the Division of Neurosurgery, "S. Chiara Hospital" (Trento, ITALY) for the testing of the three patients and in the Impact laboratory (CRNL, INSERM U1028, Lyon, FRANCE) for the testing of the healthy subjects.

For P1 and P2, one confederate, one female, took part in the study. For P3, in addition to the female confederate, a male confederate also took part in the study. For the healthy subjects, as for P3, the two confederates took part in the study. The confederates were unfamiliar to the patients and healthy subjects. During the experiment, the confederate wore neutral casual clothes without accessories. They were instructed to maintain a neutral expression, to keep their gaze on the chest of the participant and to move at roughly the same speed and arm swing while walking.

Procedure

The experiment was divided into two blocks, one active approach condition and one passive approach condition. In the active approach, the confederate remained motionless and participants walked towards them until they stopped. In the passive approach, participants stood still and saw the confederate walking towards them until they stopped the confederate.

In the passive condition, the instructions to the participants were similar to Exp. 1 (i.e., "stop the confederate as soon as the distance between you and the confederate makes you feel uncomfortable"). In the active condition, the instructions were to "stop as soon as the distance between you and the confederate makes you feel uncomfortable".

The starting distance from participant to confederate was counterbalanced among 2.8, 3 and 3.2 m (as in the first experiment in VR). For P1 and P2, a total of 10 trials were performed with the female confederate (5 trials in passive approach and 5 trials in active approach). For P3 and healthy subjects, a total of 20 trials was performed, 10 trials with each male or female confederate (5 trials in passive approach and 5 trials in active approach). Once the participant stopped the confederate (passive-approach) or himself (active-approach), the chin-to-chin participant-confederate distance was measured using a digital laser distance measurer (Bosch GLM 20 Blaze 65'). At the end of each trial, the participant and confederate came back to the starting point. The Order of blocks was counterbalanced across participants.

Data and statistical analysis for experiment 1 and 2

All behavioral and physiological signal (i.e. heart rate) were analyzed with the open-source software R (The R Core Team, 2013).

Data analysis

Interpersonal distance response for VR paradigm task. The distance (in meter) at which the participant stopped the virtual face was recorded. The mean distance was also computed according to the different parameters of the task: 1) Feature of faces presented (Happy, neutral and angry emotions), 2) Sex of faces (male or female) and 3) Identity of faces (ID 1 to ID 6). Patient P2 reported not feeling uncomfortable with the face stimuli moving forward and never pressed the key to stop the face stimuli. In this case, negative values were obtained as the face crossed the boundary of the screen. The same happened in some trials with P3. We replaced negative values by 0 to facilitate graphical representation.

*Interpersonal distance response for real paradigm task***.** The mean participant-to-confederate distance (in m) was computed across conditions. The mean distance was also computed under each passive and active approach condition and depending on the experimenter (i.e. male or female).

Heart rate. The heart rate signal recorded during the experiment was analyzed with AcqKnowledge software (Biopac) to obtain averaged heartbeat per minute (bpm) for each participant in each trial. For that, we first detected all the inter-beat RR peaks automatically. Then, we manually inspected the signal and corrected for any mistakes with the automatic identification. The number of R peaks for 1 minute corresponds to the number of contractions (beats) of the heart per minute (bpm), i.e. heart rate frequency (HR). We computed the averaged heartbeat per minute (i.e. mean HR) during each entire period of stimuli presentation (i.e. interval of 6 sec) and also during each fixation cross period presented before the stimuli presentation in order to obtain baseline periods (i.e. interval of 4 sec). Then, for each participant and for each trial, we computed the mean delta HR by subtracting each mean HR obtained during period of stimulation by mean HR obtained in each baseline periods. The delta HR allow to determine the effect of faces stimuli presentation on participants' HR and to be able to compare these fluctuations between individuals. As for the mean preferred distance, we also computed delta HR according to the different parameters of the task (i.e. feature of faces presented, sex of faces and identity of faces).

Statistical analysis: Comparison between patients and controls

Analysis of single-case studies requires special statistical methods (McIntosh & Brooks, 2011). The interpersonal distance response obtained in stop-distance paradigm tasks (i.e. with real confederate or in virtual reality) or the delta HR was compared with the averaged interpersonal distance response or delta HR of the healthy control group using modified paired t-test designed specifically for case report studies and allowing to control for type I errors when comparing the patient's and controls' performance scores (Bayesian Test of Deficit). The method described by Crawford & Garthwaite (2007) and Crawford et al. (2010) estimates, within a Bayesian framework, the point of abnormality of the patient's score and the associated 95% credible limits (CL). In addition, the patient's score provides the percentage of the healthy population obtaining a score lower than the patients. When appropriate, we also included covariates (i.e. level of education and age of healthy subjects and patients) in our Bayesian Test of Deficit (Crawford et al., 2011). After having tested the normality distribution of our variables, non-parametric spearman test was performed to compute correlations between our variables of interest (i.e. comfort distance and delta HR) with each covariate. As recommended in Crawford et al. 2011, we chose to add a covariate when the correlation of a covariate with the dependent variable exceeded 0.3. To perform Bayesian Test of Deficit with or without

covariates we used the package *singcar* implemented on R studio with "BTD()" and "BTD_cov()" functions.

Given the complexity of the design of the stop distance tasks, we also compared the patients' and controls' performances (i.e. preferred distance and delta HR) with mixed-effect multiple regression models using the lm4 package for R (Bates et al., 2015). We used a Linear Mixed-effect Models, a powerful tool in the analysis of single-case data allowing to compare the patients' and controls' performances even in complex study designs (Huber et al., 2015; Wiley & Rapp, 2019), on the interpersonal response distance and delta HR. As a first step, we defined a model containing the most appropriate random and fixed effects with respect to our previous study (Dureux et al., 2021). For the VR stop distance task, the final model included the participant, the sex of face stimuli and their starting distance of stimuli as random factors and the group (i.e. patient and controls), the emotion type and their interaction as fixed factors. For the real stop distance task in a real setting, the final model included as fixed factors the group, the condition (i.e. passive or active) and their interaction and as random factors the subject and the experimenter (i.e. male or female). All post-hoc analyses for significant tests were computed on the basis of least-squares means (Lenth, 2016), using False Discovery Rate (FDR, Benjamini & Hochberg, 1995) correction for multiple tests. In all tests used (i.e. Bayesian Test of Deficit and Linear Mixed-effect Models) p-values $< .05$ were considered significant.

To assess that performance in VR and real-life was related, we performed Pearson correlations tests between mean interpersonal distance of patients and control group obtained in the two settings.

2.2.2 Evaluation of emotional rating: validation task (VT)

We presented 18 stimuli sequentially, among which the four face stimuli that were used in experiment 1, on a 2D monitor screen and asked subjects to judge whether the displayed emotion was neutral, happy or angry using a 9 points Likert scale (range: -4 - +4) presented below each face stimulus. In the scale, the minimum value (-4) indicated an angry face, the maximum (+4) a happy one, with intermediate values indicating neutral expressions. The open-source OpenSesame software (Mathôt et al., 2012) was used to display stimuli and collect responses. No time-limit was given. This task was presented after the first experiment (i.e. stop distance VR task) and the aim was to ensure the categorization of emotion depicted by faces.

Results were analyzed with the open-source software R (The R Core Team, 2013). The rating score obtained for each emotion was compared between the control group and each patient using a modified Bayesian test designed specifically for case report studies (Crawford and Garthwaite, 2007) in order to determine if there is any difference in facial emotional rating between groups.

3. Results

3.1. Behavioral data: evaluation of interpersonal distances with the stop distance tasks

Experiment 1: stop distance virtual reality task with looming faces stimuli

Firstly, we assessed the relationship between the participants' age and level of education with their behavioural results on the stop distance task. The level of education was negatively correlated with the mean preferred distance (r= -0.56, *p*=0.093, BF=1.1), while the age was not correlated (r= -0.10, *p*=0.78, BF=0.51). As suggested by Crawford et al. (2011), for the statistical comparison between controls and patients, we decided to include the level of education as a covariate as its correlation with our dependent variable exceeded 0.3. Figure 2A represents the interpersonal distance responses of the control group and patients. Table 2 reports the results obtained when comparing the mean preferred distances for each patient (P1 to P3) and control group regardless of the facial emotional expression presented. Overall, all patients have a mean preferred distance shorter as compared to the control group, which were significant for P2 and P3 [M ± SD = 0.77 m ± 0.30, P1 = 0.42, Zcc = -1.87, PA= 7.27, *p*= 0.07; P2 = 0.06, Zcc= -3.25, PA= 1.14, *p*= 0.01; P3= 0.27, Zcc= -4.28, PA= 2, *p*= 0.02]. P2 reported not feeling uncomfortable hence he did not press the key to stop the face stimuli moving forward, with mean preferred distance close to 0 meter (Table 2). A similar trend is observed for P1 with a shorter mean preferred distance compared to the control group, albeit not significant (Table 2).

Table 2. Results of the comparison between patients' (P1, P2, P3) and controls group' (n=10) interpersonal response distance obtained with Bayesian Test of Deficit (Crawford and Garthwaite, 2007).

			Control group			One-tailed test	Estimated percentage of the control population obtaining a lower score than the patient (PA)		Estimated effect size (Z_{cc})	
Task		**Patient's distance**	**n**	**Mean**	**SD**	***p***	**Point**	**(95% CI)**	**Point**	**(95% CI)**
SD – VR paradigm *	**P1**	0.42	10	0.77	0.30	0.07	7.27	(0.17 to 29.36)	-1.865	(-2.94 to -0.54)
	P2	0.06				****0.01**	1.14	(0.00 to 9.16)	-3.247	(-4.77 to -1.33)
	P1	0.27				***0.02**	2	(0.00 to 21.78)	-4.284	(-7.22 to -0.78)
SD – real paradigm	**P1**	0.19	10	0.71	0.23	***0.028**	2.79	(0.02 to 14.16)	-2.291	(-3.49 to -1.07)
	P2	0.29				***0.05**	5.44	(0.21 to 21.43)	-1.863	(-2.87 to -0.79)
	P3	0.28				***0.05**	5.43	(0.18 to 21.99)	-1.868	(-2.91 to -0.77)

**We included the level of education as covariate in the test as it correlated with Distance response (r>0.3). Estimated effect size in this case corresponded to Z_{ccc}*

***PA**, point of abnormality of the patient's score*

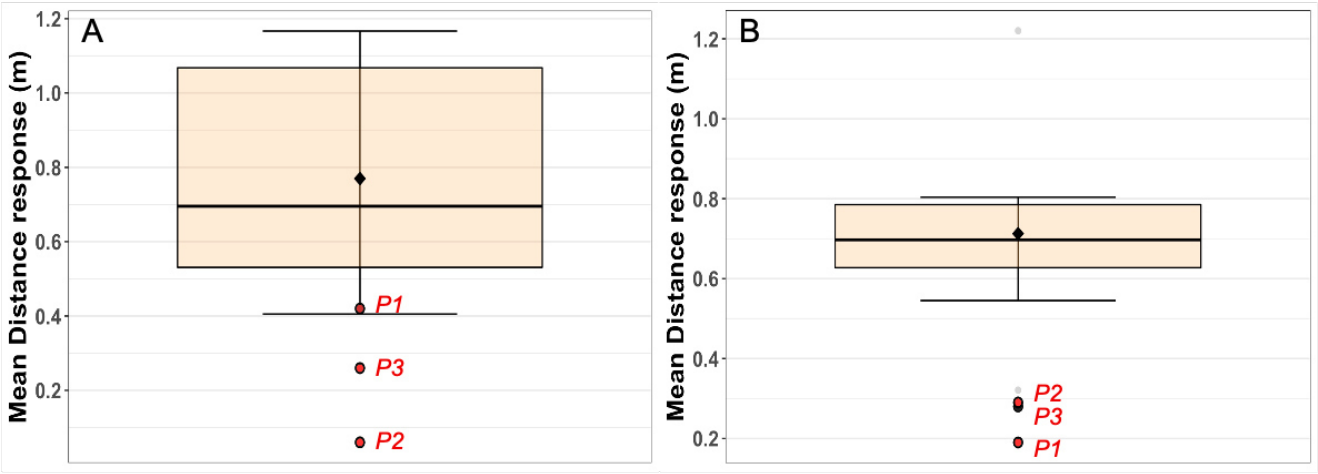

Figure 2. Behavioral results of stop distance virtual reality (A, experiment 1) and real setting (B, experiment 2) tasks: interpersonal distance in control group (n=10) and in patients P1, P2 and P3. **A:** Box-plot depicting control group' interpersonal response distances in meter from the virtual reality stop distance task. **B:** Box-plot depicting control group' interpersonal response distances in meters from the stop distance real setting task. In these plots, the mean interpersonal distance is represented by the black diamond in each fill box. The three red points outside each boxplot represent the mean interpersonal distance for each patient (P1, P2 and P3). The vertical length of each box represents the interquartile range, the thick horizontal line represents the median, and the whiskers indicate the full range of values. Grey dots outside the whiskers represent values exceeding 1.5 times the interquartile range.

The mixed-effect generalized linear model revealed a significant main effect of Group [$F(1,11.02)=7.89$, $p= 0.02$] and Emotion [$F(2, 1328.73)=14.58$, $p<0.001$] and a significant interaction of Group *Emotion [$F(2, 1328.73)= 4.04$, $p=0.02$]. Healthy subjects preferred larger distances compared to patients (controls-patients: $z= 2.81$, $p=0.005$). Post-hoc test indicated that this difference between controls and patients in interpersonal distances was observed for each emotion (angry: $z=2.99$, $p=0.003$; happy: $z= 2.60$, $p=0.009$; neutral: $z=2.81$, $p=0.005$). Moreover, as illustrated in Figure 3, the control group exhibited significant differences in their preferred distances according to the emotion presented. In particular, they preferred larger distances when angry faces were approaching compared to happy and neutral faces (angry-neutral: $z=3.49$, $p=0.0007$; angry-happy: $z=6.059$, $p<0.0001$). By contrast, the patients displayed no significant difference in preferred distance depending on the emotion presented (all $|z|<0.5$, $p=0.89$).

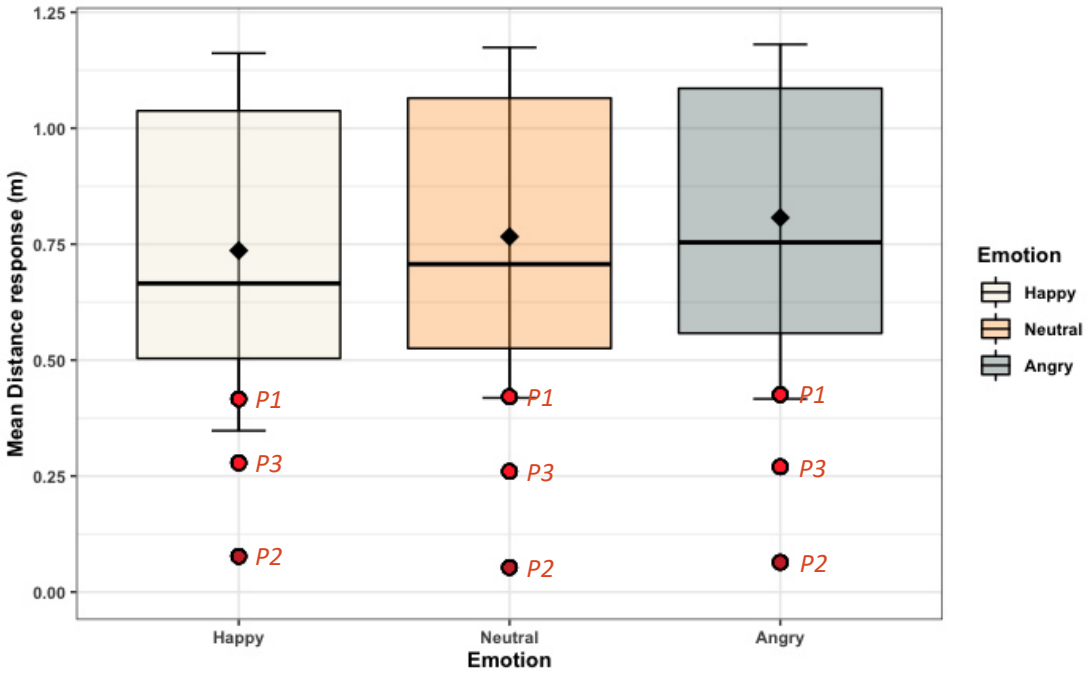

Figure 3. Behavioral results of stop distance computerized virtual reality task (experiment 1): interpersonal distance in control group (n=10) and in patients P1, P2 and P3 according to the emotion depicted by faces. Box-plots depicting the control group' preferred distance in meters as a function of the emotion depicted by faces (happy, neutral and angry). The mean interpersonal distance is represented by the black diamond in each fill box. The red points outside each boxplot represent the mean interpersonal distance for each patient according to the emotion.

Experiment 2: stop distance real setting task with confederates

In experiment 2, we performed the same task in real conditions, with confederates rather than virtual faces. For P1 and P2, only a female confederate participated in the experiment while for P3 and healthy control subjects, we introduced a male confederate in addition to the female confederate to account for any sex difference. The confederates displayed a neutral facial expression and were unfamiliar to the participants. As for experiment 1, we assessed the interpersonal distance of each patient (P1, P2 and P3) and of the control group (n=10) when confederate walked towards the participants (i.e. passive approach condition) or, inversely, when participants walked towards the confederate (i.e. active approach condition).

As for experiment 1, we estimated the relationship between the participants' age and level of education (i.e. covariates) with their behavioral results on the stop distance task. The correlation between the level of education or the age with the mean preferred distance did not reach the assumption described by Crawford et al. (2011) to be included as a covariate in the Bayesian Test of Deficit (i.e., no correlation exceeded 0.3; age: r= 0.28, p=0.43, BF=0.62; level of education: r= -0.22, p=0.53, BF=0.6). Table 2 and Figure 2B report the results obtained when comparing the mean preferred distances for each patient (P1 to P3) and control group regardless of the condition or the experimenter. As observed for the VR task, all the three patients had a mean interpersonal distance significantly shorter compared to the controls group [M ± SD = 0.71 m ± 0.23, P1 = 0.19, Zcc = -2.29, PA= 2.79, *p*= 0.03; P2 = 0.29, Zcc= -1.86, PA= 5.44, *p*= 0.05; P3= 0.28, Zcc= -1.87, PA= 5.43, *p*= 0.05].

The mixed-effect generalized linear model revealed a significant main effect of Group [F(1,11.16)=10.68, p= 0.007] and Condition [active-passive : F(1, 224.04)=20.24, p<0.001]. No significant interaction between Group and Condition was found [F(1, 224,04)= 0.82, p=0.37]. As observed with Bayesian Test of Deficit (Crawford and Garthwaite, 2007), post-hoc analysis revealed larger interpersonal distances for control subjects compared to patients (controls-patients: z= 3.27, p=0.001). The analysis also showed larger interpersonal distances in the passive condition compared to the active condition but only in the control group (active-passive: controls z= -4.48 p<0.0001; patients z=-1.01 p=0.31).

Finally, we performed correlations between mean interpersonal distance of patients and the control group obtained in the stop distance paradigm in VR and in real conditions. The analysis

revealed a significant and strong correlation between mean interpersonal distance to faces stimuli during VR stop distance task and mean interpersonal distance with real experimenter (r = 0.76, BF = 14, p = 0.0026), confirming that performance in the virtual environment was related to real-life distance.

3.2. Physiological data: heart rate modulation with looming faces stimuli in stop distance virtual reality task (experiment 1)

In experiment 1, we recorded the participants' HR frequency during the presentation of the looming faces. We computed the mean HR frequency for each participant during the entire presentation of the stimuli (i.e. interval of 6 sec) and the mean HR frequency during the baseline period of cross fixation presented before each stimulation period (i.e. 4 sec of cross presentation). In order to determine the effect of faces stimuli presentation on participants' HR and to be able to compare these fluctuations between individuals, we computed the difference in HR frequency between the period of stimulation and the baseline period (i.e. delta HR). Firstly, we wanted to test if there was a significative difference in HR during the presentation of looming stimuli by testing if the delta HR was different from 0 using one student t-test for each group. Overall, we observed a significant difference only for control group showing lower delta HR when faces where presented (delta HR: -0.58 bpm, t (971) = -3.25, p=0.001) whereas the patients didn't show difference in their delta HR with the presentation of faces (delta HR: 0.54 bpm, t (240) = 1.04, p=0.29). Then, using Bayesian Test of Deficit (Crawford and Garthwaite, 2007), we compared delta HR of control group with those of each patient (Table 3). No correlations exceeded 0.3 between delta HR and participant's level of education or age so we didn't consider any covariates (age: r= -0.084, p=0.83, BF=0.51; level of education: r= -0.35, p=0.36, BF=0.53). The analysis of delta HR frequency only shows a significant difference between delta HR of P1 and control group [M ± SD = -0.58 bpm ± 0.64, P1 = 0.77, Zcc = 2.12, PA= 3.99, p= 0.04; P2 = 0.37, PA= 9.63, Zcc= 1.49, *p*= 0.09; P3= 0.33, PA= 10.73, Zcc= 1.42, *p*=0.11]. The resulting delta HR for the control group and for each patient is depicted in the Figure 4.

Additionally, the mixed model analysis revealed that there was a significant effect of Group (F (1, 13.64) = 6.36, *p*=0.02) with no significant effect of Emotion (F (2, 1197.9) = 1.43, *p*=0.24) nor any significant interaction between Group and Emotion (F (2, 1198.06) = 1.38, *p*=0.25). Healthy subjects had significant lower delta HR frequency compared to patients (controls-patients: z=-2.51, p=0.01).

Table 3. Mean HR during faces stimulation period or baseline and results obtained with Bayesian Test of Deficit (Crawford and Garthwaite, 2007) between patients' (P1, P2, P3) and controls group' (n=9) delta HR (i.e. mean HR- mean Baseline

	Patients			Control group					One-tailed test	Estimated percentage of the control population obtaining a lower score than the patient (PA)		Estimated effect size (Z_{cc})	
	Mean HR	**Mean Baseline**	**Delta HR**	**n**	**Mean HR**	**Mean Baseline**	**Delta HR**	**SD**	***p***	**Point**	**(95% CI)**	**Point**	**(95% CI)**
P1	79.68	78.91	**0.77**	9	71.52	72.10	**-0.58**	0.64	0.04 *	3.99	(0.05 to 18.82)	2.12	(0.88 to 3.29)
P2	65.70	65.33	**0.37**						0.09	9.63	(0.69 to 30.18)	1.49	(0.52 to 2.46)
P3	104.06	103.73	**0.33**						0.11	10.73	(0.99 to 32 .12)	1.42	(0.46 to 2.33)

PA*, point of abnormality of the patient's score*

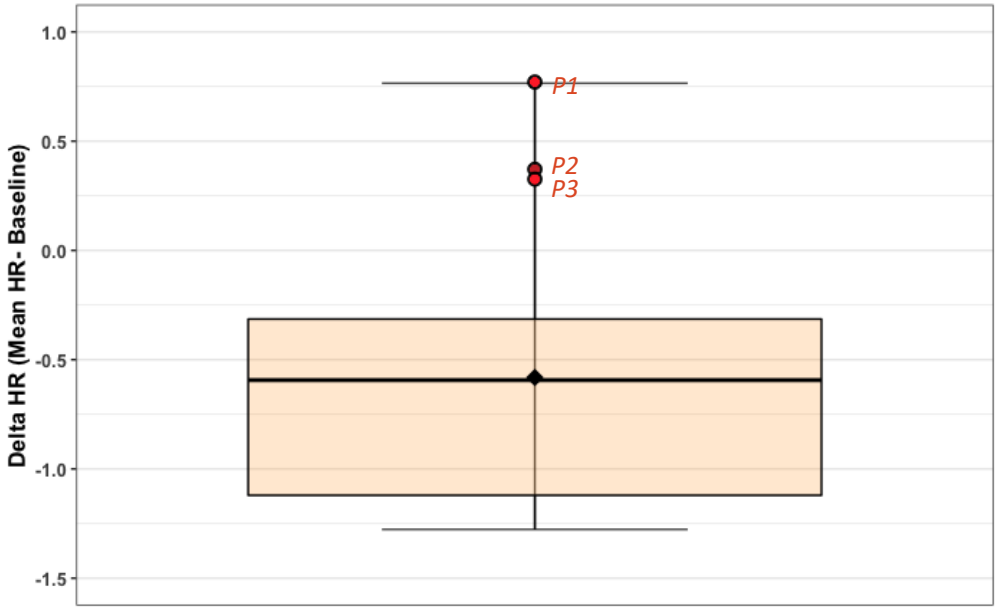

Figure 4. Physiological responses during stop distance virtual reality task (experiment 1): delta of Heart Rate frequency in Control group (n=9) and in patients P1, P2 and P3. Box-plot depicting control group' delta HR in bpm (i.e. mean HR during faces presentation – mean HR during Baseline). In the plot, the mean delta HR is represented by the black diamond in the fill box. The three red points outside the box-plot represent the mean delta HR for each patient. The vertical length of the box represents the interquartile range, the thick horizontal line represents the median, and the whiskers indicate the full range of values.

3.3. Evaluation of emotional rating: validation task (VT)

As illustrated in Figure 5, the results show that all three patients as well as the control group correctly categorized happy, neutral and angry emotions. Emotions were clearly clustered such that angry faces obtained strongly negative rankings, happy faces strongly positive rankings, and neutral ones clustered around zero. Note that for P3, there was a large variability in the rating of neutral faces, ranking on average towards the angry side.

As reported in the Table 4, the rating of emotion did not differ from that of healthy controls in any of the emotions investigated, highlighting that the patients were not impaired in recognizing facial emotions (all ps > 0.05).

Table 4. Results of emotional rating in validation task and their comparison between patients (P1, P2, P3) and controls group (n=10) with Bayesian Test of Deficit (Crawford and Garthwaite, 2007).

	ANGRY				NEUTRAL				HAPPY			
	Patient's score	**Control's score**	**Zcc, PA**	***p****	**Patient's score**	**Control's score**	**Zcc, PA**	***p****	**Patient's score**	**Control's score**	**Zcc, PA**	***p****
P1	-2.55	-2.12 ± 0.48	-0.89, 20.90	0.21	-0.25	-0.31 ± 0.69	0.09, 53.41	0.53	3.05	2.44 ± 0.47	1.32, 87.97	0.88
P2	2.65		-1.1, 16.08	0.16	-0.10		0.30, 61.18	0.61	2.55		0.25, 58.92	0.59
P3	-2.20		-0.17, 43.93	0.44	-0.95		-0.93, 19.9	0.2	2.55		0.25, 58.91	0.59

***** *One-tail T-test;* ***Zcc,*** *effect size;* ***PA****, point of abnormality of the patients' score*

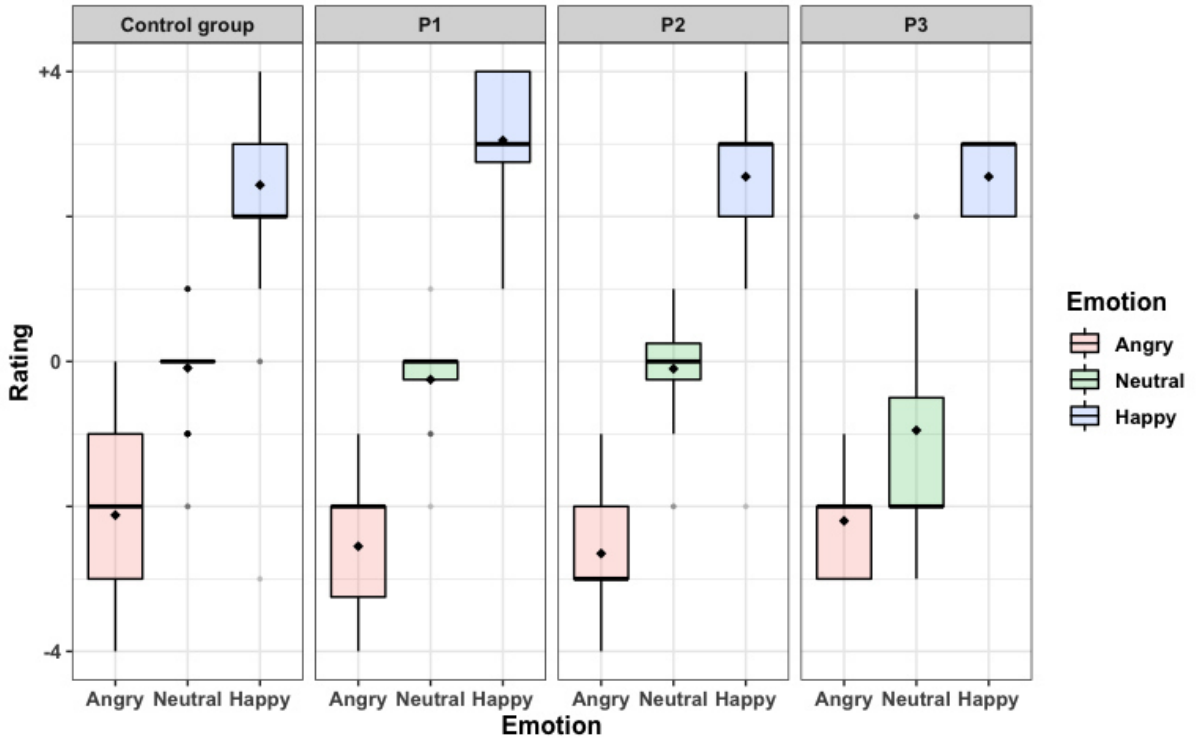

Figure 5. Emotional rating for faces used in stop distance VR task (experiment 1) for Control group (n=10) and patients P1, P2 and P3. Box-plots depicting the scores obtained for each emotion during validation task using a 9 points scale. In the scale, the minimum value (-4) indicated an angry face, the maximum (+4) a happy one, with intermediate values indicating neutral expressions. The mean score for each emotion is represented by the black diamond in each fill box for the control group and the three patients. The vertical length of the boxes represents the interquartile range, the thick horizontal line represents the median, and the whiskers indicate the full range of values. Dots outside the whiskers represent values exceeding 1.5 times the interquartile range.

4. Discussion

The present study demonstrates the reduction of interpersonal space following unilateral (left- or right-sided) medial-temporal lesions extending even beyond the amygdala. In particular, compared to healthy individuals, patients with left (P1 and P2) or right (P3) medial-temporal lesions display shorter interpersonal distances on two versions of the stop distance paradigm, with VR (experiment 1) and in real conditions (experiment 2). The lesion extent varied across patients and included a large portion of the amygdala in P1, whereas in P2 and P3 the lesion spared most or all of the amygdala, respectively, affecting other regions of the temporal lobe. This indicated that the regulation of the interpersonal distance does not depend only upon the integrity of the amygdala; rather, a unilateral lesion within the temporal lobe might be sufficient to affect the regulation of social distances. Moreover, significant HR

differences between patients and controls emerged in response to approaching faces in the VR setting.

4.1. A shorter interpersonal space in patients with unilateral temporal lesion

The actual interpersonal distances of healthy participants found in the present study in both the virtual and real settings are in line with those previously reported in the literature (Iachini et al., 2014, 2015, 2016; Ruggiero et al., 2017). As previously reported (Cartaud et al., 2018; Ruggiero et al., 2017), we also found significant differences in interpersonal distances depending on facial emotion, with larger interpersonal distances for angry faces compared to happy and neutral faces. This finding suggests that angry faces favor avoidant behaviors, in turn enlarging interpersonal distances. Indeed, the increased distance in response to angry approaching confederates can be viewed as an avoidance reaction to the violation of the body space, an important biological adaptive mechanism to ensure the survival of the organisms (Adams et al., 2006; Darwin et al., 1872; Hediger, 1955; Van Dantzig et al., 2008). Instead, when other persons communicate positive feelings, we tend to approach and interact with them (Seidel et al., 2010). Emotional signals during social interactions, thus, help us anticipate others' intentions by regulating spatial distances around us (Knutson, 1996; Ruggiero et al., 2017).

Of relevance, this adaptive behavior was abolished following damage to the temporal lobe. Indeed, all three patients displayed shorter interpersonal distances between themselves and a confederate (i.e. between 19 and 29 cm in real condition and between 6 and 42 cm in VR condition) compared to the control group (i.e. mean of 71 cm with real paradigm and 77 cm with VR paradigm). Interestingly, the interpersonal distances obtained for the three patients were similar to that obtained in the single case patient (SM) suffering from the Urbach-wiethe disease leading to a selective bilateral damage to the amygdala (i.e., patient SM: 34 cm; Kennedy et al., 2009). Also similar to that report, P1 and P2 explicitly reported not to feel uncomfortable at any proximal distance. Yet, contrary to SM, all patients had unilateral lesions that, in addition, were not confined to the amygdala. Instead, here, the three patients had unilateral medial-temporal damage following the surgery. This finding indicates that a unilateral medial-temporal lesion might be sufficient to disrupt the regulation of social distances, regardless of the side of the hemispheric damage.

The second major result of this study is that, contrary to healthy controls, patients' interpersonal distance was not modulated by the emotion displayed by the approaching faces. Again, this finding suggests that damage to temporal brain regions not limited to the amygdala can impair the ability to adjust behaviour appropriately to social situations. Noteworthy, all three patients correctly categorized the facial emotional expressions, ruling out the possibility that the lack of modulation by facial emotional expression reflected a deficit in emotion recognition.

The amygdala plays a key role in understanding social situations (Martin & Weisberg, 2003; Noack et al., 2015) and in detecting social violations (Bas-Hoogendam et al., 2017). Focusing on the extent of amygdala lesions in each patient, we note that P1 has a large part of his left amygdala affected (64% of lesioned voxels), while in P3 the right amygdala was largely spared by the lesion (1% of lesioned voxels) and in P2 the amygdala was intact. In addition, the time interval between surgery and testing differed between patients (1 - 60 months), the longer time interval being for P1. This difference could explain why P1 stands out from the other two patients as he had the furthest interpersonal distance compared to P2 and P3 (i.e., closest interpersonal distance in the stop distance real paradigm and farthest interpersonal distance in stop distance VR paradigm). Yet, these results further indicate that other regions of the temporal lobe, including the parahippocampal cortex, the hippocampus, the fusiform gyrus, the temporal pole and the middle temporal gyrus, might participate in the regulation of interpersonal distances. Alternatively, it is possible that the resection of temporal lobe tissue in the three patients, and perhaps more so in P2 and P3, may have led to a disconnection of the amygdala, through damage to white matter tracts (Sarubbo et al., 2015, 2020).

Recent studies have used direct electrical stimulation applied to both the cortical and subcortical levels during awake brain surgery to identify the role of white matter connections on mentalizing processes, defined as the propensity that social agents have to reflect on others psychological states, and that could serve to regulate interpersonal distances. Yordanova et al. (2017) have shown that functional disconnection of the inferior fronto-occipital fasciculus (IFOF) during temporal subcortical stimulation and of the superior longitudinal fasciculus/arcuate fasciculus (SLF/AF) during prefrontal subcortical stimulations impair the ability to accurately infer complex mental states. In the same vein, Herbet et al. (2015) have shown that functional disruption of the mirror network (i.e. the SLF/AF pathway connecting

the rostral posterior parietal cortex and the intraparietal sulcus to anterior mirror areas) influences higher order mentalistic inferences. The IFOF show a direct connection between frontal and occipital lobe which is in direct contact with Inferior Longitudinal Fasciculus (ILF) tract, an associative white matter pathway that connects the occipital and temporal-occipital areas to the anterior temporal areas and therefore to the amygdala. It has been shown that microstructural changes in the IFOF and/or the ILF disrupt emotional processes (Herbet et al., 2018). The SLF/AF is a large bundle of association fibers in the white matter of each cerebral hemisphere which connects the frontal, occipital, parietal and temporal lobes and facilitates the formation of a bidirectional neural network necessary for core processes (Schmahmann et al., 2008). Anomalies in the microstructural organization of inter-hemispheric white matter tracts is one of the most frequently reported features of autism spectrum disorder (Herbet et al., 2018) and that many white matter pathways connecting the fronto-parietal control network and fronto-temporal network are associated to antisocial personality disorders and to risky behaviors (Jiang et al., 2017). In keeping with these reports, our findings may support the view that social interpersonal behaviours, with their underlying mechanisms (among which the regulation of interpersonal space), rely on interactions within an interconnected network.

4.2. No modulation of HR response in patients with unilateral temporal lesion

Healthy participants show a modulation HR when viewing approaching faces, while no changes were detectable in patients' HR. The results in healthy participants are in line with evidence showing a proximity-induced modulation of physiological responses with social stimuli. In particular, an increase of HR frequency has been reported for faces presented in close compared to far space (Dureux et al., 2021), and a more specific increase of electrodermal activity by angry faces in close proximity (Cartaud et al., 2018). With respect to interpersonal space, Candini et al. (2021) observed a gradual increase of skin conductance response as a confederate moves closer to participants. However, in our study an opposite trend was found, featured by a HR decrease of when faces moved closer to the participants. The apparently contrasting effect could be due to methodological differences, such as the type of presented stimuli (e.g. Cartaud et al. (2018) used human-like point-light displays, Candini et al. (2021) used real confederates at five spatial positions).

Importantly, when looking at patients' responses, higher delta HR compared to healthy subjects emerged. As discussed in the introduction, these changes in HR might result from

increased activity within different parts of the medial temporal cortex such as the amygdala (Inman et al. (2019)) or the temporal pole (Gloor et al. (1982)). The differences in HR between controls and patients might thus be related to the impact of the lesion in the medial temporal lobe onto the regulation of the autonomic responses. P1 stands out compared to the other two patients with higher delta HR compared to P2 and P3. As observed with our behavioral results, this difference observed between patients could be explained by the degree of damage to the amygdala. P1 has his left amygdala highly impacted (64%) whereas P2 has no lesion on his left amygdala and P3 has 1% of his right amygdala lesioned. These physiological results suggest that correct autonomic regulation during social interaction should not be explained by a single brain area but possibly by a set of regions interconnected to the amygdala by the white matter pathways.

In conclusion, our behavioral and physiological results provide the first evidence of an involvement of a medial-temporal brain network interconnected to the amygdala to regulate appropriate interpersonal distances during social interactions. In our study, the behavioral and physiological deficits induced by medial-temporal brain lesions support the fact that brain damage could emerge through a mechanism of interaction which is not only restricted to the amygdala already shown to be implicated in social approach and avoidance (Capitanio et al., 2006; Emery et al., 2001; Kennedy et al., 2009). A unilateral damage to the medial-temporal lobe appears to be sufficient to cause inappropriate regulation of social distances, due to a reduction of the personal space extension along with changes in autonomic responses to social cues, which could affect the establishment of appropriate social interactions.

5. References

Adams, R. B., Ambady, N., Macrae, C. N., & Kleck, R. E. (2006). Emotional expressions forecast approach-avoidance behavior. Motivation and Emotion, 30(2), 179–188. https://doi.org/10.1007/s11031-006-9020-2

Adolphs, R. (2010). What does the amygdala contribute to social cognition? In Annals of the New York Academy of Sciences (Vol. 1191, Issue 1, pp. 42–61). Blackwell Publishing Inc. https://doi.org/10.1111/j.1749-6632.2010.05445.x

Adolphs, R., Russell, J. A., & Tranel, D. (1999). A role for the human amygdala in recognizing emotional arousal from unpleasant stimuli. Psychological Science, 10(2), 167–171. https://doi.org/10.1111/1467-9280.00126

Adolphs, R., Tranel, D., & Damasio, H. (2001). Emotion recognition from faces and prosody following temporal lobectomy. Neuropsychology, 15(3), 396–404. https://doi.org/10.1037//0894-4105.15.3.396

Adolphs, R., Tranel, D., Damasio1s2, H., & Damasio1', A. R. (1995). Fear and the Human Amygdala.

Alberici, A., Geroldi, C., Cotelli, M., Adorni, A., Calabria, M., Rossi, G., Borroni, B., Padovani, A., Zanetti, O., & Kertesz, A. (2007). The Frontal Behavioural Inventory (Italian version) differentiates frontotemporal lobar degeneration variants from Alzheimer's disease. Neurological Sciences 2007 28:2, 28(2), 80–86. https://doi.org/10.1007/S10072-007-0791-3

Bas-Hoogendam, J. M., Steenbergen, H. Van, Kreuk, T., Van Der Wee, N. J. A., & Westenberg, P. M. (2017). How embarrassing! the behavioral and neural correlates of processing social norm violations. PLoS ONE, 12(4), e0176326. https://doi.org/10.1371/journal.pone.0176326

Bates, D., Mächler, M., Bolker, B. M., & Walker, S. C. (2015). Fitting linear mixed-effects models using lme4. Journal of Statistical Software, 67(1). https://doi.org/10.18637/jss.v067.i01

Benjamini, Y., & Hochberg, Y. (1995). Controlling the False Discovery Rate: A Practical and Powerful Approach to Multiple Testing. Journal of the Royal Statistical Society: Series B (Methodological), 57(1), 289–300. https://doi.org/10.1111/j.2517-6161.1995.tb02031.x

Bucher, K., Myers, R. E., & Southwick, C. (1970). Anterior temporal cortex and maternal behavior in monkey. Neurology, 20(4), 415. https://europepmc.org/article/med/4998075

Candini, M., Battaglia, S., Benassi, M., di Pellegrino, G., & Frassinetti, F. (2021). The physiological

correlates of interpersonal space. Scientific Reports, 11(1), 2611. https://doi.org/10.1038/s41598-021-82223-2

Capitanio, J. P., Machado, C. J., & Amaral, D. (2006). Amygdalectomy and responsiveness to novelty in Rhesus monkeys (Macaca mulatta): Generality and individual consistency of effects. https://doi.org/10.1037/1528-3542.6.1.73

Cartaud, A., Ruggiero, G., Ott, L., Iachini, T., & Coello, Y. (2018). Physiological Response to Facial Expressions in Peripersonal Space Determines Interpersonal Distance in a Social Interaction Context. Frontiers in Psychology, 9(MAY), 657. https://doi.org/10.3389/fpsyg.2018.00657

Charles Darwin, B., Society Hardwicke, R., & Fritz Muller, B. (n.d.). With illustrations. 2 vols. 8vo. 24s. Murray, 1871. THE VARIATION OF ANIMALS AND PLANTS UNDER DOMESTICATION. Third Thousand. With Illustrations. 2 vols. 8vo. 28s. Murray, 1868. Effects of Crossing. With Woodcuts.

Crawford, J. R., & Garthwaite, P. H. (2007). Comparison of a single case to a control or normative sample in neuropsychology: Development of a Bayesian approach. Cognitive Neuropsychology, 24(4), 343–372. https://doi.org/10.1080/02643290701290146

Crawford, J. R., Garthwaite, P. H., & Ryan, K. (2011). Comparing a single case to a control sample: testing for neuropsychological deficits and dissociations in the presence of covariates. Cortex; a Journal Devoted to the Study of the Nervous System and Behavior, 47(10), 1166–1178. https://doi.org/10.1016/j.cortex.2011.02.017

Crawford, J. R., Garthwaite, P. H., & Wood, L. T. (2010). Inferential methods for comparing two single cases. Cognitive Neuropsychology, 27(5), 377–400. https://doi.org/10.1080/02643294.2011.559158

Dallabona, M., Sarubbo, S., Merler, S., Corsini, F., Pulcrano, G., Rozzanigo, U., Barbareschi, M., & Chioffi, F. (2017). Impact of mass effect, tumor location, age, and surgery on the cognitive outcome of patients with high-grade gliomas: A longitudinal study. Neuro-Oncology Practice, 4(4), 229–240. https://doi.org/10.1093/nop/npw030

Davis, M., & Whalen, P. J. (2001). The amygdala: Vigilance and emotion. In Molecular Psychiatry (Vol. 6, Issue 1, pp. 13–34). https://doi.org/10.1038/sj.mp.4000812

Duffau, H. (2021). Updated perspectives on awake neurosurgery with cognitive and emotional assessment for patients with low-grade gliomas. In Expert Review of Neurotherapeutics (Vol. 21, Issue 4, pp. 463–473). Taylor and Francis Ltd. https://doi.org/10.1080/14737175.2021.1901583

Dureux, A., Blini, E., Grandi, L. C., Bogdanova, O., Desoche, C., Farnè, A., & Hadj-Bouziane, F. (2021). Close facial emotions enhance physiological responses and facilitate perceptual discrimination. Cortex, 138, 40–58. https://doi.org/10.1016/j.cortex.2021.01.014

Emery, N. J., Capitanio, J. P., Mason, W. A., Machado, C. J., Mendoza, S. P., & Amaral, D. G. (2001). The Effects of Bilateral Lesions of the Amygdala on Dyadic Social Interactions in Rhesus Monkeys (Macaca mulatto) of the amygdala may be particularly important. Mem. Behavioral Neuroscience, 115(3), 515–544. https://doi.org/10.I037//0735-7044.I15.3.515

Fowler, H. L., Baker, G. A., Tipples, J., Hare, D. J., Keller, S., Chadwick, D. W., & Young, A. W. (2006). Recognition of emotion with temporal lobe epilepsy and asymmetrical amygdala damage. https://doi.org/10.1016/j.yebeh.2006.04.013

Friston, K., Ashburner, J., Kiebel, S., Nichols, T., and Penny, W. (2007). Statistical Parametric Mapping. London: Elsevier. doi: 10.1016/B978-0-12-372560-8.X5000-1

Gloor, P., Olivier, A., Quesney, L. F., Andermann, F., & Horowitz, S. (1982). The role of the limbic system in experiential phenomena of temporal lobe epilepsy. Annals of Neurology, 12(2), 129–144. https://doi.org/10.1002/ana.410120203

Goeleven, E., De Raedt, R., Leyman, L., & Verschuere, B. (2008). The Karolinska directed emotional faces: A validation study. Cognition and Emotion, 22(6), 1094–1118. https://doi.org/10.1080/02699930701626582

Hall, E. T., Birdwhistell, R. L., Bock, B., Bohannan, P., Diebold, A. R., Durbin, M., Edmonson, M. S., Fischer, J. L., Hymes, D., Kimball, S. T., La Barre, W., McClellan, J. E., Marshall, D. S., Milner, G. B., Sarles, H. B., Trager, G. L., & Vayda, A. P. (1968). Proxemics [and Comments and Replies]. Current Anthropology, 9(2/3), 83–108. https://doi.org/10.1086/200975

Hayduk, L. A. (1983). Personal space: Where we now stand. Psychological Bulletin, 94(2), 293–335. https://doi.org/10.1037/0033-2909.94.2.293

Herbet, G., Lafargue, G., Moritz-Gasser, S., Bonnetblanc, F., & Duffau, H. (2015). Interfering with the neural activity of mirror-related frontal areas impairs mentalistic inferences. Brain Structure and Function, 220(4), 2159–2169. https://doi.org/10.1007/s00429-014-0777-x

Huber, S., Klein, E., Moeller, K., & Willmes, K. (2015). Comparing a single case to a control group - Applying linear mixed effects models to repeated measures data. Cortex, 71, 148–159. https://doi.org/10.1016/j.cortex.2015.06.020

Iachini, T., Coello, Y., Frassinetti, F., & Ruggiero, G. (2014a). Body space in social interactions: A

comparison of reaching and comfort distance in immersive virtual reality. PLoS ONE, 9(11). https://doi.org/10.1371/journal.pone.0111511

Iachini, T., Coello, Y., Frassinetti, F., & Ruggiero, G. (2014b). Body Space in Social Interactions: A Comparison of Reaching and Comfort Distance in Immersive Virtual Reality. PLOS ONE, 9(11), e111511. https://doi.org/10.1371/JOURNAL.PONE.0111511

Iachini, T., Coello, Y., Frassinetti, F., Senese, V. P., Galante, F., & Ruggiero, G. (2016). Peripersonal and interpersonal space in virtual and real environments: Effects of gender and age. Journal of Environmental Psychology, 45, 154–164. https://doi.org/10.1016/j.jenvp.2016.01.004

Iachini, T., Ruggiero, G., Ruotolo, F., Schiano di Cola, A., & Senese, V. P. (2015). The influence of anxiety and personality factors on comfort and reachability space: a correlational study. Cognitive Processing, 16, 255–258. https://doi.org/10.1007/s10339-015-0717-6

Inman, C. S., Bijanki, K. R., Bass, D. I., Gross, R. E., Hamann, S., & Willie, J. T. (2020). Human amygdala stimulation effects on emotion physiology and emotional experience. Neuropsychologia, 145. https://doi.org/10.1016/j.neuropsychologia.2018.03.019

Kennedy, D. P., Gläscher, J., Tyszka, J. M., & Adolphs, R. (2009). Personal space regulation by the human amygdala. Nature Neuroscience, 12(10), 1226–1227. https://doi.org/10.1038/nn.2381

Kling, A., & Steklis, H. D. (1976). A neural substrate for affiliative behavior in nonhuman primates. Brain, Behavior and Evolution, 13(2–3), 216–238. https://doi.org/10.1159/000123811

Knutson, B. (1996). Facial expressions of emotion influence interpersonal trait inferences. Journal of Nonverbal Behavior, 20(3), 165–182. https://doi.org/10.1007/bf02281954

Ledoux, J. E., & Brown, R. (2017). A higher-order theory of emotional consciousness. Proceedings of the National Academy of Sciences of the United States of America, 114(10), E2016–E2025. https://doi.org/10.1073/pnas.1619316114

Lenth, R. V. (2016). Least-squares means: The R package lsmeans. Journal of Statistical Software, 69. https://doi.org/10.18637/jss.v069.i01

Lipson, S. E., Sacks, O., & Devinsky, O. (2003). Selective emotional detachment from family after right temporal lobectomy. Epilepsy and Behavior, 4(3), 340–342. https://doi.org/10.1016/S1525-5050(03)00081-7

Martin, A., & Weisberg, J. (2003). Neural foundations for understanding social and mechanical concepts. In Cognitive Neuropsychology (Vol. 20, Issues 3–6, pp. 575–587). NIH Public Access.

https://doi.org/10.1080/02643290342000005

Masaoka, Y., Hirasawa, K., Yamane, F., Hori, T., & Homma, I. (2003). Effects of left amygdala lesions on respiration, skin conductance, heart rate, anxiety, and activity of the right amygdala during anticipation of negative stimulus. Behavior Modification, 27(5), 607–619. https://doi.org/10.1177/0145445503256314

Mathôt, S., Schreij, D., & Theeuwes, J. (2012). OpenSesame: An open-source, graphical experiment builder for the social sciences. In Behavior Research Methods (Vol. 44, Issue 2, pp. 314–324). Behav Res Methods. https://doi.org/10.3758/s13428-011-0168-7

McIntosh, R. D., & Brooks, J. L. (2011). Current tests and trends in single-case neuropsychology. Cortex, 47(10), 1151–1159. https://doi.org/10.1016/j.cortex.2011.08.005

Noack, J., Murau, R., & Engelmann, M. (2015). Consequences of temporary inhibition of the medial amygdala on social recognition memory performance in mice. Frontiers in Neuroscience, 9(APR), 152. https://doi.org/10.3389/fnins.2015.00152

Rolls, E. T., Huang, C. C., Lin, C. P., Feng, J., & Joliot, M. (2020). Automated anatomical labelling atlas 3. NeuroImage, 206, 116189. https://doi.org/10.1016/j.neuroimage.2019.116189

Ruggiero, G., Frassinetti, F., Coello, Y., Rapuano, M., di Cola, A. S., & Iachini, T. (2017). The effect of facial expressions on peripersonal and interpersonal spaces. Psychological Research, 81(6), 1232–1240. https://doi.org/10.1007/s00426-016-0806-x

Ruggiero, G., Rapuano, M., & Iachini, T. (2019). Perceived temperature modulates peripersonal and interpersonal spaces differently in men and women. Journal of Environmental Psychology, 63, 52–59. https://doi.org/10.1016/j.jenvp.2019.04.004

Sarubbo, S., Annicchiarico, L., Corsini, F., Zigiotto, L., Herbet, G., Moritz-Gasser, S., Dalpiaz, C., Vitali, L., Tate, M., De Benedictis, A., Amorosino, G., Olivetti, E., Rozzanigo, U., Petralia, B., Duffau, H., & Avesani, P. (2021). Planning Brain Tumor Resection Using a Probabilistic Atlas of Cortical and Subcortical Structures Critical for Functional Processing: A Proof of Concept. Operative Neurosurgery, 20(3), E175–E183. https://doi.org/10.1093/ons/opaa396

Sarubbo, S., De Benedictis, A., Merler, S., Mandonnet, E., Balbi, S., Granieri, E., & Duffau, H. (2015). Towards a functional atlas of human white matter. Human Brain Mapping, 36(8), 3117–3136. https://doi.org/10.1002/hbm.22832

Sarubbo, S., Tate, M., De Benedictis, A., Merler, S., Moritz-Gasser, S., Herbet, G., & Duffau, H. (2020). Mapping critical cortical hubs and white matter pathways by direct electrical stimulation: an original functional atlas of the human brain. NeuroImage, 205, 116237. https://doi.org/10.1016/j.neuroimage.2019.116237

Seidel, E. M., Habel, U., Kirschner, M., Gur, R. C., & Derntl, B. (2010). The Impact of Facial Emotional Expressions on Behavioral Tendencies in Women and Men. Journal of Experimental Psychology: Human Perception and Performance, 36(2), 500–507. https://doi.org/10.1037/a0018169

Studies of the psychology and behavior of captive animals in zoos and circuses. - PsycNET. (n.d.). Retrieved May 26, 2021, from https://psycnet.apa.org/record/1956-08075-000

Van Dantzig, S., Pecher, D., & Zwaan, R. A. (2008). Approach and avoidance as action effects. Quarterly Journal of Experimental Psychology, 61(9), 1298–1306. https://doi.org/10.1080/17470210802027987

Vilasboas, T., Herbet, G., & Duffau, H. (2017). Challenging the Myth of Right Nondominant Hemisphere: Lessons from Corticosubcortical Stimulation Mapping in Awake Surgery and Surgical Implications. In World Neurosurgery (Vol. 103, pp. 449–456). Elsevier Inc. https://doi.org/10.1016/j.wneu.2017.04.021

Wiley, R. W., & Rapp, B. (2019). Statistical analysis in Small-N Designs: using linear mixed-effects modeling for evaluating intervention effectiveness. Aphasiology, 33(1), 1–30. https://doi.org/10.1080/02687038.2018.1454884

Yordanova, Y. N., Duffau, H., & Herbet, G. (2017). Neural pathways subserving face-based mentalizing. Brain Structure and Function, 222(7), 3087–3105. https://doi.org/10.1007/s00429-017-1388-0

Zacà, D., Corsini, F., Rozzanigo, U., Dallabona, M., Avesani, P., Annicchiarico, L., Zigiotto, L., Faraca, G., Chioffi, F., Jovicich, J., & Sarubbo, S. (2018). Whole-brain network connectivity underlying the human speech articulation as emerged integrating direct electric stimulation, resting state FMRI and tractography. Frontiers in Human Neuroscience, 12, 405. https://doi.org/10.3389/fnhum.2018.00405

Zigiotto, L., Annicchiarico, L., Corsini, F., Vitali, L., Falchi, R., Dalpiaz, C., Rozzanigo, U., Barbareschi, M., Avesani, P., Papagno, C., Duffau, H., Chioffi, F., & Sarubbo, S. (2020). Effects of supra-total resection in neurocognitive and oncological outcome of high-grade gliomas comparing asleep and awake surgery. Journal of Neuro-Oncology, 148(1), 97–108. https://doi.org/10.1007/s11060-020-03494-9

Chapitre 4 :

Discussion générale

Dans la première partie de mon introduction, j'ai exposé l'origine de l'espace péri-personnel (EPP) et comment cette région 'spéciale' de l'espace proche du corps avait été définie fonctionnellement par des études neurophysiologiques chez le macaque, de neuroimagerie chez l'homme et des études comportementales chez les patients et les sujets sains.
En particulier, les premières études menées en électrophysiologie chez le macaque ont permis d'identifier des neurones dans des régions cérébrales prémotrices et pariétales spécifiques répondant préférentiellement à des stimulations dans l'espace proche du corps. Plus tard, l'imagerie par IRMf a permis d'identifier un réseau avec des propriétés similaires chez l'homme. Bien que cet espace ait été d'abord défini comme un espace d'action permettant d'interagir physiquement avec les éléments présents dans l'environnement, c'est tout naturellement que des études se sont penchées sur la question du rôle de cet espace dans nos interactions sociales.
Dans la deuxième partie de mon introduction, j'ai identifié les récentes recherches comportementales et physiologiques menées sur cette composante sociale de l'EPP ainsi que les études qui ont tenté de comparer cette dimension de l'EPP avec l'espace personnel, un espace défini à l'origine par des psychologues comme la zone de confort pour réguler les distances entre les individus afin d'éviter l'inconfort et l'anxiété. Bien que ce dernier ait été récemment exploré en neuroimagerie, les corrélats neuronaux associés à l'EPP dans un contexte social restent encore incertains.

Dans ce cadre, au travers de mon travail de thèse, mes objectifs étaient 1) d'identifier les homologies concernant les réseaux neuronaux impliqués dans la représentation de l'EPP chez l'homme et le macaque (études 1 et 2) ; puis chez l'homme de : 2) caractériser l'impact de la présence de visages émotionnels dans l'EPP sur les réponses comportementales et physiologiques (étude 3), 3) identifier le réseau neuronal impliqué dans le traitement de visages émotionnels dans l'EPP (étude 4), 4) comparer ces réseaux neuronaux en fonction du contexte (social ou non-social) et identifier si ces réseaux possèdent une représentation somatotopique (études 1, 2 et 4) et 5) identifier des régions neuronales clés de l'espace personnel, permettant une régulation appropriée des distances entre les individus (étude 5).

I. Quelles sont les homologies concernant les réseaux neuronaux de la représentation de l'EPP chez l'homme et le singe ?

Dans les études 1 et 2 de ma thèse, en utilisant des méthodologies similaires en IRMf chez l'homme et le macaque, j'ai pu identifier les corrélats neuronaux de la représentation de l'EPP chez ces deux espèces. Ces études constituent une première tentative de comparer directement le réseau de l'EPP en utilisant la même technique de neuroimagerie et des protocoles expérimentaux similaires. Dans la première étude, à travers un protocole d'adaptation où un objet réel était présenté proche (2 cm) ou loin (100 cm) du visage des sujets, nous avons identifié chez les deux espèces un réseau fronto-pariétal impliquant des régions prémotrices et pariétales. La comparaison entre les résultats obtenus chez l'homme et le macaque a permis de mettre en évidence un chevauchement important des réponses neuronales lors de la stimulation pour la balle réelle proche du visage (voir Figure 23 ci-dessous). Ce chevauchement était d'autant plus important lorsque nous avons, à l'aide d'un classifier, pu décoder un modèle neuronal sensible à la distance (proche *vs.* loin) dans les régions du cortex prémoteur ventral et dorsal, dans le lobule pariétal supérieur (SPL), le long du sillon intrapariétal (IPS), et plus en particulier dans l'aire ventrale intrapariétale (VIP), dans l'aire latérale intrapariétale (LIP) et dans l'aire médiale intrapariétale (MIP) mais également dans l'aire 7 du lobule pariétal inférieur (IPL) ainsi que dans le putamen.

Dans la deuxième étude, à l'aide d'une tâche de visualisation passive en réalité virtuelle, j'ai pu identifier chez les deux espèces un réseau préférentiel pour les objets virtuels présentés proche des sujets (30 cm) comparé à loin (300 cm) dans l'environnement virtuel, qui impliquait principalement les aires visuelles, des régions du cortex pariétal postérieur (PPC), en particulier au niveau du sillon pariéto-occipital (V6/V6A) et le long de l'IPS (VIP, LIP, MIP), les régions prémotrices dorsales et ventrales (PMd, PMv et F4/F5 pour le singe) et des régions préfrontales comprenant le frontal eye field (FEF). De la même manière que dans la première étude, lorsque la même analyse sur des régions d'intérêts (ROIs) a été réalisée, j'ai retrouvé les activations communes aux deux espèces dans les régions du cortex prémoteur (parties ventrales et dorsales)

et dans certaines régions du PPC, dans le sillon intrapariétal (LIP, VIP), bien qu'aucune activation n'ait été rapportée dans le putamen.

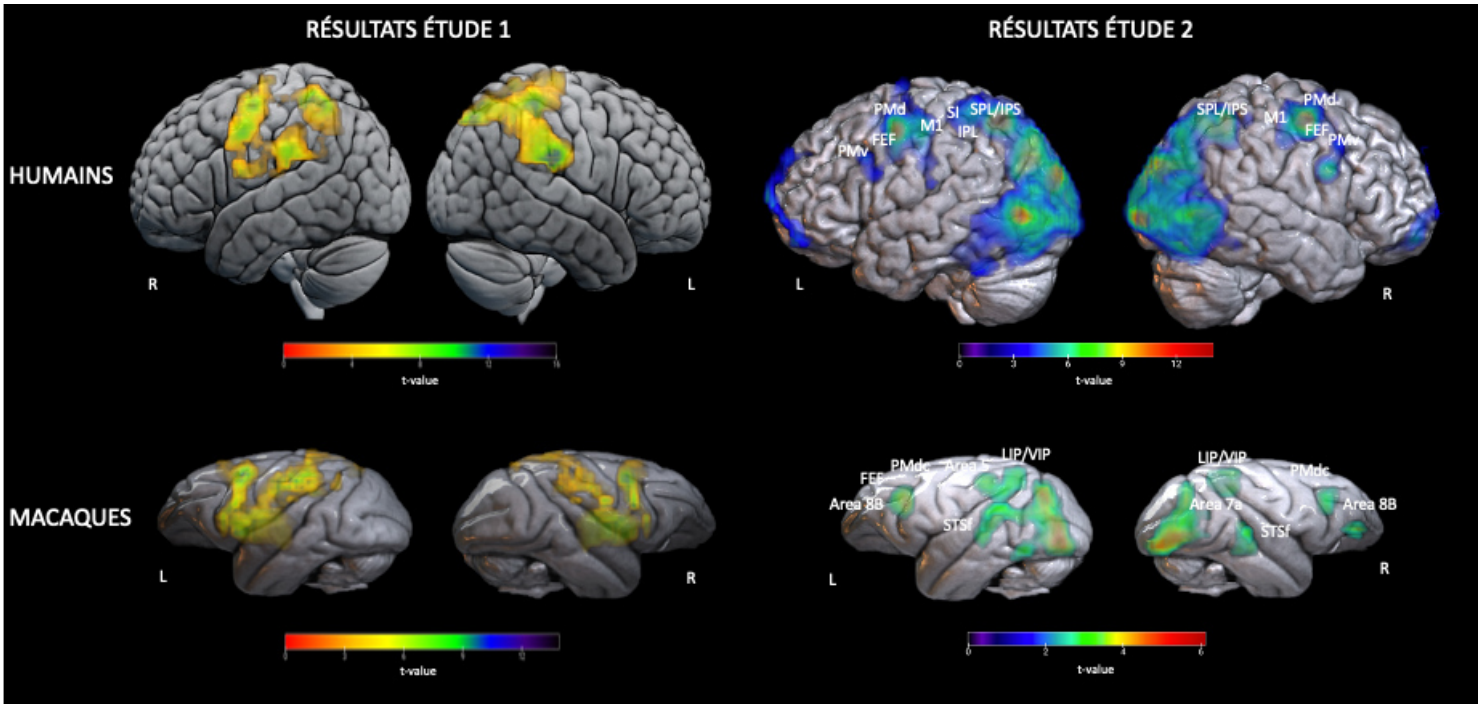

Figure 23. Résumé des résultats obtenus dans les études 1 (avec objet réel) et 2 (avec objet virtuel) chez le singe et chez l'homme. Régions cérébrales montrant une réponse significativement plus importante lors de la présentation d'un objet réel (étude 1) ou virtuel (étude 2) proche par rapport à loin (méthode d'analyse univariée, contraste proche > loin pour les deux études). Les cartes d'activations représentent les résultats obtenus pour un participant humain et un sujet macaque dans chaque étude. Voir chaque étude pour plus de détails.

Mes résultats peuvent être reliés aux études antérieures sur les bases neurales de l'EPP menées chez le singe en électrophysiologie ainsi qu'aux résultats plus récents en neuroimagerie chez l'homme et dans une étude chez le singe, la seule connue à ce jour. Dans cette partie, je me concentrerai uniquement sur la comparaison entre les réseaux de l'homme et du singe.

Tout d'abord, si je me focalise sur les lobes pariétaux et frontaux, puisque l'analyse de ROIs se concentrait essentiellement sur ces aires, nous avons mis en évidence dans les deux études, à la fois chez l'homme et le singe, des activations principalement dans le PCC et le long de l'IPS. Chez le singe, je peux relier ces résultats à ceux obtenus en électrophysiologie, identifiant que les neurones du VIP répondaient préférentiellement aux objets réels présentés dans l'espace proche du visage du singe (Colby et al., 1993 ; Duhamel et al., 1998), mais également dans la région MIP lors de stimulation proche du bras (Colby & Duhamel, 1996), et

qui possédaient également un taux de décharge plus élevé lors de fixations se déroulant dans l'espace proche (Bhattacharyya et al., 2009). Une propriété similaire avait été observée dans les neurones de la région LIP, possédant des réponses plus importantes lorsque les stimuli visuels était présentés entre le corps du singe et un point de fixation situé dans l'espace d'atteinte de l'animal (Genovesio & Ferraina, 2004 ; Gnadt & Mays, 1995). Ces mêmes résultats étaient également observés en IRMf lorsqu'un cube réel était présenté proche du visage (Cléry et al., 2018), cependant cette même étude n'a pas retrouvé d'activations préférentielles pour l'espace proche dans le LIP. Également, mes résultats ainsi que ceux de Cléry et al. (2018) indiquent un recrutement de la partie antérieure de l'IPS, la région AIP. Bien que celle-ci n'a pas été directement reliée avec l'EPP dans les études en électrophysiologie, ces neurones ont été identifiés comme possédant un codage pour la structure en 3D ainsi que sa position en profondeur (Durand et al., 2007 ; Srivastava et al., 2009a) mais également 'préférant' la présentation d'objets saisissables (Fogassi et al., 2001 ; Murata et al., 2000).

Chez l'homme, les activations que j'ai identifiées dans l'IPS (VIP, MIP, LIP, AIP) peuvent être reliées à celles observées dans la littérature, bien que ces études aient rapporté des activations avec un niveau de précision inférieur, en rapportant un recrutement de l'IPS en général (Huang et al., 2012 ; Sereno & Huang, 2006), soit dans la section antérieure (Brozzoli et al., 2011 ; Gentile et al., 2011, 2013) ou au fond de l'IPS (Makin et al., 2007). Cependant, il faut prendre quelques précautions dans la comparaison de ces différentes structures de l'IPS entre l'homme et le singe puisque l'aire VIP a été à plusieurs reprises identifiée comme homologue putatif du VIP singe à différentes localisations (Foster et al., 2021). Néanmoins, les activations identifiées dans les études 1 et 2 dans les régions VIP, LIP et AIP semblent cohérentes avec l'étude de Orban (2016) qui a identifié les homologies fonctionnelles entre les zones pariétales de l'homme et du macaque.

Toujours dans le cortex pariétal, les activations dans les aires 7a et 7b (uniquement 7a dans l'étude 2) sont en lien avec les études neurophysiologiques ayant identifié une augmentation des réponses dans les neurones de la région 7b par la présence de stimuli multisensoriels proche de différentes parties du corps (Graziano & cooke, 2006 ; Hyvärinen & Poranen, 1974 ; Leinonen et al., 1979 ; Leinonen & Nyman, 1979 ; Robinson & Burton, 1980) ainsi qu'une majorité des neurones dans la région 7a préférant des fixations dans l'espace proche du visage du singe (Sakata et al., 1980). Ces régions n'avaient cependant jamais été identifiées en IRMf chez le singe. Les mêmes activations dans l'aire 7A ont été retrouvées chez l'homme, et également dans le complexe PF/PFt du supramarginal gyrus (SMG), la région qui semblerait

homologue à l'aire 7b chez le singe (Caspers et al., 2011). Enfin, l'aire 5 (aires PE, PEa) était toujours activée dans les études 1 et 2 chez le singe lors de la stimulation proche, pourtant non identifiée jusqu'à présent comme préférentiellement activée par des distances proches mais possédant des neurones s'activant par des mouvements d'atteintes actifs (Breveglieri et al., 2006 ; Sakata et al., 1973). Chez l'homme, l'aire 5L dans l'étude 1 était également recrutée, considérée comme l'homologue putatif de l'aire PE chez le singe (Scheperjans, Grefkes, et al., 2005 ; Scheperjans, Palomero-Gallagher, et al., 2005).

Si je regarde maintenant plus en détail le lobe frontal, à chaque fois dans les deux études, les régions prémotrices ventrales et dorsales ont pu être identifiées : PMv et PMd chez l'homme ainsi que F4/F5 et PMdc chez le singe. Ces régions avaient déjà été mises en évidence chez l'homme (Bremmer et al., 2001 ; Brozzoli et al., 2011, 2012 ; Ferri et al., 2015 ; Gentile et al., 2011, 2013 ; Makin et al., 2007) et chez le singe avec les études en électrophysiologie montrant que les neurones F4 répondaient sélectivement et de manière graduelle aux objets présentés proche de l'animal (Gentilucci et al., 1983, 1988 ; Graziano et al., 1994 ; Graziano et al., 1997 ; Rizzolatti et al., 1981) ou spécifiquement dans l'espace d'atteinte pour les neurones de la région F5 (Gentilucci et al., 1988) mais également avec l'étude en IRMf pour les régions F4/F5 et F2 (PMd) (Cléry et al., 2018). Dans l'étude 2, lorsque les analyses ont été effectuées sur le cerveau entier, j'ai également identifié chez les deux espèces la région du frontal eye field (FEF), impliquée dans les mouvements oculaires, en particulier le système de vergence qui correspond aux mouvements oculaires conjugués permettant aux deux yeux de se focaliser sur un objet visuel donné (Alkan et al., 2011). Chez l'homme, j'ai aussi identifié la région du premotor eye field (PEF) ainsi que dans l'étude 2, également, le supplementary eye field (SEF). Ces résultats ne sont pas surprenants puisque nos deux paradigmes dans chacune des études impliquent des indices oculomoteurs. Dans la tâche en RV, les sujets devaient fixer l'objet en question dont sa position variait dans l'espace, alors que dans la première tâche les sujets devaient fixer un point de fixation qui était situé entre la présentation de l'objet proche et loin. Dans la littérature, la modulation de la réponse neuronale par les indices de vergence et de disparité binoculaire a été documentée dans plusieurs régions corticales qui contribuent au traitement de l'EPP. C'est le cas notamment de la région V6/V6A, située dans le sillon pariéto-occipital (POS) (Luppino et al., 2005), qui possèderait une proportion de neurones modulée par la position du regard dans l'espace 3D ainsi que par les signaux de vergence, c'est-à-dire par la localisation en profondeur de l'objet visuel (Breveglieri et al., 2012 ; Hadjidimitrakis et al., 2011, 2012). Chez l'homme, il a également été démontré que la région dorsale du POS, une

région qui semblerait homologue à la région V6A chez le singe, possédait des activations neuronales préférentielles à la présence d'un objet s'approchant (Quinlan & Culham, 2007). Puisque cette région n'était pas comprise dans le masque de ROIs utilisé dans nos analyses pour l'étude 1, cette région a été reportée uniquement dans l'étude 2, chez les deux espèces.

Si je reviens sur les régions identifiées dans le lobe frontal, l'analyse sur le cerveau entier (étude 2) a également permis de mettre en évidence un ensemble de régions dans le cortex préfrontal (PFC, dans le gyrus frontal médian) et dans le cortex orbitofrontal chez l'homme et le singe ou encore dans l'opercule frontal chez l'homme. D'une façon assez rare dans les études ayant caractérisé la représentation neuronale de l'EPP chez l'homme, il a été observé parfois des activations dans le gyrus frontal médian mais il n'était jamais indiqué à quelle(s) région(s) ces activations se référaient (Ferri et al., 2015 ; Wittmann et al., 2010). Chez le singe, certaines de ces régions ont seulement été observées en IRMf (une région du PFC ainsi que dans le cortex orbitofrontal (Cléry et al., 2018)).

Dans l'étude 2 en RV, les objets en 3D apparaissant dans l'EPP recrutaient également une partie importante du lobe occipital avec des fortes activations dans les aires visuelles V1, V2, V3, V4 et V3A chez le macaque mais également certaines régions du lobe temporal, en particulier la jonction temporo-occipitale temporale (TPO) et l'aire temporale médiale supérieure (MST) ou encore dans le sillon supérieur temporal (STS) et le lobe temporal médian (MT) également chez le singe. Certaines études impliquant uniquement des stimulations visuelles chez l'homme avaient également identifié quelques régions dans le gyrus occipital inférieur et médian (Brozzoli et al., 2011) mais également dans la région latérale du cortex occipital (LOC ; Gentile et al., 2013 ; Makin et al., 2007). Dans le cortex temporal, il a été rapporté uniquement des activations dans le STS chez l'homme et le singe en IRMf (Cléry et al., 2018 ; Ferri et al., 2015; Tyll et al., 2012).

Enfin, d'autres régions comme le gyrus cingulaire (Tyll et al., 2012 ; Wittmann et al., 2010), le putamen (Brozzoli et al., 2011 ; Gentile et al., 2011, 2013 ; Graziano & Gross, 1993), l'insula (Cléry et al., 2018 ; Gentile et al., 2011, 2013) et le cervelet (Brozzoli et al., 2011 ; Gentile et al., 2011, 2013) étaient rapportées comme étant impliquées dans la représentation neuronale de l'EPP. Plus spécifiquement, à travers nos paradigmes, j'ai identifié une préférence pour l'objet proche dans le putamen chez les deux espèces seulement dans l'étude 1. Dans la deuxième étude en RV, les sujets humains présentaient également des préférences à l'objet proche dans le gyrus cingulaire, le cervelet ainsi que dans le thalamus, le putamen et l'insula pour un des trois participants.

En résumé, tout d'abord mes résultats montrent des activations assez similaires dans les régions prémotrices et pariétales impliquées dans le traitement de l'EPP, que l'espace proche des sujets soit stimulé par un objet réel à 2 cm du visage ou par un objet 3D proche du corps à l'aide de la RV à 30 cm dans l'environnement virtuel. Cependant, l'analyse réalisée sur le cerveau entier dans l'étude 2 a également permis de révéler un ensemble de régions occipitales, temporales et frontales certaines connues comme étant impliquées dans le traitement de l'information visuelle en générale (aires visuelles) ou dans le système de vergence et de disparité binoculaire certainement recrutées puisque notre tâche en RV impliquait à la fois des indices oculomoteurs et perceptifs de profondeur.
Ensuite, les régions montrant une préférence pour les stimulations visuelles proches comparées à loin dans chacune des espèces homme et singe, possédaient des localisations très similaires, ce qui indique la présence d'homologies fonctionnelles à travers ces différentes régions impliquées dans la représentation de l'EPP (voir Figure 23 et 24). Ces réseaux identifiés chez l'homme et le singe suggèrent donc un réseau central et commun de l'EPP qui serait recruté lors d'un événement survenant proche du corps (dans notre cas, lors de la présence d'un objet neutre réel ou virtuel).

La distinction entre les voies dorsales et ventrales du traitement visuel, proposée pour la première fois par Mishkin & Ungerleider (1982) puis affinée par Goodale & Milner (1992) a été considérablement élaborée ces dernières années. Traditionnellement, la voie ventrale a été décrite comme provenant du cortex visuel primaire vers une série d'aires visuelles telles que V2 et V4 et s'étendant ensuite le long de la surface ventrale dans le cortex temporal jusqu'au cortex temporal antérieur inférieur (aire TE), permettant d'identifier l'identité des objets visuels alors que la voie dorsale relie le cortex visuel primaire au cortex pariétal, permettant la localisation des objets visuels et des actions dirigées vers ces objets. Chez le singe, un grand nombre de zones corticales extrastriées interconnectées dans le cortex pariétal constituent la voie dorsale, comprenant le MST, le gyrus temporal supérieur (aire FST), les régions VIP, LIP, MIP et AIP et l'aire inféro-pariétale PF (ou aire 7b). Il y a de plus en plus de preuves qu'à l'intérieur de cette voie dorsale, il existe une subdivision anatomique et fonctionnelle, et en particulier des voies multiples occipito-pariéto-frontales (Rizzolatti & Matelli, 2003). Rizzolatti et Matelli (2003) ont suggéré que les circuits pariéto-frontaux seraient organisés dans une voie dorso-dorsale, allant de V3/V3A à V6 pour atteindre V6A et MIP dans le SPL qui ont de fortes

connexions avec le cortex prémoteur dorsal (F2) et dans une voie ventro-dorsale, qui passerait par l'intermédiaire de AIP ou de l'aire PF située dans la convexité du PCC (aire 7b), étant toutes deux connectées avec la région F5 du prémoteur ventral. Toujours dans ce circuit ventro-dorsal, des entrées afférentes visuelles provenant de l'aire temporale supérieure médiale (MT/MST) ou du cortex somatosensoriel (SI), rejoindraient la région VIP de l'IPS qui aurait elle-même une connexion directe avec la partie caudale du cortex prémoteur ventral F4 ou une connexion par l'intermédiaire de l'aire PEa et de l'aire 5 (Murata et al., 2016).

Chez l'homme, les données de neuroimagerie indiquent une similitude dans l'organisation des aires fonctionnelles à celle du singe au niveau du cortex pariétal (Grefkes & Fink, 2005) avec une décomposition de la voie dorsale en deux sous-circuits : un circuit dorso-dorsal allant de l'aire visuelle V6 passant par V6A au SPL (MIP, VIP, LIP) et un circuit ventro-dorsal allant de V6 ou MT à plusieurs régions pariétales notamment dans l'IPL (Grefkes & Fink, 2005). Comme pour le singe, ces voies dorso-dorsale et ventro-dorsale seraient ensuite reliées aux régions corticales prémotrices à travers deux entrées séparées : une reliant le SPL, à partir de V6A et MIP, à l'aire prémotrice dorsale (PMd) et l'autre reliant la région VIP à l'aire prémotrice ventrale (PMv) ou encore par l'intermédiaire de l'IPL (comme les régions AIP et le SMG). Il a donc été proposé que ces deux sous-circuits pourraient médier différents objectifs comportementaux : la voie dorso-dorsale concernée par le contrôle de l'action « en ligne » (pendant que l'action est en cours) et la voie ventro-dorsale pour la perception de l'espace et la « compréhension de l'action » (Rizzolatti & Matelli, 2003). Enfin, ces deux circuits de la voie dorsale seraient ensuite reliés aux zones corticales frontales préfrontales comme le FEF à travers la région VIP ou la région LIP elle-même connectée aux région MT/MST ou V6. Enfin un troisième circuit pariéto-temporal médial existerait, reliant l'IPL (aire PG) au cortex parahippocampique et à l'hippocampe (Kravitz et al., 2011), et pourrait jouer un rôle dans la navigation spatiale. Ainsi, la plupart des connexions de la voie ventrale atteignent la partie ventrale de la voie dorsale (le sous-circuit ventro-dorsal). Le sous-circuit ventro-dorsal semble donc constituer une interface entre les voies ventrales et dorsales lors du traitement de l'information visuelle. Ce mode d'échange d'informations entre les voies dorsales et ventrales est particulièrement intéressant puisqu'il est très probable que ces circuits traitent les mêmes informations visuelles mais pour des objectifs comportementaux différents (Binkofski & Buxbaum, 2013).

Par conséquent, je peux suggérer que de la même manière chez l'homme et le singe, le circuit de la voie ventrale reliant V1 aux autres aires visuelles jusqu'à la région temporale TE

enverrait des informations à la voie dorsale qui permettrait de traiter l'information visuelle survenant dans l'EPP à travers deux sous-circuits commençant soit par l'aire visuelle V6 et s'étendant ensuite vers les aires pariétales pour se terminer au niveau de l'aire PMd (voie dorso-dorsale) ou passant par l'intermédiaire de l'aire V6 ou par les régions temporales MT/MST pour relier VIP ainsi que des régions dans la partie plus inférieure du cortex pariétal (AIP, PF ou SMG) au PMv (voie ventro-dorsale). En parallèle, l'aire visuelle V6 connectée à la région pariétale LIP ou encore par l'intermédiaire de la région VIP, permettrait d'envoyer ou de recevoir des informations de la région FEF, impliquée dans les indices de vergence, ce qui pourrait permettre de transmettre des indications supplémentaires sur la profondeur et indirectement sur la distance perçue dans l'espace. C'est l'ensemble de ces connexions, ayant principalement lieu dans la voie dorsale du cerveau, qui seraient nécessaires pour réaliser nos actions et réagir rapidement dans l'EPP. Dans la Figure 24, j'ai représenté le réseau neuronal central sous tendant la représentation de l'EPP, mis en évidence chez l'homme et le singe à l'aide des études 1 et 2 ainsi que les potentiels circuits permettant de relier ces régions.

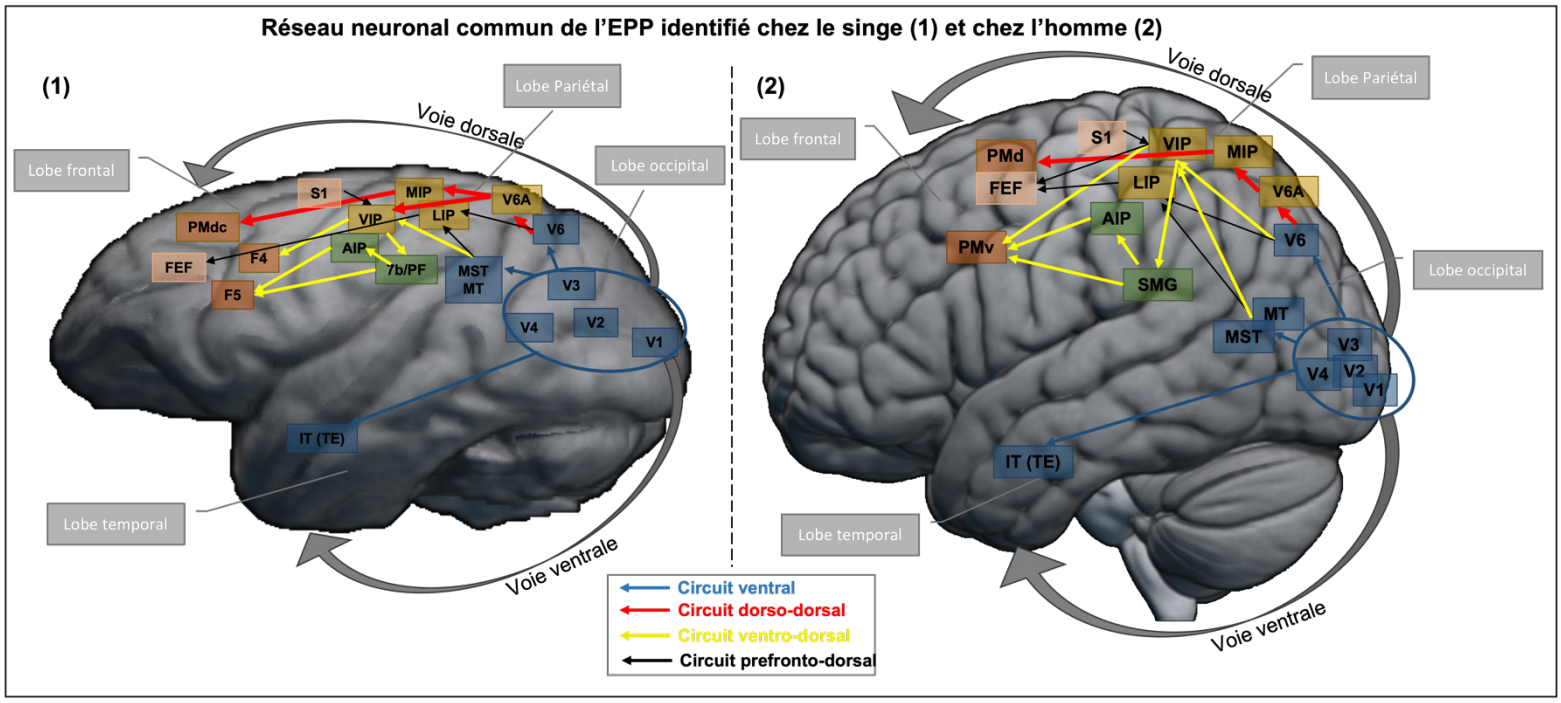

Figure 24. Homologies des réseaux fonctionnels du singe (1) et de l'homme (2) qui sous-tendent la représentation de l'EPP. Représentation schématique des régions neuronales identifiées communément dans les deux espèces qui répondaient préférentiellement soit à l'objet réel ou à l'objet virtuel présenté proche du visage ou dans l'environnement virtuel, respectivement. Les régions représentées en bleu correspondent aux régions visuelles

occipitales et temporales, les régions pariétales sont séparées en deux couleurs : en jaune celles du lobule pariétal supérieur et en vert du lobule pariétal inférieur. Enfin les régions en orange correspondent aux régions frontales, les plus foncées sont les régions prémotrices. Chez les deux espèces, nous suggérons que les régions de la voie ventrale (régions reliées par des flèches bleues) envoient les informations visuelles à la voie dorsale qui permettra ensuite de traiter cette information à travers deux circuits fonctionnant en parallèle : un circuit dorso-dorsal (représenté par les flèches rouges) et un circuit ventro-dorsal (représenté par les flèches jaunes). Ces circuits seraient également reliés aux aires préfrontales, et particulièrement à la région du FEF (circuit représenté par les flèches noires). C'est l'ensemble de ces connexions relayant l'information au sein de la voie dorsale qui nous permettrait de réagir rapidement face à la situation survenant dans notre EPP et ainsi de réaliser l'action nécessaire.

II. Comment l'information sociale module nos capacités de perception, notre état physiologique et notre activité cérébrale ?

Dans les études 3 et 4 de ma thèse, je me suis focalisée sur l'aspect social de l'EPP et plus particulièrement j'ai essayé d'identifier l'impact que pouvait avoir un visage émotionnel inconnu dans notre espace proche sur notre comportement, notre état physiologique et le réseau neuronal sous-jacent. Au travers de la littérature sur l'EPP, mon hypothèse était que l'information sociale dans notre EPP induirait une facilitation de la discrimination visuelle, une augmentation de nos signaux internes, et recruterait un réseau central prémoteur-pariétal, similaire à celui observé comme impliqué dans la représentation de l'EPP pour les indices non sociaux.

Dans l'étude 3 de ma thèse, j'ai testé l'impact de visages avec des expressions émotionnelles apparaissant dans l'espace proche sur les capacités de discrimination visuelle et les mesures physiologiques, à savoir le diamètre pupillaire et le rythme cardiaque. En présentant les visages proches (50 cm) ou éloignés (30 cm) dans un environnement de RV immersif, j'ai identifié une facilitation de la discrimination des visages hommes/femmes lorsque ceux-ci étaient proches (dans l'EPP) (expérience 1), c'est-à-dire un temps de réaction plus rapide comparé à lorsque ces mêmes visages étaient discriminés loin. Cette facilitation pour la

discrimination des visages proches était toujours présente lorsque nous avons corrigé la taille rétinienne pour les visages proche et loin (expérience 2). Autre résultat important : la discrimination visuelle des visages dépendait également de l'émotion véhiculée par le visage (heureux, neutre ou en colère) mais aussi du sexe de l'image et celui du participant. Notamment, les participants étaient plus rapides pour discriminer les visages heureux dans l'EPP et plus lents pour les visages en colère dans l'espace loin. Enfin, nous avons mis en évidence un impact de la distance sur les réponses physiologiques avec, en particulier, une constriction de la pupille pour les visages proche et une dilatation pour les visages loin (expérience 1 et 2), mais également, une augmentation du rythme cardiaque lors de la visualisation passive des visages dans l'EPP (expérience 3). De la même manière que pour les réponses comportementales, ces modulations par la distance variaient également en fonction du sexe du visage et celui du participant.

Ces résultats comportementaux et physiologiques soutiennent l'idée que la représentation de l'EPP est sensible à la fois aux aspects externes du milieu mais également à l'état interne (Bufacchi & Iannetti, 2018). Tout d'abord, la facilitation observée dans les réponses comportementales démontre que la simple présence d'un visage émotionnel semble capturer les mêmes caractéristiques de l'EPP qui ont jusqu'à présent été observées avec des tâches multisensorielles dans un contexte social (Pellencin et al., 2018 ; Teneggi et al., 2013). De plus, la modulation des performances de discrimination par l'émotion ou le sexe suggère que les stimuli complexes apparaissant dans l'EPP bénéficient d'un traitement visuel beaucoup plus fin que ce que l'on pensait. Notamment, la facilitation que nous avons observée pour les visages heureux comparé aux autres émotions pourrait résulter des informations saillantes extraites au niveau de la bouche du visage, ce qui pourrait expliquer l'accélération du traitement de l'information sensorielle (Calvo et al., 2010).

Ensuite, la modulation du diamètre pupillaire ainsi que du rythme cardiaque ajoute une nouvelle preuve d'une modulation des signaux internes du corps qui dépendrait de la distance, comme il a pu l'être récemment identifié à travers l'activité électrodermale (Cartaud et al., 2018 ; Rossetti et al., 2015), bien que ces études aient plus particulièrement observé une augmentation de ces signaux par des stimuli menaçants. La constriction de la taille de la pupille pour les stimuli proches accompagnée par une augmentation du rythme cardiaque suggère une stimulation de la branche sympathique du système nerveux autonome qui pourrait permettre de

préparer le corps à une réaction rapide, particulièrement important pour les évènements survenant dans notre EPP. Également, la constriction/dilatation pupillaire observée pour les visages apparaissant dans l'espace proche ou loin pourrait être reliée à la focalisation des yeux à différentes distances reflétant le couplage entre la taille de la pupille et le système de vergence (Feil et al., 2017). Nous avons également mis en évidence une modulation de ces signaux par l'émotion mais qui ne variait pas en fonction de la distance, en particulier une dilatation de la pupille pour les visages en colère et une augmentation de la variabilité de la fréquence cardiaque (HRV) par les visages heureux. Ces résultats suggèrent que notre état interne serait sensible différemment en fonction de l'émotion, indiquant un niveau « d'excitation » (« arousal » en anglais) différent en fonction de l'émotion.

Dans l'ensemble, ces résultats démontrent que cette représentation de l'espace proche du corps nous permet d'adapter notre réponse comportementale et d'interagir avec les différents éléments de notre environnement en fonction du contexte, d'une manière flexible. Comme je l'ai montré dans le paragraphe précédent, plusieurs études neurophysiologiques et de neuroimagerie ont identifié un ensemble de substrats neuronaux avec une activité sélective en réponse aux stimuli non-sociaux qui étaient présentés dans l'EPP, comprenant des régions prémotrices et pariétales. J'ai donc souhaité étudier la dynamique de ce réseau dans un contexte social, lorsque des visages émotionnels apparaissent dans notre EPP et comment celui-ci, par l'interaction supposée avec d'autres régions neuronales, et par la transmission de nos réponses physiologiques, était impliqué dans la régulation de notre comportement. C'est la question à laquelle j'ai tenté de répondre avec l'étude 4 de ma thèse.

Dans cette quatrième étude, j'ai identifié le réseau neuronal de la représentation de l'EPP dans un contexte social à travers une tâche de discrimination en RV où les participants devaient discriminer entre des stimuli non-sociaux (objets de formes géométriques) ou sociaux (visages véhiculant des émotions) présentés proche dans l'environnement virtuel (30 cm) ou loin (300 cm) (version modifiée de la tâche de discrimination utilisée dans l'étude 3). J'ai donc également comparé ces réseaux neuronaux en fonction du stimulus utilisé, social ou non-social, mais cette dernière partie sera discutée dans le paragraphe suivant.

D'une manière assez similaire aux activations obtenues dans mes études 1 et 2 décrites dans le paragraphe précédent, les visages apparaissant dans l'EPP ont suscité des réponses dans un certain nombre de régions, recrutant un réseau assez large qui comprenait des régions

occipitales, temporales, pariétales et frontales et quelques régions du système limbique comme le gyrus parahippocampique, et l'hippocampe mais également le mésencéphale dans le tronc cérébral et le cervelet situé juste derrière le tronc cérébral. En particulier, des fortes activations étaient observées dans le cortex occipital (inférieur, médian et supérieur), dans la scissure calcarine et le gyrus lingual, comprenant un certain nombre d'aires visuelles (V1, V2, V3, V4, V3A, V3B). Dans le cortex temporal, plusieurs régions étaient recrutées au niveau médian (MST, MT, TPO) puis plus en particulier dans le complexe inféro-temporal postérieur (OFA) et dans le gyrus fusiforme, en particulier dans l'aire fusiforme des visages (« fusiform face area » en anglais ou FFA). Au niveau du cortex pariétal, les activations commençaient au niveau du sillon pariéto-occipital avec les régions V6 et V6A puis dans le SPL et l'IPL où la majeure partie des activations se situait dans l'IPS (régions LIP, MIP, VIP, AIP), et dans le SMG. Enfin dans le cortex frontal, la majeure partie des activations se situait dans le gyrus postcentral (SI), dans le cortex prémoteur (PMv et PMd) et dans les régions préfrontales FEF et PEF ainsi que dans le gyrus frontal médian (dans l'aire 55b). Il est important de noter que ces mêmes régions étaient décodées comme possédant un pattern spatial spécifique entre les conditions proches et lointaines.

Contrairement aux quelques études ayant tenté d'identifier les marqueurs neuronaux de l'espace personnel chez le sujet sain (Holt et al., 2014 ; Vieira et al., 2017, 2020) ou chez les patients (Holt et al., 2015 ; Schienle et al., 2016) utilisant des stimuli dont la taille s'élargissait ou diminuait sur un écran pour les faire apparaitre de manière illusoire comme s'approchant ou s'éloignant du corps, notre paradigme impliquait des apparitions abruptes de visages émotionnels proches ou loin dans un environnement virtuel. Bien que nos paradigmes soient différents, j'ai pu identifier des similitudes dans le recrutement des régions à l'approche des visages, en particulier dans les régions pariétales (SPL, IPL et particulièrement dans l'IPS) (Holt et al., 2014, 2015 ; Schienle et al., 2016 ; Vieira et al., 2017, 2020) et prémotrices (PMd, PMv) (Holt et al., 2014, 2015 ; Vieira et al., 2017, 2020) ainsi que dans le FFA (Holt et al., 2015), le cortex SI (Schienle et al., 2016) et dans le cervelet (Holt et al., 2014 ; Vieira et al., 2017, 2020). De la même manière que Vieira et al. (2020) nous avons également observé une activation accrue dans le tronc cérébral/mésencéphale lors de la présence des visages proches. Cependant, des différences majeures peuvent être également pointées du doigt comme par exemple l'approche des visages qui entrainait une augmentation des réponses neuronales dans l'amygdale (Vieira et al., 2017), dans l'insula (Schienle et al., 2016 ; Vieira et al., 2017, 2020)

ou encore dans le cortex préfrontal (Schienle et al., 2016 ; Vieira et al., 2017, 2020) et le thalamus (Vieira et al., 2020), que nous n'avons pas retrouvé dans cette analyse.

Toutefois, lorsque j'ai identifié les réseaux de l'EPP pour chacune des émotions, en particulier pour l'émotion heureuse, en plus de la majorité des régions déjà identifiées dans les aires occipitales, pariétales et prémotrices, j'ai également observé une augmentation de l'activité dans l'insula, dans le cortex dorsolatéral préfrontal, dans le rolandic operculum, dans le cortex cingulaire et dans le complexe rétrosplénial pour cette émotion. Ces régions n'étaient pas retrouvées pour les autres émotions, neutre et en colère. Il a été montré que l'insula possède des connexions privilégiées avec le cortex cingulaire et l'amygdale mais également avec d'autres structures corticales et sous-corticales et contribuerait à l'expérience consciente des émotions. L'insula, recevant des entrées intéroceptives de l'ensemble du corps jouerait un rôle dans la perception des réactions corporelles provoquées par les émotions comme le montrent certaines études à travers une activation de l'insula qui covarie avec des sensations subjectives reflétées par l'intensité du stimulus (revue Gogolla, 2017).

Mes résultats reflètent donc un réseau beaucoup plus étendu lors du traitement des visages heureux dans l'EPP, suggérant qu'il se passe un traitement « particulier » lors de la perception de cette émotion, comme j'ai pu également l'observer à travers mes résultats comportementaux et physiologiques obtenus dans l'étude 3. Comme déjà évoqué plus haut dans le paragraphe, il est possible que la différence des performances obtenue dans la tâche de discrimination spécifiquement pour les visages heureux pouvait s'expliquer par la présence de la saillance véhiculée au niveau de la bouche (Calvo & Nummenmaa, 2011).

Comme je l'ai suggéré dans le paragraphe précédent, la contribution des voies ventrales et dorsales, et plus spécifiquement d'un échange des informations visuelles dans différents sous circuits de la voie dorsale, constitueraient les processus cérébraux impliqués pour traiter l'information dans l'EPP et ainsi adapter un comportement approprié. Cependant, lors de la visualisation d'éléments sociaux, la voie visuelle ventrale jouerait un rôle d'autant plus important lors de l'élaboration de l'information visuelle puis de la transmission de ces informations à la voie dorsale et plus particulièrement aux régions pariétales et prémotrices. En effet, un réseau spécifique dans la voie visuelle ventrale serait recruté lors du traitement des visages. Il a été suggéré que ce système serait composé de deux voies distinctes : une voie plus dorsale allant de l'aire occipitale des visages (OFA) au STS et une voie ventrale partant de la même région mais se projetant jusqu'au gyrus fusiforme (FFA). Ces deux voies joueraient des

rôles différents dans le traitement des visages : tandis que le premier serait impliqué dans le traitement des aspects changeants des visages (expression, regard, mouvement des lèvres), le second comprenant la région du FFA serait spécialisé dans le traitement de l'identité du visage (Haxby et al., 2000 ; O'Toole et al., 2002). Récemment, une troisième voie visuelle, sur la face latérale du cerveau a été mise en évidence cohérente avec les entrées neuroanatomiques et fonctionnelles qui se projettent de V1, via la zone temporale moyenne (MT), jusqu'au STS et serait principalement engagée dans les aspects dynamiques de la perception sociale (Pitcher & Ungerleider, 2021).

Par conséquent, mes résultats suggèrent qu'un circuit ventral reliant la région FFA serait nécessaire pour relayer l'information sociale, survenant dans l'EPP, jusqu'aux circuits ventro et dorso-dorsal permettant de connecter les aires pariétales aux régions prémotrices et préfrontales (FEF). L'ensemble de ces connexions constitueraient un système d'échange complexe pour traiter les informations visuelles sociales apparaissant dans l'EPP afin de nous permettre de réagir rapidement, comme observé à travers la facilitation de nos performances de discrimination (étude 3).

Néanmoins, le recrutement de régions supplémentaires observé pour les visages heureux, comme l'insula, ainsi que l'activation du système autonome via une modulation des signaux physiologiques (étude 3) suggèrent que le traitement de l'information ne se limite pas à ces circuits, et que d'autres interactions ont probablement lieu pour permettre de réagir face à certains éléments sociaux, comme un visage émotionnel particulier, ou face à certaines situations survenant dans notre EPP. Je peux par exemple supposer que lors de l'activation du système autonome, les signaux intéroceptifs ascendants seraient transmis à plusieurs noyaux du tronc cérébral, y compris le noyau du tractus solitaire (NTS), le noyau parabrachial (PB) et la matière grise périaqueducale (PAG) qui à leur tour réguleraient les entrées neuromodulatrices vers les régions cérébrales sous-corticales et corticales (Azzalini et al., 2019 ; Critchley & Harrison, 2013). Les signaux intéroceptifs ascendants pourraient donc être envoyés aux régions sous-corticales impliquées dans la régulation autonome, comme par exemple l'hypothalamus, l'amygdale, le striatum et le cervelet (Azzalini et al., 2019 ; Critchley & Harrison, 2013) mais également vers de nombreuses voies corticales qui reçoivent des entrées viscérales comme le cortex somatosensoriel primaire, l'insula, le cortex cingulaire et le cortex préfontral ventromédian (Amassian, 1951 ; Azzalini et al., 2019 ; Cechetto & Saper, 1987 ; Dum et al., 2009). L'hippocampe reçoit également des entrées du tronc cérébral via une voie

multisynaptique (Castle et al., 2005). En effet, bien que l'hippocampe soit surtout impliqué dans la mémoire épisodique et dans la navigation spatiale, c'est aussi une région clé dans le réseau cérébral émotionnel qui joue un rôle important dans la cognition sociale, en particulier dans la régulation des émotions en réponse à des images ou des stimuli émotionnels positifs (Palomero-Gallagher & Amunts, 2021). Bien que cette région n'ait pas été, jusqu'à présent, particulièrement reliée au traitement de l'EPP, son activation accrue par les stimuli sociaux proches, dans mes résultats, suggère que cette région pourrait jouer un rôle par exemple dans la transmission des informations intéroceptives puisque cette même région est ensuite reliée à un ensemble de structures corticales et en particulier à l'aire PG du cortex pariétal inférieur, elle-même connectée à l'ensemble du réseau identifié comme le réseau central pariéto-premoteur de l'EPP.

Toutefois, l'insula pourrait être considérée comme une région majeure pour intégrer les entrées sensorielles extéroceptives et les signaux intéroceptifs (Uddin et al., 2017) envoyés ensuite au réseau de l'EPP, puisque comme je l'ai montré, cette région joue un rôle important dans la perception des réactions corporelles (Gogolla, 2017) mais possèdent également une activation accrue lors de l'approche de visages émotionnels (Schienle et al., 2016 ; Vieira et al., 2017, 2020), également observée à travers mes résultats pour les visages heureux proches. Connue comme possédant de fortes connexions avec le cortex pariétal, frontal ainsi qu'avec des régions sous-corticales comme l'hippocampe et l'amygdale (Showers & Lauer, 1961), il a également été récemment montré que le cortex insulaire était anatomiquement connecté avec l'IPL, le PMv et l'aire 46 similairement chez l'homme et le singe (Di Cesare et al., 2019), bien que ces connexions avec le circuit pariéto-frontal aient été déjà établies chez le singe, particulièrement dans l'aire AIP/PF, dans l'aire prémotrice F5 et l'aire préfrontale 46v (Bruni et al., 2017).

Ces interactions cerveau-viscères me laissent donc penser que les signaux viscéraux intéroceptifs communiqueraient avec le réseau pariétal-premoteur-prefrontal, codant la représentation de l'EPP, pour moduler directement ou indirectement son activité à travers un ensemble de régions corticales (comme l'insula) et/ou sous-corticales (comme l'hippocampe ou l'amygdale) pour former un seul système complexe permettant de façonner nos réponses comportementales en fonction du contexte social (voir Figure 25).

III. Les réponses cérébrales de la représentation de l'EPP sont-elles influencées en fonction de la nature de l'information (sociale vs non-sociale) ?

Après avoir identifié le réseau neuronal fonctionnel impliqué dans le traitement des informations sociales dans l'EPP, c'est naturellement que je me suis posée la question des similitudes et différences avec celui recruté par les éléments non-sociaux.

Tout d'abord, si je compare les activations neuronales obtenues dans l'étude 4 avec celles identifiées dans l'étude 1 lors de la présentation d'une balle réelle et dans l'étude 2 avec la présentation d'une balle virtuelle chez l'homme, je peux souligner une grande similarité dans les régions. En effet, les activations au niveau du cortex occipital, et dans le sillon occipito-pariétal semblent cohérentes (V1, V2, V3, V4, V6, V6A). Ensuite, je peux également observer des activations similaires dans la jonction pariéto-temporo-occipitale ainsi que dans l'aire médiale temporale supérieure (MST). Cependant les régions OFA et FFA sembleraient être uniquement recrutées en condition sociale, un résultat supposé attendu puisque ces régions ont été démontrées comme faisant partie d'un réseau spécifique dans le traitement des visages (Haxby et al., 2000). Dans le PCC, la seule différence qui semble émerger serait au niveau du cortex pariétal inférieur et plus en particulier la région AIP ainsi que les régions 7a et 7PC qui sembleraient recrutées uniquement par les stimuli non-sociaux. Ce résultat suggère que la région AIP pourrait être recrutée uniquement dans le traitement des objets et non des visages, peut-être par son rôle dans l'identité tridimensionnelle d'un objet telle que sa forme, son orientation et sa taille (Murata et al., 2000). Enfin, contrairement à nos études avec stimuli non-sociaux, plus particulièrement observé dans l'étude 1, le putamen n'était également jamais recruté avec les stimuli sociaux.

Comme mentionné dans le paragraphe précédent, dans la tâche utilisée dans l'étude 4, les participants devaient discriminer entre les visages émotionnels d'hommes et de femmes mais également entre des formes géométriques qui étaient présentées proche ou loin dans l'environnement virtuel, les mêmes stimuli 3D non sociaux qu'utilisés dans l'étude 2 en version passive. Ainsi, la présence de ces deux types de stimuli dans une même étude m'a permis de

comparer directement les activations pour chaque type d'information dans une même tâche. Plus particulièrement, j'ai déterminé si le modèle/pattern de décodage de la distance était similaire pour les stimuli sociaux et non sociaux en entrainant une catégorie et en testant si ces informations de distance pouvaient être décodées sur l'autre catégorie. Ces résultats ont montré que les informations liées à la distance pouvaient être décodées pour les informations sociales ou non sociales dans la plupart des régions cérébrales occipitales, pariétales et prémotrices identifiées précédemment pour chacune des catégories. Ce décodage de la distance dans les deux catégories a particulièrement été identifié dans les aires visuelles (V1, V2, V3, V4, V6), dans les régions du cortex pariétal supérieur V6A, MIP, VIP, LIP, dans le cortex somatosensoriel (SI), dans les régions du cortex prémoteur (PMv et PMd), dans le FEF, dans l'aire 55b du gyrus frontal médian et dans le cervelet. En d'autres termes, l'activité au sein de ce réseau contiendrait des informations de distance qui ne font pas de distinction entre les catégories sociales et non sociales. Ce résultat confirme donc mes observations faites lors de la comparaison entre les résultats obtenus dans les études 1, 2 et 4 avec une différence majeure qui se situe essentiellement au niveau du cortex temporal et au niveau du cortex inférieur de l'aire pariétale mais également dans le putamen. Dans l'IPL en particulier, ni la région AIP, ni le SMG (aires PF/PFG) ne permettait de décoder la distance à la fois pour les deux catégories.

Ces résultats appuient le fait que les sous-circuits dorso-dorsal et ventro-dorsal de la voie dorsale reliant le cortex pariétal et les régions prémotrices, discutés dans les paragraphes précédents, contribueraient à la perception de l'espace avec différents rôles. Je peux suggérer que le cortex pariétal postérieur contribuerait à un traitement spatial multimodal avec la plus grande partie des régions étant impliquées dans le traitement visuospatial de la représentation de l'EPP en général, notamment à travers la voie dorso-dorsale ainsi que le circuit de la voie ventro-dorsale reliant la région VIP jusqu'au PMv. Cependant, d'autres régions du cortex pariétal seraient impliquées dans la traduction d'informations visuelles en représentations adaptées pour guider des actions (Culham & Valyear, 2006) comme la région AIP de la voie ventro-dorsale qui possèderait des représentations/caractéristiques des objets en 3D adaptés pour pouvoir guider la main et les doigts vers un objet (Durand et al., 2007 ; Murata et al., 2000 ; Orban, 2016 ; Srivastava et al., 2009b) et des régions adjacentes de la partie rostrale de l'IPL (comme l'aire PF/PFG, encore appelée SMG) qui contiennent des représentations multimodales complexes comme l'organisation de l'action dans l'espace relatif au bras et à la main (Rozzi et al., 2008).

Il a notamment été montré que l'AIP contribuerait à l'étape de planification initiale du mouvement vers l'objet en incorporant à la fois des preuves spatiales et des connaissances sur la configuration d'objets familiers (Verhagen et al., 2012) suggérant que la région AIP permettrait d'établir un plan moteur basé sur ces différentes sources d'informations provenant de l'affordance de l'objet. Arbib & Mundhenk (2005) ont notamment proposé que l'affordance perceptive pour atteindre l'objectif d'action pour manipuler l'objet serait sélectionnée dans la région AIP, selon un signal du cortex préfrontal. Ces études suggèrent donc que des fonctions spatiales et non-spatiales seraient représentées dans le PPC avec un gradient s'étendant du SPL, au travers de l'IPS, à l'IPL de fonctions spatiales à non spatiales (Husain & Rorden, 2003) et quelques régions intermédiaires dans l'IPS présentant des fonctions à la fois spatiales et non spatiales. Selon ce modèle, le SPL, faisant partie du système dorso-dorsal pourrait être dédié au contrôle de l'action dans l'EPP (par exemple comme observé à travers les facilitations des réponses comportementales), tandis que l'IPL faisant partie de la voie ventro-dorsale serait nécessaire dans la perception spatiale mais également à la compréhension de l'action (Murata et al., 2016).

De plus, comme je l'ai montré à travers ces résultats, la région sous-corticale du putamen dans les ganglions de la base serait également uniquement recrutée dans le cas d'informations non-sociales présentées dans l'EPP suggérant que cette région pourrait encoder la localisation de l'objet permettant de réaliser les actions en lien avec la coordination sensorimotrice en fonction de la partie du corps ciblée (Graziano & Gross, 1993), à partir de projections de l'aire 7b chez le singe (ou PF) (Cavada & Goldman-Rakic, 1989). En effet, il a notamment été montré que cette région posséderait un cadre de coordonnées visuelles ancrées sur différentes parties du corps, comme la main ou le visage dans le but d'encoder la cible pour permettre ensuite de réaliser l'action sensori-motrice dans l'EPP (Graziano & Gross, 1996).

Ces cadres de coordonnées visuelles fixées sur différentes parties de la surface du corps dans le but de réaliser des actions dans l'espace proche de la partie du corps ont été décrits dans plusieurs régions prémotrices et pariétales par les études en électrophysiologie chez le singe. Notamment, les neurones de l'aire intrapariétale VIP ou de l'aire 7b qui possédaient une représentation de leurs champs récepteurs distribuée sur la main, le bras, le visage et la tête (Colby et al., 1993 ; Duhamel et al., 1998) ou les neurones de la partie ventrale du cortex

prémoteur (aire 6) qui possédaient des champs récepteurs autour de la main, du bras, du cou et du visage (Fogassi et al., 1996 ; Graziano et al., 1994).

Chez l'homme, l'ensemble des études sur l'EPP utilisaient jusqu'à présent des stimulations proches de la main ou du visage, mais il n'a jamais été testé directement si la représentation de l'EPP pouvait avoir une organisation somatotopique dans le réseau neuronal de l'EPP. Dans l'étude 1 de ma thèse, j'ai testé cette idée en présentant une balle réelle proche de différentes parties du corps, en particulier de la main, du visage et du tronc. Mes résultats indiquent une activation préférentielle pour les stimuli proches du corps, quelle que soit la partie du corps stimulée, au niveau du sillon intrapariétal et des zones pariétales supérieures environnantes mais également dans le SMG. Ces régions ont souvent été rapportées dans les études sur l'EPP chez l'homme, en relation avec des stimulations proches de la main (Brozzoli et al., 2011, 2012 ; Gentile et al., 2011, 2013 ; Makin et al., 2007), ou du visage (Bremmer et al., 2001 ; Holt et al., 2014 ; Huang et al., 2012 ; Sereno & Huang, 2006) ou à d'autres parties du corps (Huang et al., 2012), et est l'une des zones également rapportée dans la méta-analyse (Grivaz et al., 2017). Cependant, ces résultats montrent quelques spécificités intéressantes en fonction des parties du corps, en particulier dans les régions prémotrices. En effet, ces régions qui s'activaient à la fois par les stimuli proche du visage et de la main recrutaient une partie commune mais également des parties spécifiques à l'intérieur de cette même région, avec un gradient antéro-postérieur, la partie plus antérieure possédant des réponses spécifiques à l'espace proche du visage et la partie plus postérieure des réponses spécifiques à l'espace proche de la main.

Ces résultats fournissent une preuve que chez l'homme, des populations de neurones dans les régions prémotrices et pariétales impliquées dans le traitement de l'EPP coderaient similairement et spécifiquement l'espace proche de certaines parties du corps comme observé dans les régions pariétales pour le visage, la main et le tronc et dans les régions prémotrices pour la main et le visage, validant le fait que le réseau neuronal de l'EPP possèderait une représentation somatotopique fine et probablement efficace pour nous permettre de réagir plus rapidement en fonction du contexte.

Par conséquent, la mise en évidence d'un réseau neuronal occipital-pariéto-prémoteur commun pour le traitement des informations sociales et non sociales dans l'EPP et codant l'espace proche de plusieurs parties du corps par sa représentation somatotopique fine et spécifique suggère qu'un « noyau » commun dans la voie dorsale impliquant spécifiquement les circuits reliant les régions du SPL et du sillon intrapariétal aux régions prémotrices, aurait

un rôle fondamental pour les actions survenant dans l'EPP, quelles soient sociales ou non-sociales.

IV. Mécanisme neuronal de l'espace personnel pour réguler les distances entre individus

Bien que le réseau neuronal qui nous permet de réagir face à un visage émotionnel apparaissant proche de notre corps a pu être identifié (étude 4), dans la vie de tous les jours, nous faisons souvent face à des situations sociales où nous devons interagir avec des individus. Ces interactions sociales nécessitent aux individus d'ajuster automatiquement leurs distances en fonction de leurs relations mais également du contexte où se déroule l'interaction afin d'éviter l'inconfort. Comment notre cerveau permet de maintenir et réguler de façon appropriée cette distance de confort, appelé espace personnel ? Est-ce le même réseau neuronal que celui recruté par les éléments sociaux dans l'EPP ?

Des études antérieures ont indiqué que l'amygdale, qui contribue de manière générale au traitement des informations sociales (Adolphs, 2010 ; Hadj-Bouziane et al., 2012 ; Martin & Weisberg, 2003), était une région essentielle pour réguler les distances, observé à travers une réduction de l'espace personnel chez une patiente qui présentait des lésions bilatérales de l'amygdale comparé aux sujets contrôles (Kennedy et al., 2009) mais également à travers son rôle dans l'approche sociale et l'évitement social (Capitanio et al., 2006 ; Emery et al., 2001).

Dans l'étude 5 de ma thèse, j'ai cherché à étendre notre compréhension de la régulation de l'espace personnel en testant trois patients qui possédaient des lésions unilatérales temporales (incluant le cortex parahippocampique, l'hippocampe, l'amygdale, le gyrus fusiforme, le pole temporal et le MT) dont un avec une lésion qui était entièrement confinée à l'amygdale gauche, dans des tâches de distance d'arrêt en RV ou en version réelle où les sujets devaient arrêter des visages émotionnels ou l'expérimentateur lorsqu'ils commençaient à se sentir mal à l'aise avec la proximité de l'individu.

J'ai pu montrer que les trois patients avec une lésion unilatérale du lobe temporal médian arrêtaient les visages ainsi que l'expérimentateur plus proche d'eux, par rapport aux sujets contrôles, signifiant des distances interpersonnelles plus courtes chez ces patients de la même

manière que l'étude de Kennedy et al. (2009). Également, par rapport aux sujets sains, les patients n'ajustaient jamais leur distance en fonction de l'expression émotionnelle du visage malgré une capacité préservée à catégoriser l'émotion. Ces déficits de régulation des distances identifiés chez ces patients étaient accompagnés d'une modification de la fréquence cardiaque comparé aux sujets sains lors de l'approche des visages.
L'étendue de la lésion variait d'un patient à l'autre incluant une grande partie de l'amygdale chez un patient, alors que pour les deux autres, la lésion épargnait la plupart ou la totalité de l'amygdale, affectant de plus grandes parties des autres régions temporales. Ces résultats ont donc permis de mettre en évidence que la régulation de l'espace personnel ne dépendait pas seulement de l'intégrité de l'amygdale et qu'une lésion dans le lobe temporal, touchant notamment le cortex parahippocampique, l'hippocampe, le gyrus fusiforme, le pôle temporal et le gyrus temporal moyen, affectait également la régulation des distances sociales, quel que soit le côté de la lésion.

Mes résultats soutiennent donc l'idée que l'espace personnel pourrait reposer sur des interactions au sein d'un réseau interconnecté (Sarubbo et al., 2015, 2020) et qu'une lésion dans l'une de ces régions temporales perturberait ce réseau ce qui amènerait à une modification des comportements appropriés lors de la régulation des distances sociales. Néanmoins, la présence de lésions unilatérales chez ces patients et non bilatérales, comme dans l'étude de Kennedy et al. (2009), suggèrent que même le maintien d'une amygdale intacte ne permet pas de réguler à elle seule l'espace personnel. Également, le fait que, contrairement aux sujets sains, la distance interpersonnelle de ces patients n'était pas modulée par l'émotion et que la régulation des signaux physiologiques semblait affectée ajoute une preuve supplémentaire au fait que ces régions pourraient permettre d'ajuster le comportement de manière appropriée aux situations sociales.

Comme je l'ai exposé dans le paragraphe 2, de récentes études en neuroimagerie ont tenté d'identifier les corrélats neuronaux de l'espace personnel lors de l'approche de visage, en mettant en évidence un certain nombre de régions pariétales (SPL, IPL et particulièrement dans l'IPS) (Holt et al., 2014, 2015 ; Schienle et al., 2016 ; Vieira et al., 2017, 2020) et prémotrices (PMd, PMv) (Holt et al., 2014, 2015 ; Vieira et al., 2017, 2020) que j'ai également pu identifier comme jouant un rôle dans la représentation de l'EPP à la fois dans un contexte social et non-social (paragraphes 2 et 3). Des régions étaient également recrutées uniquement par les stimuli sociaux, comme la région FFA, le cortex parahippocampique, l'hippocampe et le tronc cérébral

mais également l'insula uniquement avec les visages heureux, dont certaines de ces régions ont également été identifiées dans les études sur la représentation neuronale de l'espace personnel (Holt et al., 2015, FFA ; Schienle et al., 2016, Insula ; Vieira et al., 2017, 2020, tronc cérébral, insula). Néanmoins, ces études ont aussi mis en évidence des activations neuronales dans l'amygdale (Vieira et al., 2017) et dans le thalamus (Vieira et al., 2020), indiquant que ces régions joueraient un rôle précis dans la représentation de l'espace personnel, comme déjà évoqué pour l'amygdale (Kennedy et al., 2009).

Il est important de noter que certaines de ces régions mises en évidence dans des contextes sociaux du traitement de l'EPP et/ou de l'espace personnel, sont interconnectées anatomiquement et fonctionnellement. Par exemple, l'insula est fonctionnellement et anatomiquement liée à l'amygdale (Mufson et al., 1981 ; Uddin et al., 2017), qui jouerait un rôle dans la régulation des distances lors des interactions sociales comme observé à travers mes résultats obtenus chez les patients et dans l'étude de Kennedy et al. (2009) ou encore observé présentant une activité atypique chez les sujets autistes (Lough et al., 2015) qui serait également liée à une diminution anormale de la distance personnelle (Kennedy & Adolphs, 2014 ; Massaccesi et al., 2021). Cette région serait également liée au lobule pariétal, au PMv (Gerbella et al., 2014) et à la région FFA où une récente étude a mis en évidence une augmentation de la connectivité fonctionnelle entre l'amygdale, l'IPS et la région du FFA chez les patients autistes comparés aux sujets sains (Massaccesi et al., 2021). Dans cette pathologie, une intéroception atypique a été identifiée (Mul et al., 2019 ; Quadt et al., 2018) ce qui pourrait être lié à une altération de la représentation de l'EPP et de l'espace personnel (Mul et al., 2019 ; Noel et al., 2017). Dans cette même lignée, Holt et al. (2015) ont rapporté une réduction du couplage fonctionnel entre l'IPS et l'aire FFA chez les patients schizophrènes lors de l'approche de visages, une pathologie qui a récemment été associée à une modification de la représentation de l'EPP (Lee et al., 2021) mais également à un déficit de leur espace personnel (Corbo et al., 2017 ; Di Cosmo et al., 2018) par rapport aux sujets sains.

L'ensemble de ces études suggèrent qu'un dialogue 'anormal' entre les régions impliquées dans le traitement et la reconnaissance des visages et les régions identifiées comme jouant un rôle dans la représentation de l'EPP et celle de l'espace personnel pourrait entraîner des difficultés dans l'interaction avec les éléments sociaux dans notre environnement proche, y compris durant nos interactions sociales.

Par conséquent, mes résultats obtenus dans les études 4 et 5 ainsi que les données existantes de la littérature suggèrent que les mécanismes sous-jacents de la représentation de l'EPP partageraient des points communs avec ceux de l'espace personnel en recrutant un réseau neuronal principal occipito-parieto-premoteur, déjà identifié comme le réseau cœur de l'EPP impliqué dans n'importe quelle situation intervenant dans l'espace proche dans les paragraphes précédents (sociale/non-sociale), mais également en recrutant un réseau d'aires temporales pour traiter en particulier l'information sociale. La différence dans la représentation neuronale de ces deux espaces semblerait plus subtile, observé à travers le recrutement supplémentaire de certaines régions, comme l'amygdale, mais cette différence pourrait provenir de la fonction ciblée ou plus généralement de l'information sociale véhiculée, comme observé à travers avec le recrutement de l'insula pour les visages heureux dans l'étude 4. Par conséquent ces différences seraient-elles simplement dues à la tâche demandée ?

En effet, comme je l'ai exposé dans l'introduction, même au sein des études comportementales utilisées pour étudier la fonction sociale de l'EPP, une divergence des résultats pouvait être observée allant dans des sens différents en fonction du paradigme expérimental, à savoir en fonction de l'utilisation de la tâche de jugement d'atteinte (Iachini et al., 2014, 2015, 2016 ; Ruggiero et al., 2017) ou de la tâche d'interaction multisensorielle (Pellencin et al., 2018 ; Teneggi et al., 2013). De la même manière, au laboratoire, les tâches utilisées pour étudier l'espace personnel et l'EPP utilisent des paradigmes expérimentaux qui peuvent être assez éloignés puisque dans les tâches utilisées pour étudier l'espace personnel il est demandé à l'individu de juger ou d'arrêter le congénère face à lui à partir du moment où il commence à ressentir de l'inconfort par rapport à la proximité, l'individu étant donc totalement conscient de la distance de la personne face à lui, de la même manière d'ailleurs que pour la tâche de jugement d'atteinte, alors que dans la tâche d'interaction multisensorielle ou dans nos tâches de discrimination visuelle, l'individu doit détecter la stimulation tactile ou discriminer entre deux catégories, et ne prend donc pas en considération consciemment la distance du stimulus visuel. Bien que les tâches en laboratoire semblent cibler des fonctions différentes à travers ces paradigmes expérimentaux, l'EPP et l'espace personnel ont pourtant tous deux été décrits comme des zones de confort puisqu'il a été suggéré que l'EPP possédait une fonction défensive, permettant de réagir rapidement pour se protéger dans certaines situations. Cette fonction de défense pourrait être reliée à la fonction de régulation des distances au cours des interactions sociales avec des inconnus, nous permettant de garder ces individus hors de cette zone pour nous protéger de l'inconfort ou d'un danger. Il est donc difficile de conclure sur le fait que ces

espaces soient strictement similaires mais il est possible d'affirmer que ces espaces partagent des points communs, déjà observé à travers certaines études comportementales qui ont tenté de comparer ces deux espaces mais surtout à travers les études 4 et 5 de ma thèse qui ont permis d'identifier un chevauchement clair des régions sous-tendant la représentation de ces deux espaces. Ainsi, la dimension sociale de l'EPP et l'espace personnel recruteraient de la même manière un réseau central interconnecté avec d'autres régions corticales et sous-corticales pour nous permettre de réaliser une réponse rapide ou un ajustement de nos distances lors des interactions sociales. En effet, nous avons vu que l'information visuelle sociale mais également la variation de nos signaux physiologiques dans certaines situations (une personne trop proche ou une situation émotionnelle) recruterait un ensemble d'autres régions qui permettrait de relayer ces informations spécifiques au réseau central de l'EPP afin d'affiner notre comportement lorsqu'il est nécessaire mais également de maintenir de façon appropriée les distances sociales (voir Figure 25).

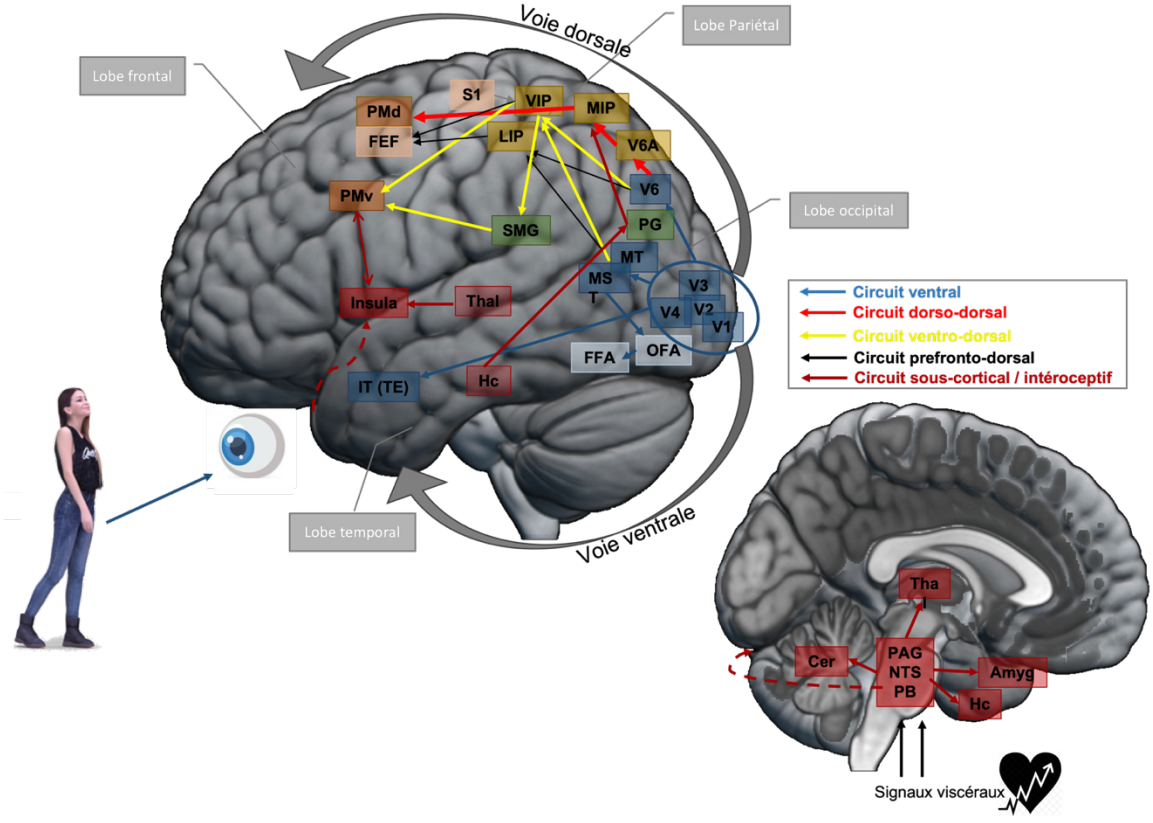

Figure 25. Réseau neuronal sous-tendant la représentation de l'EPP dans un contexte social. Représentation schématique des régions neuronales recrutées par des visages émotionnels présentés proche du corps mises en évidence dans l'étude 4, des régions identifiées

dans l'étude 5 comme jouant un rôle important dans la régulation appropriée des distances ainsi que des régions permettant de transmettre les signaux intéroceptifs.
Les régions cérébrales représentées en bleu correspondent aux aires visuelles occipitales et temporales, les régions en bleu claires constituant le réseau impliqué dans le traitement des visages. Les régions pariétales sont séparées en deux couleurs : en jaune celles du lobule pariétal supérieur et en vert celles du lobule pariétal inférieur. Les régions frontales sont représentées en orange, les plus foncées correspondant aux régions prémotrices. Les régions en rose correspondent aux régions sous-corticales ou corticales impliquées uniquement dans la transmission des signaux intéroceptifs ou ayant été identifiées comme jouant un rôle particulier lors du traitement des informations sociales et/ou émotionnelles. Je suggère qu'un réseau central comprenant un ensemble de régions interconnectées occipitales, pariétales et frontales permettrait de traiter l'information visuelle, qu'elle soit sociale ou non sociale, à travers deux circuits fonctionnant en parallèle : un circuit dorso-dorsal (représenté par les flèches rouges) et un circuit ventro-dorsal (représenté par les flèches jaunes). Ces circuits seraient également reliés aux aires préfrontales, et particulièrement à la région du FEF (circuit représenté par les flèches noires). C'est l'ensemble de ces connexions relayant l'information au sein de la voie dorsale qui nous permettrait de réagir rapidement face à une situation survenant dans notre EPP et ainsi de réaliser l'action nécessaire. L'information sociale en particulier recruterait également un ensemble de régions permettant d'envoyer un signal spécifique pour réagir en conséquence. Ces informations spécifiques seraient envoyées à la fois par le circuit du traitement des visages dans la voie ventrale (circuit représenté en bleu) et par un circuit sous-cortical/cortical qui permettrait de relayer l'information intéroceptive provenant des signaux viscéraux (circuit représenté en rose). Ce dernier circuit permettrait de communiquer ces signaux, qui seraient par exemple modulés par une information émotionnelle spécifique, au réseau pariétal-prémoteur central codant pour la représentation de l'EPP, nous permettant ainsi de façonner nos réponses comportementales, et donc de réaliser rapidement l'action nécessaire ou pour réguler nos distances en conséquence au cours des interactions sociales.

V. Perspectives

Pour donner suite à la découverte de ces résultats, plusieurs questions persistent. Notamment, mes résultats montrent un réseau neuronal central et commun permettant de traiter l'information dans l'EPP quel que soit le type d'information (social/non-social) et j'ai proposé, à travers les connexions anatomiques et/ou fonctionnelles existantes entre ces régions, une dynamique d'interactions à l'intérieur de ce réseau de l'EPP et également avec d'autres aires cérébrales recrutées ensuite spécifiquement en fonction du contexte (EPP social/non-social et espace personnel). Mais comment 'discutent' réellement ces régions ? Et interagissent-elles différemment en fonction de l'information perçue ou de la tâche à accomplir dans l'EPP ou

pendant la régulation de nos distances sociales, même dans le réseau « cœur » commun à toutes ces situations ? Pour répondre à ces questions, il serait intéressant d'analyser les changements de connectivité fonctionnelle entre ces régions à travers l'analyse d'interaction psychophysiologique généralisée (PPI) (O'Reilly et al., 2012) permettant d'étudier les changements spécifiques à une tâche à travers la relation entre l'activité des différentes aires neuronales, ou encore à travers la méthode DCM (Dynamic Causal Modelling) (Friston et al., 2003) permettant de tester plusieurs modèles d'interactions neuronales, à l'aide de la comparaison de modèles bayésiens, à travers les connexions entre ces régions évoquées dans cette discussion. Par conséquent, ces analyses pourraient être réalisées pour identifier l'effet du stimulus sur la communication entre ces régions, à l'aide des données acquises dans mes études 2 et 4, mais également pour comparer les réseaux neuronaux des espèces homme et singe afin d'obtenir une mesure quantitative de ces similitudes entre espèces, à travers les données des études 1 et 2. Ainsi, ces analyses permettraient de renforcer nos conclusions sur la présence d'homologies fonctionnelles claires entre les réseaux de l'EPP chez ces deux espèces.

Dans la continuité de la comparaison neuronale des réseaux fonctionnels entre l'homme et le singe et pour donner suite à nos découvertes concernant la dimension sociale de l'EPP chez l'homme, il serait également intéressant de réaliser des tâches similaires impliquant des informations sociales à connotation émotionnelles présentées proche ou loin dans l'environnement virtuel chez le singe afin d'identifier le réseau neuronal de la représentation sociale de l'EPP du singe. J'avais d'ailleurs déjà commencé à entreprendre ce travail à la fin de ma thèse.

VI. Conclusion

Au travers de mon travail de thèse, j'ai ainsi pu apporter de nouvelles réponses sur différents questionnements qui restaient en suspens concernant la représentation de l'EPP. J'ai ainsi pu combler le fossé entre les données qui étaient existantes à ce jour sur les propriétés enregistrées dans les neurones du singe et l'activité cérébrale identifiée en neuroimagerie chez l'homme en identifiant un réseau occipito-prémoteur-pariétal homologue possédant des propriétés similaires pour le traitement des objets apparaissant dans l'EPP chez les deux espèces. Son rôle dans les interactions physiques et non-sociales étant déjà bien établi, j'ai ensuite réalisé un ensemble de travaux qui m'ont permis de caractériser le fonctionnement de

cet espace dans les situations sociales et émotionnelles en combinant des mesures comportementales, physiologiques et neuronales, afin de mieux comprendre son fonctionnement au cours des interactions sociales. J'ai ainsi pu montrer qu'un réseau neuronal central permettrait de traiter n'importe quelle information survenant dans notre espace proche, qu'elle soit sociale ou non sociale, notamment pour réagir rapidement en fonction de la tâche à réaliser, par exemple pour attraper un objet, ou pour réagir face à une personne inconnue en face de nous. C'est cependant avec l'interaction de régions neuronales supplémentaires interconnectées, permettant de relayer d'autres informations essentielles à ce réseau central comme nos signaux intéroceptifs, que nos actions seraient affinées pour faire face à certaines situations intervenant dans notre espace proche, par exemple si la personne inconnue présente une émotion particulière qui pourrait nous faire réagir différemment. Nos signaux internes nous aideraient donc dans l'affinement de ces actions, et c'est l'intégration de ces signaux avec ce réseau central mais également avec le recrutement d'autres régions connues comme étant impliquées dans le traitement des visages et des émotions, qui nous permettrait de réagir rapidement et différemment en fonction du contexte ou pour garder des distances appropriées en fonction de l'individu.

C'est donc ce réseau neuronal central, avec la combinaison des signaux externes de l'environnement et des signaux internes de l'intérieur du corps, qui nous permettrait de réagir de manière appropriée dans notre vie de tous les jours, soit avec les objets présents dans l'espace qui nous entoure soit avec nos congénères.

Bibliographie

Adams, R. B., Ambady, N., Macrae, C. N., & Kleck, R. E. (2006). Emotional expressions forecast approach-avoidance behavior. *Motivation and Emotion*, *30*(2), 179–188. https://doi.org/10.1007/s11031-006-9020-2.

Adolphs, R. (2010a). What does the amygdala contribute to social cognition? In *Annals of the New York Academy of Sciences* (Vol. 1191, Issue 1, pp. 42–61). Blackwell Publishing Inc. https://doi.org/10.1111/j.1749-6632.2010.05445.x.

Adolphs, R. (2010b). Emotion. In *Current Biology* (Vol. 20, Issue 13, pp. R549–R552). Cell Press. https://doi.org/10.1016/j.cub.2010.05.046.

Adolphs, R., Russell, J. A., & Tranel, D. (1999). A role for the human amygdala in recognizing emotional arousal from unpleasant stimuli. *Psychological Science*, *10*(2), 167–171. https://doi.org/10.1111/1467-9280.00126.

Adolphs, R., Tranel, D., & Damasio, H. (2001). Emotion recognition from faces and prosody following temporal lobectomy. *Neuropsychology*, *15*(3), 396–404. https://doi.org/10.1037//0894-4105.15.3.396.

Adolphs, R., Tranel, D., Damasio1s2, H., & Damasio1', A. R. (1995). *Fear and the Human Amygdala*.

Alberici, A., Geroldi, C., Cotelli, M., Adorni, A., Calabria, M., Rossi, G., Borroni, B., Padovani, A., Zanetti, O., & Kertesz, A. (2007). The Frontal Behavioural Inventory (Italian version) differentiates frontotemporal lobar degeneration variants from Alzheimer's disease. *Neurological Sciences 2007 28:2*, *28*(2), 80–86. https://doi.org/10.1007/S10072-007-0791-3.

Alkan, Y., Biswal, B. B., & Alvarez, T. L. (2011). Differentiation between vergence and saccadic functional activity within the human frontal eye fields and midbrain revealed through fMRi. *PLoS ONE*, *6*(11). https://doi.org/10.1371/JOURNAL.PONE.0025866.

Amassian, V. E. (1951). CORTICAL REPRESENTATION OF VISCERAL AFFERENTS. *Https://Doi.Org/10.1152/Jn.1951.14.6.433*, *14*(6), 433–444. https://doi.org/10.1152/JN.1951.14.6.433.

Andersen, R., & Buneo, C. (2002). Intentional maps in posterior parietal cortex. *Annual Review of Neuroscience*, *25*, 189–220. https://doi.org/10.1146/ANNUREV.NEURO.25.112701.142922.

Andersen, R., Snyder, L., Bradley, D., & Xing, J. (1997). Multimodal representation of space in the posterior parietal cortex and its use in planning movements. *Annual Review of Neuroscience*, *20*, 303–330. https://doi.org/10.1146/ANNUREV.NEURO.20.1.303.

Arbib, M. A., & Mundhenk, T. N. (2005). Schizophrenia and the mirror system: an essay. *Neuropsychologia*, *43*(2), 268–280. https://doi.org/10.1016/J.NEUROPSYCHOLOGIA.2004.11.013.

Ardizzi, M., & Ferri, F. (2018). Interoceptive influences on peripersonal space boundary. *Cognition*, *177*, 79–86. https://doi.org/10.1016/J.COGNITION.2018.04.001.

Aspell, J. E., Lavanchy, T., Lenggenhager, B., & Blanke, O. (2010). Seeing the body modulates audiotactile integration. *European Journal of Neuroscience*, *31*(10), 1868–1873. https://doi.org/10.1111/J.1460-9568.2010.07210.X.

Avillac, M., Ben Hamed, S., & Duhamel, J. (2007). Multisensory integration in the ventral intraparietal area of the macaque monkey. *The Journal of Neuroscience : The Official Journal of the Society for Neuroscience*, *27*(8), 1922–1932. https://doi.org/10.1523/JNEUROSCI.2646-06.2007.

Azzalini, D., Rebollo, I., & Tallon-Baudry, C. (2019). Visceral Signals Shape Brain Dynamics and Cognition. *Trends in Cognitive Sciences*, *23*(6), 488–509. https://doi.org/10.1016/J.TICS.2019.03.007.

Baayen, R. H., Davidson, D. J., & Bates, D. M. (2008). Mixed-effects modeling with crossed random effects for subjects and items. *Journal of Memory and Language*, *59*(4), 390–412. https://doi.org/10.1016/J.JML.2007.12.005.

Baldwin, J. D., & Baldwin, J. I. (1974). THE DYNAMICS OF INTERPERSONAL SPACING IN MONKEYS AND MAN. *American Journal of Orthopsychiatry*, *44*(5), 790–806. https://doi.org/10.1111/J.1939-0025.1974.TB01157.X.

Banati, R., Goerres, G., Tjoa, C., Aggleton, J., & Grasby, P. (2000). The functional anatomy of visual-tactile integration in man: a study using positron emission tomography. *Neuropsychologia*, *38*(2), 115–124. https://doi.org/10.1016/S0028-3932(99)00074-3.

Bas-Hoogendam, J. M., Steenbergen, H. Van, Kreuk, T., Van Der Wee, N. J. A., & Westenberg, P. M. (2017). How embarrassing! the behavioral and neural correlates of processing social norm violations. *PLoS ONE*, *12*(4), e0176326. https://doi.org/10.1371/journal.pone.0176326.

Bates, D., Mächler, M., Bolker, B. M., & Walker, S. C. (2015). Fitting linear mixed-effects models using lme4. *Journal of Statistical Software*, *67*(1). https://doi.org/10.18637/jss.v067.i01.

Becker, E., & Karnath, H.-O. (2007). Incidence of Visual Extinction After Left Versus Right Hemisphere Stroke. *Stroke*, *38*(12), 3172–3174. https://doi.org/10.1161/STROKEAHA.107.489096.

Bender, M. B. (2011). Disorders in perception: With particular reference to the phenomena of extinction and displacement. *Disorders in Perception: With Particular Reference to the Phenomena of Extinction and Displacement.* https://doi.org/10.1037/13218-000.

Benjamini, Y., & Hochberg, Y. (1995). Controlling the False Discovery Rate: A Practical and Powerful Approach to Multiple Testing. *Journal of the Royal Statistical Society: Series B (Methodological)*, *57*(1), 289–300. https://doi.org/10.1111/j.2517-6161.1995.tb02031.x.

Berger, M., Neumann, P., & Gail, A. (2019). Peri-hand space expands beyond reach in the context of walk-and-reach movements. *Scientific Reports*, *9*(1). https://doi.org/10.1038/S41598-019-39520-8.

Berti, A., & Frassinetti, F. (2000). When far becomes near: Remapping of space by tool use. *Journal of Cognitive Neuroscience*, *12*(3), 415–420. https://doi.org/10.1162/089892900562237.

Beschin, N., & Robertson, L. (1997). Personal versus extrapersonal neglect: a group study of their dissociation using a reliable clinical test. *Cortex; a Journal Devoted to the Study of the Nervous System and Behavior*, *33*(2), 379–384. https://doi.org/10.1016/S0010-9452(08)70013-3.

Bhattacharyya, R., Musallam, S., & Andersen, R. A. (2009). Parietal reach region encodes reach depth using retinal disparity and vergence angle signals. *Journal of Neurophysiology*, *102*(2), 805–816. https://doi.org/10.1152/JN.90359.2008.

Binkofski, F., & Buxbaum, L. J. (2013). Two action systems in the human brain. *Brain and Language*, *127*(2), 222. https://doi.org/10.1016/J.BANDL.2012.07.007.

Bisiach, E., Perani, D., Vallar, G., & Berti, A. (1986). Unilateral neglect: personal and extra-personal. *Neuropsychologia*, *24*(6), 759–767. https://doi.org/10.1016/0028-3932(86)90075-8.

Bisio, A., Garbarini, F., Biggio, M., Fossataro, C., Ruggeri, P., & Bove, M. (2017). Dynamic Shaping of the Defensive Peripersonal Space through Predictive Motor Mechanisms: When the "Near" Becomes "Far." *Journal of Neuroscience*, *37*(9), 2415–2424. https://doi.org/10.1523/JNEUROSCI.0371-16.2016.

Blanke, O. (2012). Multisensory brain mechanisms of bodily self-consciousness. *Nature Reviews Neuroscience 2012 13:8*, *13*(8), 556–571. https://doi.org/10.1038/nrn3292.

Blini, E., Desoche, C., Salemme, R., Kabil, A., Hadj-Bouziane, F., & Farnè, A. (2018). Mind the Depth: Visual Perception of Shapes Is Better in Peripersonal Space. *Psychological Science*, *29*(11), 1868–1877. https://doi.org/10.1177/0956797618795679.

Bodegård, A., Geyer, S., Naito, E., Zilles, K., & Roland, P. (2000). Somatosensory areas in man activated by moving stimuli: cytoarchitectonic mapping and PET. *Neuroreport*, *11*(1), 187–191. https://doi.org/10.1097/00001756-200001170-00037.

Bogdanova, O. V., Bogdanov, V. B., Dureux, A., Farnè, A., & Hadj-Bouziane, F. (2021). The Peripersonal Space in a social world. *Cortex*, *142*, 28–46. https://doi.org/10.1016/J.CORTEX.2021.05.005.

Bonini, L., Maranesi, M., Livi, A., Fogassi, L., & Rizzolatti, G. (2014). Space-Dependent Representation of Objects and Other's Action in Monkey Ventral Premotor Grasping Neurons. *Journal of Neuroscience*, *34*(11), 4108–4119. https://doi.org/10.1523/JNEUROSCI.4187-13.2014.

BRAIN, W. R. (1941). VISUAL DISORIENTATION WITH SPECIAL REFERENCE TO LESIONS OF THE RIGHT CEREBRAL HEMISPHERE. *Brain*, *64*(4), 244–272. https://doi.org/10.1093/BRAIN/64.4.244.

Bremmer, F., Schlack, A., Kaminiarz, A., & Hoffmann, K. P. (2013). Encoding of movement in near extrapersonal space in primate area VIP. *Frontiers in Behavioral Neuroscience*, *0*(JANUARY 2013), 8. https://doi.org/10.3389/FNBEH.2013.00008.

Bremmer, F., Schlack, A., Shah, N. J., Zafiris, O., Kubischik, M., Hoffmann, K. P., Zilles, K., & Fink, G. R. (2001). Polymodal motion processing in posterior parietal and premotor cortex: A human fMRI study strongly implies equivalencies between humans and monkeys. *Neuron*, *29*(1), 287–296. https://doi.org/10.1016/S0896-6273(01)00198-2.

Breveglieri, R., Galletti, C., Gamberini, M., Passarelli, L., & Fattori, P. (2006). Somatosensory cells in area PEc of macaque posterior parietal cortex. *Journal of Neuroscience*, *26*(14), 3679–3684. https://doi.org/10.1523/JNEUROSCI.4637-05.2006.

Breveglieri, R., Hadjidimitrakis, K., Bosco, A., Sabatini, S. P., Galletti, C., & Fattori, P. (2012). Eye Position Encoding in Three-Dimensional Space: Integration of Version and Vergence Signals in the Medial Posterior Parietal Cortex. *Journal of Neuroscience*, *32*(1), 159–169. https://doi.org/10.1523/JNEUROSCI.4028-11.2012.

Brozzoli, C, Gentile, G., Bergouignan, L., & Ehrsson, H. (2013). A shared representation of the space near onself and others in the human premotor cortex. *Curr Biol*, *23*..

Brozzoli, Claudio, Gentile, G., & Ehrsson, H. H. (2012). That's Near My Hand! Parietal and Premotor Coding of Hand-Centered Space Contributes to Localization and Self-Attribution of the Hand. *Journal of Neuroscience*, *32*(42), 14573–14582. https://doi.org/10.1523/JNEUROSCI.2660-12.2012.

Brozzoli, Claudio, Gentile, G., Petkova, V. I., & Ehrsson, H. H. (2011). fMRI Adaptation Reveals a Cortical Mechanism for the Coding of Space Near the Hand. *Journal of Neuroscience*, *31*(24), 9023–9031. https://doi.org/10.1523/JNEUROSCI.1172-11.2011.

Bruni, S., Gerbella, M., Bonini, L., Borra, E., Coudé, G., Ferrari, P. F., Fogassi, L., Maranesi, M., Rodà, F., Simone, L., Serventi, F. U., & Rozzi, S. (2017). Cortical and subcortical connections of parietal and premotor nodes of the monkey hand mirror neuron network. *Brain Structure and Function 2017 223:4*, *223*(4), 1713–1729. https://doi.org/10.1007/S00429-017-1582-0.

Bucher, K., Myers, R. E., & Southwick, C. (1970). Anterior temporal cortex and maternal behavior in monkey. *Neurology*, *20*(4), 415. https://europepmc.org/article/med/4998075.

Bufacchi, R. J. (2017). Control of Movement: Approaching threatening stimuli cause an expansion of defensive peripersonal space. *Journal of Neurophysiology*, *118*(4), 1927. https://doi.org/10.1152/JN.00316.2017.

Bufacchi, Rory J., & Iannetti, G. D. (2018). An Action Field Theory of Peripersonal Space. *Trends in Cognitive Sciences*, *22*(12), 1076–1090. https://doi.org/10.1016/J.TICS.2018.09.004.

Bufalari, I., Porciello, G., Sperduti, M., & Minio-Paluello, I. (2015). Self-identification with another person's face: the time relevant role of multimodal brain areas in the enfacement illusion. *Https://Doi.Org/10.1152/Jn.00872.2013*, *113*(7), 1962–2015. https://doi.org/10.1152/JN.00872.2013.

Bushara, K. O., Grafman, J., & Hallett, M. (2001). Neural Correlates of Auditory–Visual Stimulus Onset Asynchrony Detection. *The Journal of Neuroscience*, *21*(1), 300. https://doi.org/10.1523/JNEUROSCI.21-01-00300.2001.

Calvo, M. G., & Nummenmaa, L. (2011). Time course of discrimination between emotional facial expressions: The role of visual saliency. *Vision Research*, *51*(15), 1751–1759. https://doi.org/10.1016/J.VISRES.2011.06.001.

Calvo, M. G., Nummenmaa, L., & Avero, P. (2010). Recognition advantage of happy faces in extrafoveal vision: Featural and affective processing. *Http://Dx.Doi.Org/10.1080/13506285.2010.481867*, *18*(9), 1274–1297. https://doi.org/10.1080/13506285.2010.481867.

Candini, M., Battaglia, S., Benassi, M., di Pellegrino, G., & Frassinetti, F. (2021). The physiological correlates of interpersonal space. *Scientific Reports*, *11*(1), 2611. https://doi.org/10.1038/s41598-021-82223-2.

Candini, M., Giuberti, V., Santelli, E., di Pellegrino, G., & Frassinetti, F. (2019). When social and action spaces diverge: A study in children with typical development and autism. *Autism*, *23*(7), 1687–1698. https://doi.org/10.1177/1362361318822504.

Canzoneri, E., Magosso, E., & Serino, A. (2012). Dynamic Sounds Capture the Boundaries of Peripersonal Space Representation in Humans. *PLOS ONE*, *7*(9), e44306. https://doi.org/10.1371/JOURNAL.PONE.0044306.

Canzoneri, E., Ubaldi, S., Rastelli, V., Finisguerra, A., Bassolino, M., & Serino, A. (2013). Tool-use reshapes the boundaries of body and peripersonal space representations. *Experimental Brain Research*, *228*(1), 25–42. https://doi.org/10.1007/S00221-013-3532-2.

Capitanio, J. P., Machado, C. J., & Amaral, D. (2006). *Amygdalectomy and responsiveness to novelty in Rhesus monkeys (Macaca mulatta): Generality and individual consistency of effects*. https://doi.org/10.1037/1528-3542.6.1.73.

Cardini, F., Costantini, M., Galati, G., Romani, G. L., Làdavas, E., & Serino, A. (2011). Viewing One's Own Face Being Touched Modulates Tactile Perception: An fMRI Study. *Journal of Cognitive Neuroscience*, *23*(3), 503–513. https://doi.org/10.1162/JOCN.2010.21484.

Cartaud, A., Ott, L., Iachini, T., Honoré, J., & Coello, Y. (2020). The influence of facial expression at perceptual threshold on electrodermal activity and social comfort distance. *Psychophysiology*, *57*(9), e13600. https://doi.org/10.1111/PSYP.13600.

Cartaud, A., Ruggiero, G., Ott, L., Iachini, T., & Coello, Y. (2018). Physiological Response to Facial Expressions in Peripersonal Space Determines Interpersonal Distance in a Social Interaction Context. *Frontiers in Psychology*, *9*(MAY), 657. https://doi.org/10.3389/fpsyg.2018.00657.

Caspers, S., Eickhoff, S. B., Rick, T., von Kapri, A., Kuhlen, T., Huang, R., Shah, N. J., & Zilles, K. (2011). Probabilistic fibre tract analysis of cytoarchitectonically defined human inferior parietal lobule areas reveals similarities to macaques. *NeuroImage*, *58*(2), 362–380. https://doi.org/10.1016/J.NEUROIMAGE.2011.06.027.

Castle, M., Comoli, E., & Loewy, A. D. (2005). Autonomic brainstem nuclei are linked to the hippocampus. *Neuroscience*, *134*(2), 657–669. https://doi.org/10.1016/J.NEUROSCIENCE.2005.04.031.

Cavada, C., & Goldman-Rakic, P. S. (1989). Posterior parietal cortex in rhesus monkey: II. Evidence for segregated corticocortical networks linking sensory and limbic areas with the frontal lobe. *Journal of Comparative Neurology*, *287*(4), 422–445. https://doi.org/10.1002/CNE.902870403.

Cechetto, D. F., & Saper, C. B. (1987). Evidence for a viscerotopic sensory representation in the cortex and thalamus in the rat. *Journal of Comparative Neurology*, *262*(1), 27–45. https://doi.org/10.1002/CNE.902620104.

Cléry, J., Guipponi, O., Odouard, S., Wardak, C., & Ben Hamed, S. (2018). Cortical networks for encoding near and far space in the non-human primate. *NeuroImage*, *176*, 164–178. https://doi.org/10.1016/j.neuroimage.2018.04.036.

Cléry, J., Guipponi, O., Wardak, C., & Ben Hamed, S. (2015). *Neuronal bases of peripersonal and extrapersonal spaces, their plasticity and their dynamics: knowns and unknowns*. https://doi.org/10.1016/j.neuropsychologia.2014.10.022.

Colby, C. L., Duhamel, J. R., & Goldberg, M. E. (1993). Ventral intraparietal area of the macaque: Anatomic location and visual response properties. *Journal of Neurophysiology*, *69*(3), 902–914. https://doi.org/10.1152/JN.1993.69.3.902.

Colby, Carol L., & Duhamel, J. R. (1996). Spatial representations for action in parietal cortex. *Cognitive Brain Research*, *5*(1–2), 105–115. https://doi.org/10.1016/S0926-6410(96)00046-8.

Cooke, D. F., & Graziano, M. S. A. (2003). Defensive Movements Evoked by Air Puff in Monkeys. *Https://Doi.Org/10.1152/Jn.00513.2003*, *90*(5), 3317–3329. https://doi.org/10.1152/JN.00513.2003.

Corbo, M., Di Cosmo, G., Ferri, F., Salone, A., Carlesi, D., Centofanti, M., Cipollone, F., Costantini, M., Di Iorio, G., Martinotti, G., & di Giannantonio, M. (2017). Peripersonal space and schizophrenia: Looking for the self boundaries. *European Psychiatry*, *41*(S1), S806. https://doi.org/10.1016/J.EURPSY.2017.01.1561.

Cowey, A., Small, M., & Ellis, S. (1994). Left visuo-spatial neglect can be worse in far than in near space. *Neuropsychologia*, *32*(9), 1059–1066. https://doi.org/10.1016/0028-3932(94)90152-X.

Cox, R. W. (1996). AFNI: Software for analysis and visualization of functional magnetic resonance neuroimages. *Computers and Biomedical Research*, *29*(3), 162–173. https://doi.org/10.1006/cbmr.1996.0014.

Crawford, J. R., & Garthwaite, P. H. (2007). Comparison of a single case to a control or normative sample in neuropsychology: Development of a Bayesian approach. *Cognitive Neuropsychology*, *24*(4), 343–372. https://doi.org/10.1080/02643290701290146.

Crawford, J. R., Garthwaite, P. H., & Ryan, K. (2011). Comparing a single case to a control sample: testing for neuropsychological deficits and dissociations in the presence of covariates. *Cortex; a Journal Devoted to the Study of the Nervous System and Behavior*, *47*(10), 1166–1178. https://doi.org/10.1016/j.cortex.2011.02.017.

Crawford, J. R., Garthwaite, P. H., & Wood, L. T. (2010). Inferential methods for comparing two single cases. *Cognitive Neuropsychology*, *27*(5), 377–400. https://doi.org/10.1080/02643294.2011.559158.

Critchley, H. D., & Harrison, N. A. (2013). Visceral Influences on Brain and Behavior. *Neuron*, *77*(4), 624–638. https://doi.org/10.1016/J.NEURON.2013.02.008.

Culham, J. C., & Valyear, K. F. (2006). Human parietal cortex in action. *Current Opinion in Neurobiology*, *16*(2), 205–212. https://doi.org/10.1016/J.CONB.2006.03.005.

Dallabona, M., Sarubbo, S., Merler, S., Corsini, F., Pulcrano, G., Rozzanigo, U., Barbareschi, M., & Chioffi, F. (2017). Impact of mass effect, tumor location, age, and surgery on the cognitive outcome of patients with high-grade gliomas: A longitudinal study. *Neuro-Oncology Practice*, *4*(4), 229–240. https://doi.org/10.1093/nop/npw030.

Darwin, C.B., Society Hardwicke, R., & Fritz Muller, B. (1875). *With illustrations. 2 vols. 8vo. 24s. Murray, 1871. THE VARIATION OF ANIMALS AND PLANTS UNDER DOMESTICATION. Third Thousand. With Illustrations. 2 vols. 8vo. 28s. Murray, 1868. Effects of Crossing. With Woodcuts*.

Davis, M., & Whalen, P. J. (2001). The amygdala: Vigilance and emotion. In *Molecular Psychiatry* (Vol. 6, Issue 1, pp. 13–34). https://doi.org/10.1038/sj.mp.4000812.

de Haan, B., Karnath, H., & Driver, J. (2012). Mechanisms and anatomy of unilateral extinction after brain injury. *Neuropsychologia*, *50*(6), 1045–1053. https://doi.org/10.1016/J.NEUROPSYCHOLOGIA.2012.02.015.

de Vignemont, F, & Iannetti, G. (2015). How many peripersonal spaces? *Neuropsychologia*, *70*, 327–334. https://doi.org/10.1016/J.NEUROPSYCHOLOGIA.2014.11.018.

de Vignemont, Frédérique. (2018). Peripersonal perception in action. *Synthese 2018 198:17*, *198*(17), 4027–4044. https://doi.org/10.1007/S11229-018-01962-4.

Di Cesare, G., Pinardi, C., Carapelli, C., Caruana, F., Marchi, M., Gerbella, M., & Rizzolatti, G. (2019). Insula Connections With the Parieto-Frontal Circuit for Generating Arm Actions in Humans and Macaque Monkeys. *Cerebral Cortex*, *29*(5), 2140–2147. https://doi.org/10.1093/CERCOR/BHY095.

Di Cosmo, G., Costantini, M., Salone, A., Martinotti, G., Di Iorio, G., Di Giannantonio, M., & Ferri, F. (2018). Peripersonal space boundary in schizotypy and schizophrenia. *Schizophrenia Research*, *197*, 589–590. https://doi.org/10.1016/J.SCHRES.2017.12.003.

Di Pellegrino, G., & De Renzi, E. (1995). An experimental investigation on the nature of extinction. *Neuropsychologia*, *33*(2), 153–170. https://doi.org/10.1016/0028-3932(94)00111-2.

Di Pellegrino, Giuseppe, Basso, G., & Frassinetti, F. (1997). Spatial extinction on double asynchronous stimulation. *Neuropsychologia*, *35*(9), 1215–1223. https://doi.org/10.1016/S0028-3932(97)00044-4.

di Pellegrino, Giuseppe, & Làdavas, E. (2015). Peripersonal space in the brain. In *Neuropsychologia* (Vol. 66, pp. 126–133). Elsevier Ltd. https://doi.org/10.1016/j.neuropsychologia.2014.11.011.

Duffau, H. (2021). Updated perspectives on awake neurosurgery with cognitive and emotional assessment for patients with low-grade gliomas. In *Expert Review of Neurotherapeutics* (Vol. 21, Issue 4, pp. 463–473). Taylor and Francis Ltd. https://doi.org/10.1080/14737175.2021.1901583.

Duhamel, J., Bremmer, F., Ben Hamed, S., & Graf, W. (1997). Spatial invariance of visual receptive fields in parietal cortex neurons. *Nature*, *389*(6653), 845–848. https://doi.org/10.1038/39865.

Duhamel, J. R., Colby, C. L., & Goldberg, M. E. (1998). Ventral intraparietal area of the macaque: Congruent visual and somatic response properties. *Journal of Neurophysiology*, *79*(1), 126–136. https://doi.org/10.1152/JN.1998.79.1.126.

Dum, R. P., Levinthal, D. J., & Strick, P. L. (2009). The Spinothalamic System Targets Motor and Sensory Areas in the Cerebral Cortex of Monkeys. *Journal of Neuroscience*, *29*(45), 14223–14235. https://doi.org/10.1523/JNEUROSCI.3398-09.2009.

Duncan, J. (1996). Cooperating Brain Systems in Selective Perception and Action. *Attention and Performance*, *16*, 547–578. https://doi.org/10.7551/MITPRESS/1479.003.0033.

Durand, J.-B., Nelissen, K., Joly, O., Wardak, C., Todd, J. T., Norman, J. F., Janssen, P., Vanduffel, W., & Orban, G. A. (2007). Anterior Regions of Monkey Parietal Cortex Process Visual 3D Shape. *Neuron*, *55*(3), 493. https://doi.org/10.1016/J.NEURON.2007.06.040.

Dureux, A., Blini, E., Grandi, L. C., Bogdanova, O., Desoche, C., Farnè, A., & Hadj-Bouziane, F. (2021). Close facial emotions enhance physiological responses and facilitate perceptual discrimination. *Cortex*, *138*, 40–58. https://doi.org/10.1016/j.cortex.2021.01.014.

Ehrsson, H. H., Holmes, N. P., & Passingham, R. E. (2005). Touching a Rubber Hand: Feeling of Body Ownership Is Associated with Activity in Multisensory Brain Areas. *The Journal of Neuroscience*, *25*(45), 10564. https://doi.org/10.1523/JNEUROSCI.0800-05.2005.

Ehrsson, H. H., Spence, C., & Passingham, R. E. (2004). That's My Hand! Activity in Premotor Cortex Reflects Feeling of Ownership of a Limb. *Science*, *305*(5685), 875–877. https://doi.org/10.1126/SCIENCE.1097011.

Ellena, G., Starita, F., Haggard, P., & Làdavas, E. (2020). The spatial logic of fear. *Cognition*, *203*, 104336. https://doi.org/10.1016/J.COGNITION.2020.104336.

Emery, N. J., Capitanio, J. P., Mason, W. A., Machado, C. J., Mendoza, S. P., & Amaral, D. G. (2001). The Effects of Bilateral Lesions of the Amygdala on Dyadic Social Interactions in Rhesus Monkeys (Macaca mulatto) of the amygdala may be particularly important. Mem. *Behavioral Neuroscience*, *115*(3), 515–544. https://doi.org/10.I037//0735-7044.I15.3.515.

Essen, D. C. Van, & Dierker, D. L. (2007). Surface-Based and Probabilistic Atlases of Primate Cerebral Cortex. *Neuron*, *56*(2), 209–225. https://doi.org/10.1016/J.NEURON.2007.10.015.

Farnè, A, & Làdavas, E. (2002). Auditory peripersonal space in humans. *Journal of Cognitive Neuroscience*, *14*(7), 1030–1043. https://doi.org/10.1162/089892902320474481.

Farnè, Alessandro, Demattè, M. L., & Làdavas, E. (2005). Neuropsychological evidence of modular organization of the near peripersonal space. *Neurology*, *65*(11), 1754–1758. https://doi.org/10.1212/01.WNL.0000187121.30480.09.

Farnè, Alessandro, Iriki, A., & Làdavas, E. (2005). Shaping multisensory action–space with tools: evidence from patients with cross-modal extinction. *Neuropsychologia*, *43*(2), 238–248. https://doi.org/10.1016/J.NEUROPSYCHOLOGIA.2004.11.010.

Feil, M., Moser, B., & Abegg, M. (2017). The interaction of pupil response with the vergence system. *Graefe's Archive for Clinical and Experimental Ophthalmology 2017 255:11*, *255*(11), 2247–2253. https://doi.org/10.1007/S00417-017-3770-2.

Ferraina, S., Paré, M., & Wurtz, R. (2000). Disparity sensitivity of frontal eye field neurons. *Journal of Neurophysiology*, *83*(1), 625–629. https://doi.org/10.1152/JN.2000.83.1.625.

Ferri, F, Tajadura-Jiménez, A., Väljamäe, A., Vastano, R., & Costantini, M. (2015). Emotion-inducing approaching sounds shape the boundaries of multisensory peripersonal space. *Neuropsychologia*, *70*, 468–475. https://doi.org/10.1016/J.NEUROPSYCHOLOGIA.2015.03.001.

Ferri, Francesca, Costantini, M., Huang, Z., Perrucci, M. G., Ferretti, A., Romani, G. L., & Northoff, G. (2015). *Behavioral/Cognitive Intertrial Variability in the Premotor Cortex Accounts for Individual Differences in Peripersonal Space*. https://doi.org/10.1523/JNEUROSCI.1696-15.2015.

Ferri, S., Peeters, R., Nelissen, K., Vanduffel, W., Rizzolatti, G., & Orban, G. A. (2015). A human homologue of monkey F5c. *Neuroimage*, *111*, 251. https://doi.org/10.1016/J.NEUROIMAGE.2015.02.033.

Filimon, F. (2010). Human cortical control of hand movements: parietofrontal networks for reaching, grasping, and pointing. *The Neuroscientist : A Review Journal Bringing Neurobiology, Neurology and Psychiatry*, *16*(4), 388–407. https://doi.org/10.1177/1073858410375468.

Fogassi, L., Gallese, V., di Pellegrino, G., Fadiga, L., Gentilucci, M., Luppino, G., Matelli, M., Pedotti, A., & Rizzolatti, G. (1992). Space coding by premotor cortex. *Experimental Brain Research 1992 89:3*, *89*(3), 686–690. https://doi.org/10.1007/BF00229894.

Fogassi, L., Raos, V., Franchi, G., Gallese, V., Luppino, G., & Matelli, M. (1999). Visual responses in the dorsal premotor area F2 of the macaque monkey. *Experimental Brain Research 1999 128:1*, *128*(1), 194–199. https://doi.org/10.1007/S002210050835.

Fogassi, L, Gallese, V., Fadiga, L., Luppino, G., Matelli, M., & Rizzolatti, G. (1996). Coding of peripersonal space in inferior premotor cortex (area F4). *Journal of Neurophysiology*, *76*(1), 141–157. https://doi.org/10.1152/JN.1996.76.1.141.

Fogassi, Leonardo, Gallese, V., Buccino, G., Craighero, L., Fadiga, L., & Rizzolatti, G. (2001). Cortical mechanism for the visual guidance of hand grasping movements in the monkeyA reversible inactivation study. *Brain*, *124*(3), 571–586. https://doi.org/10.1093/BRAIN/124.3.571.

Fossataro, C., Sambo, C., Garbarini, F., & Iannetti, G. (2016). Interpersonal interactions and empathy modulate perception of threat and defensive responses. *Scientific Reports*, *6*. https://doi.org/10.1038/SREP19353.

Foster, C., Sheng, W.-A., Heed, T., & Hamed, S. Ben. (2021). *The macaque ventral intraparietal area has expanded into three homologue human parietal areas*. https://doi.org/10.31219/OSF.IO/6MEYW.

Fowler, H. L., Baker, G. A., Tipples, J., Hare, D. J., Keller, S., Chadwick, D. W., & Young, A. W. (2006). *Recognition of emotion with temporal lobe epilepsy and asymmetrical amygdala damage*. https://doi.org/10.1016/j.yebeh.2006.04.013.

Friston, K. J., Harrison, L., & Penny, W. (2003). Dynamic causal modelling. *NeuroImage*, *19*(4), 1273–1302. https://doi.org/10.1016/S1053-8119(03)00202-7.

Galletti, C., Fattori, P., Kutz, D. F., & Gamberini, M. (1999). Brain location and visual topography of cortical area V6A in the macaque monkey. *European Journal of Neuroscience*, *11*(2), 575–582. https://doi.org/10.1046/J.1460-9568.1999.00467.X.

Genovesio, A, & Ferraina, S. (2004). Integration of retinal disparity and fixation-distance related signals toward an egocentric coding of distance in the posterior parietal cortex of primates. *Journal of Neurophysiology*, *91*(6), 2670–2684. https://doi.org/10.1152/JN.00712.2003.

Gentile, G., Björnsdotter, M., Petkova, V. I., Abdulkarim, Z., & Ehrsson, H. H. (2015). Patterns of neural activity in the human ventral premotor cortex reflect a whole-body multisensory percept. *Neuroimage*, *109*, 328. https://doi.org/10.1016/J.NEUROIMAGE.2015.01.008.

Gentile, G., Guterstam, A., Brozzoli, C., & Ehrsson, H. H. (2013). *Disintegration of Multisensory Signals from the Real Hand Reduces Default Limb Self-Attribution: An fMRI Study*. https://doi.org/10.1523/JNEUROSCI.1363-13.2013.

Gentile, Petkova, & Ehrsson. (2011). Integration of visual and tactile signals from the hand in the human brain: an FMRI study. *Journal of Neurophysiology*, *105*(2), 910–922. https://doi.org/10.1152/JN.00840.2010.

Gentilucci, M., Fogassi, L., Luppino, G., Matelli, M., Camarda, R., & Rizzolatti, G. (1988). Functional organization of inferior area 6 in the macaque monkey. *Experimental Brain Research 1988 71:3*, *71*(3), 475–490. https://doi.org/10.1007/BF00248741.

Gentilucci, M., Scandolara, C., Pigarev, I., & Rizzolatti, G. (1983). Visual responses in the postarcuate cortex (area 6) of the monkey that are independent of eye position. *Experimental Brain Research*, *50*(2–3), 464–468. https://doi.org/10.1007/BF00239214.

Gerbella, M., Borra, E., Rozzi, S., & Luppino, G. (2014). Connections of the macaque Granular Frontal Opercular (GrFO) area: a possible neural substrate for the contribution of limbic inputs for controlling hand and face/mouth actions. *Brain Structure and Function 2014 221:1*, *221*(1), 59–78. https://doi.org/10.1007/S00429-014-0892-8.

Ghuman, A. S., Brunet, N. M., Li, Y., Konecky, R. O., Pyles, J. A., Walls, S. A., Destefino, V., Wang, W., & Richardson, R. M. (2014). Dynamic encoding of face information in the human fusiform gyrus. *Nature Communications*, *5*, 5672. https://doi.org/10.1038/ncomms6672.

Glasser, M. F., Smith, S. M., Marcus, D. S., Andersson, J., Auerbach, E. J., Behrens, T. E. J., Coalson, T. S., Harms, M. P., Jenkinson, M., Moeller, S., Robinson, E. C., Sotiropoulos, S. N., Xu, J., Yacoub, E., Ugurbil, K., & Essen, D. C. Van. (2016). The Human Connectome Project's Neuroimaging Approach. *Nature Neuroscience*, *19*(9), 1175. https://doi.org/10.1038/NN.4361.

Gloor, P., Olivier, A., Quesney, L. F., Andermann, F., & Horowitz, S. (1982). The role of the limbic system in experiential phenomena of temporal lobe epilepsy. *Annals of Neurology*, *12*(2), 129–144. https://doi.org/10.1002/ana.410120203.

Gnadt, J., & Mays, L. (1995). Neurons in monkey parietal area LIP are tuned for eye-movement parameters in three-dimensional space. *Journal of Neurophysiology*, *73*(1), 280–297. https://doi.org/10.1152/JN.1995.73.1.280.

Goeleven, E., De Raedt, R., Leyman, L., & Verschuere, B. (2008). The Karolinska directed emotional faces: A validation study. *Cognition and Emotion*, *22*(6), 1094–1118. https://doi.org/10.1080/02699930701626582.

Gogolla, N. (2017). The insular cortex. *Current Biology*, *27*(12), R580–R586. https://doi.org/10.1016/J.CUB.2017.05.010.

Goodale, M. A., & Milner, A. D. (1992). Separate visual pathways for perception and action. *Trends in Neurosciences*, *15*(1), 20–25. https://doi.org/10.1016/0166-2236(92)90344-8.

Graziano, & Gross, C. (1996). *Attention and Performance XVI*. MIT Press.

Graziano, M. S. A., & Gandhi, S. (2000). Location of the polysensory zone in the precentral gyrus of anesthetized monkeys. *Experimental Brain Research 2000 135:2*, *135*(2), 259–266. https://doi.org/10.1007/S002210000518.

Graziano, Michael S.A., Hu, X. T., & Gross, C. G. (1997). Visuospatial properties of ventral premotor cortex. *Journal of Neurophysiology*, *77*(5), 2268–2292.

Graziano, MS, & Cooke, D. (2006). Parieto-frontal interactions, personal space, and defensive behavior. *Neuropsychologia*, *44*(13), 2621–2635. https://doi.org/10.1016/J.NEUROPSYCHOLOGIA.2005.09.011.

Graziano, MS, & Gross, C. (1993). A bimodal map of space: somatosensory receptive fields in the macaque putamen with corresponding visual receptive fields. *Experimental Brain Research*, *97*(1), 96–109. https://doi.org/10.1007/BF00228820.

Graziano, MS, Yap, G., & Gross, C. (1994). Coding of visual space by premotor neurons. *Science*, *266*(5187), 1054–1057. https://doi.org/10.1126/SCIENCE.7973661.

Grefkes, C., & Fink, G. R. (2005). REVIEW: The functional organization of the intraparietal sulcus in humans and monkeys. *Journal of Anatomy*, *207*(1), 3–17. https://doi.org/10.1111/J.1469-7580.2005.00426.X.

Grill-Spector, K., Weiner, K. S., Kay, K., & Gomez, J. (2017). The Functional Neuroanatomy of Human Face Perception. In *Annual Review of Vision Science* (Vol. 3, pp. 167–196). Annual Reviews Inc. https://doi.org/10.1146/annurev-vision-102016-061214.

Grivaz, P., Blanke, O., & Serino, A. (2017). Common and distinct brain regions processing multisensory bodily signals for peripersonal space and body ownership. *NeuroImage*, *147*, 602–618. https://doi.org/10.1016/j.neuroimage.2016.12.052.

Gross, C. G., & Graziano, M. S. A. (1995). Review ■ : Multiple Representations of Space in the Brain. *The Neuroscientist*, *1*(1), 43–50. https://doi.org/10.1177/107385849500100107.

Hadj-Bouziane, F., Liu, N., Bell, A. H., Gothard, K. M., Luh, W.-M., Tootell, R. B. H., Murray, E. A., & Ungerleider, L. G. (2012). *Amygdala lesions disrupt modulation of functional MRI activity evoked by facial expression in the monkey inferior temporal cortex*. https://doi.org/10.1073/pnas.1218406109.

Hadjidimitrakis, K., Breveglieri, R., Bosco, A., & Fattori, P. (2012). Three-dimensional eye position signals shape both peripersonal space and arm movement activity in the medial posterior parietal cortex. *Frontiers in Integrative Neuroscience*, *0*(JUNE 2012), 37. https://doi.org/10.3389/FNINT.2012.00037.

Hadjidimitrakis, K., Breveglieri, R., Placenti, G., Bosco, A., Sabatini, S. P., & Fattori, P. (2011). Fix Your Eyes in the Space You Could Reach: Neurons in the Macaque Medial Parietal Cortex Prefer Gaze Positions in Peripersonal Space. *PLOS ONE*, *6*(8), e23335. https://doi.org/10.1371/JOURNAL.PONE.0023335.

Hall, E. T., Birdwhistell, R. L., Bock, B., Bohannan, P., Diebold, A. R., Durbin, M., Edmonson, M. S., Fischer, J. L., Hymes, D., Kimball, S. T., La Barre, W., McClellan, J. E., Marshall, D. S., Milner, G. B., Sarles, H. B., Trager, G. L., & Vayda, A. P. (1968). Proxemics [and Comments and Replies]. *Current Anthropology*, *9*(2/3), 83–108. https://doi.org/10.1086/200975.

Halligan, P., & Marshall, J. (1991). Left neglect for near but not far space in man. *Nature*, *350*(6318), 498–500. https://doi.org/10.1038/350498A0.

Hartig, R., Glen, D., Jung, B., Logothetis, N. K., Paxinos, G., Garza-Villarreal, E. A., Messinger, A., & Evrard, H. C. (2021). The Subcortical Atlas of the Rhesus Macaque (SARM) for neuroimaging. *NeuroImage*, *235*, 117996. https://doi.org/10.1016/J.NEUROIMAGE.2021.117996.

Haxby, J. V., Hoffman, E. A., Gobbini, M. I., (2000). The distributed human neural system for face perception. *Trends in Cognitive Sciences*, *4*(6), 223–233. https://doi.org/10.1016/S1364-6613(00)01482-0.

Hayduk, L. A. (1983). Personal space: Where we now stand. *Psychological Bulletin*, *94*(2), 293–335. https://doi.org/10.1037/0033-2909.94.2.293.

Hediger, H. (1955). Studies of the psychology and behavior of captive animals in zoos and circuses. Criterion Books, Inc. from https://psycnet.apa.org/record/1956-08075-000.

Heed, T., Habets, B., Sebanz, N., & Knoblich, G. (2010). Others' actions reduce crossmodal integration in peripersonal space. *Current Biology : CB*, *20*(15), 1345–1349. https://doi.org/10.1016/J.CUB.2010.05.068.

Herbet, G., Lafargue, G., Moritz-Gasser, S., Bonnetblanc, F., & Duffau, H. (2015). Interfering with the neural activity of mirror-related frontal areas impairs mentalistic inferences. *Brain Structure and Function*, *220*(4), 2159–2169. https://doi.org/10.1007/s00429-014-0777-x

Hobeika, L., Taffou, M., Carpentier, T., Warusfel, O., & Viaud-Delmon, I. (2020). Capturing the dynamics of peripersonal space by integrating expectancy effects and sound propagation properties. *Journal of Neuroscience Methods*, *332*. https://doi.org/10.1016/J.JNEUMETH.2019.108534.

Holmes, N., Calvert, G., & Spence, C. (2004). Extending or projecting peripersonal space with tools? Multisensory interactions highlight only the distal and proximal ends of tools. *Neuroscience Letters*, *372*(1–2), 62–67. https://doi.org/10.1016/j.neulet.2004.09.024.

Holt, D. J., Boeke, E. A., Coombs, G., Decross, S. N., Cassidy, B. S., Stufflebeam, S., Rauch, S. L., & Tootell, R. B. H. (2015). Abnormalities in personal space and parietal–frontal function in schizophrenia. *NeuroImage: Clinical*, *9*, 233–243. https://doi.org/10.1016/J.NICL.2015.07.008.

Holt, D. J., Cassidy, B. S., Yue, X., Rauch, S. L., Boeke, E. A., Nasr, S., Tootell, R. B. H., & Coombs Iii, G. (2014). *Neural Correlates of Personal Space Intrusion*. https://doi.org/10.1523/JNEUROSCI.0686-13.2014.

Huang, R.-S., Chen, C., Tran, A. T., Holstein, K. L., & Sereno, M. I. (2012). Mapping multisensory parietal face and body areas in humans. *Proceedings of the National Academy of Sciences*, *109*(44), 18114–18119. https://doi.org/10.1073/PNAS.1207946109.

Huber, S., Klein, E., Moeller, K., & Willmes, K. (2015). Comparing a single case to a control group - Applying linear mixed effects models to repeated measures data. *Cortex*, *71*, 148–159. https://doi.org/10.1016/j.cortex.2015.06.020.

Husain, M., & Rorden, C. (2003). Non-spatially lateralized mechanisms in hemispatial neglect. *Nature Reviews Neuroscience 2003 4:1*, *4*(1), 26–36. https://doi.org/10.1038/nrn1005.

Hyvärinen, J., & Poranen, A. (1974). function of the parietal associative area 7 as revealed from cellular discharges in alert monkeys. *brain*, *97*(1), 673–692. https://doi.org/10.1093/brain/97.1.673.

Iachini, T., Coello, Y., Frassinetti, F., & Ruggiero, G. (2014). Body space in social interactions: A comparison of reaching and comfort distance in immersive virtual reality. *PLoS ONE*, *9*(11). https://doi.org/10.1371/journal.pone.0111511.

Iachini, T., Coello, Y., Frassinetti, F., Senese, V. P., Galante, F., & Ruggiero, G. (2016). Peripersonal and interpersonal space in virtual and real environments: Effects of gender and age. *Journal of Environmental Psychology*, *45*, 154–164. https://doi.org/10.1016/j.jenvp.2016.01.004.

Iachini, T., Pagliaro, S., & Ruggiero, G. (2015). Near or far? It depends on my impression: Moral information and spatial behavior in virtual interactions. *Acta Psychologica*, *161*, 131–136. https://doi.org/10.1016/j.actpsy.2015.09.003.

Iachini, T., Ruggiero, G., Ruotolo, F., Schiano di Cola, A., & Senese, V. P. (2015). The influence of anxiety and personality factors on comfort and reachability space: a correlational study. *Cognitive Processing*, *16*, 255–258. https://doi.org/10.1007/s10339-015-0717-6.

Inman, C. S., Bijanki, K. R., Bass, D. I., Gross, R. E., Hamann, S., & Willie, J. T. (2020). Human amygdala stimulation effects on emotion physiology and emotional experience. *Neuropsychologia*, *145*. https://doi.org/10.1016/j.neuropsychologia.2018.03.019.

Iriki, A., Tanaka, M., & Iwamura, Y. (1996). Coding of modified body schema during tool use by macaque postcentral neurones. *Neuroreport*, *7*(14), 2325–2330. https://doi.org/10.1097/00001756-199610020-00010.

Ishida, H., Nakajima, K., Inase, M., & Murata, A. (2010). Shared Mapping of Own and Others' Bodies in Visuotactile Bimodal Area of Monkey Parietal Cortex. *Journal of Cognitive Neuroscience*, *22*(1), 83–96. https://doi.org/10.1162/JOCN.2009.21185.

Jacobs, S., Brozzoli, C., Hadj-Bouziane, F., Meunier, M., & Farnè, A. (2011). Studying Multisensory Processing and Its Role in the Representation of Space through Pathological and Physiological Crossmodal Extinction. *Frontiers in Psychology*, *2*(MAY). https://doi.org/10.3389/FPSYG.2011.00089.

Jaeger, T. F. (2008). Categorical Data Analysis: Away from ANOVAs (transformation or not) and towards Logit Mixed Models. *Journal of Memory and Language*, *59*(4), 434. https://doi.org/10.1016/J.JML.2007.11.007.

Janssen, P., Vogels, R., & Orban, G. A. (1999). Macaque inferior temporal neurons are selective for disparity-defined three-dimensional shapes. *Proceedings of the National Academy of Sciences of the United States of America*, *96*(14), 8217. https://doi.org/10.1073/PNAS.96.14.8217.

Jung, B., Taylor, P. A., Seidlitz, J., Sponheim, C., Perkins, P., Ungerleider, L. G., Glen, D., & Messinger, A. (2021). A comprehensive macaque fMRI pipeline and hierarchical atlas. *NeuroImage*, *235*, 117997. https://doi.org/10.1016/J.NEUROIMAGE.2021.117997.

Kennedy, D. P., & Adolphs, R. (2014). Violations of Personal Space by Individuals with Autism Spectrum Disorder. *PLOS ONE*, *9*(8), e103369. https://doi.org/10.1371/JOURNAL.PONE.0103369.

Kennedy, D. P., Gläscher, J., Tyszka, J. M., & Adolphs, R. (2009). Personal space regulation by the human amygdala. *Nature Neuroscience*, *12*(10), 1226–1227. https://doi.org/10.1038/nn.2381.

Khalsa, S. S., Adolphs, R., Cameron, O. G., Critchley, H. D., Davenport, P. W., Feinstein, J. S., Feusner, J. D., Garfinkel, S. N., Lane, R. D., Mehling, W. E., Meuret, A. E., Nemeroff, C. B., Oppenheimer, S., Petzschner, F. H., Pollatos, O., Rhudy, J. L., Schramm, L. P., Simmons, W. K., Stein, M. B., … participants, the I. S. 2016. (2018). Interoception and Mental Health: A Roadmap. *Biological Psychiatry. Cognitive Neuroscience and Neuroimaging*, *3*(6), 501. https://doi.org/10.1016/J.BPSC.2017.12.004.

Kling, A., & Steklis, H. D. (1976). A neural substrate for affiliative behavior in nonhuman primates. *Brain, Behavior and Evolution*, *13*(2–3), 216–238. https://doi.org/10.1159/000123811.

Knutson, B. (1996). Facial expressions of emotion influence interpersonal trait inferences. *Journal of Nonverbal Behavior*, *20*(3), 165–182. https://doi.org/10.1007/bf02281954.

Kravitz, D. J., Saleem, K. S., Baker, C. I., & Mishkin, M. (2011). A new neural framework for visuospatial processing. *Nature Reviews. Neuroscience*, *12*(4), 217. https://doi.org/10.1038/NRN3008.

Làdavas, E, & Farnè, A. (2004). Visuo-tactile representation of near-the-body space. *Journal of Physiology, Paris*, *98*(1–3), 161–170. https://doi.org/10.1016/J.JPHYSPARIS.2004.03.007.

Làdavas, E, Zeloni, G., & Farnè, A. (1998). Visual peripersonal space centred on the face in humans. *Brain : A Journal of Neurology*, *121 (Pt 1*(12), 2317–2326. https://doi.org/10.1093/BRAIN/121.12.2317.

Làdavas, Elisabetta. (2002). Functional and dynamic properties of visual peripersonal space. *Trends in Cognitive Sciences*, *6*(1), 17–22. https://doi.org/10.1016/S1364-6613(00)01814-3.

Làdavas, Elisabetta, & Serino, A. (2010). Action-dependent plasticity in peripersonal space representations. *Http://Dx.Doi.Org/10.1080/02643290802359113*, *25*(7–8), 1099–1113. https://doi.org/10.1080/02643290802359113.

Lara, A. H., Cunningham, J. P., & Churchland, M. M. (2018). Different population dynamics in the supplementary motor area and motor cortex during reaching. *Nature Communications 2018 9:1*, *9*(1), 1–16. https://doi.org/10.1038/s41467-018-05146-z.

Lebert, A., Chaby, L., Garnot, C., & Vergilino-Perez, D. (2020). The impact of emotional videos and emotional static faces on postural control through a personality trait approach. *Experimental Brain Research 2020 238:12*, *238*(12), 2877–2886. https://doi.org/10.1007/S00221-020-05941-5.

Ledberg, A., O'Sullivan, B., Kinomura, S., & Roland, P. (1995). Somatosensory activations of the parietal operculum of man. A PET study. *The European Journal of Neuroscience*, *7*(9), 1934–1941. https://doi.org/10.1111/J.1460-9568.1995.TB00716.X.

Ledoux, J. E., & Brown, R. (2017). A higher-order theory of emotional consciousness. *Proceedings of the National Academy of Sciences of the United States of America*, *114*(10), E2016–E2025. https://doi.org/10.1073/pnas.1619316114.

Lee, H.-S., Hong, S.-J. J., Baxter, T., Scott, J., Shenoy, S., Buck, L., Bodenheimer, B., & Park, S. (2021). Altered Peripersonal Space and the Bodily Self in Schizophrenia: A Virtual Reality Study. *Schizophrenia Bulletin*, *47*(4), 927–937. https://doi.org/10.1093/SCHBUL/SBAB024.

Leinonen, L., Hyvärinen, J., Nyman, G., & Linnankoski, I. (1979). I. Functional properties of neurons in lateral part of associative area 7 in awake monkeys. *Experimental Brain Research 1979 34:2*, *34*(2), 299–320. https://doi.org/10.1007/BF00235675.

Leinonen, L., & Nyman, G. (1979). II. Functional properties of cells in anterolateral part of area 7 associative face area of awake monkeys. *Experimental Brain Research 1979 34:2*, *34*(2), 321–333. https://doi.org/10.1007/BF00235676.

Lenth, R. V. (2016). Least-squares means: The R package lsmeans. *Journal of Statistical Software*, *69*. https://doi.org/10.18637/jss.v069.i01.

Lipson, S. E., Sacks, O., & Devinsky, O. (2003). Selective emotional detachment from family after right temporal lobectomy. *Epilepsy and Behavior*, *4*(3), 340–342. https://doi.org/10.1016/S1525-5050(03)00081-7.

Longo, M., & Lourenco, S. (2006). On the nature of near space: effects of tool use and the transition to far space. *Neuropsychologia*, *44*(6), 977–981. https://doi.org/10.1016/J.NEUROPSYCHOLOGIA.2005.09.003.

Lough, E., Hanley, M., Rodgers, J., South, M., Kirk, H., Kennedy, D. P., & Riby, D. M. (2015). Violations of Personal Space in Young People with Autism Spectrum Disorders and Williams Syndrome: Insights from the Social Responsiveness Scale. *Journal of Autism and Developmental Disorders 2015 45:12*, *45*(12), 4101–4108.

Lourenco, S., Longo, M., & Pathman, T. (2011). Near space and its relation to claustrophobic fear. *Cognition*, *119*.

Luppino, G., Hamed, S. Ben, Gamberini, M., Matelli, M., & Galletti, C. (2005). Occipital (V6) and parietal (V6A) areas in the anterior wall of the parieto-occipital sulcus of the macaque: a cytoarchitectonic study. *European Journal of Neuroscience*, *21*(11), 3056–3076. https://doi.org/10.1111/J.1460-9568.2005.04149.X.

Magosso, E. (2010). Integrating information from vision and touch: A neural network modeling study. *IEEE Transactions on Information Technology in Biomedicine*, *14*(3), 598–612. https://doi.org/10.1109/TITB.2010.2040750.

Magosso, E., Serino, A., Pellegrino, G. di, & Ursino, M. (2010). Crossmodal Links between Vision and Touch in Spatial Attention: A Computational Modelling Study. *Computational Intelligence and Neuroscience*, *2010*, 13. https://doi.org/10.1155/2010/304941.

Magosso, E., Zavaglia, M., Serino, A., di Pellegrino, G., & Ursino, M. (2010). Visuotactile Representation of Peripersonal Space: A Neural Network Study. *Neural Computation*, *22*(1), 190–243. https://doi.org/10.1162/NECO.2009.01-08-694.

Maister, L., Cardini, F., Zamariola, G., Serino, A., & Tsakiris, M. (2015). Your place or mine: Shared sensory experiences elicit a remapping of peripersonal space. *Neuropsychologia*, *70*, 455–461. https://doi.org/10.1016/J.NEUROPSYCHOLOGIA.2014.10.027.

Makin, T., Holmes, N., & Ehrsson, H. (2008). On the other hand: dummy hands and peripersonal space. *Behavioural Brain Research*, *191*(1), 1–10. https://doi.org/10.1016/J.BBR.2008.02.041.

Makin, T. R., Holmes, N. P., & Zohary, E. (2007). Is That Near My Hand? Multisensory Representation of Peripersonal Space in Human Intraparietal Sulcus. *Journal of Neuroscience*, *27*(4), 731–740. https://doi.org/10.1523/JNEUROSCI.3653-06.2007.

Maravita, A., & Iriki, A. (2004). Tools for the body (schema). *Trends in Cognitive Sciences*, *8*(2), 79–86. https://doi.org/10.1016/J.TICS.2003.12.008.

Maravita, A., Spence, C., & Driver, J. (2003). Multisensory integration and the body schema: close to hand and within reach. *Current Biology*, *13*(13), R531–R539. https://doi.org/10.1016/S0960-9822(03)00449-4.

Maravita, A., Spence, C., Kennett, S., & Driver, J. (2002). Tool-use changes multimodal spatial interactions between vision and touch in normal humans. *Cognition*, *83*(2), B25–B34. https://doi.org/10.1016/S0010-0277(02)00003-3.

Mars, R. B., Jbabdi, S., Sallet, J., O'Reilly, J. X., Croxson, P. L., Olivier, E., Noonan, M. P., Bergmann, C., Mitchell, A. S., Baxter, M. G., Behrens, T. E. J., Johansen-Berg, H., Tomassini, V., Miller, K. L., & Rushworth, M. F. S. (2011). Diffusion-Weighted Imaging Tractography-Based Parcellation of the Human Parietal Cortex and Comparison with Human and Macaque Resting-State Functional Connectivity. *Journal of Neuroscience*, *31*(11), 4087–4100. https://doi.org/10.1523/JNEUROSCI.5102-10.2011.

Martin, A., & Weisberg, J. (2003). Neural foundations for understanding social and mechanical concepts. In *Cognitive Neuropsychology* (Vol. 20, Issues 3–6, pp. 575–587). NIH Public Access. https://doi.org/10.1080/02643290342000005.

Masaoka, Y., Hirasawa, K., Yamane, F., Hori, T., & Homma, I. (2003). Effects of left amygdala lesions on respiration, skin conductance, heart rate, anxiety, and activity of the right amygdala during anticipation of negative stimulus. *Behavior Modification*, *27*(5), 607–619. https://doi.org/10.1177/0145445503256314.

Massaccesi, C., Groessing, A., Rosenberger, L. A., Hartmann, H., Candini, M., Di Pellegrino, G., Frassinetti, F., & Silani, G. (2021). *Neural correlates of interpersonal space permeability and flexibility in autism spectrum disorder Running Title: Interpersonal space regulation in autism*. https://doi.org/10.1101/2020.10.14.339291.

Mathôt, S., Schreij, D., & Theeuwes, J. (2012). OpenSesame: An open-source, graphical experiment builder for the social sciences. In *Behavior Research Methods* (Vol. 44, Issue 2, pp. 314–324). Behav Res Methods. https://doi.org/10.3758/s13428-011-0168-7.

Mattingley, J., Driver, J., Beschin, N., & Robertson, L. (1997). Attentional competition between modalities: extinction between touch and vision after right hemisphere damage. *Neuropsychologia*, *35*(6), 867–880. https://doi.org/10.1016/S0028-3932(97)00008-0.

McIntosh, R. D., & Brooks, J. L. (2011). Current tests and trends in single-case neuropsychology. *Cortex*, *47*(10), 1151–1159. https://doi.org/10.1016/j.cortex.2011.08.005.

Mishkin, M., & Ungerleider, L. G. (1982). Contribution of striate inputs to the visuospatial functions of parieto-preoccipital cortex in monkeys. *Behavioural Brain Research*, *6*(1), 57–77. https://doi.org/10.1016/0166-4328(82)90081-X.

Monaco, S., Cavina-Pratesi, C., Sedda, A., Fattori, P., Galletti, C., & Culham, J. C. (2011). Functional magnetic resonance adaptation reveals the involvement of the dorsomedial stream in hand orientation for grasping. *Https://Doi.Org/10.1152/Jn.01069.2010*, *106*(5), 2248–2263. https://doi.org/10.1152/JN.01069.2010.

Mufson, E. J., Mesulam, M. M., & Pandya, D. N. (1981). Insular interconnections with the amygdala in the rhesus monkey. *Neuroscience*, *6*(7), 1231–1248. https://doi.org/10.1016/0306-4522(81)90184-6.

Mul, C., Cardini, F., Stagg, S. D., Esfahlani, S. S., Kiourtsoglou, D., Cardellicchio, P., & Aspell, J. E. (2019). Altered bodily self-consciousness and peripersonal space in autism: *Https://Doi.Org/10.1177/1362361319838950*, *23*(8), 2055–2067. https://doi.org/10.1177/1362361319838950.

Murata, A., Fadiga, L., Fogassi, L., Gallese, V., Raos, V., & Rizzolatti, G. (1997). Object Representation in the Ventral Premotor Cortex (Area F5) of the Monkey. *Https://Doi.Org/10.1152/Jn.1997.78.4.2226*, *78*(4), 2226–2230. https://doi.org/10.1152/JN.1997.78.4.2226.

Murata, A., Gallese, V., Luppino, G., Kaseda, M., & Sakata, H. (2000). Selectivity for the Shape, Size, and Orientation of Objects for Grasping in Neurons of Monkey Parietal Area AIP. *Https://Doi.Org/10.1152/Jn.2000.83.5.2580*, *83*(5), 2580–2601. https://doi.org/10.1152/JN.2000.83.5.2580.

Murata, A., Wen, W., & Asama, H. (2016). The body and objects represented in the ventral stream of the parieto-premotor network. *Neuroscience Research*, *104*, 4–15. https://doi.org/10.1016/J.NEURES.2015.10.010.

Naghavi, H., Eriksson, J., Larsson, A., & Nyberg, L. (2007). The claustrum/insula region integrates conceptually related sounds and pictures. *Neuroscience Letters*, *422*(1), 77–80. https://doi.org/10.1016/J.NEULET.2007.06.009.

Neubert, F. X., Mars, R. B., Thomas, A. G., Sallet, J., & Rushworth, M. F. S. (2014). Comparison of Human Ventral Frontal Cortex Areas for Cognitive Control and Language with Areas in Monkey Frontal Cortex. *Neuron*, *81*(3), 700–713. https://doi.org/10.1016/J.NEURON.2013.11.012.

Nichols, T. E., & Holmes, A. P. (2002). Nonparametric permutation tests for functional neuroimaging: A primer with examples. *Human Brain Mapping*, *15*(1), 1–25. https://doi.org/10.1002/hbm.1058.

Nishihara, R., & Okubo, M. (2015). A Study on Personal Space in Virtual Space based on Personality. *Procedia Manufacturing*, *3*, 2183–2190. https://doi.org/10.1016/J.PROMFG.2015.07.359.

Noack, J., Murau, R., & Engelmann, M. (2015). Consequences of temporary inhibition of the medial amygdala on social recognition memory performance in mice. *Frontiers in Neuroscience*, *9*(APR), 152. https://doi.org/10.3389/fnins.2015.00152.

Noel, J.-P., Cascio, C. J., Wallace, M. T., & Park, S. (2017). The Spatial Self in Schizophrenia and Autism Spectrum Disorder. *Schizophrenia Research*, *179*, 8. https://doi.org/10.1016/J.SCHRES.2016.09.021.

Noel, J. P., Grivaz, P., Marmaroli, P., Lissek, H., Blanke, O., & Serino, A. (2015). Full body action remapping of peripersonal space: The case of walking. *Neuropsychologia*, *70*, 375–384. https://doi.org/10.1016/J.NEUROPSYCHOLOGIA.2014.08.030.

Noel, J. P., Park, H. D., Pasqualini, I., Lissek, H., Wallace, M., Blanke, O., & Serino, A. (2018). Audio-visual sensory deprivation degrades visuo-tactile peri-personal space. *Consciousness and Cognition*, *61*, 61–75. https://doi.org/10.1016/J.CONCOG.2018.04.001.

Noel, J. P., Pfeiffer, C., Blanke, O., & Serino, A. (2015). Peripersonal space as the space of the bodily self. *Cognition*, *144*, 49–57. https://doi.org/10.1016/J.COGNITION.2015.07.012.

O'Reilly, J. X., Woolrich, M. W., Behrens, T. E. J., Smith, S. M., & Johansen-Berg, H. (2012). Tools of the trade: psychophysiological interactions and functional connectivity. *Social Cognitive and Affective Neuroscience*, *7*(5), 604. https://doi.org/10.1093/SCAN/NSS055.

O'Toole, A. J., Roark, D. A., & Abdi, H. (2002). Recognizing moving faces: a psychological and neural synthesis. *Trends in Cognitive Sciences*, *6*(6), 261–266. https://doi.org/10.1016/S1364-6613(02)01908-3.

Oosterhof, N. N., Connolly, A. C., & Haxby, J. V. (2016). CoSMoMVPA: Multi-modal multivariate pattern analysis of neuroimaging data in matlab/GNU octave. *Frontiers in Neuroinformatics*, *10*(JUL), 27. https://doi.org/10.3389/fninf.2016.00027.

Orban, G. A. (2011). The Extraction of 3D Shape in the Visual System of Human and Nonhuman Primates. *Http://Dx.Doi.Org/10.1146/Annurev-Neuro-061010-113819*, *34*, 361–368. https://doi.org/10.1146/ANNUREV-NEURO-061010-113819.

Orban, G. A. (2016). Functional definitions of parietal areas in human and non-human primates. *Proceedings of the Royal Society B: Biological Sciences*, *283*(1828). https://doi.org/10.1098/RSPB.2016.0118.

Ortigue, S., Mégevand, P., Perren, F., Landis, T., & Blanke, O. (2006). Double dissociation between representational personal and extrapersonal neglect. *Neurology*, *66*(9), 1414–1417. https://doi.org/10.1212/01.WNL.0000210440.49932.E7.

Palomero-Gallagher, N., & Amunts, K. (2021). A short review on emotion processing: a lateralized network of neuronal networks. *Brain Structure and Function 2021*, *1*, 1–12. https://doi.org/10.1007/S00429-021-02331-7.

Parker, A. J. (2007). Binocular depth perception and the cerebral cortex. *Nature Reviews Neuroscience 2007 8:5*, *8*(5), 379–391. https://doi.org/10.1038/nrn2131.

Patané, I., Farnè, A., & Frassinetti, F. (2017). Cooperative tool-use reveals peripersonal and interpersonal spaces are dissociable. *Cognition*, *166*, 13–22. https://doi.org/10.1016/j.cognition.2017.04.013.

Pavani, F., Spence, C., & Driver, J. (2000). Visual capture of touch: out-of-the-body experiences with rubber gloves. *Psychological Science*, *11*(5), 353–359. https://doi.org/10.1111/1467-9280.00270.

Pellencin, E., Paladino, M. P., Herbelin, B., & Serino, A. (2018). Social perception of others shapes one's own multisensory peripersonal space. *Cortex*, *104*, 163–179. https://doi.org/10.1016/J.CORTEX.2017.08.033.

Petkova, V. I., & Ehrsson, H. H. (2008). If I Were You: Perceptual Illusion of Body Swapping. *PLOS ONE*, *3*(12), e3832. https://doi.org/10.1371/JOURNAL.PONE.0003832.

Petkova, V. I., Khoshnevis, M., & Ehrsson, H. H. (2011). The Perspective Matters! Multisensory Integration in Ego-Centric Reference Frames Determines Full-Body Ownership. *Frontiers in Psychology*, *2*(MAR). https://doi.org/10.3389/FPSYG.2011.00035.

Pitcher, D., & Ungerleider, L. G. (2021). Evidence for a Third Visual Pathway Specialized for Social Perception. *Trends in Cognitive Sciences*, *25*(2), 100–110. https://doi.org/10.1016/J.TICS.2020.11.006.

Pitzalis, S., Sereno, M. I., Committeri, G., Fattori, P., Galati, G., Tosoni, A., & Galletti, C. (2013). The human homologue of macaque area V6A. *NeuroImage*, *82*. https://doi.org/10.1016/j.neuroimage.2013.06.026.

Prescott, M. J., & Poirier, C. (2021). The role of MRI in applying the 3Rs to non-human primate neuroscience. *NeuroImage*, *225*, 117521. https://doi.org/10.1016/J.NEUROIMAGE.2020.117521.

Quadt, L., Critchley, H. D., & Garfinkel, S. N. (2018). The neurobiology of interoception in health and disease. *Annals of the New York Academy of Sciences*, *1428*(1), 112–128. https://doi.org/10.1111/NYAS.13915.

Quesque, F., Ruggiero, G., Mouta, S., Santos, J., Iachini, T., & Coello, Y. (2017). Keeping you at arm's length: modifying peripersonal space influences interpersonal distance. *Psychological Research*, *81*(4), 709–720. https://doi.org/10.1007/s00426-016-0782-1.

Quinlan, D. J., & Culham, J. C. (2007). fMRI reveals a preference for near viewing in the human parieto-occipital cortex. *NeuroImage*, *36*(1), 167–187. https://doi.org/10.1016/J.NEUROIMAGE.2007.02.029.

Rabellino, D., Frewen, P. A., McKinnon, M. C., & Lanius, R. A. (2020). Peripersonal Space and Bodily Self-Consciousness: Implications for Psychological Trauma-Related Disorders. *Frontiers in Neuroscience*, *14*, 586605. https://doi.org/10.3389/fnins.2020.586605.

Raos, V., Umiltá, M.-A., Murata, A., Fogassi, L., & Gallese, V. (2006). Functional Properties of Grasping-Related Neurons in the Ventral Premotor Area F5 of the Macaque Monkey. *Https://Doi.Org/10.1152/Jn.00463.2005*, *95*(2), 709–729. https://doi.org/10.1152/JN.00463.2005.

Reveley, C., Gruslys, A., Ye, F. Q., Glen, D., Samaha, J., E. Russ, B., Saad, Z., K. Seth, A., Leopold, D. A., & Saleem, K. S. (2017). Three-Dimensional Digital Template Atlas of the Macaque Brain. *Cerebral Cortex*, *27*(9), 4463–4477. https://doi.org/10.1093/CERCOR/BHW248.

Rizzolatti, G, Camarda, R., Fogassi, L., Gentilucci, M., Luppino, G., & Matelli, M. (1988). Functional organization of inferior area 6 in the macaque monkey. II. Area F5 and the control of distal movements. *Experimental Brain Research*, *71*(3), 491–507. https://doi.org/10.1007/BF00248742.

Rizzolatti, G, & Craighero, L. (2004). THE MIRROR-NEURON SYSTEM. *Annu. Rev. Neurosci*, *27*, 169–192. https://doi.org/10.1146/annurev.neuro.27.070203.144230.

Rizzolatti, G & Matelli, M. (2003). Two different streams form the dorsal visual system: anatomy and functions. *Experimental Brain Research 2003 153:2*, *153*(2), 146–157. https://doi.org/10.1007/S00221-003-1588-0.

Rizzolatti, G, Scandolara, C., Matelli, M., & Gentilucci, M. (1981). Afferent properties of periarcuate neurons in macaque monkeys. II. Visual responses. *Behavioural Brain Research*, *2*(2), 147–163. https://doi.org/10.1016/0166-4328(81)90053-X.

Robinson, C. J., & Burton, H. (1980). Organization of somatosensory receptive fields in cortical areas 7b, retroinsula, postauditory and granular insula of M. fascicularis. *Journal of Comparative Neurology*, *192*(1), 69–92. https://doi.org/10.1002/CNE.901920105.

Robinson, D. L., Goldberg, M. E., & Stanton, G. B. (1978). Parietal association cortex in the primate: sensory mechanisms and behavioral modulations. *Https://Doi.Org/10.1152/Jn.1978.41.4.910*, *41*(4), 910–932. https://doi.org/10.1152/JN.1978.41.4.910.

Rolls, E. T., Huang, C. C., Lin, C. P., Feng, J., & Joliot, M. (2020). Automated anatomical labelling atlas 3. *NeuroImage*, *206*, 116189. https://doi.org/10.1016/j.neuroimage.2019.116189.

Rossetti, A., Romano, D., Bolognini, N., & Maravita, A. (2015). Dynamic expansion of alert responses to incoming painful stimuli following tool use. *Neuropsychologia*, *70*, 486–494. https://doi.org/10.1016/J.NEUROPSYCHOLOGIA.2015.01.019.

Rozzi, S., Ferrari, P. F., Bonini, L., Rizzolatti, G., & Fogassi, L. (2008). Functional organization of inferior parietal lobule convexity in the macaque monkey: electrophysiological characterization of motor, sensory and mirror responses and their correlation with cytoarchitectonic areas. *European Journal of Neuroscience*, *28*(8), 1569–1588. https://doi.org/10.1111/J.1460-9568.2008.06395.X.

Ruggiero, G., Frassinetti, F., Coello, Y., Rapuano, M., di Cola, A. S., & Iachini, T. (2017). The effect of facial expressions on peripersonal and interpersonal spaces. *Psychological Research*, *81*(6), 1232–1240. https://doi.org/10.1007/s00426-016-0806-x.

Ruggiero, G., Rapuano, M., & Iachini, T. (2019). Perceived temperature modulates peripersonal and interpersonal spaces differently in men and women. *Journal of Environmental Psychology*, *63*, 52–59. https://doi.org/10.1016/j.jenvp.2019.04.004.

Sakata, H, Shibutani, H., & Kawano, K. (1980). Spatial properties of visual fixation neurons in posterior parietal association cortex of the monkey. *Journal of Neurophysiology*, *43*(6), 1654–1672. https://doi.org/10.1152/JN.1980.43.6.1654.

Sakata, Hideo, Takaoka, Y., Kawarasaki, A., & Shibutani, H. (1973). Somatosensory properties of neurons in the superior parietal cortex (area 5) of the rhesus monkey. *Brain Research*, *64*(C), 85–102. https://doi.org/10.1016/0006-8993(73)90172-8.

Sallet, J., Mars, R. B., Noonan, M. P., Neubert, F.-X., Jbabdi, S., O'Reilly, J. X., Filippini, N., Thomas, A. G., & Rushworth, M. F. (2013). The Organization of Dorsal Frontal Cortex in Humans and Macaques. *Journal of Neuroscience*, *33*(30), 12255–12274. https://doi.org/10.1523/JNEUROSCI.5108-12.2013.

Sambo, C. F., Liang, M., Cruccu, G., & Iannetti, G. D. (2012). Defensive peripersonal space: the blink reflex evoked by hand stimulation is increased when the hand is near the face. *Https://Doi.Org/10.1152/Jn.00731.2011*, *107*(3), 880–889. https://doi.org/10.1152/JN.00731.2011.

Sambo, Chiara F., & Iannetti, G. D. (2013). Better Safe Than Sorry? The Safety Margin Surrounding the Body Is Increased by Anxiety. *The Journal of Neuroscience*, *33*(35), 14225. https://doi.org/10.1523/JNEUROSCI.0706-13.2013.

Sarubbo, S., Annicchiarico, L., Corsini, F., Zigiotto, L., Herbet, G., Moritz-Gasser, S., Dalpiaz, C., Vitali, L., Tate, M., De Benedictis, A., Amorosino, G., Olivetti, E., Rozzanigo, U., Petralia, B., Duffau, H., & Avesani, P. (2021). Planning Brain Tumor Resection Using a Probabilistic Atlas of Cortical and Subcortical Structures Critical for Functional Processing: A Proof of Concept. *Operative Neurosurgery*, *20*(3), E175–E183. https://doi.org/10.1093/ons/opaa396.

Sarubbo, S., De Benedictis, A., Merler, S., Mandonnet, E., Balbi, S., Granieri, E., & Duffau, H. (2015). Towards a functional atlas of human white matter. *Human Brain Mapping*, *36*(8), 3117–3136. https://doi.org/10.1002/hbm.22832.

Sarubbo, S., Tate, M., De Benedictis, A., Merler, S., Moritz-Gasser, S., Herbet, G., & Duffau, H. (2020). Mapping critical cortical hubs and white matter pathways by direct electrical stimulation: an original functional atlas of the human brain. *NeuroImage*, *205*, 116237. https://doi.org/10.1016/j.neuroimage.2019.116237.

Scandola, M., Aglioti, S. M., Lazzeri, G., Avesani, R., Ionta, S., & Moro, V. (2020). Visuo-motor and interoceptive influences on peripersonal space representation following spinal cord injury. *Scientific Reports 2020 10:1*, *10*(1), 1–16. https://doi.org/10.1038/s41598-020-62080-1.

Schaefer, M., Heinze, H.-J., & Rotte, M. (2012). Close to You: Embodied Simulation for Peripersonal Space in Primary Somatosensory Cortex. *PLOS ONE*, *7*(8), e42308. https://doi.org/10.1371/JOURNAL.PONE.0042308.

Scheperjans, F., Grefkes, C., Palomero-Gallagher, N., Schleicher, A., & Zilles, K. (2005). Subdivisions of human parietal area 5 revealed by quantitative receptor autoradiography: a parietal region between motor, somatosensory, and cingulate cortical areas. *NeuroImage*, *25*(3), 975–992. https://doi.org/10.1016/J.NEUROIMAGE.2004.12.017.

Scheperjans, F., Palomero-Gallagher, N., Grefkes, C., Schleicher, A., & Zilles, K. (2005). Transmitter receptors reveal segregation of cortical areas in the human superior parietal cortex: Relations to visual and somatosensory regions. *NeuroImage*, *28*(2), 362–379. https://doi.org/10.1016/J.NEUROIMAGE.2005.06.028.

Schienle, A., Wabnegger, A., Leitner, M., & Leutgeb, V. (2016). *Neuronal correlates of personal space intrusion in violent offenders*. https://doi.org/10.1007/s11682-016-9526-5.

Seidel, E. M., Habel, U., Kirschner, M., Gur, R. C., & Derntl, B. (2010). The Impact of Facial Emotional Expressions on Behavioral Tendencies in Women and Men. *Journal of Experimental Psychology: Human Perception and Performance*, *36*(2), 500–507. https://doi.org/10.1037/a0018169.

Sereno, M. I., & Huang, R.-S. (2006). *A human parietal face area contains aligned head-centered visual and tactile maps*. https://doi.org/10.1038/nn1777.

Serino, A, Bassolino, M., Farnè, A., & Làdavas, E. (2007). Extended multisensory space in blind cane users. *Psychological Science*, *18*(7), 642–648. https://doi.org/10.1111/J.1467-9280.2007.01952.X.

Serino, A. (2019). Peripersonal space (PPS) as a multisensory interface between the individual and the environment, defining the space of the self. *Neuroscience & Biobehavioral Reviews*, *99*, 138–159. https://doi.org/10.1016/J.NEUBIOREV.2019.01.016.

Serino, A, Alsmith, A., Costantini, M., Mandrigin, A., Tajadura-Jimenez, A., & Lopez, C. (2013). Bodily ownership and self-location: Components of bodily self-consciousness. *Consciousness and Cognition*, *22*(4), 1239–1252. https://doi.org/10.1016/J.CONCOG.2013.08.013.

Serino, A, Canzoneri, E., Marzolla, M., di Pellegrino, G., & Magosso, E. (2015). Extending peripersonal space representation without tool-use: evidence from a combined behavioral-computational approach. *Frontiers in Behavioral Neuroscience*, *0*(FEB), 4. https://doi.org/10.3389/FNBEH.2015.00004.

Serino, A, Noel, J.-P., Galli, G., Canzoneri, E., Marmaroli, P., Lissek, H., & Blanke, O. (2015). Body part-centered and full body-centered peripersonal space representations. *Scientific Reports 2015 5:1*, *5*(1), 1–14. https://doi.org/10.1038/srep18603.

Showers, M. J. C., & Lauer, E. W. (1961). Somatovisceral motor patterns in the insula. *Journal of Comparative Neurology*, *117*(1), 107–115. https://doi.org/10.1002/CNE.901170109.

Spence, C, Pavani, F., & Driver, J. (2000). Crossmodal links between vision and touch in covert endogenous spatial attention. *Journal of Experimental Psychology. Human Perception and Performance*, *26*(4), 1298–1319. https://doi.org/10.1037//0096-1523.26.4.1298.

Spence, Charles, Pavani, F., & Driver, J. (2004). Spatial constraints on visual-tactile cross-modal distractor congruency effects. *Cognitive, Affective and Behavioral Neuroscience*, *4*(2), 148–169. https://doi.org/10.3758/CABN.4.2.148.

Srivastava, S., Orban, G. A., Mazière, P. A. De, & Janssen, P. (2009). A Distinct Representation of Three-Dimensional Shape in Macaque Anterior Intraparietal Area: Fast, Metric, and Coarse. *Journal of Neuroscience*, *29*(34), 10613–10626. https://doi.org/10.1523/JNEUROSCI.6016-08.2009.

Stanton, G., Deng, S., Goldberg, M., & McMullen, N. (1989). Cytoarchitectural characteristic of the frontal eye fields in macaque monkeys. *The Journal of Comparative Neurology*, *282*(3), 415–427. https://doi.org/10.1002/CNE.902820308.

Teneggi, C., Canzoneri, E., Pellegrino, G. di, & Serino, A. (2013). Social modulation of peripersonal space boundaries. *Curr Biol*, *23*.

Thier, P., & Andersen, R. (1998). Electrical microstimulation distinguishes distinct saccade-related areas in the posterior parietal cortex. *Journal of Neurophysiology*, *80*(4), 1713–1735. https://doi.org/10.1152/JN.1998.80.4.1713.

Tsakiris, M. (2010). My body in the brain: A neurocognitive model of body-ownership. *Neuropsychologia*, *48*(3), 703–712. https://doi.org/10.1016/J.NEUROPSYCHOLOGIA.2009.09.034.

Tyll, S., Bonath, B., Schoenfeld, A., Heinze, H.-J., Ohl, F. W., & Noesselt, T. (2012). *Neural basis of multisensory looming signals*. https://doi.org/10.1016/j.neuroimage.2012.09.056.

Uddin, L. Q., Nomi, J. S., Hebert-Seropian, B., Ghaziri, J., & Boucher, O. (2017). Structure and function of the human insula. *Journal of Clinical Neurophysiology : Official Publication of the American Electroencephalographic Society*, *34*(4), 300. https://doi.org/10.1097/WNP.0000000000000377.

Van Dantzig, S., Pecher, D., & Zwaan, R. A. (2008). Approach and avoidance as action effects. *Quarterly Journal of Experimental Psychology*, *61*(9), 1298–1306. https://doi.org/10.1080/17470210802027987.

Verhagen, L., Dijkerman, H. C., Medendorp, W. P., & Toni, I. (2012). Cortical Dynamics of Sensorimotor Integration during Grasp Planning. *Journal of Neuroscience*, *32*(13), 4508–4519. https://doi.org/10.1523/JNEUROSCI.5451-11.2012.

Verhoef, B.-E., Vogels, R., & Janssen, P. (2016). Binocular depth processing in the ventral visual pathway. *Philosophical Transactions of the Royal Society B: Biological Sciences*, *371*(1697). https://doi.org/10.1098/RSTB.2015.0259.

Vernet, M., Quentin, R., Chanes, L., Mitsumasu, A., & Valero-Cabré, A. (2014). Frontal eye field, where art thou? Anatomy, function, and non-invasive manipulation of frontal regions involved in eye movements and associated cognitive operations. *Frontiers in Integrative Neuroscience*, *0*(AUG), 66. https://doi.org/10.3389/FNINT.2014.00066.

Vieira, J. B., Pierzchajlo, S. R., & Mitchell, D. G. V. (2020). Neural correlates of social and non-social personal space intrusions: Role of defensive and peripersonal space systems in interpersonal distance regulation. *Social Neuroscience*, *15*(1), 36–51. https://doi.org/10.1080/17470919.2019.1626763.

Vieira, J. B., Tavares, T. P., Marsh, A. A., & Mitchell, D. G. V. (2017). Emotion and personal space: Neural correlates of approach-avoidance tendencies to different facial expressions as a function of coldhearted psychopathic traits. *Human Brain Mapping*, *38*(3), 1492–1506. https://doi.org/10.1002/hbm.23467.

Vilasboas, T., Herbet, G., & Duffau, H. (2017). Challenging the Myth of Right Nondominant Hemisphere: Lessons from Corticosubcortical Stimulation Mapping in Awake Surgery and Surgical Implications. In *World Neurosurgery* (Vol. 103, pp. 449–456). Elsevier Inc. https://doi.org/10.1016/j.wneu.2017.04.021.

Vuilleumier, P., Valenza, N., Mayer, E., Reverdin, A., & Landis, T. (1998). Near and far visual space in unilateral neglect. *Annals of Neurology*, *43*(3), 406–410. https://doi.org/10.1002/ANA.410430324.

Wiley, R. W., & Rapp, B. (2019). Statistical analysis in Small-N Designs: using linear mixed-effects modeling for evaluating intervention effectiveness. *Aphasiology*, *33*(1), 1–30. https://doi.org/10.1080/02687038.2018.1454884.

Wise, S. (1985). The primate premotor cortex: past, present, and preparatory. *Annual Review of Neuroscience*, *8*(1), 1–19. https://doi.org/10.1146/ANNUREV.NE.08.030185.000245.

Wittmann, M., Van Wassenhove, V., Craig, B., & Paulus, M. P. (2010). The neural substrates of subjective time dilation. *Frontiers in Human Neuroscience*, *0*, 2. https://doi.org/10.3389/NEURO.09.002.2010.

Xu, T., Nenning, K. H., Schwartz, E., Hong, S. J., Vogelstein, J. T., Goulas, A., Fair, D. A., Schroeder, C. E., Margulies, D. S., Smallwood, J., Milham, M. P., & Langs, G. (2020). Cross-species functional alignment reveals evolutionary hierarchy within the connectome. *NeuroImage*, *223*, 117346. https://doi.org/10.1016/J.NEUROIMAGE.2020.117346.

Yamane, Y., Carlson, E. T., Bowman, K. C., Wang, Z., & Connor, C. E. (2008). A neural code for three-dimensional object shape in macaque inferotemporal cortex. *Nature Neuroscience*, *11*(11), 1352. https://doi.org/10.1038/NN.2202.

Yordanova, Y. N., Duffau, H., & Herbet, G. (2017). Neural pathways subserving face-based mentalizing. *Brain Structure and Function*, *222*(7), 3087–3105. https://doi.org/10.1007/s00429-017-1388-0.

Zacà, D., Corsini, F., Rozzanigo, U., Dallabona, M., Avesani, P., Annicchiarico, L., Zigiotto, L., Faraca, G., Chioffi, F., Jovicich, J., & Sarubbo, S. (2018). Whole-brain network connectivity underlying the human speech articulation as emerged integrating direct electric stimulation, resting state FMRI and tractography. *Frontiers in Human Neuroscience*, *12*, 405. https://doi.org/10.3389/fnhum.2018.00405.

Zanini, A., Patané, I., Blini, E., Salemme, R., Koun, E., Farnè, A., & Brozzoli, C. (2021). Peripersonal and reaching space differ: Evidence from their spatial extent and multisensory facilitation pattern. *Psychonomic Bulletin & Review 2021*, 1–12. https://doi.org/10.3758/S13423-021-01942-9.

Zigiotto, L., Annicchiarico, L., Corsini, F., Vitali, L., Falchi, R., Dalpiaz, C., Rozzanigo, U., Barbareschi, M., Avesani, P., Papagno, C., Duffau, H., Chioffi, F., & Sarubbo, S. (2020). Effects of supra-total resection in neurocognitive and oncological outcome of high-grade gliomas comparing asleep and awake surgery. *Journal of Neuro-Oncology*, *148*(1), 97–108. https://doi.org/10.1007/s11060-020-03494-9.